UNIVERSIDAD DE GRANADA

FACULTAD DE BELLAS ARTES

Departamento de Escultura

Efecto de los ciclos de humedad-sequedad en el deterioro de rocas ornamentales que contienen minerales de la arcilla

Inmaculada Jiménez González

TESIS DOCTORAL

Granada, 2008

Editor: Editorial de la Universidad de Granada
Autor: Inmaculada Jiménez González
D.L.: GR.1776-2008
ISBN: 978-84-691-5461-8

Memoria presentada por Inmaculada Jiménez González para aspirar al grado de Doctor por la Universidad de Granada y realizada bajo la dirección de los Doctores: Carlos M. Rodríguez Navarro, Catedrático del Departamento de Mineralogía y Petrología de la Universidad de Granada; George W. Scherer, Catedrático de Ingeniería Civil y Ambiental de la Universidad de Princeton (NJ), EE.UU. y George S. Wheeler, Catedrático de la Universidad de Columbia (NYC), EE.UU. y Científico del Metropolitan Museum de Nueva York.

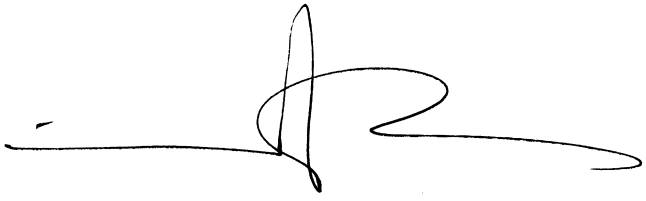

Fdo. Inmaculada Jiménez González

DIRECTORES:

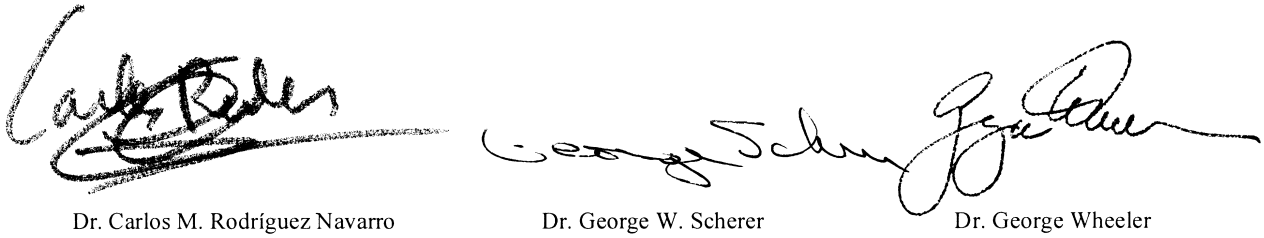

Dr. Carlos M. Rodríguez Navarro | Dr. George W. Scherer | Dr. George Wheeler

A mi bailaora Sophie,
a mi cajonista Robert,
al "ritmo" que llevo dentro
y a mis padres…
¡Gracias, va por vosotros!

Agradecimientos

Empezaré diciendo que nunca esperé que mi tesis pudiera convertirse en un trabajo “tan próximo al ámbito de la Ciencia de los materiales”.

Comencé alegremente la misma familiarizándome con el espacio del laboratorio y sus instrumentos y realizando algunos ensayos fáciles y relativamente comunes en el ámbito de la conservación de la piedra. La dificultad llegó cuando empecé a obtener resultados inesperados (ej. valores de módulos de elasticidad “intrigantes” durante las medidas con ultrasonidos o “descubrir” un comportamiento viscoelastico de las piedras con las que trabajaba). Todo ello desviaba mi investigación hacia temas más propios de la Ciencia de los materiales.

Como conservadora/restauradora, con una formación, desde el punto de vista académico, no científica; el poder entender y controlar en profundidad aquellos “descubrimientos” no era algo fácil, sin embargo, todo ello se proponía como un puro desafío intelectual. Así que intenté asumirlo a través de la dedicación de largas horas para aprender sobre los principios básicos y mecanismos físicos que rigen los comportamientos de la piedra, así como sobre sus propiedades mecánicas y las complicaciones inherentes a las mismas.

Este preámbulo se hace entonces necesario para expresar desde la más profunda modestia y sinceridad, mi agradecimiento a todas aquellas entidades y personas que me han ayudado, desde diferentes puntos de vista o ámbitos, a llevar a cabo este proyecto.

Mi investigación ha sido llevada a cabo en las Universidades de Granada, Princeton (NJ, EE.UU.) y el “Expert Center for Built Cultural Heritage” (Escuela Politécnica Federal en Lausanne, Suiza). La misma ha sido financiada por la fundación Samuel H. Kress (Nueva York) y VIP Restoration INC. A ambas entidades les agradezco el soporte económico recibido, sin el cual este trabajo no hubiera sido posible.

Tampoco lo hubiera sido, por supuesto, sin la guia de mis tres directores de tesis. A ellos agradezco el haber depositado su confianza en mí, ofrecido su amistad e inspirado durante todo este tiempo. De forma muy especial expreso mi agradecimiento al Dr. George W. Scherer por su optimismo, entusiasmo contagioso y curiosidad

intelectual que no sólo han amenizado y motivado mi estancia en Princeton desde un principio, sino que han sido los responsables de que incluso haya llegado a pensar como él… that “Science is beautiful”…, aunque no siempre lo diga!. Es de agradecer la forma en la que está introduciendo su amplio conocimiento en Ciencia de los materiales en el ámbito de la Conservación de materiales pétreos; pero si hay algo que me ha marcado sobremanera es su generosidad intelectual, de la cual espero haberme contagiado.

Del mismo modo quedo agradecida al Dr. Carlos M. Rodríguez Navarro por su enorme disponibilidad, asistencia e interés en este proyecto. Su vasto conocimiento sobre materiales pétreos ha ofrecido una dimensión adicional a este trabajo. Asimismo, su crítica, siempre muy constructiva, ha sido esencial a la hora de aclarar conceptos y explicaciones cruciales en esta tesis.

Al Dr. George Wheeler, le expreso mi gratitud por su orientación, asesoramiento y por haber sido el promotor del tema de mi investigación. Su gran experiencia y conocimiento en el ámbito de la conservación de rocas ornamentales fue esencial a la hora de identificar una piedra de gran importancia en el patrimonio construido norteamericano y potencialmente candidata al tipo de degradación que se planteó estudiar en esta tesis.

Expreso también mi agradecimiento al Dr. Miguel Barranco López, mi tutor en el programa de doctorado del Dpto. de Escultura al cual estoy adscrita, por su disponibilidad, ayuda y por animarme siempre en esta aventura. Asimismo, quedo sinceramente agradecida a este Departamento, por su apoyo y por haberme siempre permitido y facilitado el llevar a cabo este proyecto.

Durante mi estancia en la Universidad de Princeton, agradezco a mis colegas y u otros profesionales ligados al Dpto. de Ingeniería Civil y Ambiental la colaboración prestada. En especial:

A Tim Wangler, por haberme ayudado a terminar algunos ensayos que había dejado “aún en el horno” al abandonar EE.UU.

A la Dra. Wilasa Vichit-Vadakan, por el interés demostrado en mi trabajo, por introducirme en algunas técnicas de laboratorio muy importantes para mi tesis, y por su ayuda y apoyo en general en múltiples ocasiones.

A los Dres. John Valenza y Hang-Shing Ma, por su ayuda y asesoramiento técnico en temas de ensayos de flexión por tres puntos y adsorción de nitrógeno, respectivamente y a Megan Higgins, por haber sido una “cool Senior thesis student” con quien trabajar y compartir laboratorio.

A Joe Vocaturo por su ingenio y brillantez técnica a la hora de convertir los proyectos en papel o verbales en verdaderas obras de arte (ej: máquina para someter probetas a ciclos de humedad /sequedad) además de por el trato siempre amable recibido; el mismo que recibí de Larry McIntyre y Barry Runner, a los cuales he de agradecer su buenas ideas y excepcional destreza en la fabricación y modificación de instrumentos cruciales en mi trabajo. A George Rose le doy las gracias por su asistencia técnica en el laboratorio de piedra y por permitirme siempre el acceso al mismo y poner todo su instrumental a mi servicio.

La finalización de una parte importante de mi tesis ha tenido lugar al volver a Europa y responsable de ello ha sido la generosidad del Dr. Andreas Queisser (Expert Center, EPFL, Suiza) al acogerme en su grupo y proporcionarme material pétreo e información concerniente al mismo. A Jérôme Constantin le doy las gracias por la atención y ayuda prestadas. A Fred Girardet, por proporcionarme información muy útil. Su profundo sentido de la observación y excepcional uso del sentido común para deducir el proceso de degradación de las obras in situ son, sencillamente, dignos de admiración.

Agradezco asimismo:

A la Dra. Lucia Fernández por su ayuda, asesoramiento en los análisis de DRX y proceso de separación de arcillas, asi como por su amistad y el apoyo ofrecido.

A Ivan Myjer por su generosidad al compartir material fotográfico e información sobre aspectos particulares de la conservación de la piedra más estudiada en mi tesis.

A los Dres. David Benavente García (Universidad de Alicante) y Costanza Miliani (CNR de Perugia) por su compañerismo, amistad y por empujarme a que termine este proyecto.

A “Tita tzara, Tata igit, Tonton Shel y Grandpapa Ené” por su gran comprensión, apoyo y por algunos “baby-sittings” decisivos durante la redacción de esta memoria.

A Marthy Scherer por sus ánimos y por recordarme…to “keep calm!”

Mil gracias a mi familia, en especial a la abuela, por su continuo interés en mi trayectoria académica y su constancia en recordarme lo que he de terminar y a los amigos de aquí, de allá, recientes y particularmente a esos de toda la vida, por su apoyo moral, su amistad y paciencia demostrada al aguantarme durante este periodo y aceptar mis recurrentes “no” a tomar una caña o a “irse de marcha”.

Agradezco a la música en general, por el mero hecho de existir y a sus artistas, especialmente a Mario Conte, Mariza, Juan Perro, Kronos Quartet y Glenn Gould por producirme esos “picos en el ánimo” que asiduamente se necesitan, recordándome que debo dedicarles más tiempo en el futuro.

De todo corazón, le agradezco a mi hermano su ayuda inestimable, sus consejos, optimismo, disponibilidad extrema y sus enormes esfuerzos e interés para hacer que esas cosas imprevistas y de “último minuto” sean siempre posibles.

Por supuesto, la conclusión de este trabajo hubiera sido imposible sin la ayuda inestimable y gran apoyo de mis padres, en fin que puedo decir… sus sacrificios, esfuerzos, generosidad, dedicación, continuos puentes aéreos Granada-Zurich y todo el cariño y cuidado que han dado a su nieta… y mucho más, han sido cruciales en todo este tiempo.

Por último agradeceré siempre a mi niña Sophie por permitirme “robarte tiempo” para llevar a cabo ese último “ensayo” que ha venido demorándose -a pesar de tus innumerables ¡“mamos…mamos”!- por mi empeño en mantenerte a mi lado en todo momento y que ha consistido en finalizar la redacción de esta memoria. Para concluir, como no, a Robert, siempre y para siempre, por tu optimismo, tus espléndidos consejos, tozuda insistencia en algunos temas y por aguantar “el tirón”. No encuentro palabras adecuadas para agradecerte TANTO en ninguna lengua…bueno, espero que quizás el alemán, con sus palabras tan largas, me permita algún día expresarlo!. Perdón también por el tiempo usurpado! y muchas gracias por estar siempre ahí, “clavao” a mi lado, en los momentos más delicados.

Resumen

Esta tesis afronta uno de los mecanismos de deterioro menos estudiados que afecta al patrimonio construido y obras de arte realizadas en piedra que contiene minerales de la arcilla: la expansión y contracción del material al ser expuesto a episodios de humedad y sequedad.

El hecho de que ciertos minerales de la arcilla sufran expansión en presencia de agua y contracción durante el secado es un fenómeno conocido, como también lo es la deformación ocasionada a los materiales pétreos naturales que los contienen. También se sabe que determinadas rocas con contenidos altos (10-15 %) de estos filosilicatos y provenientes de ambientes muy secos (ej. Egipto) puedan llegar a descomponerse literalmente cuando son sumergidas en agua (Rodríguez Navarro et al., 1997, 1998; Zehnder et al., 2000). Sin embargo, sólo se han encontrado pocos estudios que parecen mostrar de forma convincente que el tipo de daño estudiado puede producirse también de forma menos espectacular, aunque no por ellos menos dañina (Langella et al., 2000; Topal and Doyuran, 1998; Wendler et al., 1996). No obstante, este tipo de degradación se menciona frecuentemente en la literatura; aunque no se han encontrado estudios de detalle sobre como ocurren estos daños, lo que ha provocado que no existan hasta el momento medios o tratamientos eficaces para paliarlos.

Este trabajo aborda el "vacío de conocimiento" que supone este tema en el campo de la conservación de la piedra e intenta contribuir a una mejor comprensión y cuantificación de este mecanismo de deterioro. Para ello, se han investigado sistemáticamente los factores que controlan el impacto de los minerales de la arcilla sobre las propiedades de la piedra y como las variaciones dimensionales experimentadas por los mismos pueden producir tensiones en el material. Los litotipos seleccionados y estudiados en detalle en esta tesis son los siguientes: arenisca *Portland Brownstone* (EE.UU.), *molasa de Villarlod* (Suiza) y *arenisca de Tarifa* (España). Aunque los resultados/conclusiones obtenidos en esta tesis se refieren estrictamente a tales materiales pétreos, se asume el hecho de que los mismos puedan ser representativos de las piedras que contienen minerales de la arcilla en general. En este trabajo, también se estudian algunos tratamientos de materiales pétreos basados en la aplicación de productos inhibidores del hinchamiento y consolidantes, como opción

para prevenir el daño y restablecer la resistencia a los materiales en el caso de que estos se hayan deteriorado.

Un factor de estudio fundamental en esta investigación es el coeficiente de deformación por expansión libre. Esta propiedad de la piedra depende de la naturaleza de los minerales de la arcilla así como de su cantidad y distribución. Si estos se encuentran como inclusiones en los espacios vacíos entre los granos o recubriendo las paredes de los poros, entonces su presencia no tendría mucho efecto en las propiedades de la piedra y probablemente su expansión no causaría el hinchamiento del material propiamente dicho. Sin embargo, lo contrario sucedería si estos se encuentran como fase cementante, es decir conectando los granos entre ellos. En este caso, es importante subrayar que la expansión de una piedra es mucho más pequeña que aquella experimentada por este tipo de filosilicatos.

El hinchamiento de los minerales de la arcilla de tipo expansivo está compuesto de dos fases sucesivas. La primera es denominada “expansión cristalina” y se produce cuando las moléculas de agua se sitúan de forma ordenada dentro de las partículas (en la intercapa) de estos minerales. En este caso, la deformación por expansión resultante no es muy grande, sin embargo las presiones requeridas para evitarla serían elevadas. La segunda fase es de tipo osmótico y depende mucho de la naturaleza y concentración de los cationes presentes en solución y adsorbidos en la superficie de las partículas de arcilla (Madsen and Müller-Vonmoos, 1985). En este caso, las moléculas de agua no se organizan de forma ordenada y la expansión puede ser virtualmente infinita, es decir, que las deformaciones por expansión producidas podrían ser muy grandes. Por otra parte, las presiones necesarias para evitarla serían mucho más pequeñas que aquellas requeridas para prevenir la expansión cristalina. De hecho, cuanto mayor sea la expansión, menor será la presión necesaria para prevenir la continuación de la misma. Sin embargo, en una piedra, su “esqueleto” (es decir, la estructura rígida que une unos granos con otros) limitaría la magnitud de la expansión en la fase osmótica.

La cuestión que esta tesis se propone responder es conocer si los esfuerzos que se desarrollan durante estos cambios dimensionales pueden realmente degradar un cierto material pétreo. Para afrontarla, se ha desarrollado un nuevo planteamiento donde el cálculo de dichas tensiones requiere la caracterización previa de las propiedades de la piedra (coeficiente de deformación por expansión libre y módulo de elasticidad). Posteriormente, los esfuerzos calculados se comparan con las propiedades mecánicas identificadas que controlan la resistencia de la piedra durante los ciclos de humidificación y secado, es decir, con la resistencia mecánica a la compresión y a la

tracción, respectivamente. La determinación o medida de estas propiedades, junto con otras, ha permitido una mejor cuantificación del riesgo de daño, además de la obtención de otros resultados señalados más abajo.

Una contribución importante de esta tesis en el ámbito de la conservación de la piedra ha sido el demostrar que si bien los esfuerzos pueden ser estimados simplemente como el producto del módulo de elasticidad y el coeficiente de expansión linear; dicho resultado es realístico sólo si se hace uso del valor del módulo de elasticidad obtenido a través de métodos estáticos en vez de dinámicos. Es más, se ha mostrado que las piedras que contienen minerales de la arcilla presentan la habilidad de relajar esfuerzos (comportamiento viscoelástico). Por lo tanto, se han llevado a cabo ensayos específicos de relajación de esfuerzos para cuantificar este fenómeno. Con los resultados obtenidos, ha sido posible explicar de forma cuantitativa la magnitud de las presiones de hinchamiento medidas experimentalmente.

También ha sido posible calcular el potencial de daño tras incluir las variaciones experimentadas por el material con la humedad relativa y el grado de saturación. Una de las conclusiones obtenidas, por ejemplo, en el caso de la arenisca *Portland Brownstone*, es que el fisurado debido al secado de la piedra sería posible sólo en elementos protuberantes y/o de escaso grosor. En este caso, las fisuras deberían producirse principalmente siguiendo los planos de sedimentación de la piedra. La confirmación de estas observaciones la proporcionan los ejemplos encontrados in situ, lo cual indica que el método/modelo propuesto en esta memoria es fiable.

Otra aportación importante de esta tesis ha sido la introducción en este trabajo de una nueva técnica denominada “ensayo de pandeo” o técnica del “3 en 1”, con la que se puede medir simultáneamente el coeficiente de expansión libre, la razón del módulo saturado respecto al seco y el coeficiente de absorción capilar. Esta técnica presenta las ventajas de ser no destructiva y de poder ser usada para caracterizar, por ejemplo, la evolución de una probeta antes y después de un tratamiento o durante los ciclos de envejecimiento. Por esta razón, su uso es muy apropiado en este trabajo para poder examinar el efecto de los tratamientos aplicados, lo cual ha constituido otra parte importante de esta investigación.

Una forma de prevenir el daño durante los ciclos de humidificación y secado consiste en reducir el coeficiente de expansión lineal del material. Esto se ha logrado con el uso de diamino alcanos (Wendler et al., 1991) y aminoalcoholes. Los productos aplicados se seleccionaron individualmente para cada tipo de piedra tras comprobar

cual/cuales de ellos producían la máxima reducción del hinchamiento sin inducir a cambios cromáticos evidentes y sin modificar el coeficiente de absorción capilar de los litotipos. Los resultados han mostrado reducciones entorno al 50 % o más -dependiendo de la piedra- las cuales son suficientes, en general, para mantener los esfuerzos potencialmente causantes de deterioro por debajo de los límites críticos.

También se ha encontrado que estos tratamientos son muy beneficiosos si se aplican previamente a la consolidación del material con silicatos de etilo. En este caso, la pérdida de resistencia que muestran las piedras consolidadas poco después de ser sometidas a los primeros ciclos de humidificación y secado (Félix and Furlan, 1994) es mucho menor. Esta sinergia debería ser explotada en un futuro como una opción para conseguir una mayor durabilidad en este tipo de materiales.

Resumiendo, esta tesis ha introducido un nuevo enfoque investigador que permite analizar de forma cuantitativa la susceptibilidad de una roca ornamental a sufrir degradación durante los ciclos de humedad/sequedad. Este diagnóstico puede ser mejorado con la consideración de parámetros/factores ambientales para obtener así unas conclusiones más realistas. Es más, el mismo ayuda a identificar qué propiedades de los materiales deberían ser modificadas y cuanto para evitar el daño.

Todo este trabajo está apoyado por la introducción y uso de técnicas experimentales que son innovadoras o poco comunes en el campo de la conservación de patrimonio.

La mayor parte de los resultados de esta tesis están recogidos en un total de seis publicaciones que han sido (5) o están siendo (1) evaluadas por diversos comités científicos y que en el caso de dos articulos se han publicado en revistas internacionales recogidas en el JCR. Entre ellas, la autora de esta memoria, dada su formación académica como conservadora/restauradora, desea destacar la titulada: “Factors affecting the durability of *Portland Brownstone*: a review” por considerarla particularmente importante ya que examina el tema de la conservación de la piedra desde una perspectiva más general intentando así, el que los resultados más relevantes de esta investigación sean accesibles a una audiencia más amplia.

Summary

This thesis deals with one of the less studied decay mechanisms that affect the built heritage and works of art made of stone: the swelling and shrinkage that stone can suffer when it contains clay minerals and is exposed to wetting/drying events.

The fact that certain clay minerals expand in the presence of water and contract during drying is well established, and so is the fact that stones containing such clays do the same. It is also known that rocks with high contents of those phyllosilicates (10-15%) and coming from very dry environments such as Egypt, can virtually decompose when submerged in water (Rodríguez Navarro et al. 1998; Zehnder et al., 2000). However, a few studies appear to convincingly show that the studied damage can also happen in a less spectacular way (Langella et al., 2000; Topal and Doyuran, 1998; Wendler et al., 1996). In spite of this, this type of degradation is often mentioned in the conservation literature. However, the mechanisms leading to such damage are not well known. This has prevented the development and application of effective conservation treatments aimed at halting or mitigating this type of damage.

This thesis addresses this "knowledge gap" in stone conservation and tries to contribute to a better understanding and quantification of this mechanism of damage. For this, the ways in which clay minerals impact stone properties and how their dimensional variations produce stresses have been investigated systematically on: *Portland Brownstone* (USA), *Villarlod molasse* (Switzerland) and *Tarifa sandstone* (Spain). Although, strictly speaking, the findings of this thesis only apply to these stones, it is assumed that they are representative of clay bearing stones in general. This thesis also addresses stone treatments as swelling inhibition and consolidation, with a perspective of both, preventing damage and restoring strength if it has already taken place.

A key factor in this study is the swelling strain. It is recalled that this property of a stone depends on the nature of the clay minerals it contains, their amount and distribution. If they are found as inclusions in vacancies between grains, or they just coat pore walls, then they would not have much effect on stone properties and would probably not cause any swelling. On the other hand, the opposite would be true if they are located in the cementing phase connecting grains to each other. In any case, it is

important to emphasize that the swelling of a stone is very much smaller than that of the clay minerals themselves.

The expansion of swelling clay minerals is composed of two successive steps. The first one is called crystalline swelling and is produced by water molecules getting into the clay particles in an ordered way. The resulting expansion is not very large, but large pressures are required to avoid it. The second portion of the swelling is of osmotic nature and depends very much on the nature of the cations adsorbed onto the clay particles as well as their concentration in the pore solution (Madsen and Müller-Vonmoos 1985). It does not lead to ordering of water molecules and can be virtually infinite, which means that large swelling strains can be expected. On the other hand, pressures much lower than those for crystalline swelling are needed to prevent it. In fact, the greater the swelling, the lower is the pressure needed to prevent further expansion. In a stone, obviously the "skeleton" (consisting of rigid clay-free joints between grains) would try to resist this osmotic swelling.

The question this thesis tries to answer is whether the stresses that develop during these dimensional changes can actually damage a given stone. For this, a new approach has been developed where those stresses are calculated based on stone properties (swelling strain and elastic modulus) and then compared with the mechanical properties identified as controlling the stone resistance in cycles of wetting and drying (compressive and tensile strength respectively). These material properties, as well as some others, have been measured. This allowed better quantification of damage risks and also brought a couple additional findings that are outlined below.

An important contribution of this thesis to the field of conservation has been to show that, although stresses could be estimated by simply multiplying the elastic modulus by the free swelling strain, the result is only realistic if one uses a modulus determined by static rather than by dynamic methods. Furthermore, it was shown that these clay-bearing stones have the ability to relax stresses (viscoelastic behaviour). Specific experiments of stress relaxation were performed to quantify this phenomenon. With these results, it was possible to account quantitatively for the magnitude of experimentally measured swelling pressures.

The calculation of damage potential was also done by including variations of material properties with relative humidity and degree of saturation. This led, for example, to the conclusion that cracking from drying should only be seen in protruding and/or thin elements and that, in the case of *Portland Brownstone*, cracks should

mainly appear parallel to the bedding planes. The fact that both these observations are confirmed by field observation indicates that the approach proposed in this thesis is reliable.

Another important contribution of this thesis has been to introduce a new technique we call “warping” or the “3 in 1” test, that provides a simultaneous measurement of swelling strain, ratio of wet to dry modulus and sorptivity. This technique has the advantage of being non-destructive and can be used to characterise the evolution of a sample before and after a treatment, as well as during aging cycles. For this reason, it is well adapted to examine the effect of treatments, which has constituted another important part of this thesis.

A way of preventing the damage during wetting and drying cycles is to reduce the swelling strain of the material. This was achieved with diamino-alkanes (Wendler et al., 1991) and aminoalcohols. The products used have been selected in a case by case basis for each stone to obtain the maximum swelling reduction without notable colour change and without modifying the stone sorptivity. They lead to swelling reductions on the order of 50% or more depending on the stone, which is found to be sufficient to keep stress below damaging limits in general.

It was also found that these treatments are very beneficial if applied prior to consolidation treatments based on ethyl silicates. In such cases, the loss of strength that consolidated stones show after only a few cycles of wetting and drying (Félix and Furlan, 1994) is much reduced. This synergy is something that should be exploited in the future for long-lasting strengthening of clay-bearing stones.

In summary, this thesis has introduced a new research approach, which allows the quantitative assessment of a stone susceptibility to damage during wetting and drying cycles. This diagnosis can be fed with environmental parameter so to obtain more realistic conclusions. Furthermore, it helps identify which material properties should be changed and by how much to avoid damage.

All this work is supported by the introduction and use of experimental techniques that are either innovative or uncommon in the field of stone conservation.

Most of this work is reported in a total of six publications that have been (5) or are being (1) peer reviewed. With respect to the author’s background as a conservator, the publication: “Factors affecting the durability of *Portland Brownstone*: a review” is felt to be particularly important. Indeed, it examines stone conservation from a broader

perspective and attempts to make the main scientific findings of this thesis accessible to a larger audience.

Tabla de contenidos

Lista de Figuras

Documento principal

indican aquellos efectos que no lo han sido.

Anexo 1. Materials and methods

Lista de tablas

Documento principal

Anexo 1. Materials and methods

Lista de notaciones

$\perp$, $\parallel$		dirección perpendicular y paralela a los planos de sedimentación respectivamente
a, b	[GPa]	parámetros de ajuste que caracterizan la relajación de esfuerzos del módulo viscoelástico seco.
d	[-]	profundidad relativa de penetración del agua en un ensayo de pandeo ($d = h_w / h$)
E^{din}, E^{est}	[GPa]	módulos de elasticidad obtenidos con medidas dinámicas (ultrasonidos) y estáticas (flexión en tres puntos) respectivamente
E_{sec}, E_{sat}	[GPa]	módulos de elasticidad del material seco y saturado respectivamente
$E_{(t)}$, $E_{(0)}$	[GPa]	módulos de elasticidad en función del tiempo o "módulo viscoelástico" y extrapolado a t = 0 ó "módulo inicial" respectivamente
h	[cm]	grosor de la probeta en un ensayo de pandeo
h_w	[cm]	zona saturada del grosor de la probeta en un ensayo de pandeo
L	[cm]	grosor de un bloque pétreo
L_{sat}	[cm]	zona saturada del grosor de un bloque pétreo
r	[-]	razón del módulo de elasticidad del material saturado respecto al mismo en seco (E_{sat} / E_{sec})
$R_{(t)}$	[-]	función de relajación hidrodinámica (describe la redistribución del agua durante una medida de módulo de elasticidad estático de una probeta saturada)
S	[cm/s$^{1/2}$]	coeficiente de succión capilar
S_0 , S_μ	[cm/s$^{1/2}$]	coeficientes de succión capilar a t = 0 y a tiempos largos respectivamente
t	[s]	tiempo
w	[cm]	luz en un ensayo de pandeo
$W_{(t)}$, $W_{(0)}$	[g]	cargas en un ensayo de flexión a tres puntos a tiempo t y a t = 0 (carga inicial) respectivamente

Δ	[cm] o [µm]	deflexión en un ensayo de pandeo
Δ_s	[cm]	es la ordenada en el origen de la regresión linear de la curva de ascenso capilar cuando se representa como la altura del frente capilar respecto a la raíz cuadrada del tiempo
e_S , $e_{S(t)}$	[-] o [µm/m]	coeficientes de deformación por expansión libre y en función del tiempo (usado en la noción de expansión retardada), respectivamente
n_{sec}, n_{sat}	[-]	coeficientes de Poisson del material seco y saturado respectivamente
s_{sec} , $s_{sec,\,2}$	[MPa]	esfuerzos máximos de tracción en la zona "seca" y más exterior en un bloque pétreo que está total o parcialmente saturado respectivamente
s_{sat}	[MPa]	esfuerzo máximo de compresión en la zona saturada
s_T	[MPa]	resistencia mecánica máxima a la tracción
s_C , $s_{C(sat)}$, $s_{C(sec)}$	[MPa]	resistencias mecánicas máximas a la compresión en general, del material saturado y seco respectivamente
t_{VE}	[s]	tiempo característico para la relajación viscoelástica de una probeta saturada
$y_{(t)}$	[-]	función que caracteriza la velocidad de relajación de esfuerzos en probetas secas y saturadas
a	[$s^{-1/2}$]	parámetro de ajuste de la función de succión capilar que es equivalente a $(S_0 - S_\mu)/\Delta_s$
b	[-]	parámetro de ajuste de la función de relajación de esfuerzos en la piedra saturada
q_d, q_{d1}, q_{d2}	[s]	parámetros de ajuste que caracterizan la relajación de esfuerzos del módulo viscoelástico seco.

Capítulo 1. Introducción

1.1 Antecedentes históricos

El tema de la durabilidad de materiales pétreos ha sido objeto de preocupación desde tiempos muy remotos. De hecho ya en el siglo I a. C, Marco Vitruvio Pollione, en el capitulo VII del libro II de su obra "Los diez libros de Arquitectura" (Oliver Domingo, 1997) da algunas indicaciones sobre como seleccionar y "curar" la piedra con objeto de tener edificios más duraderos:

…Podemos concluir estas cualidades fijándonos en los monumentos que se encuentran cerca de Ferente, labrados con piedras de estas canteras. Allí se levantan magníficas y excelentes estatuas y pequeñas figuritas, e incluso flores y acantos tallados primorosamente; aunque son antiguos, parecen realmente recientes, como si los acabaran de tallar. Igualmente, los fundidores de bronce hacen sus moldes con piedras de estas canteras, pues poseen importantes propiedades para la fundición del bronce. Si estuvieran cerca de Roma, merecería nuestro elogio el que se concluyeran todos los edificios precisamente con piedras de estas canteras pero, debido a la proximidad, la necesidad nos impone usar las canteras de piedra roja, las de Palla y otras que encontramos cerca de aquí. Si queremos concluir las obras sin ningún defecto, deben prepararse las piedras de antemano de la siguiente manera: se extraerán las piedras en bruto con una antelación de dos años antes del momento de edificar; se extraerán en el verano y no durante el invierno. Y amontonadas en tierra se mantendrán a cielo raso. Las que durante estos dos años queden dañadas por los temporales, colóquense en los cimientos; las restantes, que estén intactas, como probadas por la misma naturaleza, darán solidez y firmeza en las construcciones que se levanten a lo alto. Estas precauciones deben tenerse en cuenta también con las piedras para la mampostería…

A pesar de la temprana toma de conciencia histórica sobre el problema del deterioro de la piedra, no será hasta el siglo XIX cuando se den grandes pasos en el entendimiento de las causas que ocasionan el mismo. De hecho, los primeros trabajos conocidos que estudian el mecanismo de generación de presiones por cristalización de sales, se atribuyen a Lavalle (1853) y Taber (1916). En ellos se expresa de forma clara y científica los modos en los que las sales ejercen presiones aunque no se propone un modelo cuantitativo de predicción de las mismas. Será más tarde, bien adentrado el siglo XX, cuando a través del uso de la termodinámica se consiga derivar expresiones cuantitativas de las mencionadas presiones de cristalización ejercidas tanto por sales (Mortensen, 1933; Correns, 1949) como por el agua en su transformación en hielo

(Everett, 1961). Ello supondrá un evidente avance respecto a los tradicionales estudios de investigación llevados a cabo hasta entonces siguiendo la más pura línea geológica y constituirá un complemento a estos últimos más que un reemplazo de los mismos.

Pese a que estas últimas investigaciones conducen a la predicción de presiones, realmente ninguna de ellas llega a establecer una relación entre los esfuerzos generados y las propiedades de la piedra que permita conocer la potencialidad de deterioro de la misma. A este asunto tan sólo se le ha prestado más atención recientemente desde el ámbito de la Ciencia de los Materiales. De hecho Scherer (1999) explica como las presiones generadas durante la cristalización de sales o formación de hielo se pueden relacionar con la resistencia mecánica a la tracción de la piedra para determinar la posibilidad de degradación. Este planteamiento ha sido también aplicado a la cristalización de sulfato de sodio por Flatt (2002). En su estudio queda demostrado que durante la transformación de tenardita (sulfato de sodio anhidro) en mirabilita (sulfato de sodio decahidrato) por procesos de disolución/precipitación en ambientes húmedos (Rodríguez Navarro y Doehne, 1999), se generan presiones de cristalización que exceden los valores de resistencia a la tracción de las piedras considerados como típicos (2-6 MPa para areniscas según Knöfel et al., 1987). En relación con este tema, un estudio más reciente y elaborado basado en el uso de ciclos de impregnación en soluciones salinas y secado ha sido publicado por Coussy (2006).

A pesar del gran progreso realizado en este campo, no todos los mecanismos de deterioro de la piedra se conocen con el mismo nivel de profundidad. Así, uno de los que parecen haber sido menos analizados sería el de la expansión hídrica y/o hígrica sufrida por los materiales pétreos que contienen minerales de la arcilla en su matriz y/o cemento. La importancia de examinar dicho mecanismo es evidente si se considera el número de referencias bibliográficas que apuntan a la expansión/contracción cíclica de estos minerales como causa de deterioro de la piedra a largo plazo (Abd El Hady, 1988; Beloyiannis et al., 1988; Bradley y Middleton, 1988; Brattli y Broch, 1995; Caner y Seeley, 1978; Delgado Rodrigues, 2001; Dunn y Hudec, 1966; Esbert et al., 1981; Fascina y Cherido, 1985; Félix, 1988, 1994, 1995; Félix y Furlan, 1994; Franzini et al., 2007; Helmi, 2000; Iñigo et al., 2003; Kühnel et al., 1994; Madsen y Müller-Vonmoos, 1985; McGreevy y Smith, 1984; Pye y Mottershead, 1995; Rodríguez Navarro et al., 1997, 1998; Veniale et al., 2001; Vicente, 1983; Vincente y Brufau, 1986; Winkler, 1986, 1993; Wüst y McLane, 2000; Zehnder et al., 2000).

Pese a la frecuencia con que la literatura menciona este argumento, apenas existen estudios que demuestren de forma directa el daño que este mecanismo puede ocasionar a los materiales pétreos.

Rodríguez Navarro et al. (1997, 1998) estudiaron un caso muy peculiar donde el material pétreo analizado se descompone espectacularmente después de ser sumergido en agua como consecuencia de la expansión sufrida por minerales de la arcilla. Se precisa que la piedra estudiada es una caliza egipcia con un porcentaje relativamente elevado de arcillas ($\geq$ 10 % en peso). Zehnder et al. (2000) también observan un fenómeno parecido en calizas margosas egipcias que contienen alrededor del 15% de esmectitas. Del mismo modo, Brattli y Broch (1995) observaron la desintegración de pizzarras poco después de sumergirlas en agua.

Topal y Doyuran (1998) estudian la durabilidad de las famosas "Chimeneas de hada" de Capadocia las cuales muestran un nivel de degradación mucho menos espectacular que las calizas egipcias mencionadas. Estas formaciones rocosas están constituidas por toba volcánica cuyo contenido en arcillas (principalmente esmectitas) oscila entre 2 y 7 % llegando en algunas zonas al 14 % según las estimaciones de dichos autores. En su estudio sometieron probetas de toba a ciclos de cristalización de sales, de hielo/deshielo y de humidificación/secado y midieron durante los mismos algunas propiedades físicas de la piedra. Sus resultados muestran como los dos primeros ensayos, es decir, aquellos que implican mecanismos de cristalización, parecen deteriorar la piedra de forma más severa que los ciclos de humedad/sequedad. No obstante, conviene señalar que las condiciones de los ensayos de cristalización de sales que hacen uso del sulfato de sodio son muy extremas y muy poco representativas de lo que ocurre en la realidad. Algo parecido ocurre con los ciclos de hielo/deshielo, durante los cuales la piedra se ve sometida a enormes choques térmicos. En cuanto a los ciclos de humedad/sequedad, los autores demuestran como estos afectan tanto a la resistencia a la compresión de la piedra como a la velocidad de los ultrasonidos aplicados durante y después del ensayo, produciendo una sustancial reducción de los valores iniciales.

Delgado Rodríguez (1988) estudia rocas carbonatadas donde uno de los litotipos, con un contenido en arcillas de alrededor del 7-8%, se descompone después de ser sometido a ciclos de humidificación/sequedad. Sin embargo, otras rocas con contenidos en arcillas mucho más altos (hasta ~50 %) parecen no mostrar este tipo de degradación. En un contexto más general, los valores de 7-8 % citados, no sólo pueden ser considerados como relativamente altos, sino también como un factor

potencial de deterioro. Por lo tanto, este estudio muestra que el daño del material pétreo no está relacionado únicamente con la cantidad de arcillas, como ya había sido indicado por Dunn y Hudecc (1966). De hecho, Delgado Rodríguez indica que estas últimas se concentran en pequeñas venas de la piedra, lo que según el autor, incrementaría el grado de daño durante los ciclos de h/s. El tipo de degradación observado en este estudio es muy severo, por lo que dichos materiales no resistirían mucho tiempo a la intemperie.

Langella et al. (2000) estudian la durabilidad de rocas ornamentales usadas en monumentos de algunas ciudades de la región de Campania (Italia). Una de ellas en particular -una toba volcánica napolitana- muestra degradación después de ser sometida a unos 10-30 ciclos de h/s. Prueba de ello es por ejemplo la reducción (~50 %) de su resistencia a la compresión o en la velocidad de propagación de ultrasonidos. Otros cambios observados fueron un ligero incremento tanto de la porosidad como de la absorción de agua por inmersión total, al igual que una pérdida de masa de alrededor del 3%.

Por último, Wendler et al. (1996) examinan una situación que puede ser bastante habitual, donde un número sustancial de ciclos de humedad/secado (ciclos de h/s) serán necesarios para generar degradación tan sólo en la zona más superficial del material pétreo. En este último caso, los autores examinan el envejecimiento de la piedra (toba volcánica) utilizada en la creación de algunos de los mohai de la Isla de Pascua. En primer lugar observan que la resistencia al taladrado (*drilling resistance*) del material original es mucho más baja en la capa más superficial que en la subyacente o interna[1]. Para averiguar si tal alteración podría estar inducida por ciclos de h/s, sometieron probetas procedentes tanto de la cantera como de la obra a dichos ciclos. Cada uno tuvo una duración de doce horas: durante una hora, las probetas permanecieron completamente sumergidas en agua a 20° C y durante las once restantes fueron sometidas a desecación a temperaturas de 40° C y a 18 % de humedad relativa. Después de seiscientos ciclos de h/s, las probetas mostraron un drástico descenso en la resistencia al taladrado en sus primeros 1-1.5 mm, es decir, en la capa más superficial o externa, mientras que el interior de las mismas permaneció inalterado (Figura 1-1).

[1] Las probetas se obtuvieron de trozos fragmentados de esculturas de Tongariki ahu, las cuales fueron destruidas por un tsunami en 1960.

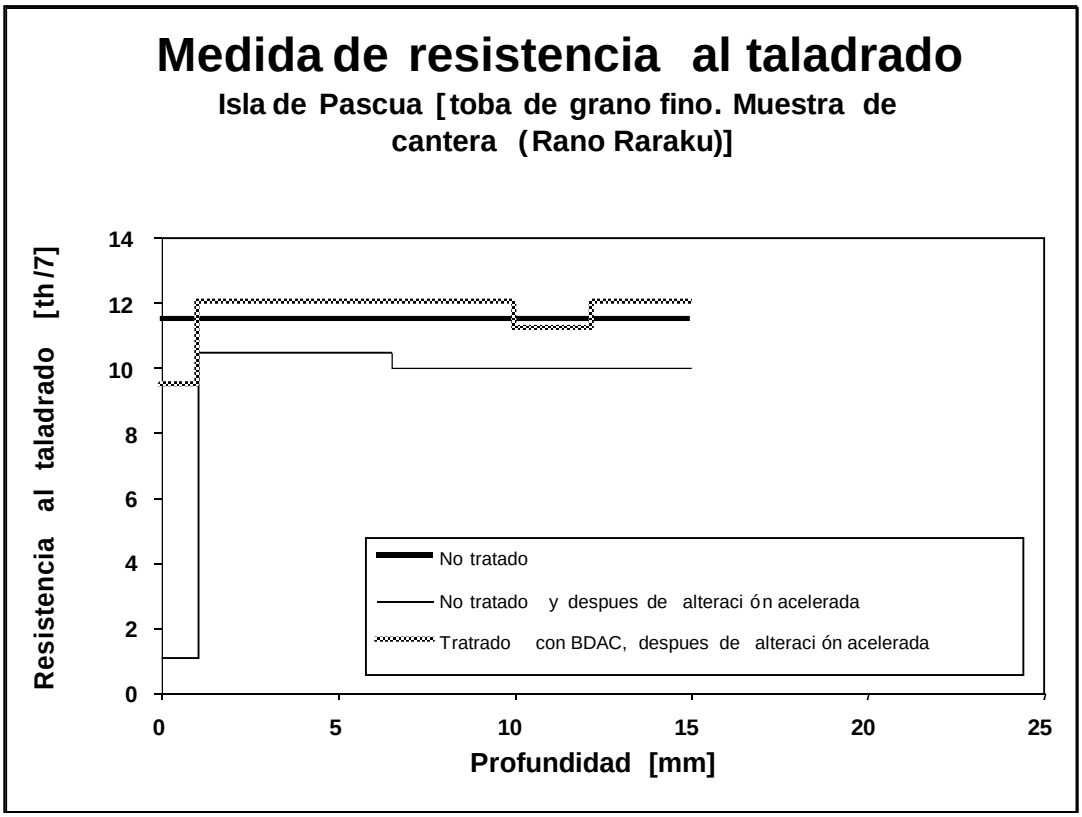

Figura 1-1. Adaptación del gráfico procedente de Wendler et al. (1996). Comparación de las medidas de resistencia al taladrado entre probetas de toba de grano fino tratadas y no tratadas, deterioradas y no deterioradas provenientes de la cantera de Rano Raraku, en la Isla de Pascua. El daño es provocado sometiendo las probetas a 600 ciclos de h/s en los que durante 1 hora son sumergidas totalmente en agua a 20° C y posteriormente sufren una fase de secado durante 11 horas a una temperatura de 40° C y a 18 % de humedad relativa. Las unidades del eje Y [Th/7] provienen de una función empírica que relaciona la resistencia al taladrado con la resistencia a la flexión de la piedra (Wendler et al., 1996).

Otro aspecto interesante de este estudio consiste en el tratamiento de una serie adicional de probetas del mismo lipotipo con un agente inhibidor de la dilatación, concretamente un diaminobutano di-hidroclórico (Wendler et al., 1991; Snethlage y Wendler, 1991). Dicho tratamiento no modificó el ingreso de agua o la porosidad en la probeta pero redujo significativamente la expansión hídrica de la misma. Posteriormente, las probetas tratadas fueron sometidas al mismo tipo de ensayo empleado con las no tratadas, es decir, a 600 ciclos de h/s. Tras este, se comprobó

como la resistencia al taladrado de la parte más externa de las mismas sufrió tan sólo una ligera reducción, demostrando por consiguiente la acción “protectora” del tratamiento (Figura 1-1).

Este ensayo establece de forma evidente que los ciclos de h/s pueden degradar el material pétreo que experimenta expansión en contacto con agua. Aunque esta misma referencia no menciona explícitamente la palabra “arcillas o minerales de la arcilla” sino “minerales reactivos”, se entiende que la expansión es debida a la presencia de minerales de la arcilla. En particular, la elección de productos inhibidores de la expansión sigue una lógica de control de la expansión de minerales de la arcilla que algunos de estos autores mencionan explícitamente en otros trabajos (Wendler et al., 1991; Snethlage y Wendler, 1991). En cuanto a la composición de la toba volcánica, se dice estar formada por una matriz vítrea con plagioclasa, clinopiroxeno, olivino y limonita como componentes minerales. También este estudio demuestra que los productos usados como inhibidores de la expansión pueden activamente contribuir a la reducción del deterioro, si bien no lo previenen totalmente. Como contraparte, el uso de estos últimos no permite elaborar un pronóstico cuantitativo de la reducción del daño que se alcanzaría en el material pétreo. De cualquier modo, este estudio indica claramente que el daño producido por este mecanismo (al menos durante el número de ciclos estudiado) se limita a la parte más superficial del material. Debido a ello, la relevancia de este tipo de deterioro en un muro de un edificio podría ser limitada, pero la pérdida de un milímetro en una escultura o elemento decorativo comprometería directamente su valor estético y por lo tanto sería más crítico. Esto último distingue en cierto modo el daño ocasionado por los ciclos de h/s de aquel producido por la formación de hielo o cristalización de sulfato de sodio, ya que estos últimos mecanismos pueden causar un deterioro de más envergadura y/o espectacular, particularmente cuando se realizan ensayos acelerados en laboratorio (Scherer, 1999; Flatt, 2002; Rodríguez-Navarro et al., 2000).

Otro aspecto importante a destacar en este tipo de rocas es la pérdida relativamente rápida del efecto alcanzado tras su consolidación con silicatos de etilo. Según varios autores (Félix y Furlan, 1994; Félix, 1994, 1995), esta se produce después de un limitado número de ciclos de h/s. Este efecto ha sido atribuido a la incapacidad del consolidante a resistir la expansión hídrica y/o hígrica de los minerales de la arcilla y en consecuencia a fisurarse. De todos modos, se recuerda que algunos estudios ya mencionados [e.g. Wendler et al. (1996)] muestran como materiales pétreos no consolidados también sufren deterioro por dichos ciclos (ver Figura 1-1) pero después de un número mucho mayor de ellos (600 ciclos).

1.2 Propósito y estructura de la tesis

La investigación llevada a cabo en esta tesis supone un avance en el conocimiento del daño sufrido por la piedra con minerales arcillosos a consecuencia de la acción de ciclos de h/s. La mayor parte de los resultados conseguidos son relativos al material pétreo mas utilizado en nuestro estudio, una arenisca conocida comúnmente como *Portland Brownstone* que protagoniza un importante papel en el panorama arquitectónico en piedra del Noreste de los EE.UU. (Anexo 7). También han sido examinadas otras piedras aunque en menor profundidad. Sería el caso de la *molasa de Villarlod*, una arenisca muy usada en la meseta suiza y que es ampliamente representativa de otros muchos litotipos usados profusamente en el patrimonio arquitectónico del país y de cuyo estudio se ha encargado con cierta profundidad el Dr. C. Félix. La otra roca sedimentaria estudiada y referida en este trabajo como *arenisca de Tarifa* es el principal material constitutivo de la fachada principal de la Iglesia de S. Mateo, en Tarifa (Cádiz), la cual presenta un estado de deterioro avanzado atribuido principalmente a la expansión de los minerales de la arcilla que la componen. A pesar de las particularidades ofrecidas por cada tipo de material pétreo estudiado en esta tesis, existe un interés primordial por extraer/identificar principios y recomendaciones de carácter general cuya aplicación pueda ser extendida a otros materiales pétreos que contengan minerales de la arcilla así como extrapolarla a otras situaciones o circunstancias y ambientes físicos. En el afán de conseguirlo, se espera que este trabajo no contribuya al malestar generalizado existente respecto al contenido de muchas de las publicaciones dedicadas a la conservación de piedra y que ha sido expresado por Price (1996) en los siguientes términos:

"…La literatura esta llena de artículos dedicados a la caracterización de la piedra. Coge cualquier volumen de comunicaciones de conferencia y encontrarás numerosos estudios que describen en primer lugar la situación e historia de algún monumento en particular y después continúan con las propiedades físicas de los materiales pétreos en sí. Habrá descripciones petrológicas seguidas por medidas de dureza superficial, porosidad, absorción de agua, capilaridad, distribución de tamaño de poro, resistencia mecánica, velocidad de ultrasonidos, resistencia a la cristalización de sales, etc. Habrá sin duda algunas fotografías tomadas al microscopio electrónico de barrido y probablemente algunos análisis de energía dispersiva de rayos X como buena medida. ¿Todo esto con que fín? la información, sin duda alguna, tendrá valor para aquellos que estén interesados en el cuidado y

manutención de ese monumento en concreto, pero es cuestionable la relevancia de todo ello para una audiencia más general a menos que las propiedades de la piedra estudiada puedan relacionarse con su comportamiento…"[2]

La modalidad elegida para la presentación de los resultados de esta tesis consiste en la compilación de trabajos de investigación -ya publicados (5) o en periodo de revisión (1)- llevados a cabo por la autora de esta tesis- en la sección de anexos de este manuscrito. Entre ellas, la autora de esta memoria, dada su formación académica como conservadora/restauradora, desea destacar la titulada: "Factors affecting the durability of *Portland Brownstone*: a review" por considerarla particularmente importante ya que examina el tema de la conservación de la piedra desde una perspectiva más general intentando así, el que los resultados más relevantes de esta investigación sean accesibles a una audiencia más amplia.

En las páginas que siguen esta introducción, se dará una justificación y visión general de los objetivos de este estudio. Le seguirá un capítulo de discusión conjunta de todos los resultados obtenidos. A continuación, en la sección de conclusiones y perspectivas del trabajo, se resaltará el significado y relevancia de los principales resultados y sus implicaciones en el campo de la conservación de piedra. A esta le seguirán los apartados de referencias y anexo de los artículos.

También se ha visto oportuno incluir un glosario, una lista de terminología técnica inglesa traducida al español, una lista de notaciones así como un capítulo dedicado a materiales y métodos empleados. Los dos primeros, se hacen necesarios para dar la posibilidad al lector de consultar aquella terminología con la cual no está familiarizado, facilitando por consiguiente la comprensión del trabajo realizado. En cuanto al capítulo de materiales y metodología (Anexo 1), se ha considerado importante incluirlo ya que son diversas las técnicas utilizadas y algunas de ellas son poco conocidas o han sido desarrolladas específicamente para este trabajo.

Por último, se cree necesario hacer una serie de precisiones sobre cierta terminología empleada en esta tesis y que puede inducir a confusión o dudas. En primer lugar, cuando se usa el término "material pétreo" se hace referencia exclusivamente a aquel de origen natural, o lo que en lenguaje común se conoce como

[2] Texto traducido del inglés por la autora de esta tesis

“piedra”, por lo tanto, quedan excluidas las cerámicas, ladrillos, hormigones, morteros, etc.

Por otro lado, se advierte que en este trabajo, el daño ocasionado por los ciclos de h/s a las piedras es evaluado considerando que su contenido en minerales de la arcilla es la única causa de la expansión y contracción sufrida por las mismas. En consecuencia, el análisis no considera el papel que pueden tener otros factores en la expansión/contracción cíclica, como pueden ser la presión negativa de capilaridad, la presencia de sales o los cambios térmicos.

Además, los diferentes vocablos usados “arcilla”, “arcilloso”, etc. hacen referencia exclusivamente a los minerales de la arcilla y en caso contrario se especifica. Por otro lado, durante la lectura de esta memoria, se apreciará como se hace un uso indiscriminado de la expresión “piedras que contienen minerales de la arcilla”. Se considera por tanto importante aclarar, que dicha expresión hace referencia exclusivamente a las piedras estudiadas en esta tesis, aunque se asume el hecho de que las mismas puedan ser representativas de aquellas que contengan minerales de la arcilla en general.

Capítulo 2. Justificación y objetivos

2.1 Justificación

Una gran parte de las obras escultóricas, monumentos y patrimonio arquitectónico están realizados en piedra, la cual muy frecuentemente contiene minerales de la arcilla en su cemento y/o matriz. Estos filosilicatos presentan la particularidad de expandirse cuando entran en contacto con el agua (principalmente en ambientes al abierto) o con humedad atmosférica (a la intemperie y/o en ambientes cerrados) y de contraerse en ambientes más secos. La alternancia de expansiones y contracciones sufrida por el material pétreo durante estos ciclos de h/s incide en su estructura, afectando por tanto su durabilidad o en el peor de los casos comprometiendo la propia integridad física de la obra de arte a la cual ofrecen soporte matérico.

Como ya ha sido indicado en el capítulo anterior, son abundantes las referencias que advierten sobre la posibilidad de deterioro presentada por dicho mecanismo. Sin embargo, no se ha encontrado en ninguna de ellas un análisis completo del problema a nivel cuantitativo. El abordar el estudio de este mecanismo de deterioro a través de la cuantificación de los esfuerzos generados durante los ciclos de h/s, se convierte por lo tanto en algo crucial para determinar sí y bajo qué condiciones estas tensiones pueden suponer una verdadera amenaza para la durabilidad de dichos materiales.

El poder satisfacer tal exigencia ha sido considerado como el primer objetivo en este trabajo y el haberlo conseguido representa una importante contribución tanto en el campo de la ciencia de la conservación como en el de la práctica de campo o in situ.

2.2 Objetivos

Como ha sido mencionado, esta tesis tiene como objetivo principal contribuir a un mayor conocimiento y entendimiento del daño producido en rocas ornamentales no consolidadas, que contienen minerales de la arcilla, como consecuencia de las expansiones/contracciones cíclicas experimentadas durante ciclos de h/s. Esto se conseguirá:

- cuantificando los esfuerzos generados durante los ciclos de h/s

- § estableciendo la relación de dichas tensiones tanto con las propiedades mecánicas del material pétreo como con las condiciones de exposición del mismo para determinar el potencial de daño.

Con esta finalidad, este trabajo se propone crear un modelo predictivo del daño potencial al que estaría expuesto este tipo de materiales pétreos usados en el patrimonio histórico-artístico. Para ello, una serie de subobjetivos han tenido que ser previamente alcanzados. Estos se clasifican en tres categorías: diagnóstico, caracterización y tratamiento.

2.2.1 Diagnóstico

Esta supone probablemente la contribución más importante de esta investigación. Consiste en proponer expresiones que caractericen los esfuerzos que pueden desarrollarse durante los ciclos de h/s, así como indicar qué propiedades del material pétreo determinan la producción de deterioro. Las formas de degradación previstas son examinadas críticamente con la finalidad de poder identificar qué proceso es el más importante en la exposición al aire libre. Una extensiva revisión de todo esto se presenta en el Anexo 7 para el caso de la arenisca denominada *Portland Brownstone*.

2.2.2 Caracterización

Los análisis que se mencionan a continuación revelan cuales son las propiedades de la piedra más importantes y determinantes del deterioro. Una extensa caracterización de las mismas es, por consiguiente, la segunda parte más importante de este trabajo. Para conseguir dicho objetivo se han usado varias técnicas experimentales, algunas de ellas poco comunes e innovadoras en el ámbito de la conservación de piedra. Entre ellas destacan:

- § **Ensayo de flexión estática por tres puntos (*Three point beam bending*)**: una técnica que permite medir el módulo de elasticidad (o módulo de Young) usando deformaciones comparables a aquellas esperadas en ciclos de h/s. También permite medir la relajación de esfuerzos del material pétreo.

- § **Pandeo (*Warping*)**: Se trata de una nueva técnica, a la cual denominamos técnica del “3 en 1”, ya que permite medir la velocidad de succión/ascenso

capilar, el coeficiente de expansión lineal y la razón del módulo de elasticidad del material saturado respecto de aquel seco (E_{sat}/E_{sec}), todo ello realizando un sólo ensayo.

§ **Presión de hinchamiento**: consiste en una versión adaptada de un ensayo ya existente con la que se consigue acelerar el tiempo empleado en medir la presión generada durante la expansión de la piedra siendo ahora diez veces menor.

2.2.3 Tratamiento

Entender como se genera el deterioro de la piedra y qué propiedades lo controlan no es de mucha utilidad si no se pretende intervenir para paliarlo. En un principio, las técnicas descritas en la sección anterior pueden ser usadas de forma directa durante las intervenciones de restauración para caracterizar adecuadamente los materiales pétreos. También esta metodología permitiría seleccionar la piedra de sustitución de elementos muy deteriorados, en el caso de que tal tipo de intervención sea necesaria, compatible no sólo según criterios estéticos sino también considerando su durabilidad.

No obstante, lo ideal sería poder emprender acciones preventivas para evitar el llegar a situaciones límite como el citado caso de sustitución de material. Es por ello, que aquí se examina el uso de agentes reductores de la expansión y su uso combinado con consolidantes de la piedra. Mientras que el uso de este tipo de productos ha sido ya objeto de numerosas referencias en la literatura, este trabajo se propone también determinar cuales son los mejores tratamientos que hacen uso de estos agentes para el material pétreo seleccionado y además, caracterizar la permanencia de dichos productos en el sustrato rocoso. Para examinar este último aspecto, se ha construido un instrumento que permite realizar numerosos ciclos de h/s de forma automática. El resultado más novedoso que se desprende de este estudio no sólo muestra que los agentes inhibidores de la expansión hídrica no son eliminados durante los ciclos, sino que además el uso de estos productos parece incrementar la resistencia del tratamiento de consolidación.

Capítulo 3. Discusión general de los resultados

3.1 Visión general

Este capítulo presenta una discusión general de los resultados obtenidos en la evaluación y cuantificación del daño producido a la piedra durante ciclos de h/s. Así mismo, en él se pone de manifiesto la contribución que este trabajo supone en el campo de la conservación de estos materiales. Este cometido se lleva a cabo de forma sintética, dejando los detalles para ser consultados en los artículos asociados en la sección de anexos.

El capítulo comienza con una visión y presentación general del tema (sección 3.1). A continuación se hará una revisión breve sobre el argumento (sección 3.2.1). Se hace preciso señalar que durante la misma no se ha encontrado publicación alguna donde se establezca una relación clara entre la degradación producida y las propiedades de los materiales y/o condiciones de exposición. La propuesta de dicho tipo de relaciones es por tanto un importante logro de esta tesis como se muestra en la sección 3.2.2.

Este análisis subraya la importancia del coeficiente de expansión lineal y de las propiedades mecánicas de los materiales pétreos que contienen minerales de naturaleza arcillosa. Así pues, la sección 3.3 está dedicada a la caracterización de dichas propiedades. En dicho apartado se subraya la necesidad de usar métodos estáticos en vez de dinámicos para determinar el módulo de Young. También se refleja como este tipo de materiales muestran claramente un comportamiento viscoelástico que no debería ser despreciado en su estudio.

La siguiente sección (3.4) trata de la caracterización del coeficiente de expansión lineal así como de su reducción a través del uso de agentes inhibidores del hinchamiento. La durabilidad de estos productos en los litotipos estudiados será evaluada con ensayos acelerados automatizados de ciclos de h/s. También se examinan en este apartado las ventajas, limitaciones y la posibilidad de hacer un uso generalizado de la innovadora técnica de pandeo o del “3 en 1” (*warping*).

El producto del coeficiente de hinchamiento lineal y el módulo de elasticidad de la piedra predice presiones de hinchamiento mucho más elevadas que las referidas en la literatura científica y que las encontradas en nuestros ensayos. La razón de ello se explica en la sección (3.5).

A continuación, la sección 3.6 estará dedicada a la predicción de daño durante los ciclos de h/s. En ella se expondrá de forma sucinta la posibilidad de que se produzca deterioro, las formas de alteración y/o degradación y las condiciones necesarias para ello.

En la sección 3.7 se afronta el tema de la consolidación de este tipo de materiales pétreos. En este apartado también se confirmarán los resultados de Félix (1994, 1995) y de Félix y Furlan (1994) sobre la incapacidad de los silicatos de etilo para resistir la expansión de la piedra, resultando en un daño extensivo después del primer ciclo de h/s al que se someten. No obstante, se ha comprobado que el tratamiento de este tipo de materiales con agentes reductores de la expansión incrementa la resistencia de los mismos a la acción de los periodos alternativos de humedad / sequedad.

Finalmente, la contribución global de esta tesis queda plasmada de forma bastante gráfica en la sección 3.8, donde se explica y hace hincapié en cual ha sido la principal línea de investigación que se ha desarrollado en esta tesis para abordar esta problemática.

A través de estas secciones, se persigue establecer una relación entre los logros obtenidos y las posibles situaciones prácticas a las que se enfrenta el conservador /restaurador de piedra. Todo ello será reflejado de forma sintética en el capítulo cuarto titulado “Conclusiones y perspectivas”.

3.2 Daño por acción de ciclos de humidificación y secado

3.2.1 Antecedentes

El hecho de que ciertos minerales de la arcilla sufran expansión en presencia de agua y contracción durante procesos de evaporación es bien conocido, como también lo es la dilatación transferida a los materiales pétreos naturales que los contienen. También es sabido que rocas con contenidos altos (10-15 %) de estos filosilicatos y provenientes de ambientes muy secos (ej. Egipto) puedan llegar a descomponerse literalmente cuando son sumergidas en agua (Rodríguez Navarro et al., 1997,1998; Zehnder et al., 2000). Sin embargo, como ya ha sido señalado, sólo se ha identificado

un número escaso de publicaciones que muestren convincentemente que este efecto pueda constituir un problema a largo plazo también en el caso de materiales pétreos que muestran una degradación menos espectacular y rápida (Langella et al., 2000; Topal y Doyuran, 1998; Wendler et al., 1996).

A pesar de ser reducido el número de estos estudios que ofrecen datos cuantitativos acerca del deterioro por expansión hídrica e hígrica, las publicaciones en el ámbito de la conservación de rocas ornamentales mencionan frecuentemente este mecanismo como una posible causa de deterioro de la piedra, como es el caso de la arenisca *Portland Brownstone*. A este punto, se hace preciso recordar que estamos hablando de un material pétreo no consolidado. De hecho, la piedra consolidada pierde casi todo el beneficio del tratamiento después de ser sometida a un limitado número de dichos ciclos (Félix y Furlan, 1994).

3.2.2 Análisis del desarrollo de esfuerzos

En esta sección, se examina desde el punto de vista conceptual la forma en la que el material pétreo natural no consolidado llega a deteriorase durante ciclos de h/s. El análisis propuesto se desarrolla de forma más completa en el Anexo 6.

En el caso de piedra no consolidada, la mayoría de las publicaciones discuten el rol de la presión de hinchamiento de los minerales de la arcilla. La clave de esta idea puede ser sintetizada de la siguiente forma: la superficie "seca"[3] de una piedra ornamental cualquiera empieza a absorber agua (Figura 3-1a). Los minerales de la arcilla en la zona húmeda empiezan a expandirse, por consiguiente esa zona saturada de la piedra (Figura 3-1b) se expandiría potencialmente también si no fuese porque su adhesión al resto del sustrato seco (mucho más voluminoso y que no se ha hinchado todavía) lo impide. Como resultado, la zona saturada ve su capacidad expansiva

[3] En realidad, en el ámbito de la conservación de piedra in situ no podemos hablar de material en estado "seco", ya que siempre contendrá algún grado de humedad (humedad de equilibrio) debido a su contacto continuo con la atmósfera. Tan sólo en casos donde se habla de situaciones más controlables (caso de ensayos en laboratorio donde después de haber sometido el material pétreo a desecación se ha mantenido aislado del contacto con la humedad atmosférica) podríamos hablar de estado seco con más propiedad.

limitada por esfuerzos de compresión (Figura 3-1c). El deterioro se produciría, por tanto, si dichos esfuerzos fuesen mayores que la resistencia máxima a la compresión de la piedra saturada.

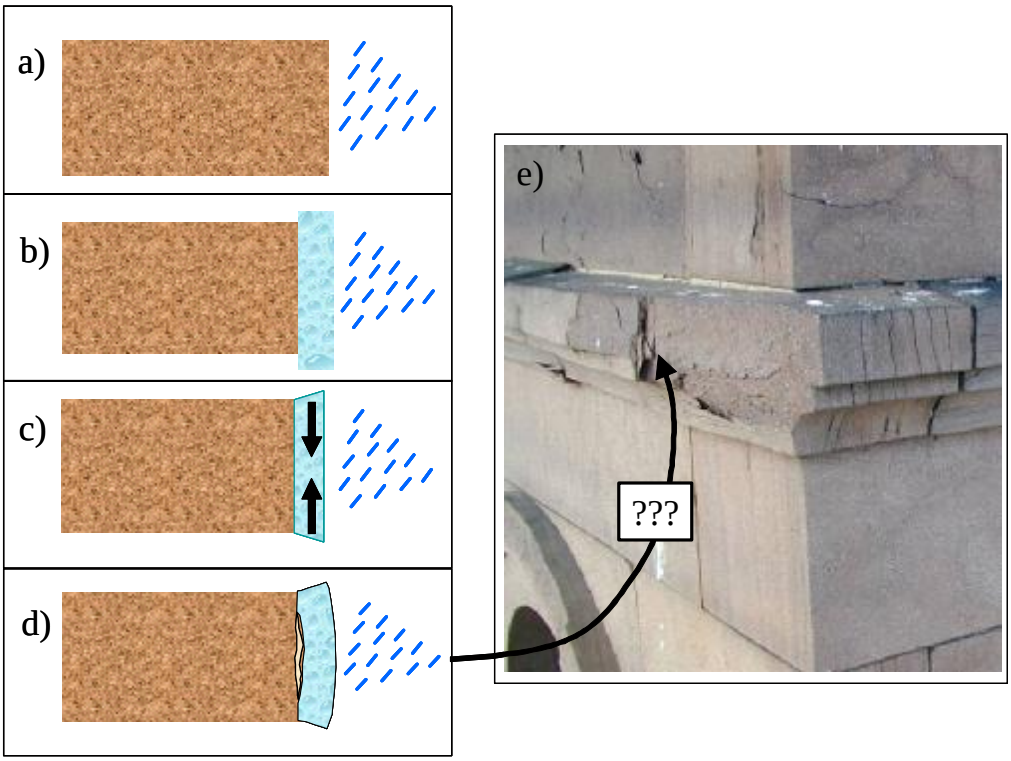

Figura 3-1. Degradación durante un ciclo de humidificación: a) la superficie exterior de un bloque pétreo está expuesta a la lluvia directa. b) La parte mojada, aún de escaso grosor, expandiría si no estuviese adherida al sustrato "seco" que es mucho más voluminoso. c) Sin embargo su adhesión al mismo hace que esté sometida a esfuerzos de compresión (simbolizados con flechas). Por lo tanto, la primera posibilidad de degradación se daría si dichos esfuerzos superasen los valores de resistencia mecánica máxima a la compresión de la piedra saturada. d) La otra posibilidad de deterioro estaría más ligada a tensiones cortantes o de cizalla que podrían ser la causa del combado/abombamiento de la zona más externa ya saturada. e) La fotografía muestra una situación donde esta última modalidad de deterioro parece tener lugar.

Otro posible mecanismo de deterioro durante ciclos de absorción de agua consistiría en el combado de la superficie pétrea húmeda. Para que este se produzca, un requisito se hace necesario y es la presencia de defectos paralelos a dicha superficie (Figura 3-1d). Estos pueden ser el resultado de otros mecanismos de deterioro o ser

inherentes al propio material rocoso (ej. anisotropía textural). Así pues, colocar bloques de piedra con los planos de sedimentación paralelos a la fachada del edificio, es decir, a contrahoja, significaría tener estas zonas de máxima debilidad en la orientación más apropiada para que los esfuerzos cortantes (*shear stresses*), en la interfase seca/saturada, propaguen dichos defectos ocasionando el combado (*buckling*) de la zona saturada. Este último caso es ilustrado en la Figura 3-1e, donde se muestra una fachada construida en *Portland Brownstone* y un posible caso de combado de la superficie pétrea.

En la situación inversa, en la que el material pétreo saturado empieza a secarse desde su superficie externa (Figura 3-2a), esta última tendería a contraerse si no estuviese adherida a la zona húmeda del material (Figura 3-2b). Sin embargo, esta adhesión a la parte mojada, mucho más voluminosa, causa el que la capa fina en fase de evaporación se encuentre sometida a esfuerzos de tensión (Figura 3-2c), por lo que el material en esta situación sufriría deterioro si dichos esfuerzos llegasen a ser mayores que la resistencia mecánica máxima de la piedra seca a la tracción.

Debido a que la resistencia mecánica a la tracción de los materiales pétreos es mucho más baja (aproximadamente entre 10-20 veces inferior) que su resistencia a la compresión, se espera que el deterioro por solicitaciones mecánicas (tensiones en este caso) durante el proceso de secado sea mucho más problemático que el deterioro debido a esfuerzos de compresión durante procesos de exposición a la humedad.

Durante los procesos de evaporación, el tipo de daño observado debería ser similar al experimentado por los terrenos arcillosos de secano (Figura 3-2d-f) donde las grietas se desarrollan perpendicularmente a la superficie de los mismos en direcciones arbitrarias, formando un entramado poligonal de tamaño característico. En piedras con gran anisotropía textural, la morfología del entramado puede ser diferente, como se explica en el Anexo 6.

No obstante, un análisis más detallado del problema nos lleva a identificar factores que pueden modificar estas expectativas en gran medida. De hecho, las tensiones de secado pueden verse limitadas por el comportamiento viscoelástico del material pétreo que contiene minerales de la arcilla, como se explica en la sección 3.3.3.

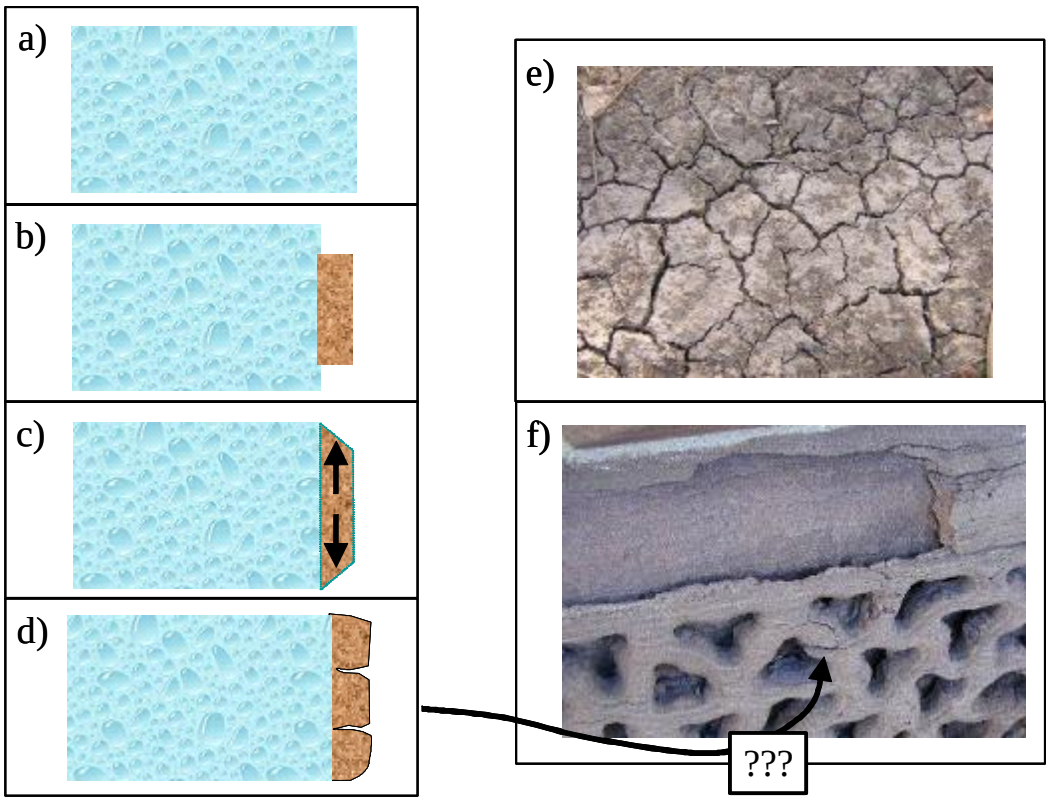

Figura 3-2. Ilustración de las formas en que pueden desarrollarse máximos esfuerzos durante el proceso de secado. Se parte de la idea de que un bloque de piedra, previamente saturado en agua (a) empieza a secarse desde el exterior y la zona, aún muy fina, una vez "seca" tendería a contraerse si no estuviese adherida a la gran masa húmeda del bloque (b) pero la adhesión impide que esto suceda y en realidad somete la fina capa "seca" a esfuerzos de tracción, simbolizados con flechas en (c). Debido a que el material pétreo es débil en tracción, podría fisurarse, exhibiendo en ese caso una forma de craquelado muy similar a la observada en los terrenos de ambientes áridos o de secano (e) donde las fisuras aparecen perpendicularmente a la superficie del bloque pétreo guardando entre ellas un espaciado característico. Una imagen de la arenisca Portland Brownstone que parece ilustrar esta tipología de deterioro se muestra en (f).

Otro factor importante a resaltar es que para que los esfuerzos de tracción se desarrollen plenamente, los bloques de piedra deben estar totalmente expandidos (Figura 3-3b) antes del secado y además, este último debería llevarse a cabo en un ambiente totalmente seco (0% RH). En la práctica, esta situación es poco frecuente, por no decir inexistente, por lo que el número de casos de daño por esfuerzos de tracción es limitado. Un caso más típico es el protagonizado por ejemplo por un

bloque de piedra en la fachada de un edificio que por su localización no llegue a estar totalmente saturado (Figura 3-3c-d). Una situación diferente cabe esperar en un bloque protuberante, relieve o por ejemplo una fina lápida, donde la mayor parte de las superficies están expuestas a la lluvia y posiblemente a succión capilar (Figura 3-3a). En tales situaciones, es más probable llegar a la saturación máxima (Figura 3-3b) y por consiguiente, a situaciones de deterioro que podrían ocasionar craquelado durante los ciclos de evaporación.

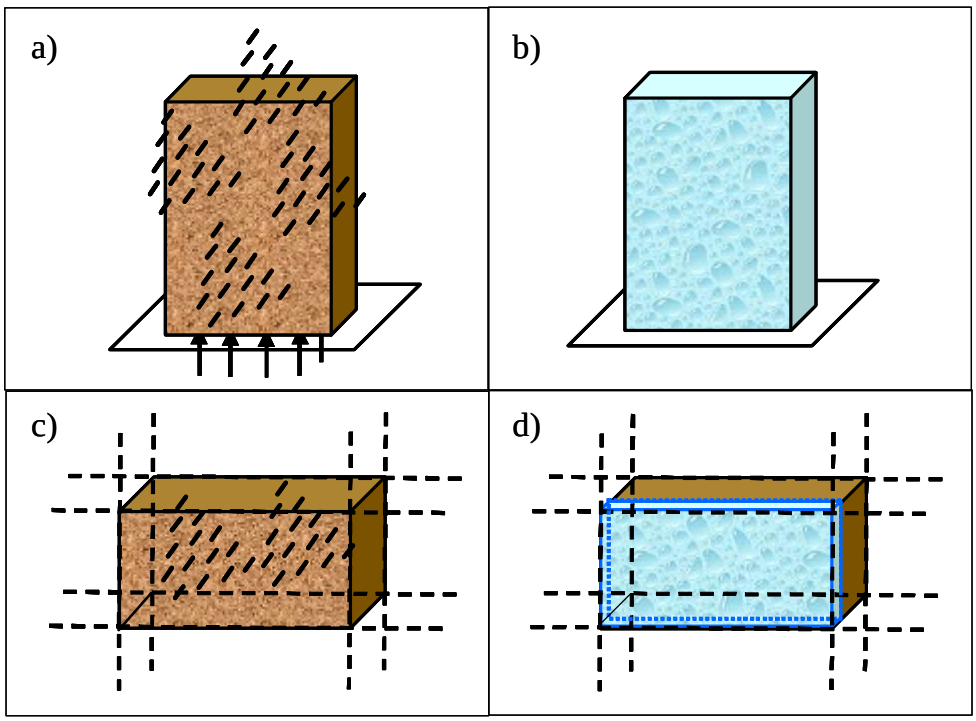

Figura 3-3. Ilustración de casos extremos de condiciones de exposición. Arriba, un bloque vertical de escaso grosor podría representar por ejemplo una lápida sometida tanto a la succión capilar en su base como a la acción de la lluvia en el resto de sus superficies (a). Como resultado, dicho bloque podría llegar a saturarse completamente (b). Un bloque pétreo en un edificio (que no sea un elemento exento o protuberante, por ejemplo en una fachada) presenta hipotéticamente sólo una superficie de exposición al agua de lluvia (c). Si excluimos la acción de la succión capilar, dicho bloque solamente se mojaría parcialmente (d).

La humedad relativa afecta a la magnitud de la retracción y al módulo elástico de la piedra, como muestra la Figura 3-4. La retracción producida durante el secado del

elemento pétreo (partiendo de situaciones iniciales de saturación total) disminuye conforme la humedad relativa aumenta. La retracción se expresa como fracción de la máxima retracción obtenida en una atmósfera completamente "seca". La disminución tanto de la deformación por retracción como del módulo de elasticidad con valores altos de humedad relativa reduciría el riesgo de daño por formación de grietas durante el proceso de secado.

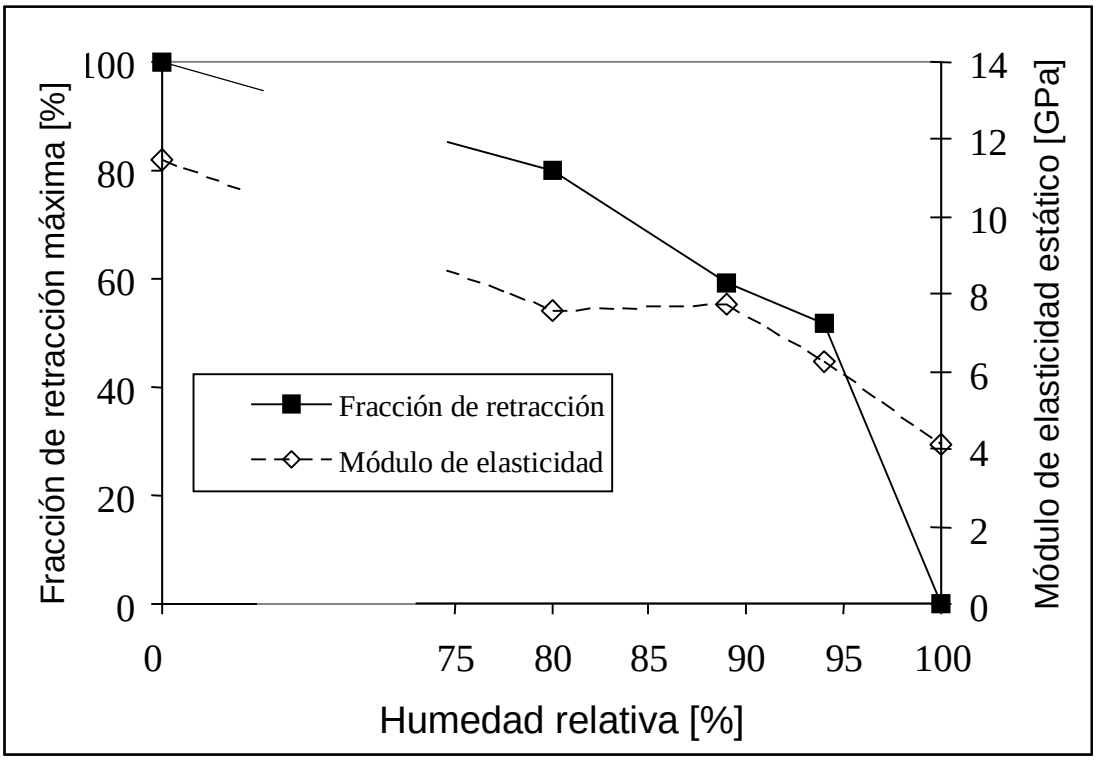

Figura 3-4 Fracción de la retracción máxima (y tensiones de secado) de la arenisca Portland Brownstone en función de la humedad relativa de la atmósfera durante el secado. Asimismo se muestra el aumento del módulo de elasticidad al disminuir la humedad relativa.

En el caso de la arenisca *Portland Brownstone*, nuestros resultados muestran que alrededor de valores de HR del 85 %, el valor de la retracción es de tan sólo el 70% de aquel alcanzado a 0% HR y el módulo de elasticidad del 67 %. Consecuentemente, durante el proceso de secado (en condiciones del 85% HR), el esfuerzo pronosticado sería de aproximadamente 2.3 MPa, y no de 5 MPa como se calcula para situaciones

con 0% HR; El valor de 2.3 MPa es también más bajo que el de la resistencia mecánica máxima a la tracción del material seco (alrededor de 4.5 MPa).

De acuerdo con la discusión precedente, el daño a las diferentes areniscas estudiadas en esta tesis dependería de una serie de factores entre los cuales se incluyen las propiedades mecánicas. Tanto los valores de resistencia mecánica como la rigidez de las piedras que contienen minerales de la arcilla y que además han absorbido agua pueden ser sustancialmente más bajos que los de la misma piedra "seca". Esto podría implicar que piedras como la *molasa de Villarlod*, la cual presenta un grado de reblandecimiento considerable, podrían llegar incluso a deshacerse durante los procesos de humidificación y no durante los de evaporación. Por otro lado, la arenisca *Portland Brownstone* es poco propensa a sufrir daño por esfuerzos de compresión durante los ciclos de humidificación. De acuerdo con nuestros cálculos, esta presión llegaría a ser de tan sólo 1-2 MPa, siendo la resistencia mecánica máxima a la compresión en las mismas condiciones de aproximadamente 35 MPa (Anexo 3).

En cualquier caso, todas las piedras ornamentales pueden sufrir daño durante los ciclos de humidificación por abombamiento, aunque como ya ha sido indicado, este requiere la existencia previa de defectos (irregularidades) o fisuras paralelas a la superficie, que dependerán o serán favorecidas por varias propiedades del material. En el caso de la molasa -la cual tiene cemento calcítico- dichos defectos pueden haber tenido origen en la pérdida del cemento calcítico seguida de la cristalización de yeso producido por la reacción de la piedra con el dióxido de azufre atmosférico. En otros casos, tales "defectos" pueden deberse a la anisotropía textural intrínseca a la roca ornamental: por ejemplo debida a la concentración de las arcillas en planos de sedimentación.

3.3 Propiedades mecánicas

3.3.1 Resistencia mecánica

La medida de la resistencia mecánica a la tracción de la piedra es de importancia crucial, al tratarse esta de un material frágil. Además, los materiales pétreos, como ya ha sido mencionado, muestran menor resistencia cuando son sometidos a esfuerzos de tracción que de compresión. De hecho, es bien sabido que los mecanismos de degradación que implican el crecimiento de cristales en el seno de los materiales, caso

de la formación de hielo o la cristalización de sales, causan tensiones de tracción en el material. En el caso que nos ocupa y como ya ha sido explicado con anterioridad, los ciclos de h/s podrían también causar fallo por esfuerzos de tracción durante los procesos de secado.

La medida directa de la resistencia a la tracción de los materiales pétreos no es trivial ya que el ensayo requiere el uso de una muestra de morfología compleja y de un sofisticado sistema de fijación de la misma al instrumento. De hecho, esta propiedad suele ser medida haciendo uso de otro método mucho más sencillo, como es el ensayo de resistencia indirecta a la tracción (también conocido como ensayo brasileño), realizado con probetas cilíndricas sobre las que se aplica una carga perpendicular al eje mayor de simetría (Anexo 1). Los valores de la resistencia mecánica máxima a la tracción en húmedo y en seco de las principales piedras estudias están indicados en Anexo 1, Table A1- 1.

La resistencia mecánica máxima a la compresión podría ser un problema en caso de litotipos que presentan una cohesión intergranular débil, ya que en determinadas circunstancias de humedad estos se “reblandecerían” mucho. Si el “reblandecimiento” llegase a adquirir cierta magnitud, se podría producir deterioro durante los ciclos de humidificación. Un buen ejemplo de ello es el protagonizado por las molasas suizas anteriormente citadas, las cuales presentan una acusada reducción de la cohesión cuando absorben agua.

Finalmente, mencionamos otro aspecto importante a considerar en el análisis de los resultados del ensayo de resistencia mecánica (tanto a la tracción como a la compresión), y es que esta depende también de la duración de la aplicación de la carga durante el ensayo. La influencia de este factor no ha podido ser analizada debido sobretodo a razones de disponibilidad instrumental, pero somos conscientes de sus implicaciones y desde aquí se recomienda la consideración del mismo en trabajos futuros. Girardet (comunicación personal, 2004) encuentra por ejemplo que cuando a una molasa “seca” se le aplica una carga de valor igual a la mitad de la magnitud de su resistencia a la compresión, durante un tiempo prolongado, la piedra se fractura después de aproximadamente 24 horas. La velocidad con la que se desarrollan los esfuerzos durante los procesos de meteorización es obviamente mucho más lenta que las velocidades de carga típicas producidas en los ensayos de laboratorio. Por esta razón, parece correcto tener en cuenta la dependencia del factor tiempo durante estos ensayos, ya que contribuiría a tener una predicción más exacta del momento en que se produciría el fallo o rotura del material *in situ*.

3.3.2 Módulo de elasticidad

El módulo de elasticidad o módulo de Young (E) de un material se define como el cociente entre el esfuerzo/tensión (s) aplicado a un material y la deformación (e) sufrida y puede ser determinado usando técnicas ultrasónicas o estáticas. En el primer caso, se diría que la propiedad medida correspondería al módulo elástico dinámico del material. En el segundo caso se mediría el módulo elástico estático del mismo.

Módulo dinámico

En este tipo de ensayo, las deformaciones producidas son extremadamente pequeñas y se encuentran en el límite elástico de la deformación del material.

La técnica ultrasónica presenta la ventaja de ser no destructiva (TND). Con ella, el módulo elástico dinámico (E^{din}) del material se calcula considerando su densidad y la velocidad con la que ondas sónicas atraviesan el mismo [ecuación (A1-2)]. Esta velocidad se calcula a partir de la medida del tiempo de transmisión de un pulso ultrasónico (onda comprimida) a través de una probeta.

El instrumento usado en este estudio proporciona un valor medio de los "caminos" más rápidos encontrados por la onda en su recorrido, es decir, detecta el tiempo mas rápido empleado por la onda sónica. Esta técnica no es sensible a la existencia de defectos superficiales o fisuras de pequeña entidad, lo cual indica que en una piedra deteriorada, los defectos o fisuras deben ser relativamente grandes para poder inducir un cambio significativo en su módulo dinámico.

A pesar de estas limitaciones, este tipo de instrumento es apreciado y usado por la comunidad de conservadores-restauradores debido tanto a su carácter no destructivo como por su fácil manejo y transporte. En el caso particular del estudio llevado a cabo en esta tesis, el hecho de poder usar un instrumento de este tipo ha sido especialmente útil, ya que determinadas probetas han podido ser medidas antes y después de ser sometidas a determinados tratamientos (ej. aplicación de productos inhibidores de la expansión o de consolidantes). Del mismo modo, el instrumento ha sido utilizado durante la realización de ensayos de envejecimiento acelerado por ciclos de

humedad/sequedad. Para este tipo de estudio de carácter comparativo, se observa que el uso de esta técnica es satisfactorio.

De cualquier modo, durante las primeras medidas efectuadas con esta técnica, pudimos observar como el módulo de elasticidad de la arenisca *Portland Brownstone* era sustancialmente más alto cuando estaba totalmente saturada en agua que cuando estaba seca. Los mismos ensayos realizados posteriormente con probetas de otros litotipos indicaron que nuestra observación era generalmente correcta para piedras que contienen minerales de la arcilla. Sin embargo, en piedras como la caliza de "Indiana" que como máximo contiene alguna traza de este tipo de minerales, el módulo dinámico elástico no experimentó cambios significativos, es decir, era independiente de las condiciones de humedad presentadas por las probetas.

Este comportamiento mostrado por las rocas que contienen minerales de la arcilla es atribuido a la reducida movilidad del agua entre las capas y/o partículas de estos minerales. Se sospecha que este factor sea el responsable de que una porción del agua localizada entre las capas de estos filosilicatos se comporte como un sólido a la velocidad de propagación de los ultrasonidos. En otras palabras, durante el tiempo en que una onda ultrasónica induce la deformación en el material saturado, las moléculas de agua no tendrían tiempo suficiente para fluir, por lo que quedarían atrapadas entre partículas de los minerales y se comportarían eventualmente como si formasen parte del "esqueleto" de la piedra, contribuyendo sustancialmente a la transmisión (más rápida) de las ondas acústicas. Se piensa que esta podría ser la razón por la cual se obtienen valores de módulo elástico del material saturado aparentemente más altos.

Se deduce por tanto, que las medidas llevadas a cabo con ultrasonidos en piedras que contienen minerales de la arcilla podrían no ser fiables, incluso en el caso de material pétreo seco. En consecuencia, debido a la importancia que tiene en nuestro estudio el conocer esta propiedad mecánica para poder así determinar los esfuerzos o tensiones generados durante los ciclos de h/s, este aspecto ha sido analizado y para ello han sido realizadas medidas estáticas del módulo de elasticidad.

Módulo estático

El método estático empleado para medir el módulo de Young se basa en la flexión de una placa que se apoya en dos puntos (ensayo de flexión por tres puntos). A la distancia entre esos dos soportes se le denomina "luz". El ensayo consiste en aplicar

una carga en la placa de piedra (en el punto medio de la luz) y en medir la deflexión o desplazamiento vertical de la misma. La carga y la deflexión están relacionadas por el módulo de Young a través de una expresión matemática (Anexo 1). Con este tipo de medidas se imponen en las probetas deformaciones de mayor magnitud que las inducidas por la técnica de ultrasonidos descrita previamente. De hecho, el uso de este ensayo tiene especial interés en este trabajo ya que permite imponer deformaciones similares a las que se espera que ocurran durante los ciclos de expansión/contracción. El módulo así medido (E^{est}) es por consiguiente más relevante a la hora de estimar los esfuerzos surgidos durante estos procesos. Es más, la técnica puede usarse también para determinar las propiedades viscoelásticas del material, tanto si este se encuentra saturado en agua o seco. La decisión de usar este ensayo y no otro para caracterizar las propiedades mecánicas de nuestros materiales constituye una novedad de esta tesis. Los resultados obtenidos al respecto han sido publicados (Anexo 3 y Anexo 4).

En la Figura 3-5a podemos observar la gran diferencia de los valores de módulos de elasticidad obtenidos con técnicas estáticas y dinámicas. Existe además una falta total de correlación entre el efecto de la saturación obtenido con ambas técnicas (representado con las razones entre módulo seco y saturado). Sin embargo, el grado de reblandecimiento de las piedras medido con la técnica estática muestra una correlación muy clara con el coeficiente de deformación por expansión (Figura 3-5b). Esto confirmaría nuestra hipótesis sobre el hecho de que en el estado de saturación, la presencia de minerales de la arcilla perturba las medidas de módulo dinámico y las hacen irrelevantes en nuestro estudio.

Aunque el uso de la técnica de flexión por tres puntos es satisfactorio, no obstante se debe puntualizar que el análisis de la flexión de probetas saturadas necesita una atención particular. La razón se debe a que durante la flexión, la fase sólida de la zona superior de la probeta se encuentra en compresión, lo cual crea presiones que se transmiten al agua contenida en su sistema poroso y que obligan a esta última a desalojar dicho espacio. Por otro lado, la mitad inferior se encuentra en tensión. En consecuencia, el líquido tiende a ser succionado en esta zona. En otras palabras, se produce una redistribución del agua a través del sistema poroso de la probeta. Este proceso requiere tiempo debido a la viscosidad del líquido. Como resultado, la carga que se aplica para producir una cierta deformación es más elevada inicialmente y decrece hasta alcanzar un valor constante en el caso de sólidos elásticos. Este valor de la carga final será usado para calcular el módulo de elasticidad del material, de la misma forma que se determina el módulo de una placa/vigueta elástica no saturada.

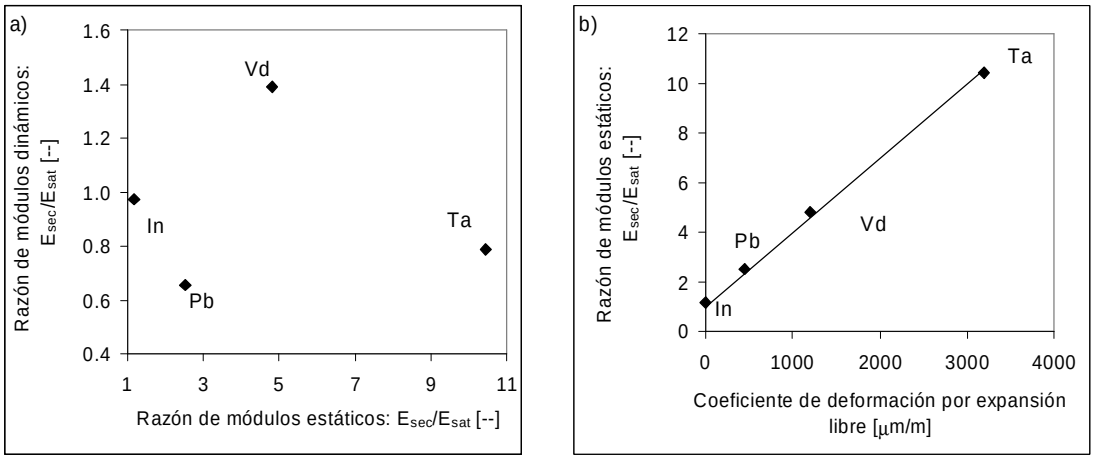

Figura 3-5. Efecto de los minerales de la arcilla en las medidas de módulo de elasticidad. a) representación de la razón (E_{sec}/E_{sat}) obtenida con medidas dinámicas respecto a aquella obtenida con medidas estáticas. Se observa la gran diferencia entre los valores ofrecidos por las dos técnicas así como la falta de correlación entre ellas. b) Efecto de la razón (E_{sec}/E_{sat}) obtenida con medios estáticos y el coeficiente de deformación por expansión libre de piedras no tratadas. La buena correlación encontrada pone de manifiesto el papel de las arcillas en el grado de reblandecimiento de cada piedra. Los litotipos representados son: caliza de "Indiana" (In), arenisca Portland Brownstone (Pb), molasa de Villarlod (Vd) y arenisca de Tarifa (Ta).

Scherer (1992) ha publicado un análisis completo de este problema. Sus ensayos muestran que la evolución de la carga con el tiempo puede estar relacionada con la permeabilidad de la probeta. Cuando esta tiene poros pequeños, la redistribución del líquido es más lenta y el tiempo empleado por la carga en alcanzar el valor constante aumenta. Los resultados que confirman esto último provienen de ensayos realizados con vidrios Vycor® y han sido publicados por Vichit-Vadakan y Scherer (2000). El análisis que realizan sobre este ensayo confirma que la teoría predice correctamente la dependencia de la evolución temporal de la carga con respecto a la viscosidad del líquido.

En general, la relajación de la carga (W) necesitada para mantener un sólido elástico saturado en agua bajo una deformación constante disminuye con el tiempo (t) de la siguiente forma:

$$\frac{E_{(t)}}{E_{(0)}} = \frac{W_{(t)}}{W_{(0)}} = R_{(t)} \tag{3-1}$$

donde $E_{(t)}$ y $E_{(0)}$ son los módulos de elasticidad respecto al tiempo t (o módulo viscoelástico) y extrapolado a t = 0 (o módulo inicial), respectivamente y $W_{(t)}$ y $W_{(0)}$ son las cargas respecto al tiempo t y extrapolada a t = 0, respectivamente.

La función $R_{(t)}$ sólo describe la redistribución del agua durante el experimento. Su expresión analítica está bien definida para viguetas tanto circulares como rectangulares y depende tanto de las propiedades del material poroso como de aquellas del líquido. A tiempos largos alcanza un valor constante que depende sólo del material poroso.

En el caso de placas viscoelásticas saturadas, la carga disminuye continuamente con el tiempo y en este caso, la función $R_{(t)}$ no es suficiente para describir tal comportamiento. Este es el caso de los materiales pétreos que contienen minerales de la arcilla, por lo que se pone de manifiesto su claro carácter viscoelástico como se verá en la siguiente sección.

3.3.3 Viscoelasticidad

Los materiales viscoelásticos experimentan deformaciones tanto reversibles como irreversibles cuando se les aplica un esfuerzo o carga. La deformación reversible se corresponde con la parte elástica de los mismos y por lo tanto puede ser analizada según los principios de elasticidad, como ya ha sido señalado anteriormente. La deformación irreversible se correspondería con la parte de comportamiento viscoso, es decir, la deformación se mantendría una vez eliminado el esfuerzo y además se incrementaría con la duración de aplicación del mismo.

Existen dos tipos principales de medidas de viscoelasticidad:

1) **Ensayo de relajación del esfuerzo (*stress relaxation*):** con este experimento se mide el esfuerzo requerido para mantener una cierta deformación (deflexión en este caso) en la probeta con respecto al tiempo. De hecho, se ha observado que dicho esfuerzo disminuye con el tiempo. Este tipo de medida es la que se

ha empleado en esta tesis haciendo uso del ensayo de flexión por tres puntos, del cual se facilita una descripción detallada en el Anexo 3 y Anexo 4.

2) **Ensayo de fluencia lenta (*creep*):** en este caso, un determinado esfuerzo es aplicado a la probeta y lo que se mide es la deformación resultante, la cual se ha observado que incrementa respecto al tiempo.

Asimismo, vale la pena subrayar, que las propiedades mecánicas de los materiales viscoelásticos dependen tanto de la frecuencia (o velocidad) como de la magnitud de la deformación aplicadas durante los ensayos. Este es también el caso para piedras que contienen minerales de la arcilla (Tutuncu et al., 1998a, b). En este último caso, el carácter viscoelástico de estos materiales explica la falta de concordancia encontrada entre los valores de módulo de Young obtenidos con métodos dinámicos (técnicas de ultrasonidos) y aquellos estáticos (ej. ensayo de flexión por tres puntos) mencionados en la sección anterior. En este contexto, se considera oportuno recordar que se atribuye el carácter viscoelástico de estas piedras al movimiento del agua en su sistema poroso.

De hecho, durante la medida con ultrasonidos, dada la alta frecuencia de las ondas aplicadas, se espera que las moléculas de agua tengan una movilidad reducida entre las partículas o capas de arcilla. Esta sería la causa por la que se cree, se produciría aparentemente un incremento del módulo dinámico en probetas saturadas. Por otra parte, en el ensayo de flexión por tres puntos, el agua tiene tiempo de redistribuirse y el módulo medido refleja realmente la rigidez del “esqueleto” del material. A tiempos más largos, es decir, a frecuencias mucho más bajas, esta parte sólida puede también exhibir relajación de esfuerzos. Se cree que esta última es favorecida por la lubricación provocada por la presencia de agua entre las partículas o capas de las arcillas. Esto es congruente con el hecho de que las piedras que contienen este tipo de filosilicatos muestran relajación de los esfuerzos tanto si están “secas” como saturadas, siendo el proceso mucho más rápido en este último estado. Esta relajación del “esqueleto pétreo” será por tanto, la que afecte a los ciclos de h/s si estos son lo suficientemente largos.

Placas "secas" viscoelásticas

La viscoelasticidad de placas/viguetas no saturadas es examinada siguiendo la relajación de la carga que debe ser aplicada a una probeta para mantener una deflexión específica respecto al tiempo. El módulo de elasticidad es entonces una función del tiempo, por lo que podríamos denominarlo "módulo viscoelástico" y es simbolizado por $E_{(t)}$. Además, cuando este último se divide por el módulo inicial $E_{(0)}$, se obtiene como resultado la misma función adimensional dependiente del tiempo $y_{(t)}$ que la obtenida cuando la carga $W_{(t)}$ es dividida por la carga inicial $W_{(0)}$:

$$\frac{E_{(t)}}{E_{(0)}} = \frac{W_{(t)}}{W_{(0)}} = y_{(t)} \tag{3-2}$$

donde $y_{(t)}$ es una función que caracteriza la relajación viscoelástica de la probeta seca y depende del material empleado en el ensayo. En esta tesis, las funciones para los litotipos estudiados fueron identificadas y se encuentran definidas en el Anexo 3.

En los casos de la arenisca *Portland Brownstone* y la *molasa de Villarlod*, se ha encontrado que la relajación de las probetas no saturadas muestra una disminución casi lineal en escala logarítmica (Anexo 3). Este comportamiento de relajación de esfuerzos puede ser ajustado con la siguiente función logarítmica:

$$E_{(t)} = E_{(0)} - a\ln\left(1 + \frac{t}{q_d}\right) \tag{3-3}$$

donde tanto a como q_d son parámetros de ajuste. Claramente, esta función no es válida para tiempos largos, ya que generaría valores de módulo negativos; de todas formas, ofrece un ajuste adecuado en la escala de tiempo considerada. Una vez que $t >> q_d$, obtenemos:

$$E_{(t)} \cong E_{(0)} - a\ln(t) + a\ln(q_d) \tag{3-4}$$

así que el parámetro a es el que verdaderamente caracteriza la velocidad de relajación del esfuerzo.

En el caso de probetas de *Portland Brownstone*, se han obtenido diferentes valores del módulo de elasticidad. Esto ha permitido examinar si existe una correlación entre los parámetros de ajuste. De hecho, los símbolos de fondo blanco en la Figura

3-6, sugieren que hay una relación lineal entre el parámetro *a*, que controla la velocidad de relajación, y el módulo inicial, $E_{(0)}$.

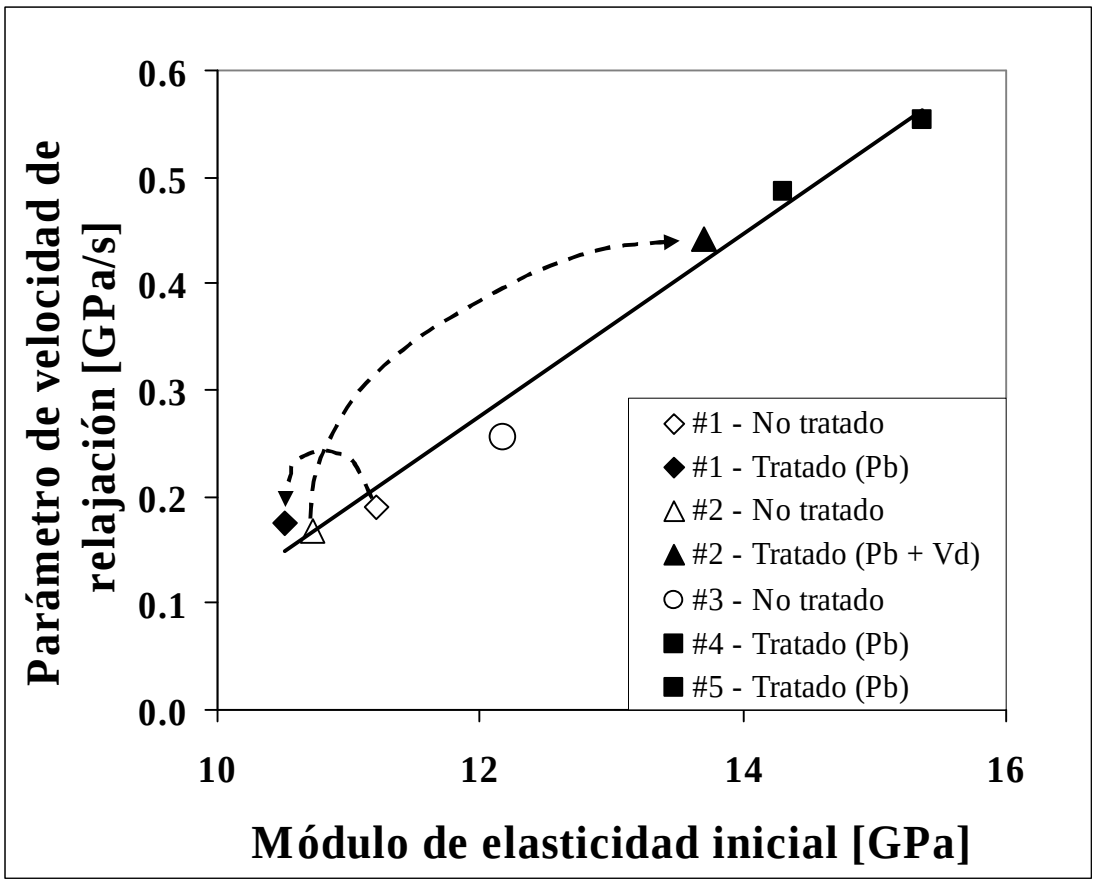

Figura 3-6. Correlación entre el parámetro que define la velocidad de relajación, a, *y el módulo de elasticidad inicial,* $E_{(0)}$*, medidos en cinco probetas de arenisca Portland Brownstone. Los símbolos de fondo blanco y aquellos de fondo negro representan respectivamente medidas obtenidas antes y después del tratamiento con productos inhibidores de la expansión. Las probetas #1 y #2 han sido medidas previa y posteriormente a la aplicación del tratamiento (indicado con el uso de flechas discontinuas). En la mayoría de los casos se ha usado el tratamiento habitualmente aplicado para la arenisca Portland Brownstone (Pb). La probeta #2 recibió un tratamiento adicional con una mezcla de diaminoalcanos usada para el tratamiento de la molasa de Villarlod (Vd, ver Tabla 3-1 y Anexo 3).*

En la misma figura, los símbolos de fondo negro representan probetas tratadas con productos inhibidores de la expansión. Las muestras que han sido medidas previa y posteriormente a la aplicación del tratamiento se señalan en el gráfico a través de flechas discontinuas. Si observamos el gráfico, es interesante señalar como la velocidad de relajación del esfuerzo aumenta conforme lo hace el módulo de elasticidad.

La velocidad de relajación de esfuerzos experimentado por la *arenisca de Tarifa* es bilineal a escala logarítmica (Anexo 3) y esto podría sugerir la implicación de dos procesos de relajación consecutivos (con tiempos característicos q_{d1} y q_{d2}). Se ha encontrado que la siguiente función proporciona un ajuste óptimo de las curvas obtenidas:

$$E_{(t)} = E_{(0)} - a\ln\left(1+\frac{t}{q_{d1}}\right) - b\ln\left(1+\frac{t}{q_{d2}}\right) \tag{3-5}$$

En este caso, la relajación inicial esta gobernada por a y la posterior por b.

La razón por la cual esta piedra muestra un comportamiento que sugiere la existencia de dos procesos de relajación con tiempos característicos diferentes es desconocida. Sólo se observa que los datos experimentales pueden ser bien ajustados considerando esa hipótesis.

Placas saturadas viscoelásticas

En el caso de sólidos viscoelásticos saturados, el análisis es más complejo. De hecho, en dichos materiales y para una determinada deflexión, la disminución de la carga respecto al tiempo depende tanto de la redistribución del líquido a través del sistema poroso como de la deformación irreversible de la probeta.

Este caso ha sido analizado también por Scherer (1992). Los experimentos que han validado el análisis teórico realizado por este autor han sido efectuados igualmente haciendo uso de geles de sílice. Posteriormente, Vichit-Vadakan y Scherer (2003) mostraron que el mismo análisis es válido también en el caso de la pasta de cemento. El estudio de Vichit-Vadakan (2002) presenta más detalles sobre la técnica empleada y su uso para la caracterización de las propiedades viscoelásticas de este último material.

El cambio respecto al tiempo, tanto del módulo de Young como de la carga necesaria para mantener un desvío constante, se indica como el producto de la función de la relajación hidrodinámica, $R_{(t)}$, y de una función de relajación viscoelástica, $y_{(t)}$.

$$\frac{E_{(t)}}{E_{(0)}} = \frac{W_{(t)}}{W_{(0)}} = R_{(t)} y_{(t)} \tag{3-6}$$

Se hace preciso señalar que $y_{(t)}$ en este caso -y en contraste con la ecuación. (3-2)- caracteriza la velocidad de relajación de la probeta saturada y no seca. La determinación de esta función para los diferentes materiales pétreos estudiados es otra contribución original de esta tesis.

Se ha encontrado que la velocidad de relajación de esfuerzos de la roca saturada es cualitativamente diferente a la de la piedra no saturada. Los mejores resultados de ajuste se han obtenido cuando y es representada por una función de estiramiento exponencial (también conocida como función de Kohlrausch-Williams-Watts):

$$y = \exp\left(-\left(\frac{t}{t_{VE}} \right)^{b} \right) \tag{3-7}$$

donde t_{VE} es el tiempo de relajación viscoelástico y b es un parámetro de ajuste que caracteriza la función de relajación.

Cuando la piedra está saturada, se observa que el efecto del tratamiento con productos inhibidores de la expansión depende de la combinación específica del tratamiento y la piedra. Por ejemplo, la *arenisca de Tarifa* muestra una aceleración espectacular de la velocidad de relajación de esfuerzos en condiciones de saturación después del tratamiento (Figura 3-7).

Por otra parte, en las mismas condiciones de humedad, la *molasa de Villarlod* tratada muestra sólo un modesto aumento de dicha velocidad, mientras que la arenisca *Portland Brownstone* tratada no muestra aceleración alguna. El gran efecto que tiene la combinación específica: producto inhibidor del hinchamiento y tipo de piedra (Tabla 3-1) indica que se trata de un problema complejo donde se necesitaría un estudio mucho más amplio para poder entender qué efectos químicos o físicos serían los responsables de esos cambios.

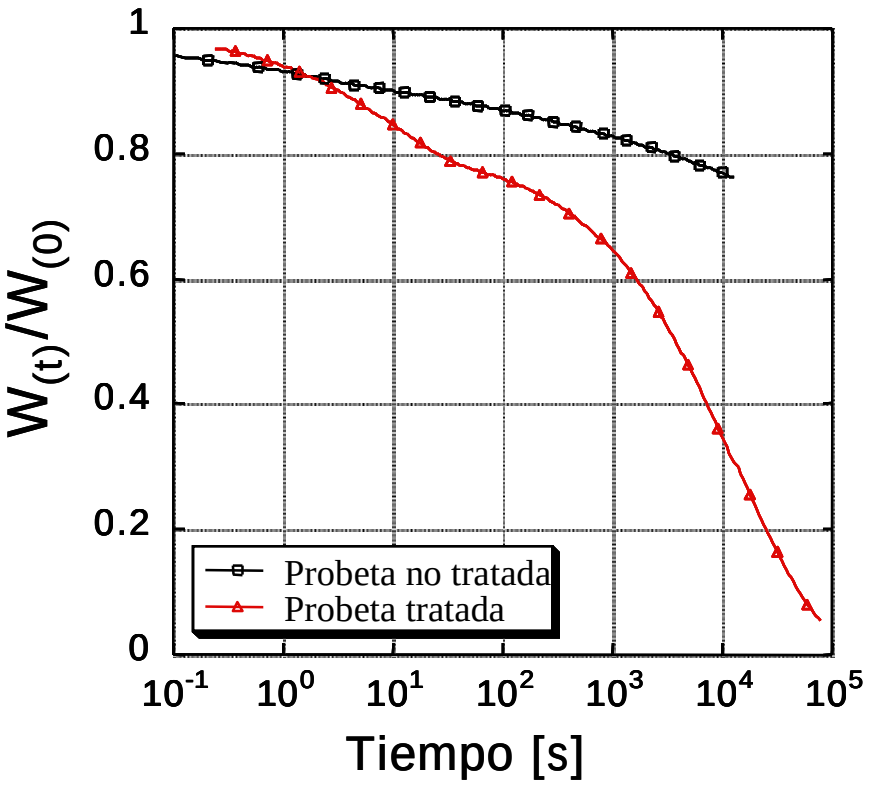

Figura 3-7. Curvas ajustadas de relajación de esfuerzos de una probeta de arenisca de Tarifa saturada en agua. La probeta ha sido medida previa (cuadrados) y posteriormente (triángulos) a ser tratada con agentes inhibidores de la expansión seleccionados para esta piedra.

Sin embargo, en el contexto de esta tesis, lo importante es que estos resultados experimentales indican que estos tratamientos pueden afectar a la velocidad de relajación de esfuerzos. En cuanto a la predicción del impacto de estos cambios sobre la susceptibilidad de la piedra a ser deteriorada por ciclos de h/s, se debe decir que no es trivial, ya que la cinética de todo el proceso debe ser tenida en cuenta. Esto implica la intervención de muchos más factores, como por ejemplo la velocidad de secado y/o saturación. Se supone que un incremento de la velocidad de relajación será beneficioso, por lo menos a corto plazo, aunque se necesitaría estudiar el posible cambio de resistencia mecánica que tales tratamientos podrían causar. A más largo plazo, una acumulación de microdeformaciones irreversibles, resultantes de este comportamiento viscoelástico, podría causar una reducción de la resistencia mecánica máxima del material.

Nuestra propuesta de interpretación sobre la capacidad mostrada por este tipo de materiales pétreos para relajar esfuerzos, tanto si están saturados como no, considera la existencia de un deslizamiento entre las capas o superficies de los minerales de la arcilla. El hecho de que la velocidad de relajación de esfuerzos sea más rápida en estado húmedo tiende a confirmar esta hipótesis. Como se verá más adelante, este mismo comportamiento también se dará en medidas de presiones de hinchamiento. De hecho, en estos últimos ensayos, la fuerza requerida para prevenir la expansión de la probeta es sustancialmente menor que la esperada debido a la existencia de este proceso de relajación de esfuerzos.

3.4 Expansión hídrica

3.4.1 Expansión libre e inhibidores del hinchamiento

La magnitud de la expansión de la piedra depende tanto de la naturaleza y cantidad de minerales de la arcilla que contiene como de la distribución de estos en el sustrato pétreo. Como ejemplo a título ilustrativo del efecto de la distribución de arcillas, considéranos dos casos extremos. En el primero, los minerales de la arcilla se encontrarían solamente recubriendo las paredes de los poros (Figura 3-8a), por lo que no formarían parte de la fase cementante que conecta los granos entre ellos. En este caso, las arcillas probablemente no tendrían mucho efecto tanto en la expansión como en el reblandecimiento de la piedra. Sin embargo, lo contrario sucedería en el caso de que estos minerales se encontrasen en el cemento rocoso que une los granos de la roca (Figura 3-8b).

En cualquier modo cabe señalar que la magnitud de expansión de la piedra es generalmente mucho más pequeña que aquella de los minerales de la arcilla. Por ejemplo, si el grosor de la fase cementante es del 1 % del tamaño de grano y las arcillas contenidas en el mismo expanden un 10 %, entonces la piedra dilataría tan sólo el 0.1 % (ó 1000 μm/m).

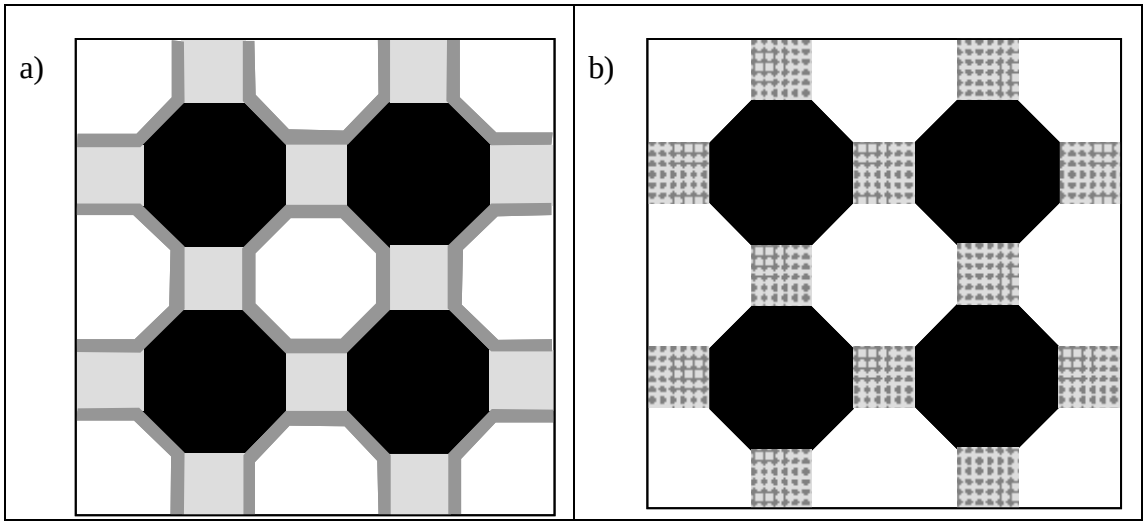

Figura 3-8. Ilustración de posibles casos extremos de distribución de minerales de la arcilla en la piedra: a) las arcillas (en gris oscuro) recubren las paredes de los poros en (blanco) y los granos (en negro) se conectan entre sí a través de una fase cementicia no expansiva (en gris claro), b) las arcillas están localizadas ahora exclusivamente en el cemento entre los granos.

Las piedras estudiadas ofrecen una amplia gama de coeficientes de deformación por expansión lineal (Figura 3-9).

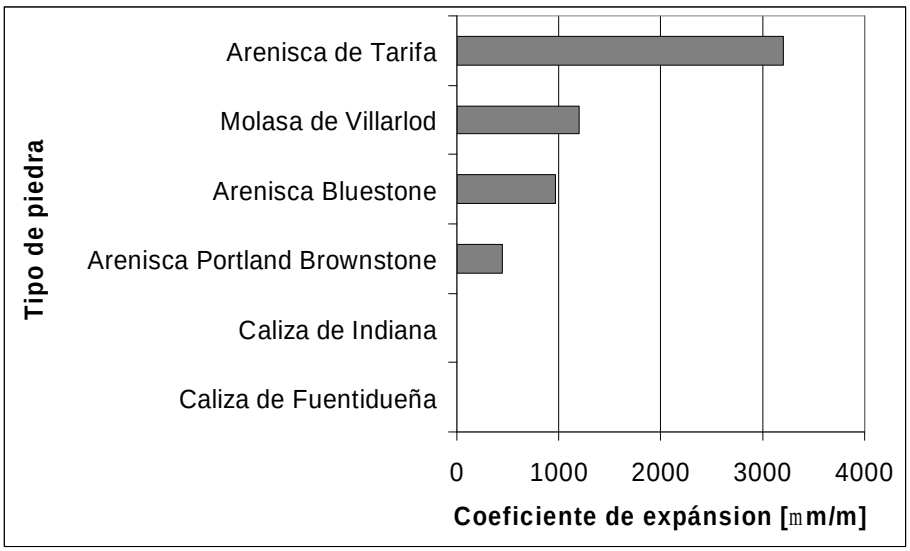

Figura 3-9. Coeficientes de deformación por expansión hídrica medidos en las diferentes piedras estudiadas en esta tesis.

De los tres materiales pétreos estudiados en detalle, el valor más bajo (valor medio de 450 μm/m) corresponde a la arenisca *Portland Brownstone*, al cual le sigue el de la *molasa de Villarlod* con aproximadamente 1200 μm/m y finalmente el de la *arenisca de Tarifa* que muestra una media de 3200 μm/m, como indica la Tabla 3-1 y Anexo 3. Recordamos que para estas piedras se ha encontrado una clara relación entre el grado de reblandecimiento de las mismas y sus coeficientes de deformación por expansión (Figura 3-5b). Esto claramente sugiere que el reblandecimiento del material debe estar producido por la saturación de la fracción de los minerales de la arcilla localizada en espacios intergranulares. De hecho, serían sólo estas arcillas y no las situadas en las paredes de los poros, las presuntas responsables del hinchamiento de la piedra.

Como ya ha sido mencionado, la expansión hídrica puede ser reducida usando tratamientos específicos. En nuestro estudio, el tratamiento de cada litotipo ha sido seleccionado de acuerdo con los mejores resultados obtenidos de ensayos preliminares con diferentes productos y sus combinaciones. Tanto los productos como el efecto conseguido se muestran en la Tabla 3-1. Asimismo, los detalles sobre la selección de tratamientos se encuentran en el Anexo 3. Las mezclas usadas están compuestas por soluciones acuosas que no superan el 5 % en peso con objeto de no inducir cambios colorimétricos en nuestros especímenes. Es evidente que el hecho de no aplicar la misma combinación de productos a todas las piedras dificulta la comprensión sobre el porqué de la eficacia de la misma. Sin embargo, visto que uno de nuestros objetivos principales es ver el efecto macroscópico que la aplicación de dichos agentes tiene en los diferentes sustratos pétreos, nos ha parecido más relevante a nivel práctico trabajar con los productos que podrían proporcionar la mayor reducción de expansión.

Las soluciones utilizadas para estos tratamientos presentan un pH variado. Los diamino-alcanos dihidroclóricos presentan un valor medio de pH ligeramente ácido (5) muy similar al pH del agua de lluvia. Por otro lado, el aminoalcohol tiene pH básico (10). En un principio, el tratamiento de nuestros litotipos con estos productos no debería entonces plantear problema alguno, incluso en el caso de las *arenisca de Tarifa y molasa de Villarlod*, ambas de cemento calcítico.

Como puede observarse, la reducción de la expansión para las areniscas *Portland Brownstone* y *de Tarifa* es aproximadamente del 50%, siendo este valor un poco más elevado (65%) en el caso de la *molasa de Villarlod*. Wangler et al. (2006) han llevado a cabo tratamientos con productos similares a los descritos en esta tesis pero en

diferentes rocas y con concentraciones más elevadas, obteniendo reducciones de los coeficientes de expansión libre de alrededor del 80 %.

Tabla 3-1. Tratamientos inhibidores del hinchamiento seleccionados y sus efectos en las tres piedras estudiadas. Las siglas F-C hacen referencia a un aminoalcohol (Anexo 3).

Piedra	Tratamiento	Hinchamiento [μm/m]	
		No tratado	Tratado
Portland Brownstone	1,3 diaminopropano dihidroclórico +F-C Una impregnación con una solución al 2.5% y 0.5% de estos productos respectivamente	446	212
Molasa de Villarlod	1,3 diaminopropano dihidroclórico + 1,2 diaminoetano dihidroclórico Una impregnación con una solución al 2.5% de cada producto	1200	422
Arenisca de Tarifa	1,2 diaminoetano dihidroclórico Dos impregnaciones con una solución al 5%	3200	1620

El hecho de haber logrado reducir la deformación por hinchamiento constituye un aspecto positivo para la conservación de obras y estructuras en piedra ya que, en una primera aproximación y según lo explicado en la sección 3.2.2 y Anexo 3, los esfuerzos son proporcionales al coeficiente de hinchamiento lineal. Por consiguiente, una disminución de este último valor en el orden del 50 % o más implicaría una disminución de los esfuerzos resultantes en el mismo orden de magnitud.

Según el conocimiento de la autora de esta tesis, los primeros autores en demostrar que cierto tipo de moléculas podrían ser usadas para reducir la deformación por expansión en obras en piedra y patrimonio construido han sido Wendler et al. (1991) y Snethlage y Wendler (1991). La idea general se basa en reemplazar los cationes adsorbidos en las superficies de las partículas de los minerales de la arcilla por moléculas orgánicas, típicamente aminas protonadas que deberían prevenir la expansión tanto por su facultad de no disociarse como por ser capaces de evitar el que las moléculas de agua sean absorbidas en la estructura de estos minerales.

En un principio, Snethlage y Wendler (1991) realizaron ensayos con tensoactivos que son conocidos por intercalarse entre las capas de los minerales de la arcilla, pero no obtuvieron buenos resultados ya que la aplicación de los mismos provocó un daño sustancial en las rocas tratadas. La explicación que estos autores ofrecen a este hecho es que la cola hidrófoba de los tensoactivos se orienta perpendicularmente a la superficie. La interacción entre dos partículas de arcilla con moléculas de este tipo adsorbidas en sus superficies provoca una repulsión estérica, induciendo así una expansión importante en el material, el cual incluso llega a destruirse.

Después de estos ensayos iniciales, prestaron más atención a otro tipo de productos, los diamino-alcanos dihidroclóricos, que finalmente demostraron ser una elección mucho mejor. Estas moléculas no presentan la estructura típica de los productos tensoactivos, ya que no tienen una cola hidrófoba y una cabeza polar.

Snethlage y Wendler (1991) sugieren que los diamino-alcanos dihidroclóricos son inhibidores del hinchamiento efectivos ya que pueden "enlazar" capas opuestas de minerales de la arcilla a través de un grupo amino adsorbido en cada superficie como se ilustra en la Figura 3-10. De todas formas, la veracidad de este supuesto ha sido examinada de forma más crítica por Wangler y Scherer (comunicación personal del Prof. G. Scherer, 2008), los cuales han encontrado que los grupos amino se sitúan más o menos de forma paralela a las capas de los minerales de la arcilla y entre las mismas.

Para que estas moléculas sean adsorbidas en las superficies (001) de carga negativa de los minerales de la arcilla, los grupos amino necesitan estar protonados ($-NH_3^+$). La protonación depende del pH, así que cuanto más elevado sea el valor de este último, mayor será la desprotonacion ($-NH_2$). Sin embargo, debido al carácter "ácido" de las superficies de estos minerales, se podría esperar esta protonación molecular en más casos.

Dichos diamino-alcanos han sido utilizados en esta tesis para reducir la expansión de nuestros litotipos (Tabla 3-1). Sin embargo, en el caso de la *Portland Brownstone,* la aplicación de un amino-alcohol junto a un diamino-alcano dihidroclórico ha producido los mejores resultados.

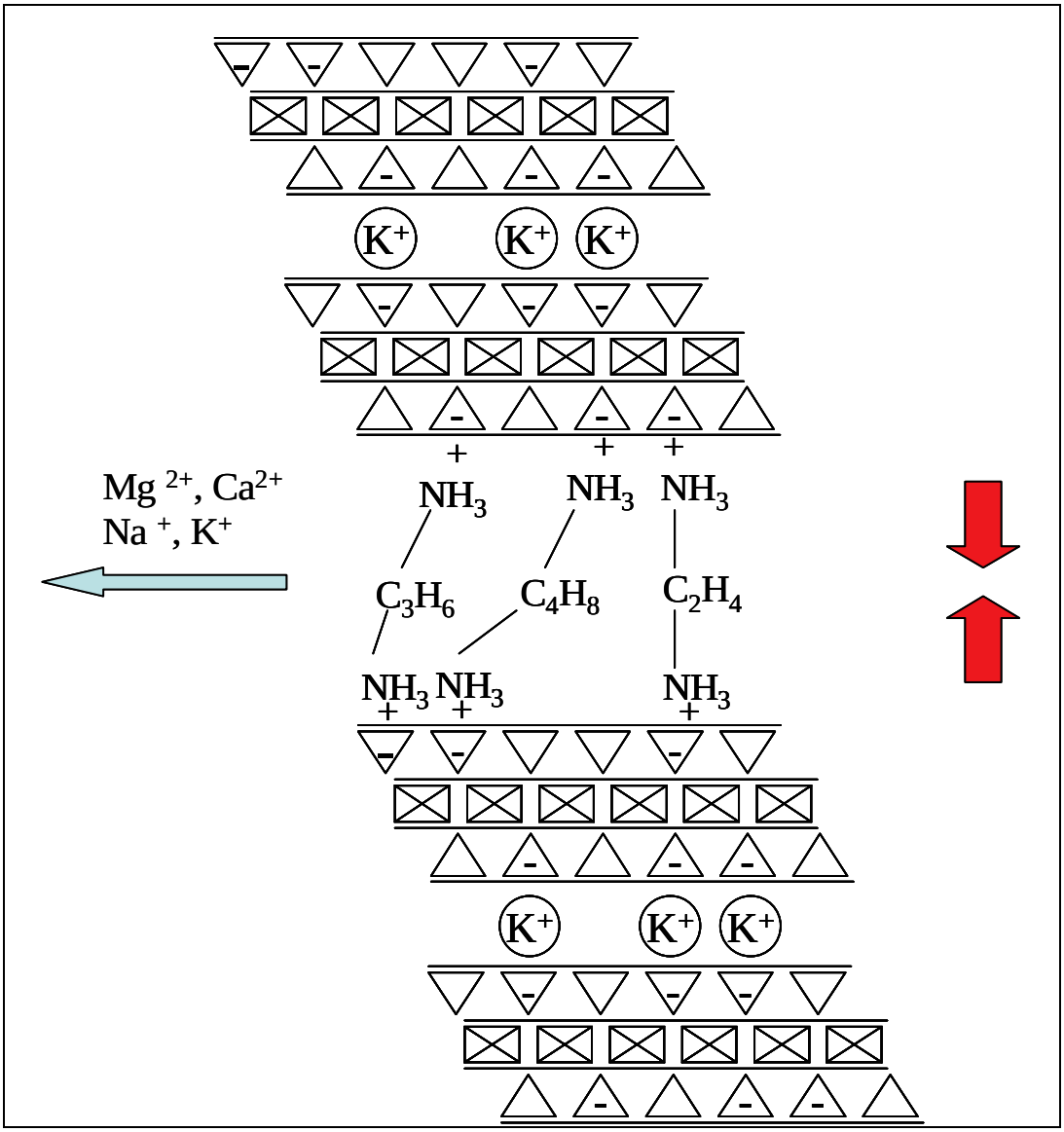

Figura 3-10. Ilustración de la acción de productos inhibidores de la expansión según proponen Snethlage et al. (1991), donde los diamino-alcanos "enlazan" las superficies de las partículas de los minerales de la arcilla. Los triángulos y rectángulos representan átomos de silicio y aluminio tetraédrica y octaédricamente coordinados, respectivamente, en minerales de la arcilla de tipo 2:1

3.4.2 Durabilidad del tratamiento inhibidor de la expansión

En la práctica, una vez corroborada la eficacia de un producto inhibidor de la expansión, el hecho de poder saber si este ofrece una durabilidad efectiva en el tiempo, se convierte obviamente en una información de importancia capital. Una respuesta

parcial a esta pregunta se obtendría tras examinar la permanencia de estos productos después de someter piedras tratadas con los mismos a numerosos ciclos de h/s. De hecho, esto ha sido experimentado en nuestro laboratorio con probetas de *Portland Brownstone*. Con dicho propósito se ha diseñado y construido una máquina que permite someter un gran número de probetas (finos paralelepípedos) a múltiples ciclos de h/s de forma automatizada. Una vez finalizado el ensayo, el coeficiente de expansión lineal de las probetas vuelve a ser medido (Anexo 5).

Se ha encontrado que después de 700 ciclos, la expansión de todas las probetas (tratadas y no tratadas) ha aumentado ligeramente (Figura 3-11). Visto que el incremento se observa también en el caso de las probetas de referencia, podemos inferir que la causa del aumento de la expansión en las probetas tratadas se tiene que buscar en otros fenómenos y no tanto en la posible eliminación del tratamiento durante los ciclos. Se podría pensar por lo tanto, que podría tratarse de una degradación por fatiga mecánica. Una forma más directa de tener información sobre la permanencia de los productos inhibidores en las probetas podría haber sido la de medir la concentración de aminas en el agua. Sin embargo, en nuestro caso, esto no hubiera sido muy relevante ya que el equipo usado en nuestro ensayo esta diseñado para proporcionar un flujo continuo de agua corriente, por lo que la concentración de aminas en el agua habría sido demasiado baja como para ser detectada con fiabilidad.

En cualquier caso, el resultado importante de nuestra evaluación sobre la durabilidad de los agentes inhibidores en el sustrato pétreo es que al final del ensayo, los valores de los coeficientes de expansión lineal de las probetas tratadas aún permanecen bastante por debajo de aquellos iniciales medidos en las probetas no tratadas. Esto indica que los productos no son eliminados fácilmente durante estos ciclos (Figura 3-11).

Mientras que los ensayos de expansión se presentan como pruebas suficientes para poder inferir diferencias en la durabilidad de nuestros materiales; una medida de la degradación más directa podría obtenerse a través de ensayos de resistencia mecánica al taladrado, como indican Wendler et al. (1996) en su estudio donde hacen uso de los mismos. En nuestra opinión, la combinación de esta última técnica con nuestros ensayos acelerados de ciclos de h/s, supondría una forma óptima y útil de presentar datos por ejemplo a la comunidad de conservadores-restauradores ante su manifiesta preocupación por la evolución de las capas más externas de las superficies pétreas del patrimonio histórico-artístico.

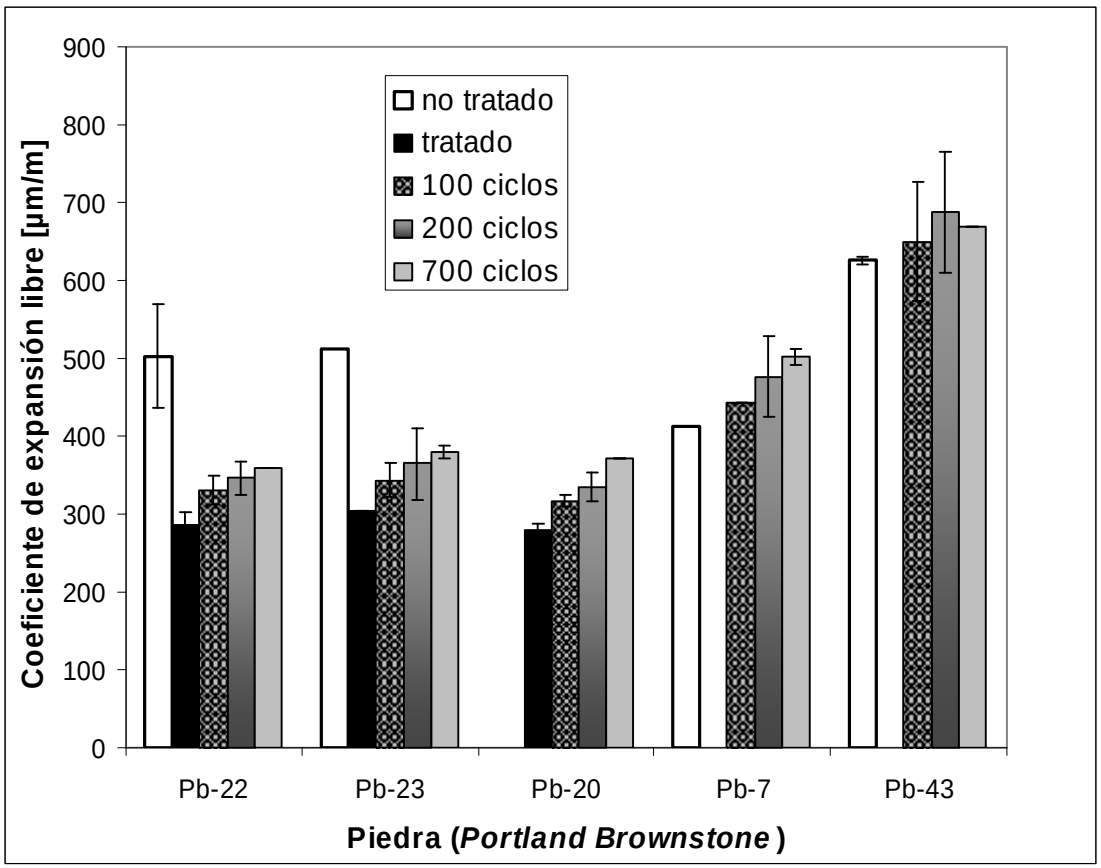

Figura 3-11. Efecto de los ciclos de h/s en el coeficiente de deformación por expansión libre (medido perpendicularmente a la dirección de los planos de sedimentación) de la arenisca Portland Brownstone (Anexo 5). Las probetas Pb-22, Pb-23 y Pb-20 han sido tratadas con productos inhibidores de la expansión (el efecto del tratamiento se puede observar por la diferencia entre la barra de color blanco y aquella negra). Las probetas Pb-7 y Pb-43 son muestras de referencia por lo que no han sido tratadas con productos inhibidores de la expansión (ausencia de barra de color negro). Se señala asimismo que el coeficiente de expansión lineal de la muestra Pb-20 no ha sido medido previamente al tratamiento. Destacamos que en este gráfico, la reducción relativa de expansión mostrada por las probetas Pb-22 y Pb-23 es un poco menor que la media indicada en la tabla Tabla 3-1 (40 % en vez de 50 %).

3.4.3 Pandeo (Warping)

La técnica de pandeo (*warping*) o del "3 en 1", que ha sido incorporada en esta tesis como método de caracterización de los materiales pétreos, se describe en el anexo dedicado a materiales y métodos (Anexo 1). Muy resumidamente se puede decir que consiste en medir la deformación (deflexión) sufrida por una placa fina de piedra que se apoya horizontalmente en dos soportes y que se pandea hacia arriba como resultado de añadir agua en su superficie superior[4]. El combado sufrido, que es dependiente del tiempo, es así medido por un sensor, más exactamente un Transductor Diferencial Variable Lineal (TDVL) (ver Anexo 1 y Figure A1- 23). Un análisis matemático de la deflexión por pandeo, el cuál será descrito posteriormente, proporcionará las ecuaciones que permitan extraer de las curvas experimentales los valores del coeficiente de deformación por expansión libre, e_S del coeficiente de succión capilar, S, así como aquel de la razón $r = E_{sat}/E_{sec}$.

Análisis básico

El análisis básico de este ensayo es una adaptación sencilla del tratamiento clásico de este tipo de experimento (Anexo 2). Su uso ofrece las siguientes expresiones para la deflexión por pandeo, Δ, sufrida por la probeta en función de la profundidad de penetración del agua:

$$\Delta = \left(\frac{3w^2 e_S}{4h} \right) \left(\frac{r(1-d)d}{d^4(1-r)^2 - 4d^3(1-r) + 6d^2(1-r) - 4d(1-r) + 1} \right) \tag{3-8}$$

donde w es la luz, e_S es el coeficiente de deformación por expansión libre, h es la altura (grosor) de la probeta, $d = h_w/h$, es la profundidad de penetración del agua, h_w, normalizada respecto a h y r, la razón entre el módulo de Young de la piedra saturada y el de la misma en seco.

[4] En nuestro ensayo, se usó como barrera alrededor de la probeta un material elástico y moldeable para impedir que el agua se derramase por los bordes de la misma. Dicho material descrito en el Anexo 1 no impide el pandeo de la probeta.

La relación entre la profundidad de penetración, *d*, alcanzada por el agua a lo largo del tiempo, *t*, y el coeficiente de succión capilar, *S*, queda así establecida:

$$d = \frac{h_w}{h} = \frac{S}{h}\sqrt{t} \tag{3-9}$$

Las curvas de deflexión por pandeo respecto al tiempo pueden por lo tanto ajustarse para obtener los parámetros mencionados anteriormente. Debido a las variaciones de probeta a probeta, las medidas de expansión libre y de módulo de Young se han realizado en los mismos especímenes usados en los ensayos de pandeo. Solamente en el caso de las medidas del coeficiente de succión capilar, exigencias técnicas (incompatibilidad entre las morfologías de las probetas) nos han obligado a usar otras muestras.

En el caso de la *arenisca de Tarifa*, este tipo de análisis básico resulta ser altamente satisfactorio (Anexo 6). La aplicación del mismo comienza con el cálculo de la deflexión máxima, Δ_{max} extraído de la ecuación (3-8). Esto requiere que la derivada de esta ecuación (o pendiente) con respecto a *d* sea igual a cero. De este modo se obtiene un valor de *d*, que una vez sustituido en la ecuación (3-8) proporciona una deflexión máxima que depende sólo de la expansión y no de la razón del módulo de elasticidad saturado respecto al seco, *r*:

$$\Delta_{max} = \left(\frac{3w^2 e_S}{16h} \right) \tag{3-10}$$

Con esta última ecuación y el valor Δ_{max} de la curva experimental de pandeo, se calcula el coeficiente de deformación por expansión. Los valores de e_S así obtenidos (Tabla 3-2) concuerdan muy bien con aquellos proporcionados por las medidas directas realizadas con las mismas probetas (~10 %). Después, la curva ha podido ser ajustada variando los valores de $r = E_{sat}/E_{sec}$ y S (Figura 3-12). Este ajuste no cubre la última parte de la curva de deflexión por pandeo, donde se asume que otros fenómenos (como pueden ser los de expansión retardada de los minerales de la arcilla, presión capilar, etc.) podrían ser responsables de la forma que adquiere la misma algo después de que se alcance la deflexión máxima. Lo importante aquí es que el valor de la razón *r*, obtenido del ajuste, concuerda bastante bien (~7 %) con el valor proporcionado por medidas independientes, en este caso con la técnica de flexión por tres puntos (Anexo 1).

En cuanto al coeficiente de succión capilar, *S*, los valores obtenidos de la curva de pandeo son más bajos (~50%) que los valores obtenidos haciendo uso de medidas directas (Anexo 1). Sin embargo, se ha encontrado una concordancia muy buena con el coeficiente de succión capilar obtenido a través de la medida directa de las presiones de expansión (Tabla 3-2), descrita en la sección 3.5.

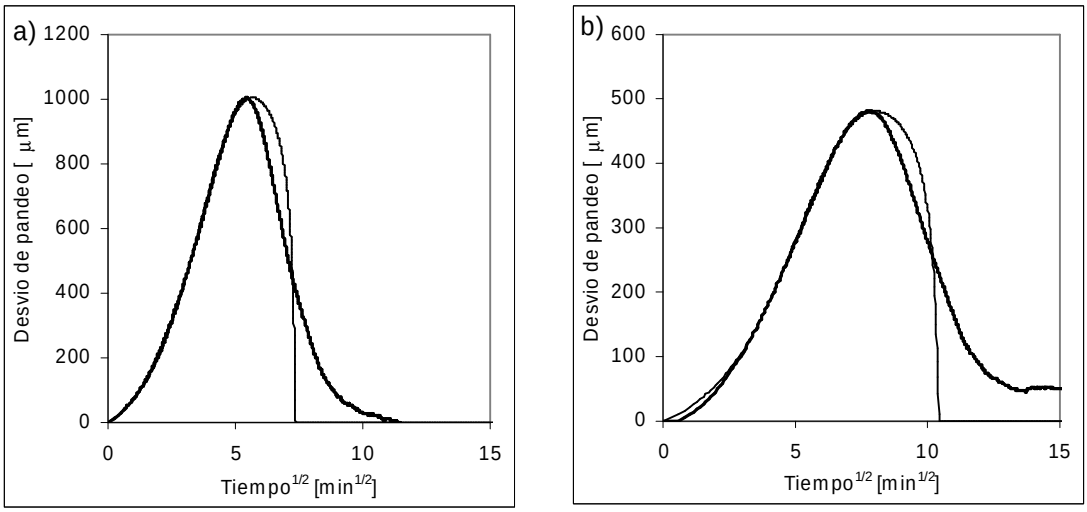

Figura 3-12. Curvas de pandeo de dos probetas de arenisca de Tarifa. En a) la probeta presenta los planos de estratificación paralelos a la dirección de ingreso del agua. En b) los planos de estratificación son perpendiculares a la dirección de ingreso del agua. La línea más gruesa indica los datos experimentales y la más delgada el ajuste (Anexo 6).

Sin embargo, este análisis no tiene el mismo éxito cuando lo aplicamos a la arenisca *Portland Brownstone* (Tabla 3-2), la cual requiere un análisis más sofisticado (Anexo 5) que incluye ciertas modificaciones que mejoran la correlación entre los datos obtenidos con esta técnica y aquellos procedentes de medidas independientes. Todo ello se explicará más adelante, aunque también se ofrece un tratamiento más detallado en el Anexo 5.

Tabla 3-2. Correlación entre los valores aproximados de coeficiente de succión capilar, S, la razón $r = E_{sat}/E_{sec}$ y del coeficiente de deformación por expansión libre, e_S, obtenidos a través de medidas independientes y aquellos estimados por la técnica de pandeo. Los valores caracterizan la Portland Brownstone y arenisca de Tarifa.

	S [cm/s$^{1/2}$]		$r = E_{sat}/E_{sec}$ [-]		ε_S [μm/m]	
	directa	pandeo	directa	pandeo	directa	pandeo
Portland Brownstone	0.01	0.025	0.35	0.6	513	300
Arenisca de Tarifa	0.0065-0.0082* 0.013**	0.0072	0.095	0.088	3200	2900

* Obtenido de la medida de presión de expansión; ** Obtenido con medidas independientes

Análisis refinado

A continuación se presenta el tipo de análisis que mejor caracteriza la deformación por pandeo de la arenisca *Portland Brownstone*. En esta piedra, las diferencias o falta de correlación entre los parámetros anteriormente mencionados podría ser justificada de la siguiente forma: inicialmente, se observa que las probetas que tienen mayores valores de dilatación muestran los valores más bajos de coeficiente de succión capilar, mientras la razón de los módulos de elasticidad es relativamente constante. Esto ha sido comprobado con medidas de penetración de agua por ascenso capilar efectuadas separadamente. Estas muestran la existencia de una etapa inicial donde el frente de agua accede al material con mayor velocidad (Figura 3-13)[5]. Este hecho dificulta el análisis de los ensayos de pandeo ya que requiere la introducción de una expresión que considere los cambios en dicho coeficiente y la velocidad de la dilatación, las cuales no están necesariamente relacionadas de una forma trivial. Por otro lado, existe igualmente la posibilidad de que el reblandecimiento del material

[5] Los resultados de las medidas de masa de agua absorbida se han convertido en alturas alcanzadas por el agua haciendo uso de la superficie de la base de la probeta, su porosidad y la densidad del líquido.

pétreo saturado dependa del tiempo, lo cual justificaría también la discrepancia encontrada en las razones de módulos elásticos (saturado respecto al seco). De hecho, el ensayo de pandeo es rápido, por lo que la piedra podría no llegar a su grado máximo de reblandecimiento. Esto no sucede en la medida directa del módulo estático en probetas saturadas, ya que estas han tenido tiempo suficiente de reblandecerse antes de la medida. Esto explicaría el hecho de que el valor de la razón, *r*, obtenido durante el ensayo de pandeo, sea mayor que aquel obtenido por medidas directas (Tabla 3-2).

La más simple de las aproximaciones supone que tanto la cinética de succión capilar como la de expansión dependen de la raiz cuadrada del tiempo a corto y a largo plazo. Basados en este supuesto, las curvas de ascenso capilar están bien ajustadas, según se ilustra en la Figura 3-13, si se hace uso de la siguiente ecuación modificada para el coeficiente de succión capilar:

$$d = \left(\frac{\Delta_S a \sqrt{t}}{1 + a\sqrt{t}} + S_\infty \sqrt{t} \right) \frac{1}{h} \qquad (3\text{-}11)$$

donde d es la profundidad de penetración del agua normalizada con respecto al grosor de la probeta, h; Δ_S es la ordenada en el origen de la regresión lineal de la curva de ascenso capilar cuando se representa como la altura del frente capilar respecto a la raíz cuadrada del tiempo, $\Delta_S a$ es la diferencia entre el coeficiente de succión capilar a tiempo cero, S_0, y aquella a largo plazo, $S_¥$ (Figura 3-13).

Una forma de justificar este hecho se ilustra en la Figura 3-14. La idea básica es que la presencia de minerales de la arcilla afecta la distribución del tamaño de poro (ver Figura 3-16, Figura 3-17, y discusión en página 91) incrementando la cantidad de poros pequeños y reduciendo el tamaño efectivo de los poros que controlan la velocidad de ascenso capilar. Esto reduce la velocidad del transporte de agua a través del material y también incrementa la altura máxima de ascenso capilar. En el caso de la arenisca *Portland Brownstone*, se piensa que durante la absorción de agua tiene lugar una expansión "retardada" de los minerales de la arcilla que es la responsable de la reducción del tamaño de poro en función del tiempo. Esto produce el que la velocidad de ingreso del agua en el material, que es bastante alta inicialmente, disminuya más rápido que si el coeficiente de succión fuese constante. De hecho, si dichos minerales empiezan a hincharse tan pronto entran en contacto con el agua, el gráfico de absorción capilar (Figura 3-14, caso b) se parecería mucho más a un gráfico ordinario (Figura 3-14, caso a). En todo caso, ambos mostrarían una velocidad de ascenso

capilar proporcional a la raíz cuadrada del tiempo. Sin embargo, si los minerales de la arcilla no se expanden inmediatamente, la reducción del tamaño efectivo de poro se vería retardada. En consecuencia, se esperaría obtener un gráfico de penetración de agua por absorción capilar que mostrara dos regiones diferentes, cada una con su propia dependencia de la raíz cuadrada del tiempo (ver gráfico añadido a la derecha en la Figura 3-13 y Figura 3-14, caso c).

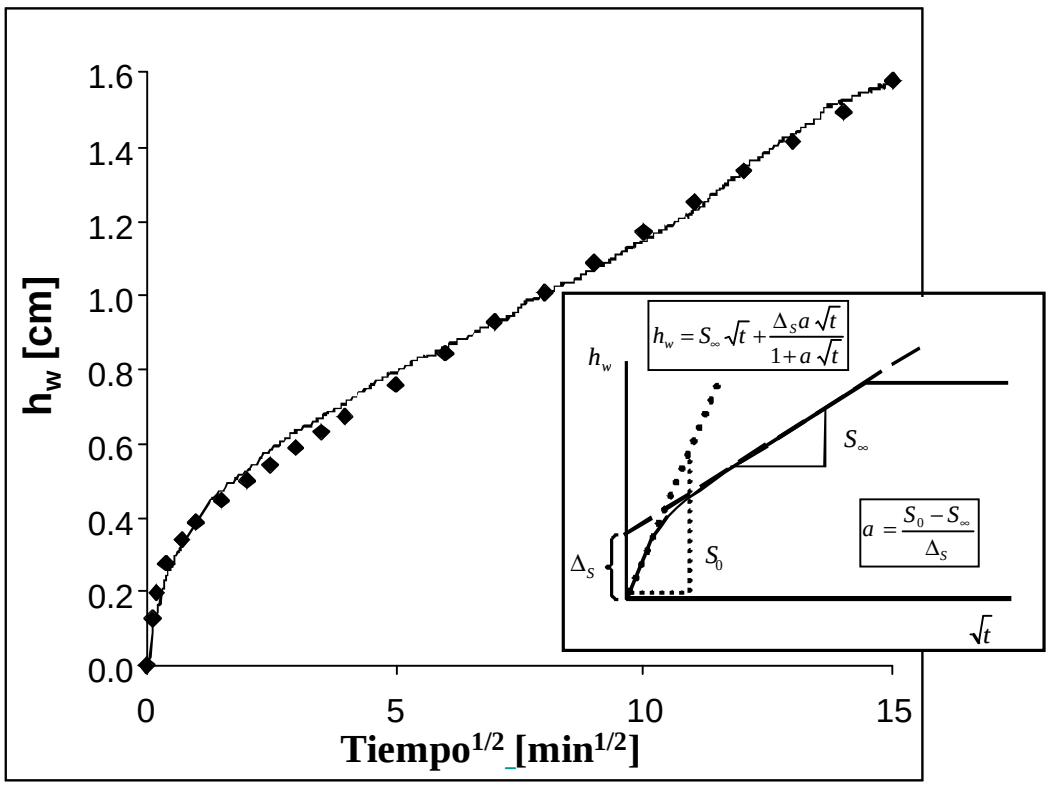

Figura 3-13. Ilustración de una curva de ascenso capilar ajustada con la ecuación (3-11). Los datos se muestran como la altura h_w alcanzada por el agua en la probeta. La línea continua muestra los datos experimentales y los diamantes representan el ajuste obtenido para un limitado número de puntos (requisito a título ilustrativo). En el gráfico añadido a la derecha se indican los diferentes parámetros de la ecuación (3-11).

En realidad, el efecto de la expansión de los minerales de la arcilla no puede ser tan dramático como sugiere la Figura 3-14, en la cual se hace una gran simplificación principalmente con fines ilustrativos. De hecho, más que un cambio en el tamaño principal de poro, se producirían cambios en los cuellos estrechos de los poros, lo cual podría tener un efecto mayor sobre el coeficiente de succión capilar.

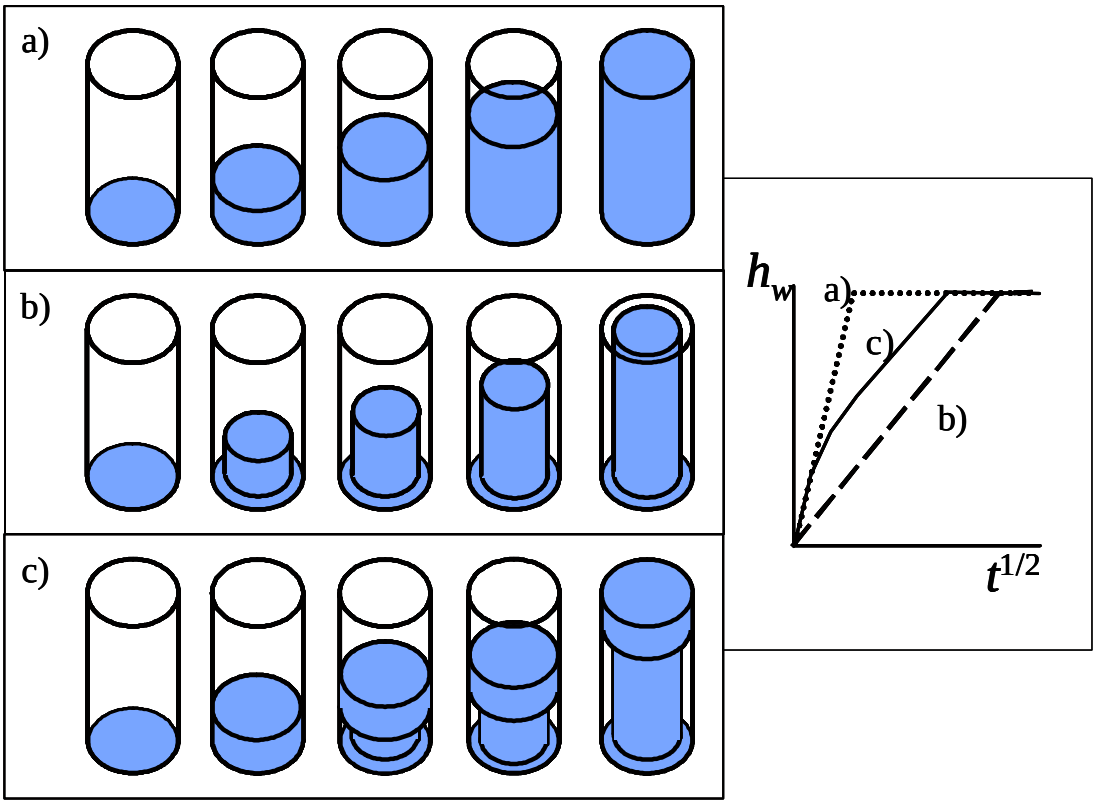

Figura 3-14. Ilustración esquemática de tres situaciones diferentes de ascenso capilar. a) caso normal/típico, donde el tamaño de poro es constante durante todo el experimento; b) caso en que los minerales de la arcilla se expanden inmediatamente después de entrar en contacto con el agua. En este caso, el tamaño de poro se reduce pero es constante durante todo el periodo de ascenso capilar; c) en este caso se considera la expansión retardada como la responsable de que el frente de agua "vea" un mayor tamaño de poro que la parte más baja o final del mismo. La figura de la derecha muestra esquemáticamente como serían las curvas de ascenso capilar en cada uno de los casos considerados (usando el mismo valor de saturación).

Se considera oportuno señalar que en el gráfico añadido a la derecha en la Figura 3-14, se muestran tres curvas representando la altura de succión capilar respecto a la raíz cuadrada del tiempo. En dicho gráfico se ve como en los tres casos se llega al mismo valor de saturación, que se corresponde con la altura de la probeta. En el caso de que la representación utilizase el cambio de masa respecto a la raíz cuadrada del tiempo, la cantidad de agua absorbida por cada probeta también sería la misma, ya que la reducción del volumen de la porosidad capilar (ilustrada en la Figura 3-14) se vería compensada con agua movilizada dentro de los minerales de la arcilla. Por lo tanto, el

volumen total de agua absorbida es igual, en todos los casos, a la porosidad inicial (si se obvia la variación de volumen debida a la expansión de la roca en contacto con el agua).

A este punto, se hace necesario introducir la noción de expansión retardada, $e_{S(t)}$ como el producto del coeficiente de deformación por expansión libre, e_S, y la parte hiperbólica de la ecuación (3-11):

$$e_{S(t)} = e_S \frac{a\sqrt{t}}{1 + a\sqrt{t}} \tag{3-12}$$

Así, la misma ecuación usada para calcular la deflexión por pandeo se escribe ahora:

$$\Delta = \left(\frac{3w^2 e_{S(t)}}{4h} \right) \left(\frac{r(1-d)d}{d^4(1-r)^2 - 4d^3(1-r) + 6d^2(1-r) - 4d(1-r) + 1} \right) \tag{3-13}$$

que ha sido calculada haciendo uso de la ecuación (3-11) para determinar el valor de d en función del tiempo.

Usando un valor medio de 0.013 cm/s$^{1/2}$ para $S_{¥}$, los valores correspondientes de e_S y la razón E_{sat}/E_{sec} procedente de medidas independientes, se ajusta la parte inicial de la curva cambiando los valores de los parámetros de ajuste, Δ_S y a. La concordancia es buena, pero claramente insuficiente para ensayos más largos (Figura 3-15) como sucede también en el caso de la *arenisca de Tarifa*. Cualquier otro intento encaminado a mejorar el ajuste de la curva después de que la probeta haya alcanzado el máximo desvío por pandeo empeora el ajuste de la misma a tiempos cortos.

Considerando los parámetros de ajuste Δ_S y a, se puede predecir el tiempo que sería necesario para que la probeta de *Portland Brownstone* alcance la saturación completa, que en el caso representado en la Figura 3-15 sería de ~280 s. Teniendo en cuenta la pendiente obtenida al representar el desvío medido respecto al tiempo (eje de ordenadas derecho en Figura 3-15), se obtiene un mínimo a 230 s que puede ser razonablemente atribuido a un posible cambio experimentado en el mecanismo responsable de la deflexión por pandeo aproximadamente cuando el frente de agua

alcanza la superficie opuesta de la probeta. Este cambio en la velocidad de la deflexión podría deberse a:

1. la continuación de la expansión de la parte de la piedra que está ya totalmente saturada

2. la expansión retardada de la parte de piedra recientemente saturada.

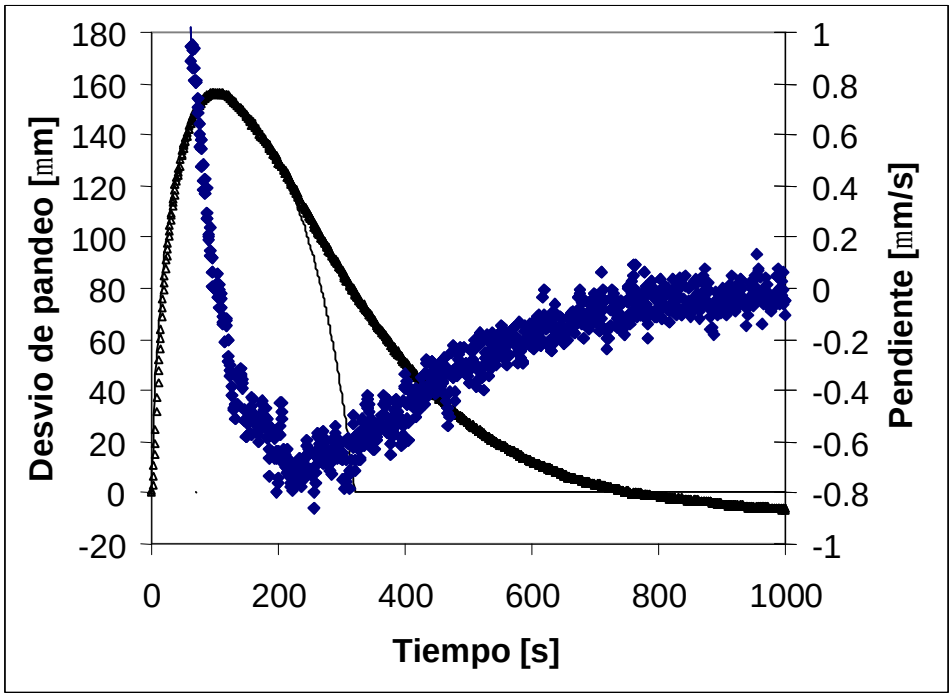

Figura 3-15. Comparación de la curva experimental de deflexión por pandeo medido en la arenisca Portland Brownstone (triángulos) con aquella obtenida de la función ajustada (línea continua fina) calculada con las ecuaciones (3-11) a (3-13); los diamantes azules (referidos al eje de ordenadas derecho) representan la pendiente de la deflexión medida experimentalmente (Anexo 5).

El análisis básico del ensayo de pandeo asume que la piedra alcanzaría instantáneamente la saturación total, por lo que su módulo de elasticidad disminuiría hasta un valor mínimo (módulo de elasticidad saturado) al instante en el que el agua llega. Basados en la reducción de la velocidad de la "disminución de la deflexión" (indicada por los valores de la pendiente de la deflexión que se convierten en negativos), concluimos que este supuesto no es válido. La relativamente buena

correlación entre el tiempo en el cual los datos experimentales muestran el mínimo en la velocidad de deflexión y el tiempo en el cual se predice la saturación por el ajuste parecen confirmar esta conclusión.

Los resultados de Wangler (comunicación personal, 2005) sugieren que otros factores, como el enfriamiento por evaporación del líquido acumulado en la parte superior de la muestra, la presión de capilaridad del agua en el sistema poroso y el efecto de la tensión o esfuerzo en la velocidad de la absorción de agua por los minerales de la arcilla pueden contribuir a la lenta reducción de deflexión observada después de alcanzar su valor máximo (*post-peak deflection*). Este aspecto sigue siendo objeto de investigación en la actualidad. De hecho, resultados muy recientes del grupo de investigación del mencionado autor parecen indicar que el efecto de la presión en la velocidad de absorción es la razón más probable para explicar este retardo (comunicación personal del Prof. Scherer, 2007). Esto significa, que la flexión de la probeta reduce el esfuerzo de compresión en la parte superior de la misma, lo cual permite a los minerales de la arcilla en esa zona absorber más agua; al mismo tiempo, la flexión impone esfuerzos de compresión en la zona inferior de la placa de piedra, inhibiendo la absorción (y el hinchamiento) en esa zona. La combinación de estos efectos retarda el aplanamiento de la probeta ya que la mitad superior de la misma permanece más expandida con el agua que la parte inferior.

El concepto de expansión retardada y su relación con la porosidad

En la sección anterior hemos descrito un “análisis refinado” para tratar el pandeo de la arenisca *Portland Brownstone*. Este análisis se basa en una observación experimental durante la realización de los ensayos de succión capilar de esta piedra. En ellos, observamos que al representar el incremento de masa de la probeta respecto a la raíz cuadrada del tiempo, la pendiente es inicialmente alta y después disminuye hasta llegar a un valor constante. La existencia de este cambio en el coeficiente de succión capilar nos ha llevado a pensar en un posible rol de la expansión de los minerales de la arcilla. Basados en esta hipótesis, usamos más adelante la misma cinética para describir la expansión retardada de los mismos. Este enfoque ha permitido ajustar los datos experimentales relativamente bien haciendo uso de un número limitado de parámetros de ajuste.

El interrogante que se plantea ahora es si el mecanismo que proponemos se corresponde con el real y si lo hace, si este podría estar soportado por otras medidas

realizadas para caracterizar la porosidad de esta piedra. Antes de entrar en esta discusión, se debe señalar que este aspecto es bastante complejo y que actualmente es objeto de estudio en otros proyectos del grupo del Prof. G. W. Scherer. Dentro del ámbito de esta tesis, debemos decir que el cambio en el coeficiente de succión capilar durante el experimento es un argumento que podría sugerir el rol de la expansión de los minerales de la arcilla en el cambio de las propiedades de transporte en el sistema poroso. Esto podría ser investigado usando líquidos que no causen expansión alguna (por ejemplo decano). En cuanto a los tipos de ensayo a emplear, serían principalmente dos los más apropiados: uno de succión capilar y otro de flexión por tres puntos que haga uso de la probeta saturada y sumergida en el líquido elegido. Ensayos de este último tipo han ofrecido valores de permeabilidad para esta piedra de alrededor de 0.15 nm^2 cuando se satura la probeta en agua (Anexo 4). Por lo tanto, sería importante el poder determinar si este valor cambia cuando se usa un líquido que no causa expansión.

Vale la pena señalar que la permeabilidad puede ser usada conjuntamente al coeficiente de succión capilar (correspondiente a periodos largos de tiempo) para determinar un valor medio de diámetro de poro. Esto se ha calculado para el caso de la arenisca *Portland Brownstone* encontrándose un tamaño medio de 80 nm (Anexo 4). Es interesante observar como en los resultados de porosimetría de inyección de mercurio (Figura 3-16a), los poros menores de este tamaño representan aproximadamente el 25-30 % del volumen de poros. Además, la Figura 3-16b muestra una categoría de poros relativamente bien definidos de 100 a 8 nm y centrados alrededor de los 30 nm, lo cual cubre el tamaño medio de poro estimado con la combinación de los métodos de succión capilar y flexión por tres puntos en condiciones de saturación.

Sin embargo, el hecho de que estos poros puedan "cerrarse o bloquearse" lo suficientemente debido simplemente a la expansión de las arcillas parece plausible, considerando que el tamaño de poro es de 30-80 nm. De hecho, a título ilustrativo, una montmorillonita sódica, hidratada con tan sólo dos capas de agua, presenta una distancia basal de 1.5 nm, la cual puede aumentar hasta 2.5 nm sólo por expansión intracristalina (Madsen y Müller Vonmoos, 1989). Como simplificación, podemos entonces considerar que cada capa de arcilla puede expandirse un 50 %. En consecuencia, si las paredes de los poros están constituidas de partículas de minerales de la arcilla con un espesor de unos 60 nm (tamaño más que típico en estos filosilicatos), el hinchamiento de las mismas causaría por lo tanto una reducción considerable del tamaño de los poros mencionado anteriormente (30-80 nm). De

hecho, muchos de estos quedarían prácticamente cerrados y el tamaño máximo sería de alrededor de 20 nm.

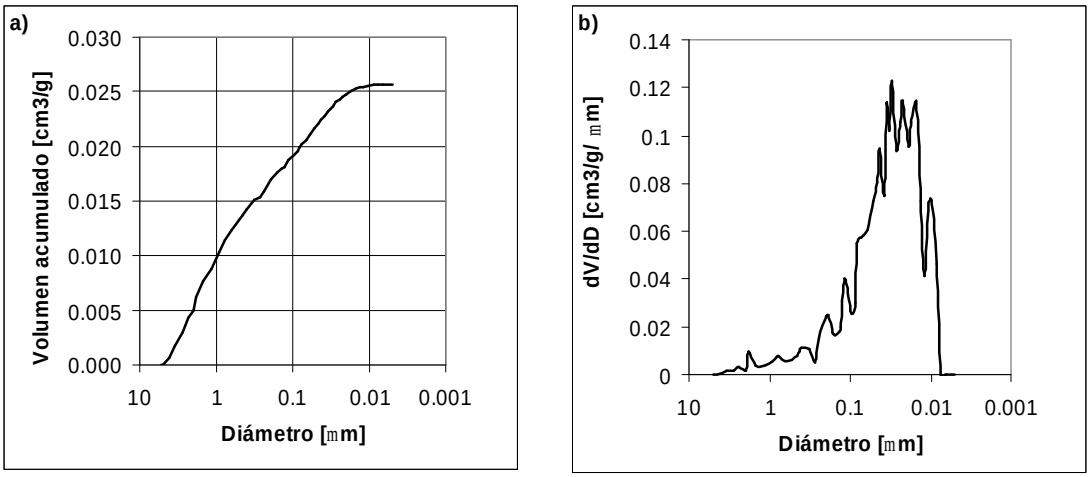

Figura 3-16. Resultado del análisis por porosimetría de inyección de mercurio en la arenisca Portland Brownstone. a) Volumen de poro acumulado, b) Distribución de tamaño de acceso de poro.

Como ha sido mencionado anteriormente, la realización de ensayos de permeabilidad con un líquido que no cause expansión se sigue perfilando como la forma más apropiada de abordar este tema. Mientras tanto, también vale la pena destacar que nuestras medidas de desorción de nitrógeno muestran claramente una clase de poros de 4 nm que puede estar probablemente asociada con la presencia de los minerales de la arcilla (Figura 3-17a y b). Estos poros también verían su tamaño claramente reducido por la expansión de estos minerales.

Podemos por tanto conjeturar que la expansión de los minerales de la arcilla podría causar una reducción en el tamaño de poro suficiente como para ralentizar de forma notable el transporte total de agua a través del sistema poroso. De todas formas, llegados a este punto, debemos reconocer que nuestra propuesta modificada para el análisis de los ensayos de pandeo de la arenisca *Portland Brownstone* ("análisis refinado") caracteriza correctamente el fenómeno principal, aunque insistimos en que el mecanismo real es ciertamente más complicado que aquel sugerido en la Figura 3-14, del cual recordamos su carácter meramente ilustrativo.

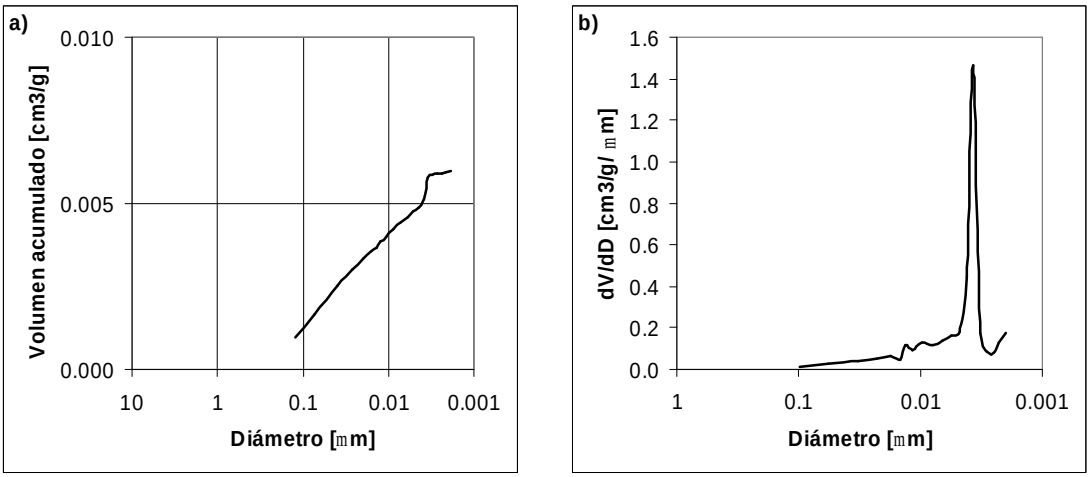

Figura 3-17. Resultados del análisis de tamaño de poro a través de ensayos de desorción de nitrógeno en Portland Brownstone. a) Volumen de poro acumulado, b) Distribución de tamaño de poro. El cálculo de la distribución de tamaño de poro se efectuó según el método BJH.

Posibilidades de un uso generalizado de la técnica de pandeo

Como se ha podido comprobar, la técnica del "3 en 1" es muy eficaz en los casos donde el modelo de análisis básico puede ser aplicado (ej. *arenisca de Tarifa*).

Para otros casos (ej. *Portland Brownstone*), el ajuste de la curva de pandeo obtenido usando las ecuaciones (3-11) y (3-8) podría optimizarse disminuyendo el grosor de las probetas. En aquellas más gruesas, el análisis simplificado debería ser por consiguiente mucho más preciso. Este hecho es interesante ya que permite prescindir de los parámetros de ajuste adicionales descritos anteriormente. De hecho, esto ha sido confirmado por el grupo de investigación del Prof. G. Scherer (comunicación personal del Prof. G. Scherer, 2006).

Para demostrar la influencia del grosor de la probeta, se han calculado las curvas de pandeo/combado, normalizadas para el desvío máximo esperado, considerando el análisis básico [ecuación (3-10)].

Para facilitar la representación, usamos un desvio de pandeo normalizado con respecto a la deflexión máxima obtenida del análisis básico. Además, estos valores se representan con respecto a la profundidad relativa de penetración del agua, *d*. Bajo

estas condiciones, el desvío máximo proporcionado por el análisis básico (sin expansión retardada) es igual a uno (línea continua en la Figura 3-18). En este gráfico también se han calculado varias curvas de pandeo/combado asumiendo que todas las probetas de *Porland Brownstone* presentan la misma velocidad de ascenso capilar inicial, que como ya ha sido mencionado, es muy rápida. Los diferentes símbolos representan valores teóricos calculados para diferentes grosores de probetas. La razón del módulo saturado respecto al seco considerada es 0.35 (valor obtenido mediante ensayos independientes realizados en probetas de *Portland Brownstone*).

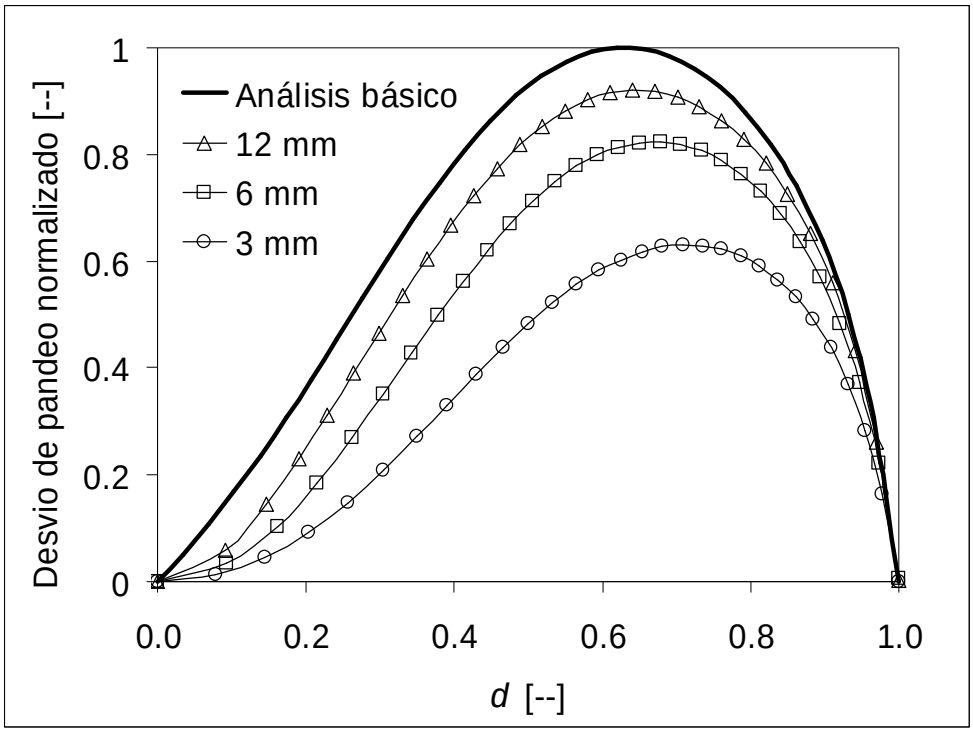

Figura 3-18. Curvas normalizadas de la deflexión por pandeo sufrida por probetas de Porland Brownstone en un ensayo de pandeo. La línea continua muestra el análisis básico [ecuaciones (3-8) y (3-9)]. Los diferentes símbolos muestran los resultados de la modelización utilizando las ecuaciones (3-11) a (3-13) para probetas con diferentes grosores (expresados en la leyenda). La razón entre el módulo saturado y el seco es 0.35.

Debido a que la curva de referencia en la Figura 3-18 caracteriza el análisis básico [definido por las ecuaciones (3-8) y (3-9)], se puede observar que las probetas

de mayor grosor se ajustan mejor teniendo en cuenta un coeficiente de succión capilar constante. En consecuencia, el uso de la técnica de pandeo se simplifica mucho con el uso de probetas gruesas, como ya hemos mencionado. Sin embargo, esta solución presenta una dificultad experimental ya que el desvío absoluto (no normalizado) disminuye con el grosor de la probeta. Consecuentemente no es posible usar probetas muy gruesas, aunque si este es el caso, siempre se podría recurrir a aumentar la luz entre los apoyos [ver ecuación (3-10)]. Esto significaría que habría muchos casos donde el ensayo de pandeo podría hacer uso del análisis básico, por lo que se convertiría así en una técnica rápida para determinar la expansión, el coeficiente de absorción capilar y la razón de los módulos, r, con una sola medida. En general, este análisis básico proporciona un ajuste correcto siempre y cuando se aplique a los datos anteriores al alcance del desvío máximo.

3.5 Presiones de expansión

El hinchamiento de los minerales de la arcilla de tipo expansivo tiene lugar en dos etapas sucesivas: una denominada “cristalina” y otra conocida como “osmótica”. La primera consiste en la incorporación ordenada de moléculas de agua en la intercapa. La deformación por expansión resultante en este primer paso es finita y limitada a aproximadamente 3-4 capas de moléculas de agua por capa de arcilla. Conviene senalar que la expansión depende mucho de la naturaleza de los cationes de la intercapa y disminuye según la secuencia Na > Ca > Cs. La fuerza motriz de esta parte del hinchamiento es sin embargo extremadamente grande y se estima que serían necesarias presiones superiores a 100 MPa para prevenir esta porción de la expansión, por ejemplo en el caso de montmorillonitas (Madsen y Müller-Vonmoos, 1985).

La segunda etapa es de naturaleza osmótica. Esta no conlleva la incorporación ordenada de las moléculas de agua. Por ejemplo, la expansión, virtualmente infinita, que se puede observar en el caso de la montmorillonita sódica (Norrish, 1954) resulta principalmente de este tipo de hinchamiento. Por tanto se podría esperar que, en un material pétreo, la deformación por expansión provocada por este mecanismo pudiera ser virtualmente infinita, aunque obviamente, la propia cohesión interna del material resistiría dicha deformación. De hecho, cuanto mayor sea el hinchamiento, menor será la presión que el material tiene que ejercer para resistir a un incremento adicional de la expansión. Es decir, una vez alcanzada una cierta deformación, el propio material impediría la continuación de la misma. Esto también explica el que en una piedra, las

presiones necesarias para prevenir la expansión osmótica sean mucho más pequeñas que aquellas requeridas para impedir la expansión cristalina.

Afortunadamente para la conservación de los materiales pétreos, la completa desorción de los minerales de la arcilla requiere temperaturas que no son alcanzadas en las obras in situ. De hecho, el agua que contribuye a la expansión cristalina es la adsorbida o coordinada a los cationes de la intercapa, que se pierde totalmente sólo al calentar entre 100-110 ºC. El agua estructural la constituyen los grupos hidróxidos (OH^-) de la capa octaédrica y se elimina con temperaturas mucho más altas (Velde 1992); por lo tanto no participa en el hinchamiento del material in situ. Esto significa que parte de la primera, y potencialmente más peligrosa, etapa de la expansión puede ya haberse dado parcialmente. Hecha esta observación, parece que in situ, la expansión estaría ocasionada por la aún restante hidratación de los cationes en la intercapa, posiblemente combinada con el hinchamiento osmótico entre partículas de minerales arcillosos (Salles et al., 2008). En el caso de la arenisca *Portland Brownstone*, que presenta una expansión lineal bastante limitada para ser una piedra que contiene minerales de la arcilla, incluso en condiciones de saturación completa, se piensa que algún tipo de restricción debe ser la causa de tal limitación. Nuestros experimentos con esta arenisca parecen indicar que la expansión osmótica en la intercapa no llega a producirse o si lo hace podría ser ignorada. Esto lo corrobora el hecho de que las medidas de expansión realizadas tanto en soluciones salinas (NaCl, 1 M; KCl, 1 M; $CaCl_2$, 0.1 M) como en agua, proporcionan el mismo resultado, a pesar de que en un proceso osmótico, el aumento de la concentración de sales tendría que reducir la expansión. Este resultado podría explicarse considerando las siguientes hipótesis:

1. que el hinchamiento osmótico de esta piedra no consiga superar la restricción propia del esqueleto pétreo. La piedra podría entonces tener tendencia a hincharse por repulsión osmótica, por ejemplo, entre partículas de minerales de la arcilla considerados como “no expansivos”, pero no conseguiría hacerlo.

2. que la piedra contenga ya una cierta cantidad de sales y por lo tanto no le afecte la nueva cantidad añadida. Esto también implicaría que en el caso de hinchamiento máximo del material, este no opusiera resistencia interna a la expansión.

En el primer caso, es conveniente señalar, que una fracción de los minerales de la arcilla podría estar recubriendo las paredes de los poros. Al contrario de lo que

sucedería a las arcillas en posición intergranular, estas no tendrían su expansión limitada por el esqueleto sólido. En tal situación, la saturación de la piedra podría producir una reducción del tamaño de los poros y por consiguiente del coeficiente de succión capilar que es compatible con el modelo descrito en la Figura 3-14.

Por lo tanto, cuanto mayor sea la expansión de la piedra, mayor será la resistencia ejercida por la rigidez del sólido (módulo de elasticidad). Al contrario, la presión de expansión (presión que hay que ejercer para impedir un incremento de la expansión) disminuiría con la misma expansión. En consecuencia, la deformación por hinchamiento libre de la probeta se alcanzaría una vez que se llegase a un equilibrio entre la presión de expansión y la de restricción. Entonces, en cualquier piedra, el producto del módulo de elasticidad, E, y el coeficiente de expansión lineal, e_S, debería determinar la presión de hinchamiento, P:

$$P = E\, e_S \tag{3-14}$$

Para medir directamente esta presión se determina previamente aquella que debe ser aplicada a una probeta para evitar su expansión. Madsen (1979) y Madsen y Müller-Vonmoos (1985) han publicado estudios que se ocupan de este tema y que constituyen además referencias importantes en este campo. En ellos se describe el procedimiento a seguir para realizar este tipo de medida. Este consiste en colocar la probeta en un soporte metálico con forma cilíndrica con el objetivo de confinarla lateralmente, de este modo sólo se permite una expansión uniaxial. El instrumento utilizado está dotado de una celda de carga que permite ir incrementando la carga en la probeta en una única dirección y llevarla gradualmente a su dimensión inicial. Las presiones de expansión medidas de este modo han proporcionado valores de entre aproximadamente 100 y 2200 kN/m^2 (0.1 y 2.2 MPa respectivamente).

En el caso de la arenisca *Portland Brownstone*, nuestros ensayos revelan valores similares a los apenas citados (en nuestro caso, 0.75 MPa). Sin embargo, usando la ecuación (3-14), el módulo de elasticidad estático de la piedra saturada (de ~ 4 Gpa), el coeficiente de deformación por expansión libre (4.5 10^{-4}) y el coeficiente de Poisson (0.2), obtenemos una presión de aproximadamente 1.8 MPa. La diferencia entre los valores de presión calculados y el valor de 0.75 MPa medido directamente puede explicarse si se tiene en consideración la relajación de los esfuerzos por parte del material (Anexo 4).

Tampoco se ha encontrado una concordancia directa entre los valores de presión de expansión medidos (0.84 MPa) y aquellos estimados (2.62 MPa) para la ***arenisca de Tarifa*** (Anexo 6). En este caso, esta discrepancia no puede ser justificada ni tan siquiera teniendo en cuenta la relajación de esfuerzos del material pétreo (cuya consideración nos llevaría a presiones de aproximadamente 2.18 MPa). Sin embargo, observando la curva de la Figura 3-19 se puede apreciar como la evolución de la presión de hinchamiento no es totalmente lineal respecto a la raíz cuadrada del tiempo, como predice la teoría (Anexo 4). Si consideramos sólo la parte lineal como correcta (ya que la no linealidad de la parte inicial de la curva podría deberse a problemas de índole técnico, como se señala en el Anexo 6) y la extrapolamos a $t = 0$, esto nos llevaría a valores de presión de hinchamiento de alrededor de 1.43 MPa, valor que se aproxima al de 2.18 MPa obtenido considerando la viscoelasticidad del material[6].

La inclusión (a nivel cuantitativo) del carácter viscoelástico del material en este análisis resulta ser bastante compleja (ver Anexo 4 para una descripción detalla de este aspecto). Describiéndolo en breves líneas, el ensayo para medir la presión por hinchamiento se basa en que el agua es absorbida por la probeta a una velocidad que es determinada por el coeficiente de succión capilar. La parte saturada de la piedra intenta dilatar pero encuentra oposición por el instrumento, el cual está programado para mantener una posición constante. Si el material es puramente elástico, se espera que el esfuerzo aumente hasta un máximo y permanezca invariable una vez la probeta está totalmente saturada.

Si el material es viscoelástico, este se deformaría (debido por ejemplo al deslizamiento entre las capas de arcilla) de forma que sería requerida una presión más baja para mantener una cierta posición. Un modo simple de verificar este efecto consistiría en prolongar el tiempo experimental. En tal caso, si encontramos que el esfuerzo disminuye, en vez de permanecer invariable, después de alcanzar un valor máximo, entonces estaríamos ante un fenómeno de relajación de esfuerzos.

[6] Vale la pena mencionar que los tiempos estimados para alcanzar la expansión máxima de la probeta, en la Figura 3-19, se pueden usar para calcular el coeficiente de succión de la piedra y además los valores obtenidos, grosso modo concuerdan con aquellos medidos directamente mediante el ensayo de pandeo. En realidad, los valores de coeficiente de succión que se obtienen de este gráfico son más bajos que los obtenidos directamente mediante ensayos hídricos, lo cual sugiere la no inmediatez del proceso de expansión (Anexo 7).

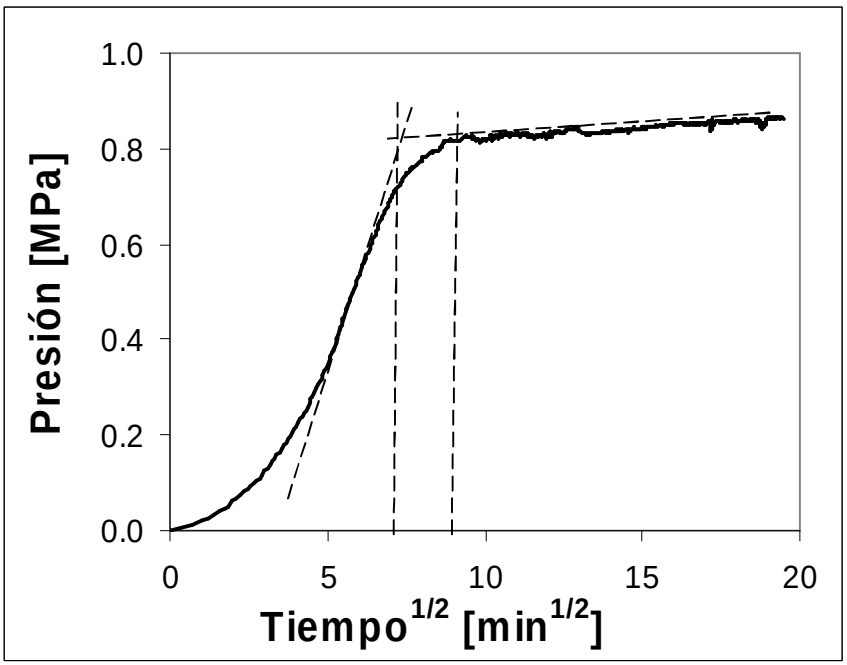

Figura 3-19. Evolución de la presión de hinchamiento respecto a la raíz cuadrada del tiempo para una probeta de arenisca de Tarifa. La línea discontinua inclinada representa la zona de incremento lineal de esta presión. Las líneas discontinuas verticales representan los tiempos estimados para alcanzar la máxima expansión.

Usando las medidas de relajación de esfuerzos descritas anteriormente ha sido posible calcular exactamente a qué velocidad se producen los esfuerzos en estos ensayos. Este tipo de medida se ilustra en la Figura 3-20, donde los símbolos circulares indican valores experimentales y la línea discontinua indica la curva calculada. Conviene señalar que los valores usados para los otros parámetros (coeficientes de absorción capilar y de expansión libre) son compatibles con aquellos proporcionados por medidas independientes.

La reproducibilidad de este tipo de experimentos es sin embargo poco satisfactoria y siempre proporciona valores de esfuerzos menores que aquellos previstos. Parte del problema es que el valor de la fuerza medida se encuentra muy cerca del límite inferior de la celda de carga del instrumento. Por ejemplo, la expansión libre total esperada en el caso de la arenisca *Portland Brownstone* es de ~20-25 μm (para probetas que tienen 5 cm de altura), entonces un pequeño movimiento de los

platos del instrumento o la irregularidad de las superficies de la mismas probetas afectarían sustancialmente el esfuerzo medido.

Este ensayo "acelerado" que proponemos para medir directamente las presiones de expansión es por lo tanto rico en información y además mucho más rápido que los ensayos de este tipo comúnmente referidos en la literatura (Madsen, 1979, Madsen y Müller-Vonmoos, 1985), sin embargo, pese a estas ventajas, resulta "relativamente" lento si lo comparamos con la duración del ensayo de pandeo. Además, es de difícil ejecución y requiere un instrumento costoso. Los instrumentos usados para medir las propiedades mecánicas más ordinarias no ofrecen necesariamente demasiadas garantías para realizar este tipo de ensayo donde se requiere mantener las dimensiones de la probeta fijas (con pequeñas variaciones de micras). Esto implicaría por lo tanto la construcción de un equipo especializado. Es más, el experimento requiere el uso de una cantidad relativamente grande de piedra (especialmente si se hace uso de una máquina de ensayos mecánicos con una gran celda de carga) lo cual puede ser problemático si la piedra procede directamente de la obra en estudio (por ejemplo, un edificio histórico).

Sin embargo, estos ensayos son satisfactorios en cuanto a que muestran la importancia de la viscoelasticidad para reducir la presión de expansión aparente, es decir, aquella a nivel macroscópico. Este descubrimiento hace aun más complicada la evaluación del criterio de daño y también trae a colación el tema de la resistencia mecánica de la piedra y su dependencia del tiempo. A título ilustrativo y para subrayar la necesidad de que este aspecto sea investigado con detalle en el futuro, señalamos que ensayos (con resultados no publicados) realizados por Girardet (*Expert Center for Built Cultural Heritage*, Lausanne, Suiza) con probetas de naturaleza similar a las de la *molasa de Villarlod*, indican que si los especímenes se dejan cargados a la mitad del valor nominal de su resistencia mecánica a la compresión, estos se fracturan después de 24 horas (normalmente un ensayo de este tipo en el laboratorio suele tener un duración de un par de minutos). Por lo tanto, para predecir correctamente la durabilidad de los materiales pétreos in situ, es necesario tener en cuenta este tipo de comportamiento (Anexo 7).

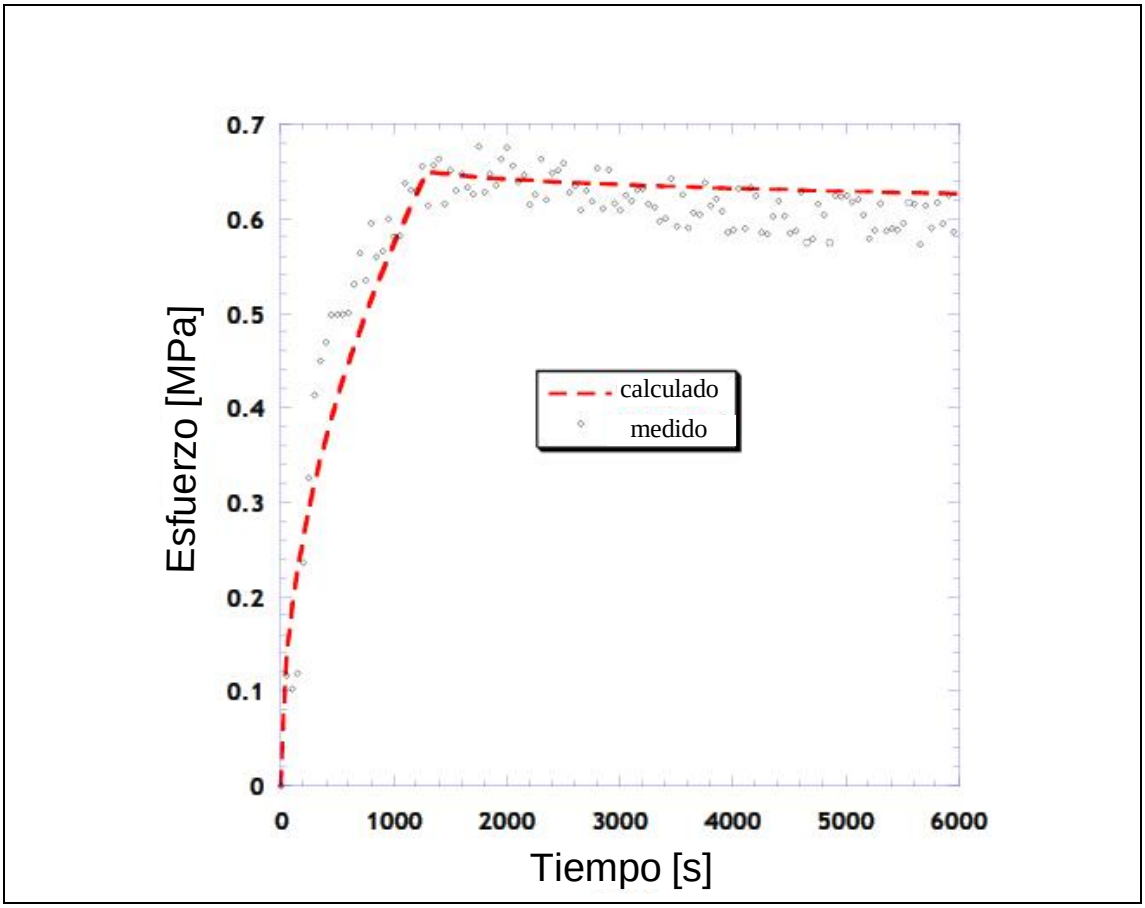

Figura 3-20. Medida directa de la presión de hinchamiento de la arenisca Portland Brownstone. En este ensayo, las probetas se encuentran confinadas entre los platos de la máquina usada. La curva de línea discontinua se ha calculado incluyendo la relajación de esfuerzos por parte del material (Anexo 4).

3.6 Predicción de daño en los distintos litotipos sometidos a ciclos de h/s

Para evaluar el daño potencial que los ciclos de h/s podrían ocasionar a los materiales pétreos estudiados, debemos comparar las propiedades mecánicas de los mismos con los esfuerzos que podrían desarrollarse durante dichos ciclos.

Durante los ciclos de humidificación, la zona más exterior de un bloque pétreo, es decir, aquella que absorbe el agua, sufriría esfuerzos máximos de compresión, s_{sat}, los cuales podrían ser estimados de la siguiente forma:

$$s_{sat} = \frac{E_{sat} e_S}{1 - n_{sat}} \tag{3-15}$$

donde se tiene en cuenta el módulo de elasticidad estático de la piedra saturada, E_{sat}, el coeficiente de expansión libre, e_S y el coeficiente de Poisson, n_{sat} del material saturado. Con estos parámetros podemos calcular los esfuerzos máximos producidos durante el periodo de saturación. Estos últimos deberían ser por tanto comparados con la resistencia mecánica máxima a la compresión del material saturado.

Del mismo modo, cuando el material empieza a secarse, los esfuerzos máximos desarrollados son de tracción, s_{sec} y pueden ser estimados de una forma similar a la descrita con la ecuación anterior:

$$s_{sec} = \frac{E_{sec} e_S}{1 - n_{sec}} \tag{3-16}$$

En este caso, se consideraría evidentemente el módulo de elasticidad estático de la piedra y el coeficiente de Poisson, E_{sec} y n_{sec} respectivamente, del material "seco".

En la Tabla 3-3 se presentan los valores medidos de los parámetros descritos, así como la estimación de los esfuerzos máximos producidos para las piedras: arenisca *Portland Brownstone, arenisca de Tarifa* y *molasa de Villarlod.*

Antes de proceder con el análisis, conviene señalar que dada la imposibilidad[7] de medir el módulo estático "seco" de la *arenisca de Tarifa* (Ta) en la dirección paralela a los planos de estratificación, este dato ha debido ser estimado. Para ello nos basamos en la semejanza encontrada en las razones entre los módulos "secos" en direcciones paralela y perpendicular, medidos tanto con métodos estáticos como dinámicos. En el caso de la *Portland Brownstone* (Pb), se encuentra que la razón entre el módulo elástico dinámico medido en dirección paralela a los planos de sedimentación y aquel medido en la dirección perpendicular es de 0.69, muy similar a aquella encontrada para las mismas condiciones pero usando medidas estáticas (0.80).

[7] Dicha medida requería una cierta dimensión de probeta que no pudo ser obtenida de los bloques de piedra proporcionados.

Tabla 3-3. Comparación de los esfuerzos calculados, s_{sec} y s_{sat}, con las resistencias mecánicas máximas a la tracción, s_T y a compresión, s_C, respectivamente. Se proporcionan asimismo los datos requeridos por las ecuaciones (3-17) y (3-18) es decir, los valores de módulo de elasticidad estático y de coeficiente de expansión libre, para las piedras: arenisca Portland Brownstone (Pb), arenisca de Tarifa (Ta) y molasa de Villarlod (Vd). Conviene señalar que el coeficiente de Poisson en todos los casos es de 0.2. Los símbolos ∥ y ⊥ indican propiedades medidas en la dirección paralela y perpendicular respecto a los planos de sedimentación respectivamente.

			SECADO			**HUMIDIFICACION**		
		e_S	E_{sec}	s_{sec}	s_T	E_{sat}	s_{sat}	s_C
		[µm/m]	[GPa]	[MPa]	[MPa]	[GPa]	[MPa]	[MPa]
Pb	∥	168	14.3	3.0	6.7	7.7	1.6	58#
	⊥	446	11.5	6.4	4.5	4.1	2.3	-
Ta	∥	1200	17.4*	26.1	6.9	1.7	2.5	-
	⊥	2900	9.4	34.1	5.3	0.9	3.3	14
Vd	∥	1400	3.9	6.8	2.6	0.9	1.6	20.3
	⊥	1200	2.4	3.6	1.2	0.5	0.75	22.1

** Valor estimado usando la ecuación* (3-17)

 # Valor estimado usando la ecuación (3-18)

En el caso de la *molasa de Villarlod* (Vd), encontramos la misma semejanza: (0.63) sería la razón entre los módulos dinámicos considerando ambas direcciones y 0.62 aquella entre los módulos estáticos. Por lo tanto, el módulo estático para la *arenisca de Tarifa* en dirección paralela a los planos de estratificación, $E^{est}_{\mathrm{sec},//}$ se puede estimar de la siguiente forma:

$$E^{est}_{\mathrm{sec},//} = E^{est}_{\mathrm{sec},\perp} \frac{E^{din}_{\mathrm{sec},//}}{E^{din}_{\mathrm{sec},\perp}} \qquad (3\text{-}17)$$

donde $E^{sta}_{sec,\perp}$ es el módulo estático "seco" en la dirección perpendicular y $E^{din}_{sec,\perp}$ y$E^{din}_{sec,//}$ son los módulos dinámicos "secos" en la dirección perpendicular y paralela respectivamente.

En cuanto al módulo de la piedra saturada (1.7 GPa), asumimos que la razón de los módulos seco respecto al saturado es independiente de la orientación con respecto a los planos de sedimentación. Señalamos igualmente que la resistencia mecánica a la compresión de la arenisca *Portland Brownstone* saturada ha sido estimada haciendo uso de la ecuación (3-18) que usa la proporcionalidad entre la resistencia a la compresión y la raíz cuadrada del módulo estático. Esta relación es confirmada de forma muy satisfactoria en la arenisca de Villarlod, donde la razón de resistencia es de 2.1 ± 0.2 y la raíz cuadrada de la razón de los módulos estáticos es de 2.1 ± 0.1:

$$s_{C,sat} = s_{C,sec}\sqrt{\frac{E^{est}_{sat}}{E^{est}_{sec}}} \qquad (3\text{-}18)$$

donde $s_{C,sat}$ y $s_{C,sec}$ son las resistencias mecánicas a la compresión del material saturado y "seco" respectivamente.

Según los datos de la Tabla 3-3, a simple vista se podría descartar la posibilidad de fallo por esfuerzos de compresión durante los ciclos de humidificación en las tres piedras. De todas formas, no se debe olvidar que los valores de resistencias mecánicas máximos podrían ser más bajos si consideramos que esta medida depende del tiempo de aplicación de la carga. Por lo tanto, una velocidad baja de aplicación de la carga y la propia viscoelasticidad de la piedra, especialmente cuando está saturada (Anexo 6), serían los responsables de tal disminución de resistencia mecánica del material. Valdría la pena, por lo tanto, examinar esta posibilidad particularmente en los casos de la *molasa de Villarlod* y *arenisca de Tarifa* que muestran un grado de reblandecimiento muy alto después de los periodos de humidificación.

Como ya ha sido señalado anteriormente, estos resultados tampoco excluyen la posibilidad de fallo debido a esfuerzos cortantes, que producirían el combado de la superficie mojada (Scherer, 2006), y el posterior desplacado de la misma (ver sección 3.2.2). Este caso se ilustra también en la Figura 3-1, Figura 3-21a y Figura 3-22a, donde se sugiere que este mecanismo es importante in situ. Desafortunadamente, el fallo debido a esfuerzos cortantes no es fácil de cuantificar (Duffus et al., 2008).

Finalmente conviene recordar, que la preexistencia de grietas responsables del proceso de combado pueden ser el resultado de otros mecanismos de deterioro como aquellos de cristalización de sales o de hielo/deshielo (McGreevy y Smith, 1984). Sin embargo, en el caso de la *arenisca de Tarifa*, ninguno de estos mecanismos parece ser desencadenante del deterioro observado en edificios históricos (Sebastián et al., 2008). De todos modos, si consideramos que la cristalización de sales tendría sólo que iniciar el daño; el papel de este mecanismo podría ser, a priori, mucho más importante de lo que se piensa cuando se le considere como la única causa de deterioro.

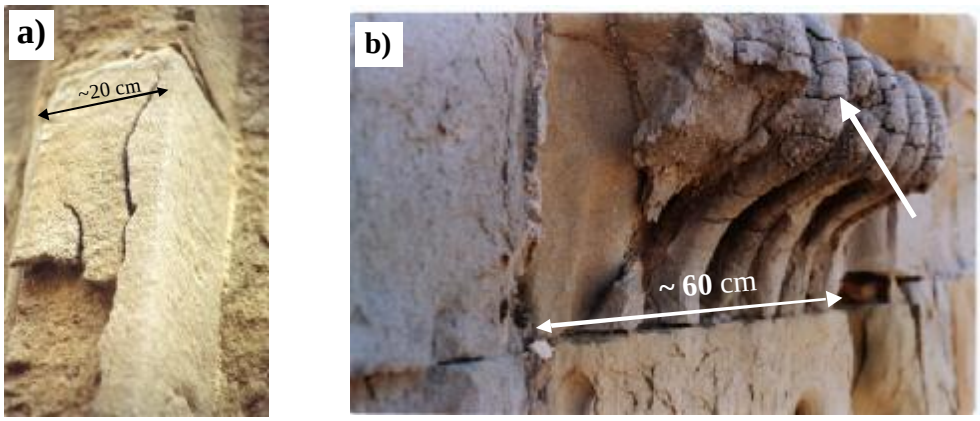

Figura 3-21. Formas de deterioro posiblemente debidas a ciclos de h/s en la arenisca de Tarifa (Portada de la Iglesia de S. Mateo, Tarifa, Cádiz). a) Efectos del combado de la superficie de la piedra durante la humidificación. b) fisurado de la superficie pétrea siguiendo un entramado poligonal de tamaño característico (típico de terrenos de secano) indicado con la flecha en el capitel de la pilastra y un descamado múltiple (en la parte superior del fuste de la pilastra). Fotografías proporcionadas por los Dres. C. Rodríguez Navarro y E. Sebastián Pardo.

En los casos de la *arenisca de Tarifa* y la molasa suiza, parece más probable que el daño ocurra durante los ciclos de secado por fallo debido a esfuerzos de tracción.

Sin embargo, para que se produzcan dichos esfuerzos, la piedra inicialmente debe estar casi, por no decir totalmente saturada. Hemos ya indicado que esto es bastante

improbable en el caso de los sillares de un muro, al menos que por alguna razón estos permanezcan mojados de forma persistente. Sin embargo, estos esfuerzos podrían producirse en el caso de elementos exentos de escaso grosor (ej. esculturas, columnas o lápidas).

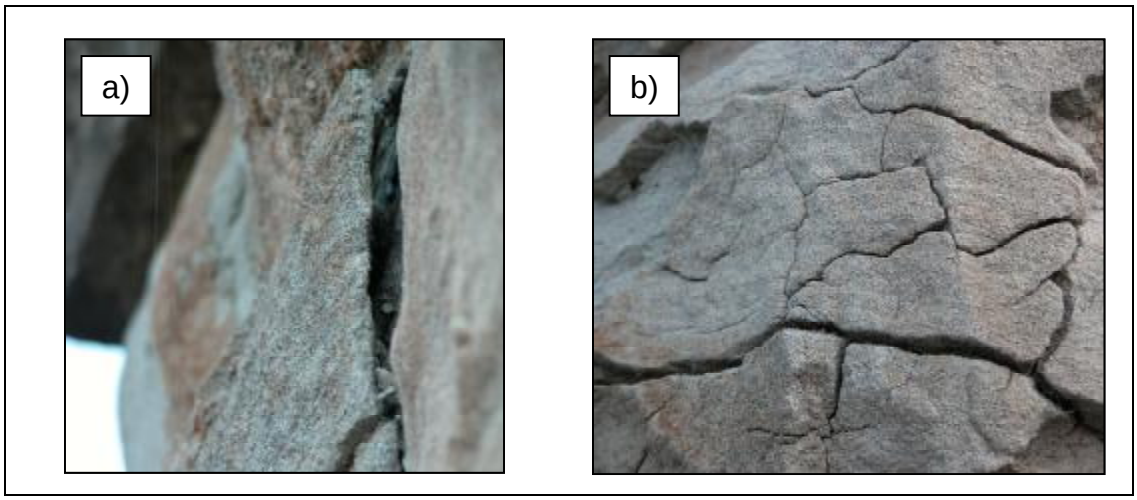

Figura 3-22. Formas de deterioro de la molasa de Villarlod posiblemente debidas a los ciclos de h/s. a) combado de la superficie, b) fisuras de secado.

De hecho, para una cierta profundidad de penetración de agua, L_{sat}, en un bloque pétreo de grosor L, los esfuerzos de tracción se calculan con la siguiente expresión:

$$s_{\sec,2} = \frac{E_{\sec} e_S}{1 - n_{\sec}} \left(\frac{r}{r + \frac{L - L_{sat}}{L_{sat}}} \right) \qquad (3\text{-}19)$$

donde $s_{sec,2}$ es el esfuerzo a la tracción en la zona más exterior durante el proceso de secado; n_{sec} es el coeficiente de Poisson para la piedra seca, r es la razón E_{sat} / E_{sec}, y e_s el coeficiente de expansión libre de la piedra.

Por ejemplo, a titulo ilustrativo y según la ecuación (3-19), ante un episodio de lluvia directa, en un bloque de *arenisca de Tarifa* de 25 cm de grosor, y con un coeficiente de expansión máximo (es decir, medido en la dirección perpendicular a los planos de sedimentación), el agua debería alcanzar una profundidad de alrededor 16 cm para que fuera después susceptible al daño durante el secado. Por otro lado,

considerando el coeficiente de succión capilar de este material, podríamos calcular además el tiempo de lluvia mínimo requerido para alcanzar tal profundidad. El resultado sugiere, por tanto, que se necesitarían 13 días de lluvia ininterrumpida, lo cual es un hecho muy poco probable, y aun más en esta zona de Andalucía.

Este pequeño cálculo a nivel ilustrativo refuerza lo anteriormente mencionado sobre el hecho de que este tipo de daño pueda ser más relevante para elementos ornamentales, de escaso grosor, o elementos exentos o protuberantes susceptibles de saturarse completamente en periodos de tiempo mucho más cortos que los anteriormente descritos. Ejemplos de ello se muestran en las Figura 3-2f, Figura 3-21b, Figura 3-22b y Figura 3-23 donde se puede observar ese entramado de pequeñas grietas característico de este tipo de fallo por esfuerzos de tracción.

Figura 3-23. Ilustración de un caso probable de degradación durante el secado en la arenisca Portland Brownstone. En consonancia con lo indicado en la Tabla 3-3, las grietas se producen siguiendo los planos de sedimentación del material, lo que corresponde a esfuerzos dañinos en la dirección perpendicular a dichos planos. Este capitel, perteneciente a la fachada de la "Victoria Mansion" (en Portland, Maine, EE.UU.), parece mostrar esta forma de degradación (foto proporcionada por I. Myjer).

Vale la pena señalar que en los dos casos donde se ilustra este tipo de deterioro en la arenisca *Portland Brownstone* (Figura 3-2f y Figura 3-23), la formación de grietas tiene lugar principalmente en la dirección paralela a los planos de sedimentación. Esto indica que los esfuerzos de tracción que causan la degradación son principalmente perpendiculares a los planos de sedimentación. Esto concuerda con los resultados de la Tabla 3-3, los cuales indican que los esfuerzos podrían superar la resistencia máxima a la tracción del material en esa dirección pero no en aquella perpendicular.

Otros factores que pueden reducir los esfuerzos calculados durante el secado son:

- una velocidad de secado baja (que permita la relajación viscoelástica del material)
- una humedad ambiental alta (que haga que el secado y las contracciones asociadas no sean completas)

Para el caso de la *arenisca de Tarifa*, ninguna de estas circunstancias son muy relevantes ya que la ciudad de Tarifa es precisamente una de las ciudades europeas con más viento y al mismo tiempo, para estar situada en la costa no es por cierto demasiado húmeda (75%, RH según Hoyos et al., 1999).

En resumidas cuentas, para esta piedra, el principal factor limitante de los esfuerzos generados durante el secado parece ser la profundidad de penetración del agua.

Para concluir esta sección, debemos decir que en nuestros cálculos hemos asumido la homogeneidad de las propiedades de los materiales pétreos estudiados. En la práctica, sabemos que dicha premisa no concuerda en la mayoría de los casos con la realidad, sobretodo en el caso de rocas sedimentarias donde la heterogeneidad es muy común. En consecuencia, se debe señalar la posibilidad de que en dichos materiales se desarrollen esfuerzos locales de entidad considerable debidos a deformaciones diferenciales a escala milimétrica. Estos últimos también podrían ser responsables de un ligero pero irreversible movimiento de los granos conectados entre sí a través de cemento arcilloso, los cuales podrían rotar o deslizarse durante el hinchamiento. Esto implicaría el que la piedra no recuperase su estado inicial. Aunque esto no se ha observado en ciclos individuales, no podemos excluir que después de un número

elevado de los mismos, la piedra pudiera experimentar una expansión gradual debido al movimiento local de los granos y que esto produjera un tipo de daño por fatiga.

3.7 Consolidación

3.7.1 Evolución de la consolidación

Se ha estudiado el efecto de un tipo de consolidantes (silicatos de etilo) sobre probetas prismáticas (mismo tipo de vigueta o placa fina usada para los ensayos de pandeo o flexión en tres puntos) de arenisca *Portland Brownstone*. El consolidante, comercialmente conocido como *Conservare® OH*, fue aplicado por inmersión total de las muestras en el mismo, siguiendo una de las opciones de aplicación del producto descritas por el fabricante. Posteriormente las probetas se dejaron secar. La elección de la geometría de las muestras se ha basado en la posibilidad de poder medir algunas propiedades como el módulo de elasticidad estático previa y posteriormente al tratamiento. Durante el periodo de desecación y curación, sus pesos fueron medidos periódicamente. La pérdida de peso inicial puede ser debida a la evaporación del disolvente contenido en estos productos, pero a largo plazo, la atribuimos a la formación (y evaporación) de etanol producido por la reacción de condensación de los silicatos de etilo. Consecuentemente, la pérdida de peso es un indicador claro del progreso de la condensación.

Tanto el avance como el grado de la consolidación se caracterizaron mediante medidas del módulo de elasticidad dinámico (medido por ultrasonidos) y estático, usando el ensayo de flexión de tres puntos como se muestra en la Figura 3-24. En este gráfico, la pérdida de peso respecto al tiempo se expresa como fracción de la cantidad de consolidante que inicialmente ha sido absorbido por la piedra. En la Figura 3-24a se representa una probeta de arenisca *Portland Brownstone* directamente consolidada. La Figura 3-24b muestra otra probeta consolidada de la misma piedra pero en este caso, ésta fue tratada previamente con un producto inhibidor de la expansión.

Los datos muestran claramente que el módulo de elasticidad estático continúa evolucionando, mientras que aquel obtenido con medidas dinámicas llega a estabilizarse. Aún más interesante es observar como esta evolución del módulo estático se correlaciona con la pérdida de peso de las probetas. Por lo tanto, cualquiera de estas

dos medidas parece ser un indicador del progreso de la reacción de condensación de los silicatos más fiable que la técnica de ultrasonidos.

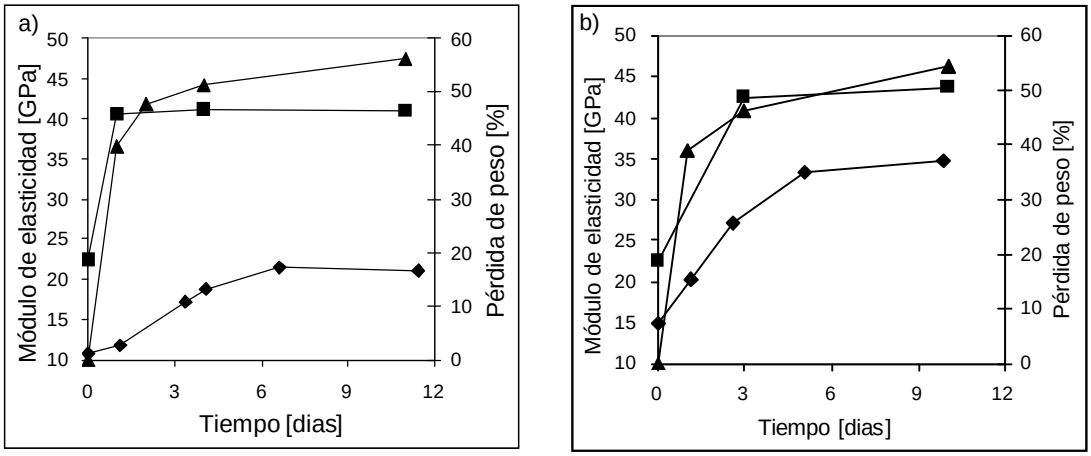

Figura 3-24. Evolución del proceso de consolidación de la arenisca Portland Brownstone con un silicato de etilo (Conservare^{Ò} OH), a) representa una probeta directamente consolidada, b) representa una probeta consolidada y tratada previamente con productos inhibidores de la expansión. Los símbolos triangulares representan la fracción del peso del consolidante aplicado que se ha perdido. Los cuadrados y diamantes representan el módulo de elasticidad dinámico y estático respectivamente.

Está claro que en un monumento, este tipo de medidas (flexión por tres puntos o pérdida de peso) no son operativas. De todos modos, para poder saber cual sería el número apropiado de aplicaciones del consolidante sobre una obra, para poder obtener el mejor incremento de resistencia mecánica, se debería considerar la realización de ambos ensayos en el laboratorio con suficiente antelación. En este caso, los experimentos deberían ser efectuados bajo unas condiciones ambientales (temperatura, humedad, velocidad de circulación de aire, etc.) representativas del ambiente propio de la obra a tratar. Además, se debería usar una técnica de aplicación del consolidante similar a la que se prevea emplear en la obra in situ. Las opciones mencionadas se consideran opciones más validas que el confiar solamente en las medidas ultrasónicas in situ, ya que nuestros resultados ponen en duda la pertinencia de esta técnica durante el seguimiento del proceso de consolidación.

3.7.2 Pérdida del efecto de la consolidación

Como ya ha sido citado al inicio del capítulo, Félix (1994, 1995) y Félix y Furlan (1994) han estudiado de forma bastante exhaustiva la pérdida del efecto consolidador del silicato de etilo aplicado en piedras areniscas (molasas) que contienen minerales de la arcilla procedentes de la Meseta o "Plateau" suizo. Sus ensayos muestran que tan sólo unos pocos ciclos de h/s son suficientes para casi anular cualquier beneficio obtenido de la consolidación. Lo mismo ocurre en el caso de la arenisca *Portland Brownstone*, como muestra la Figura 3-25. Recientemente también Wheeler (2005) ha publicado resultados en este ámbito y para esta misma piedra, aunque sus valores muestran que la pérdida del efecto de la consolidación requiere alrededor de 10 ciclos en vez de los 2-3 medidos en nuestros ensayos. En los experimentos de este último autor, vale la pena señalar que no se ha observado diferencia alguna en cuanto a la pérdida de eficacia del tratamiento consolidante llevado a cabo tanto con un silicato de etilo como puede ser el ya mencionado *Conservare*^{Ò} *OH* o con uno parcialmente hidrófobo, *Conservare*^{Ò} *H*.

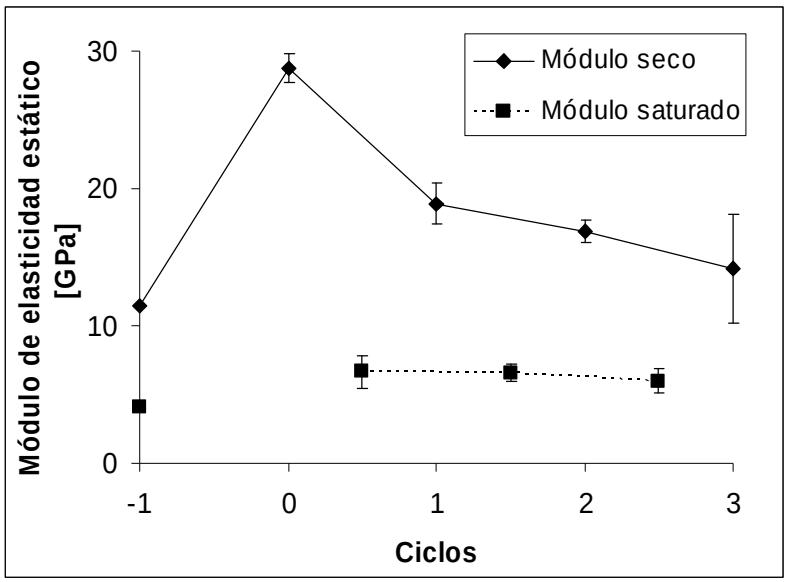

Figura 3-25. Evolución del módulo de elasticidad estático de la arenisca Portland Brownstone consolidada, durante ciclos de h/s. El ciclo –1 muestra los valores del módulo antes de la aplicación del tratamiento de consolidación. El ciclo 0 muestra el módulo de la piedra después del tratamiento. Las medidas del módulo de elasticidad en probetas saturadas se simbolizan con cuadrados. Las barras de error corresponden a un intervalo de confianza del 95%.

La pérdida del efecto de la consolidación se debe a que la expansión de los minerales de la arcilla rompe la estructura del gel de sílice formado tras la condensación del tratamiento, rotura que impide la cohesión entre los granos de cuarzo (o feldespatos) de la arenisca, lo que provoca que el tratamiento sea ineficaz. Según el trabajo de Wangler y Scherer (2008a), donde se distingue entre zonas intergranulares ricas y pobres en arcillas, se supone que este fenómeno es particularmente importante en las zonas intergranulares ricas en estos filosilicatos. Sin embargo, en aquellas menos ricas, este fenómeno sería mucho más lento. De hecho, la progresión de la degradación en estas últimas zonas requeriría de un número elevado de ciclos donde esta vez, no sólo los episodios de saturación, sino también los de secado contribuirían a la fisuración (Yang et al., 1998).

Además, se observa que el módulo de elasticidad estático de la piedra en estado seco decrece continuamente durante los ciclos de h/s, mientras que no sucede lo mismo con aquel en el estado saturado. Una explicación de este fenómeno se puede proponer recordando que el módulo saturado está limitado por las conexiones intergranulares ricas en arcillas. Entonces, siguiendo el razonamiento precedente, se puede suponer que estas conexiones pierden el efecto de la consolidación ya en el primer ciclo de saturación. Sin embargo, durante los siguientes ciclos de h/s, la reducción del módulo de la parte del esqueleto granular, excluyendo los "puentes" intergranulares ricos en arcillas, es mucho menor. Sería entonces la consolidación de este "esqueleto" lo que explicaría tanto el aumento inicial del módulo en el estado saturado como el hecho de que este sea vea menos afectado por los ciclos de h/s.

3.7.3 Efecto de los agentes inhibidores de la expansión

En la sección 3.4.1 se ha visto que los productos inhibidores de la expansión son efectivos en reducir la deformación por expansión libre de litotipos no consolidados. Aquí se muestra que dichos tratamientos, aplicados previamente a la consolidación, pueden incrementar la resistencia de la arenisca *Portland Brownstone* a los efectos de los ciclos de h/s (Snethlage y Wendler 1991; Wendler et al. 1991). Los resultados ilustrados en la Figura 3-26 muestran la evolución del módulo estático en muestras de esta piedra.

Estos resultados ponen en evidencia que los ciclos de h/s reducen el módulo de elasticidad estático de la piedra consolidada tanto si esta se encuentra seca (Figura

3-26a) como saturada (Figura 3-26b) e incluso aún habiendo sido esta tratada con un inhibidor de la expansión previamente a la consolidación. De cualquier modo, se observa que el módulo de elasticidad de una probeta que ha recibido una doble aplicación del tratamiento inhibidor, permanece sustancialmente más alto que el valor de referencia. Este aumento en el valor del módulo se desarrolla ya durante la consolidación, sugiriendo la existencia de alguna sinergia específica entre el producto inhibidor y el consolidante. Dada la información de la que disponemos, sería "demasiado especulativo" atribuir una razón de índole química para este fenómeno. De todas formas, es un efecto que merece la pena estudiar en un futuro ya que puede mejorar el impacto de tales tratamientos. Además, la ventaja que representa el tratamiento con productos inhibidores de la expansión previamente al de consolidación está corroborada tanto por la permanencia del efecto después de los ciclos de h/s como por el incremento de la resistencia mecánica mostrado por la piedra saturada.

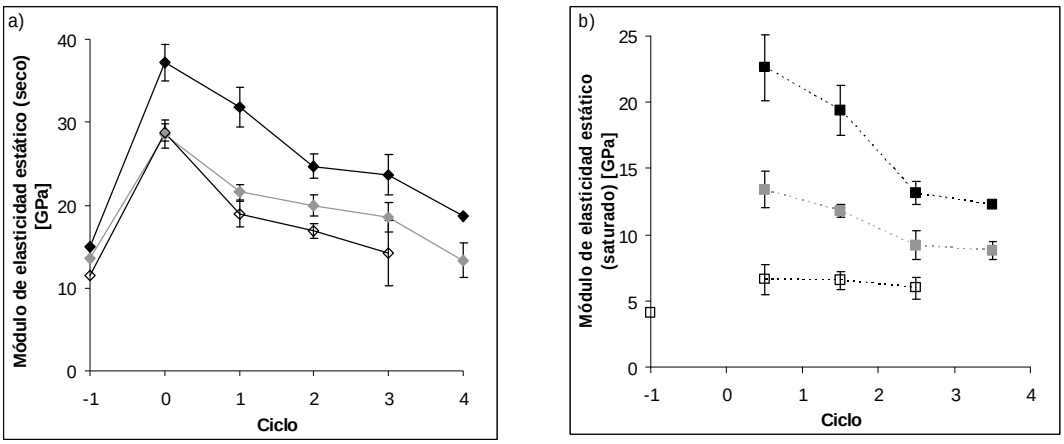

Figura 3-26. Evolución del módulo de elasticidad estático en probetas consolidadas de Portland Brownstone (en los estados seco y saturado) sometidas a ciclos de h/s. a) probetas medidas en seco, b) probetas medidas cuando están saturadas. Los símbolos vacíos representan piedras que no recibieron tratamiento con agentes reductores de la expansión previamente a la consolidación. Los símbolos grises representan a probetas que han recibido una aplicación de inhibidores de la expansión y los símbolos negros representan a aquellas que recibieron dos aplicaciones de dichos productos. Las barras de error corresponden a un intervalo de confianza del 95% determinado con la media de cuatro probetas medidas en cada ciclo. Tanto en el gráfico a) como en el b), los datos son medias de dos probetas (excepto para el último valor de módulo seco que corresponde a una sola probeta tratada con una concentración más elevada en aminoalcohol).

Además, también queda claro que el módulo estático de la piedra saturada permanece sustancialmente más alto en la probeta tratada una sola vez con un producto inhibidor de la expansión.

En términos de aplicación de estos productos in situ, el beneficio a largo plazo que se esperaría conseguir, al administrar un tratamiento inhibidor de la expansión previamente al de consolidación, aún necesita ser confirmado, dado que los presentes resultados sólo hacen referencia a los cuatro primeros ciclos. Sin embargo, considerando que estos son siempre los más devastadores (Félix et al., 2000) hay buenas razones para esperar que dichos tratamientos puedan ser beneficiosos.

El hecho de que las probetas tratadas con productos inhibidores de la expansión y posteriormente consolidadas, permanezcan más resistentes (como podría insinuar su gran rigidez), particularmente en condiciones de saturación, podría ser beneficioso en especímenes muy deteriorados. De hecho, en tales casos, podría ser problemático el fallo por esfuerzos de compresión durante el proceso de humidificación. Otra ventaja que muestra la resistencia de las probetas saturadas sería la de evitar la propagación de fisuras en el proceso de combado del material pétreo in situ. En este último caso, un factor crítico para asegurar el éxito de este tipo de tratamientos sería el asegurarse de que la consolidación sea aplicada de tal modo que sea efectiva a la profundidad donde tiene lugar la propagación de fisuras. En una primera aproximación, se podría decir que esta profundidad sería como máximo igual a la profundidad de saturación alcanzada después de un episodio de lluvia directa.

La razón del aumento del módulo estático de las piedras consolidadas y tratadas previamente con agentes inhibidores de la expansión no se conoce; y aunque se sabe que estas moléculas se intercalan en los minerales de la arcilla, no se han encontrado hasta el momento estudios que demuestren que lo mismo sucede en el caso de los silicatos de etilo. Por lo tanto, suponemos que los agentes inhibidores de la expansión son los responsables de un aumento inicial de módulo por intercalación. Posteriormente, el consolidante actuaría en un sustrato más rígido, lo que ocasionaría la sinergia de los tratamientos observada.

3.8 Contribución global de esta tesis

Como bien se ha podido observar en este capítulo, uno de los objetivos fundamentales en esta tesis ha sido el desarrollar un “modelo” de daño del material

pétreo expuesto a ciclos de h/s. Este "modelo" queda esquemáticamente representado en la Figura 3-27, la cual ha sido introducida al final de este capítulo en la tentativa de expresar aún de forma más gráfica y clara cuales son realmente los "caminos más directos a seguir para alcanzar nuestro objetivo".

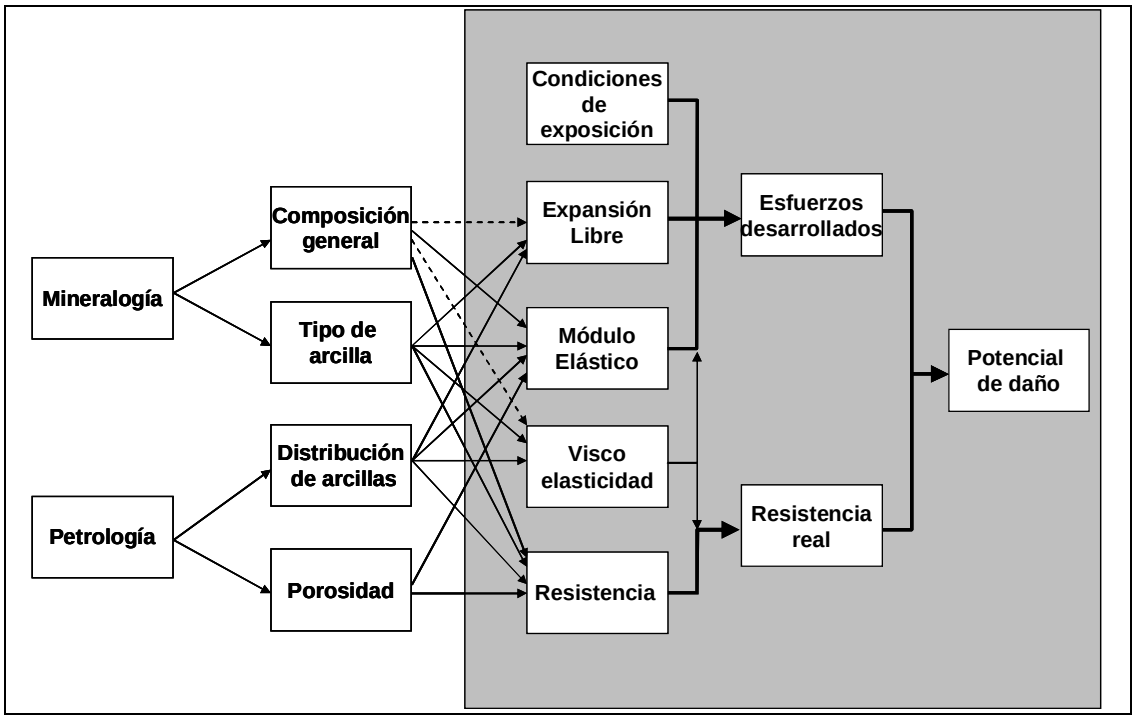

Figura 3-27. Representación esquemática del "modelo" de predicción de daño. El bloque con sombreado gris indica el procedimiento seguido en esta tesis. Dentro de este bloque, lo indicado en la columna más a la izquierda ha sido estimado con la realización de ensayos y no a través de las complejas combinaciones de factores resultantes de caracterizaciones mineralógico-petrográficas. Esto ha sido fruto de una decisión deliberada en esta tesis.

Dentro del bloque gris, el recuadro más a la derecha indica nuestro objetivo final: obtener una indicación sobre la posibilidad de producción de deterioro. Esta información nos la proporcionan dos factores, por una parte el cálculo de los esfuerzos desarrollados y por otra, la resistencia mecánica máxima del material.

En esta ilustración introducimos el término "resistencia mecánica real" para hacer referencia a la resistencia mecánica máxima del material en el caso de que la

carga sea aplicada durante un periodo largo de tiempo. En estas condiciones, el material podría fallar o fracturarse con cargas sustancialmente más bajas que aquellas a las que se ve sometido en los ensayos de laboratorio (realizados con velocidades de carga más altas) y que proporcionan los valores de resistencia nominal de la misma. La causa de ello hay que buscarla en el carácter viscoelástico del material. De hecho, el haber demostrado la existencia de una respuesta viscoelástica en estos materiales sugiere fuertemente que este factor debería ser tomado en consideración.

La viscoelasticidad también influye sobre la magnitud de los esfuerzos calculados. En algunos casos, este factor ha sido incluido explícitamente en nuestros cálculos, pero por lo general hemos despreciado su contribución, particularmente en nuestro análisis para la predicción de daño. Como resultado, nuestros cálculos generalmente proporcionan valores que constituyen el límite superior de los esfuerzos desarrollados.

Estos esfuerzos son, fundamentalmente, el resultado de la combinación de tres factores: el módulo de elasticidad, el coeficiente de expansión libre y las condiciones de exposición del material. Este último factor puede ser muy decisivo en nuestro análisis. De hecho, la humedad relativa ambiental podría modificar el coeficiente de expansión lineal. También las condiciones de exposición podrían, por ejemplo, determinar la profundidad de penetración del agua en el bloque pétreo o el tiempo que esta podría permanecer en el interior del material contribuyendo a su saturación.

Todos estos factores se encuentran dentro del bloque gris, que define las fronteras de lo tratado directamente en esta tesis. Es importante señalar que las propiedades más a la izquierda dentro del mismo marco (coeficiente de expansión libre, módulo de elasticidad, viscoelasticidad y resistencia,) han sido obtenidas con medidas directas sobre probetas. Evidentemente hubiera sido muy deseable el haber podido obtener todas estas propiedades también a través de caracterizaciones mineralógico-petrográficas. Sin embargo, esto es bastante complejo ya que diferentes factores como por ejemplo el tipo de minerales de la arcilla, su distribución y la porosidad del material afectan a muchas de las propiedades macroscópicas necesarias para cuantificar los esfuerzos desarrollados.

Estas relaciones, no sólo son numerosas, como bien se ilustra en la misma figura, sino también difíciles de cuantificar. De hecho, no conocemos ningún método fiable que lo permita, es más, creemos que esto no sería posible ni tan siquiera a través de la caracterización mineralógico-petrográfica del material. En consecuencia, los

límites/fronteras establecidos en esta tesis son fruto de una elección pragmática, donde la información mínima necesaria se obtiene de la caracterización del material a nivel macroscópico.

Otro aspecto importante de esta tesis es el examen de los tratamientos que podrían ser usados una vez se ha producido el daño o el potencial de daño haya sido reconocido. Así, nuestro bloque gris se expande ahora totalmente hacia la izquierda para albergar otro tema al cual se ha prestado atención en este estudio: el uso de productos inhibidores de la expansión, consolidantes y la combinación de ambos (Figura 3-28).

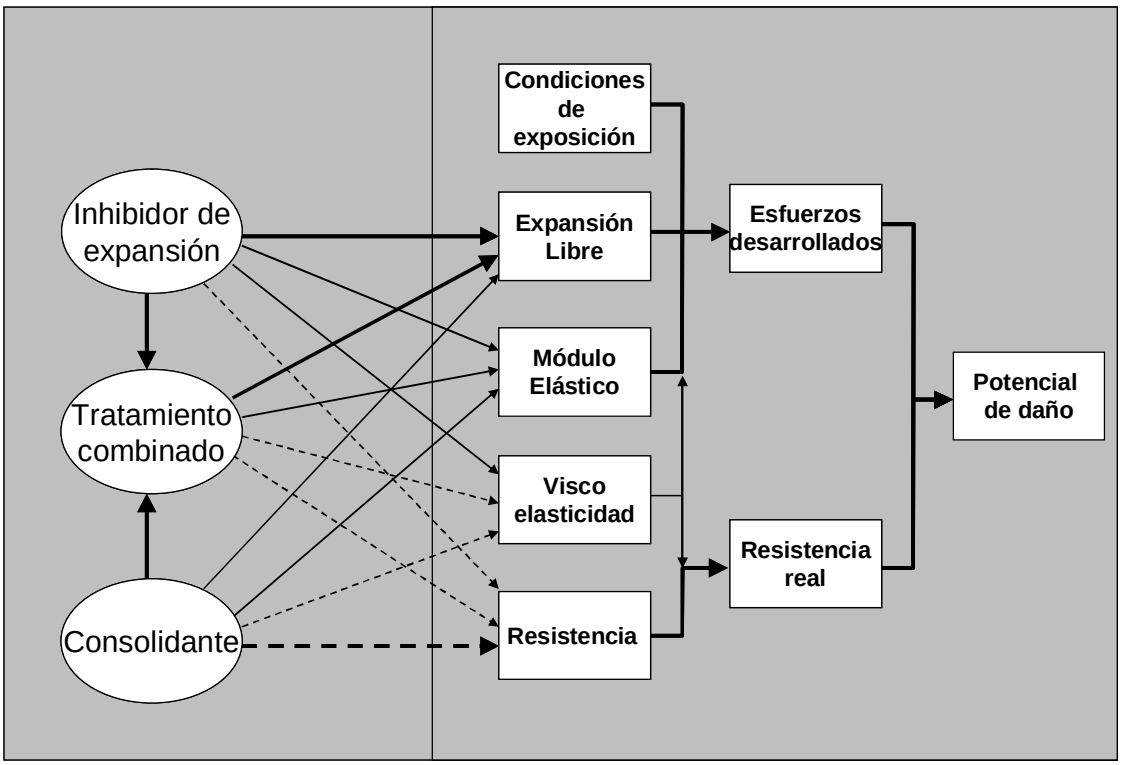

Figura 3-28. Representación esquemática de las relaciones entre varios tratamientos y su impacto sobre nuestra evaluación del potencial de daño. Las flechas continuas indican lo estudiado en esta tesis, mientras que las discontinuas indican aquellos efectos que no lo han sido.

Se considera oportuno subrayar que el interés principal en estudiar estos tratamientos ha sido el de evaluar su efecto directo en la expansión del material. Sin

embargo, esto no nos ha impedido examinar también en cierto grado los efectos sobre otras propiedades importantes que controlan los resultados de nuestra evaluación de daño (ver flechas continuas en Figura 3-28). Por otro lado, los efectos que no han sido específicamente examinados en esta tesis, pero que merecerían serlo en un futuro, han sido indicados con flechas discontinuas.

Aquí, de nuevo hemos tomado una posición pragmática, en cuanto a que los productos inhibidores de la expansión han sido seleccionados después de realizar un estudio exploratorio (*screening*). Con este se han identificado los mejores resultados ofrecidos por la aplicación de los productos o combinaciones entre los mismos en probetas de cada tipo de piedra.

En este trabajo, se ha considerado que era más importante determinar en un primer momento si estos tratamientos, optimizados para reducir la expansión, podrían afectar otras propiedades de forma negativa. Por ejemplo, se ha encontrado que estos productos pueden cambiar la viscoelasticidad del material. De hecho, esto tendría un impacto tanto sobre el cálculo de los esfuerzos como sobre la "resistencia mecánica real" de la piedra, según lo ilustrado en la Figura 3-28. Por lo tanto, un incremento de la velocidad de relajación viscoelástica podría en principio reducir ambos, y el resultado dependería entonces de la duración de los esfuerzos. Este tema puede ser crítico para otros mecanismos de deterioro como pueden ser la cristalización de sales y la formación de hielo, donde los esfuerzos podrían mantenerse durante periodos de tiempo más largos. Pese a todo esto, el impacto real de estos tratamientos sobre nuestra predicción de daño final es difícil de evaluar.

En cuanto a la aplicación de consolidantes, hemos confirmado el hecho de que el tratamiento pierde su eficacia en piedras que contienen minerales de la arcilla después de que estas sufran sólo unos pocos ciclos de humidificación. Sin embargo, se ha demostrado que un tratamiento preliminar con agentes reductores del hinchamiento podría reducir este inconveniente.

Capítulo 4. Conclusiones y perspectivas

4.1 Impacto de los minerales de la arcilla en la degradación de la piedra

4.1.1 Comentarios generales sobre la cuantificación

Esta tesis propone una metodología que permite cuantificar la susceptibilidad de materiales pétreos que contienen minerales de la arcilla al deterioro por ciclos de expansión/contracción. Esta incluye la caracterización de la magnitud de la deformación por expansión hídrica así como de las propiedades mecánicas del material. La idea básica es que el producto del módulo de elasticidad (E) y de la deformación por expansión (ε_S) proporciona una estimación de los esfuerzos que pueden ser generados de acuerdo con nuestras previsiones. Es más, la comparación de estos con la resistencia mecánica de la piedra proporcionaría un buen criterio para saber si se produciría el deterioro o fallo de la misma. Sin embargo, la situación no es tan simple y algunos factores como son las condiciones de exposición y viscoelasticidad del material tienen que ser tomados en consideración. A continuación se señalan las tres situaciones estimadas como potenciales fuentes de daño por ciclos de h/s:

- fallo por esfuerzos de tracción (*tensile failure*) en la zona más exterior (seca) durante el proceso de evaporación
- fallo por esfuerzos de compresión (*compressive failure*) en la zona más exterior (saturada) durante el proceso de mojado
- combado por fallo debido a esfuerzos cortantes (*buckling from shear failure*) desarrollados paralelamente a la superficie exterior también durante el proceso de humidificación.

4.1.2 Fallo por esfuerzos de tracción durante el secado

Durante el proceso de evaporación de bloques de piedra totalmente saturados, se pueden generar esfuerzos máximos de tracción en la capa exterior donde tiene lugar el secado. Si dichos esfuerzos son mayores que la resistencia mecánica máxima de la piedra "seca" a la tracción, estos pueden producir fisuras o grietas siguiendo un modelo de craquelado típico de suelos arcillosos (*mud-cracking pattern*) (Figura 3-2). Dicha morfología de fisurado ha sido identificada en zonas protuberantes (*Portland*

Brownstone, Figura 3-2f y Figura 3-23), elementos semiexentos decorativos (*arenisca de Tarifa*, Figura 3-21b) y en estructuras exentas (*molasa de Villarlod*, Figura 3-22b). Sin embargo, este tipo de daño es relativamente poco común en elementos no exentos o de gran grosor (ej. un muro) ya que raramente llegan a saturarse completamente (ver sección 3.2).

4.1.3 Fallo por esfuerzos de compresión durante la humidificación

Es el caso contrario al descrito en la sección anterior. Ahora un bloque de piedra que se halla totalmente "seco" empieza a absorber humedad. En esta situación, los esfuerzos máximos de compresión se generarían en la capa fina exterior mojada. En principio, muy pocas piedras serían candidatas a padecer degradación por esfuerzos de compresión, por ser estos mucho más pequeños (factor de ~15) que la resistencia mecánica a la compresión de la piedra saturada. Sin embargo, estos serían probablemente preocupantes en el caso de aquellos materiales pétreos que se reblandecen mucho cuando se encuentran saturados (ej. molasas suizas). En estos casos, la resistencia mecánica a la compresión podría disminuir considerablemente en el estado saturado si el esfuerzo se mantiene durante largos periodos (lo que implicaría el que la piedra permaneciese sólo parcialmente mojada durante mucho tiempo). La otra posibilidad de daño durante la humidificación es descrita en la siguiente sección.

4.1.4 Combado por fallo debido a tensiones cortantes durante la humidificación

Durante el proceso de absorción de agua de un bloque de piedra "seco", aparte del fallo por compresión mencionado, puede tener lugar otro proceso quizás más problemático. Se trata del generado por tensiones cortantes en la interfase zona seca/saturada, y que provoca el combado o abombamiento (*buckling*) de la capa exterior del bloque pétreo (Figura 3-1) como consecuencia de las fisuras existentes debajo de esa superficie. Desde el punto de vista mecánico, este tipo de fractura o fallo es difícil de tratar con un criterio simple ya que su iniciación depende en gran parte de la existencia previa de defectos (Scherer, 2006; Hutchinson et al., 2000). El origen de tales defectos puede ser variado (ej. planos de sedimentación o fisuras generadas por

otros mecanismos de degradación), por lo que este mecanismo resulta bastante más difícil de cuantificar que los dos anteriores.

En este caso, el hinchamiento de los minerales de la arcilla junto con otros mecanismos de deterioro ya mencionados (cristalización de sales y/o formación de hielo) incrementarían sustancialmente la envergadura del daño y la posibilidad de pérdida de detalles superficiales y u ornamentales. En consecuencia, el hecho de tratar la piedra para prevenir la expansión, se perfila como una importante contribución para la preservación de la apariencia estética de elementos pétreos de valor histórico-artístico.

4.1.5 Factores limitantes

En todas las situaciones indicadas anteriormente, la magnitud de los esfuerzos se encuentra limitada por la viscoelasticidad de la piedra. Es más, tanto la humedad inicial de la piedra como la de la atmósfera durante el proceso de desecación afectan los valores de los esfuerzos máximos, de modo que no sólo la naturaleza de la piedra es determinante sino también las condiciones de exposición (ambientales, de orientación, la geometría y dimensiones, etc.) de la misma. En el caso especifico de los esfuerzos generados durante la fase de evaporación, el grado de saturación de la piedra previo al comienzo del secado debe ser igualmente considerado.

Viscoelasticidad

Para obtener una buena estimación de los esfuerzos que pueden ser generados durante las expansiones /contracciones cíclicas, no basta con calcular el simple producto de la deformación por expansión libre y el módulo de elasticidad. También se deben tener en cuenta las propiedades viscoelásticas de la piedra (sección 3.3.3 y Anexo 3). Estas reducen la magnitud de los esfuerzos que se desarrollan tanto en la parte saturada como "seca" del material pétreo durante los ciclos de h/s, aunque la relajación de los esfuerzos es más importante cuando la zona que se halla bajo esfuerzos está saturada. La importancia de esto último a nivel cuantitativo ha sido demostrada a través de medidas de presión de hinchamiento en los casos de las areniscas *Portland Brownstone* y de *Tarifa*.

Humedad relativa (HR)

Las condiciones ambientales durante el proceso de evaporación deben ser igualmente consideradas ya que pueden limitar la magnitud de los esfuerzos de tracción generados. En el caso de un bloque totalmente saturado que empieza el proceso de secado en una atmósfera "totalmente seca" (0 % HR), se llegan a valores máximos tanto de deformación como de esfuerzos durante la retracción. Si la desecación tiene lugar en una atmósfera húmeda, el cambio en el contenido de humedad de la piedra es menor, por lo que la retracción será más pequeña. En la práctica, esto significa que las condiciones locales de humedad relativa en un monumento, es decir, su microclima, deberían también ser consideradas al evaluar los posibles esfuerzos/solicitaciones a los que se verá sometido un material pétreo ornamental tras un proceso de humidificación y secado. Tales valores permitirían establecer el umbral mínimo de resistencia mecánica para que, por ejemplo, un tratamiento de consolidación sea eficaz.

Grado de humedad preexistente

La magnitud de los esfuerzos de tracción durante el secado se ve limitada por el grado de absorción de agua por parte del material, el cual depende de la localización, condiciones de exposición (accesibilidad directa del agua de lluvia y/o de ascenso capilar) y grosor de la piedra. Estos esfuerzos serán máximos en piedras totalmente saturadas, como podría ser el caso de elementos exentos (ej. una lápida, columna o escultura) o de elementos artísticos y/o decorativos protuberantes y de escaso grosor y (ej. una moldura). Sin embargo, los mismos presentaran menor importancia en los muros de un edificio o bloques de gran grosor (ej. sillares) que no favorezcan la saturación total.

4.1.6 Otras preocupaciones

Fatiga mecánica

En rocas que no tienen un contenido excepcionalmente alto de minerales de la arcilla, el daño debido a ciclos de h/s aparecerá sólo a largo plazo.

Algunos estudios, como el de Wendler et al. (1996), demuestran el efecto nocivo de dichos ciclos en la piedra que contiene arcillas no consolidada. Es por esto, que el equipo diseñado específicamente en esta tesis pare someter automáticamente diversas probetas a numerosos ciclos de h/s es importante para estudiar este tipo de degradación, por ejemplo para estudiar la permanencia de tratamientos inhibidores de la expansión de los materiales pétreos (Anexo 5 y sección 3.4.2).

Las medidas directas de la deformación por expansión en probetas no tratadas muestran un aumento de este parámetro con el número de ciclos de h/s. Esto probablemente significa que existe daño que se genera progresivamente por fatiga. Los ensayos para evaluar la susceptibilidad de los materiales pétreos a la acción de los ciclos de h/s deberían incluir, por lo tanto, este tipo de experimento que permite realizar muchos más ciclos que de forma manual y en un tiempo razonable (Anexo 5 y sección 3.4.2).

Otros mecanismos

Otros mecanismos, como la formación de hielo y cristalización de sales, podrían ser más peligrosos o perjudiciales que los ciclos de h/s para las rocas que contienen minerales de la arcilla. Esto es debido a que la presencia de estos minerales implica necesariamente la existencia de una fracción de poros muy pequeños y este tipo de porosidad es la que genera preferiblemente altas presiones de cristalización. Por ejemplo, se puede calcular que si la formación de hielo tiene lugar en poros cilíndricos de diámetro inferior a ~20 nm en la arenisca *Portland Brownstone*, se generarían presiones de cristalización superiores a su resistencia máxima a la tracción. De hecho, como se observa en la Figura 3-16b, esta arenisca tiene una clase de poros bien definidos alrededor de este tamaño, aunque la misma representa sólo una pequeña fracción de la porosidad total (Figura 3-16a). En consecuencia, estas piedras presentan una susceptibilidad inherente a ser dañadas por dichos mecanismos. Es más, se ha encontrado que estos últimos actúan en sinergia con los ciclos de h/s, siendo la causa de la formación de fisuras y por consiguiente siendo los precursores del combado (*buckling*) de superficies pétreas durante los ciclos de humedad (Anexo 7).

4.2 Impacto de los minerales de la arcilla en las propiedades de la piedra

4.2.1 Hinchamiento

Ciertas rocas ornamentales experimentan un cambio de volumen en presencia de agua líquida o vapor de agua (expansión hídrica o hígrica, respectivamente). Esto sucede si estos materiales contienen minerales expansivos de la arcilla. Ocasionalmente, rocas que contienen esta clase de minerales, pero aquellos de tipo "no expansivo" también pueden hincharse. En estos casos, la expansión será sólo de carácter intercristalino u osmótico.

En el material pétreo más estudiado en esta tesis (*Portland Brownstone*), la expansión no parece ser de naturaleza osmótica, sino intracristalina. De hecho, nuestros ensayos llevados a cabo con diferentes soluciones salinas (NaCl, KCl y $CaCl_2$) no han mostrado reducciones en el coeficiente de hinchamiento lineal (sección 3.5 y Anexo 2).

4.2.2 Propiedades mecánicas

Los ensayos de expansión libre son insuficientes por sí mismos para juzgar la importancia de la presencia de los minerales de la arcilla en la durabilidad de la piedra ornamental. Por lo tanto, las propiedades mecánicas del material deben ser caracterizadas.

En esta memoria se ha comprobado como los valores de algunas de estas propiedades, como el módulo de elasticidad estático y la resistencia mecánica a la tracción pueden disminuir sustancialmente en piedras que se encuentran saturadas. En el caso del módulo de Young estático, la razón (E_{sec}/E_{sat}) se puede relacionar con el coeficiente de hinchamiento del material.

4.2.3 Viscoelasticidad

Nuestros ensayos muestran que no sólo la expansión de las arcillas localizadas en los espacios intergranulares causa el reblandecimiento de la piedra, sino también, que

la presencia de estas es responsable de que el material tenga un carácter viscoelástico en vez de elástico. Una consecuencia de esto es que los módulos de elasticidad medidos usando la técnica de ultrasonidos (que emplea deformaciones muy pequeñas y una frecuencia alta) y aquellos obtenidos con el ensayo de flexión por tres puntos (donde las deformaciones aplicadas son muy grandes y a baja frecuencia) sean diferentes en estos tipos de piedra. Esta diferencia es aún más acentuada cuando el material se encuentra saturado en agua.

Las citadas diferencias en los valores de módulo se atribuyen al movimiento del agua localizada entre los contactos intergranulares del material, lo cual proporciona resiliencia (*compliance*) a bajas frecuencias de carga, no teniendo lugar a frecuencias altas. Desde el punto de vista de la durabilidad, interesa conocer las solicitaciones generadas durante periodos largos de tiempo bajo deformaciones substanciales, en el orden de magnitud de aquellas experimentadas durante los fenómenos de hinchamiento. Consecuentemente, sólo los valores ofrecidos por las medidas del módulo de elasticidad estático son relevantes.

Otra consecuencia de la viscoelasticidad de las piedras que contienen minerales de la arcilla es su habilidad para relajar esfuerzos. En términos de durabilidad, esto es muy importante ya que así se puede evitar el que solicitaciones potencialmente peligrosas (como son por ejemplo las de cristalización de sales y de hielo) alcancen un umbral crítico. En esta tesis se ha podido cuantificar la importancia de esta relajación de esfuerzos a través de la medida de la presión de hinchamiento para la arenisca *Portland Brownstone* y aquella de *Tarifa*.

4.3 Caracterización de las propiedades

Las solicitaciones producidas durante la expansión de los materiales pétreos que contienen minerales de la arcilla pueden llegar a ser bastante importantes. Estas también pueden llegar a ser problemáticas en el caso de piedras que no presentan un coeficiente de deformación por expansión muy elevado (ej. *Portland Brownstone*). Para la evaluación de estos casos, el conocimiento de diversas propiedades del material se hace imprescindible. Para alcanzar este objetivo, en esta tesis se han introducido técnicas innovadoras que han permitido caracterizar el material pétreo de la forma más adecuada.

4.3.1 Técnica de Pandeo o del “3 en 1” (*warping*)

La técnica de pandeo o del “3 en 1” ha sido utilizada por primera vez en el ámbito de la conservación de piedra en esta tesis. Con ella se puede obtener una estimación rápida del coeficiente de expansión libre (e_S), coeficiente de absorción capilar (S) y de la razón entre los módulos de elasticidad del material saturado respecto al seco (E_{sat}/E_{sec}). No obstante, dependiendo de la naturaleza de la piedra, es posible que para alcanzar resultados fiables, se requiera el uso de probetas de grosor y longitud superiores a los que han sido señalados como típicos.

En todo caso, el hecho de que una vigueta o barra fina de piedra se combe sustancialmente cuando su superficie superior absorbe agua, demuestra los elevados esfuerzos generados por la expansión de los minerales de la arcilla contenidos en la misma. En edificios, el grosor de los bloques o sillares de un muro previene el pandeo, pero la generación de esfuerzos en las capas exteriores de los mismos -que tienden a retraerse o expandirse- no puede ser evitada y por lo tanto puede ser una causa de deterioro.

4.3.2 Ensayo de flexión por tres puntos

Módulo de elasticidad

Los esfuerzos generados durante las expansiones/contracciones cíclicas de la piedra se desarrollan lentamente. Debido al carácter viscoelástico de estas piedras, las propiedades del material necesarias para el cálculo de los esfuerzos, también tienen que ser representativas de procesos lentos para que los resultados sean realísticos. Esta es la razón por la que en el caso del módulo de elasticidad, se necesita medir aquel estático. El uso de la técnica de flexión por tres puntos en esta tesis ha sido, por lo tanto, muy adecuada para determinar este valor tanto en probetas saturadas como secas. Así mismo, el uso de este ensayo ha ayudado a entender las importantes diferencias de rigidez entre material seco y saturado debidas a la presencia de minerales de la arcilla en el material pétreo.

Relajación de esfuerzos

La misma técnica (ensayo de flexión por tres puntos) ha sido usada para caracterizar el comportamiento viscoelástico de las piedras que contienen minerales de

la arcilla. Con ella se ha podido constatar la capacidad de relajación de esfuerzos que tienen las mismas y que esta existe tanto si el material se encuentra en estado “seco” como saturado. Esta propiedad es muy importante ya que contribuye a limitar el grado de deterioro producido durante la generación de esfuerzos en los ciclos de h/s.

4.3.3 Medida directa de la presión de hinchamiento

En esta investigación se ha revisado el tipo de ensayo tradicional más común para medir directamente las presiones de hinchamiento. Nuestra evaluación del mismo ha permitido reducir el tiempo experimental en aproximadamente 10 veces, lo cual hace su uso más atractivo. Otra ventaja de esta técnica es la gran cantidad de información que ofrece, sobre todo a la hora de cuantificar la importancia del carácter viscoelástico de la piedra. De hecho, con ella podemos observar la importancia que tiene la velocidad de relajación de esfuerzos por parte del material. No obstante, algunos inconvenientes como la baja reproducibilidad ofrecida (atribuida a problemas de carácter técnico), que son, hasta el momento insalvables la convierten en poco satisfactoria.

4.4 Conservación y restauración de piedra que contiene minerales de la arcilla

4.4.1 Material pétreo no tratado

Se ha visto como para pronosticar la susceptibilidad del material pétreo a ser dañado por ciclos de h/s, se necesita realizar medidas del módulo de elasticidad estático y del coeficiente de expansión del material. Una evaluación más refinada requiere cálculos más complejos que tienen en cuenta la relajación de esfuerzos. Sin embargo, ninguna de estas técnicas puede realizarse de forma no destructiva directamente en el monumento u obra artística.

Por lo tanto, nuestra propuesta de evaluación sería operativa en el ámbito preventivo, por ejemplo, en la toma de decisiones sobre el tipo de piedra a usar en una obra de nueva creación o en operaciones de restauración que implican la sustitución de algunos bloques o fragmentos pétreos. Para materiales pétreos que son irremplazables y que por lo tanto deben permanecer in situ, uno debería realizar ensayos para

determinar el contenido, tipo, cantidad y distribución de minerales de la arcilla. En estos casos, una alternativa consistiría en recolectar pequeñas muestras procedentes de zonas de la obra que así lo posibiliten y sin que esto comprometa la apariencia estética de la misma, para realizar mínimas investigaciones como por ejemplo medidas del coeficiente de deformación por expansión.

En el caso en que el uso de nuestro modelo diagnostique el daño potencial que la expansión de las arcillas pueda ocasionar al material, el tratamiento del mismo con productos inhibidores de la expansión puede resultar efectivo, como se describe a continuación.

4.4.2 Agentes inhibidores de la expansión

En esta tesis se ha demostrado que ciertos aminoalcoholes y diaminoalcanos ensayados son efectivos como productos inhibidores de la expansión. Para una cierta cantidad de producto, algunas combinaciones tienden a ofrecer mejores resultados que el uso del producto individualmente. Un factor importante a tener en cuenta es que las moléculas seleccionadas no modifiquen las propiedades hidrófilas, la velocidad de ingreso del agua en el sistema poroso de la probeta y el color del material. Para las dosis usadas (~5% en peso de soluciones acuosas), la reducción del coeficiente de expansión ha sido de aproximadamente entre el 50-65%. Esto se traduce directamente en una reducción “casi equivalente” de los esfuerzos previstos durante los ciclos de h/s. En el caso de la arenisca *Portland Brownstone*, la reducción conseguida es suficiente para que los esfuerzos generados durante la desecación no excedan los valores de resistencia máxima a la tracción de la piedra “seca”, eliminando eventualmente el deterioro por este tipo de mecanismo. Es más, se ha encontrado que al menos hasta 700 ciclos de h/s el producto permanece en el sustrato pétreo tratado (en este caso, la arenisca *Portland Brownstone*), por lo que cabe esperar que su efecto sea prolongado tras su aplicación in situ.

El tratamiento con estos productos también afecta a otras propiedades de la piedra. Por ejemplo, en algunos casos se ha observado que incrementan ligeramente el módulo de elasticidad en probetas secas (de 2.5 GPa a 4 GPa), lo cual es sólo realmente importante en el caso de materiales pétreos particularmente poco resistentes como las *molasas de Villarlod*. Sin embargo el tratamiento no parece afectar el módulo de elasticidad de probetas saturadas. Los agentes reductores del hinchamiento

también modifican las velocidades de relajación de esfuerzos, aunque nuestros resultados no han ofrecido tendencias claras y todo parece depender de las combinaciones específicas piedra-producto. Estos tratamientos se presentan entonces como un instrumento de gran utilidad y potencialidad en el ámbito preventivo de la conservación de este tipo de materiales pétreos, aunque serían necesarias más investigaciones sistemáticas sobre los posibles efectos secundarios que su aplicación pueda producir.

4.4.3 Consolidantes

Los resultados de esta tesis confirman que los materiales pétreos formados por minerales de la arcilla y sometidos a un tratamiento de consolidación con silicatos de etilo, pierden rápidamente el efecto otorgado por dicho tratamiento al someterse a un número limitado de ciclos de h/s. Cualquier tentativa de consolidación de este tipo de rocas ornamentales debería por lo tanto ejecutarse sólo en combinación con un agente reductor de la expansión, siempre que el material vaya a estar expuesto a la humedad. Nuestros resultados sugieren que con esta combinación de tratamientos, la pérdida de resistencia mecánica es menor. También indican que existe una cierta sinergia entre los silicatos de etilo y algunos inhibidores de la expansión, lo que parece incrementar el efecto de la consolidación.

Es más, es bien sabido que los consolidantes basados en silicatos de etilo sólo son efectivos en enlazar las paredes separadas por espacios del orden de 50 μm. Los espacios más grandes, que pueden desarrollarse por ejemplo debido al proceso de combado, no disfrutarían del efecto de dichos consolidantes. Esto muestra de nuevo el claro beneficio que proporciona un uso preventivo de los productos inhibidores del hinchamiento para evitar tener que tratar el daño ocasionado por el combado de superficies. Estos tratamientos presentan, por tanto, un gran potencial que habría que explorar y seguir estudiando para poder garantizar así el éxito de su uso.

4.5 Perspectivas

La investigación llevada a cabo en este estudio ha permitido establecer las bases para la cuantificación de los esfuerzos que pueden desarrollarse en piedras que contienen minerales de la arcilla durante ciclos de h/s. Para situaciones que implican

estrictamente estos ciclos, se podría por lo tanto proponer un criterio cuantitativo, aunque llegados a este punto, se deberían llevar a cabo más trabajos de investigación para incorporar el papel de las propiedades viscoelásticas del material in situ. Con respecto a esto último, la dependencia de la resistencia mecánica (a la compresión, tracción y esfuerzos cortantes) de las velocidades de aplicación de la carga, debería ser examinada para definir mejor el criterio de rotura.

En situaciones donde otros mecanismos actúan conjuntamente, es probable que la expansión de los minerales de la arcilla provoque combado de las superficies pétreas una vez que los otros mecanismos han creado los defectos iniciales. El análisis cuantitativo de este mecanismo es más complejo y merecería ser llevado a cabo de forma más completa en un futuro ya que al menos en el caso de la *Portland Brownstone*, podría ser la principal forma por la cual la expansión de las arcillas podría causar deterioro.

En cuanto a la posible aplicación de nuestro estudio sobre agentes inhibidores de la expansión, en la conservación de este tipo de rocas ornamentales; los resultados obtenidos indican que las reducciones en expansión son sustanciales y además suficientes para mantener los esfuerzos dañinos por debajo de los límites de fallo del material. Estos productos permanecen en el material después de ser este sometido a ciclos de h/s, no le otorgan propiedades hidrófobas y además, no producen un cambio de color en los mismos (al menos a simple vista), si bien esto último debería ser examinado con los correspondientes ensayos de colorimetría. De todos modos, nuestros resultados indican que el uso de inhibidores de la expansión podría ser considerado apropiado, particularmente si se tiene previsto llevar a cabo un tratamiento de consolidación con silicatos de etilo. Los efectos que estos tratamientos tienen en las propiedades viscoelásticas de los materiales pétreos estudiados deberían ser por tanto examinados con más profundidad. Así se podría evitar seleccionar productos que limitarían la habilidad inherente de estos materiales a relajar esfuerzos dañinos. Es más, la combinación de ciertas moléculas orgánicas seleccionadas y su interacción con consolidantes se ha identificado como una opción real para mejorar la resistencia de la piedra a la acción de los ciclos de h/s. Por lo tanto, un estudio más detallado sobre estas sinergias, se perfila entonces como una muy buena opción de poder identificar tratamientos realmente efectivos y duraderos para la conservación de estos materiales in situ. En dichos estudios sería recomendable realizar ensayos que permitan seguir los cambios en la resistencia mecánica de las superficies pétreas durante los ciclos de h/s, por ejemplo a través de medidas de resistencia al taladrado. También, durante estas investigaciones sería muy interesante poder relacionar la

reducción de expansión tanto con la composición química del agente inhibidor del hinchamiento como con la naturaleza de los minerales de la arcilla. Asimismo, se podrían determinar las composiciones óptimas de tales productos conociendo la composición mineralógica de la piedra, lo cual evitaría la realización sistemática de estudios exploratorios de tipo “prueba y equivócate”.

Llegados a este punto, y a propósito del uso de estos agentes reductores de la expansión, debe hacerse un comentario respecto a las rocas que experimentan expansiones muy importantes (ej. algunos litotipos egipcios que llegan incluso a la descomposición literal cuando absorben humedad). En estos casos, la aplicación de estos productos debería llevarse a cabo usando mezclas de alcohol y agua como disolvente, aunque las proporciones óptimas de dicha combinación necesitarían ser cuidadosamente determinadas previamente.

Por último, expresar nuestra esperanza de que el tipo de planteamiento desarrollado en este trabajo facilite la toma de decisiones adecuadas al conservador/restaurador que tenga que enfrentarse día a día al difícil reto que le plantea cada obra de arte.

Chapter 4. Conclusions and perspectives

4.1 Impact of clay minerals on stone degradation

4.1.1 General statements about quantification

In this thesis a methodology to quantify the susceptibility of clay-bearing stones to damage by wetting and drying cycles is proposed. In order to do this, the magnitude of the swelling strain and the mechanical properties of the stone have been characterized. The basic idea is that the product of the elastic modulus (E) and the swelling strain (ε_S) gives a good estimate of the stresses that can be expected. Furthermore, comparing this to the mechanical strength of the stone considered should provide a failure criterion. However, the situation is not so simple, and a number of factors, such as exposure conditions and viscoelasticity, must be taken into account. In what follows, the three situations considered as potential sources of damage from wetting and drying cycles are outlined:

- tensile failure in the outermost zone (dry) during drying,
- compressive failure in the outermost zone (saturated) during wetting,
- buckling from shear failure developed parallel to the exterior surface during wetting.

4.1.2 Tensile failure during drying

Maximum drying stresses can be generated in situations where fully saturated thick stone blocks start drying. If these stresses become larger than the dry tensile strength of the stone they can produce cracking that should develop perpendicularly to the stone surface following a mud-cracking pattern (Figura 3-2). This kind of cracking has been identified in protruding structures (*Portland Brownstone*, Figura 3-2f f and Figura 3-23) and in semi-isolated elements (*Villarlod molasse*, Figura 3-22b). However, this type of damage is relatively uncommon on non-isolated or thick blocks (e.g. a wall building) because they rarely get fully saturated (section 3.2).

4.1.3 Compressive failure during wetting

This is the opposite case to the one just described. What happens during the wetting of a “completely dry” clay-bearing stone is that the swelling of the outer layer is suppressed by the dry stone core that puts the outer layer into compression. In principle, very few stones are candidates to suffer degradation by compressive stresses, due to the fact that these are much smaller (by factor of ~15) than the typical wet compressive strength of these stone. This indicates that damage under these conditions is probably of concern only in the case of stones that get very weak when wet (e.g., Swiss molasse). In these cases the compressive strength could significantly decrease if the stresses are maintained during long periods (which would imply that the stone remains partially wet for a long time). The other possibility of damage during wetting is described in the following section.

4.1.4 Buckling from shear failure during wetting

During the wetting of a “dry” stone, a process other than compressive failure is probably more problematic. It comes from the shear forces at the dry/wet stone interface and results in the buckling of an exterior layer as a consequence of the cracking occurring below that stone surface (Figura 3-1). From a mechanical point of view, this type of failure is difficult to treat with a simple criterion, since its initiation requires the previous existence of flaws (Scherer 2006, Hutchinson et al. 2000). The origin of such as defects can be multiple (e.g. stratification planes or cracks generated by other degradation mechanisms), therefore it is substantially more difficult to quantify that the above two cases.

In this case, where the clay swelling works together with other damage mechanisms already mentioned (salt crystallization and/or freezing), the extent of damage and possibly the loss of superficial and/or ornamental details would increase substantially. Therefore treating the stone to prevent swelling is an important contribution for the preservation of the aesthetic appearance of historic-artistic objects.

4.1.5 Limiting factors

In all the situations discussed above, the magnitude of the stresses is limited by the viscoelasticity of the stone. Furthermore, the relative humidity either of the stone before wetting or of the atmosphere during drying affects the maximum stresses, so that not only the nature of the stone, but also the exposure conditions (environment, orientation, geometry and dimensions, ecc.), must be taken into account. In the specific case of drying stresses, the extent of wetting before the start of drying must also be considered.

Viscoelasticity

To obtain a good estimation of the stresses that can be generated during swelling/shrinkage cycles, it is not sufficient to simply multiply the swelling strain by the elastic modulus. It has been shown that the viscoelastic properties of the stone must be taken into account (section 3.3.3 and Anexo 3). These reduce the magnitude of the stresses that develop during wetting and drying cycles, both in the wet and dry part of the stone, although this stress relaxation is more important when the stressed zone is wet. It is possible to demonstrate the importance of this quantitatively through direct measurements of the swelling pressure, as we have done in the case of *Portland Brownstone* and *Tarifa sandstone*.

Relative humidity (RH)

The environmental conditions during drying play a role in limiting the magnitude of the tensile stresses generated. In the case of a fully saturated block that starts drying in a totally dry atmosphere (0 % RH), maximum shrinkage strain and drying stresses are found. If the drying takes place in a humid atmosphere, the change in moisture content of the stone is less, so the shrinkage is smaller. In practice, this means that local conditions of relative humidity of a monument (its microclimate) should also be taken into account. These local conditions would be used to calculate the stresses developed in that particular location and thereby define stresses that a consolidation treatment would have to provide in order not to be damaged in situ during those cycles.

Extent of pre-existing wetting

The magnitude of the tensile drying stresses is limited by the extent of wetting of the stones, which depends on the location, exposure conditions (accessibility of the rain or capillary rise water) and thickness of the stones. Maximum stresses develop in fully saturated stones as could be protruding elements (e.g. tombstones, columns or sculptures) or thin decorative motives (e.g. mouldings). On the other hand, the tensile stresses should be much smaller in a building wall or thick blocks (e.g. ashlars) that are unlikely to get completely saturated.

4.1.6 Other concerns

Fatigue

In stones that do not have exceptionally high clay-content, damage from wetting and drying will appear only in the long term.

The study by Wendler et al. (1996) demonstrates that wetting and drying cycles can damage unconsolidated clay-bearing stones. Thus the machine built in this thesis to automatically subject samples to many wetting and drying cycles is important for studying this type of degradation, for example to study the permanence of swelling inhibitors treatments in the stones (Anexo 5 and section 3.4.2).

Direct measurement of swelling strain on untreated samples shows an increase of strain with the number of cycles. This probably means that progressive damage is happening by fatigue. Testing of susceptibility of stones to wetting and drying cycles should therefore involve such testing that allows many more cycles than can be done manually and in a reasonable amount of time (Anexo 5 and section 3.4.2).

Other mechanisms

Other mechanisms, such as freezing and salt crystallization, could be more harmful, because stones containing clays necessarily contain a fraction of very small pores, and these are the pores most likely to generate high crystallization pressure. For example, in the case of *Portland Brownstone*, it can be calculated that if ice formation takes place in cylindrical pores of diameter smaller than 20 nm, crystallization pressures larger than the tensile strength of the material could be generated. In fact, as shown in Figura 3-16b, this sandstone has a class of pores well defined around this size, although they only represent a small fraction of the total porosity. (Figura 3-16a). Consequently, such stones are inherently susceptible to damage by these mechanisms. Furthermore, these mechanisms were found to act in synergy with wetting/drying cycles in clay bearing stones, being the cause of crack formation and therefore the precursors of buckling of surfaces during the wetting cycles (Anexo 7).

4.2 Impact of clay minerals on stone properties

4.2.1 Swelling

Some ornamental stones swell in the presence of liquid water or in humid environments (hydric and hygric swelling, respectively). This happens if the stones contain swelling clay minerals. Occasionally, stones containing clays considered to be of the non-swelling type are also found to swell. In those cases, the swelling is only intercrystalline or osmotic.

In the case of *Portland Brownstone*, the expansion does not seem to be of osmotic origin but intracrystalline. In fact, our tests performed with different salt solutions (NaCl, KCl, $CaCl_2$) did not show any reduction on swelling strain (Anexo 2).

4.2.2 Mechanical properties

The swelling strain measurements alone are quite insufficient to judge the importance of clays for stone durability. Therefore, the stone mechanical properties must be characterized.

We have corroborated how the values of some mechanical properties such as elastic modulus and tensile strength can substantially decrease in wet stones. In the case of static Young modulus, the dry to wet modulus ratio (E_{dry}/E_{wet}) can be related to the swelling strain of the stone.

4.2.3 Viscoelasticiy

Our tests show that not only the swelling of the intergranular clays causes the stone to soften, but also the presence of such clays causes the stone to have a viscoelastic, rather than an elastic behavior. A consequence of this is that elastic moduli measured by the acoustic pulse delay (very small strain and high frequency) and the one obtained by beam bending (very large strain and very low frequency) are different in clay bearing stones. This difference is enhanced when the stones are wet.

These differences in modulus are attributed to the movement of water between clay surfaces, which provides compliance at low frequencies of loading, but which cannot occur at high frequencies. From the point of view of durability, what is of interest is stresses generated over a long period of time under substantial strains, on the order of those experienced during swelling. Consequently, only the static modulus data are relevant.

Another consequence of the viscoelasticity of the clay-bearing stones is their ability to relax stresses. In terms of durability, this is very important, because in this way, potentially dangerous stresses arising from salt crystallization and freezing, for example, could be prevented from reaching a critical threshold. In this thesis, we quantified the importance of the stress relaxation by measuring the swelling pressure on *Portland Brownstone* and *Tarifa sandstone*

4.3 Characterization of stone properties

The stresses generated during the expansion of clay-bearing stones can be quite important. They can also be problematic in the case of stones that do not show a very high swelling strain (i.e *Portland Brownstone*). To evaluate these cases, it is mandatory to know some stone properties. To reach this objective, some innovative techniques have been introduced in order to characterize the stone in the most appropriate way.

4.3.1 Warping

The warping, or “three in one”, technique has been used for the first time in the Conservation field in this thesis. It is a very convenient technique to obtain a quick estimation of changes of free swelling strain (e_S), sorptivity (S), and the ratio of wet to dry modulus (E_{wet}/E_{dry}). However, depending on the stone nature, it is possible that the use of samples thicker and longer than those indicated as typical in this thesis need to be used in order to reach reliable results.

In any case, the fact that a plate of stone, although thin, can warp substantially when wetted from above, demonstrates that high stresses arise from the swelling of clays contained in stones. On buildings, the thickness of the wall blocks or ashlars prevent warping, but leads to stresses in the expanding or shrinking outer layers which may cause damage.

4.3.2 Beam bending (three point beam bending)

Elastic modulus

The stresses from cyclic expansion and shrinkage develop slowly. Because of viscoelasticity of these stones, the material properties necessary for the stress calculation must also be measured at slow rates, for results to be relevant to practice. It is for this reason that the static modulus had to be measured. Three point bending was therefore a very adequate method to use for determining moduli of samples both, wet and dry. This helped to understand the important differences in the stiffness of wet and dry stones due to the presence of clay minerals.

Stress relaxation

The same three point bending technique was also used to characterize the viscoelastic behaviour of clay bearing stones. It was possible to show that they can relax stresses both in the wet and the dry state. This property is important, in that it can contribute to limiting damage from wetting and drying cycles.

4.3.3 Direct measurement of swelling pressure

In this research, the generally quoted technique to directly measure swelling pressure was revised. This led to having experiments last about 10 times less, which makes it much more attractive. Another advantage of this technique is that it can contribute to quantifying the viscoelastic character of the stones. In fact, with it, we can observe the importance of the rate of stress relaxation. However, it does have some inconveniences, such as low reproducibility (attributed to technical problems) that are currently not resolved and make it unsatisfactory.

4.4 Conservation and restoration of clay bearing stones

4.4.1 Untreated stones

It was shown how in order to predict the susceptibility of stone to damage by wetting and drying cycles, it is necessary to perform measurements of static modulus and swelling strain. More refined evaluations require more sophisticated calculations involving stress relaxation. However, none of these techniques can be done in a non-destructive way directly on a monument or on a sculpture.

Therefore, our proposed evaluation could be applied in preventive conservation, for example for deciding which stones to use in new buildings or in restoration interventions that imply the substitution of blocks or stone elements. For stones that must remain in place, one might have to rely on a mineralogical investigation to determine whether the stone contains clay minerals and if so their type, amount and distribution. Alternatively, small samples may be removed from hidden places for minimum investigations, such as swelling strain measurements.

In the case that swelling is diagnosed to be an issue with the support of the above described approach, a treatment with swelling inhibitors may be effective, as described below.

4.4.2 Swelling inhibitors

Aminoalcohols and diamino-alkanes are found to be effective swelling inhibitors on the stones used in this thesis. For a given amount of product, combinations tend to work better than single molecules taken alone. An important point is that the molecules selected do not modify the hydrophilicity, rate of water ingress, the porosity or the color of the sample. For the dosages used (~5 wt% solutions in water), the swelling strain reduction was around 50-65%. This translates directly into a comparable reduction of the predicted stresses during wetting and drying cycles. In the case of *Portland Brownstone*, where drying stresses can exceed the tensile strength of the dry stone, such a reduction brings the stresses well below the dry tensile strength and removes the eventuality of damage by this mechanism. Furthermore, it was found that up 700 wetting and drying cycles do not succeed in washing the product out and cancelling its effect on *Portland Brownstone* samples, indicating that the treatment should be long lasting on site.

These swelling inhibitors also affect other stone properties. In some cases a minor increase of the elastic modulus (2.5 GPa to 4 Gpa) is found, which is only really important for particularly weak stones, such as the *Villarlod molasse*. No such effect is seen for the wet modulus. The swelling reducing agents modified rates of stress relaxation, but the trends were not very clear and appear to depend on the specific combinations of stone and swelling inhibitor. Therefore, the treatments present themselves as very useful and with a big potential in the field of preventive conservation. However, more systematic research about the possible secondary effects produced by their application would be necessary.

4.4.3 Consolidants

Results of this thesis confirmed that clay-bearing stones consolidated with ethyl silicate rapidly lose any benefit of consolidation with a limited number of cycles of wetting and drying. Any consolidation attempt on clay bearing stones that will be exposed to water should therefore be considered only in combination with a swelling inhibitor. Results in this thesis suggest that, with such a combination of treatments, the loss of strength is reduced. They also indicate that there might also be a certain synergy between ethyl silicates and some specific swelling inhibitors, which seems to increase the consolidation effect.

Furthermore, it is known that ethyl silicate consolidants are only effective in bridging small gaps on the range of 50 µm. Larger gaps that can develop by the buckling process described above would therefore not be bridged by ethyl silicates. There is therefore a clear benefit in using swelling inhibitors early enough to prevent this buckling. These treatments show a big potential that should be explored and studied in order to guarantee the success of their use.

4.5 Perspectives

The work in this thesis has laid the basis for the quantification of the stresses that can develop in clay-bearing stones during cycles of wetting and drying. For situations strictly involving wetting and drying, a quantitative criterion could be proposed, although further work is now needed to incorporate the role of viscoelasticity in field conditions. In this respect the dependence of mechanical strength (compressive, tensile and shear) on loading rates should be examined to better define this failure criteria.

In situations where other mechanisms are acting as well, it is probable that clay swelling would lead to buckling after the other mechanisms would have created initial flaws. The quantification of this mechanism is more complicated and would deserve further investigation since, at least in the case of *Portland Brownstone*, it may be the main way in which clay dilation could cause damage.

For conservation purposes, results of this thesis indicate that swelling inhibitors can lead to substantial swelling reduction and bring the damaging stresses well below the failure threshold. These products do not get washed out, or render the stone hydrophobic. There is no net color, change although more detailed examinations by colorimetry could be recommended. Nevertheless, such treatments can already, in our opinion, be considered as suitable for clay-bearing stones, particularly if a consolidation with ethyl silicates is under consideration. The effects that these treatments have on viscoelastic properties should however be examined in further detail, to avoid selecting products that might limit the inherent ability of these stones to relax damaging stresses. Furthermore, the combination of the organic molecules selected and their interaction with consolidants has been identified as a real option to improve the resistance of the stones to these cycles. Therefore, a more detailed study about these synergies appears to be a good way of identifying really effective and durable treatments for the conservation of these materials in situ. In such studies it

would be recommended to follow changes in the surface strength of stones during wetting and drying, for example by drill resistance. Also during this type of research it would be very interesting to be able to relate the swelling reduction to both the chemical composition of the swelling inhibitor agent and the nature of the clay minerals. Likewise, it could be very convenient to determine the optimal compositions of such products for particular stone mineralogical compositions, which would avoid the systematic repetition of trial and error studies.

With respect to the use of such as products, a comment should be made concerning stones that swell so much that they virtually decompose upon wetting, such as some Egyptian stones. In those cases, swelling inhibitors might be applied by using mixtures of alcohol and water as solvents, but the optimum proportions would need to be determined carefully first.

Finally, we express our hope that this approach will contribute to providing sound decisions for conservators/restorers in their daily decision making for stone conservation.

Referencias

Abd El Hady, M.M. (1988): “Durability of monumental sandstone in Upper Egypt” In *Proc. Int. Symposium Engineering Geology of Ancient Works, Monuments and Historical Sites*, Marinos & Koukis (eds) Balkema, Rotterdam, v.2: 825-831

Alcalde, M. and Martin, A. (1990): “Examen visual de las alteraciones que presentan las obras de piedra de interes historico artistico”. In Ensayos y Experiencias de Alteracion en la Conservacion de Obras de Piedra de Interes Historico Artistico, ed. A. Martin. Centro de Estudios Ramon Areces, Madrid. Ch. 3 p.117-239.

Arnold, A. and Zehnder, K. (1990): “Salt weathering on monuments”. In *First International Symposium on the Conservation of Monuments in the Mediterranean Basin*, ed. F.Zezza. Brescia: Grafo. 31–58

Bailey, S.W. (1980): “Summary of recommendations of AIPEA Nomenclature Committee on clay minerals”, *American Mineralogist*; 65 [1-2]: 1-7

Beloyiannis, N.; Theoulakis, P. and Haralambides, L. (1988): “Causes and mechanism of stone alteration at the temple of Apollo Epicuros”. In *Engineering Geology of Ancient Works, Monuments and Historic Sites*. Marinos and Koukis, eds., Balkema, Rotterdam, 763-770

Bowles, O. (1939): “The stone industries: Dimension stone – crushed stone – geology – technology – distribution – utilization”, 2nd Ed., McGraw Hill, New York, 519 p.

Bradley, S.M. and Middleton, A.P.(1988): "A study of the deterioration of egyptian limestone sculpture" *JAIC* 27: 64-86

Brattli, B. and Broch, E. (1995): "Stability problems in water tunnels caused by expandable minerals. Swelling pressure measurements and mineralogical analysis". Engineering Geology, 39: 151-169

Camuffo, D. (1998): “Microclimate for cultural heritage”, Elsevier, Amsterdam, 390 p.

Caner, E. N. and Seeley, N. J. (1978): “The clay minerals and the decay of limestone”. In *Int. Symp. Deterioration and Protection of stone Monuments.* Unesco-Rilem, Paris, 2: 5-3, 34 p.

Correns, C.W. (1949): “Growth and dissolution of crystals under linear pressure”, *Disc. Faraday Soc.*, 5: 267–271.

Coussy, O. (2006): “Deformation and stress from in-pore drying-induced crystallization of salt”. *Journal of the Mechanics and Physics of Solids*, 54: 1517–1547

Crosby, W.O. and Loughlin, G.F. (1904): “The Building Stones of Boston and Vicinity”, *Tech. Quarterly*, 17: 165-185

Delgado Rodrigues, J. (2001): “Evaluación del comportamiento expansivo de las rocas y su interes en conservacion” “Swelling behaviour of stones and its interests in conservation. An appraisal”. *Materiales de Construcción,* 51 [263-264]: 183-195

Duffus, P; Wangler, T. and Scherer, G.W. (2008): "Swelling damage mechanism for clay-bearing sandstones", submitted

Dunn, J.R. and Hudec, P.P. (1966): "Water clay and rock Soundness". *The Ohio Journal of Science* 66 [2]:153-168

Esbert, R. M.; Ordaz, J.; Alonso, F.J.; Alba, J.M. (1981): "Petrographic and physical study of the building stones from Leon cathedral (Spain)" In *Int. symp The conservation of the ston*e. *II*. Bologna, 27-30 Oct-1981. Part A: deterioration. Part B: Treatment, 285-298

Esbert, R.M.; Ordaz, J.; Alonso, F.J.; Montoto, M.; Gonzáles, T. y Alvaréz del Buergo, M.. (1997): “Manual de diagnosis y tratamiento de materiales pétreos y cerámicos”. Ed. Colegio de Aparejadores y Arquitectos Técnicos de Barcelona.

Everett, D.C. (1961): “The thermodynamics of frost damage to porous solids”. *Trans. Faraday Soc.*, 57: 1541-1551

Fassina, V. and Cherido, M. (1985): "The nanto stone deterioration and restoration of Loggia Cornaro in Padova" In *Proc. Vth Intern Con. On Deterioration and conservation of stone*. Lausanne 25-27-Sep-1985. v.1. Labortoire de conservation de la pierre. Ecole Polytechnique Federal de Lausanne.

Félix, C. (1988): "Comportement des grès en construction sur le plateau suisse (Performance of Sandstones in Construction on the Swiss Plateau)". In *LCP Publications 1975-1995*, Montreux, R. Pancella Ed., EPFL, 833-841

Félix, C. (1994): "Déformation des grès consecutive à leur consolidation avec un silicate d'ethyle", In *7th Int. Congress of the association of engineering geology*, Lisboa, Ed. R. Oliveria, L.F. Rodrigues, A.G. Coehlo and A.P. Cunha,. Rohterdam: A.A. Balkema, 3543-50

Félix, C. (1995): "Peut-on consolider les grès tendres du Plateau suisse avec le silicate d'éthyle? (Can one consolidate the soft sandstones of the Swiss plateau with ethyl silicate?)", In *Preservation and restoration of cultural heritage*, ed. R. Pancella, Proc. LCP Congress, Montreux, 267-274

Félix, C. and Furlan, V. (1994): "Variations dimensionnelles des gres et calcaires liees a leur consolidation avec un silicate d'ethyle (Dimensional changes of sandstones and limestones related to their consolidation with an ethyl silicate)". In *3rd international Symposium on the conservation of Monuments in the Mediterranean Basin*. Edited by V. Fassina, F. Zezza. Venice, 22-25-June, 855-859

Félix, C.; Ferrari, P. and Queisser, A. (2000): "Déconsolidation par absorption d'eau de grès traités avec le silicate d'éthyle. Mesures non destructives de E, G et v". *In Procc. 9th Int.Cong. on deterioration and conservation of stone,* v.2. (V. Fassina, ed.), Elsevier, Amsterdam, 288-295

Flatt, R.J. (2002): "Salt damage in porous materials: how high supersaturations are generated". *J. Crystal Growth*, 242: 435–454.

Folk, R.L. (1980): "The Petrology of Sedimentary Rocks", Hemphill Publishing, Austin, Texas, 184 p.

Franzini, M.; Leoni, L.; Lezzerini, M. and Cardelli, R. (2007): Relationships between mineralogical composition, water absorption and hydric dilatation in the "Macigno" sandstones from Lunigiana (Massa, Tuscany), *Eur. J. Mineral*, 19: 113-123

Helmi, F.M. (2000): "Geoegyptology of Al-Muzawaka tombs, Dakhla oases, Egypt", *In Procc. 9th Int.Cong. on deterioration and conservation of stone*, v 1. (V. Fassina, ed.), Elsevier, Amsterdam, 99-107

Hoyos, M.; Sanchez-Moral, S.; Sanz-Rubio, E. and Cañaveras, J.C. (1999): "Alteration causes and processes in the stone material from the pavement in Baelo Claudia archaeological site, Cádiz/Spain". *Materiales de construccion*, 49: 5-19.

Hutchinson, J.W.; He, M.Y. and Evans, A.G. (2000): "The influence of imperfections on the nucleation and propagation of buckling driven delaminations" *J. Mech. Physics Solids*, 48: 709-734

Iñigo A.C.; García-Talegón J.; Trujillano R.; Molina E. and Rives V. (2003): "Evolution and decay processes in the Villamayor and Zamora sandstones", In *Applied Study of Cultural Heritage and Clays* (JL Perez-Rodríguez, Ed.) CSIC, 47-57

Kelly, W. M. (2005): "Petrology and chemistry of 'bluestone' in New York State". 40th Annual Meeting of the Geological Society of America, 37[1]: 63, http://gsa.confex.com/gsa/2005NE/finalprogram/abstract_82929.htm

Knöfel, D. K.; Hoffmann, D. and Snethlage, R. (1987): "Physico-chemical weathering reactions as a formulary for time-lapsing ageing tests". *Mater Struct* 20[2]:127–145

Kühnel, R.A.; Van der Gaast, S.J.; Brych, J.; Laan, G.J and Kulnig, H. (1994): "The role of clay minerals in durability of rocks: Observation on basaltic rocks". *Applied Clay Science*, 9: 225-237

Langella, A., Calcaterra, D., Cappelletti, P., Colella, A., de'Gennaro M. and de'Gennaro, R. (2000): "Preliminary contribution on durability of some macroporous monumental stones used in historical towns of Campania region, southern Italy", *In Procc. 9th Int.Cong. on deterioration and conservation of stone*, v.2. (V. Fassina, ed.), Elsevier, Amsterdam, 59-67

Lavalle, J. (1853): “Recherches sur la formation lente des cristaux à la température ordinaire” (Research on the slow growth of crystals at ambient temperature), *Compt Rend,* 34: 493–495.

Loughlin, G.F. (1903): “The building stones of Boston and vicinity”, Ph.D. Dissertation, MIT (Boston, MA/ USA), 109 p.

Lowell, S. and Shields, J.E. (1984): “Powder Surface Area and Porosity”, Chapman and Hall, New York, 87-120

McGreevy, J.P. and Smith, B.J. (1984): “The possible role of clay minerals in salt weathering”. *Catena*, 11: 169-175

Madsen, F.T. (1979): “Determination of the swelling pressure of claystones and marlstones using mineralogical data”. In *Proc. 4th Cong. ISRM*, 1: 237-243

Madsen, F.T. and Müller-Vonmoos, M. (1985): “Swelling pressure calculated from mineralogical properties of a Jurassic opalinum shale, Switzerland”. *Clays and Clay Minerals*, 33 [6]: 501–509

Madsen, F.T. and Müller-Vonmoos, M. (1989): “The swelling behavior of clays”. *Applied Clay Science* 4: 143–156

Matero, F.G. and Teutonico, J. M. (1982): “The use of architectural sandstone in New York City in the 19th century”. *Bull. of the Association for Preservation Technology,* 14 [2]: 11-17

Mortensen, H. (1933): “Die Salzsprengung“ und ihre Bedeutung für die regiona1klimatische Gliederung der Wüsten”. *Petermanns Geogr. Mitt.,* 5/6: 130-135

Mindess, S. and Young, J.F. (1981): “Concrete”. Prentice-Hall, Englewood Cliffs, NJ, 425–427

Norrish, K. (1954): “The swelling of montmorillonite”. *Discuss. Faraday Soc.* 18:120-134

Oliver Domingo, J.L. (1997): “Los diez libros de arquitectura”. Traducción de la obra original de Marco Vitruvio Polion. Ed. Alianza Editorial, Madrid, 400 p

Price, C.A. (1996): “Stone Conservation: An Overview of Current Research “, In *Research in Conservation series* edited by the J. Paul Getty Trust, Santa Monica (CA, USA), 72p.

Pye, K. and Mottershead, D. N. (1995): “Honeycomb weathering of Carboniferous sandstone in a sea wall at Weston-super-Mare, UK”. *Q. J. Eng. Geol*., 28*:* 333-347

Rodríguez-Navarro, C.; Hansen, E.; Sebastián Pardo, E. and Ginell, W. S. (1997): “The role of clays in the decay of ancient Egyptian limestone sculptures”. *J. Am. Inst. for Conservation* 36 [2]: 151-163.

Rodríguez-Navarro, C.; Sebastián Pardo, E.; Doehne, E. and Ginell, W. S. (1998): “The role of sepiolite-palygorskite in the decay of ancient Egyptian limestone sculptures”. *Clays and Clay Minerals,* 46 [4]: 414-422.

Rodríguez-Navarro, C. and Doehne, E. (1999): “Salt weathering: Influence of evaporation rate, supersaturation and crystallization pattern”. *Earth Surf. Process. Landforms*, 24 [3]: 191-209.

Rodríguez-Navarro, C.; Doehne, E.; Sebastián Pardo, E. (2000): “How does sodium sulfate crystallize? Implications for the decay and testing of building materials”. *Cement. Concr. Res.*, 16 [3]: 947-954

Salles, F.; Beurroies, I.; Bildstein, O.; Jullien, M.; Raynal, J.; Denoyel, R. and Van Damme, H. (2008): “A calorimetric study of mesoscopic swelling and hydration sequence in solid Na-montmorillonite”, in press

Scherer, G.W. (1992): “Bending of gel beams: method of characterizing mechanical properties and permeability”. *Journal of Non-Crystallyne Solids* 142 [1-2]: 18–35.

Scherer, G.W. (1999): “Crystallization in pores”. *Cem. Concr. Res.* 29: 1347–1358.

Scherer, G.W. (2006): "Internal stress and cracking in stone and masonry", In *Measuring, Monitoring and Modeling Concrete Properties*, edited by M.S. Konsta-Gdoutos, Springer, Dordrecht, The Netherlands, 633-641.

Sebastián, E.; Cultrone, G.; Benavente, D.; Fernández, L.L.; Elert, K. and Rodríguez-Navarro, C. (2008): "Swelling damage in clay-rich sandstones used in Architectural Heritage". *J. Cultural Heritage* 9: 66-76.

Snethlage, R. and Wendler, E. (1991): "Surfactants and adherent silicon resins—New protective agents for natural stone". In *Mat. Res. Soc. Symp. Proc.*, Pittsburgh, PA, 185: 193–200.

Taber, S. (1916): "The growth of crystals under external pressure". *Am J. Sci* 41: 532–556.

Topal, T. and Doyuran, V. (1998): "Analyses of deterioration of the Cappadocian tuff, Turkey". *Env. Geol.* 34 [1]: 5-20

Tutuncu, A.N.; Podio, A.L.; Gregory, A.R. and Sharma, M.M. (1998a): "Nonlinear viscoelastic behavior of sedimentary rocks, Part I: Effect of frequency and strain amplitude". *Geophysics* 63 [1]: 184-194

Tutuncu, A.N., Podio, A.L. and Sharma, M.M. (1998b): "Nonlinear viscoelastic behavior of sedimentary rocks, Part II: Hysteresis effects and influence of type of fluid on elastic moduli". *Geophysics* 63 [1]: 195-203

Velde B. (1992): "Introduction to clay minerals: Chemistry, origins, uses and environmental significance", Chapman & Hall, London, 198 p.

Velo-Simpson, M. L. (2004): "Falling apart: Understanding the damage mechanism of Bollingen and Krauchthal stone". Undergraduate Thesis, Princeton University (Princeton, NJ/ USA), 87 p.

Veniale, F.; Setti, M.; Rodríguez-Navarro, C. and Lodola, S. (2001): "Procesos de alteración asociados al contenido de minerales arcillosos en materials pétreos (Role of clay constituents in stone decay processes)". *Materiales de Construcción* 51 [263-264]: 163–182.

Vicente, M.A. (1983): “Clay mineralogy as the key factor in weathering of ‘Arenisca dorada’ (Golden sandstone) of Salamanca, Spain”. *Clay Minerals* 18: 215-217.

Vicente M.A. and Brufau, A. (1986): “Weathering of the Villamayor arkosic sandstone used in buildings under a continental semi-arid climate". *Applied Clay Scienc*e. Elsevier Science Publishers B.V., Amsterdam, 1 [3]: 265-272.

Vichit-Vadakan, W. (2002): “Measuring permeability, Young Modulus and Stress relaxation by the Beam-Bending technique”. Ph.D. Dissertation, Princeton University (Princeton, NJ/ USA), 153 p.

Vichit-Vadakan, W. and Scherer, G.W. (2000): “Measuring permeability of rigid materials by a beam-bending method: II. Porous glass”. *J. Am. Ceram. Soc.* 83 [9]: 2240– 2245.

Vichit-Vadakan, W. and Scherer, G.W. (2003): “Measuring permeability and stress relaxation of young cement paste by beam bending”. *Cem. Concr. Res.* 33: 1925–1932

Wangler, T.P.; Wylykanowitz, A. K. and Scherer, G.W. (2006): “Controlling stress from swelling clay”, In *Measuring, Monitoring and Modeling Concrete Properties*, ed. M.S. Konsta-Gdoutos), Springer, Dordrecht, The Netherlands, 703-708.

Wangler, T.P. and Scherer, G.W. (2008a): “Controlling swelling of Portland Brownstone”, submitted.

Wendler, E., Klemm, D.D. and Snethlage, R. (1991): “Consolidation and hydrohobic treatment of natural stone”, in *Proc. 5th Int. Conf. on Durability of Building Materials and Components*, eds. J.M. Baker, P.J. Nixon, A.J. Majumdar, and H. Davies (Chapman & Hall, London), 203-212

Wendler, E.; Charola, A. E. and Fitzner, B. (1996): “Easter Island tuff: Laboratory studies for its consolidation”. In *Proc. 8th International Congress on Deterioration and Conservation of Stone*, ed J. Riederer. Berlin, Germany 2: 1159-1170.

Wheeler, G. (2005): “Alkoxysilanes and the Consolidation of Stone”, *Getty Conservation Institute*, Los Angeles, 196 p.

Winkler, E.M. (1986): "A durability index for stone". *Bull. Assoc. Eng. Geol.*, 23: 344-347

Winkler, E.M. (1993) "Discussion and reply on "The durability of sandtone as a building stone, especially in urban environments",. *Bull. Assoc. Eng. Geol.*, 30: 99-101

Winkler, E.M. (1997): "Stone in architecture", 3rd Ed. Springer, Berlin, 309 p.

Wüst, R.A.J. and McLane J. (2000): "Rock deterioration in the Royal Tomb of Seti I, Valley of the Kings, Luxor, Egypt", *Eng. Geol.*, 58: 163-190.

Yang, G.W., Scherer, G.W. and Wheeler, G. (1998): "Compatible consolidants". In *Compatible materials for the protection of European cultural heritage*, eds. G. Biscontin, A. Moropoulou, M. Erdik, and J. Delgado Rodrigues, PACT 56, Athens: Technical Chamber of Greece, 201-208.

Zehnder, K., Arnold, A. and Küng, A. (2000) "Weathering of painted marly limestones in the temple green of Merenptah, Qurna/Luxor (Egypt)", In *Procc. 9th Int.Cong. on deterioration and conservation of stone*, v.2. (V. Fassina, ed.), Elsevier, Amsterdam, 749-757

Anexo 1. Materials and methods

A1.1 Materials

A1.1.1 Stone

Various stones types were studied in this thesis. They were chosen for their swelling properties and relevance to particular conservation cases where swelling was suspected to be an issue. Some were chosen to serve as reference because of virtually nonexistent swelling.

This thesis focuses mainly on sandstone degradation and more specifically on the case of *Portland Brownstone*. Systematic measurements were also done on two other types of sandstones: the *Villarlod molasse* and the *Tarifa sandstone*. Some other stones were also listed but are only used for a very limited number of experiments.

The stones used were the following:

Portland Brownstone

It is a coarse-grained arkose sandstone with marked bedding planes and whose dark reddish-brownish color is due to the content of hydrous ferric oxide (Matero and Teutonico, 1982). It is principally composed of quartz with a variable amount of feldspar and mica (flakes of muscovite) and mainly clays, hematite and albite as a binding phase (Figure A1- 1 and Anexo 7).

The amount of expandable clays does not seem to be very high (~2%). However this content by volume is given with respect to the whole stone, therefore, when reported with respect to the binding phase, in which most of the clays appear to be located, it becomes more considerable (8.3%). As far as the clay fraction is concerned, an XRD analysis (Figure A1- 2) identified the following clay minerals: montmorillonite, illite and possibly kaolinite-smectite mixed layer. A scanning electron microscope image of these clays can be seen in Figure A1- 3.

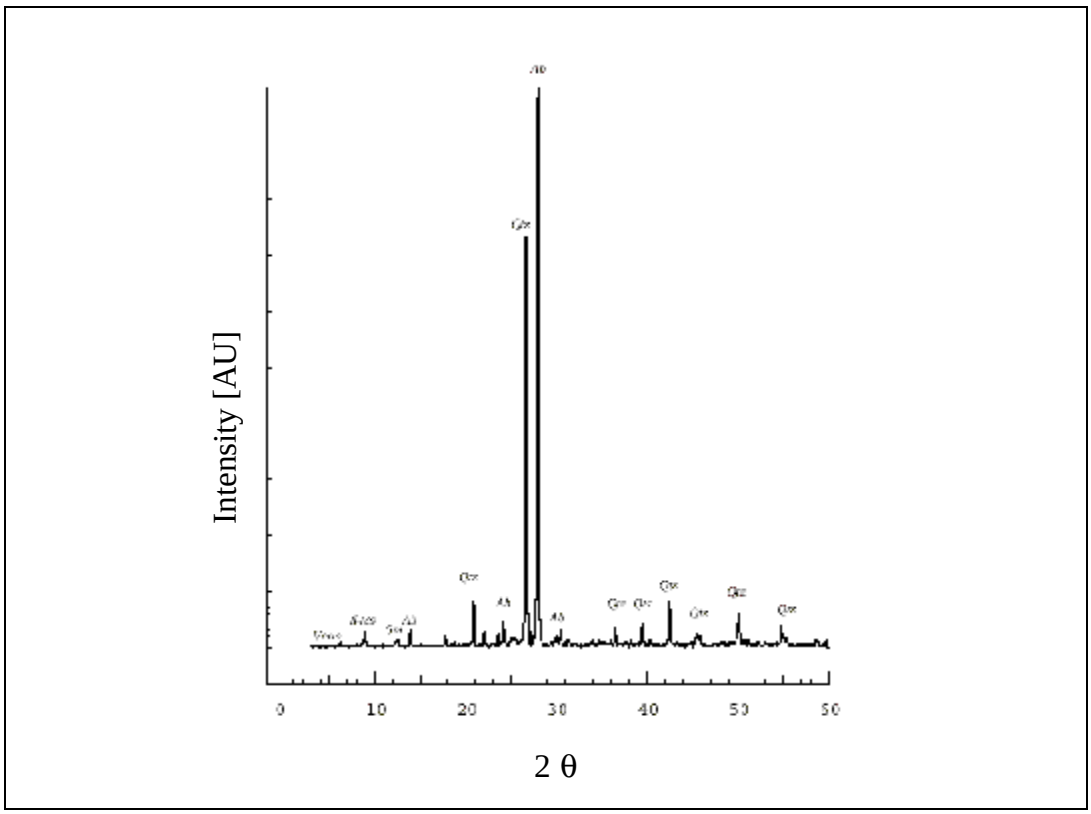

Figure A1- 1. XRD pattern of Portland Brownstone used for our investigations. Peaks highlighted correspond to Albite (Ab), Quartz (Qtz), Vermiculite (Verm), Smectite (Sm), Illite (Il) and Muscovite-mica (Ms).

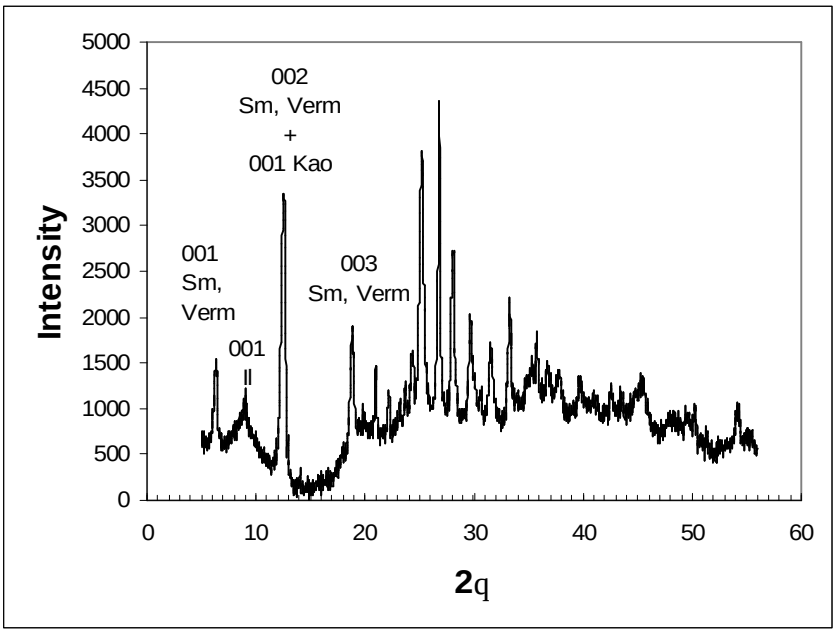

Figure A1- 2. XRD analysis of the clay fraction of Portland Brownstone. Sm: smectite, Il: illite, Kao: kaolinite.

a)

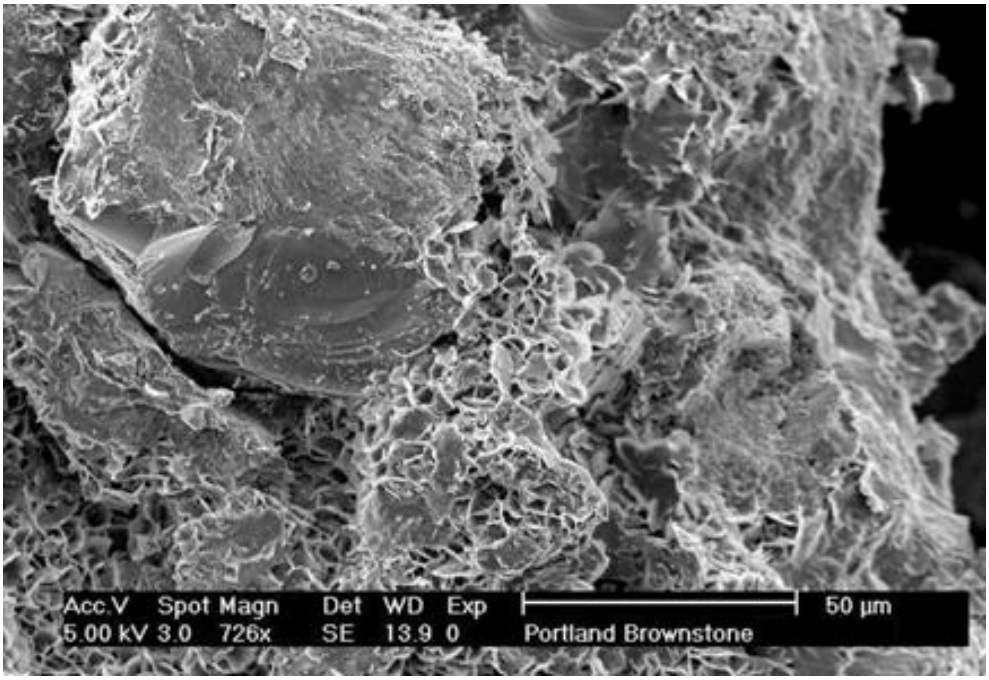

b)

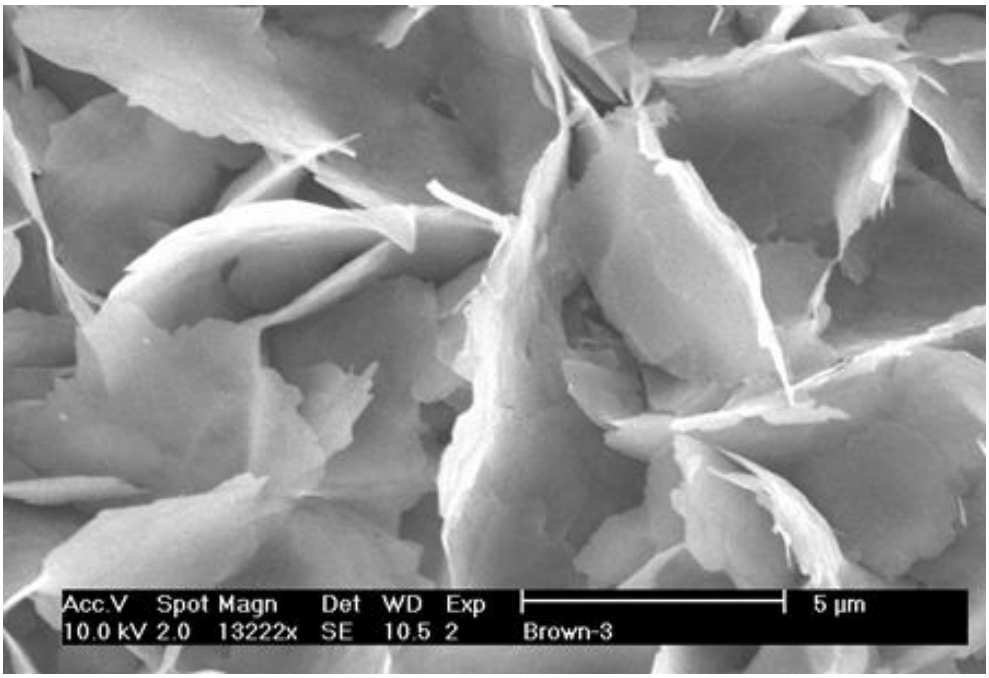

Figure A1- 3. SEM images of Portland Brownstone showing the presence of clay minerals. a) low magnification image showing clays surrounding grains. b) detailed view of clay minerals.

The polarized light optical microscopy analysis of a thin section of *Portland Brownstone* also shows evidence of mica beds and probably some clays, as indistinct material at grain boundaries (Figure A1- 4). The parallel colored lines result from the high birefringence of these layered minerals (principally muscovite).

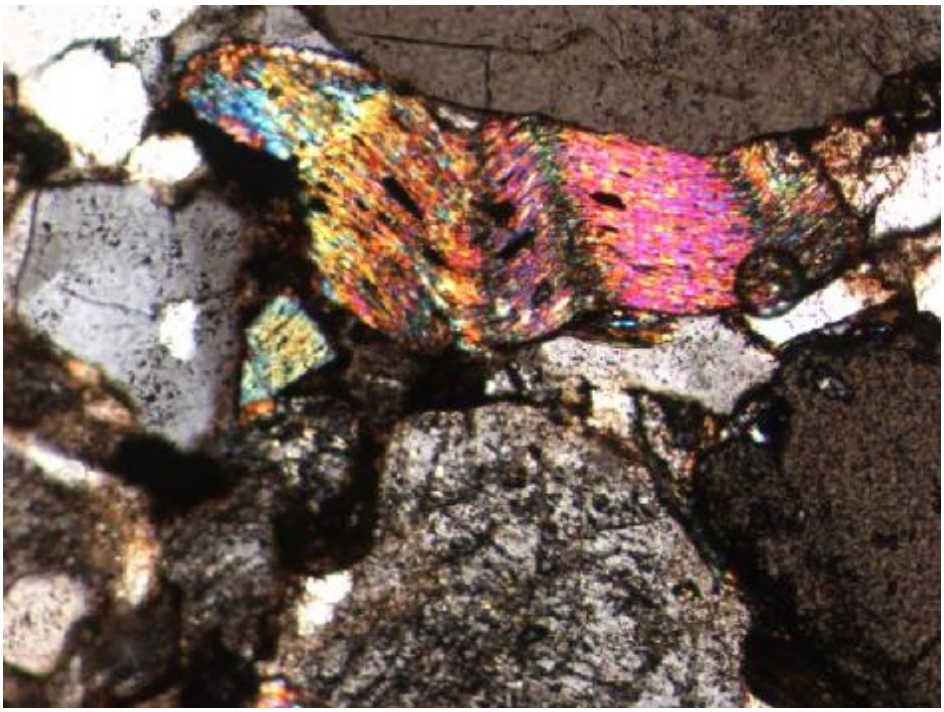

Figure A1- 4. Optical microscope image of a thin section of Portland brownstone taken under cross-polarized light. The birefringence of the mica grains is evident in the coloured layers seen in the top part of the image.

The binding phase may be viewed as the weakest link in stone microstructure, particularly when swelling clays are present. Consequently, one may be tempted to try relating the binding phase composition to stone durability. However other factors such as porosity and grain size should be at least as important as the mineralogy of the binding phase, so that no simple relation is expected. However, what can be stated, and is pertinent in the case of *Portland Brownstone*, is that a stone is weakened by a high content of swelling clays in the binder.

Portland Brownstone exhibits very marked bedding planes, which confer rather anisotropic properties and weaken the stone. They often alternate in fine and coarse

grains. This heterogeneity, perfectly apparent to the naked eye, not only poses an experimental challenge, but also limits the extent to which results obtained with one source of *Portland Brownstone* can be generalized to other sources. Furthermore, quarried stones show little homogeneity.

Crosby and Loughlin (1904) distinguish four grades of quarried brownstone:

a) medium-grained (first quality) brownstone, used in high-class architectural work; b) fine-grained (second quality) brownstone, richest in clay and mica, and most subject to injury by frost action; c) brownstone of uneven, laminated and shaly texture (third quality) d) coarse brownstone (conglomerate), used for rough stone work and bridges.

b) This anisotropy has a significant effect on swelling, sorptivity, elastic modulus and tensile strength as shown in (Table A1- 1). Whereas for heterogeneity the use of large samples or a large number of samples should reduce errors, anisotropy causes systematic differences according to the direction in which a property is measured. This is true however large the samples are or however many samples are measured.

The *Portland Brownstone* we studied shows a bimodal pore size distribution with about a third of the pore volume centered around 1 μm and the remainder averaging about 0.05 μm in diameter. The water accessible porosity of the *Portland Brownstone* is on the order of 8% by volume, while the total porosity is slightly higher, about 11% (Anexo 7).

Portland Brownstone is a very widely used stone in the northeast of the USA, particularly in the New York area, where the conservation of many buildings made of this stone has received particular interest. Owing to this, and because it seems to degrade due to swelling clays, this stone appeared to be a good candidate to study in this project.

Samples were taken from plates of about 25×25×5 cm that were acquired from Pasvalco Co. (Closter, New Jersey, USA).

More information and details about this stone can be found in Anexo 7. Its basic materials properties are given in Table A1- 1.

Villarlod Molasse.

This sandstone comes from Switzerland and is representative of the sandstones of the Swiss plateau. Félix (1988) distinguishes two types of Villarlod molasse: the "blue" and "yellow" varieties. The one used here is the "blue" one. The stone has been the subject of numerous studies due to the extensive use of these molasses as a building material and the evident degradation suffered by most of them. The swelling behavior of this stone has been highlighted as an important factor of degradation (Félix 1994).

This stone was kindly supplied by the "Expert Center pour la Conservation du Patrimoine Bâti" of Lausanne (Switzerland) in blocks of approximately 25×10×5 cm.

Regarding the clay mineral content of this stone, general information about Swiss molasse composition is given by Félix (1988), who indicates that the average mineralogical composition of these types of stone is quite constant and that the clay fraction in the matrix varies from 2-10%. Among these clays, there are swelling clays, such as smectites (montmorillonite), (30%), as well as illite (40-50%), chlorite (15-30%) and kaolinite (0-20%).

Some physical-mechanical properties of this stone are listed in Table A1- 1.

Tarifa Sandstone

This stone was studied in detail by the group of Dr. Sebastián Pardo / Dr. Rodríguez-Navarro at the department of Mineralogy and Petrology of the University of Granada. That work was commissioned because a church mostly built with this stone showed extensive degradation (southern Spanish city of Tarifa, Cádiz). In absence of any clear denomination for this stone, we just refer to it as *Tarifa sandstone* in this thesis.

Concerning the relevance of studying this stone in this thesis, it must be pointed out that the work by Dr. Sebastián Pardo / Dr. Rodríguez-Navarro concluded that the particularly high content of swelling clays in this stone is the cause of the extensive damage observed on the above-mentioned building (S. Mateo Church).

The *Tarifa sandstone* is a grayish arkose sandstone composed mainly of quartz and a matrix or cementing phase were clays prevail together with a small proportion of carbonates. In lesser amounts are feldspars, calcite and phyllosilicates, including muscovite, biotite and chlorite (Anexo 6). Generally, two varieties have been distinguished by Sebastián et al. (2008): the light brown and the grey variety, the first one being the closest to the one used in this study.

Figure A1-5a shows XRD patterns of the clay fraction. Smectite-chlorite mixed layers (corrensite) and minor amounts of illite are the main clay minerals present, which shows average values of 7 wt % (Anexo 6).

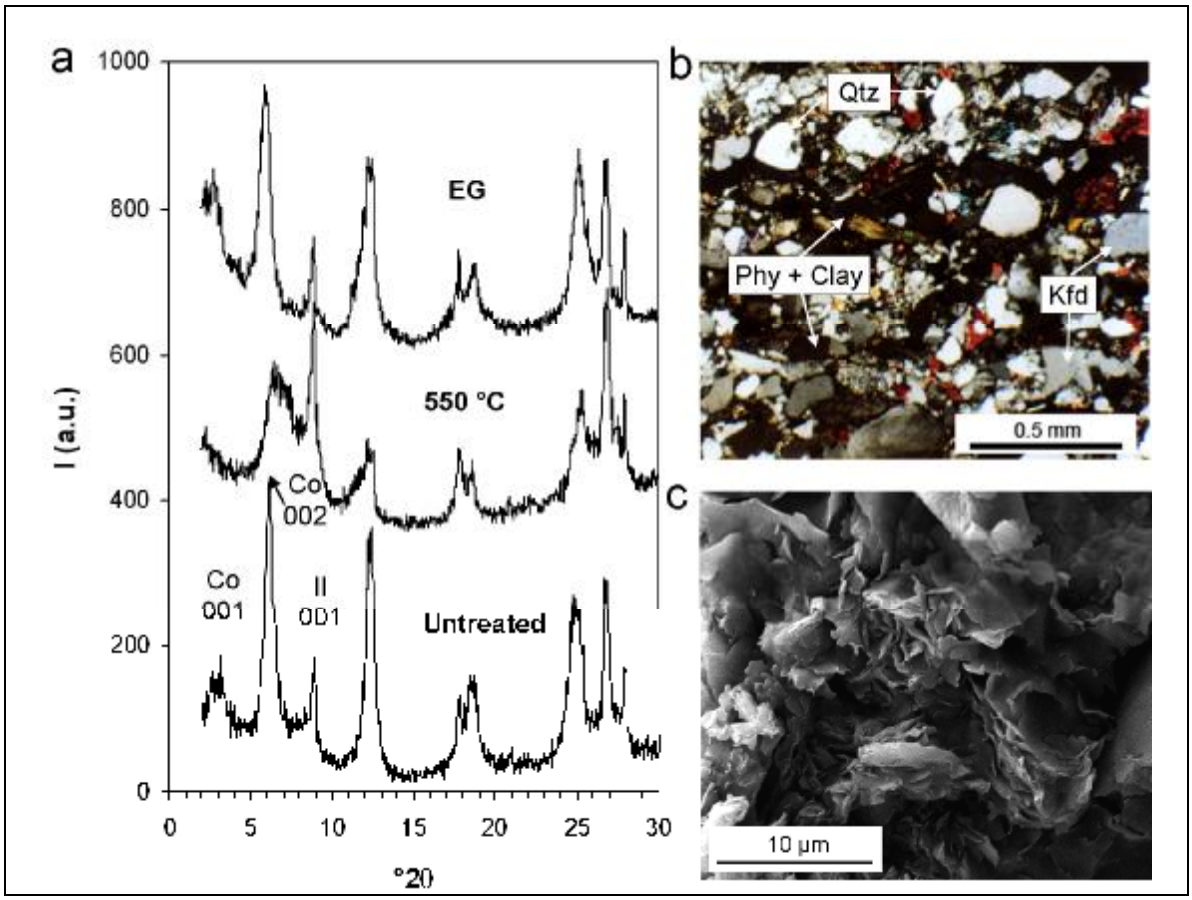

Figure A1-5. Mineralogy and texture of Tarifa sandstone: a) XRD patterns of oriented aggregates showing illite (Il) 001 reflection and corrensite (Co) 001 and 002 reflections and their change upon glycolation (EG) and thermal treatment (550 C); b) representative OM photomicrograph (crossed polars) showing quartz (Qtz), potassium feldspar (Kfd) and phyllosilicates plus clays (Phy+clay) oriented along bedding planes (horizontal); and c) SEM photomicrograph of the clay minerals.

Blocks of different sizes that were obtained from the quarries (currently closed) located near Tarifa were kindly supplied to us by Dr. Rodríguez-Navarro.

The most relevant material properties -from a conservation point of view- of those stones are given in Table A1- 1.

About the clay distribution, optical microscopy and SEM observations show that the phyllosilicates display a preferred planar orientation along the stone bedding planes (Figure A1-5b and c). The latter is responsible for the marked textural and structural anisotropy of this stone (Sebastián et al., 2008). The pore system of the sandstone is characterized by submicron pores (pore radii 0.5-0.02 μm) having an average total porosity of around 8-11 % (Sebastián et al., 2008).

Fuentidueña limestone

Another stone to which special attention was paid at the beginning of this research is a dolomitic limestone from the Spanish city of Fuentidueña (Segovia), which is referred to in this thesis as "Fuentidueña limestone".

It had initially been observed that the effect of consolidation with different products (ethyl silicates and acryloid B72^{TM}) on this stone was short lived and it was suspected that swelling of clays might be one of the causes. A 5 cm sided cube of that type of stone was obtained from the Department of Conservation of Objects of the Metropolitan Museum of Art (New York City).

Quarries of this type of stone do not exist anymore. The sample belonged to the monument[8], a Spanish apse that originally was part of the church "S. Martin de Fuentidueña", located in Fuentidueña, Segovia (Spain). The church -a Rockefeller JR acquisition- was dismantled stone by stone around 1954. Currently it is part of the Metropolitan Museum of Art branch: "The Cloisters", placed in Fort Tryon, Manhattan (New York City).

[8] The sample was not taken from the monument. It belonged to an original ashlar never used after the apse was rebuilt in New York.

Table A1- 1. Material properties of the Portland Brownstone, Villarlod Molasse and Tarifa sandstone.

TECHNIQUE	Bedding orientation	Conditions	Portland Brownstone	Villarlod molasse	Tarifa sandstone
Static Modulus [GPa]	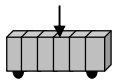	**Untreated: dry**	11.5	2.4	9.4
		wet	4.1	0.5	0.9
		75.3 % RH	7.6	n.a.	n.a
		84.3 % RH	7.7	n.a.	n.a
		91.4% RH	6.3	n.a.	n.a
		Consolidated: dry	29.8	15.9	14.6
		Treated: dry	12.5	4.1	9.4
		wet	4.1	0.5	n.a
		Treated and consolidated: dry	31.6	16.8	20.6
	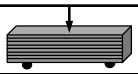	**Untreated: dry**	14.3	3.9	n.a
		wet	7.7	0.9	n.a
Dynamic Modulus [GPa]	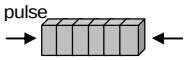	**Untreated: dry**	24	7.5	15.4
		wet	36.5	5.4	19.6
		75.3 % RH	18.7	n.a.	n.a.
		84.3 % RH	18.6	n.a.	n.a.
		91.4% RH	17.7	n.a.	n.a.
		Consolidated: dry	42	21.4	18.6
		Treated: dry	n.a.	n.a.	n.a.
		wet	n.a.	n.a.	n.a.
		Treated and consolidated: dry	42.5	21	23
	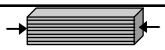	**Untreated: dry**	35	12	28.4
		wet	44	9.7	27.5
Tensile Strength [MPa]	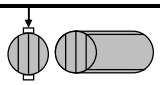	**Untreated: dry**	4.5	1.2*	5.3
		wet	n.a.	n.a.	n.a.
		Consolidated: dry	n.a.	n.a.	n.a.
		Treated: dry	n.a.	n.a.	n.a.
	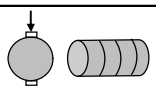	**Untreated: dry**	6.7	2.6	6.9
		wet	5.2	2.6*	n.a.
		Consolidated: dry	11.9	n.a.	n.a.
		Treated: dry	n.a.	n.a.	n.a.
Compressive Strength [MPa]		**Untreated: dry**	n.a.	37.5*	n.a.
		wet	n.a.	20.3*	n.a.
		**Untreated: dry**	79 $	50.9*	31.16 #
		wet	n.a.	22.1*	14.41 #
Sorptivity [cm/sec^1/2]		**Untreated:**	0.012	0.0352+	0.013
		Treated (swelling inhibitors)	0.010	n.a.	n.a.
		**Untreated:**	0.0079	0.0307+	0.008 #
		Treated:	n.a.	n.a.	n.a
Density [g/cm3]	apparent		2.4	2.3	2.1
	skeletal		2.7	2.7	2.6
Porosity [%]		Apparent (plateau sorptivity)	8	13.8	12 (4 #)
		Total (vacuum impregnation)	8.7	15.9	9.7 #
		Total (Hg porosimetry)	6.5	17	10 #
Swelling strain [µm/m]	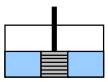	**Untreated: water saturation**	446	1200 (1700+)	(2900-3200)
		75.3 % RH	533	n.a.	n.a.
		84.3 % RH	330	n.a.	n.a.
		91.4% RH	306	n.a.	n.a.
		ethanol saturation	365	n.a.	n.a.
		isopropanol sat.	99	n.a.	n.a.
		salt solutions	no change	n.a.	n.a.
		Treated: water saturation	212	422	1620
	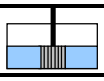	**Untreated: water saturation**	168	1400+	1200
		Treated: water saturation	n.a.	n.a.	n.a.

* Félix (1977)
\+ Velo-Simpson (2004)
\# Sebastian et al. (2008)
$ Crosby and Loughlin (1904)

The stone composition is mainly dolomite (90-94 %), jasper (3-4 %) and calcite (0-2 %) (Prof. G. Wheeler, personal communication). It was found to exhibit no swelling (Anexo 2) so that nothing more was said about it.

Indiana Buff limestone

Indiana limestone is a calcite cemented calcareous stone formed of shells and shell fragments. It is found in massive deposits located almost entirely in Lawrence, Monroe and Owen counties in Indiana. Chemically it is almost pure limestone, with a composition of 98% fine-grained calcite ($CaCO_3$) and dolomite grains ($Ca\ Mg(CO_3)_2$). Because of this high purity, the Indiana Geological survey qualifies this material as a chemical stone.

It is a typical freestone, which means that it exhibits no preferential direction of splitting and can, therefore, be cut and carved in an almost limitless variety of shapes and sizes. It does not show stratification planes, and its texture and structure are very uniform. The variety used in this work was the one that has light buff color. Its main properties are listed in Table A1- 2 (table2).

Indiana limestone has been used widely in North America, for example: the Empire State Building (NYC); the Tribune Tower in Chicago, Illinois; and the National Cathedral in Washington, D.C.

It was selected for this study as a reference material for the case of no textural anisotropy, no-clay content and, thus, no potential problems connected to clays.

Bluestone sandstone

The denomination “Bluestone” is known commercially as a type of sandstone that can be typically defined as an indurated arkose with the capacity to split into thin slabs. The bluestone is a fine-grained, dense, tough sandstone of even texture and bedding and has a dark blue-gray color in this case. Even if it has a high content in clays, it is *“so compact that it is non absorptive”* according to Loughlin (1903). The author pointed out that *“the fine particles of clay are arranged among the sand*

grains that the pores are practically closed". It has been extensively used for flagging, curbs, sills, steps, etc. It is quarried chiefly in New York and Pennsylvania.

Bowels (1939) has reported that the mineralogical composition of the bluestone from Ulster County (N.Y) consists of feldspars, quartz, sericite, chlorite, calcite, clay, and a little pyrite. The stone shows angular grains held together with a strong, siliceous cement. A quantitative determination of the rock composition is given by Kelly (2005) who reported it to be "*predominantly quartz (43%) and rock fragments (15%) with interstitial "sericite" (22%), chlorite (8%), muscovite (4%) and plagioclase, K-feldspar, biotite, and opaque phases (<2% each)*". The same author also indicated that apatite, calcite, ferromagnesian silicates, and zircons were present in trace amounts.

This stone has not been much studied in this thesis where the main property measured was its swelling strain. Other basic properties are, however, given Table A1-2.

For all stones, the blocks (25x5x5 cm) cut parallel and perpendicular to the bedding planes were ordered so that long samples could be obtained for characterizing properties (e.g.: static elastic modulus, warping) in both directions. There was however some minor deviation to be noted with respect to ideal orientation. An effort was made to choose homogeneous blocks. However, inhomogeneity and spread of results could not be avoided.

Table A1- 2. Main properties measured of Indiana Buff limestone and Bluestone sandstone.

TECHNIQUE	Bedding orientation	Conditions	Indiana limestone	Bluestone sandstone
Static Modulus [GPa]	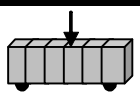	Untreated: Dry	26.8#	n.a
		Wet	22.8#	n.a.
	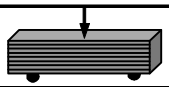	Untreated: Dry	n.a	n.a.
		Wet	n.a	n.a.
Dynamic Modulus [GPa]	puls 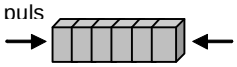	Untreated: Dry	44.8#	31.8
		Wet	46#	n.a
		Untreated: Dry	46.7	49.6
		Wet	46.7	n.a.
Tensile Strength [MPa]	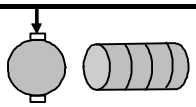	Untreated: Dry	6.3	18.2
		Wet	n.a.	n.a.
Sorptivity [cm/sec^1/2]		Untreated: Dry	0.007	n.a.
		Untreated: Dry	n.a.	n.a.
Density [g/cm3]	apparent		2.3	2.59
	skeletal		2.69	2.74
Porosity [%]		Apparent (plateau sorptivity)	8.5	n.a.
		Total (vacuum impregnation)	12.4	2.90
		Total (Hg porosimetry)	n.a.	2.85
Swelling strain [µm/m]	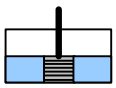	Untreated: water saturation	does not swell	968
	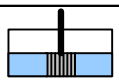	Untreated: water saturation	n.a.	252

\# little or no anisotropy

A1.1.2 Swelling inhibitors

Swelling inhibitors were used to limit or eliminate the amount of swelling of stones that expand in contact with humidity due to the swelling clays they contain. Various classes of molecules with radically different structures were tested. Many of these were commercially available products and the information given below is that provided by the manufacturer. These classes of molecules were:

Zonyl® Fluorosurfactants

This group of products is generally used at low concentrations (below 100 ppm) to reduce the surface tension of aqueous systems. They were obtained from DuPont™ Zonyl® (DE, USA). The name of the products tested and their structure were as follows:

Zonyl® FSH [$R_fCH_2CH_2O(CH_2CH_2O)_xH$]

Zonyl® FSA [$R_fCH_2CH_2S\ CH_2CH_2COO^-Li^+$]

Zonyl® FSP [$(R_fCH_2CH_2O)_aPO(O^-NH_4^+)_b$]

Zonyl® FSJ [$(R_fCH_2CH_2O)_aPO(O^-NH_4^+)_b$]

Zonyl® 9361 [$(R_fCH_2CH_2O)_aPO(O^-N^+H_2(CH_3CH_2OH)_2)_b$]

All of them are anionic except Zonyl® FSH which is non-ionic. In addition, Zonyl® 9361 contains also a nonfluorinated surfactant. Regarding their structure, the notations used above have the following meaning:

$R_f = F(CF_2\ CF_2)_x$, with X=1 to about 7, average 4; a+b=3; x<y<z and x, y, or z= 0 to about 25.

Corrosion inhibiting admixtures

These products were supplied by Sika Technology AG (Zurich, Switzerland). They are from the Ferrogard® line of products. We later refer to those products as F-A, F-B, F-C. They are aqueous solutions usually used as corrosion inhibitors for the steel reinforcement of hardened concrete structures. Some of these products are applied to the surface of concrete and the active substance diffuses to the rebar while others can be added directly to concrete while mixing. In all cases, the active substances are aminoalcohols. They are meant to adsorb onto the iron and create a passive film. These products were selected because after their adsorption, the surface remained hydrophilic, which contrasted with the Zonyl® products above. We examined whether mixed aminoalcohols could also be active as swelling inhibitors without making the stone hydrophobic. In this thesis the commercially formulated products

were used and found to have an effect. This work was continued by Velo-Simpson (2004) in her undergraduate thesis using only the active aminoalcohols.

Diamino alkanes

The use of diamino-alkanes as swelling inhibitors was first suggested by Wendler et al. (1991) and Snethlage and Wendler (1991). Two types of such swelling inhibitors were obtained from Sigma/Aldrich Chemical Co. (WI, USA) and Across Organics N.V. (NJ, USA) respectively: 1,3 Diaminopropane dihydrochloride ($H_2N(CH_2)3NH_2$. 2HCl) and Ethylnediamine dihydrochloride ($C_2H_8N_2$. 2HCl). Their structures are represented in Figure A1- 6-d.

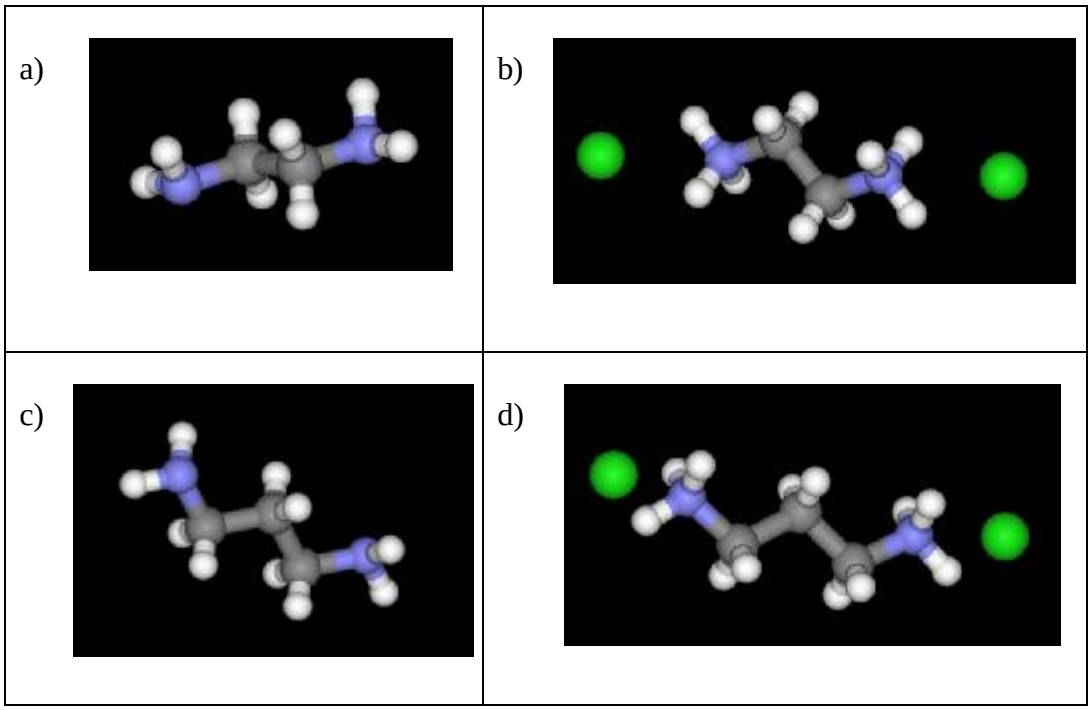

Figure A1- 6. Structure of the diaminoalkanes used as swelling inhibitors.

(a) diaminoethane or ethylenediamine ($C_2H_8N_2$),
(b) acidified version of (a): ethylenediamine dihydrochloride ($C_2H_8N_2$. 2HCl)
(c) 1-3 diaminopropane ($H_2N(CH_2)3NH_2$).
(d) acidified version of (c): 1,3 Diaminopropane dihydrochloride ($H_2N(CH_2)3NH_2$. 2HCl).

CTAB

Hexadecyltrimethylammomium bromide ($CH_3(CH_2)_{15}$ $N(CH_3)_3$ Br), known as CTAB is a cationic surfactant that is very widely used in many applications. It was tested in this work for its ability to prevent swelling and was obtained from Across Organics N.V. (NJ, USA).

A1.1.3 Consolidants

The ready-to-use product used as consolidant in our tests on sandstones is commercially known as Conservare® OH 100 (PROSOCO, Inc). It is composed of a solvent added to extremely small oligomers of ethyl silicate for allowing a good penetration into the deteriorated material while limiting volatility. The product is commonly used by conservators to strengthen weathered stones by allowing the formation of a new binder, a silica gel between the stone grains. The silica content of Conservare® OH 100 is about 40% by mass. It also contains dibutyltin dilaurate in small amounts as a catalyst (Wheeler, 2005).

A1.1.4 Brine solutions

Solutions of sodium chloride (NaCl), 1 M, potasium chloride (KCl), 1 M, and calcium chloride ($CaCl_2$), 0.1 M have been used to impregnate samples of *Portland Brownstone*. They all have a high solubility in water and were chosen to test their capability of reducing the swelling of this stone. The salts used to prepare these solutions were all analytical grade from Fisher Scientific Co (PA, USA).

A1.1.5 Organic solvents

Isopropyl alcohol (C_3H_8O) and ethanol (C_2H_6O) 99.5 % purity were used to demonstrate the importance of water in swelling. These polar alcohols only caused minor swelling, which points to the importance of the hydration of charge balancing cations in the clays. They were obtained from Fisher Scientific Co, (PA, USA).

A1.2 Methods

A1.2.1 Stone sample preparation

General considerations

Commercial and homemade instruments were used in order to characterize stone properties. Each technique required a specific size and geometry of the sample. These are specified in this section, when each technique is described.

Parallelepiped samples were cut wet with different diamond saws. One saw with a coarser blade was used for the larger samples. Smaller samples were cut on a smaller bench top saw. For each of these saws, sample holders were specifically designed and built to ensure the best possible cuts. In addition, some samples were cut with a high precision saw at the labs of the Conservation Department of the Metropolitan Museum of Modern Art in New York City.

Great care and precision was necessary to prepare thin (3 mm) and long plates (~150 mm) used in warping experiments and beam bending.

A core drill was used for producing the cylindrical samples. Most of these were drilled from plates five centimeters thick. A limited number of these samples were drilled with diameters of about 0.5 cm. They were later cut down to smaller lengths and used for free swelling experiments. Most samples had 2 cm Ø and 5 cm length and were used for tensile strength measurements. Finally, a limited number of cylinders about 5 cm length and about 4 cm diameter were cored after having drilled a 2 cm diameter hole in their center. These samples were used for the measurement of swelling pressure.

As a general routine, prior to each experiment, the sample to be used was oven dried at 60˚C in a circulating air oven to constant weight and then left to cool down to room temperature in a closed container.

Clay separation for XRD analysis

The procedure below was recommended by Dr. Rodríguez Navarro in order to obtain the clay fraction of a stone. It was carried for *Portland Brownstone* as follows:

A piece of stone of 50 g was first crushed and then ground into a fine powder using an agate mortar and pestle. About 100 ml of deionized water were poured into a 500 ml container to disperse the clay particles.

At that moment, a solution of acetic acid (20 % by volume) was added to dissolve any carbonates. The solution was then vigorously shaken every 30 minutes approximately. This operation was repeated until no more effervescence was observed (in our case very little effervescence was observed). Once this operation finished, the dispersed sample was left to stand over night in a large beaker to obtain the clay fraction (particles less than 2 μm in diameter). Afterwards, the liquid was decanted and fresh water was poured on the particles. Once again, the sample was left to settle and then the water discarded. This operation has to be repeated several times to ensure that all the acid has been eliminated.

Once the sample has been washed out of the acid, 2 ml of sodium hexametaphosphate (commercially known as “calgon”) at 10 wt% in water, was added to disperse the clay particles. This suspension was shaken for a couple of minutes and then left to settle for approximately 4 hours. After that, the first 4 cm of the clay suspension were decanted into another container of about 2000 ml capacity. After another 4 hours, the top 5 cm were eliminated and so on. Once this was complete, more water was added to the remaining sample and shaken. The process above was repeated as many times as required until reaching a totally transparent suspension. This indicated that no more clays remained in the main suspension and that they were all in the dilute suspension composed of the successively removed portions of liquid. To concentrate the clay fraction in that suspension and to accelerate the evaporation process, the container was placed in the oven (60°C).

Once the clays were concentrated, around 4 ml of suspension was taken and deposited on a thin section. This last one (suspension) was left to evaporate and therefore the clays orient with their (001) faces lying down on the thin sections. Both, thin sections and clays left to evaporate in a petry dish were analyzed by XRD by Dr. Fuellman (EPFL, Switzerland). A similar procedure was used in the case of the ***Tarifa sandstone***. Clay samples (oriented aggregates) were analyzed using XRD by Dr. Rodríguez Navarro (Granada University, Spain).

A1.2.2 Swelling behavior

The methods described in this section serve to characterize the free swelling of stone samples. By free swelling one means that the sample has no external constraints that limit its swelling.

Differential mechanical analyser (DMA)

In a first series of experiments, the stone free swelling was measured with a differential mechanical analyser (DMA) from Perkin Elmer™ (model 7e; Boston, MA, USA). This instrument is usually used to measure thermal expansion and mechanical properties (modulus, creep) as a function of temperature**,** time, frequency, stress or a combination of these parameters. In this case it was used to determine the change over time in the length of a stone sample after it was submerged in water. In terms of displacement, the instrument can measure from 100 nm to 24 mm, with a sensitivity of 50 nm.

The instrument is illustrated in Figure A1- 7. The whole instrument is shown in Figure A1- 7a and the sample holder in Figure A1- 7b. In that figure, a sample can be seen in the glass sample holder. On the top of it is the tip of the glass push rod that serves to measure the displacement. In Figure A1- 7a, the block at the bottom of the instrument is a bath that serves as temperature controlling unit. It can be raised to surround the sample holder and control its temperature. In this unit is a small metal cup that surrounds the sample holder. In our experiments, this cup contained deionized water and it was the raising of the bath that caused the submersion of the sample and the start of the swelling.

Samples with different bedding orientation and geometries were used: cylinders (0.5 Ø cm×1.8 cm) and parallelepipeds (0.5×0.5×1.8 cm). Prior to each experiment, the samples were oven dried at 60˚C to constant weight and then left to cool down to room temperature in a closed container. At that point, a sample was then placed in the quartz holder and the push rod was lowered until it touched the sample surface (Figure A1- 7a). A static force in the range from 150 to 500 mN was then applied to hold the sample in place. The data logging of the push rod position was initiated.

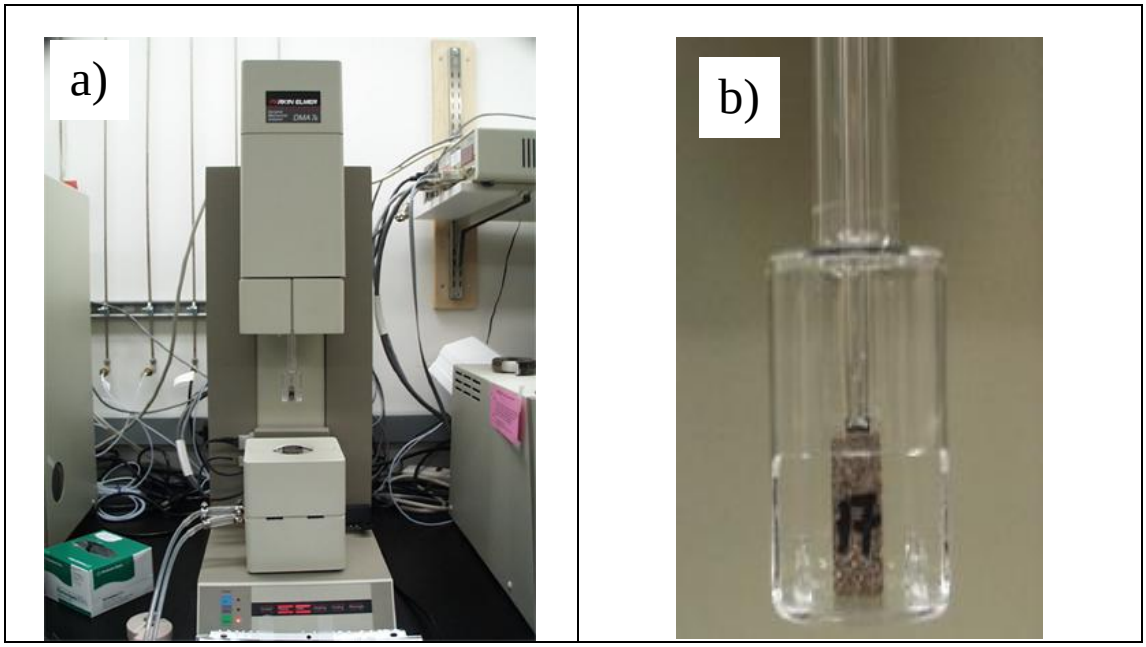

Figure A1- 7. Image of DMA: a) whole instrument, b) sample holder.

The temperature of 20˚C was maintained during the whole test. For this, cold water was circulating continuously in the temperature-controlling unit. After that, this unit in which the cup has been previously filled with water was raised. The amount of water was chosen so that only the top surface of the sample was not submerged. As soon as the sample contacted the water, expansion could be detected. The submersion of the sample can however be considered as instantaneous with respect to the total duration of the swelling.

The test was stopped once the expansion finished, which was revealed by the plateau shown on the graph of position versus time.

In addition to water, polar liquids (ethanol and isopropanol) and brines ($CaCl_2$, NaCl, KCl) were used to determine the importance of water activity and the capacity of swelling reduction in the case of salt solutions.

Homemade dilatometer

A homemade instrument was used to measure the linear expansion of most samples. It is illustrated in Figure A1- 8[9]. The measuring device consists of a pushrod that passes through a cylinder containing a linear variable differential transformer (LVDT). It is mounted in the center of the pushrod and allows the LVDT to measure its displacement, transforming it into electrical output (one mm corresponds to one volt). The cylinder, furthermore, contains two ball bearings above and below to allow optimal alignment of the pushrod without friction. The LVDT is connected to a computer that uses an analog connection with WorkBench™ data acquisition software for Macintosh (Strawberry Tree Incorporated, California, USA). The computer has an already installed data acquisition card.

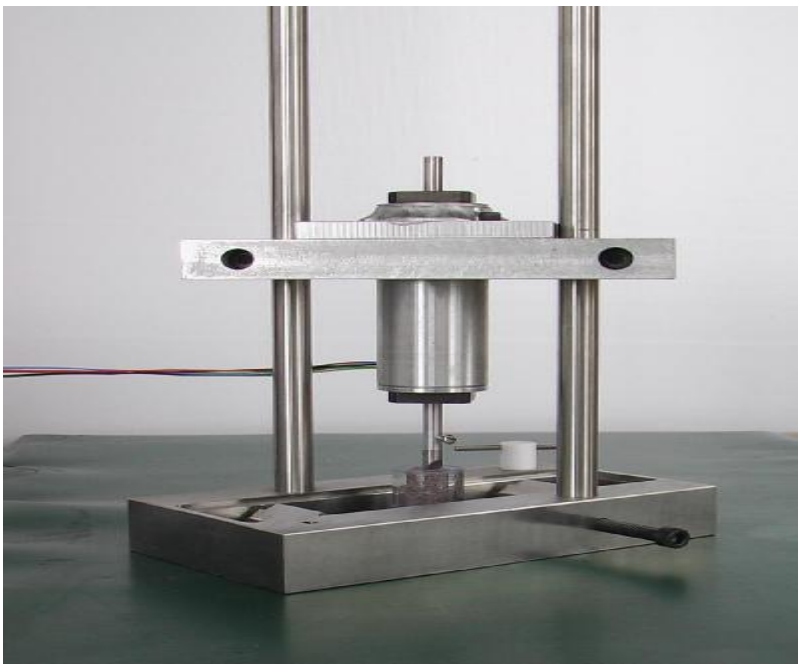

Figure A1- 8. Homemade dilatometer for measuring free swelling.

[9] The picture shows that the set up includes a metallic bath. This is not necessary for measuring the swelling and comes from the requirement of another experiment that uses the same frame.

The tests were performed by using mostly parallelepiped samples about 25×6×6 mm. Some of them were untreated and others were treated with swelling inhibitors and/or brine solutions. The samples were placed to stand on their smallest surface in a glass container, as illustrated in Figure A1- 9. The swelling was measured in both bedding orientations, meaning that two sets of samples were cut for this purpose. The sample was placed in a glass container and the pushrod lowered on top of it. Once the data acquisition was started, deionized water was poured around the sample until it reached the upper surface of the sample without covering it. As soon as the surface got wet, the sample started swelling.

This technique measured only the linear change of length experienced by the sample when in contact with water, and was plotted versus time by the computer.

Figure A1- 9. Detail of the pushrod tip and LVDT used for measuring the free swelling of stone sample, which was placed in a glass container.

Calipers for measuring swelling

This is a very simple and direct method developed to measure the swelling capacity of stone samples quickly. Despite being much less accurate than the above

techniques, it is much faster and is sufficient to screen treatments aimed at reducing swelling.

Electronic stainless steel calipers (Mitotuyo) that measure up to 150 mm with 0.01 mm resolution were used. For these experiments, they were placed in a holder in order to keep them in a fixed position as shown in Figure A1- 10. A parallelepiped sample (12-14×1×1 cm) was placed on a specially built stainless steel support in a container. The calipers were zeroed and placed into tight contact at each end of the 14 cm long sample. In most cases this measurement was done for samples whose bedding planes were orientated perpendicularly to the sample length. Once the set-up was ready, deionized water was poured into the container until it covered the whole sample except the upper surface. The sample started swelling and the caliper displayed the length change. The stainless steel support facilitated solution access to the bottom of the sample.

Figure A1- 10. Caliper set-up for quick measurements of swelling.

A1.2.3 Elastic modulus

Measurements of the elastic deformation of the sample were made to determine the modulus of elasticity or so-called Young's modulus of the stone. For that purpose, dynamic and static techniques were used and the results of both methods compared.

Both techniques have been used to measure the stiffness of untreated as well as treated (with swelling inhibitors and /or consolidants) samples of the main stones used in this thesis.

Dynamic elastic modulus

The elastic modulus can be measured by ultrasound propagation velocity. In this case, one refers to the measured property as the dynamic elastic modulus. The deformations produced in the sample by this technique are extremely small and well within the elastic limit of the material.

The instrument used is a portable PUNDIT (CNS Electronics, London, England) with a resolution of 0.1 μs. It is composed of two 54 kHz interchangeable transducers (emitter and receptor) covered by a stainless steal casing, a pulse generator, a timer, an amplifier and a filtering and registering system.

To obtain reliable measurements there must be good transmission of the ultrasound between the transducers and the sample. For this, vacuum grease is usually applied at the interface to provide a good contact. However, this is not desirable in this case because many samples undergo subsequent treatments such as impregnation by aqueous solutions. For this reason, nitrile pads were used (CNS Farnell Limited, Elstree Business Centre, Elstree Way, Borehamwood, Herts, England. WD6 1RX). Before applying the pads, the sample surfaces were dusted.

Apart from using a good coupling material, a sufficient force must be applied to allow a good transmission of the sound wave. To obtain reproducible results, a homemade aluminum and stainless steel frame was built (Figure A1- 11). It allows to read from a gauge cell the force applied when pressing the sample between the two transducers. These transducers are inserted into plastic casings to limit acoustic transmission to the frame. The force that is usually sufficient to get a good contact is about 100 N and is kept constant during the measurement. The measuring capacity of the gauge is 200 N.

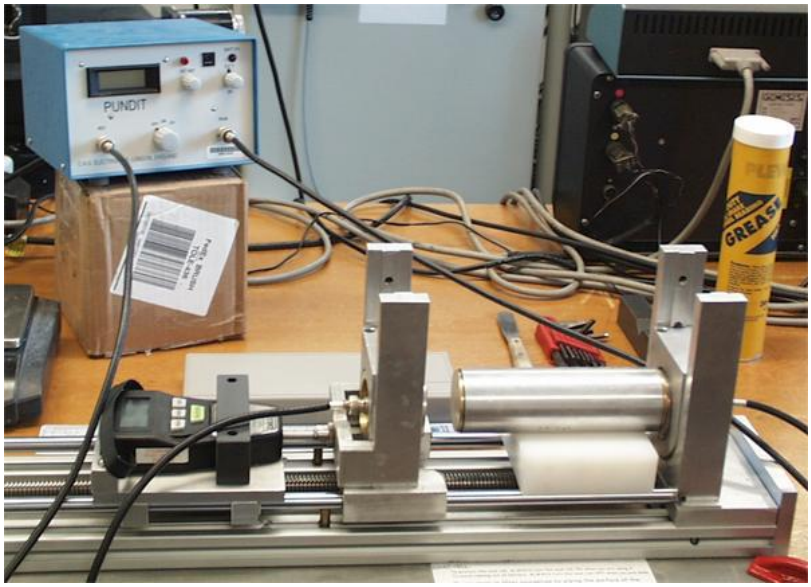

Figure A1- 11. Pulse delay measurement device showing the Pundit and the calibration bar on the homemade frame allowing to read the applied pressure (black gauge to the left).

Under these conditions, the instrument provides a reliable measurement of the transit time (Δt) in µs. It corresponds to the time needed for the fastest sound wave to travel through the sample and the pads. To determine the sound velocity through the sample alone, the transit time through the pads is deducted. This value was obtained as indicated below.

Before each measurement session, the instrument was calibrated by adjusting the transit time through a calibration bar to a known value (25.8 µs). In doing so, the coupling was done with Castrol® water pump grease. After this, the grease was removed and the measurement was repeated with nitrile pads as coupling agents. The transit time was systematically higher (by about 1.2 µs). Taking the difference between both transit times gives the transit time (Δt_0) through the nitrile pads.

With the sample length (L) and the transit time (Δt) through both, the sample and pads, the pulse velocity (v) can be determined by:

$$v = \frac{L}{\Delta t - \Delta t_0} \tag{A1-1}$$

Having determined the pulse velocity, the dynamic elastic modulus (*E*) can be easily calculated by using equation (A1-2) that takes into account the bulk density of the sample (r) that we measured.

$$E = r v^2 = r\left(\frac{L}{\Delta t - \Delta t_0}\right)^2 \quad \text{(A1-2)}$$

This equation shows that if two stones composed of the same mineral have identical sound velocity, they could still have different elastic moduli if their bulk densities were different. In such a case, the stone with equal composition but higher porosity would have the lower elastic modulus.

Dry and wet samples have been tested. For the wet measurements, the samples were previously saturated with water under vacuum or spontaneously (i.e., by capillary rise). To keep wet samples saturated, a wet sponge was placed around the sample during the short time the measurement lasted.

Elastic modulus by static measurement

In the present work, two homemade beam benders were used (Figure A1- 12 and Figure A1- 13). The same instruments were also used to measure stress relaxation and this is described later. These beam benders have computer controlled stepper motors (Ultra Motion, Mattituck, NY) capable of moving up to 3.75 mm/s as well as two type K thermocouples (one on the frame and one in the bath). This motor displaces a load cell, on which a push rod is mounted that feeds through an LVDT (Macrosensors, Pennsauken, NJ) allowing displacements to be measured over 10 mm with a resolution of 0.2 μm (Figure A1- 12). The software DaisyLab 5.0 (lotech, Cleveland, OH) is used to computer-control these motors from a Microsoft Windows 98SE platform. The load cells are from SENSOTEC (Columbus, OH, USA) and have capacities of ± 50, ± 250 and ± 1000 g. Two counterweights fixed to the load cells (± 250 and ± 1000 g) were also used when required to increase the measuring range with the given load cell. Known weights were used to check the calibration of each load cell by fixing them on the pushrod.

To optimize the stability of the stone plate, the best supports were a stainless steel cylinder about 6.3 mm in diameter at one end and a stainless steel sphere also about 6.3 mm in diameter at the other end. The cylindrical support was confined in a

slot allowing only slight rotation without translation. The spherical support was held in a hemispherical cavity. The position of these supports could be changed to adjust the length of the span. The tip of the push rod was a half sphere also of 6.3 mm diameter.

The push rod included an iron core section, which allowed its motion to be detected by the coil of the LVDT. The frame that supported the LVDT, motor and load cell was designed to provide optimum dimensional stability and allow optimal alignment.

The stainless-steel bath that hosted the sample rested on a rubber pad to minimize vibrations. The whole set-up was placed inside an incubator kept at a constant temperature of 28°C. It was checked for dimensional and thermal stability (about 0.1°C) as well as alignment. Further details on this instrument were given by Vichit-Vadakan (2002).

Figure A1- 12. Home made beam bender apparatus and equipment in the incubator.

The stone plates used in these experiments were typically 12 cm long, 2.5 cm wide and 3-4 mm thick. After placing them carefully on the supports, the pushrod was lowered until it contacted with the sample surface at mid-distance between the two supports. For runs under saturated conditions, the sample was previously vacuum impregnated and left under water until the test was performed. Before this, the bath was filled with de-mineralized water. A plexiglas cover allowing free movement of the pushrod was used to reduce evaporation from the bath. The samples were left in the incubator for a few hours to equilibrate before beginning the experiment.

The experiment was started when the baseline drift was negligible. For this, the desired deflection was input into the computer and the program initiated. This directed the pushrod to move up and down by the desired deflection at least 7 times at an average velocity of 28 microns/ second. The maximum deflection was chosen based on the beam dimensions and an estimated modulus, so that the stress did not exceed the tensile strength of the stone; the minimum deflection was greater than zero, to insure that the pushrod remained in contact with the sample at the top of the cycle.

Load versus deflection data were used to calculate the Young's modulus (E^{est}) of the samples according to the following equation:

$$E^{est} = \frac{Ww^3}{4ch^3\Delta} \qquad \text{(A1-3)}$$

where w is the span or distance between the supports, c is the width of the plate, h is its thickness, Δ is the deflection and W is the load needed to obtain that deflection.

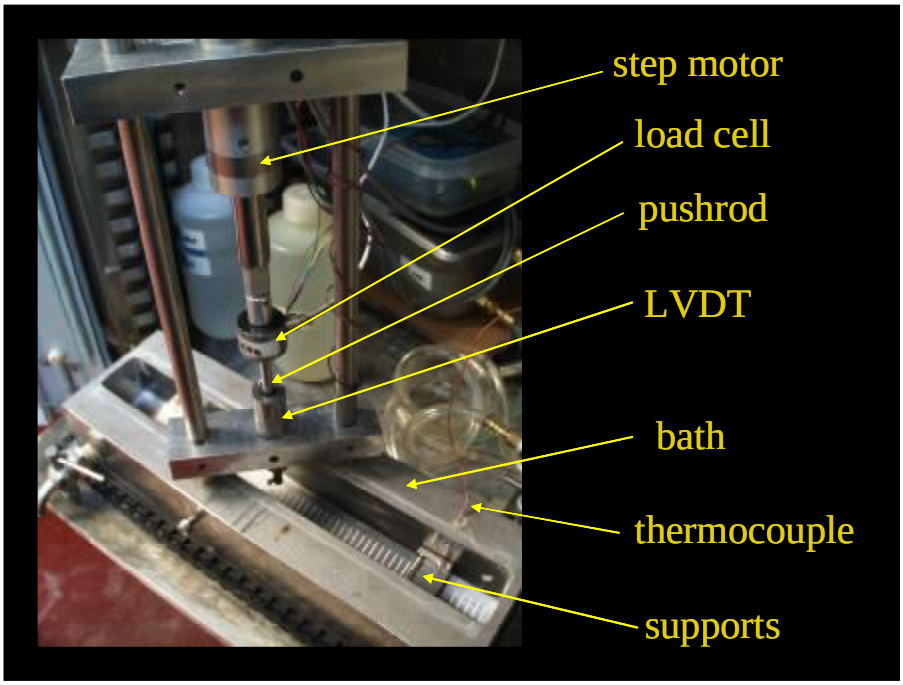

Figure A1- 13. Close-up of one of the beam bending apparatus used. The measurement set up is inline.

A1.2.4 Tensile strength

Indirect tensile strength test (also known as Brazilian test) was made to measure the tensile strength of the stone specimens under tension. It was performed on an INSTRON® testing machine (Instron Corp., Norwood MA, USA), with the testing software to control the loading and data acquisition as well as to calculate the peak load. The displacement resolution of the machine is 2.54 µm. The samples were 2 cm in diameter f and 5 cm in length L.

In the case of *Portland Brownstone*, *Villarlod Molasse* and *Tarifa sandstone*, samples were cut both parallel and perpendicular to the bedding planes. These tests were done on dried samples for all those stones. Only in the case of *Portland Brownstone*, wet tensile strengths were measured.

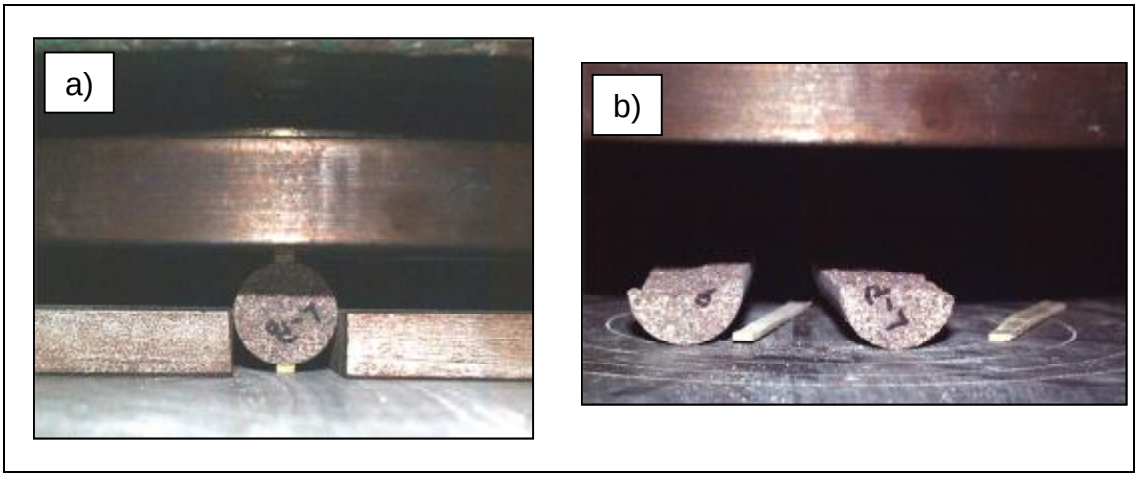

Figure A1- 14. Cylindrical stone sample between loading plates of an INSTRON® testing machine. Thin balsa wood sticks were used to insure homogeneous stress distribution along the sample length in contact with the plates. a) The picture shows how the sample was positioned when bringing the upper plate into contact before starting the test. b) Split sample at the end of the test.

Cylindrical samples with a 2 cm diameter (f) and a length (L) of 5 cm were placed horizontally between the two loading plates (called *platens*) of the Instron machine. At the sample/platen contacted surface, two balsa wood sticks[10] were placed parallel to the length of the specimen, below and above it. They were 5 cm long and around 3 mm wide and preloaded before use. To prevent the sample from rolling aside, two metal blocks were used. The upper platen was gently brought down until getting close to the wooden stick. At that point the upper platen had to be reoriented until it was perfectly parallel to the sample; otherwise the load distribution was uneven and the result was unreliable. The lowering of the platen continued until touching the balsa stick on top of the sample (Figure A1- 14a). No load should be applied at that moment, just enough to keep the sample in a balanced position. Then, the metal blocks already mentioned were removed. At that point, the load was progressively increased by raising the lower platen at a constant rate of 2.5 mm /minute, which typically caused

[10] These sticks permit a good contact between the surfaces in contact. Because of their capacity of deforming, they allow the pressure to be uniform along the stone. Their width must cover a region not bigger than 1/6 of the diameter of the sample to ensure homogeneous application of the load along the cylinder edge.

failure in less than one minute. A computer recorded the evolution of the load as a function of displacement. Once the sample broke, it split in two as shown in Figure A1-14. The load then suddenly dropped and the experiment finished. Through the Partner™ Materials Testing Software (Instron Corp., Norwood MA, USA), the computer gave the peak load (P_{max}), which was used to calculate the tensile strength (s) of the material according to the well-established expression (Mindess and Young, 1981):

$$s = \frac{2P_{\max}}{p f L} \tag{A1-4}$$

A1.2.5 Stress relaxation

The same homemade beam benders previously described in the section dedicated to static measurement of the elastic modulus were used to determine stress relaxation. They were built with particular care to fit the requirements of long relaxation measurements. The set-up and sample preparation for both wet and dry samples was basically the same as for the static modulus measurements described previously. In addition, when performing the wet stress relaxation tests for runs over 24 hours, a gravity-based refill system was used with the beam bender. The bath was fed from an external reservoir whose level was controlled by a float valve, while minimizing disturbance of the liquid in the bath.

The main difference with respect to the measurement of the modulus was that in this case, when the run started, the computer imposed the desired deflection and maintained it for a long period of time (typically up to a maximum of 22 hours, although some tests were done up to about 120 hours).

The data of load versus time were analyzed to extract the viscoelasticity parameters defined in Vichit-Vadakan and Scherer (2003).

A1.2.6 Fatigue resistance (Wetting and drying cycles)

It is well known that cyclic processes even in very strong and stable material can eventually cause damage by fatigue. It is expected that this may be the case for wetting and drying cycles of clay containing stones. To measure the resistance to that process,

we built a machine that allowed automatically subjecting *Portland Brownstone* samples to such cycles, which made it much easier to test the effect of many cycles. This was necessary, because the initial manual testing with up to about 20 cycles did not show any significant change in mechanical properties of this stone and testing after much more cycles was required.

The machine is illustrated in Figure A1- 15 and consists of two parallel belts on which rings of stainless steel springs allow to fix thin stone plates. Rotation of the wheels on which the belts are fixed brings the samples successively into a water bath and a zone in which fans dry the samples. In our experiments, the motor speed was set so as to complete one wetting/drying cycle per hour (for testing thin plates of *Portland Brownstone*). Given their sorptivity, these samples that were only 3 to 4 mm thick saturated in about 1 to 2 minutes, so the duration of these cycles was considered to be sufficient both for the wetting and the drying. Further information about this technique and its use is given in Anexo 5.

Figure A1- 15. Illustration of the wetting and drying machine.

A1.2.7 Sorptivity

Sorptivity experiments were done with a Denver Instrument XL-410 electronic balance with a 0.001 g resolution. This was connected to a computer and the data were

acquired with Software Wedge. The samples had different sizes in the cm range. They were connected to a metal holder fixed to the bottom of the balance. Below this, there was a large glass dish containing water and placed on a screw jack. After initiating the data acquisition, the screw jack was raised to contact the water with the bottom of the sample (Figure A1- 16). The last millimeters before contact, the rate of rise was reduced to avoid instability of the water surface. The sample then started soaking up the water and the increase in mass was recorded as a function of the time.

The vertical sides of the sample were coated with grease prior to the experiment. On one hand this was done to prevent water evaporation from the sample and on the other, it limited sudden suction of the sample from wetting of the sample perimeter. In order to avoid evaporation of the water reservoir, the glass dish was covered with plexiglas plates. The samples were left until the weight stopped increasing, indicating that saturation was complete.

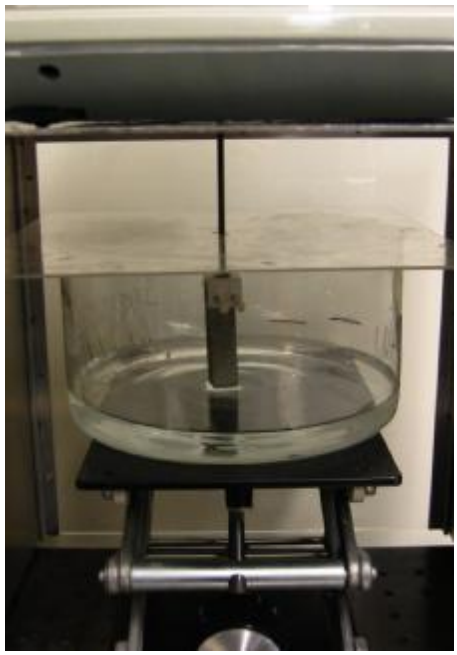

Figure A1- 16. Illustration of the sorptivity set-up. The vertical bar is connected to the bottom of the scale, which is not shown in this picture.

A1.2.8 Vacuum impregnation

The porosity obtained from the saturation plateau in the sorptivity experiment described above might not correspond to the total volume of pores, since some air can get trapped inside and prevent water from entering certain parts of the sample. To determine the "real" total open porosity, the stone was subjected to vacuum and impregnated with water.

Samples with different geometries and sizes were used. They were weighed and measured before the impregnation started. Then, the stones were placed in a desiccator that was connected through one tube to a vacuum line (where a pump draws the air that the stone contains) and to a water supply (Figure A1- 17) through another tube. During the application of vacuum (about 15 minutes) the water supply tube was closed. When the sample was ready for impregnation, the vacuum line was closed. The water line was slowly opened and water was drawn in until it completely submerged the samples. The atmospheric pressure was then re-established inside the vessel and the samples were left at least overnight for full saturation.

Figure A1- 17. Apparatus for vacuum impregnation.

Knowing the water density (r_{water}) and the volume of the stone sample (V_{stone}), the porosity, ($ø$) is given from the impregnated mass (Δm) of water by the following equation:

$$f = \frac{\Delta m}{V_{stone}\, r_{water}} \tag{A1-5}$$

A1.2.9 Mercury intrusion porosimetry

The volume of pores and their size is important information for evaluating the durability of porous materials. The technique most widely used to characterize both these properties is mercury intrusion porosimetry (MIP).

The principle of the technique is that mercury has a high surface tension and is a non-wetting liquid for most of the surfaces. Pressure must therefore be applied to force mercury into a porous material (Lowell and Shields, 1984). The pressure (P) at which mercury intrudes is related to the pore radius, r, according to:

$$P = -2\frac{g_{LV}}{r}\cos(q) \tag{A1-6}$$

where g_{LV} is the liquid/vapor interfacial energy of mercury and q is the wetting or contact angle. Since mercury is non-wetting, q is greater than 90˚ (usually the instrument assumes a q ~130˚).

The amount of mercury that enters at a given pressure gives the volume of pores of that size. By progressively increasing the pressure, one gradually fills the material with mercury, starting from the larger pores and finishing with the narrower ones.

The instrument used (Figure A1- 18) is an AutoPore 9420 from Micromeritics® (Narcross, GA, USA) that can go up to pressures of 414 MPa (60,000 psia). It features two low-pressure ports and one high-pressure chamber. In the low-pressure ports, it measures from 0 to 345 kPa (50 psia) with a resolution of 69 Pa (0.01 psi). This corresponds to pore diameter between 360 µm and 3.6 µm. In the high-pressure port, it measures from 0.1 MPa (14 psi) to 414 MPa (60,000psia) with the following resolutions: 2070 Pa (0.3 psi) from 34 MPa (5000 psia) to 414 MPa (60000 psia) and 207 Pa (0.03 psi) from atmospheric pressure to 34 MPa (5000 psi). Theoretically, it has the possibility to measure pore diameters of 6 to 0.003 (3nm) µm.

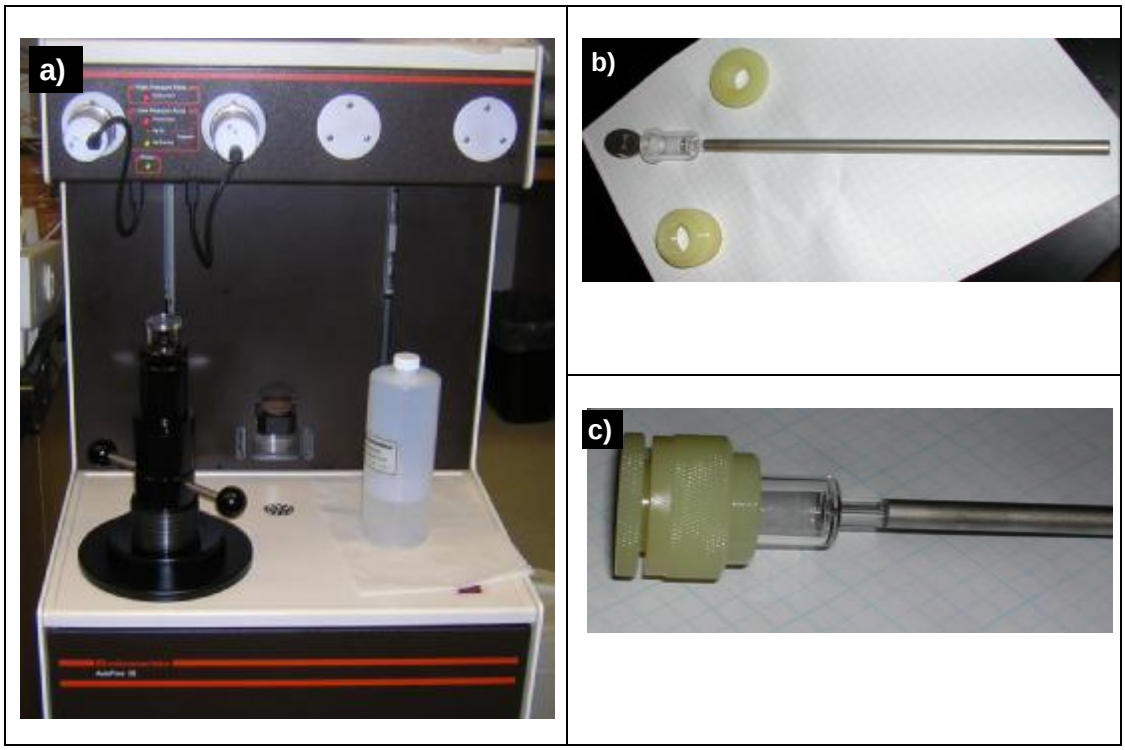

Figure A1- 18. Picture of the porosimeter (a) the penetrometer (b) and detail of the penetrometer sample holder (c).

A1.2.10 Helium pycnometry

The porosimetry measurement techniques described above require knowledge of the skeletal density of the material in order to express porosity as a volume fraction rather than in units of pore volume per unit mass. The skeletal density is the density of the material itself in its non-porous state.

The technique used to measure this parameter on our samples is helium pycnometry (Figure A1- 19). The instrument is an Accupyc 1330 from Micromeritics® (Narcross, GA, USA).

An oven dried and weighed sample was placed into a sample chamber of volume V_1. That chamber was flushed with helium and then pressurized with the same gas to an initial pressure P_1. The law of ideal gases allows writing:

$$P_1(V_1 - V_S) = nRT \qquad \text{(A1-7)}$$

where V_S is the volume of the sample skeleton (without its porosity), n is the number of moles of helium (He) introduced, R is the gas constant and T the absolute temperature.

Once the pressure has equilibrated, a valve that communicates between the sample chamber and another chamber of volume V_2 is opened. A new pressure, P_2, is established. The following equation can then be written:

$$P_2\left(V_1 + V_2 - V_S\right) = nRT \tag{A1-8}$$

This allows to calculate the sample volume as:

$$V_S = V_1 - V_2 \frac{P_2}{P_1 - P_2} \tag{A1-9}$$

Figure A1- 19. Picture of the Helium Pycnometer.

A1.2.11 Nitrogen Sorption

The technique of mercury porosimetry described previously is quoted to determine the volume and size of pores in a material down to sizes of about 3 nm. In fact, the measurements in the low pore size range are questionable; because the high pressure needed to penetrate such small pores can damage the sample. These sizes are important for the issues of wetting and drying cycles, because such porosity can be expected in and among clay particles. The technique of nitrogen adsorption can

provide more reliable porosity measurement in this range. For the instrument described below the range accessible by this technique is from 1 to 50 nm.

The nitrogen sorption instrument used is an ASAP (Accelerated Surface Area and Porosimetry system) 2010 from Micromeritics® (Narcross, GA, USA).

It contains two sample conditioning ports, an analyzer, a control module, which enables to enter analysis and report options and an interface, which controls the analyses. The whole instrument can be seen in Figure A1- 20.

Samples were first oven dried at 105°C and then ground into a fine powder using an agate mortar and pestle. The powder was placed into the glass sample holder, which was then fixed onto the instrument where it was degassed at 105°C. A heating mantle was fixed on the sample holder during this operation. This degassing lasted until a stable pressure of 5 µm of mercury (0.67 Pa) was obtained. The heating mantle could then be removed and the sample holder placed on the analysis port. The experiment can then be launched from the Autopore software. It began by drawing vacuum on the sample and then bringing it down to 77 °K by raising a platform on which a container with liquid N_2 was placed.

Controlled doses of nitrogen were then introduced into the sample tube and the equilibrium pressure was measured. This wet on until nitrogen condensation (100% vapor pressure), so that the sample holder was filled with liquid nitrogen. Desorption was then initiated. The pressure was reduced by steps, which allowed vaporization of condensed molecules and desorption of the adsorbed ones. From the adsorption process, the software calculated the Brunauer, Emmett, and Teller (BET) surface area.

$$\frac{P_a}{V\left(P_0 - P_a\right)} = m_1 \frac{P_a}{P_0} + m_2 \qquad \text{(A1-10)}$$

where P_0 and P_a are respectively the saturation pressure and the actual pressure of adsorbate gas, V is the volume of the adsorbed gas while m_1 and m_2 are fitting parameters.

The volume of gas needed to form a complete monolayer is $1/(m_1+m_2)$. Knowing the surface that one nitrogen molecule occupies (0.162 nm^2), it can be converted to a specific surface.

Capillary condensation causes the adsorbed gas to be bound more tightly in smaller pores. This is the basis for determining pore size distribution, best done from

desorption experiments. The radius r_p of pores in which capillary condensation takes place is linked to the pressure P_a through the BJH equation:

$$\frac{-2g_{LV}}{r_p - d} = \frac{RT}{v_l} \ln\left(\frac{P_a}{P_0}\right) \qquad \text{(A1-11)}$$

where g_{lv} is the liquid/vapor interfacial energy, r_p is the pore radius, d is thickness of the adsorbed layer on a flat surface, R is the universal gas constant, T is the absolute temperature, and v_l is the molar volume of the adsorbate in liquid state.

Figure A1- 20. Nitrogen sorption instrument.

A1.2.12 RH-sample equilibration

To equilibrate samples at selected relative humidities before running certain experiments, samples were stored in boxes insuring stable relative humidity and good convection (see Figure A1- 21). Recommendations by Mr. F. Girardet of the "*Expert Center pour la Conservation du Patrimoine Bâti"* of Lausanne (Switzerland) were followed. On the bottom of each box, a container with a saturated salt solution was placed (i.e. with an excess of the dissolved salt). These boxes were perfectly hermetic. Above the salt containers there were shelves on which the samples were placed. A hole about 5 cm in diameter was drilled in their centers. Below them, fans were fixed to

ensure good convection in the chambers. A thermo-hygrometer was placed in each chamber and the humidity was regularly checked for stability. The precision (+/- 1-5%) of these hygrometers was too low to insure that the exact expected humidity was achieved, however it was sufficient to check that no significant drift was taking place.

The previously dried samples that were stored in these chambers were parallelepipeds and cylinders that were subsequently measured for their swelling. In addition, plates used for warping and bending were also equilibrated in these chambers. For these test on the role of RH only *Portland Brownstone* samples were used.

The saturated salt solutions used were of sodium sulphate decahydrate (or mirabilite, $Na_2SO_4 \cdot 10H_2O$), potassium chloride (or silvite, KCl) and sodium chloride (or halite, NaCl), giving relative humidities at the lab temperature (25°C) of respectively 91.4%, 84.3% and 75.3% (Arnold and Zehnder, 1990).

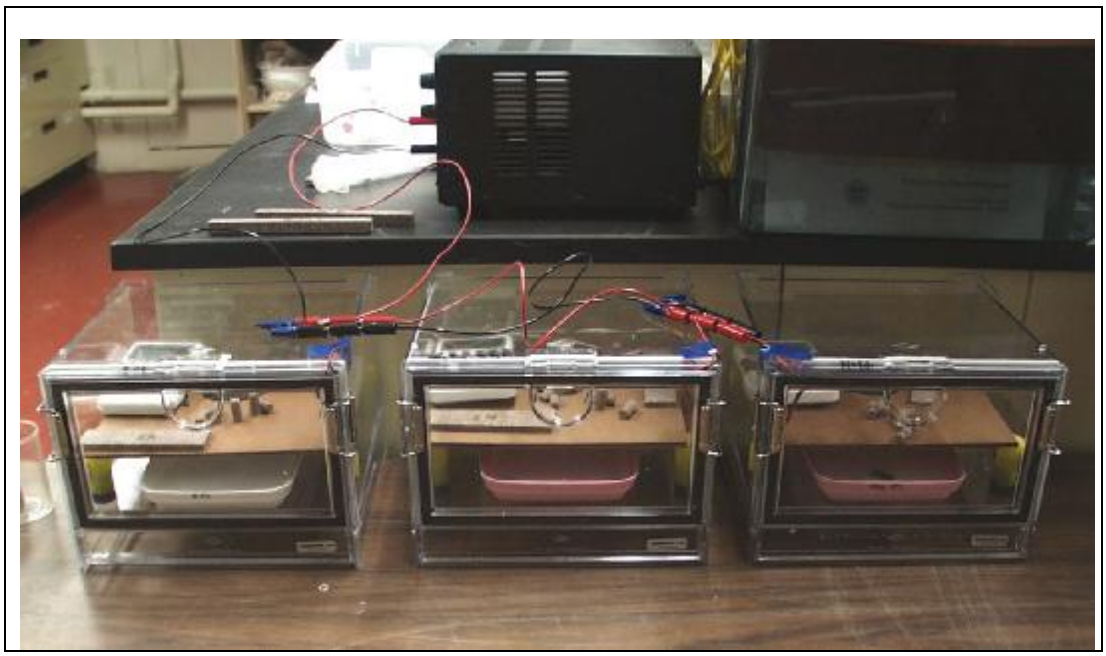

Figure A1- 21. Humidity boxes showing the plate on which samples were placed and the container with a saturated salt solution to regulate relative humidity. The centre of the plate contained a hole below which a fan was placed for good air circulation.

A1.2.13 Direct measure of swelling pressure

In this section, a technique is described to measure the pressure that a stone exerts when it tries to swell, but is prevented from doing so by an externally applied load. The technique is adapted from a frequently quoted study by Madsen and Müller-Vonmoos (1985) on this topic. However, some changes were introduced in terms of sample size and geometry for this experiment to last a few hours instead of two weeks as in the previously mentioned study.

The tests were performed on *Portland Brownstone*, *Villarlod molasse*, and *Tarifa sandstone* samples. Parallelepipeds (5×3×3 cm) and cylindrical (5 cm ∅ and 5 cm height) sample geometries were used to perform this type of test. In both cases, the center of the sample was drilled out by using a core drill with a diameter of 2 cm.

The hollowed sample was placed between two stainless steel cylinders (8 cm ∅ and 3 cm height) that were drilled in their centers as well as laterally. The sample plus the cylinders were placed in a specially designed container that had a stainless steel base (12 cm ∅ and 2.5 cm height) and plastic walls (Figure A1- 22b). The whole set up was then placed between two metal plates of the INSTRON® machine described before, paying attention that they would only exert a very small pressure on the stone sample, just enough to establish a contact such that pressure would be measured as soon as the sample started to swell.

After placing the sample under that slight load- which was set manually- the test began. This consisted in the machine increasing its load until about 50 N. At that point, the position was set to zero and the machine was instructed to maintain that position. Because the loading did not stop immediately, the position was overshot and some time was needed to regain that position. Once it was clear that position and load were stabilized, deionized water from a bottle was quickly introduced into the container through a plastic tube fixed at the bottom of the bottle. As soon as the liquid contacted the sample, surrounding it and flowing in also through the hollowed core (Figure A1-22a), the stone started to try to swell. However, this was prevented by the INSTRON® testing machine, which increased its load to keep the sample to its initial dimensions. The load increased over time to a maximum value that could be used to determine the swelling pressure. The kinetics of this process were analyzed and linked to sorptivity, stress relaxation and free swelling strain as explained in Anexo 4.

The reason for having a drilled sample and the metallic cylinders with several holes (one at their centers and the rest at their walls) was for the water to have a faster

ingress in the stone, saturating the sample in a record time- 10 times less than the time required if the center of the sample was not previously core drilled in its center.

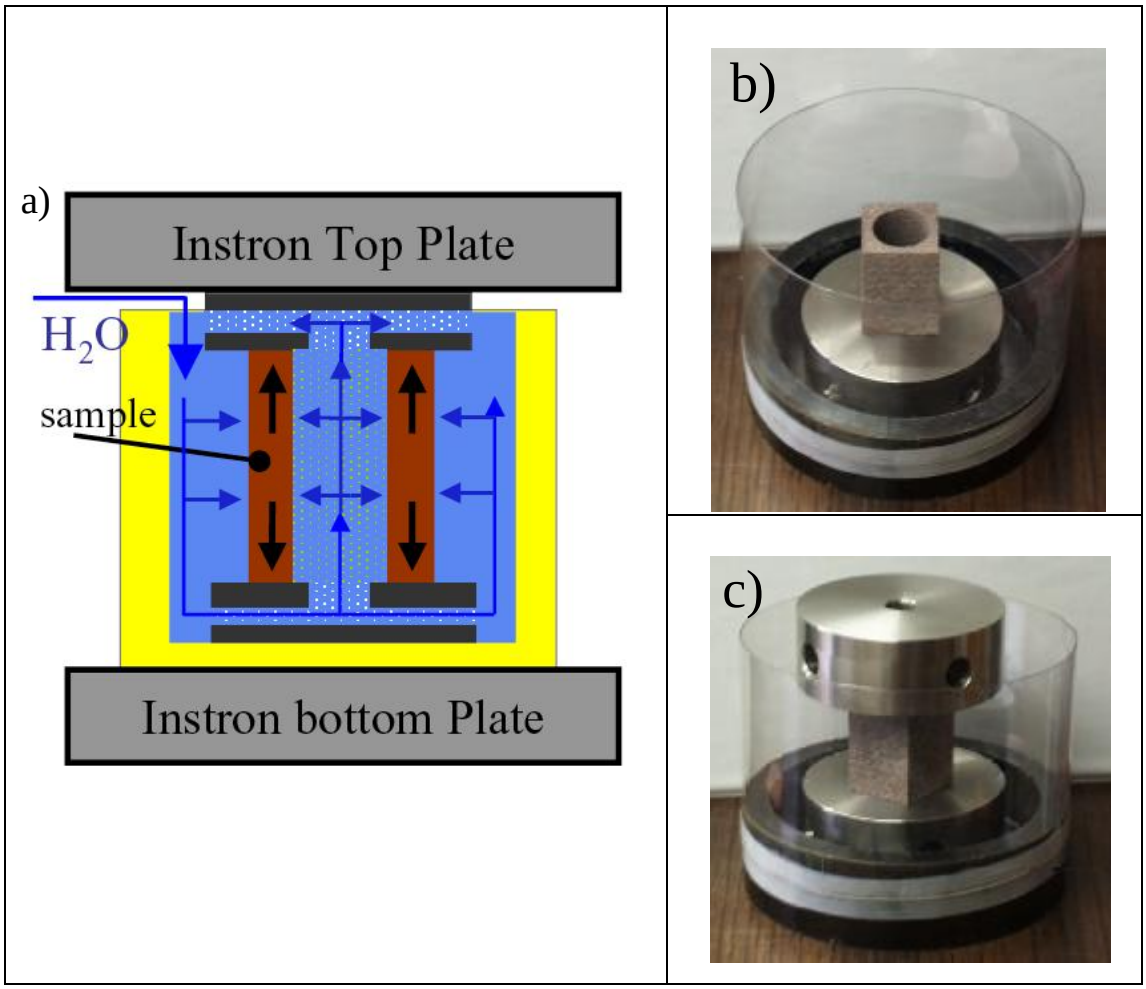

Figure A1- 22. Illustration of the direct measure of swelling pressure set-up: a) sketch showing how water infiltrates the sample core, b) image of the cored sample resting on the stainless steel perforated base, c) image of the sample as placed in the Instron machine.

A1.2.14 Warping device

The application of a warping technique to the study of stone swelling has been an innovation in this thesis and various papers have reported the results obtained (Anexo 2, 4-7).

The simplest illustration of warping comes from a plate composed of two layers of materials with different thermal dilatation coefficients. When the temperature changes, the material with the largest thermal dilatation coefficient wants to expand more than the other. A stress balance leads the plate to bend in one direction if heated and in the other if cooled. The extent of the bending depends of the thermal dilatation coefficients, the elastic modulus and thickness of the layers.

Various variations around exploiting this type of behavior can be found in other fields. They use the mathematical analysis of the deflection as a way to characterize at least one of the material properties.

With clay bearing stones, it is not the thermal expansion that causes expansion of a layer, but the wetting of the upper portion of the stone. Indeed, the wet part wants to expand, while this is not the case for the dry part. In these experiments, water is added on the top of a stone plate and progresses through the plate as time passes.

The samples which are long and thin plates were placed horizontally on two supports and a dam was created on its top surface to prevent the added water from running down the sides (Figure A1- 23a). In the first tests, this was done with a grease strip. Later the solution of a sealant “barrier” with an elastic and soft material called “caulk tip” was preferred. Indeed, this material could be easily removed once the test was complete, allowing the sample to be reused more easily than if grease was used. At the same time it did not prevent the sample from warping when in contact with water[11]. Therefore the role of this “dam” was just to retain the water on the upper sample surface without interfering otherwise with the experiment. Such a sealant barrier is illustrated in Figure A1- 24.

[11] This is shown by comparing results with tests done previously, which used grease instead of this sealant material.

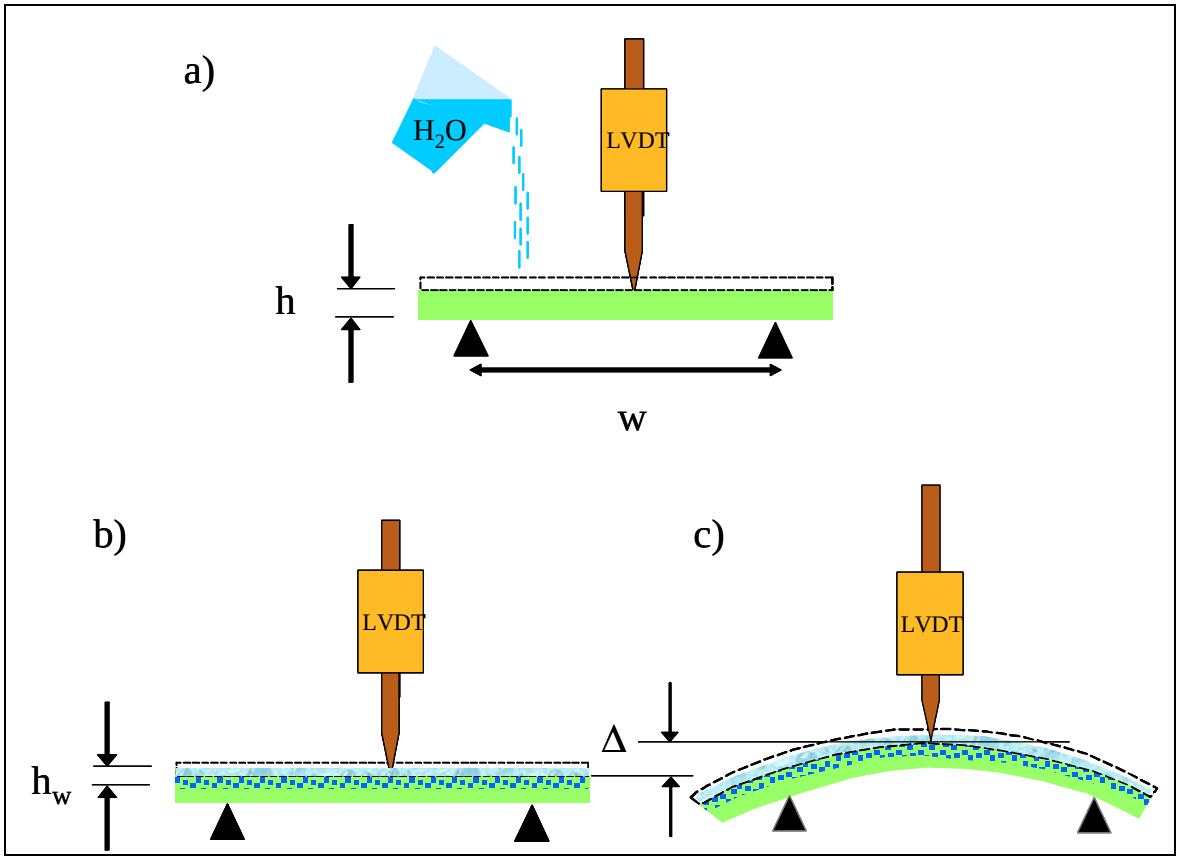

Figure A1- 23. Schematic representation of a warping experiment. a) sample of thickness h placed on two supports separated by a span w. The tip of a pushrod going through an LVDT rests on the sample. The discontinuous line on the top of the sample symbolizes the dam. The experiment starts when water is poured on the sample. b) as water progresses through the sample, the wet zone tries to expand, c) this causes a deflection, Δ, of the plate that is measured by the LVDT and depends on the depth h_w reached by the water at the time of measurement.

The samples were typically 10 cm long, 2.5 cm wide and between 2 and 6 mm thick. The thickness was chosen depending on the swelling and mechanical properties of the particular stone to give sufficient deflection during the experiment. A homogeneous thickness, smooth on its upper and lower surfaces and free of cutting defects is very important for this test. Thus great care always has to be taken when cutting these thin samples. Specially made fixtures were used on the saws to increase the quality of the cuts.

Most of the tests were performed using samples with their bedding perpendicular to the sample length. In only a few cases the deflection was measured on samples with their bedding planes parallel to the sample length.

Figure A1- 24. Warping device set up. Detail of the sample preparation before pouring the water. The perimeter of the sample is surrounded with a sealant material in order to keep the water on the top surface during the whole test.

The test started when water was poured into the dam on top of the samples. For the reasons explained above, the plate started to bend upwards and the deflection was measured (Figure A1- 23b, c). This was done in two different ways. The first one was with an optical probe and only concerned the first measurements. The optical probe (MTI 1000, MTI Inst.) was mounted below the plate. The displacement was obtained by a measurement of the light intensity that was reflected by a small piece of reflective foil glued to the bottom of the plate. A description of the how the probe operates can be found in (http://www.mtiinstruments.com/gaging/products/mti-2000.html). This

technique was borrowed from experiments done in the same lab on samples of cement paste submitted to freezing.

Later, the deflection measurement was carried out with the same homemade instrument (using an LVDT) and software described for the free swelling strain measurement (case in Figure A1- 23). The only new elements incorporated were the two metallic supports for the sample at the base of the set-up (Figure A1- 24 and Figure A1- 25). This second technique was found to be more convenient in our experiments that do not have the problem of the formation of an ice layer on the top of the sample surface as in the cement case experiments from which the first set up was initially taken.

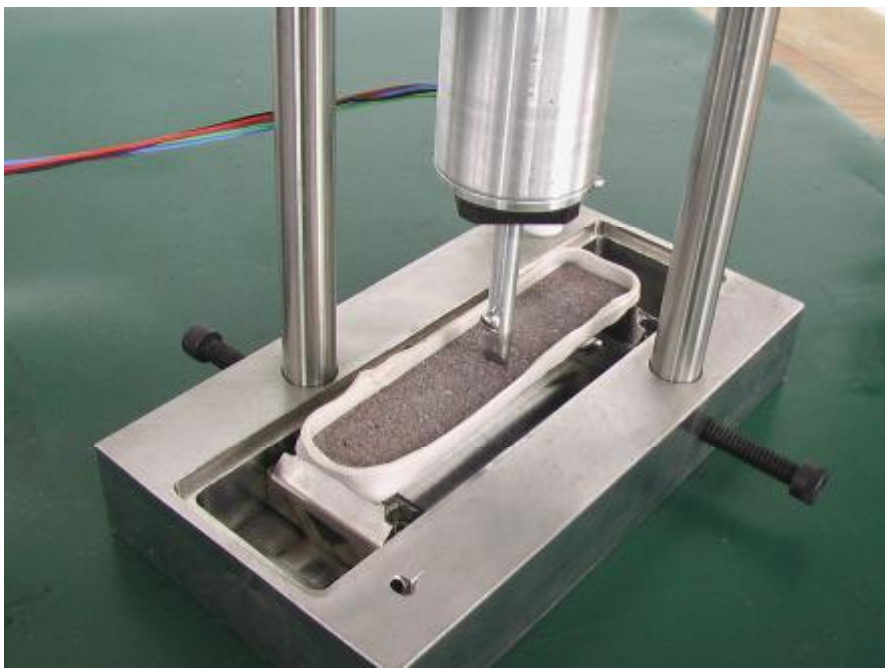

Figure A1- 25. Illustration of the warping set up.

These supports are equidistant from the vertical axis of the pushrod. Before the experiment started, the free pushrod (ended in a knife-edge tip) was placed in contact with the sample surface (the knife-edge was oriented perpendicularly to the sample length). As for the free swelling, the LVDT transforms an electrical signal from the displacement of the iron core on the push rod to produce an electrical output for displacement (1 mm correspond to 1 V).

The analysis of this process is presented in detail in Anexo 4 and in Anexo 6; a condensed way in Anexo 5.

A1.2.15 Scanning Electron Microscopy (SEM)

Imaging

Scanning electron microscopy (SEM) is a widely used technique, which, for stones, is mainly used to study the morphology and particle size of the grains. This is the main use of this technique made in this thesis. It is noted that SEM can also be used to study porosity on polished sections.

For morphological examination, the samples were small crushed pieces. For examination of the clays, samples were either a finer powder of the stone ground in an agate mortar and pestle or the pure clay fraction obtained following the procedure described previously. Finally, in order to examine the state of the consolidant in consolidated samples, the samples were small pieces that did not need any crushing (a few mm in dimension). In some cases they were split. This was done so that any cracking in the consolidant from sample preparation would be minimized.

Dried samples were mounted on an aluminum pin mount stub holder. In order to provide a conductive path for the electrons, a double-sided sticky carbon tape was placed on the holder surface, then, the specimen was stuck onto it. In the case of samples that were particularly thick (around 3-4 mm) the conduction from the sample to the support had to be enhanced. This was done in one of the two following ways. The first solution was to apply carbon paint between sample and the carbon tape. The second method was to fix some strips of carbon tape leading from the stub surface to the upper surface of the sample. In addition, in both cases these specimens were sputter coated. In most of the cases, carbon was used and applied by a standard carbon coater giving a layer of about 30 to 60 nm. In a few other cases, when analyzing very small clay particles, thinner and more homogeneous coatings were obtained with an IBS/ TM 200S Ion-beam Sputter (VCR Group, South San Francisco, CA). They were either carbon or iridium and their thickness was about 5 nm. Typical coating times were about 1 hour for carbon and 200 s for iridium.

The coated samples were inserted in the chamber of a Philips XL 30 FEG-SEM. After applying vacuum, imaging was performed using a secondary electron detector.

Typical imaging conditions were 10 kV for the acceleration voltage and about 10 mm for the working distance. Additional SEM images of the *Tarifa sandstone* were acquired on a Zeiss 900 from the *Centro de instrumentación Científica* of Granada University (Spain).

Elemental analysis

The Philips XL 30 also was equipped with an Energy Dispersive X-ray Spectrometer (EDS) detector that was used in some cases to perform an elemental composition analysis of the specimen. This was used for spot analysis, bearing in mind that the probed volume was much larger than the beam size. The technique is often described as semi-quantitative with errors estimated at 10%.

A1.2.16 Application of treatments

Impregnation by surfactants and swelling inhibitors

The effectiveness of various surfactants for reducing the swelling of *Portland Brownstone*, *Villarlod molasse* and *Tarifa sandstone* was tested. After an initial screening which ruled out products that made the stone hydrophobic or did not reduce swelling, a more elaborate screening was done on *Portland Brownstone* to identify the most efficient of the remaining products and their combinations.

In this procedure, the samples were (35×10×10) bars. Solutions of surfactants at 1 and 5% by weight were prepared. The samples were treated with 1% aqueous solutions, tested their swelling strain and then retreated with the same products at 5% and retested.

For the treatments that used mixtures of surfactants, the solutions of the products selected during the screening were mixed 50% by weight. This was done to avoid exceeding 5% concentration of total product in one treatment. Additional treatment by these mixtures did not increase the swelling reduction, so that these concentrations were sufficient.

The soaking procedure was as follows: oven-dried stone samples were placed horizontally in small containers where they were partially submerged in the surfactant solution. Each container was hermetically sealed to avoid evaporation. Samples were left to soak up the product until saturation, ensured by the constant sample weight. Soaking times for the three types of stones varied between 6 hours for *Villarlod molasse* and 20 hours for *Tarifa sandstone*. Once the impregnation was complete, samples were removed and left to dry under the hood for approximately 1 hour. Afterwards, they were placed in the oven to dry at 60°C.

Consolidation of samples

The samples to be consolidated were placed horizontally in a covered container containing the previously described ethyl silicate product Conservare® OH (not diluted) reaching one-third the height of the samples. In the case of the very thin plates used for bending and warping, this condition was difficult to satisfy and most samples were submerged. The samples remained in the Conservare® OH until they reached constant weight. After this, they were allowed to dry for about a week under a lab hood.

Anexo 2. Publicación nº.1

"Hygric swelling of Portland Brownstone"

Jiménez González, I.; Higgins, M. and Scherer, G.W.

in Materials Issues in Art & Archaeology VI, MRS Symposium Proc. (2002) Vol 712,

eds P.B. Vandiver, M. Goodway and J.L. Mass (Material Res. Soc.),

Warrendale, PA, pp. 21-27

Materials Issues in Art & Archaeology VI, MRS Symposium Proc. Vol. 712, eds. P.B. Vandiver, M. Goodway, and J.L. Mass (Materials Res. Soc., Warrendale, PA, 2002)

Hygric Swelling of Portland Brownstone

Inmaculada Jimenez Gonzalez, Megan Higgins, and George W. Scherer

Princeton University, Eng. Quad. E-319, Princeton, NJ 08544 USA

ABSTRACT

Portland Brownstone (PB) is a widely used building material, particularly in New York City, that is susceptible to severe deterioration from weathering. This stone contains clays that may cause damage by dilating during wetting/drying cycles. We have measured the swelling strain of PB in aqueous solutions to determine the effect of ionic strength (of KCl and $CaCl_2$) and water activity (in isopropanol solutions). We have also measured the stress exerted during swelling when the expansion is constrained. These data permit calculation of the stresses produced during wetting/drying cycles, which are found to be comparable to the tensile strength of the stone.

INTRODUCTION

Many types of stone contain inclusions of clay that dilate with changes in humidity. In some cases this leads to deterioration of the stone[1]; it can also result in destruction of consolidants[2]. This paper presents the results of preliminary investigations of the effect of swelling in a particular stone, Portland Brownstone, that is widely used as a building material in the eastern United States. This is a complex sandstone containing grains of quartz and albite in a matrix including kaolinite, mica, iron oxides, illites and smectites. The clay flakes around the quartz grains are evident in Figure 1.

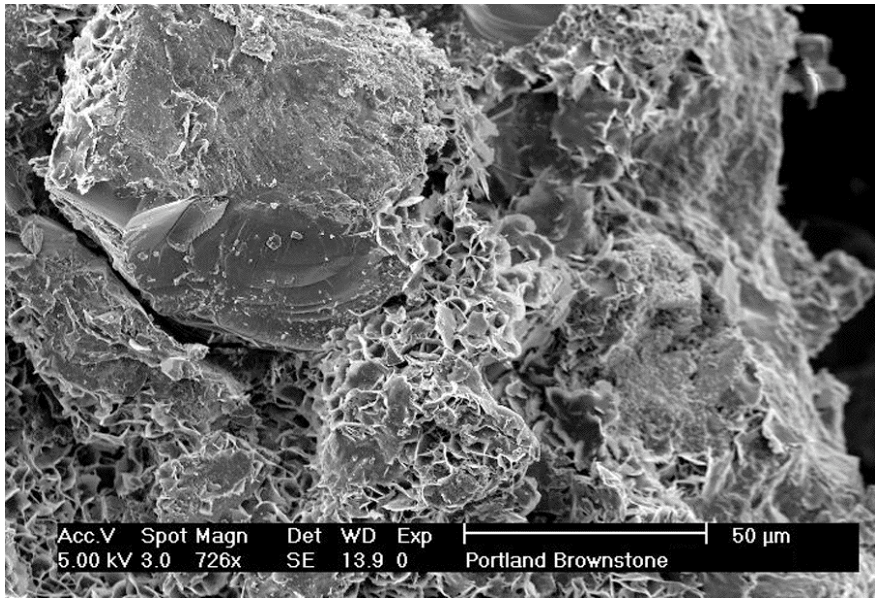

Figure 1. Scanning electron micrograph of Portland Brownstone used in this study.

Materials Issues in Art & Archaeology VI, MRS Symposium Proc. Vol. 712, eds. P.B. Vandiver, M. Goodway, and J.L. Mass (Materials Res. Soc., Warrendale, PA, 2002)

This stone is subject to relatively rapid deterioration from weathering, and swelling of the clay components has been suggested to contribute to the damage.[3] We will quantify the swelling stresses and show that they can exceed the strength of the stone.

EXPERIMENTAL PROCEDURE

Plates of Portland Brownstone (PB) were purchased from Pasvalco Co. [Closter, NJ] and samples were prepared by cutting with a diamond saw or core drill (2 cm I.D.). The pore structure was characterized by nitrogen sorption using a Micromeritics ASAP 2010 and by mercury porosimetry using a Micromeritics 9410. The dynamic elastic modulus was calculated from acoustic pulse delay, which was measured using a PUNDIT instrument. The static modulus for a fully saturated sample was determined by a 3-point bending test on a rod roughly 3 x 10 x 210 mm. Tensile strength was measured by the Brazil (or splitting) test on cylindrical samples 2 cm in diameter and 5 cm long. Sorptivity was measured by suspending samples of stone from an electronic balance so that the bottom of the stone touched a large pool of water, and recording the output from the balance continuously; the sides of the sample were coated with grease to prevent evaporation. Swelling of the stone was quantified using a Perkin-Elmer differential mechanical analyzer (DMA). Samples with a maximum height of 18 mm and diameter no more than 10 mm were placed on the sample holder that was then immersed in liquid; the length of the sample was continuously monitored before, during, and after immersion. The tests were performed in water, isopropyl alcohol, and aqueous solutions of 1 M KCl and 0.1 M $CaCl_2$. To measure the force exerted during swelling of the stone, two methods were employed. A core was cut from a cube of stone, and the hollow sample was placed in a dish between the platens of a mechanical testing machine (INSTRON); the sample stood on a plate with holes to permit water to enter the hollow core. The dish was filled with water and the force exerted by the stone on the platens was measured as a function of time. The second method employed a plate of stone about 3.5 x 10 x 100 mm. The plate was supported at the ends and a bead of vacuum grease was run around the upper edge (to act as a dam); water was poured onto the top surface and the warping of the plate was measured with an optical probe (MTI 1000, MTI Inst.) mounted below the plate. A small piece of reflective foil was glued to the bottom to improve the sensitivity of the probe. For a direct test of the effect of wetting/drying cycles on the strength of stone, cylinders were subjected to vacuum impregnation followed by drying in an oven at 60˚C. After every 5 cycles, the dynamic elastic modulus was tested and 8 samples were broken in the Brazil test.

RESULTS

The stone has evident bedding planes and the dynamic modulus is found to be 35 GPa parallel to the bedding and 24 GPa perpendicular to it; however, the static modulus is 20 GPa parallel and 13 GPa perpendicular to the bedding. The difference is attributed to water in the clays that behaves incompressibly at sonic frequencies and contributes to the apparent stiffness in the acoustic measurement. For analyzing swelling stresses, the static modulus is the relevant parameter. Measurements currently underway indicate that the modulus of the saturated stone is about half that of the dry stone, and the wet stone exhibits viscoelastic relaxation. The tensile strength was 6.8 MPa in the plane of the bedding and 4.5 MPa perpendicular to the bedding (average of 8 samples). The sorptivity was measured on 6 samples and found to be $S = 0.0092 \pm$

Materials Issues in Art & Archaeology VI, MRS Symposium Proc. Vol. 712, eds. P.B. Vandiver, M. Goodway, and J.L. Mass (Materials Res. Soc., Warrendale, PA, 2002)

0.0024 g cm^{-2} $min^{-1/2}$. The porosity found by vacuum impregnation was 8.7 %, whereas mercury penetration yielded only 6.1%. The pore size distribution shown in Figure 2 is distinctly bimodal, with a third of the pore volume centered around 10 μm and the remainder averaging 0.1 μm.

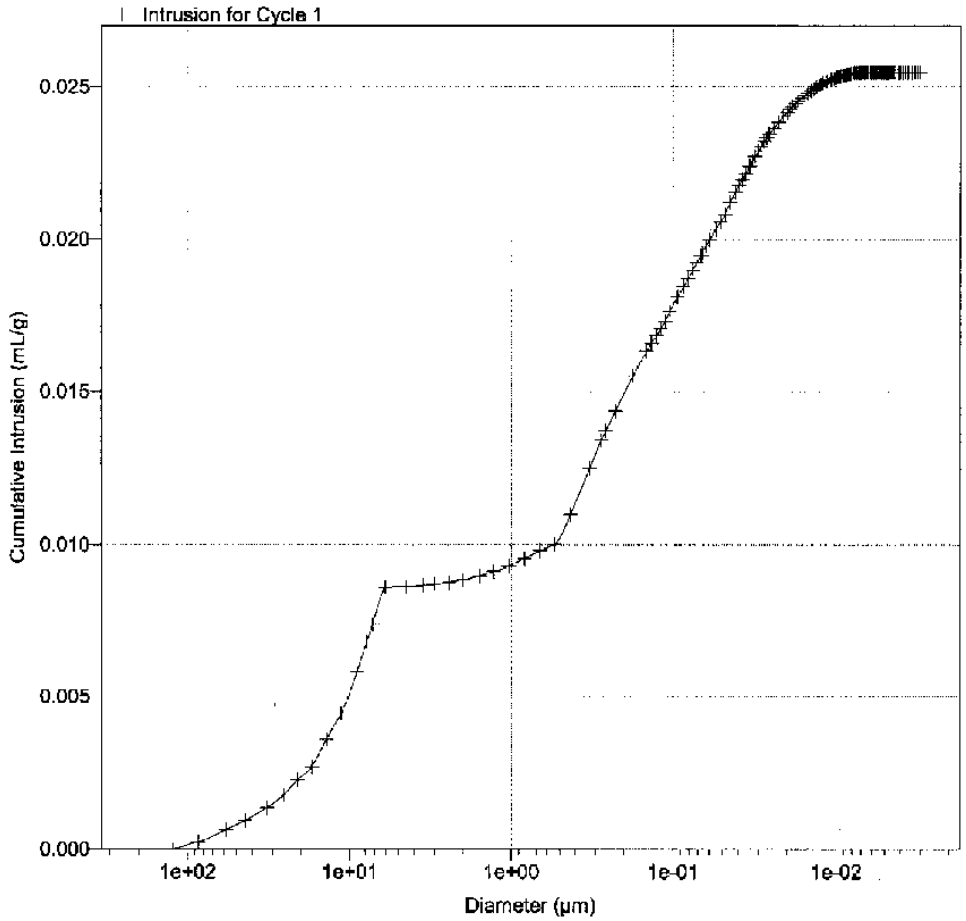

Figure 2. Pore size distribution of Portland brownstone by Hg porosimetry.

The DMA reveals that the PB expands in pure water by about 4.5±1.0 x 10^{-4} m/m perpendicular to the bedding and about 1.7 x 10^{-4} m/m parallel to the bedding. A typical curve is shown in Figure 3. In isopropyl alcohol, the expansion perpendicular to the bedding is similar to that parallel to the bedding in water. The expansion in salt solutions was the same as in pure water.

Materials Issues in Art & Archaeology VI, MRS Symposium Proc. Vol. 712, eds. P.B. Vandiver, M. Goodway, and J.L. Mass (Materials Res. Soc., Warrendale, PA, 2002)

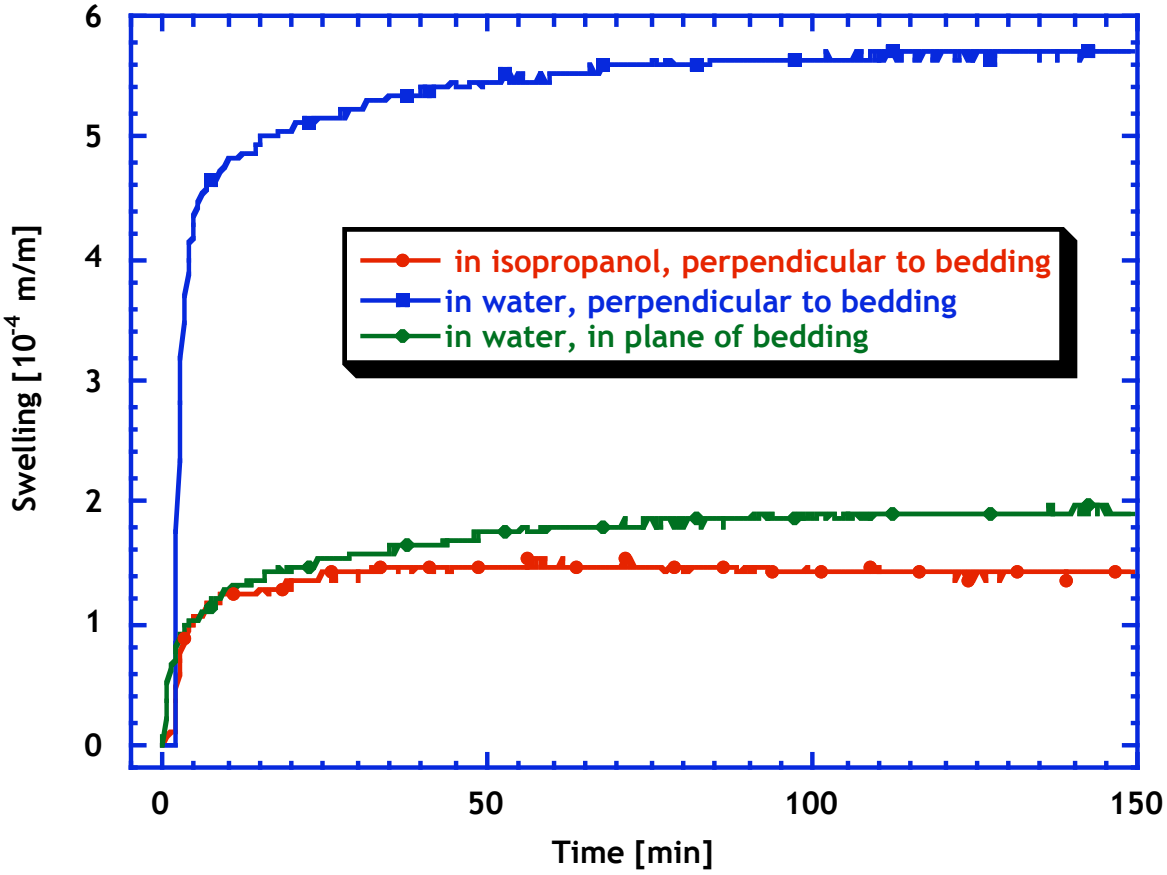

Figure 3. Expansion of Portland Brownstone in water and alcohol.

When a plate of PB is wetted only on the upper surface, the expansion of that side causes it to warp upward, as shown in Figure 4. The plate (3.5 mm thick by 10 cm long, with the bedding planes oriented vertically) deflects by about 200 μm over a period of about 2 minutes, then relaxes. The peak deflection occurs when the wet region occupies half the thickness; as the whole plate becomes saturated, the differential strain is eliminated and the warping decreases to zero.

Materials Issues in Art & Archaeology VI, MRS Symposium Proc. Vol. 712, eds. P.B. Vandiver, M. Goodway, and J.L. Mass (Materials Res. Soc., Warrendale, PA, 2002)

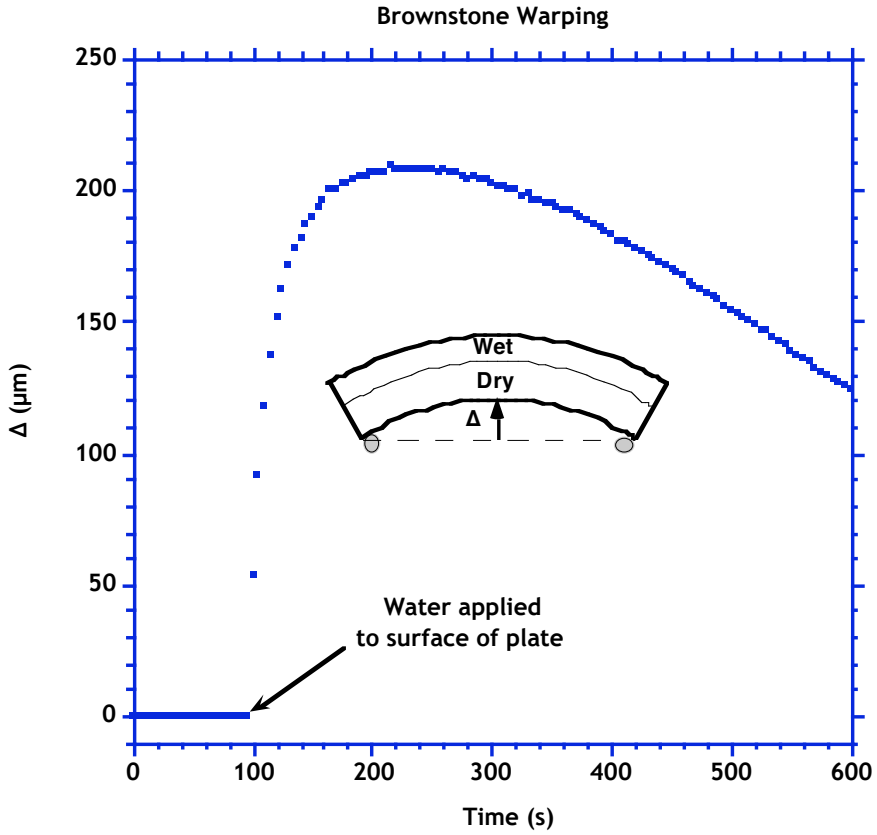

Figure 4. Deflection, Δ, of Portland Brownstone plate when top surface is exposed to water.

DISCUSSION

The stresses caused by swelling of a stone can be calculated by direct analogy to the stresses caused by thermal stress. For example, if a plate exhibits a swelling strain of ε_s, then (assuming that the elastic properties of the wet and dry stone are the same, and that the wetted region is so thin that the plate doesn't bend) the stress in the plane of the plate is[4]

$$\sigma = \frac{E\varepsilon_s}{1-\nu} \qquad (1)$$

where ν is Poisson's ratio. Our data indicate that E = 12.5 GPa and $\varepsilon_s = 4.5 \times 10^{-4}$, so if we let ν = 0.2, we find that the stress caused by swelling is about 7 MPa. During wetting, the stress in the wetted layer is compressive (because it swells relative to the dry region), but during drying the surface contracts and the tensile stress of 7 MPa considerably exceeds the measured tensile strength of 4.5 MPa. Therefore, it is evident that swelling could be a major cause of damage to PB.

To make a direct measurement of the swelling pressure, we placed a hollow sample of stone between the platens of an INSTRON testing machine, fixed the position of the platens, and

Materials Issues in Art & Archaeology VI, MRS Symposium Proc. Vol. 712, eds. P.B. Vandiver, M. Goodway, and J.L. Mass (Materials Res. Soc., Warrendale, PA, 2002)

measured the stress created when the stone was saturated. Surprisingly, the stress was only about 1 MPa, which may have resulted from the inability of the instrument to sustain a constant displacement. To confirm that the stresses are truly high, we employed a novel method that avoids the complications created by surface irregularities: we exposed the top surface of a plate of stone to water and measured the warping of the plate as the upper part of the plate expanded. The stresses and strains in a bilayer material were analyzed by Timoshenko[5]; the solution is discussed in ref. [6]. If the supports under a plate of thickness h are separated by a distance w, then the deflection Δ of the plate (see insert in Figure 4) is

$$\Delta = \left(\frac{3w^2}{4h}\right)\left(\frac{h_s}{h}\right)\left(1-\frac{h_s}{h}\right)\varepsilon_s \qquad (2)$$

where h_s is the depth of the saturated layer. The latter can be calculated as a function of time if the sorptivity is known, and the other parameters have been independently measured, therefore we can predict the expected deflection. However, the sorptivity and swelling strain vary somewhat from sample to sample, so instead we use those quantities as fitting parameters as we fit eq. (2) to the expansion shown in Figure 4. The result is shown in Figure 5. The shape of the expansion curve is quite well described by eq. (2) with $\varepsilon_s = 3.9 \times 10^{-4}$ (which controls the amplitude of the peak) and sorptivity of $S = 0.0099$ g cm^{-2} min$^{-1/2}$. Both of those values are within the range measured for this stone.

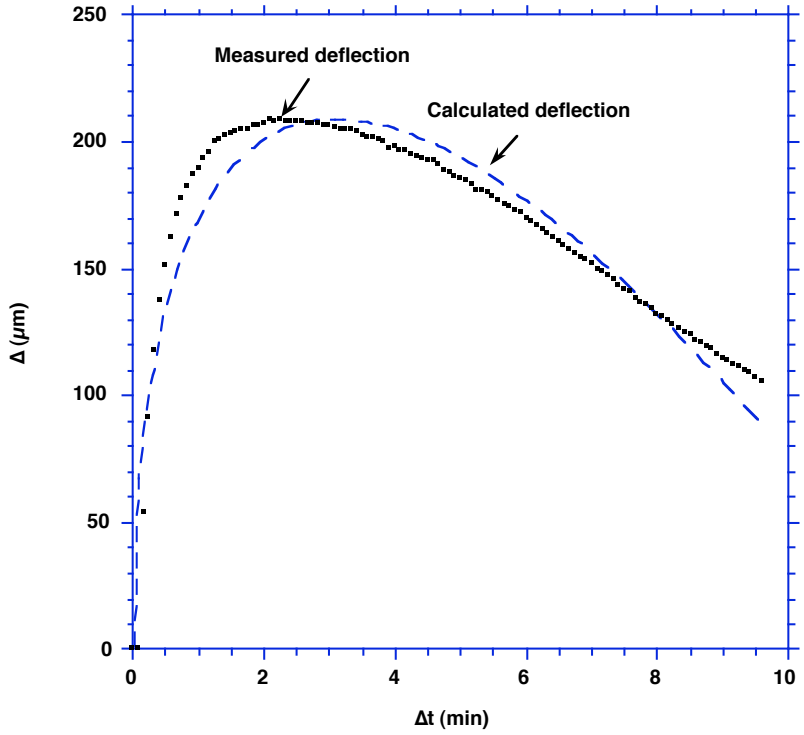

Figure 5. Warping measured for a plate of Portland Brownstone (dots) compared with theoretical curve (dashed).

Materials Issues in Art & Archaeology VI, MRS Symposium Proc. Vol. 712, eds. P.B. Vandiver, M. Goodway, and J.L. Mass (Materials Res. Soc., Warrendale, PA, 2002)

The fact that the stone plate shows the expected degree of warping indicates that the stresses are actually quite large (approaching 7 MPa in a thin dried layer); nevertheless, the direct measurement of the strength of stones subjected to wet/dry cycling show no systematic reduction in strength after 10 cycles. Given the longevity of brownstone buildings, it is likely to take many cycles to show a substantial loss in strength.

CONCLUSIONS

Portland brownstone exhibits a fractional expansion of about 4.5×10^{-4} in pure water. If the wetting of the stone is not uniform, then stresses result from differential strain, and they can be twice as large as the tensile strength of the stone. A novel method – warping – has been shown to provide quick and accurate measurement of the stress and strain resulting from wetting. We intend to use this method to examine the swelling behavior of other stones, and to evaluate the effectiveness of treatments, such as surfactants[7], that reduce the swelling of clays.

ACKNOWLEDGMENTS

Inmaculada Jimenez Gonzalez was supported by a generous grant from the Kress Foundation. We are indebted to Dr. Robert Flatt for many helpful discussions during the course of this work, and to John Valenza for his help with the warping experiment.

REFERENCES

[1] C. Rodriguez-Navarro, E. Hansen, E. Sebastian, and W.S. Ginell, J. Am. Inst. Conservation 36 [2] (1997) 151-163

[2] C. Félix, "Peut-on consolider les grès tendres du Plateau suisse avec le silicate d'éthyle? (Can one consolidate the soft sandstones of the Swiss plateau with ethyl silicate?)", pp. 267-274 in Preservation and restoration of cultural heritage, ed. R. Pancella, Proc. LCP Congress, Montreux, 1995

[3] N. Weiss, J. Teutonico, F. Matero, and R. Pepi, "Sandstone Restoration Project", Landmarks Conservancy, New York, NY. 1980

[4] G.W. Scherer, *Relaxation in Glasses and Composites* (Wiley, NY, 1986) Ch. 8

[5] S. Timoshenko, J. Opt. Soc. America 11 (1925) 233-255

[6] G.W. Scherer, *Relaxation in Glasses and Composites* (Wiley, NY, 1986) Ch. 16

[7] R. Snethlage and E. Wendler, "Surfactants and akherent silicon resins - New protective agents for natural stone", pp. 193-200 in Mat. Res. Soc. Symp. Proc. Vol. 185 (Mater. Res. Soc., Pittsburgh, PA, 1991)

Anexo 3. Publicación nº.2

"Effect of Swelling Inhibitors on the Swelling and Stress Relaxation of Clay Bearing Stone"

Jiménez González, I. and Scherer, G.W.

Environmental Geology, 46 (2004) 364-377.

Original article

Effect of swelling inhibitors on the swelling and stress relaxation of clay bearing stones

Inmaculada Jimenez Gonzalez · George W. Scherer

Abstract Clay-containing stones such as Portland Brownstone (USA), Villarlod Molasse (Switzerland) and Tarifa Sandstone (Spain), are expected to weather as a result of wetting and drying cycles. During drying events, contraction of the drying surface leads to stresses approaching the tensile strength of the stone. However, we have found that the magnitude of these stresses is reduced by the ability of the stone to undergo stress relaxation. In this paper we describe novel methods to determine the magnitude of the stresses and the rate at which they develop and relax. We also discuss the influence of swelling inhibitors on the magnitude of swelling and the rate of the stress relaxation of these stones. The implications of our findings for the understanding of damage due to swelling of clays are discussed.

Keywords Clays · Wetting/drying · Free swelling · Stress relaxation · Surfactants

Introduction

Alteration of clay-bearing stones is often attributed to stresses arising from cycles of swelling and shrinking of the clays. Despite the fact that this mechanism is so often mentioned, there is barely any direct demonstration that this process does indeed damage the material. To the best of the authors' knowledge there is only one study that successfully achieves this goal (Wendler et al. 1996). In this study, the authors examined the aging of stones from Easter Island. They first observed that the drill resistance of exposed stone was much weaker at the outside than in the inside. To test whether such an alteration could be induced by cycles of wetting and drying, they subjected samples to 11 hour cycles in which there was 1 hour complete submersion in water at 20°C, followed by 11 hours at 40°C and 18% RH. As indicated in Fig. 1 after 600 cycles, the samples showed a drastic drop in the drill resistance of the first 1–1.5 mm; the core of the sample remained unchanged. More interestingly, they treated another series of samples of the same stone with a swelling reducing agent, a di-aminobutane di-hydrochloride (Wendler et al. 1991, Snethlage and Wendler 1991). This treatment did not modify the water ingress or porosity of the sample, but significantly reduced the swelling. At the end of the same number of cycles these samples only showed a slight reduction of the drill resistance in the outer part.

This experiment clearly establishes that wetting and drying cycles can damage clay-bearing stones. Furthermore it demonstrates that swelling inhibitors may actively contribute to the reduction of this damage. However, the damage is not eliminated, and there is no prediction of the extent to which damage may be reduced by a given treatment. It also clearly indicates that damage by this mechanism is, at least during the number of cycles investigated, limited to the very exterior of the stone. This may not be too critical for a monument, but the loss of 1 mm on a sculpture will lead to considerably more esthetic damage. This clearly distinguishes wetting and drying damage from that caused by crystallization of ice or sodium sulfate, which can lead to stresses over larger portions of the sample volume (Scherer 1999, Flatt 2002), therefore leading to more spectacular damage being produced in accelerated tests carried out in the laboratory. Stones consolidated by ethyl silicate rapidly lose any benefit of consolidation with a limited number of cycles of wetting and drying (Félix and Furlan 1994, Félix 1994, 1995b). This has been attributed to the consolidant not being able to resist the swelling of clays and consequently being cracked during wetting cycles. The study by Wendler et al. (1991) shows that unconsolidated stones are also damaged by cycles of wetting and drying, but after many more cycles.

In this paper, we present a series of experiments that are aimed at establishing the stresses that may

Special Issue: Stone decay hazards

Received: 18 June 2003 / Accepted: 16 November 2003
Published online: 4 June 2004

I. Jimenez Gonzalez · G. W. Scherer (✉)
Dept of Civil & Env. Eng/ Princeton Materials Institute, Princeton University, Eng. Quad. E-319, Princeton, NJ 08544, USA
E-mail: scherer@princeton.edu

DOI 10.1007/s00254-004-1038-8

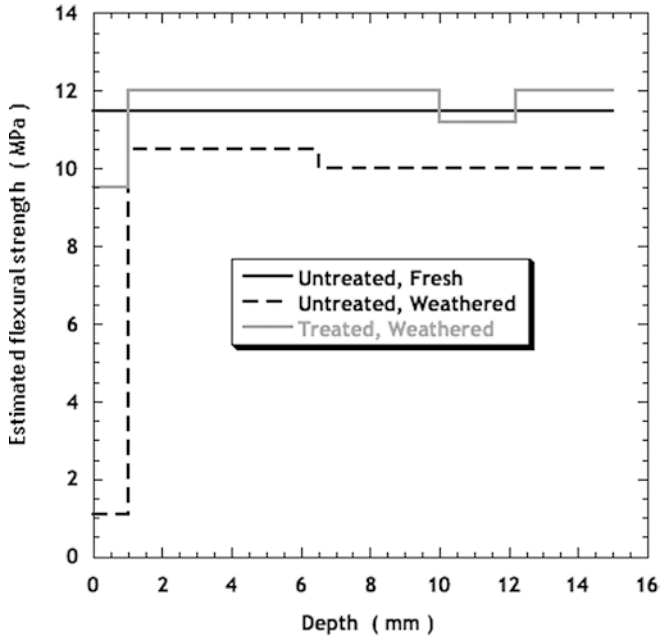

Fig. 1
Comparison of flexural strength between untreated, treated, weathered and unweathered tuff fined-grained quarry samples from (Rano Raraku), Easter Island. Strength is estimated from the drill penetration rate, based on an empirical correlation, as explained in Wendler et al. (1996), from which this figure is adapted

evolve during wetting and drying cycles and the circumstances under which they may lead to damage of stone. In a previous paper, we presented novel experiment methods along with the theoretical background necessary to analyze the stresses (Scherer and Jiménez González 2003). We demonstrated that the relaxation of stress in clay-bearing stones is an important factor that must be taken into account; otherwise significant overestimation of stress will result. This paper presents further results on three different stones. It establishes that the same phenomena (swelling, softening, viscoelastic relaxation) occur. In addition, we demonstrate the modifications of these properties by the presence of several swelling reducing agents (surfactants). Of course, clay-bearing stones tend to have a significant fraction of small pores, which makes them highly susceptible to damage from crystallization of salts and ice; however, that aspect of their behavior is not considered in the present study.

Materials and methods

Materials

Stone

Portland Brownstone is an arkose sandstone widely used in the northeastern United States in the beginning of the last century. This is a complex sandstone containing grains of quartz and albite in a matrix including kaolinite, mica, iron oxides, illites and smectites; clay flakes around the quartz grains are evident in SEM photos (Jiménez González et al. 2002). It was obtained from Pasvalco Co. (Closter, NJ). Indiana limestone is a widely used building stone in the United States. It contains few clays and exhibits no swelling upon wetting. It was also obtained from Pasvalco Co.

Villarlod Molasse is a clay-rich subarkose sandstone with a calcitic cement from Switzerland that has been widely studied for its swelling characteristics (Félix 1995a). Its composition is 50–60% quartz, 10–15% feldspars as plagioclase and orthose, 20–30% calcite as cement, 3–5 % glauconite, and some biotite, mica blanc, and epidote (Félix 1977). The mineral content of Swiss molasse is quite constant (Félix 1988): the clay fraction in the matrix varies from 2–10%, and includes ~30% swelling clays — smectites or montmorillonite — along with illite (40–50%), chlorite (15–30%) and kaolinite (0–20%). It was kindly supplied by the Expert Center on Built Cultural Heritage (EPFL, Lausanne, Switzerland).

Tarifa is an arkose sandstone from Tarifa (Cádiz), Spain, that contains quartz, feldspars, biotite (altered to chlorite), muscovite and clay minerals (smectite, chorite, illite) as cement. The large clay content has been identified as the principle cause for the deterioration of this material (Rodriguez Navarro, C., personal communication, 2002). The stone was kindly supplied by the Department of Geology of the University of Granada, Spain.

Swelling inhibitors (surfactants)

Two types of swelling inhibitors suggested by Wendler et al. (1991) and Snethlage and Wendler (1991) were obtained from Sigma/Aldrich and Across organics: 1,3-diaminopropane dihydrochloride ($H_2N(CH_2)_3NH_2{\cdot}2HCl$) and ethylenediamine dihydrochloride ($C_2H_8N_2{\cdot}2HCl$). Another surfactant, hexadecyl trimethylammomium bromide, known as CTAB ($CH_3(CH_2)_{15}N(CH_3)_3Br$) was obtained from Across organics.

We chose to examine whether mixed aminoalcohols used for steel corrosion inhibition may be also active as swelling inhibitors. The samples, from the Ferrogard$^{(r)}$ line of products, were supplied by Sika Technology AG (Zurich, Switzerland); we refer to those products as F-A, F-B, and F-C. Additionally we tested the following Zonyl$^{(r)}$ fluorosurfactants supplied by Dupont (USA): FSA, FSJ, FSP, FSH and 9361.

To screen the effectiveness of the surfactants on Portland Brownstone bars, solutions of surfactants at 1 and 5% by weight were prepared. The samples were treated with 1% solutions, tested and then retreated with the same products at 5% and retested (Table 1). For treatments that used mixtures of surfactants, the solutions of the products selected during the screening were mixed 50% by weight. We proceeded this way to avoid exceeding 5% concentration of total product in one treatment. We confirmed that additional treatment by these mixtures did not increase the swelling reduction, so that these concentrations were sufficient. The soaking procedure was as follows: stones samples (30×10×10 mm) were dried at 60°C, then placed horizontally in small containers where they were partially submerged in the surfactant solution. Each

Table 1
Results of treatment screening on Portland Brownstone

Product name	Concentration [%]	Swelling reduction [%]
DuPont Zonyl FSA	1	11
	6	11
DuPont Zonyl FSH	1	17
	6	33
CTAB	1	20
(hexadecyltrimethyl-ammonium bromide)	6	0
Sika Ferrogard F-A	1	20
	6	20
Sika Ferrogard F-B	1	41
	6	50
Sika Ferrogard F-C	1	20
	6	60
1,3 diaminopropane, dihydrochloride	1	25
	5	50
1,2 diaminoethane, dihydrochloride	1	25
	5	50

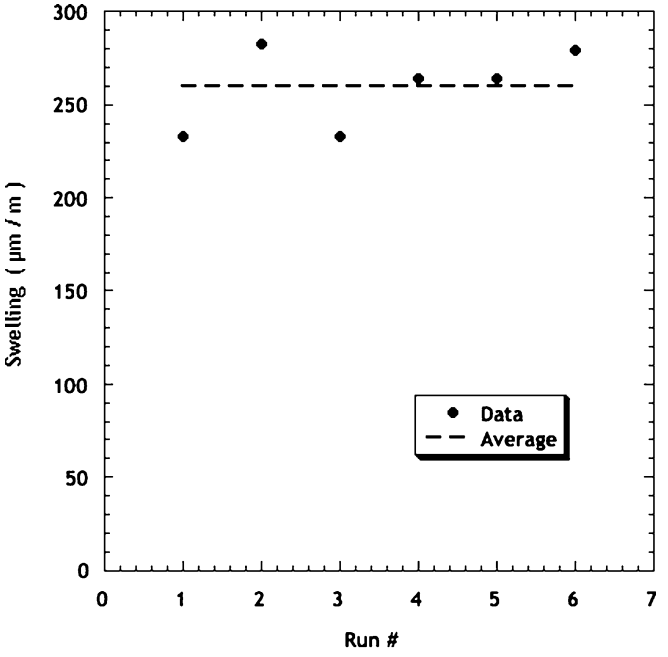

Fig. 2
Six repetitions of the swelling of treated Portland Brownstone sample as measured by LVDT

container was hermetically sealed to avoid evaporation. Samples were left to soak in the product until saturation was ensured by the constant sample weight. Measurements of expansion during soaking were obtained using calipers; the expansion was 7–54% less than the expansion in water. Soaking times for the three types of stones varied between 6 hours for Villarlod Molasse and 20 hours for Tarifa sandstone. Once the impregnation was completed, samples were removed and left to dry under the hood for approximately 1 hour. Afterwards, they were placed in the oven to dry at 60°C.

Methods

Commercial and homemade instruments have been used to characterize the mechanical properties of the stone. Each technique required the sample to have a specific size and geometry. All the samples were cut using diamond saws. A core drill was used to prepare samples used to measured tensile strength; they were drilled from a stone plate, producing cylinders ∼2 cm in diameter and ∼5 cm in length.

Freeswelling, effect of treatments

Preliminary tests of single treatments

In a first series of experiments we screened swelling inhibitor candidates using a simple test in which the swelling was measured directly using a caliper with an accuracy of ±10 µm. In these experiments, bars of Portland Brownstone (140×10×10 mm) were placed in a container and calipers were fixed on a vertical support and adjusted to the sample length. Upon addition of water, the samples began swelling and the change in sample length could be determined. The swelling of the untreated samples was remeasured between three and five times, then they were submerged in solutions containing the different candidate treatments.

Preliminary test of sequential treatments

After the preliminary screening of single treatments, the samples showing significant swelling reduction were cut into four pieces of identical length. These samples were then given a second treatment with a different product. Their swelling was measured this time using a Linear-Variable Differential Transformer (LVDT), which has a resolution of 0.2 µm. The samples were placed vertically in a small glass container having a flat base. The top of the sample was contacted with a rod linked to the iron core of the LVDT. The swelling was initiated by adding enough water to cover most of the sample, leaving the top surface exposed. This led to the identification of the best combination of swelling inhibitors. The reproducibility of the swelling measurements for treated Portland Brownstone was very good with the LVDT, as illustrated in Fig. 2.

Determination of the treatment sequence

The optimal combination of treatments was tested again, using the LVDT on samples 3 cm high. The same sequence of treatments was repeated to obtain more precise values of the swelling reduction. In addition, we tested the direct application of both surfactants simultaneously as a mixed solution.

Dynamic elastic modulus

Dynamic elastic modulus was determined from the ultrasound transmission velocity with a portable PUNDIT (CNS Electronics, London, England) instrument operating at 54 kHz. Both transducers were mounted in a homemade aluminum and stainless steel frame, shown in Fig. 3, designed so that the force applied to the samples during

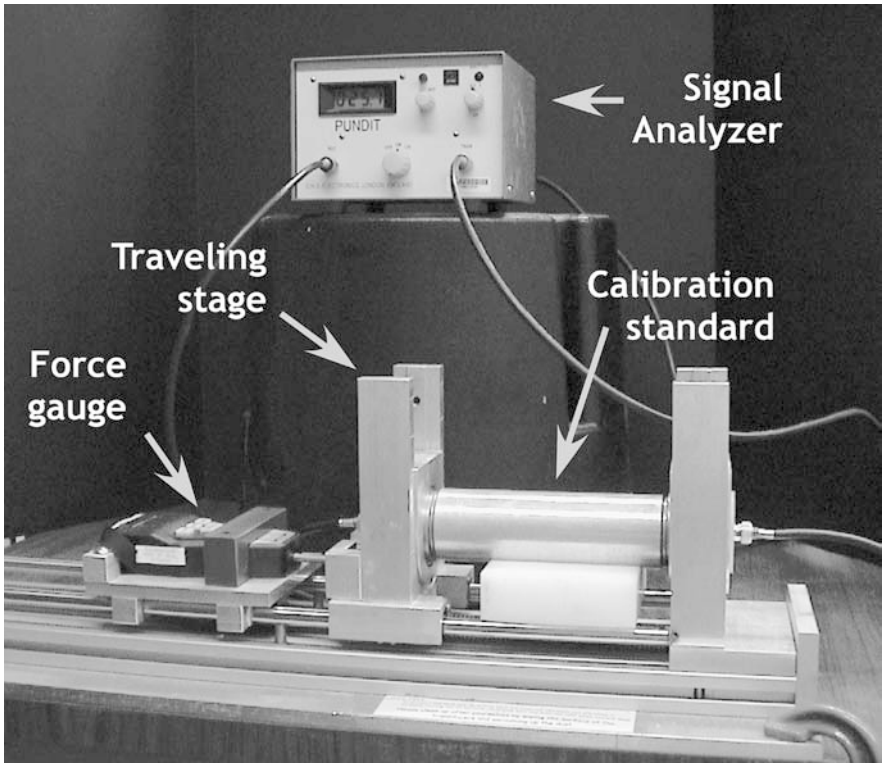

Fig. 3
Transducers are mounted in supports; the left transducer travels on a screw drive; an in-line force gauge indicates the force exerted against the sample. In this photo, the metal calibration standard is in place of the sample

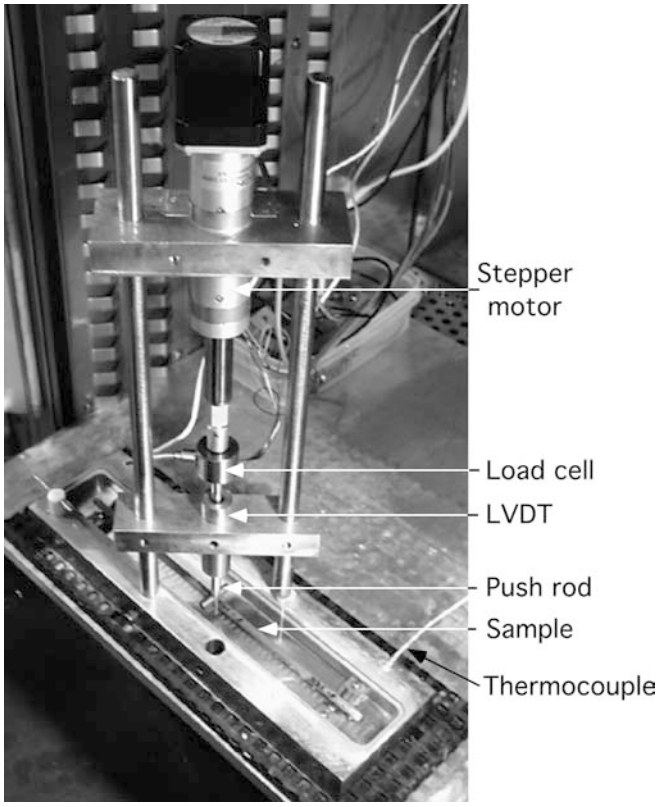

Fig. 4
Three-point bending apparatus. In this photo the sample is cylindrical, but the sample used in the present study were plates

each measurement can be determined and easily adjusted. The force was raised sufficiently so that the transit time reached a plateau. For the samples used, this typically occurred around 100 N. This procedure greatly increased the reproducibility of the method.

Prior to each measurement, the instrument was calibrated by measuring the transit time through a reference bar. In this case the contact was assured by vacuum grease. Grease contact had to be avoided on the stone, because the samples had to be water saturated for further experiments after those measurements. Therefore, the measurement of the reference was then repeated with nitrile pads as contact agents. The transit time difference was used to determine the time the sound wave takes to cross the pads (~1.1 μs). This value was then subtracted from the measurements on the stone samples, which were measured exclusively with the pads.

Beam bending

Static modulus and stress relaxation were determined by three-point bending. The beam-benders (an example is shown in Fig. 4) were homemade to suit the requirements of long relaxation measurements. They have computer controlled stepper motors (Ultra Motion, Mattituck, NY) capable of moving up to 3.75 mm/s. This motor displaces a load cell, on which a push rod is mounted that feeds through an LVDT (Macrosensors, Pennsauken, NJ) allowing displacements to be measured over 10 mm with a resolution of 0.2 μm. The load cells were from SENSOTEC (Columbus, OH, USA) and had capacities of ±50 g and ±250 g. The whole set-up which is placed inside an incubator was checked for dimensional and thermal stability (about 0.1°C) as well as alignment according to a procedure described elsewhere (Vichit-Vadakan and Scherer 2002).

The sample was placed in a stainless-steel bath on a rubber pad to minimize vibrations. For runs under saturated

conditions, the sample was previously vacuum impregnated and the bath was filled with de-mineralized water. A cover allowing free movement of the pushrod was used to prevent evaporation. For runs over 24 hours, a gravity-based refill system was used with the beam bender. A reservoir fed into an external bath whose level was controlled by a float valve, while minimizing disturbance to the liquid in the bath.

To optimize the stability of the stone plate, it was found that the best supports were a stainless steel cylinder about 6.3 mm in diameter on one end and a stainless steel sphere also about 6.3 mm in diameter on the other end. The cylindrical support was confined in a slot allowing only slight rotation without translation. The spherical support was held in a hemispherical cavity. The tip of the push rod was a half sphere of the same diameter.

The measurement was made by instructing the computer to move a certain distance (typically ~100 μm), thereby bending the plate of stone; the deflection stabilized in <0.5 s. The deflection, Δ, was held constant and the force, $W(t)$, on the sample was measured at logarithmic intervals of time. The elastic modulus is related to the force on the beam by

$$E = \frac{W\,L^3}{4\,b\,h^3\,\Delta} \tag{1}$$

where L is the distance between the supports, b is the width of the plate and h is its thickness. Since the strain is constant, the load relaxation is identical to the viscoelastic relaxation of Young's modulus:

$$\frac{W(t)}{W(0)} = \frac{E(t)}{E(0)} \equiv \psi(t) \tag{2}$$

There is an additional complication when the pores of the stone are saturated with liquid, because the deflection of the beam induces a pressure gradient in the pore liquid that causes it to flow. As the pressure in the pore liquid equilibrates, the force required to sustain a fixed deflection decreases (Scherer 2000); the kinetics of that relaxation, described by a function $R(t)$, depend on the shape and size of the sample. When beam-bending is performed on a saturated body in which the solid network is viscoelastic, then the total force relaxation is accurately approximated by the product of the functions:

$$\frac{W(t)}{W(0)} \approx R(t)\psi(t) \tag{3}$$

In tests of dry stone, the relaxation of the stress yields $\psi(t)$, but in the saturated samples, both functions are obtained.

Indirect tensile strength

The tensile strength of our samples was measured by the so-called Brazilian test (indirect tension). Cylindrical samples with a 2 cm diameter ϕ and a length L of 5 cm were placed horizontally between the two plates of an Instron machine. These were brought together until failure of the sample at a rate of 0.25 cm/min. The peak load $P_{\max}$ was used to calculate the tensile strength σ of the material according to the well established expression (Mindess and Young 1981):

$$\sigma = \frac{2P_{\max}}{\pi\phi L} \tag{4}$$

Results

Surfactant treatments

Preliminary tests of single treatments

The swelling reduction for Portland Brownstone resulting from surfactant treatments is shown in Table 1. The four products giving reduction in swelling of about 50% were chosen for further testing.

Preliminary test on sequential treatments

In Table 2, we give the results of the swelling reduction for the samples of Portland Brownstone retreated with a second product. The first two columns of results give the swelling reduction after treatments 1 and 2, respectively, as measured with calipers. Values differ from those in Table 1 because we have compared the treated samples to the average dilatation of the untreated bars to account for the inhomogeneity along those samples. The last line in the table is for a sample that was measured with the LVDT in each step. The result coincides perfectly with the average value presented in the previous line for a sample having the identical treatment. In the last column, we report swelling reduction for Portland Brownstone samples that were treated directly with the mixture of surfactants. Interestingly, the best treatment shows much better results for the mixture than for the consecutive treatments.

Table 2
Results of tests for consecutive treatments on Portland Brownstone. In the first four lines the samples were obtained from the bars measured by caliper. The last line is a sample for which all swelling measurements were done by LVDT. The last column is for LVDT measurements on samples treated directly by the mixture of products

Product 1	Product 2	Swelling reduction [%]		
		P1	P1 then P2	P1 & P2
1,2 diaminoethane, dihydrochloride	Sika Ferrogard F-B	13	24	34
Sika Ferrogard F-B	Sika Ferrogard F-C	19	37	32
1,3 diaminopropane, dihydrochloride	1,2 diaminoethane, dihydrochloride	20	29	37
Sika Ferrogard F-C	1,3 diaminopropane, dihydrochloride	25	35	52
		23	35	

Table 3
Swelling inhibition treatments and their effect for the three stones studied

Stone	Treatment	Swelling [μm/m]	
		Untreated	Treated
Portland Brownstone	1,3 diaminopropane dihydrochloride; Sika Ferrogard F-C; one impregnation with a solution of 2.5% and 0.5% of these products respectively	446	212
Villarlod Molasse	1,3 diaminopropane dihydrochloride; 1,2 diaminoethane dihydrochloride; one impregnation with a 2.5% solution of each	1200	422
Tarifa Sandstone	1,2 diaminoethane dihydrochloride; two impregnations with 5% solution.	3200	1620

In Table 3, we report the choice of swelling inhibition treatments for all three stones studied, all results having been obtained by the LVDT method. The swelling reduction for the Villarlod Molasse is about 62% and was obtained with a mixture of the two diaminoalkanes. For the Tarifa sandstone, the swelling reduction of about 50% was obtained with two treatments of the diaminoethane.

Modulus of elasticity

Comparison between techniques

The results of our modulus measurements are reported in Table 4. For all stones that contain substantial amounts of clays it is clear that the results from the two methods are not compatible. Those stones undergo an increase in dynamic modulus from the dry to the wet state, while the opposite is true for the static modulus. In contrast, measurements on stones that contain only minimal amounts of clays and do not show any swelling upon wetting, as in the case of Indiana limestone, show similar moduli by both methods for the dry and the wet samples. These moduli of clay-bearing stones are known to be sensitive to frequency and strain (Tutuncu et al. 1998a), therefore we have decided to rely on the results of the static modulus, which imposes larger strains on the material, on the order of those experienced during swelling.

Effect of surfactants

Among the stones tested, the Villarlod Molasse has the lowest modulus. Probably because of that, it shows a very clear increase in its modulus as a consequence of the swelling inhibition treatment. From the results in Fig. 5, it can be seen that the modulus goes from about 2.5 GPa to 4 GPa in its dry state. No such difference is seen for the wet modulus, however.

Table 4
Mechanical properties of stones

TECNIQUE	Bedding orientation	conditions	Portland Brownstone	Villarlod molasse	Tarifa sandstone
Static Modulus [GPa]	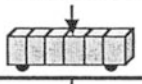	Dry	11.5	2.4	9.3
		Wet	4.1	0.5	1.1
	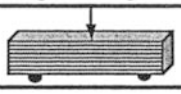	Dry	14.3	3.9	
		Wet	7.7	0.9	
Dynamic Modulus [GPa]		Dry	23	7.5	15.4
		Wet	38	5.4	19.6
		Dry	35	12	28.5
		Wet	44	9.7	27.4
Tensile Strength [MPa]	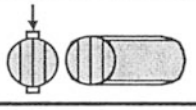	Dry	4.5	1.2*	5.3
		Wet			
	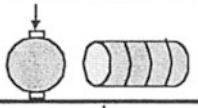	Dry	6.7	2.6 2.6*	6.9
		Wet	5.2		
Compressive Strength [MPa]		Dry		37.5*	
		Wet		20.3*	
		Dry	79 #	50.9*	
		Wet		22.1*	

* Values from Félix (1977)
\# Values from Crosby and Loughlin (1904)

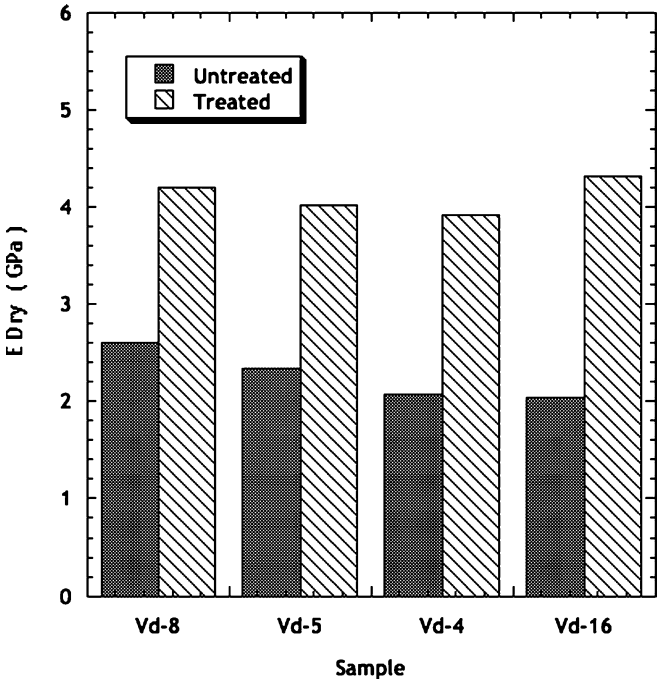

Fig. 5
Effect of swelling inhibitors on the modulus of the Villarlod Molasse

For the Portland Brownstone, there was no change in modulus when the swelling inhibition technique was applied. However, in an additional sample a double concentration treatment was applied which resulted in an increase in dry modulus from about 10 to 13 GPa. This would indicate that a minimum amount of product is needed per unit clay surface to induce this change in the dry modulus. For the Tarifa sandstone, no change was detected for either the dry or the wet modulus.

Stress relaxation

Dry stress relaxation

Untreated samples

The relaxation of the dry samples shows nearly a linear decrease on a log scale for the Portland Brownstone and the Villarlod Molasse. An example for each stone is given in Fig. 6a and b. The relaxation behavior can be fitted by the following logarithmic function:

$$E(t) = E_0 - a \ \ln\left(1 + \frac{t}{\tau}\right) \qquad (5)$$

where t is time, E_0 is the extrapolated modulus at $t = 0$, and a and τ are constants. Clearly this function does not hold at long times, since it would lead to negative modulus values; however, over the considered time scale it offers an adequate fit.

Once $t >> \tau$, eq. 3 can be approximated by:

$$E(t) \doteq E_0 - a \ \ln(t) - a \ \ln(\tau) \qquad (6)$$

so that the parameter a is the one that really characterizes the rate of stress relaxation.

The Portland Brownstone shows the same kinetics. For this stone we had enough samples with varying modulus to examine whether there was any correlation between the fitting parameters. As indicated by the open symbols in Fig. 7, there appears to be a linear relationship between the rate of relaxation and the modulus; as discussed below, this dependence is similar for the treated samples.

The relaxation of the Tarifa sandstone shows a bilinear relaxation rate on a logarithmic scale (Fig. 8). We have found that the following function, using two time constants (τ_1 and τ_2), provides a very good fit to these curves:

$$E(t) = E_0 - a \ \ln\left(1 + \frac{t}{\tau_1}\right) - b \ \ln\left(1 + \frac{t}{\tau_2}\right) \qquad (7)$$

In this case the early relaxation is governed by a and the later relaxation by b. (An equally good fit can be obtained with a stretched exponential function, as in eq. 8, so we do not ascribe any physical significance to the two time constants.)

Treated samples

In Fig. 7 treated samples of Portland Brownstone are indicated by closed symbols. Samples measured before and after treatment are linked by the arrows. The sample indicated by the triangle had been treated twice, once with the usual treatment (Table 3) and once with the same mix of diaminoalkanes as used for the Molasse. The sample receiving the usual treatment does not exhibit any change in modulus or stress relaxation. On the other hand if we consider the global picture (Fig. 7) there is a clear suggestion that treated samples have both a higher modulus and a higher rate of stress relaxation. Regardless of whether the sample is treated or not, it appears that the relaxation rate increases by about 0.084 GPa for each 1 GPa of modulus change.

The relaxation rate of the dry Villarlod Molasse sample increases with the treatment by about 0.07 GPa. This change is on the order of the one that the Portland Brownstone would undergo for about 1 GPa increase in modulus. In fact, the Villarlod Molasse modulus rises as a result of the swelling inhibition treatment by about 1.4 GPa, so it appears that the change in the dry relaxation rate of this stone is also a result of its modulus change. The Tarifa sandstone shows no clear effect of the treatments on its rate of stress relaxation or on its modulus. Relaxation rate averages for the dry samples before and after treatment are given in Table 5, along with the corresponding modulus.

Wet stress relaxation

Untreated samples

When a saturated sample is bent, two relaxation processes occur: viscoelastic relaxation of the solid and hydrodynamic relaxation in the pore fluid. For clay-bearing stones, the viscoelastic relaxation is thought to result from sliding of the clay at grain contacts. Hydrodynamic relaxation

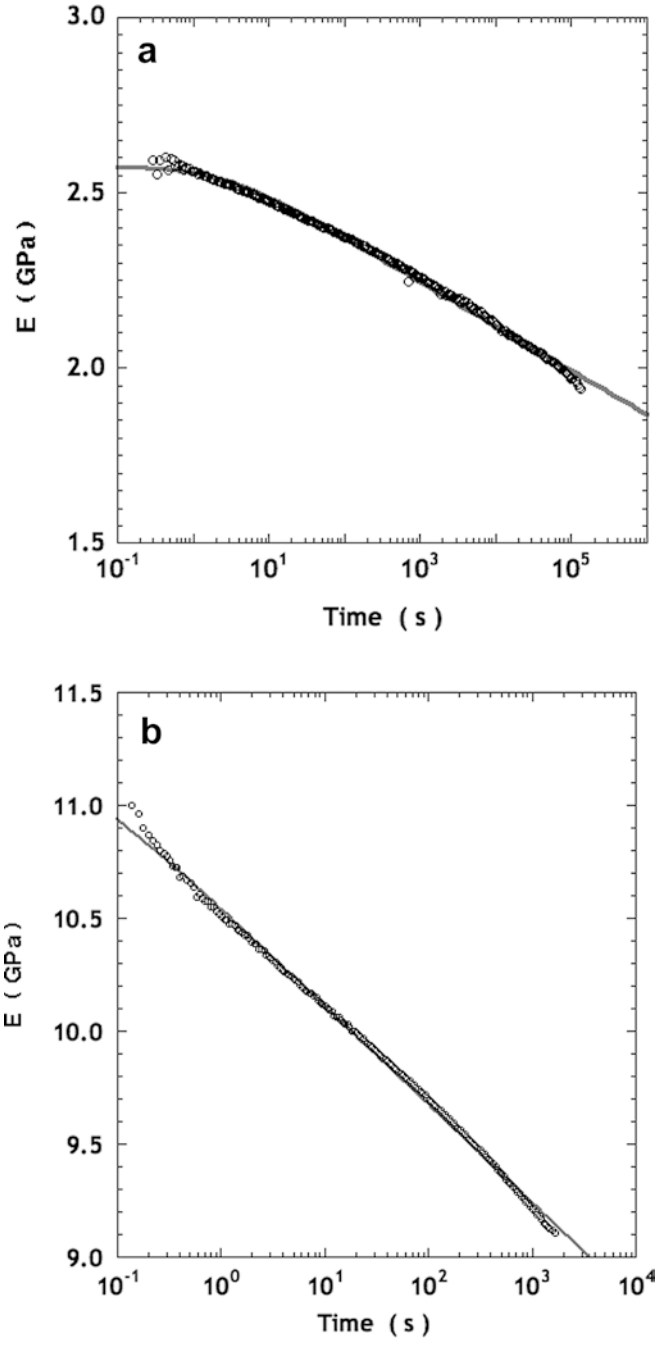

Fig. 6
Dry stress relaxation of Villarlod Molasse (**a**) and Portland Brownstone (**b**). Circles are measured values and curves are fits to eq. 5

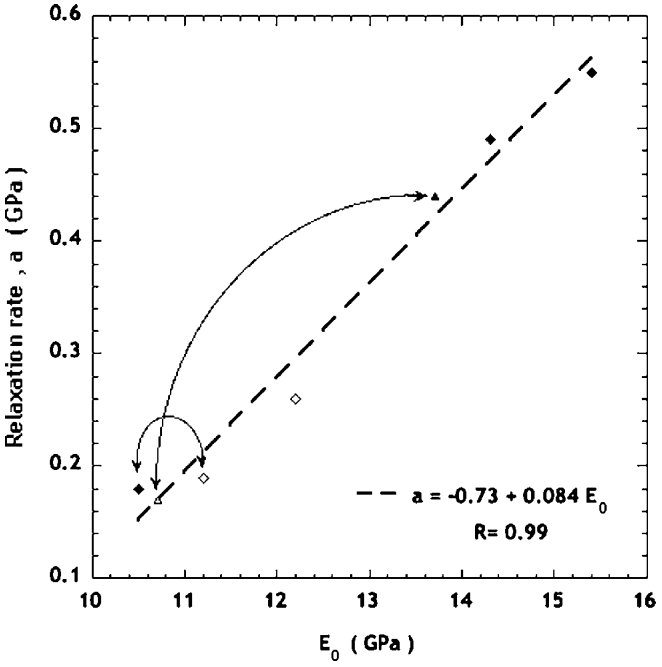

Fig. 7
Correlation of relaxation rate parameter a and initial modulus E_0, both from fits to eq. 5, for Portland Brownstone

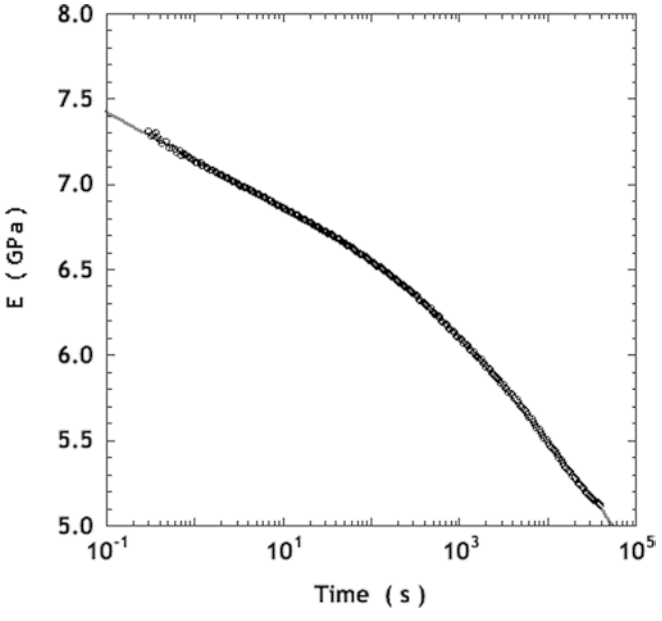

Fig. 8
Dry stress relaxation of a Tarifa sandstone sample; symbols are measured values and the curve is a fit to eq. 7

occurs because bending compresses the upper surface of the sample and stretches the bottom; this creates suction in the pore liquid in the bottom and positive pressure in the liquid near the top, so the liquid flows to relieve the pressure gradient. As the pore pressure equilibrates, the force required to sustain a fixed deflection of the sample decreases with time; by measuring the rate of relaxation of the force, it is possible to determine the permeability of the plate (Scherer 2000). This method has been tested on porous Vycor glass (Vichit-Vadakan and Scherer 2000) and cement paste (Vichit-Vadakan and Scherer 2002). Recently, the theory was extended to include transversely isotropic materials, such as sedimentary stone (Scherer 2003) and that analysis has been applied in our study (Jiménez González and Scherer 2004).

The fit to the load relaxation, $W(t)$, is the product of the hydrodynamic relaxation function, R, and the visco-

Table 5
Relaxation rate averages for the dry samples (parameters from Eqs. 5 and 7)

Dry Sample	Untreated			Treated		
	E_0 (GPa)	a (GPa)	b (GPa)	E_0 (GPa)	a (GPa)	b (GPa)
Villarlod Molasse	2.59	0.05		4.19	0.12	
Portland Brownstone	11.2	0.19		10.5	0.18	
Tarifa Sandstone	8.3	0.16	0.45	8.4	0.14	0.14

elastic stress relaxation function, ψ. In Fig. 9, the global fitted function is compared to the experimental data in the left column; in the right column, the functions R and ψ are shown separately. For the wet stone, the logarithmic function in eq. 3 does not adequately describe the relaxation; much better results are obtained when ψ is represented by a stretched exponential function:

$$\psi = \exp\left[-\left(\frac{t}{\tau_{VE}}\right)^{\beta}\right] \tag{8}$$

Fig. 10 shows that the swelling inhibition treatment causes the viscoelastic relaxation time, τ_{VE}, to increase and the exponent of the relaxation function, β, to decrease for the Molasse. Both changes decrease the rate of relaxation. As discussed later, we interpret this to mean that under saturated conditions, there is enough water to lubricate the slippage between clay surfaces. In the presence of swelling inhibitors, in the confined space between layers the frictional resistance increases, producing "stick-slip" (Tutuncu et al. 1998b). This behavior is the opposite of what we observed in the dry stones, where the swelling inhibitors seem to act as lubricants under shear. Probably, this difference arises from the fact that under saturated conditions there is enough water to lubricate slippage, so that the main effect of the swelling inhibitors is to increase stick-slip.

For the Tarifa sandstone the treatment has the opposite effect on the rate of relaxation: in this case there is a spectacular increase in the rate of relaxation in the wet state. The Portland Brownstone on the other hand does not show any significant change for the selected treatment. Relaxation rate averages for the saturated samples before and after treatment are given in Table 6 along with the corresponding moduli.

Discussion

Surfactant treatments

Single treatments

In the series of aminoalcohol mixes tested, the one with the smallest effect is based mainly on a secondary aminoalcohol. This suggests quite clearly that these molecules adsorb with that amine rather than with the alcohol function. Indeed adsorption through the amine groups would be sterically hindered by the two alkyl groups of the secondary amine, but adsorption through the alcohol function would not be affected.

Sequential and mixed treatments

It is beyond the scope of this article to determine why a particular combination of treatments is better than another. We will just remark that the optimal combination is not the same for all the stones we have examined. The other important point in these experiments is that the mixture of both products performs better than single treatments. The reason may be linked to the pH. Indeed, if the aminoalcohol adsorbs through its amine function, then a lower pH will favor its adsorption. Probably the acidity of the dihydrochloride diaminoalkane contributes to this. If such is the case, one may express concern about the durability of such treatments because repeated contact with water may neutralize the pH, thus causing progressive desorption of the swelling reducing agents. Thin (3–4 mm) plates of Portland brownstone were treated with the best surfactant combination, then subjected to sequential soaking in water (30 min) and drying under forced air (60 min). After 700 cycles, the reduction in swelling was unchanged, so the surfactant is evidently bound tightly. On the other hand, the advantage of the mixture may be that the molecules differ in size. The efficiency of ion exchange in clays is related to the size of the molecule relative to the ion spacing, and the cation sites are randomly spaced (MacEwan and Wilson 1980), so using a mixture of sizes may permit more complete exchange.

From the differences between Table 1 and Table 2 (first column of results) it must be inferred that the caliper is not an ideal measuring technique. However it is satisfactory for fast screening of treatments. The best performing treatment was correctly identified by each technique.

Modulus

Technique

The difference in static and dynamic modulus is considerable and it lies essentially in that they probe very different strains and strain rates (Tutuncu et al. 1998a). Since swelling strains are typically around 200–2000 μm/m, it is the static measurement that is most appropriate. Despite the convenience of the dynamic acoustic technique, it is not relevant. The instrument we used utilizes a single frequency. A device that spans multiple frequencies was used by Félix et al. (2000) to study the Villarlod Molasse; it yielded results for the elastic modulus closer to our static values. The dynamic modulus he measured (for an unspecified orientation) was 5 GPa for the dry sample and 0.9 GPa for the wet one. Our measurements, shown in Table 4, are comparable, being respectively 2.4 and 0.5 or

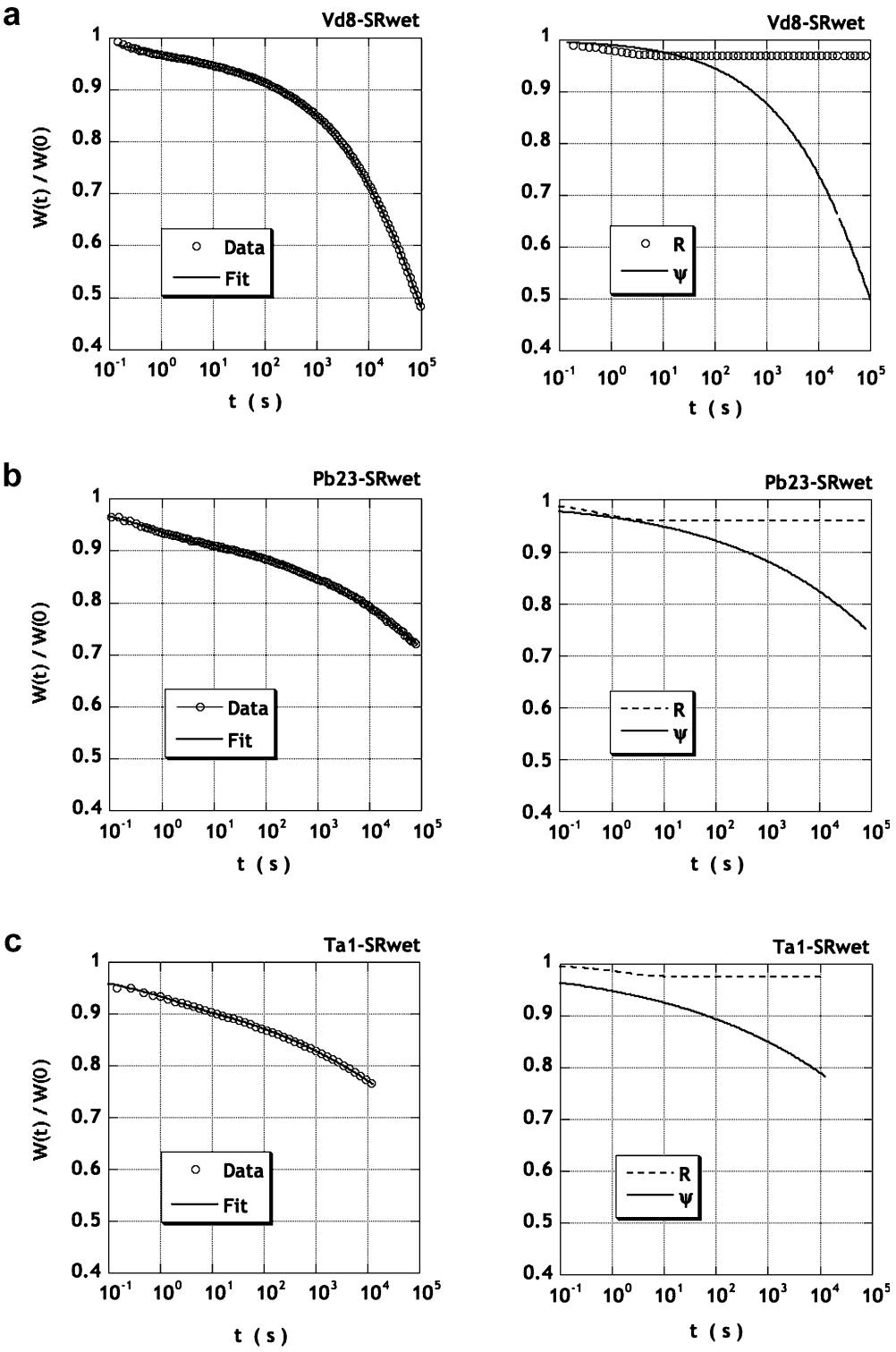

Fig. 9a–c
Stress relaxation of saturated samples. The left graphs indicate the measured force (Data) and the fit to the theory (Fit), eq. 3. The right graphs show the deconvolution of the fitting function into the hydrodynamic part (R) and the viscoelastic part (ψ). **a** Villarlod Molasse, **b** Portland Brownstone, **c** Tarifa Sandstone

3.9 and 0.9 GPa, for the two orientations. The frequency dependence of the modulus results from movement of pore liquid within grain contacts: at high frequencies, the liquid does not have time to move, so it contributes to the stiffness of the stone (Tutuncu et al. 1998a).
For the Portland Brownstone, the dynamic modulus of the wet stone is much higher than that of the dry one. This is probably a result of water behaving as a solid in the clay interlayer at the frequency of the ultrasound wave. The difference between the dynamic moduli of the dry and the wet stone is less pronounced for the Tarifa and Villarlod Molasse. However, it is more enlightening to compare the ratio of static and dynamic moduli. The dynamic moduli are 2–3 times greater than the static moduli for the dry stones, but 10–20 times larger for the wet stones; the greatest discrepancy between static and dynamic moduli

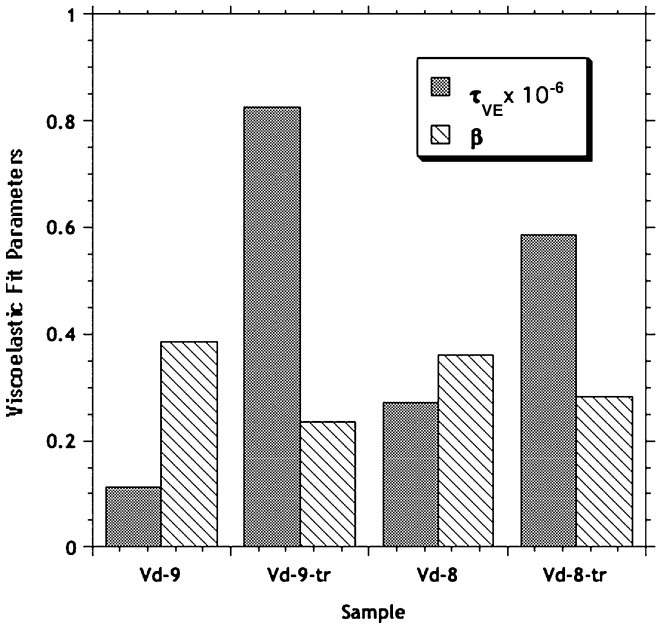

Fig. 10
Effect of swelling inhibitor on wet stress relaxation parameters, from eq. 8, of Villarlod Molasse. Treated samples are indicated by "-tr"

occurs for the Tarifa sandstone, which exhibits the greatest swelling.

Effect of swelling inhibitors

For the dry Villarlod Molasse, there is a clear increase in the static modulus of the dry stone after the treatment (Fig. 5). This effect is probably marked because this stone is very compliant to begin with. When the Portland Brownstone is given a second treatment, there is a slight increase in modulus. The surfactant molecules prevent to some extent the separation of the clay layers, but they do not significantly alter the moduli of the wet stones. This could be due to the fact that reorientation of these molecules is fast compared to time scale of bending, because water is still present between the layers of the clay. The molecular mobility might be revealed with multiple frequency acoustic techniques or NMR.

Stress relaxation

Dry stones

For the Portland Brownstone, the slope of the relaxation curve on a log-linear scale varies linearly with the instantaneous modulus (Fig. 7). A change of 1 GPa in modulus is associated with an increase of about 0.84 GPa in relaxation rate. This is true both for the untreated and the treated samples.
The Villarlod Molasse, exhibits a similar increase in stress relaxation as a result of the swelling inhibition treatment. Therefore, the surfactant must be considered to act as a lubricant increasing the relaxation rate. We believe, the Villarlod Molasse is the only stone where this effect is detected, because it has by far the lowest dry modulus. For the Portland Brownstone, the surfactant only increases the relaxation rate at high doses. The variation of relaxation rate with modulus is evident when comparing a series of treated and untreated samples (Fig. 7), but on one specific sample whose relaxation was measured before and after the treatment, we found no change in relaxation. On another sample, also measured before and after the treatment, the increase in relaxation was clearly noticeable (see samples represented by the triangle in Fig. 7). That sample received, in addition to the usual treatment indicated in Table 3, a second one with the mixture of diaminoalkanes used for the Molasse (Table 3).

Wet stones

The Tarifa sandstone shows a spectacular acceleration of the rate of stress relaxation in the wet samples, whereas Villarlod Molasse shows a modest increase and wet Portland Brownstone shows no acceleration. At this stage it is difficult to decide to what extent these differences are linked to the nature of the stone or of the swelling inhibitors, because the Tarifa sandstone was treated only with the smaller of the two aminoalkanes, while the Villarlod Molasse was treated with both molecules. However considering swelling reduction alone is not sufficient. In the next section we discuss the general route by which damage can occur and how the stresses will change as a result of viscoelastic relaxation.

Mechanism of damage

In Fig. 11 we present a schematic illustration of the development of stresses during the wetting (left: a-c) or the drying of the stone (right d-f). Let us first consider the situation of wetting. We begin with a block of thickness *L*. This block is initially dry and then its surface gets wet (Fig. 11a). As a result the wetted part will attempt to expand (Fig. 11b). However, this expansion is constrained by the bulk of the dry block, such that the wetted layer ends up in compression with respect to the dimension it would adopt if it were free to swell (Fig. 11c). The

Table 6
Relaxation rate averages for the wet samples (parameters from Eq. 8)

Wet Sample	Untreated			Treated		
	E_0 (GPa)	τ_{VE} (s)	β	E_0 (GPa)	τ_{VE} (s)	β
Villarlod Molasse	0.38	1.9E+05	0.37	0.41	7.1E+05	0.26
Portland Brownstone	4.06	6.2E+07	0.19	3.96	6.0E+07	0.17
Tarifa Sandstone	0.83	9.2E+07	0.16	0.84	1.3E+04	0.57

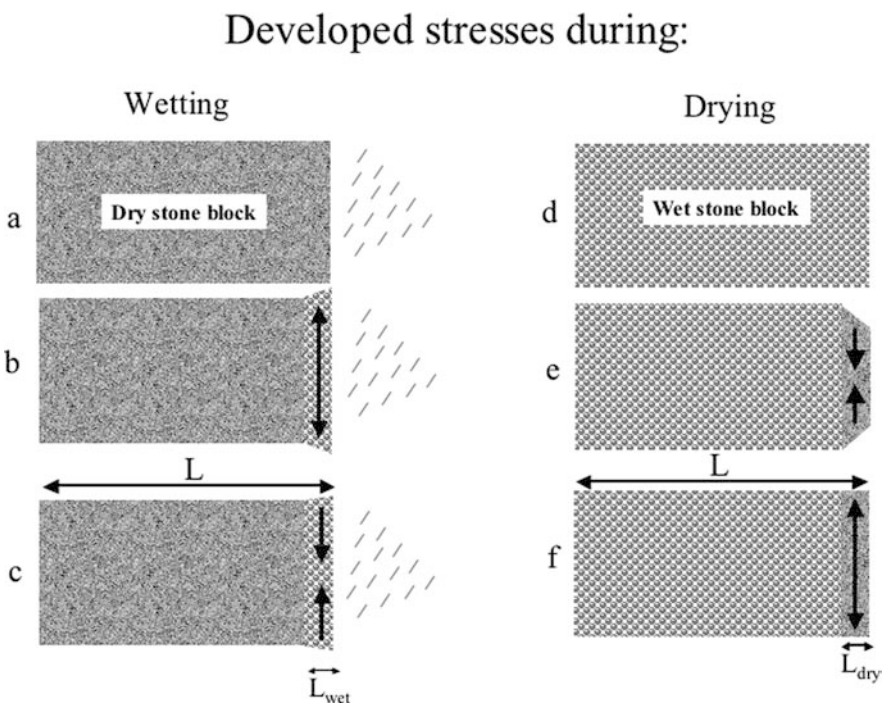

Fig. 11a–f
Illustration of stress development during wetting (**a**,**b**,**c**) and drying (**d**,**e**,**f**) cycles. Cracking is expected during the drying, because the exterior layer is then under tension, and the tensile strength is lower than the compressive strength. However, buckling of surface layers is possible during wetting, particularly if flaws exist below the surface (owing, for example, to crystallization of salts)

magnitude of the compressive stress exerted depends on the relative thickness of that layer, L_{wet}, and of the thickness of the block. If the stone is uniformly wet on opposite sides, the stresses can be calculated by analogy to the sandwich seal (Scherer 1986); if only one side is wet, then bending will occur, and the stresses and deflection can be calculated from the moduli and swelling strain (Scherer 1987). In either case, the maximum stress occurs when the swelling layer is very thin ($L_{wet} << L$), so that its expansion is completely suppressed by the larger volume of dry stone. Neglecting viscoelastic effects, for the moment, an elastic analysis of the stress in the plane of the surface yields

$$\sigma_S = -\frac{E_{wet}\,\varepsilon_S}{1 - \nu_{wet}} \tag{9}$$

where E_{wet} and ν_{wet}, are the Young's modulus and Poisson's ratio of the wet stone and ϵ_S, is the free swelling strain; the stress is compressive ($\sigma_S<0$), because the free strain is positive. We expect damage to occur when this stress exceeds the compressive strength of the wet stone. However, if there are defects below the surface of the stone (produced, for example, by crystallization of salt), then compressive stress could cause buckling of the surface layer at a stress lower than the compressive strength.

Let us now consider a bulk stone that has been wet and has expanded fully (Fig. 11d). As this block begins to dry from its surface, the exterior will attempt to shrink (Fig. 11e). As before, this dimensional change is resisted by the bulk of the stone, but in this case the exterior will be in tension (Fig. 11f). When the drying layer is very thin, the tensile stress parallel to the drying surface is given by:

$$\sigma_S = \frac{E_{dry}\,\varepsilon_S}{1 - \nu_{dry}} \tag{10}$$

where E_{dry} and ν_{dry}, are the Young's modulus and Poisson's ratio of the dry stone. In this case, damage is expected when the stress exceeds the tensile strength of the dry stone. The damage should resemble drying cracks: randomly oriented cracks running perpendicular to the surface.

Stones generally have tensile strengths that are much lower than their compressive strengths, so damage should occur during the drying cycles. Stresses calculated from eq. 7 for a thin dry layer (i.e., where $L_{dry}/L \approx 0$) are presented in Table 7. Even for the Portland Brownstone, which has the

Table 7
Calculated drying stresses and mechanical properties of stones

Stone	E_{dry}(GPa)[a]	$\varepsilon_s \times 10^3$ [b]		Tensile Stress[c] (MPa)		Tensile Strength[a] (MPa)
		Untreated	Treated	Untreated	Treated	
Brownstone	11.5	0.45	0.21	6.5	3.0	4.5
Tarifa	9.3	3.2	1.6	37	19	5.3
Villarlod	2.4	1.2	0.42	3.6	1.3	1.2

[a]From Table 4
[b]From Table 3
[c]Calculated from eq. 7, assuming ν=0.2

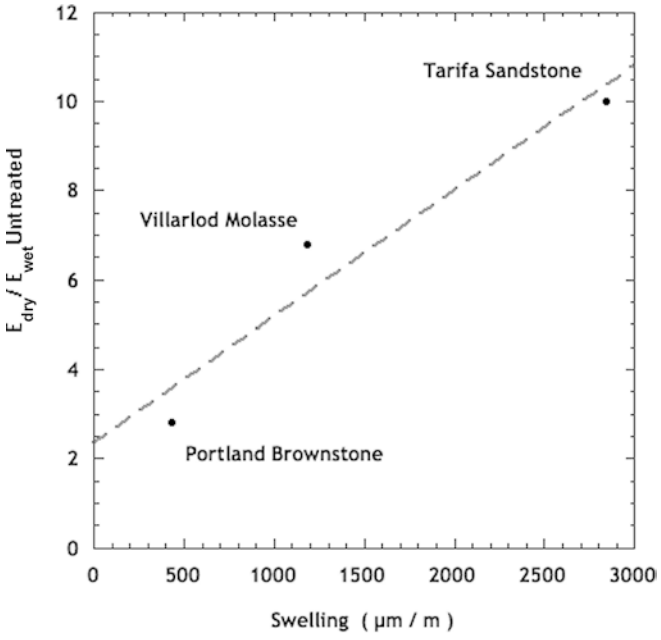

Fig. 12
Ratio of dry to wet modulus plotted against the swelling of the untreated stones

lowest expansion, the stresses evaluated are on the order of the tensile strength, σ_T, of the dry stone. Of course, this is the peak stress, not allowing for relaxation, so the stresses resulting from slow evaporation will be somewhat smaller; thus it is expected that damage will occur as a result of fatigue. For the other stones, the drying stresses are large compared to σ_T, so damage during drying is likely. After treatment with the surfactant, the stress in the Brownstone drops below σ_T, but it remains about equal to σ_T for the Molasse, and much higher for the Tarifa.

In the case of the Villarlod Molasse and the Tarifa sandstone, it is also possible that the wetting cycle may be detrimental, because these stones soften considerably during their wetting. In this connection, it is interesting to note that the samples that undergo the most swelling also show the greatest softening as a result of wetting, as indicated in Fig. 12.

For the Molasse, values reported by Félix (1994) indicate a decrease in modulus of only a factor 2–3, while the modulus decrease we observe is about a factor of 5. This does not favor the argument that damage could happen during wetting according to eq. 9. However, it must be noted that the measurements of compressive strength were carried out at high loading rates, so the strength values are probably in substantial excess of the ones that would be obtained at slower and more realistic loading rates (for the damage process considered). Therefore we cannot exclude the possibility of damage during wetting, particularly by the buckling mechanism mentioned earlier.

The equations presented above do not account for the relaxation of the material, which our experiments have demonstrated to be important. In a separate study we have shown that the low pressures obtained in classical swelling pressure measurements (Madsen and Muller-Vonmoos 1985, Jiménez González et al. 2002) can be explained using the measured values of stress relaxation (Scherer and Jiménez González 2003). From the relaxation curves in Fig. 6 and Fig. 8, we estimate that the drying stresses would relax by 20–30%, if drying occurred over the course of ~24 hours. This would be very helpful for the Brownstone and molasse, but would not be enough to protect the Tarifa. Therefore, giving a first assessment of whether or not a stone may be prone to damage by wetting or drying, or whether a specific swelling inhibition treatment is sufficient to prevent this problem, the dynamics of the process must be considered. This will involve the stress relaxation as determined in this paper, but also more realistic determination of tensile and compressive strength of these materials at realistic loading rates.

Conclusions

We applied a series of surfactants to three different stones that show expansion upon wetting. In all cases, it was found that swelling reductions on the order of 50% can be reached. This is expected to reduce the magnitude of damage during cycles of wetting and drying, provided these products are not washed out. Combinations of surfactants were more effective than any single surfactant in reducing swelling, so there is probably scope for further reductions by using optimal mixtures of surfactants. The surfactants seem to create stick-slip (attributed to the difficulty of aligning the large molecules in the confined space between layers of the clay), which raises the initial modulus. However, once slip is initiated, the surfactants seem to act as lubricants, raising the rate of stress relaxation. This is very favorable for preventing damage from weathering. Analysis of the stresses resulting from wetting/drying cycles, taking account of viscoelastic relaxation, is discussed in detail in another publication (Jiménez González and Scherer 2003).

Acknowledgements The financial support for Ms Jiménez González was provided by the Samuel Kress Foundation and VIP Restoration, Inc. Prof. Wilasa Vichit-Vadakan and Mr. John Valenza are both thanked for the help they provided with the beam-bending experiments. Prof. Carlos Rodriguez Navarro and Prof. Andréas Queisser are thanked for respectively supplying Tarifa sandstone and Villarlod Molasse as well as information pertaining to these stones. Mr. Beat Marrazni and Dr. Urs Mäder are thanked for having supplied the Ferrogard samples. Dr. Robert Flatt is thanked for constructive discussions in the preparation of this paper.

References

Crosby WO, Loughlin GF (1904) A descriptive catalogue of the building Stones of Boston and Vicinity (Mass.) Tech. Quarterly, 17:165–185

Félix C (1977) Molasses et grès de Villarlod (Fribourg) ("Molasses and Sandstones of Villarlod (Fribourg)"). LCP Publications 1975–1995. Matériaux de construction, Pierre, pollution atmosphérique, peinture murale. (Laboratoire de Conservation de la Pierre. Departement des Matériaux) MX-G Ecublens, Lausanne, article [9]

Félix C (1988) Comportement des grès utilisés en construction sur le Plateau Suisse ("Performance of Sandstones in Construction on the Swiss Plateau"). Symposium International AIGI, la geology de l'ingenieur appliquée à l'étude, à la preservation et à la protection du patrimoine historique: travaux anciens, monuments, sites historiques, Athenes, Septembre 19–23, P. Marinos et G, Koulis éd., A.A. Balkema Publ. Protection et Préservation, 2:833–841

Félix C (1994) Déformations de grès consécutives à leur consolidation avec un silicate d'éthyle ("Deformation of sandstone following their consolidation with an ethyl silicate"). In Proc. 7th Int. IAEG Congress, Lisboa, September 5–9, R. Oliveira, L.F. Rodrigues, A.G Coelho & A.P Cunha Editors, A.A. Balkema, 5:3543–3550

Félix C (1995a) Choix de gres tenders du Plateau Suisse pour les travaux de conservation ("Choice of soft sandstones from the Swiss plateau for conservation work"). Conservation et restauration des biens culturels, Actes du Congres LCP, Montreux, Septembre 1995, R. Pancella Ed., EPFL, 45–71.

Félix C (1995b) Peut-on consolider les grès tendres du plateau Suisse avec le silicate d'éthyle? ("Can one consolidate the soft sandstones of the Swiss plateau with ethyl silicate?"). Conservation et restauration des biens culturels, Actes du Congres LCP, Montreux, Septembre 1995, R. Pancella Ed., EPFL, 267–274

Félix C, Furlan V (1994) Variations dimensionnelles des gres et calcaires liees a leur consolidation avec un silicate d'ethyle ("Dimensional changes of sandstones and limestones related to their consolidation with an ethyl silicate"). In 3rd international Symposium on the conservation of Monuments in the Mediterranean Basin. Venice, June 22–25, ed by V. Fassina, F. Zezza. 855–859

Félix C, Ferrari P, Queisser A (2000) Déconsolidation par absorption d'eau de grès traités avec le silicate d'éthyle. Mesures non destructives de E, G et *v* ("Deconsolidation by absorption of water in sandstone treated with ethyl silicate. Nondestructive measurements of E, G, and *v*"). In Procc. 9th Int. Congress on deterioration and conservation of stone, Venice, June 19–24, ed V. Fassina, 2:288–295

Flatt RJ (2002) Salt damage in porous materials: How high supersaturations are generated. In J. Cryst. Growth, 242:435–454

Jiménez González I, Higgins M, Scherer GW (2002) Hygric swelling of Portland Brownstone, in Materials Issues in Art & Archaeology VI, MRS Symposium Proc., eds P.B. Vandiver, M. Goodway and J.L. Mass (Material Res. Soc.), Warrendale, PA, 12:21–27

Jiménez González I, Scherer GW (2004) Swelling of Portland Brownstone: II. Swelling mechanics, to be published

MacEwan DMC, Wilson MJ (1980) Interlayer and intercalation complexes of clay minerals, Ch. 3 in Crystal Structures of Clay Minerals and their X-ray Identification, Mineralogical Society Monograph No. 5, eds. G.W. Brindley and G. Brown (Mineralogical Soc, London)

Madsen FT, Müller-Vonmoos M (1985) Swelling pressure calculated from mineralogical properties of a jurassic opalinum shale, Switzerland. In Clays and Clay Minerals, 33 [6]: 501–509.

Mindess S, Young JF (1981) Concrete. Prentice-Hall, Englewood Cliffs, NJ, 425–427

Scherer GW (1986) Relaxation in Glass and Composites, Wiley, New York, Ch. 8

Scherer GW (1987) Drying Gels: III. Warping Plate, J. Non-Cryst. Solids 91: 83–100

Scherer GW (1999) Crystallization in pores. Cement and Concrete Research, 29:1347–1358

Scherer GW (2000) Measuring Permeability of Rigid Materials by a Beam-Bending Method: I. Theory, J. Am. Ceram. Soc. 83 [9]: 2231–2239

Scherer GW (2003) Measuring Permeability of Rigid Materials by a Beam-Bending Method: IV. Transversely Isotropic Plate, accepted to Journal American Ceramic Society.

Scherer GW, Jiménez González I (2003) Characterization of clay-bearing stone in *Stone decay and conservation*, ed. A. Turkington (Geological Soc. Am., 2003) in press

Snethlage R, Wendler E (1991) Surfactants and adherent silicon resins—New protective agents for natural stone, In Mat. Res. Soc. Symp. Proc. (Mater. Res. Soc.), Pittsburgh, PA, 185:193–200

Tutuncu AN, Podio AL, Gregory AR, Sharma MM (1998a) Nonlinear viscoelastic behavior of sedimentary rocks, Part I: Effect of frequency and strain amplitude, Geophysics 63 [1]: 184–194

Tutuncu AN, Podio AL, Sharma MM (1998b) Nonlinear viscoelastic behavior of sedimentary rocks, Part II: Hysteresis effects and influence of type of fluid on elastic moduli, Geophysics 63 [1]: 195–203

Vichit-Vadakan W, Scherer GW (2000) Measuring Permeability of Rigid Materials by a Beam-Bending Method: II. Porous Vycor, J. Am. Ceram. Soc. 83 [9]: 2240–2245

Vichit-Vadakan W, Scherer GW (2002) Measuring Permeability of Rigid Materials by a Beam-Bending Method: III. Cement Paste. J. Am. Ceram. Soc. 85 [6]: 1537–44

Wendler E, Klemm DD, Snethlage R (1991) Consolidation and hydrohobic treatment of natural stone, in Proc. 5th Int. Conf. on Durability of Building Materials and Components, eds. J.M. Baker, P.J. Nixon, A.J. Majumdar, and H. Davies (Chapman & Hall, London), 203–212

Wendler E, Charola AE, Fitzner, B (1996) Easter Island tuff: Laboratory studies for its consolidation. In Proceedings of the 8th International Congress on Deterioration and Conservation of Stone, ed J. Riederer. Berlin, Germany, 2:1159–1170

Anexo 4. Publicación nº.3

"Characterization of swelling in clay-bearing stone"

Scherer, G.W. and Jiménez González, I.

in Turkington A.V., ed., Stone decay in the architectural environment:

Geological Society of America, Special Paper 390 (2005) 51-61.

Geological Society of America
Special Paper 390
2005

Characterization of swelling in clay-bearing stone

George W. Scherer
Inmaculada Jimenez Gonzalez
Princeton University, Department of Civil & Environmental Engineering, Princeton Materials Institute, Engineering Quad. E-319, Princeton, New Jersey 08544, USA

ABSTRACT

Many sedimentary rocks contain clays that cause differential swelling upon exposure to moisture, and the resulting internal stresses are blamed for the deterioration of buildings and monuments. To predict the likelihood of damage from this mechanism, it is necessary to characterize the magnitude of the swelling and the mechanical properties of the stone. Stones that swell also exhibit viscoelastic behavior, probably owing to sliding of the clay layers. In this paper we discuss the characterization of the relaxation and swelling behavior and the estimation of stresses resulting from swelling. A new method for measuring swelling is introduced, in which warping of a plate of stone is produced by wetting one side. This method is faster than the traditional direct measurement of swelling pressure, and it also yields information about the permeability and the influence of wetting on the elastic modulus. Sample results are presented for Portland Brownstone.

Keywords: Portland Brownstone, swelling clays, viscoelastic behavior, permeability, Young's modulus of elasticity, sedimentary rocks, warping, water absorption, mechanical properties, porosity, beam-bending method, stress, strain, sorptivity, crystallization pressures.

INTRODUCTION

Many sedimentary rocks contain clays that cause the stone to swell upon exposure to moisture (Dunn and Hudec, 1966), and the resulting deformation is thought to be responsible for deterioration of buildings, monuments, and sculptures (Delgado Rodrigues, 2001; Veniale et al., 2001). Examples of susceptible stone include the brownstone widely used in the northeastern United States (Jimenez Gonzalez et al., 2002), the molasse used in the cathedral of Lausanne, Switzerland (Félix, 1994), and sandstones used in some Egyptian sculpture (Charola et al., 1982; Rodriguez-Navarro et al., 1997). Figure 1 shows damage to the molasse in the cathedral in Lausanne. On the left side of the window (Fig. 1, top photo) there are large cracks indicating separation of the surface layer from the underlying stone; on the right side (Fig. 1, bottom photo) the damage has progressed farther, and the surface layers have detached. Looking at the surface of the lower part of the column in Figure 1, it is evident that a relatively coherent surface layer >1 cm thick has detached along a circumferential plane. This is the sort of damage that would be expected if the surface expanded relative to the interior.

Although some clays exhibit enormous expansions, the greatest stress is exerted at small strains; the pressure required to suppress the expansion of clay typically drops exponentially as the volume increases (Macey, 1942; MacEwan and Wilson, 1980). However, only a small strain is required to produce stresses exceeding the tensile strength of stone, so differential swelling resulting from superficial wetting or drying of a stone surface can cause deterioration even for a stone whose swelling is on the order of 0.1%.

E-mail: scherer@princeton.edu

Scherer, G.W., and Jimenez Gonzalez, I., 2005, Characterization of swelling in clay-bearing stone, *in* Turkington, A.V., ed., Stone decay in the architectural environment: Geological Society of America Special Paper 390, p. 51–61.

Figure 1. (Upper) Cracks in stone (molasse) on left side of window in Lausanne Cathedral; (Lower) damaged stone on right side of the same window.

The goal of this research is to assess the risk of damage from swelling. The problem is complicated by the fact that stones that swell are also viscoelastic, and the dynamic elastic modulus obtained from acoustic measurements is vastly different from the static modulus that is relevant for stress development (Tutuncu et al., 1998). This paper presents analyses of swelling experiments that are useful for evaluating the stresses produced by swelling. First, the standard "direct test" is considered, where a sample of stone is held at a fixed length in a rigid frame and then saturated with water. Normally, one simply measures the force exerted by the stone against the constraint, but it is also possible to extract information about the kinetics of water movement and viscoelastic relaxation of the stone. This measurement has certain disadvantages, so a new method for evaluating swelling stress is introduced, which is to observe the warping of a thin plate of stone when water is put in contact with one side. These methods have been used in a detailed study of the behavior of Portland Brownstone and several other stones. The purpose of this paper is to examine the measurement methods in detail.

This study of swelling indicates that some stones may indeed suffer destructive stresses as a result of the differential strains produced during wetting. However, it is important to recognize that stones containing clays necessarily contain a fraction of very small pores, and these are the pores most likely to generate high crystallization pressure (Scherer, 1999). Consequently, such stones are inherently susceptible to damage from crystallization of ice and salt (McGreevy and Smith, 1984). The fact that these two mechanisms of damage are likely to act in concert makes it particularly important to evaluate their relative importance so that appropriate conservation measures can be chosen.

PORTLAND BROWNSTONE

To illustrate the application of the swelling characterization experiments, some results of experiments on Portland Brownstone are used here to offer a brief description of the materials and procedures.

Structure

Plates (25 × 25 × 5 cm) of Portland Brownstone were purchased from Pasvalco Company of Closter, New Jersey, and samples were prepared by cutting with a diamond saw or core drill (2 cm inner diameter). X-ray analysis performed on one of our samples (T.

Fuellmann, 2002, personal commun.) indicated that it consisted primarily of grains of quartz and anorthite in a matrix containing montmorillonite, kaolinite, and illite. The pore structure was characterized by nitrogen sorption using a Micromeritics ASAP 2010 and by mercury porosimetry using a Micromeritics 9410. The pore diameter distribution was found to be bimodal (Jimenez Gonzalez et al., 2002), with about half the volume around a peak near 10 μm and the rest near a peak at 0.1 μm. The latter peak was the only one detected by nitrogen sorption. The porosity of the stone, obtained by vacuum impregnation with water, is ~8.7%.

Free Swelling Strain

To measure the free expansion of the stone, rectangular parallelepipeds or core-drilled cylinders were placed into the differential mechanical analyzer (DMA, Perkin-Elmer). The maximum sample height in this instrument is limited to ~18 mm. A bath of water was raised around the sample, and the linear expansion was measured as a function of time. The swelling was found to be $4.5 \pm 1.0 \times 10^{-4}$ perpendicular to the bedding.

Sorptivity

Sorptivity was measured by suspending samples of stone from an electronic balance so that the bottom of the stone touched a large pool of water and recording the output from the balance continuously; the sides of the sample were coated with grease to prevent evaporation. The height of rise in the stone, h, is calculated from the weight gain, Δm, using

$$h = \frac{\Delta m}{\phi \rho_L A}, \tag{1}$$

where A is the area of the sample in contact with the liquid, ϕ is the porosity of the stone ($\phi = 0.087$ for the Portland Brownstone used in our study), and $\rho_L = 1.0$ g/cm^3 is the density of the liquid. The sorptivity, S, is then defined by

$$h = S\sqrt{t}, \tag{2}$$

where t is the time in seconds. The sorptivity of the Portland Brownstone was found to be $S_r \approx 0.012$ cm/s$^{1/2}$ parallel to the bedding and $S_z = 0.0079$ cm/s$^{1/2}$ perpendicular to the bedding.

For comparison to other measurements, it is useful to note that the sorptivity is related to the permeability, k. The water moves into the stone according to Darcy's law (Happel and Brenner, 1986),

$$J = -\frac{k}{\eta_L}\nabla p, \tag{3}$$

where J is the flux, η_L is the viscosity of the liquid, and ∇p is the pressure gradient. In the sorptivity experiment, the gradient is

$$\nabla p = \frac{p_c}{h} = \frac{2\gamma}{h r_m}, \tag{4}$$

where ∇p is the capillary pressure ($\nabla p < 0$), γ is the liquid-vapor interfacial energy, and r_m is the radius of the meniscus; if the contact angle of the liquid on the pore walls is zero, then r_m equals the pore radius, r_p. Recognizing that the flux in the sorptivity experiment is $\phi\, dh/dt$, the sorptivity is found to be

$$S = \sqrt{\frac{-2k\, p_c}{\phi \eta_L}} \approx \sqrt{\frac{4k\, \gamma}{\phi \eta_L r_p}}. \tag{5}$$

Elastic Modulus Measurements

The dynamic elastic modulus was calculated from the acoustic velocity at 54 KHz, measured using a commercial instrument (PUNDIT, CNS Farnell, London, UK) on stones of various sizes, wet and dry. The size of the sample is significant, because this method yields Young's modulus on very slender bodies and the longitudinal modulus on very large ones (Kolsky, 1963). More important is the effect of strain on the modulus (Tutuncu et al., 1998), because the acoustic method imposes a very small strain, and the modulus decreases as the strain increases. The frequency also has a large affect on the modulus, particularly when the sample is wet. The dynamic modulus of the dry stone was ~25 GPa and rose to 35 GPa in the wet stone. However, the static modulus (obtained from the slope of the 3-point bending curves) was only ~9.1 GPa in the dry stone and decreased to ~4.1 GPa in samples saturated with water. Similar enormous discrepancies between acoustic and static moduli have been reported (Tutuncu et al., 1998). The effect is attributed to the movement of water from grain contacts, which provides compliance at low frequencies of loading, but which cannot occur at high frequencies. Since we are interested in stresses generated over a long period of time under substantial strains, only the static modulus data are relevant.

When a plate of saturated stone is subjected to bending, the concave side of the sample is compressed and the convex side is stretched, so a pressure gradient is created in the pore liquid. The liquid flows until atmospheric pressure is restored, and the force required to sustain a fixed deflection decreases with time; this process is called hydrodynamic relaxation, because it results from flow of the pore liquid. If the solid phase in the sample is viscoelastic, then further relaxation of the force will occur. This phenomenon has been used to measure the permeability of porous bodies, including gels (Scherer, 1992), porous glass (Vichit-Vadakan and Scherer, 2000), and cement paste (Vichit-Vadakan and Scherer, 2002). For this measurement, an apparatus (Vichit-Vadakan and Scherer, 2000) with a rigid frame holding a stepper motor was used. The pushrod is driven downward by the motor; a load cell is incorporated into the pushrod to measure the applied force, and the pushrod passes through a linear variable differential transformer (LVDT) that measures the displacement. The sample was supported at one end by a roller and at the other

end by a ball, so that the plate was not subjected to twisting, even if it was not perfectly flat. The sample was immersed in liquid, so that the pore pressure was fixed at atmospheric pressure at the surfaces and liquid could freely exchange between the pores and the bath. Figure 2 shows the load relaxation of a plate of Portland Brownstone after application of a deflection of 136 μm. The fit of the theoretical curve (Scherer, 2000a) to the data is seen to be very good; it consists of the product of the hydrodynamic and viscoelastic relaxation curves, which are shown separately. The parameters of the fit include the elastic modulus of the saturated plate, $E = 3.9$ GPa, and the permeability, $k = 0.15$ nm^2. Substituting this value into Equation (5), we find that $r_p = 40$ nm, which is in very good agreement with the mean size measured by nitrogen sorption; this indicates that the smaller peak of the pore size distribution provides the driving force for capillary rise. The viscoelastic relaxation is approximated by a stretched exponential function,

$$\frac{\sigma_z(t)}{\sigma_z(0)} \equiv \Psi(t) = \exp\left[-\left(\frac{t}{\tau_{VE}}\right)^{\beta}\right], \qquad (6)$$

with $\tau_{VE} \approx 2 \times 10^{10}$ s and $\beta \approx 0.12$. Only a small part of the relaxation is observed, so the fitting parameters cannot be taken too seriously (i.e., the relaxation process would probably not take 10^5 yr), but they do accurately represent the first 15% of the relaxation, which takes ~3 h.

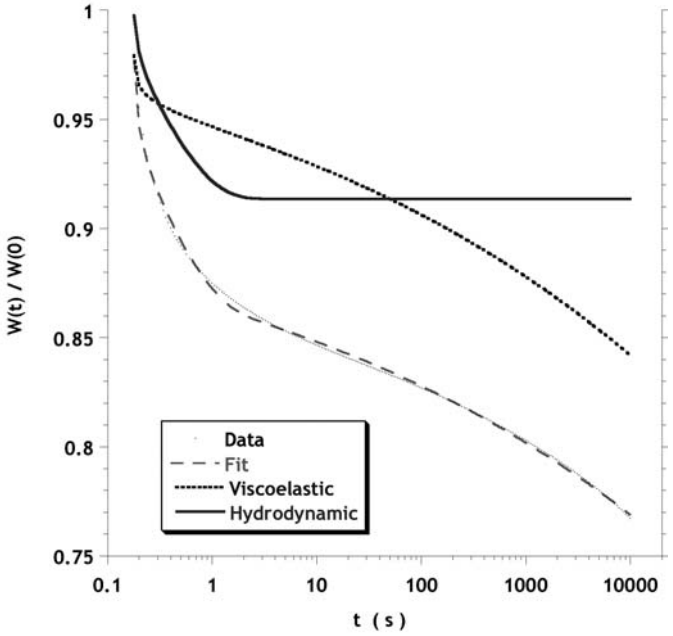

Figure 2. Relaxation of applied force at constant deflection for a plate of Portland Brownstone saturated with pure water. The dashed line is the fit of the data to the theoretical curve (Scherer, 2000a). The hydrodynamic relaxation results from equilibration of the pressure in the pore liquid, which is complete in ~2 seconds. The viscoelastic curve represents the stress relaxation produced by flow of the solid phase; the curve is given by Equation (6).

Swelling Measurements

Direct measurements of swelling were performed on a sample of Portland Brownstone ~5 cm high and 3.17 cm square, with a circular hole 2.18 cm in diameter. The arrangement, shown in Figure 3, allows water to invade the sample from the inner and outer surfaces simultaneously, while the height of the stone is fixed by the platens of the testing machine.

An alternative method for measuring expansion, discussed in detail in a later section, is to induce warping in a thin plate of stone by wetting only one side. For this purpose, a plate of Portland Brownstone 0.38 cm thick and 1.0 cm wide was placed on supports 9.3 cm apart. A bead of vacuum grease was run around the upper edge (to act as a dam); water was poured onto the top surface, and the deflection of the plate was measured with an optical probe (MTI 1000, MTI Instruments, Inc.) mounted below the plate. A small piece of reflective foil was glued to the bottom to improve the sensitivity of the probe.

THEORETICAL BACKGROUND

Direct Measurement of Swelling Pressure

The conventional method (e.g., Madsen and Müller-Vonmoos, 1989) for evaluating the swelling pressure is to place a sample of stone into a rigid frame and then saturate it with water. As the water invades the pores of the stone, the stone swells and exerts pressure on the confining frame. The objective of this measurement is usually to determine the maximum pressure exerted by the stone, but the kinetics of the increase provide information about the sorptivity of the stone. In this section, an elastic analysis of the stress is presented, then the kinetics of stress development is considered by examining the rate of penetration of the water into the stone, and the importance of viscoelastic effects is considered, given that the duration of the experiment is several hours so that substantial relaxation can occur.

The sedimentary rocks that contain clays often show strong bedding, so it should be expected that in general the stone is transversely isotropic; i.e., the properties are uniform parallel to the bedding, but different in the perpendicular direction. Let us adopt a cylindrical coordinate system with the z axis perpendicular to the bedding, and the $r - \theta$ plane parallel to the bedding. The elastic constitutive equations are

$$\varepsilon_r = \frac{du}{dr} = \varepsilon_{fr} + \frac{\sigma_r}{E_r} - \frac{v_r\sigma_\theta}{E_r} - \frac{v_z\sigma_z}{Ez} \qquad (7)$$

$$\varepsilon_\theta = \frac{u}{r} = \varepsilon_{fr} + \frac{\sigma_\theta}{E_r} - \frac{v_r\sigma_r}{E_r} - \frac{v_z\sigma_z}{E_z} \qquad (8)$$

$$\varepsilon_z = \varepsilon_{fz} + \frac{\sigma_z}{E_z} - \frac{v_z\sigma_r}{E_z} - \frac{v_z\sigma_\theta}{E_z} \qquad (9)$$

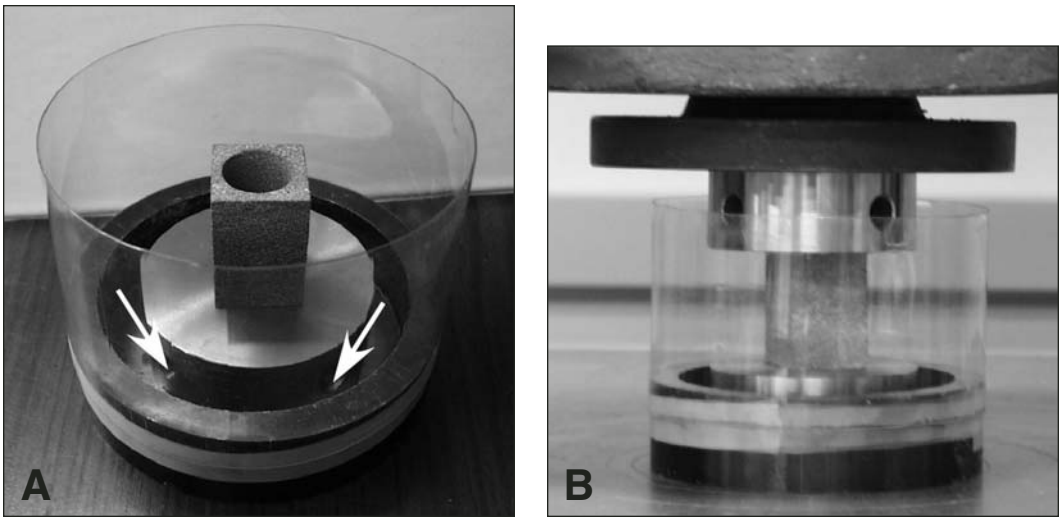

Figure 3. Setup for direct swelling measurement. (A) Hollow sample of stone rests on stainless steel platform with holes (indicated by arrows) that allow water to flow up through hole centered under sample so that water penetrates from the inner and outer surfaces of the sample. (B) Sample held to fixed length by platens of testing machine. Once the sample is arranged as in (B), water is quickly poured into the dish until the sample is submerged.

where $\varepsilon_j (j = r,\theta,z)$ are the strains, σ_j are the stresses, E_j and v_j are Young's modulus and Poisson's ratio, respectively, and u is the radial displacement. The free strain produced by swelling of the clay is ε_{fr} in the plane and ε_{fz} perpendicular to the bedding. As noted in the previous section, the latter quantity was found to be $\varepsilon_{fz} = 4.5 \pm 1.0 \times 10^{-4}$ for the Portland Brownstone used in this study. For a transversely isotropic material, Darcy's law becomes (Bear, 1972):

$$J_j = -\frac{k_j}{\eta_L}\nabla p\left(j = r,\theta,z\right), \tag{10}$$

where $k_r = k_\theta$. In the experiment described above, the bedding was perpendicular to the long axis of the plate, so the permeability obtained was k_r. For an isotropic material, Equations (7–10) still apply, with $E_r = E_z$, $v_r = v_z$, and $k_r = k_z$.

The geometry of the direct stress measurement is shown in Figure 4. The bedding is horizontal and the water invades from the inner and outer surfaces of the sample, which is in the form of a hollow cylinder. The inner wet region (Region 1) extends from $r = a$ to $r = r_1$, and the outer wet region (Region 2) extends inward from $r = b$ to $r = r_2$; the dry region lies between r_1 and r_2. In the dry region, the free swelling strain is zero and in the wet region it is ε_{fz}. Force balance in the cylinder requires:

$$\sigma_\theta = \frac{d}{dr}\left(r\sigma_r\right). \tag{11}$$

Substituting Equations (7) and (8) into Equation (11) shows that the radial displacement must have the form

$$u = c_1/r + c_2 r, \tag{12}$$

where c_1 and c_2 are constants to be determined; there are two such constants for each of the three regions. The boundary conditions required to find those constants are obtained by requiring that the radial stresses be zero at the exposed surfaces ($r = a$ and b), and that the radial stresses and displacements be continuous at r_1 and r_2. Finally, the axial strains are required to be zero in all regions, because of the constraint imposed by the testing machine. Satisfying these equations leads to expressions for the axial stress in each region. The total force, F, on the testing machine is the sum of the forces from each region:

$$F = \left(r_1^2 - a^2\right)\sigma_{z1} + \left(r_2^2 - r_1^2\right)\sigma_{zd} + \left(b^2 - r_2^2\right)\sigma_{z2}. \tag{13}$$

The complete expression for the force for a transversely isotropic body is very complicated (it would take several pages to write out the constants), but a drastic simplification is obtained if we make the reasonable assumption that the softening produced by exposure to water is the same in the radial and axial directions:

$$\frac{E_{rw}}{E_{rd}} \approx \frac{E_{zw}}{E_{zd}} \equiv f, \tag{14}$$

and that the value of Poisson's ratio is roughly the same in both directions ($v_r = v_z$) and is not significantly affected by wetting. With these approximations, Equation (13) reduces to

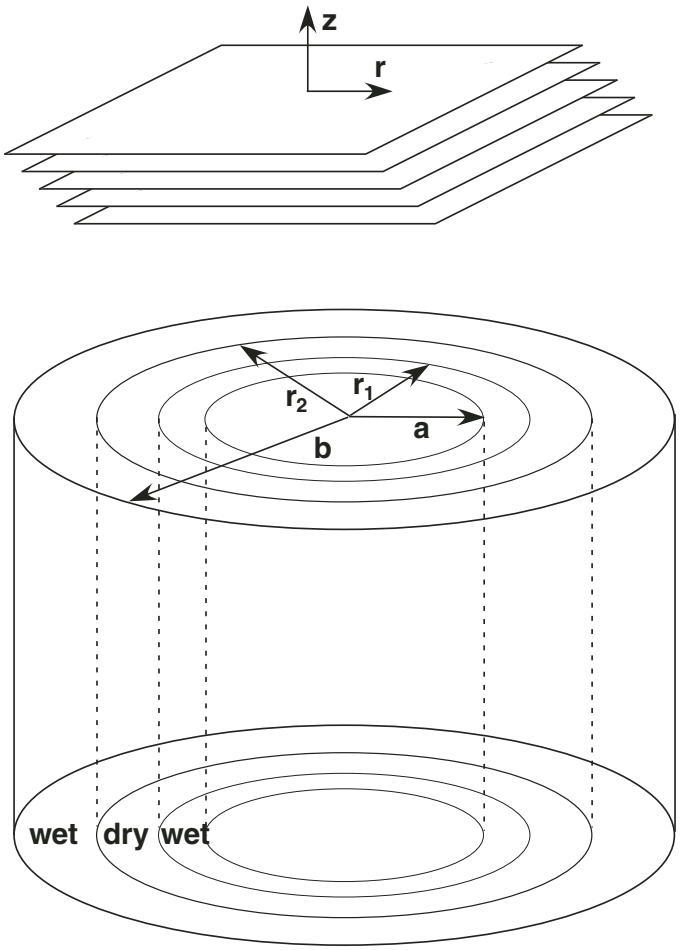

Figure 4. Schematic illustration of sample used for direct measurement of swelling pressure. The bedding is perpendicular to the axis of the cylinder as indicated at the top of the figure. Liquid invades through the inner and outer surfaces ($r = a$ and b), and the edge of the advancing fronts from the inner and outer surfaces are r_1 and r_2, respectively.

$$F = -\left(b^2 - r_2^2 + r_1^2 - a^2\right) E_{zw} \varepsilon_{fz}, \tag{15}$$

so the swelling stress is

$$\sigma_s = \frac{F}{b^2 - a^2} = -\left(\frac{b^2 - r_2^2 + r_1^2 - a^2}{b^2 - a^2}\right) E_{zw} \varepsilon_{fz}. \tag{16}$$

Once saturation is complete ($r_1 = r_2$), given the values previously cited for E_{zw} and ε_{fz}, the direct stress measurement is expected to yield $\sigma_s = -E_{zw}\,\varepsilon_{fz} \approx 1.4 - 2.3$ MPa for Portland Brownstone. The next problem is to find the rate of penetration of the water into the sample.

The water invades the sample just as in a sorptivity experiment, where the pressure gradient results from capillary pressure and the transport obeys Darcy's law. To solve for the rate of invasion, the continuity equation is solved for flow within the wet region (Scherer, 2000b):

$$\left(1 - \frac{K_p}{K_S}\right)\dot{\varepsilon} + \dot{p}\left(\frac{1 - K_p/K_S - \phi}{K_S} + \frac{\phi}{K_L}\right) = \nabla \cdot J_r, \tag{17}$$

where $\dot{\varepsilon}$ is the volumetric strain, ϕ is the volume fraction of porosity, K_L is the bulk modulus of the liquid, and liquid, K_S is the bulk modulus of the solid phase and K_p is the bulk modulus of the porous body. The maximum value for p is the capillary pressure, p_c, which is very small compared to the elastic moduli, so those terms can be neglected; similarly, the volumetric expansion is negligible (<0.1% linearly), so the equation reduces to

$$\nabla \cdot J_r = -\frac{k_r}{\eta_L} \nabla^2 p = 0. \tag{18}$$

Then, Equation (18) is solved subject to the following boundary conditions: the pore pressure at the free surfaces is zero, $p_1(a) = p_2(b) = 0$, and is equal to the capillary pressure, p_c, at the leading edge of the advancing liquid front, $p_1(r_1,t) = p_2(r_2,t) = p_c$. In region 1, the pressure is found to be

$$p_1(r,t) = \frac{p_c \ln\left[r/a\right]}{\ln\left[r_1(t)/a\right]}, \tag{19}$$

and in region 2,

$$p_2(r,t) = \frac{p_c \ln\left[b/r\right]}{\ln\left[b/r_2(t)\right]}. \tag{20}$$

The volume of water crossing the boundary of region 1 is given by

$$2\pi r_1 \frac{dr_1}{dt}\phi = 2\pi r_1 J_r(r_1,t), \tag{21}$$

which leads to

$$\int_a^{r_1} r_1 \ln\left[r_1/a\right] dr_1 = -\int_0^L \frac{k_r p_c}{\eta_L \phi} dt \tag{22}$$

and

$$\left(\frac{r_1^2}{2}\right)\ln\left[\frac{r_1}{a}\right] - \frac{r_1^2 - a^2}{4} = -\left(\frac{k_r p_c}{\eta_L \phi}\right) t. \tag{23}$$

Using Equation (5), we can define a dimensionless time:

$$\theta = \left(\frac{S_r}{a}\right)^2 t, \tag{24}$$

and Equation (23) is rewritten as

$$\frac{1}{2}\left[1-\frac{r_1^2}{a^2}+\frac{r_1^2}{a^2}\ln\left(\frac{r_1^2}{a^2}\right)\right]=\theta. \tag{25}$$

Similarly, considering the flux from region 2, Equation (26) is derived:

$$\int_b^{r_2} r_2 \ln\left[b/r_2\right] dr_2 = \int_0^t \frac{k_r p_c}{\eta_L \phi}. \tag{26}$$

So,
$$\frac{1}{2}\left[1-\frac{r_2^2}{b^2}+\left(\frac{r_2^2}{b^2}\right)\ln\left(\frac{r_2}{b^2}\right)^2\right]=\left(\frac{S_r}{b}\right)^2 t = c^2\theta, \tag{27}$$

where $c = a/b$. The sample becomes saturated when $r_1 = r_2$. Equating Equations (23) and (28), the depth at which the advancing fronts meet is

$$r_1^{sat} = r_2^{sat} = a\sqrt{\frac{1/c^2-1}{\ln\left(1/c^2\right)}}. \tag{28}$$

Substituting those dimensions into Equations (25) or (27), the time at which saturation is achieved is

$$\theta_{sat}=\left(\frac{S_r}{a}\right)^2 t_{sat}=\frac{1}{2}-\frac{1-c^2}{2c^2\log\left(1/c^2\right)}\left[\log\left(\frac{c^2\log\left(1/c^2\right)}{1-c^2}\right)+1\right]. \tag{29}$$

For $0.5 \le a/b \le 1$, θ_{sat} is approximated with less than 2% error by

$$\theta_{sat} \approx \frac{1}{4}\left(\frac{1}{c}-1\right)^2. \tag{30}$$

The measured stress depends on the volume fraction of saturation, v, which is defined as

$$v=\frac{b^2-r_2^2+r_1^2-a^2}{b^2-a^2}. \tag{31}$$

Using Equations (25) and (27) to evaluate Equation (31), when $a/b \ge 0.5$, the volume fraction saturated is given to a very high accuracy by

$$v \approx \sqrt{\frac{\theta}{\theta_{sat}}}=\sqrt{\frac{t}{t_{sat}}}. \tag{32}$$

Therefore, Equation (16) can be written as a simple function of time:

$$\sigma_z = -vE_{zw}\varepsilon_{fz} = -E_{zw}\varepsilon_{fz}\sqrt{\frac{t}{t_{sat}}}. \tag{33}$$

The advantage of this experiment is that it provides a direct measurement of the quantity $E_{zw}\,\varepsilon_{fz}$ (obtained from the final stress value); moreover, the sorptivity can be found from the time required to achieve saturation, since Equations (29) and (30) indicate that

$$t_{sat} \approx \frac{1}{4}\left(\frac{b-a}{S}\right)^2. \tag{34}$$

However, this analysis is only valid when the bedding is horizontal; otherwise, the sample is not axisymmetric, and the analysis is quite complicated. Moreover, the time required to achieve saturation is typically hours or days, during which time there will be substantial viscoelastic relaxation. Consequently, the elastic analysis presented here is not adequate to describe the kinetics.

A viscoelastic (VE) analysis can be obtained quite simply for a planar geometry, and since Equation (32) indicates that the kinetics for the approach to saturation are nearly identical for a cylinder and a plate, the planar solution should be a good approximation to the present case. First, an elastic solution for the plate is obtained, then the VE solution follows directly. Suppose that water invades the opposite faces of a plate of stone whose thickness is L, so that each side is saturated to a depth L_w and there is a dry central region of width L_d, where $L = L_d + 2L_w$. If the water is advancing parallel to the x axis and the expansion is constrained in the z direction, then the strain $\varepsilon_z = 0$ and the stresses in the unconstrained directions are $\sigma_x = \sigma_y = 0$. The constitutive equation in the z direction is given by Equation (9):

$$\varepsilon_z = \varepsilon_{fz} + \frac{\sigma_{zw}}{E_{zw}} = 0, \tag{35}$$

where σ_{zw} and E_{zw} are the stress and Young's modulus in the wet region, and ε_{fz} is the free swelling strain. In the dry interior, there is no free strain, so

$$\varepsilon_z = \frac{\sigma_{zd}}{E_{zd}} = 0. \tag{36}$$

Thus, there is no stress in the dry region, and the total stress exerted by the swelling plate is

$$\sigma_s = \left(\frac{2L_w}{L}\right)\sigma_{zw} = -\left(\frac{2L_w}{L}\right)E_{zw}\varepsilon_{fz}. \tag{37}$$

From Equation (2), $L_w = S_r\sqrt{t}$, so the elastic solution for the swelling stress is

$$\sigma_s^E = -2\left(\frac{S_r\sqrt{t}}{L}\right)E_{zw}\varepsilon_{fz}. \tag{38}$$

If the wet stone is viscoelastic, then Equation (6) indicates that E_{zw} must be replaced by $E_{zw}\psi(t)$. The water reaches a depth x at time $t' = x^2/S_r^2$, and that is the time at which relaxation begins, so the stress at any point is

$$\sigma_{zw}^{VE}(x,t) = -E_{zw}\varepsilon_{fz}\Psi\left(t - x^2/S_r^2\right). \quad (39)$$

Thus, for a VE material, Equation (38) is replaced by

$$\sigma_s^{VE} = \left(\frac{2}{L}\right)\int_0^{L_w}\sigma_{zw}dx = -\left(\frac{2}{L}\right)E_{zw}\varepsilon_{fx}\int_0^{L_w}\Psi\left(t - x^2/S_r^2\right)dx. \quad (40)$$

The integral can be written in terms of time alone, since $x = S_r\sqrt{t}$:

$$\sigma_s^{VE} = -\left(\frac{S_r}{L}\right)E_{zw}\varepsilon_{fz}\int_0^t \Psi(t-t')\frac{dt'}{\sqrt{t'}},\ t \le t_{sat}. \quad (41)$$

When the material is elastic, $\psi(t) = 1$, and Equation (41) reduces to Equation (38). Equation (41) applies until the plate becomes saturated, at time $tsat = L^2/(4S_r^2)$; thereafter,

$$\sigma_s^{VE} = -\left(\frac{S_r}{L}\right)E_{zw}\varepsilon_{fz}\int_0^{t_{sat}} \Psi(t-t')\frac{dt'}{\sqrt{t'}},\ t \le t_{sat}. \quad (42)$$

Unfortunately, if the relaxation of the stone obeys the stretched exponential function in Equation (6), Equation (41) cannot be integrated in closed form.

If the VE relaxation is slow compared to the duration of the swelling experiment, then the elastic analysis is sufficient, and one can obtain both the maximum swelling stress and the sorptivity of the sample from this measurement. If relaxation is fast, then the measurement can be used to determine Ψ by fitting the measured stress to Equation (42). The simplest way to determine whether VE relaxation is sufficient is to continue the experiment well beyond the time of saturation to see whether the stress passes through a maximum and relaxes again. This type of experiment was performed on the sample in Figure 3; the result is shown in Figure 5. The calculated curve was obtained from Equations (41) and (42), using $\psi(t)$ from Figure 2, and assuming $S = 0.012$ cm/s$^{1/2}$; the peak stress value corresponds to $E_{zw}\,\varepsilon_{fz}$ = 0.74 MPa. If E_{zw} = 3.9 GPa, as found from the fit in Figure 2, then $\varepsilon_{fz} = 1.4 \times 10^{-4}$, which is unusually small for this stone. The reproducibility of this type of experiment was poor and always yielded smaller than expected stresses. Part of the problem is that the force is at the very low end of the range of the load cell on the testing machine; moreover, the total expected free swelling is ~20 μm, so a very small movement of the platen would substantially affect the measured stress.

Although the direct stress measurement is rich in information, it is slow, difficult, and requires expensive equipment. Ordinary mechanical testing machines cannot necessarily be trusted to hold the sample dimensions fixed within a few microns, so specialized equipment should be built. Moreover, the experiment uses a relatively large amount of stone (especially if a mechanical testing machine with a large load cell is used), which may be problematic if the stone is to be taken from a monument. Therefore, it is desirable to have a test of swelling stress that is relatively fast and uses a minimal amount of stone. The warping method described in the next section satisfies those requirements.

Warping Method

A novel method for characterizing the swelling stress is presented here, based on the following principle (see Fig. 6): if one side of a thin plate of swelling stone is exposed to water, that side will swell and cause the plate to warp. The displacement of the plate is large, if the ratio of length to thickness is large, so the effect is easily measured.

An example of a warping experiment, performed on a plate of Portland Brownstone 0.38 cm thick, is shown in Figure 7. The upward deflection peaks at 155 μm ~100 s after the water is poured onto the plate; as the water proceeds through the plate, it becomes uniformly dilated, so the warping is eliminated. If the elastic properties of the wet and dry regions were equal, then the maximum deflection would occur when the water had penetrated halfway through the plate; however, the wet stone is less stiff, so the maximum is shifted. An elastic analysis of this problem is presented here; a viscoelastic treatment is not necessary, because the duration of the experiment is so short.

If, as illustrated in Figure 8, a long slender beam rests on supports with a span of L, and the plate acquires a radius of curvature R, then the deflection out of plane is Δ. If $\Delta << R$, then the geometry indicates that

$$\Delta = \frac{L^2}{8R} \quad (43)$$

.

In the present case, the radius of curvature results from the difference in free strain between the wet part (strain = ε_{fz} or ε_{fr}, according to the orientation of the sample) and the dry part (strain = zero). The warping of a composite beam was analyzed by Timoshenko (1925; see Scherer, 1992), who found that:

$$\frac{1}{R} = \frac{K_R\Delta\varepsilon_f}{h}, \quad (44)$$

where h is the thickness of the plate, $\Delta\varepsilon_f = \varepsilon_{fz}$ or ε_{fr}, and

$$K_R = \frac{6m(1+m)^2 f}{m^4 f^2 + 4m^3 f + 6m^2 f + 4mf + 1}, \quad (45)$$

where $m = h_w/h$ and $f = E_{zw}/E_{zd}$ or E_{rw}/E_{rd}, according to the orientation of the plate. According to Equation (2),

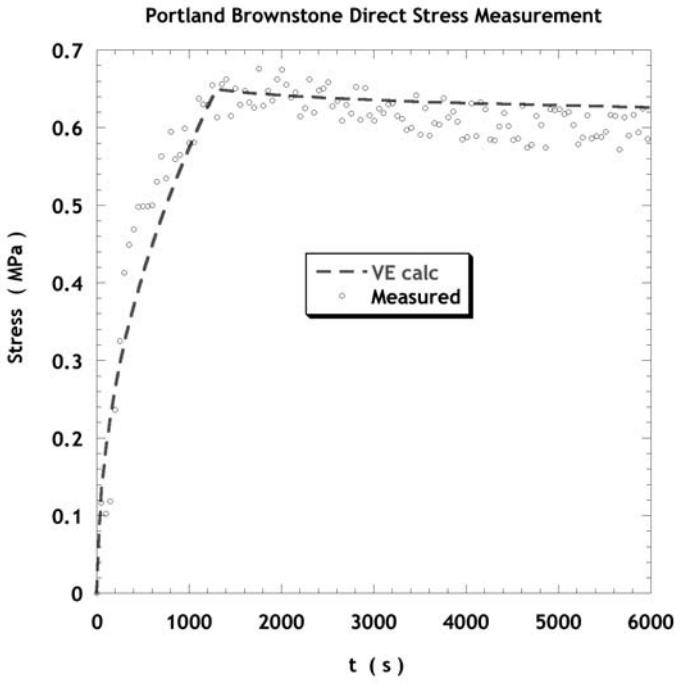

Figure 5. Direct swelling stress measurement for Portland Brownstone sample confined between platens of testing machine. The dashed curve was calculated using Equations (41) and (42), using $\psi(t)$ from Figure 2 and assuming $S = 0.013$ cm/s$^{1/2}$; the peak stress value corresponds to $E_{zw}\,\varepsilon_{fz} = 0.74$ MPa, which is smaller than expected (see text).

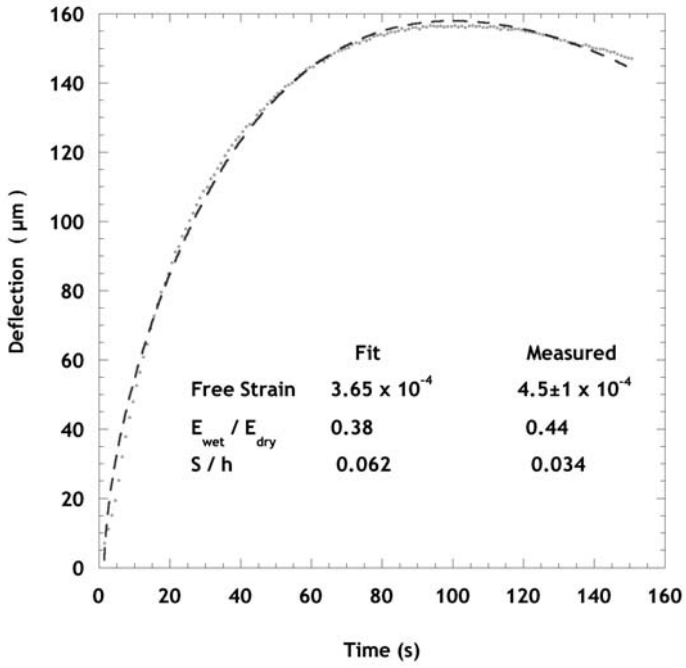

Figure 7. Measured deflection (symbols) and fit (dashed curve) to Equation (47). The fit is applied only to the data shown. At longer times, there is a discrepancy, which is shown in Figure 9.

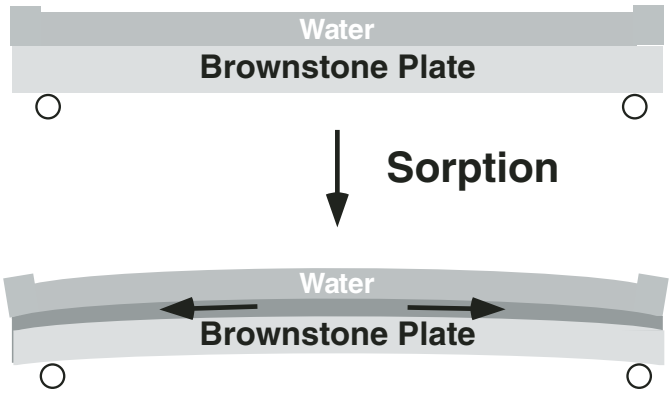

Figure 6. Schematic illustration of warping experiment. A plate of stone is supported at each end, and a dam of vacuum grease is applied around the upper edge. When water is poured on top, the upper surface of the stone expands and the plate warps; the upward deflection is measured with an optical probe (not shown) focused on the underside of the plate.

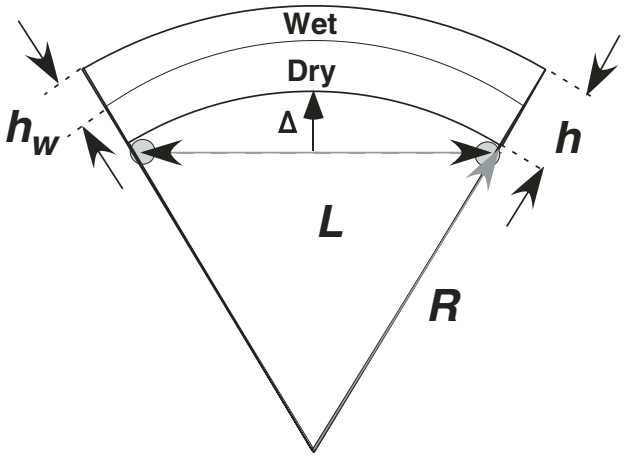

Figure 8. Schematic of warping showing radius of curvature, R, span between supports, L, and deflection, Δ; h is thickness of plate and h_w is depth of saturated zone.

$$m = \frac{h_w}{h} = \frac{S\sqrt{t}}{h} \equiv \sqrt{\theta}, \tag{46}$$

where the latter definition is analogous to Equation (24). If the bedding is perpendicular to the long axis of the plate, then $\Delta\varepsilon_f = \varepsilon_{fz}$, $S = S_r$, and $f = E_{zw}/E_{zd}$; if the bedding is parallel to the large surface of the plate, then $\Delta\varepsilon_f = \varepsilon_{fr}$, $S = S_z$, and $f = E_{rw}/E_{rd}$. With these abbreviations, Equation (43) can be written as

$$\Delta = \Delta_0 \left[\frac{4f\left(\theta^{1/2} - \theta\right)}{1 - 4(1-f)\theta^{1/2} + 6(1-f)\theta - 4(1-f)\theta^{3/2} + (1-f)^2\theta^2} \right], \tag{47}$$

where,

$$\Delta_0 = \frac{3L^2\Delta\varepsilon_f}{16h}. \tag{48}$$

By setting the derivative of Δ with respect to θ equal to zero, the maximum in Δ is equal to Δ_0, and the maximum occurs at reduced time:

$$\theta_{max} = \frac{1}{\left(1+\sqrt{f}\right)^2} \tag{49}$$

or elapsed time:

$$t_{max} = \left(\frac{h}{S\left(1+\sqrt{f}\right)} \right). \tag{50}$$

Thus, the free swelling strain of the stone can be found from the maximum deflection by using Equation (48). The quantities f and S can be obtained by fitting Equation (47) to the measured deflection, as in Figure 7. Alternatively, if the deflection is normalized by its maximum value (Δ_0) and the time is normalized by t_{max}, the resulting function depends only on f. Then it is only necessary to perform a one-parameter fit to

$$\frac{\Delta}{\Delta_0} = \left(4f\left(1+\sqrt{f}-y\right)y\right) \Big/ \left(\left(1+\sqrt{f}\right)^2 - 4\left(1+\sqrt{f}-f\right)\right.$$
$$\left. -f^{3/2}\right)y + 6(1-f)y^2 - 4\left(1-\sqrt{f}\right)y^3 + \left(1-\sqrt{f}\right)^2 y^4 \tag{51}$$

where $y = \sqrt{t/t_{max}}$. Once f is obtained from this fit, the sorptivity can be calculated from t_{max} using Equation (50). An example of a fit to normalized data is shown in Figure 9.

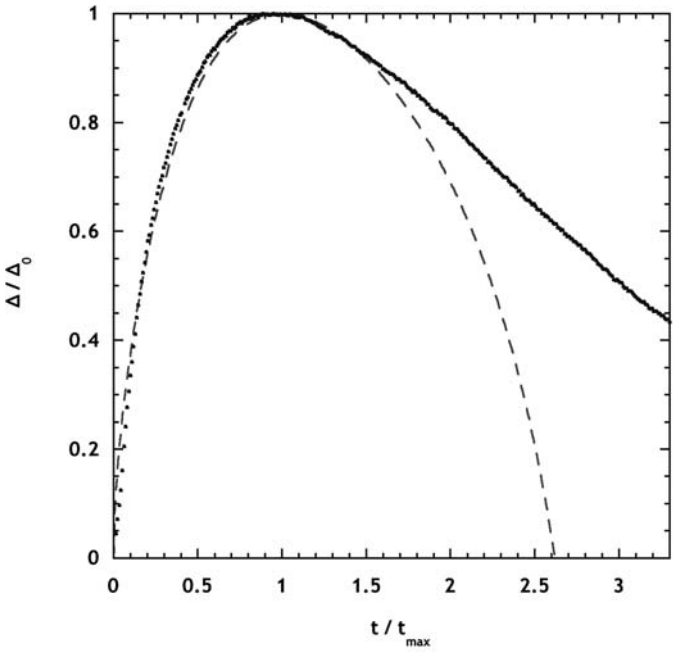

Figure 9. Data from Figure 7 normalized by the peak deflection, Δ_0, and the time of the maximum, t_{max}. The fit (dashed curve) is extrapolated to show the discrepancy between the measurement (symbols) and the fit at long times.

DISCUSSION

The fit to the warping deflection in Figure 7 yields parameters that are in good agreement with independent measurements. The plate was oriented with the bedding vertical (i.e., perpendicular to the long axis of the plate), so the free swelling strain is ε_{fz}. The fit indicates that $\varepsilon_{fz} = 3.65 \times 10^{-4}$, whereas independent measurements of free swelling described earlier give $4.5 \pm 1.0 \times 10^{-4}$. The fit yields $f = 0.38$, whereas the static modulus measurements described gave $f \approx 0.45$. The sorptivity found from the fit is almost double the average of the direct sorptivity measurements. It is not possible to obtain a good fit by reducing S_r and adjusting the other parameters, because each variable affects the shape of the curve in a different way. This particular sample might have been exceptionally permeable. Alternatively, the high value of sorptivity might reflect the relatively rapid invasion of large pores that do not percolate through the body. In a materials with a wide distribution of pore size, such as Portland Brownstone (Jimenez Gonzales et al., 2002), the water is expected to move some distance into the stone before a steady-state is reached, at which point the rate of advance is controlled by an average pore size (viz., the breakthrough radius; see Katz and Thompson, 1987). Since the warping sample is thin, the water might penetrate a significant fraction of the thickness before the steady-state sorptivity applies.

The fit was only applied to the range of data shown in Figure 7. At longer times, the relaxation of the plate is always slower than predicted, as shown in Figure 9. The effect is too large to result from viscoelastic relaxation and too persistent to result from hydrodynamic relaxation. It is suspected that the swelling strain is not achieved instantly, so the wet stone continues to

expand for some time after the advancing water front passes by. This would cause the upper surface to continue to expand relative to the lower part (which has been in contact with the water for a shorter time), so the duration of the deflection would not be entirely controlled by the sorptivity but would last longer. This would also account for the fact that the warping method usually yields a somewhat smaller free strain than the DMA measurements. This point is currently under investigation.

CONCLUSIONS

To predict whether swelling will cause damage to stone, it is necessary to know the stresses that develop and the strength of the stone. Analysis of the stresses is complicated by viscoelastic relaxation, and it can be expected that the strength of the stone will also be dependent on the rate and duration of loading. It has been demonstrated (Girardet, 2003, personal commun.) that when molasse is loaded slowly over the course of 24 h, it breaks at ~1/3 of the compressive strength measured at standard rates. In this work, methods for measuring the properties that must be known in order to calculate the stresses are discussed. The beam-bending method yields the static modulus and stress relaxation kinetics; if the measurement is performed on a saturated sample, the permeability can also be obtained from the rate of hydrodynamic relaxation. The swelling strain can be measured with a dilatometer (such as a DMA), but we find it convenient to use a simple warping experiment, which yields the swelling strain, sorptivity, and the ratio of wet to dry modulus, all in a matter of minutes. This technique is particularly useful for screening stones for swelling and for evaluating chemical treatments (such as the surfactants proposed by Snethlage and Wendler [1991]) for suppression of swelling.

ACKNOWLEDGMENTS

Inmaculada Jimenez Gonzalez thanks the Kress Foundation for their financial support of this research.

REFERENCES CITED

Bear, J., 1972, Dynamics of fluids in porous media: American Elsevier, New York, p. 124, 136.

Charola, A.E., Wheeler, G.E., and Koestler, R.J., 1982, Treatment of the Abydos reliefs: Preliminary investigations, *in* Gauri, K.L., and Gwinn, J.A., eds., Fourth International Congress on Deterioration and Preservation of Stone Objects: Louisville, Kentucky, University of Louisville, p. 77–88.

Delgado Rodrigues, J., 2001, Swelling behaviour of stones and its interest in conservation. An appraisal: Materiales de Construcción, v. 51, no. 263-264, p. 183–195.

Dunn, J.R., and Hudec, P.P., 1966, Water, clay, and rock soundness: The Ohio Journal of Science, v. 66, no. 2, p. 153–168.

Félix, C., 1994, Déformations de grès consécutives à leur consolidation avec un silicate d'éthyle (Deformation of sandstone following their consolidation with an ethyl silicate), *in* Proceedings of the 7th International IAEG Congress: Balkema, Rotterdam, p. 3543–3550.

Happel, J., Brenner, H., 1986, Low Reynolds number hydrodynamics: Dordrecht, Martinus Nijhoff, p. 389–404.

Jimenez Gonzalez, I., Higgins, M., and Scherer, G.W., 2002, Hygric Swelling of Portland Brownstone, *in* Vandiver, P.B., Goodway, M., and Mass, J.L., eds., Materials Issues in Art & Archaeology VI, MRS Symposium Proceedings 712: Warrendale, Pennsylvania, Materials Research Society, p. 21–27.

Katz, A.J., and Thompson, A.H., 1987, Prediction of rock electrical conductivity from mercury injection measurements: Journal of Geophysical Research, v. 2, no. B1, p. 599–607.

Kolsky, H., 1963, Stress waves in solids: Dover, Minneola, New York, p. 84–85.

MacEwan, D.M.C., and Wilson, M.J., 1980, Interlayer and intercalation complexes of clay minerals, *in* Brindley, G.W., and Brown, G., eds., Crystal structures of clay minerals and their X-ray identification: London, Mineralogical Society Monograph No. 5, p. 197–248.

Macey, H.H., 1942, Clay-water relationships and the internal mechanism of drying: Transactions of the British Ceramics Society, v. 41, no. 4, p. 73–121.

Madsen, F.T., and Müller-Vonmoos, M., 1989, The swelling behaviour of clays: Applied Clay Science, v. 4, p. 143–156, doi: 10.1016/0169-1317(89)90005-7.

McGreevy, J.P., and Smith, B.J., 1984, The possible role of clay minerals in salt weathering: CATENA, v. 11, p. 169–175, doi: 10.1016/0341-8162(84)90006-7.

Rodriguez-Navarro, C., Hansen, E., Sebastian, E., and Ginell, W.S., 1997, The role of clays in the decay of ancient Egyptian limestone sculptures: Journal of the American Institute of Conservation, v. 36, no. 2, p. 151–163.

Scherer, G.W., 1992, Bending of Gel Beams: method of characterizing mechanical properties and permeability: Journal of Non-Crystal: Solids, v. 142, no. 1-2, p. 18–35.

Scherer, G.W., 1999, Crystallization in pores: Cement and Concrete Research, v. 29, no. 8, p. 1347–1358, doi: 10.1016/S0008-8846(99)00002-2.

Scherer, G.W., 2000a, Measuring permeability of rigid materials by a beam-bending method: I. Theory: Journal of the American Ceramics Society, v. 83, no. 9, p. 2231–2239.

Scherer, G.W., 2000b, Thermal expansion kinetics: Method to measure permeability of cementitious materials: I, Theory: Journal of the American Ceramics Society, v. 83, no. 11, p. 2753–2761; Erratum, Journal of the American Ceramics Society, v. 87, no. 8 (2004) p. 1609–1610.

Snethlage, R., and Wendler, E., 1991, Surfactants and adherent silicon resins—New protective agents for natural stone, *in* Materials Research Society Symposium Proceedings: Pittsburgh, v. 185, p. 193–200.

Timoshenko, S., 1925, Analysis of bimetal thermostats: Journal of the Optical Society of America, v. 11, p. 233–255.

Tutuncu, A.N., Podio, A.L., Gregory, A.R., and Sharma, M.M., 1998, Nonlinear viscoelastic behavior of sedimentary rocks, Part I: Effect of frequency and strain amplitude: Geophysics, v. 63, no. 1, p. 184–194, doi: 10.1190/1.1444311.

Veniale, F., Setti, M., Rodriguez-Navarro, C., and Lodola, S., 2001, Procesos de alteración asociados al contenido de minerales arcillosos en materiales pétreos (Role of clay constituents in stone decay processes): Materiales de Construcción, v. 51, no. 263-264, p. 163–182.

Vichit-Vadakan, W., and Scherer, G.W., 2000, Measuring permeability of rigid materials by a beam-bending method: II. Porous Vycor: Journal of the American Ceramics Society, v. 83, no. 9, p. 2240–2245.

Vichit-Vadakan, W., and Scherer, G.W., 2002, Permeability of rigid materials by a beam-bending method: III. Cement Paste: Journal of the American Ceramics Society, v. 85, no. 6, p. 1537–1544.

Manuscript Accepted by the Society 19 January 2005

Anexo 5. Publicación nº.4

"Evaluating the Potential Damage to Stones from Wetting and Drying Cycles"

Jiménez González, I. and Scherer, G.W.

in proceedings of 16th European Conf. Fracture,

Measuring, Monitoring and Modeling Concrete Properties,

Ed. M.S. Konsta-Gdoutos (Springer, Dordrecht, The Netherlands)

(2006) 685-693

EVALUATING THE POTENTIAL DAMAGE TO STONES FROM WETTING AND DRYING CYCLES

Inmaculada Jiménez González [1] and George W. Scherer [2]
[1] University of Granada, Spain; [2]Princeton University, Dept of Civil & Env. Eng/ Princeton Materials Institute, Eng. Quad. E-319, Princeton, NJ 08544 USA

Abstract: The literature on stone conservation often mentions that clay-containing stones can be damaged over time through cycles of wetting and drying (Félix 1988). Several studies demonstrate the deleterious action of these cycles on stones consolidated with ethyl silicates [Félix and Furlan (1994), Félix (1995)]. However, to our knowledge, only one study (Wendler et al. 1996) demonstrates that these cycles can damage unconsolidated stone. The procedure is rather long and probably this is the reason for which so little work has been done to examine the importance of this damage mechanism.
In this paper, we present a testing machine that has been developed to automate and accelerate the rate at which stone samples may be submitted to these cycles. Direct measurement of swelling indicates that swelling increases with the number of cycles, indicating progressive damage. However, the swelling can be durably reduced, although not completely eliminated by swelling inhibitors.
We use a novel technique to examine the behavior of swelling stones, which consists in measuring the warping of a thin stone plate placed on two supports and which is wetted from above. Deflection and relaxation of the plate can be analyzed to extract free swelling, the ratio of wet to dry modulus and the sorptivity of the stone. However, agreement with separate measurements requires introducing a separate kinetic expression for the rate of swelling.

Key words: sandstone; swelling clays; consolidation; wetting and drying; swelling; sorptivity; warping; swelling inhibitors, fatigue, elastic modulus

1 INTRODUCTION

Alteration of clay-bearing stones is often attributed to stresses arising from cycles of swelling and shrinking of the clays. However, to the best of the authors' knowledge, apart from stones consolidated with ethyl silicates [Félix and Furlan (1994), Félix (1994, 1995)], only one study successfully demonstrates this [Wendler et al. (1996)].

The experiments of Wendler et al. clearly establish that wetting and drying cycles can damage clay-bearing stones. Furthermore, they demonstrate that swelling inhibitors may actively reduce this damage, although they do not eliminate it completely. In previous work we have presented analysis of the stress development during wetting and drying cycles, showing to a first approximation that stresses should increase with free swelling strain, but that those could be significantly reduced by stress relaxation, the values of which were characterized by bending techniques (Jiménez González and Scherer 2004). Based on these results, in this paper we examine the main effect of this damage mechanism by determining the evolution of free swelling during cycles of wetting and drying, as well as the effect of swelling inhibitors during such cycles.

In addition, we use the warping technique (Scherer and Jiménez González 2005) to examine the variation of sorptivity and the ratio of the wet to dry modulus during these tests.

2 MATERIALS AND METHODS

Portland Brownstone, a coarse ferruginous sandstone quarried in the Connecticut River valley and widely used in the North East of America, was obtained from Pasvalco Co. (Closter, NJ, USA). This stone has been reported to suffer extensive degradation due to swelling clays. It is mostly composed of quartz grains coated by iron oxide films with a variable amount of feldspar and mica (flakes of muscovite), with a cementing phase mostly made of silica and clays. It shows evident bedding planes and samples discussed in this paper were cut so that water ingress would take place in the direction parallel to the bedding planes

By swelling inhibitors, we refer to products that limit or eliminate the swelling that clay-bearing stones undergo when exposed to water or humidity. We have shown that best results are obtained when such products are formulated as a mixture of various small organic compounds (Jiménez González & Scherer 2004). The mixture used in this paper involves a 1,3 Diaminopropane dihydrochloride ($H_2N(CH_2)3NH_2$. 2HCl) the use of which was first suggested by Snethlage and Wendler (1991) and a corrosion inhibitor for concrete based on aminoalcohols. The stones were treated by partially submerging them in a solution after having been oven dried. Further details are available elsewhere (Jiménez González & Scherer 2004). After this treatment the samples remain hydrophilic.

A home-made dilatometer was used to measure the linear expansion of the samples (Jiménez González & Scherer 2004). Samples were plates of about 100×22×3.6 mm with the bedding perpendicular to their longest dimension. The oven-dried samples (60˚C) were placed on end in a stainless steel sample holder. They were held in place by four plastic screws, which were found to stabilize the samples without preventing their swelling. The sample and sample holder were placed in a glass container and the pushrod of an LVDT was lowered on top of the sample to allow displacement measurement. After data acquisition was started, deionized water was poured around the sample until it reached the upper surface of the sample. As soon as the surface gets wet, the sample starts swelling.

Sorptivity measurements were performed with an electronic balance with a 0.001 g resolution and connected to a computer for a data acquisition (Scherer and Jiménez González 2005). A dish of water was raised into contact with the bottom of the sample and the weight change was continuously monitored.

To test fatigue resistance to wetting and drying cycles, as well as the duration of the swelling inhibition treatments, we built a special machine that can submit stone samples to a large number of cycles. This was necessary, because the initial manual testing with up to about 20 cycles did not show any significant change in mechanical properties of the stones.

The machine is illustrated in Figure 1. It consists of two parallel belts on which rings of stainless steel springs allow to fix up to 70 thin stone plates. Rotation of the wheels on which the belts are fixed brings the samples successively into a water bath and into a zone in which fans dry the sample. The duration of the cycles can be easily adjusted. However, in our experiments, the machine was set up so that the impregnation lasted 30 minutes and drying lasted 60 minutes, for the case of Portland Brownstone. The water bath has a large volume and a constant flow of water to avoid any contamination of the untreated samples by possible washout of the swelling inhibitors from the treated samples.

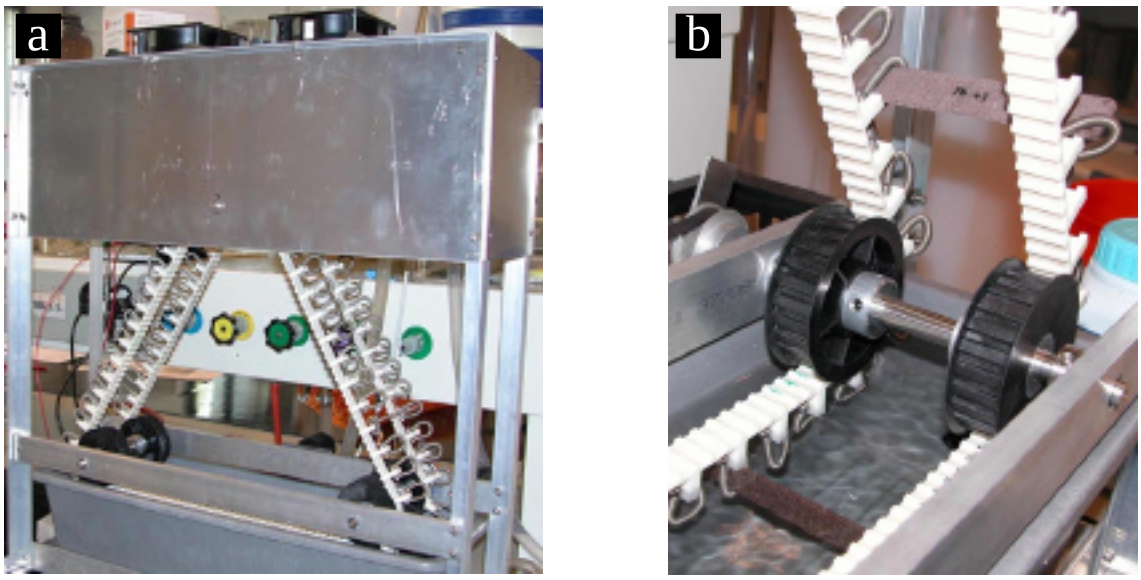

Figure 1. Wetting and drying testing machine. General view (a), detail of the bath and sample holder (b)

Details for the warping technique, which we have introduce for characterizing stones, can be found elsewhere (Scherer and Jiménez González 2005). In short, it consists in measuring the deflection of a thin plate of stone placed horizontally on two supports. The plate warps upwards as a result of adding water on its upper surface, and this is measured by a LVDT. A mathematical analysis described later gives the swelling strain, sorptivity and ratio of wet to dry modulus from the time dependent deflection of the sample.

3 RESULTS

3.1 Swelling

Results of the evolution of the free swelling strain obtained by direct measurement are reported in Figure 2. The samples Pb-22, 23 and 20 all received a treatment with the swelling inhibition mixture. The samples Pb-7 and 43 were not treated. The data indicate that this treatment reduces the initial swelling of this stone by about 42%. The data collected after 100, 200, and 700 cycles of wetting and drying show overall a gradual increase of swelling with the number of cycles regardless of whether they have been treated or not.

This increased swelling can be attributed to damage, in that a decrease of the material's stiffness will lower its ability to resist the swelling pressure caused by the wetting of the clays. From the perspective of conservation practice however, the important information of these results is that the effect of the treatment maintains the swelling of these samples well below their initial value, even after 700 cycles. Consequently, the treatment we propose reduces durably, but not indefinitely, the expansion and the associated damage. The aging of the treated samples may be due to the residual swelling strains or to a partial washout of the applied products.

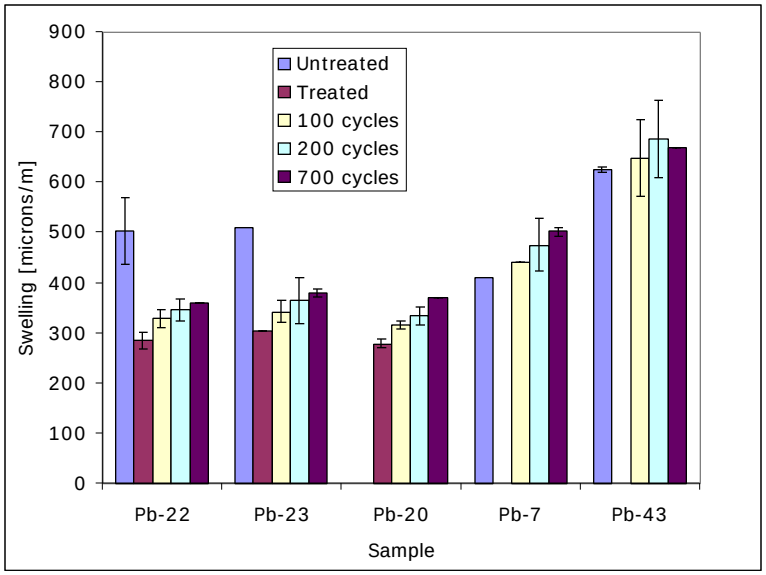

Figure 2. Evolution of the free swelling strain (direct measure) during the cycling

3.2 Warping

3.2.1 Swelling strain

In addition to doing direct measurements of swelling during these tests, we have also performed warping measurements on the same samples. The analysis of the warping experiment leads to the following expression for the height of the deflection, Δ, as a function of the depth to which the water has penetrated:

$$\Delta = \left(\frac{3w^2\varepsilon_{fw}}{4h}\right)\left(\frac{r(1-d)d}{d^4(1-r)^2 - 4d^3(1-r) + 6d^2(1-r) - 4d(1-r) + 1}\right) \quad (1)$$

where w is the span of the plate, ε_{fw} is the free swelling strain, h is the plate thickness, d is the depth of penetration normalized by h, and $r = E_{wet}/E_{dry}$ is the ratio of the wet to the dry modulus.

The maximum of this curve is given by:

$$\Delta_{max} = \left(\frac{3w^2\varepsilon_{fw}}{16h}\right) \quad (2)$$

Thus, in principle the height of the maximum deflection should be a direct measure of the free swelling strain. In fact, we find that although this measurement of the free swelling is correlated to the direct measurements discussed earlier, there is not a one-to-one relation, as can be seen in Figure 3.

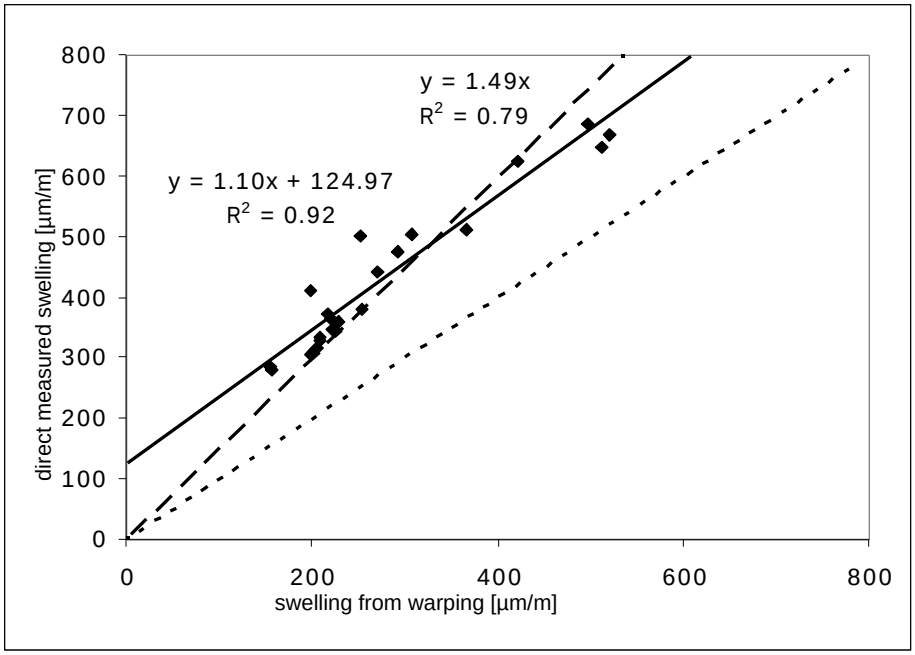

Figure 3. Relation between the free swelling strain obtained by the direct measurement and the warping measurement.

Indeed, we find that direct measurements of swelling strains are on average about 50% higher than those obtained from the warping measurement (dashed line). In fact, there is a better correlation if we admit the existence of an offset in the warping measurement. In that case the linear relation between both measurements is close to unity (solid line). Possible causes for this offset are discussed later in the paper.

3.2.2 Sorptivity and modulus ratio

Equation (1) can also be used to estimate the sorptivity and the ratio of wet to dry modulus. For this we write the rate of water ingress as:

$$d = \frac{S}{h}\sqrt{t} \tag{3}$$

where S is the sorptivity and t is the time.

It can be shown that the initial slope, a_0, of deflection versus $\sqrt{t}$ is equal to

$$a_0 \equiv \frac{d\,\Delta}{d\sqrt{t}} = \left(\frac{3\,w^2\varepsilon_{fw}}{4h}\right)\frac{r\,S}{h} = \frac{4\,\Delta_0\,r\,S}{h} \tag{4}$$

The time needed to reach the maximum deflection is:

$$t_{\Delta\max} = \left(\frac{h}{S\sqrt{1+r}}\right)^2 \tag{5}$$

Thus equations (4) and (5) can be used with the measured values of the initial slope and time to maximum deflection to obtain the ratio between wet and dry modulus, *r*, and the sorptivity *S*.

It turns out here again that there is a discrepancy between the values estimated by the warping measurement and direct measurements; however, in this case the direct measurements were performed on different samples than the warping tests, owing to experimental requirements. The values of *r* are in the range of 0.35 for direct measurement, while they are estimated at about 0.6 by warping. Direct measurement of sorptivity is in the range of 0.01 cm/s$^{1/2}$, while values from warping are about 0.025 cm/s$^{1/2}$. Possible reasons for this are discussed below.

4 DISCUSSION

4.1 Warping measurements

We have found, contrary to our preliminary experiments with this technique (Scherer and Jiménez González 2005), that there is a discrepancy between the three parameters estimated from warping measurements with respect to independent measurements of the same parameters. In the particular case of the swelling strain the situation cannot be attributed to sample-to-sample difference, because the same samples were used for both measurements. These discrepancies reveal the complexity of the kinetics of expansion, so they deserve careful study.

To analyze the possible origin of these discrepancies, we now focus our attention only on the samples measured before treatment or cycling. One way of doing this is to see whether there are dependencies among the different parameters.

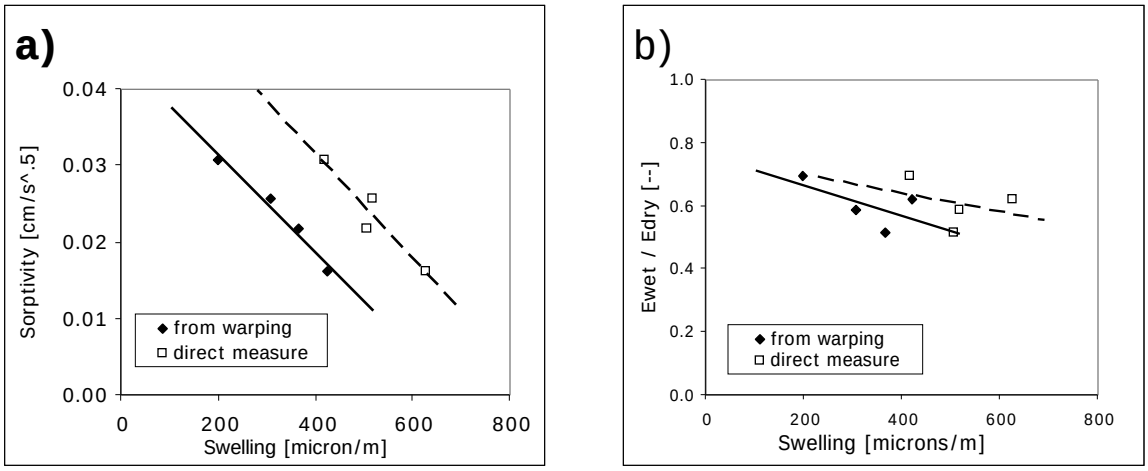

Figure 4. Dependence of sorptiviy (a) and modulus ratio, r (b) on the swelling strain. Values are plotted with respect to both the direct swelling strain measurement and the one inferred from warping

From the data in Figure 4, we can see that sorptivity clearly decreases when the swelling strain increases, while the modulus ratio is relatively unaffected by it.

Sorptivity experiments show that there is an initial stage of faster water ingress. This complicates the analysis of the water experiments by requiring the introduction of a kinetic expression for the changes in sorptivity and for the rate of expansion, which are not necessarily linked in a trivial way one to the other. Finally, there is also the possibility that the softening of

the wet stone is time dependent which would also account for the discrepancy in ratios of wet and dry modulus.

As the simplest approach, we will assume first that the kinetics of sorptivity change are the same as those of swelling. We have found that sorptivity curves could be well fitted in the following way:

$$d = \left(\frac{\Delta_s \alpha \sqrt{t}}{1+\alpha\sqrt{t}} + S\sqrt{t}\right)\frac{1}{h} \tag{6}$$

where Δ_S is the intercept of the linear regression to the sorptivity curve, when plotted as height of rise versus square root of time, and $\Delta_S\alpha$ is the difference between the sorptivity at time zero and the one at steady state.

Using, an average value of 0.13 cm/s$^{1/2}$ for the sorptivity at steady state, values from independent measurements of swelling strain and modulus ratio, we fit the initial part of the curve by adjusting the values of Δ_S and α. The agreement is good, but clearly insufficient at longer times (Figure 5).

At this stage our treatment for the delayed expansion just multiplies the swelling strain of the wet part by the hyperbolic part of the equation (6): $\alpha\sqrt{t}/\left(1+\alpha\sqrt{t}\right)$. Any further adjustment that improves the fit to the deflection after the maximum spoils the fit at short times.

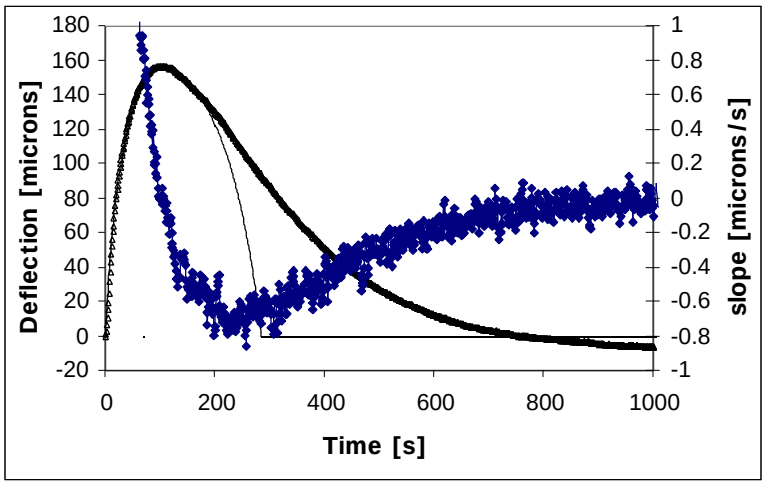

Figure 5. Comparison of a warping curve with the fitted function using the same time dependent function for sorptivity and swelling.

From the fitting parameters, we predict that the sample will be completely saturated at ~280 s. From the slope of deflection versus time (secondary axis in Figure 5), we determine a minimum at 230 s, which can reasonably be attributed to a change in deflection mechanism when the water reaches the other side of the sample. The similarity of these estimates supports the validity of the fitting parameters we obtained.

Recent results by Wangler (2005) suggest that other factors, including evaporative cooling of the liquid pool on the sample, and capillary pressure from the pore liquid, may contribute to the post-peak deflection. Studies are underway to quantify those effects.

5 CONCLUSIONS

We have examined the durability of a clay bearing stone exposed to accelerated cycles of wetting and drying. From direct measurements of swelling it appears that samples either treated or not with a swelling inhibitor, show an increased expansion over time. However, even after 700 cycles the swelling of the treated samples remains significantly under values before the application of the product, which indicates that this treatment has a durable effect in reducing damage from wetting and drying cycles which increases with the extent of swelling.

In addition we have examined in more detail the warping test by performing swelling and warping tests on the same samples. Both tests show the same trends but differ quantitatively as do values for sorptivity and modulus ratio. Agreement can be improved if the warping test is analyzed by introducing a time dependent change of sorptivity and swelling based on similar kinetics. The pertinence of the fitting parameters is strengthened by the fact that they provide a satisfactory estimate of the time the water takes to cross the sample in this test. Additional work is needed to describe the rest of the curve, taking into account of other phenomena that contribute to deformation of the sample.

Acknowledgements

The authors would like to thank Joe Vocaturo (Princeton University) for his excellent work in designing and building the wetting/drying machine. We thank Dr. Andreas Queisser, Jérôme Constantin and Dr. Bénédicte Rousset at the Expert Center pour la Conservation du Patrimoine Bâti, in Lausanne, Switzerland for providing IJG with space to perform some of the experiments. We thank Dr. Robert J. Flatt for valuable discussions regarding interpretation of the data. Financial support for Inmaculada Jiménez González was generously provided by the Samuel Kress Foundation and VIP Restoration, Inc.

References

Félix, C., 1988, Comportement des grès en construction sur le plateau suisse (Performance of Sandstones in Construction on the Swiss Plateau). In *LCP Publications 1975-1995*, Montreux, R. Pancella Ed., EPFL, 833-841

Félix, C.; Furlan, V., 1994, Variations dimensionnelles des gres et calcaires liees a leur consolidation avec un silicate d'ethyle (Dimensional changes of sandstones and limestones related to their consolidation with an ethyl silicate). In *3rd international Symposium on the conservation of Monuments in the Mediterranean Basin*. Edited by V. Fassina, F. Zezza. Venice, 22-25-June

Félix C., 1995, Choix de gres tenders du Plateau Suisse pour les travaux de conservation (Choice of soft sandstones from the Swiss plateau for conservation work). In *Conservation et restauration des biens culturels, Actes du Congres LCP*, Montreux, Septembre 1995, R. Pancella Ed., EPFL, 45-71.

Jiménez González, I.; Higgins, M. and Scherer, G.W., 2002, Hygric swelling of Portland Brownstone. In *Materials Issues in Art & Archaeology VI, MRS Symposium Proc.*, eds P.B. Vandiver, M. Goodway and J.L. Mass (Material Res. Soc.), Warrendale, PA, Vol 712: 21-27.

Jiménez González, I. and Scherer, G.W., 2004, Effect of swelling inhibitors on the swelling and stress relaxation of clay bearing stones. In *Environmental Geology*, 46: 364-377

Scherer, G.W. and Jiménez González, I., 2005, Characterization of swelling in clay-bearing stone. In Turkington A.V., ed., *Stone decay in the architectural environment:* Geological Society of America Special Paper 390: 51-61.

Wangler, T., 2005, Princeton University, private communication

Wendler, E., A. E.Charola, and B.Fitzner, 1996, Easter Island tuff: Laboratory studies for its consolidation. In *Proceedings of the 8th International Congress on Deterioration and Conservation of Stone*, ed J. Riederer. Berlin, Germany, 2, 1159-1170.

Anexo 6. Publicación nº.5

"The role of clay minerals in the physico-mechanical deterioration of sandstone"

Jiménez González, I; Rodríguez Navarro, C. and Scherer, G.W.

Journal of Geophysical Research (aceptado, en prensa)

JOURNAL OF GEOPHYSICAL RESEARCH, VOL. 113, XXXXXX, doi:10.1029/2007JF000845, 2008

Role of clay minerals in the physicomechanical deterioration of sandstone

Inmaculada Jiménez González,[1] Carlos Rodríguez-Navarro,[2] and George W. Scherer[3]

Received 1 June 2007; revised 21 January 2008; accepted 4 March 2008; published XX Month 2008.

[1] Extensive weathering suffered by sandstone in natural outcrops as well as in historical buildings could be attributed among other mechanisms to the action of wetting and drying cycles. We have recently shown how to quantify the stresses generated during such cycles to determine whether damage can take place. This procedure is further developed in this paper and applied to the Tarifa stone, a sandstone with a 7 wt % content of clay minerals and used in the main façade of the church of San Mateo in Tarifa, Cádiz, Spain, for which the relevant material properties are measured. It is shown that tensile stresses during drying can cause cracking of thin elements and that shear forces can cause buckling of wetted surfaces more generally, eventually resulting in scaling and/or contour scaling. These predictions are supported by visual observations on the monument showing degradation patterns characteristic of those types of damage. Similar weathering forms have been observed in natural sandstone landscapes. Application of swelling inhibitors (e.g., cationic surfactants) that selectively adsorb on the clay basal planes, results in a substantial swelling reduction. This confirms that the swelling clays typically present in sandstone are pivotal for its weathering and indicates that swelling inhibitors are a potentially valuable treatment to prevent or minimize damage to stone. The circumstances that would lead to weathering are discussed in relation to sandstone material properties in the wet and dry state. Clay-bearing stones are shown to exhibit softening during wetting, as well as viscoelastic stress relaxation, which is expected to limit the extent of damage. These results may aid in the better understanding of sandstone weathering both in nature and in urban environment and may help develop conservation methods to mitigate wetting/drying damage in ornamental sandstone or to prevent pore plugging in reservoir sandstones.

Citation: González, I. J., C. Rodríguez-Navarro, and G. W. Scherer (2008), Role of clay minerals in the physicomechanical deterioration of sandstone, *J. Geophys. Res., 113*, XXXXXX, doi:10.1029/2007JF000845.

1. Introduction

[2] Sandstones represent a significant volume of Earth's surface rocks. *Meybeck* [1987] estimates that they cover ca. 15% of the emerged land surface, a value nearly similar to that of granite or limestones. Sandstones are also one of the most common ornamental stones used in the built and sculptural heritage [*Winkler*, 1997]. Weathering of sandstone is a critical geomorphological phenomenon that has shaped and currently shapes the landscape and surface features of, for instance, the Grand Canyon, Zion Canyon, Monument Valley, and Arches National Park in the United States [*Bradley*, 1963; *Robinson*, 1970; *Cruikshank and Aydin*, 1994], the carved city of Petra in Jordan [*Paradise*, 2002; *Heinrichs*, 2005], or a number of cathedrals across Europe [*Vicente*, 1983]. Sandstone weathering also results in the development of striking weathering forms such as pedestal rocks [*von Engeln*, 1942], honeycombs [*Mustoe*, 1982], tafoni or caverns [*Young*, 1987; *Sancho and Benito*, 1990], scaling and contour scaling [*Snethlage and Wendler*, 1997], and polygonal cracking [*Williams and Robinson*, 1989], whose origins are still a matter of debate [*Turkington and Paradise*, 2005]. However, while study of rock weathering and stone decay has mainly focused on granite or limestone decay, sandstone still remains a relatively overlooked landscape element and building stone [*Turkington and Paradise*, 2005].

[3] In recent years, geomorphological methods and studies on natural rock weathering have gained a prominent status in the conservation of stone cultural heritage [*Pope et al.*, 2002]. Conversely, research into rock weathering has been significantly advanced through the study of urban stone decay [*McGreevy and Whalley*, 1984]. There are several reasons for the study of stone decay as a useful analogy for rock weathering in natural settings. Among them, one is the availability of easily characterized stone in a dated monu-

[1]University of Granada, Granada, Spain.
[2]Department of Mineralogy and Petrology, University of Granada, Granada, Spain.
[3]Princeton Institute for the Science and Technology of Materials, Department of Civil and Environmental Engineering, Princeton University, Princeton, New Jersey, USA.

0148-0227/08/2007JF000845$09.00

ment, which enables an accurate study of weathering processes and rates [*Dragovich*, 1978; *Meierding*, 1981; *Pope et al.*, 2002; *Hoke and Turcotte*, 2002]. Another reason is the relative ease of performing laboratory and field tests using stone samples under well-established conditions that help single out a particular weathering mechanism [*Rodríguez-Navarro and Doehne*, 1999]. In the case of sandstone, case studies, laboratory tests, and field exposure trials have focused on the study of salt weathering [*Goudie and Viles*, 1997], frost shattering [*McGreevy*, 1981], black crust (gypsum) formation [*Smith et al.*, 1994], chemical weathering (including case hardening) [*Young*, 1987], thermal weathering [*Warke and Smith*, 1998] and biodeterioration [*Mottershead et al.*, 2003]. However, other weathering mechanisms such as expansion/contraction associated with wetting/drying phenomena [*Trenhaile*, 1987; *Yatsu*, 1988] have comparatively received less attention [*Hall and Hall*, 1996; *Delgado Rodrigues*, 2001].

[4] Sandstones typically contain clays in the cement that binds the grains together [*Tallman*, 1949; *Houseknecht and Pittman*, 1992]. This type of cementing phase makes them highly susceptible to deterioration, especially under conditions of cyclic wetting and drying that cause swelling and shrinkage of clay minerals. The literature on stone conservation provides numerous studies that point to this as a durability problem for sedimentary stones [*Beloyiannis et al.*, 1988; *Caner and Seeley*, 1978; *Delgado Rodrigues*, 2001; *Iñigo et al.*, 2003; *Kühnel et al.*, 1994; *Rodríguez-Navarro et al.*, 1997, 1998; *Pye and Mottershead*, 1995; *Wust and McLane*, 2000; *Veniale et al.*, 2001; *Vicente*, 1983]. Studies on the durability of sandstones used for road pavement and other engineering purposes also suggest that clays may have a detrimental impact on their service life [*Dunn and Hudec*, 1966; *Fookes and Poole*, 1981]. Polygonal cracking [*Williams and Robinson*, 1989], tafoni [*Martini*, 1978], honeycombs [*Gill et al.*, 1980], and spalling/multiple scaling, as well as contour scaling [*Robinson and Williams*, 1994; *Heinrichs*, 2005] observed on sandstone outcrops in nature have also been related to the presence of clay minerals. However, the actual role of clays and wetting/drying events on the development of such weathering forms is a matter of controversy [*McGreevy and Smith*, 1984; *Turkington and Paradise*, 2005]. The lack of a physical-mechanical theory backed by experimental data demonstrating the actual role of the swelling/shrinking of clay minerals in weathering of sandstone, may have fostered this controversy.

[5] Clay-containing sandstones used for building purposes can develop significant swelling strain. For instance, Spanish Cervelló and Villamayor sandstones that show severe damage in some historic buildings are reported to swell respectively by 5000 and 6700 μm/m [*Esbert et al.*, 1997] in the direction perpendicular to their bedding planes. In general, swelling strain values above 1500 μm/m can be considered quite large, since the product of this strain with the elastic modulus typically exceeds the tensile strength of the stone. However, as will be explained in this paper, swelling strain alone is not sufficient to determine whether swelling may cause damage. Factors that have to be considered include elastic modulus, viscoeastic relaxation rate, tensile, shear or compressive strength of the sandstone, and relative humidity. This approach could be successfully used to identify situations where a sandstone with rather limited dilatation would get damaged. For instance, severe damage occurs in Petra sandstone, which shows a maximum swelling strain of 700 μm/m [*Heinrichs*, 2005], and in Portland Brownstone, with 500 μm/m of swelling strain (this study). As detailed in section 4.3, the stresses in the latter case can be shown to exceed the strength of the stone. The role of clay distribution in the stone has also been pointed out to be important [*Dunn and Hudec*, 1966] since inhomogeneity could give much higher local strains and stresses.

[6] Although the problem has been often mentioned, quantification of the stresses arising from such wetting/drying cycles has only been discussed recently [*Jiménez González and Scherer*, 2004; *Wangler et al.*, 2006]. Experimental evidence of the damaging character of these cycles was reported by *Rodríguez-Navarro et al.* [1997] and *Wendler et al.* [1996]. In the first case, the authors studied a clay-rich Egyptian limestone that basically decomposed when submerged in water. The study by *Rodríguez-Navarro et al.* [1998] is particularly important for museums in countries with climates more humid than Egypt. However, the properties of this stone remain very different from situations that can be encountered with building stones still in service in outdoor environments exposed to rain, or in natural outcrops. The case examined by *Wendler et al.* [1996] is closer to such situations. The authors examined the aging of stones from Easter Island by measuring the drill resistance of quarry samples subjected to wetting and drying cycles. They observed that these cycles very much reduced drill resistance in the outer layer of the samples. They also found that treating with diaminobutane dihydrochloride as a swelling inhibitor [*Wendler et al.*, 1991; *Snethlage and Wendler*, 1991] dramatically reduced the loss of drill resistance. This study highlights the fact that wetting and drying cycles can damage clay-bearing stones, but that swelling inhibitors can be used to mitigate this. Regarding the use of conventional conservation treatments, it has been reported that clay-bearing stones consolidated by ethyl silicates rapidly lose the consolidation effect after a limited number of cycles of wetting and drying, apparently as a result of hydric strain [*Félix and Furlan*, 1994; *Félix*, 1988, 1995].

[7] Over the past few years we have examined the weathering of clay-bearing stones with the objective of analyzing the stresses generated during wetting and drying cycles in order to determine their potential for damaging action [*Jiménez González and Scherer*, 2004; *Scherer and Jiménez González*, 2005]. In this process we have introduced novel characterization techniques and improved others. These include warping of thin stone plates and accelerated swelling pressure measurements [*Jiménez González et al.*, 2002; *Scherer and Jiménez González*, 2005; *Jiménez González and Scherer*, 2006]. We also applied the technique of beam bending under dry and saturated conditions to determine the viscoelastic character of these stones [*Jiménez González and Scherer*, 2004].

[8] In this paper we apply all these methodologies to study a sandstone from the South of Spain that shows substantial damage on the façade of San Mateo Church in Tarifa (Cádiz, Spain). This type of stone is also to be found

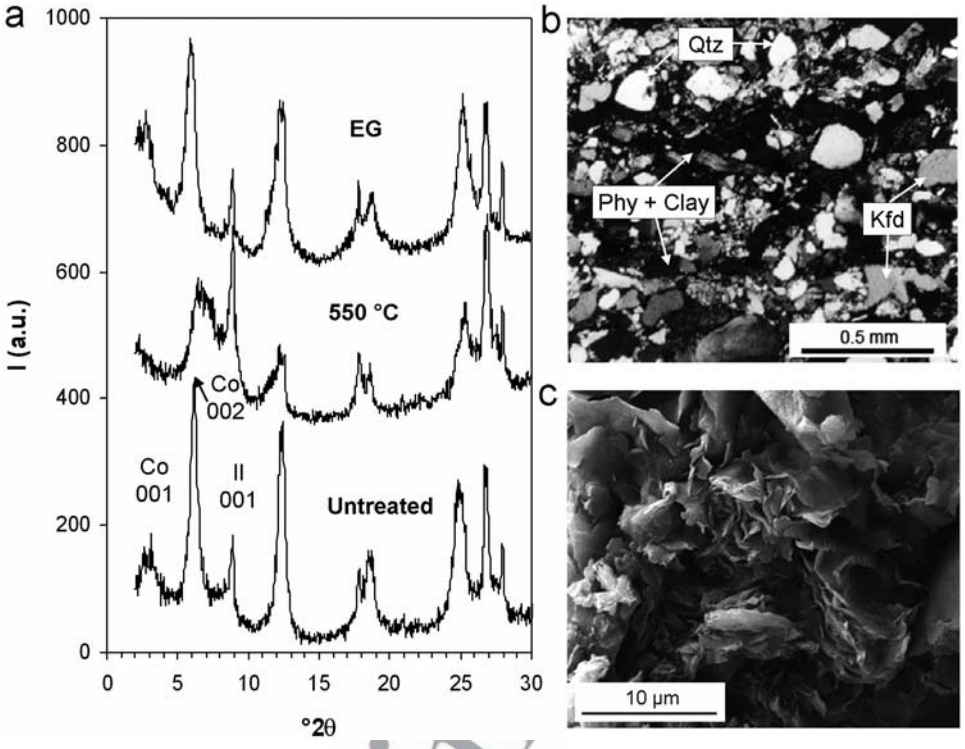

Figure 1. Mineralogy and texture of Tarifa sandstone. (a) XRD patterns of oriented aggregates showing illite (Il) 001 reflection and corrensite (Co) 001 and 002 reflections and their change upon glycolation (EG) and thermal treatment (550°C). (b) Representative optical microscopy photomicrograph (crossed polars) showing quartz (Qtz), potassium feldspar (Kfd), and phyllosilicates plus clays (Phy + clay) oriented along bedding planes (horizontal). (c) SEM photomicrograph of the clay minerals.

on the nearby Roman ruins of "Baelo Claudia," where it displays similar damage patterns [*Hoyos et al.*, 1999].

[9] Concerning the Church of San Mateo, *Sebastian et al.* [2007] describe the damage patterns as granular disintegration, flaking, scaling and "contour scaling," as well as cracking of ornamental elements. They attribute this damage to the swelling and shrinking of clays and weaknesses of the stone resulting from its high anisotropy. Furthermore, they indicate that sodium chloride aerosols increase the hygroscopicity of the stone and favor the osmotic swelling of the clays.

[10] In the present study, our experiments demonstrate that we are using a valid theoretical analysis of how stresses develop in clay-bearing stones during cycles of wetting and drying. On the basis of these results we determine under what conditions damage is likely to occur during such cycles on a monument or on a natural outcrop. We also examine the use of swelling reducing agents as a way to mitigate sandstone damage. Ultimately, we will show that the theoretical analysis and the study of the damage associated with wetting/drying of clay-bearing Tarifa sandstone could be extended to understanding sandstone weathering on Earth's surface as well as elsewhere (e.g., Mars).

2. Materials and Methods

2.1. Materials

[11] The stone object of this study is one of the most representative materials used in the main (south) façade of the San Mateo Church, in the town of Tarifa (Cádiz, Spain). It is an arkose sandstone whose matrix or cementing phase is composed prevalently of clays and a small proportion of carbonates. Generally, two varieties have been distinguished by *Sebastian et al.* [2007]: the light brown and the gray variety, the first one being the closest to the one used in this study.

[12] Samples were obtained from blocks extracted from the original quarries (currently closed) located near Tarifa. A description of these quarries is given by *Sebastian et al.* [2007]. Before all tests, the samples were oven dried (60°C) to constant weight and then stored in hermetic containers for cooling. For tests under saturated conditions, vacuum impregnation by water was additionally performed.

[13] Samples were studied by means of scanning electron microscopy (SEM; Zeiss DMS 950) and polarized light microscopy (PM; Jenapol V). Powder X-ray diffraction (XRD) analyses were performed on a Philips PW 1710 diffractometer equipped with a graphite monochromator and using Cu $K\alpha$ radiation (λ = 1.5418 Å). XRD analyses were performed on ground whole rock and oriented aggregates (untreated, ethylene glycol solvated and heated for 1 h at 550°C) of the clay fraction (size < 2 μm).

[14] This sandstone is composed mainly of quartz. Other minerals found in lesser amounts are feldspars, calcite and phyllosilicates, including muscovite, biotite and chlorite. Figure 1a shows XRD patterns of the clay fraction. Smectite-chlorite mixed layers (corrensite) and minor amounts of illite are the main clay minerals present, which shows average values of 7 wt %. The corrensite mixed layer clay

was identified by the increase in the d_{001} spacing from 28.3 Å up to 31.5 Å after glycolation and the collapse of the d_{002} spacing from 14.2 Å to a broad peak at 13 Å upon heating [*Wilson*, 1987].

[15] Clays can experience two types of swelling: intracrystalline swelling and interparticle or osmotic swelling [*Rodríguez-Navarro et al.*, 1998, and references therein]. The former is experienced by the so-called expandable or swelling clays, such as smectite or mixed layer smectite-chlorite and smectite-illite, which are very common in sandstones [*Houseknecht and Pittman*, 1992]. Intracrystalline swelling results in an increase of the d_{001} spacing when the clays are in contact with a polar liquid (e.g., water or ethylene glycol). Osmotic swelling is experienced by all clay minerals (expandable and nonexpandable clays) in the presence of an electrolyte [*Madsen and Müller-Vonmoos*, 1989]. Higher swelling strains are observed in rocks containing expandable clays than in rocks containing nonexpandable clays [*Yatsu*, 1988]. Regarding the swelling potential of corrensite, this clay was found responsible for the floor heave of tunnels in the Keuper formation of SW Germany [*Yatsu*, 1988, and references therein].

[16] Optical microscopy and SEM observations show that the phyllosilicates display a preferred planar orientation along the stone bedding planes (Figures 1b and 1c). The latter is responsible for the marked textural and structural anisotropy of this stone [*Sebastian et al. 2007*]. The pore system of the sandstone is characterized by submicron pores (pore radii 0.5–0.02 μm) having an average total porosity of around 8–11% [*Sebastian et al.*, 2007].

[17] To demonstrate unambiguously that swelling strain in clay-containing sandstone is due to clay swelling, and at the same time, to reduce or mitigate the swelling experienced by the Tarifa sandstone, we used diaminoethane dihydrochloride ($C_2H_8N_2{\cdot}2HCl$). The use of such cationic surfactants was first discussed by *Snethlage and Wendler* [1991] and considered by *Wendler et al.* [1996] for the conservation of Eastern Island Moai sculptures. This product adsorbs at the negatively charged (001) planes of clays, establishing bonds between two adjacent particles, thus preventing/minimizing swelling [*Snethlage and Wendler*, 1991]. In our study we applied the product by partially immersing the samples in 5 wt % aqueous solution, drying to constant weight (60°C) and repeating the whole operation a second time. The treatment does not have major effects on other materials properties, such as sorptivity, elastic modulus or color.

2.2. Methods

[18] The potential for damage from swelling depends on the depth to which water penetrates, the magnitude of the swelling strain, and the stiffness of the wet and dry stone, so we need to characterize all of those properties. The depth of saturation during contact with water (e.g., in a flood or rain event) depends on the sorptivity, which is the rate of uptake per unit area; if water enters the rock by capillary rise, then the distribution of moisture within the body will depend on the competition between the rate of rise and the rate of evaporation. We measure the sorptivity by a direct method described in section 2.2.1 and an indirect method, warping analysis, described in section 2.2.3. Similarly, the strain resulting from the saturation of an initially dry stone is measured directly by a dilatometric method (section 2.2.1) and indirectly by warping (section 2.2.3). If the wet surface of a dry stone expands, it creates compressive stresses; conversely, if the dry surface of a saturated stone contracts, it causes tensile stress. To calculate the stresses, we must know the mechanical properties of the rock, which we investigate by several methods, described in section 2.2.2. A convenient way to determine the elastic modulus is to calculate it from the acoustic velocity in the rock, which is quickly and easily done in the field. Unfortunately, that method gives highly unreliable results for clay-bearing stone, as we demonstrate by comparing the results of acoustic measurements with static moduli obtained by three point bending measurements. Static measurements are more appropriate for predicting swelling stresses in stone, where the duration of the process (*viz.,* wetting and drying) is on the order of hours or days. Moreover, these measurements reveal that the stone is viscoelastic, particularly when wet, and this will have an important impact on the magnitude of the swelling stresses. One might reasonably argue that it is simpler to measure the swelling stress directly, rather than calculating it from the strain and viscoelastic modulus. Such direct methods were performed, as described in section 2.2.4, but the results are disappointing, because it is difficult to confine the sample so as to prevent a strain smaller than 0.1%. This problem is avoided by the warping method, where moisture is introduced through one face of a thin plate of stone: as the wet side expands, it is resisted by the dry side, which results in warping of the plate. An elastic (or viscoelastic) analysis of this simple geometry leads to an explicit prediction of the rate and magnitude of deflection. Fitting the theoretical expression to the data (deflection versus time) yields estimates of the swelling strain, sorptivity, and ratio of elastic moduli in the wet and dry stone. This measurement is fast and requires relatively simple equipment. Finally, to predict damage we must compare the stress to the strength of the rock, so we must measure the tensile strength of the stone when wet and dry, as described in section 2.2.2.

2.2.1. Hydric Properties

[19] The rate of water intake is measured by sorptivity tests in which a sample is fixed to the bottom of an electronic balance with a 0.001 g resolution connected to a computer for the data acquisition [*Scherer and Jiménez González*, 2005]. A container with deionized water is then raised until the water touches the bottom of the sample. The mass change (Δm) per unit surface of the sample base (A) is plotted versus the square root of time and found to be linear. The height of rise, Δh, is related to the weight gain by $\Delta h = \Delta m/(A\phi\rho_L)$, where ϕ is the porosity and ρ_L is the liquid density; Δh increases in proportion to $\sqrt{t}$. From the slope and the apparent porosity determined from the mass change at the plateau, we determined the sorptivity (S) in units of cm/s$^{1/2}$ for comparison with the value obtained by applying equation (2) in the analysis of the warping experiments. Measurements were performed with the sample bedding placed normal to the water surface. Additional measurements were done with samples placed with the bedding parallel to the water surface.

[20] The linear expansion or free swelling strain (ε_s) of the stone is measured by using a homemade dilatometer [*Jiménez González and Scherer*, 2004]. Typical sample sizes

were 35 × 10 × 10 mm. The expansion was measured in directions both parallel and perpendicular to the bedding, using the following procedure: (1) the sample is placed in a glass container, (2) a pushrod mounted on an LVDT (linear variable differential transformer) is lowered on top of the sample and at that point the data acquisition starts, and (3) deionized water is poured into the container until it reaches near the upper surface of the sample (but without covering it, so that air is not trapped inside). As soon as the sample gets wet, it starts swelling. The dilatation is measured by the LVDT until it is complete. The strain difference between the initial value and the plateau value is used to calculate the linear free swelling strain.

[21] Longitudinal expansion of the long thin plates used for warping measurements was obtained using the same instrument and procedure, but a special sample holder was designed to keep the samples vertical during the measurement without preventing their swelling [*Jiménez González and Scherer*, 2006].

2.2.2. Mechanical Properties

[22] The tensile strength of the stone is obtained from indirect tensile strength tests (Brazilian tests). Cylindrical samples of 2 cm diameter and 5 cm length are placed horizontally between the two platens of an Instron® machine that compress the sample until failure [*Jiménez González and Scherer*, 2004].

[23] This property was only measured on dry samples because tensile strength is most important during drying of decorative elements, as explained below.

[24] The dynamic elastic modulus is determined from ultrasound transmission velocity measured using a portable Pundit instrument operating at 54 KHz. Nitrile pads are used instead of vacuum grease as contact agents [*Jiménez González and Scherer*, 2004]. Stones were measured both wet and dry. These measurements were performed on the received blocks before they were cut to make the smaller samples used in the other experiments. In each direction, three measurements were done and found to be very similar.

[25] Homemade three point beam benders are used for measuring static elastic modulus of oven dried and vacuum saturated samples. Typical sizes for samples were about 100 × 20 × 4 mm (dimensions are measured accurately for each sample). Each instrument is composed of a computer controlled in-line system that is placed inside an incubator [*Vichit-Vadakan*, 2002; *Jiménez González and Scherer*, 2004]. The measurements are done by applying a given displacement cyclically and measuring the corresponding load. The samples used for this test were cut such that the bedding was normal to the sample length, so we obtain Young's modulus perpendicular to the bedding.

[26] Stress relaxation tests were performed with the same benders described above. In this case, a constant displacement is applied and the load is measured over time. This measurement gives information on the viscoelastic behavior of the stones [*Jiménez González and Scherer*, 2004].

2.2.3. Warping

[27] A novel technique that we call "warping" or "the 3 in 1 test" was introduced in former studies as a quick measure of swelling strain, sorptivity and ratio of wet to dry modulus [*Scherer and Jiménez González*, 2005; *Jiménez González and Scherer*, 2006]. Briefly, it consists in measuring the upward deflection (warping) of a thin plate of a swelling stone, placed horizontally on two supports, that swells as a result of adding water on its upper surface. A piece of tape is placed around the perimeter of the plate to contain the water, and an LVDT is placed in contact with the center of the top surface of the plate. Water is quickly poured onto the upper surface and the deflection measured by the LVDT is continuously recorded by a computer. This LVDT is placed midway between the two sample supports to measure the maximum deflection during the warping process. The samples are about 100 × 20 × 4 mm (dimensions are measured accurately for each sample).

[28] This experiment can be analyzed following *Timoshenko*'s [1925] approach where the sample is considered as an assemblage of two layers (1) the wet upper layer that tries to reach the maximum swelling (free swelling strain) and (2) the dry lower layer that tries not to expand.

[29] The combination of one layer trying to expand and the other resisting leads to warping with a deflection, Δ(cm), that depends on the relative depth of water penetration, d, on the free swelling strain, ε_S, and on the ratio of wet to dry modulus, r,

$$\Delta = \left(\frac{3w^2\varepsilon_S}{4h}\right) \cdot \left(\frac{r(1-d)d}{d^4(1-r)^2 - 4d^3(1-r) + 6d^2(1-r) - 4d(1-r) + 1}\right), \quad (1)$$

where w (cm) is the span and d can be written as a function of sorptivity, S (cm/s$^{1/2}$), plate thickness, h (cm), and time, t (s),

$$d = \frac{h_w}{h} = \frac{S}{h}\sqrt{t}, \quad (2)$$

where h_w (cm) is the wet part of the sample thickness.

[30] It is important to note that we do not have an independent measure of d. Its variation with time could therefore be different from what is given in the above equation, in particular for thin samples. Such a situation was found with the Portland Brownstone and a model was proposed to analyze this [*Jiménez González and Scherer*, 2006]. However, as explained later in the paper, equation (2) can be considered suitable for analyzing Tarifa sandstone samples.

[31] The free swelling is found directly from the maximum deflection, Δ_{max} and can be calculated by

$$\varepsilon_S = \frac{16}{3}\frac{\Delta_{max} h}{w^2}. \quad (3)$$

[32] The effects of sorptivity and the modulus ratio cannot be easily separated one from the other, which is why we choose to fit the curve simultaneously for both these parameters, after having determined the free swelling strain from the maximum deflection. Samples used for warping were cut so that some had the bedding perpendicular and others had it parallel to the surface onto which the water was poured.

2.2.4. Swelling Pressure

[33] Direct measurements of swelling pressure are performed by applying an external load to prevent the sample from swelling [*Madsen and Müller-Vonmoos*, 1985]. We

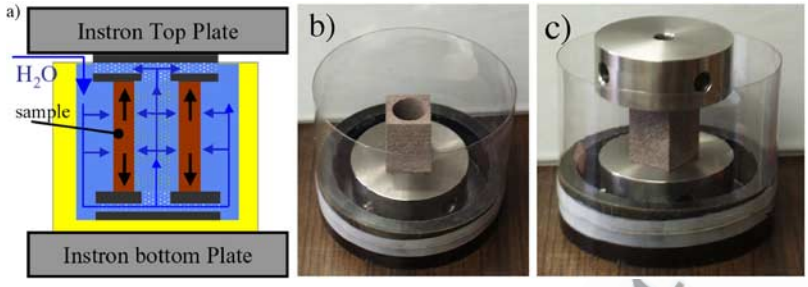

Figure 2. Illustration of the direct measure of swelling pressure setup. (a) Sketch showing how water infiltrates the sample core. (b) Image of the cored sample resting on the stainless-steel-perforated base. (c) Image of the sample as placed in the Instron machine. These pictures were taken with a sample having a square outer section unlike the one used in this study that has a circular one.

introduce changes in the sample size and geometry that greatly speed up the test (that now takes a couple hours instead of approximately two weeks). For that, we first used hollow parallelepiped samples with a square external section (as shown in Figure 2b). Afterward, as for this paper, we turned to hollow cylinders of similar dimensions (4 cm of outer diameter, 2 cm of inner diameter and 5 cm height), which facilitate the analysis of the experiment. The sample is placed between two stainless steel pieces that are drilled so as to let the water invade the sample from the inside (Figure 2a). The whole set up is placed in a container that has a stainless steel base (Figure 2c) and is positioned between two metal platens of the Instron machine described before. Initially both platens exert just enough pressure to keep the sample in place when water is added. The machine is instructed to maintain this initial position throughout the test. After adding water, the stone expands, so the load required to maintain a constant height increases and is stored on the computer. In this case the bedding planes are horizontal, so that the swelling that is restrained is the one normal to the bedding (the maximum one) and water ingress is controlled by the sorptivity in the direction parallel to the bedding.

3. Results

3.1. Hydric Properties

[34] Our tests show that the capacity of the stone to absorb water by capillarity is relatively moderate with average rates of water ingress of 0.013 $cm/s^{1/2}$, and a sorption plateau at about 12% by volume (measured with the sample bedding normal to the water surface). It has been observed that sorptivity values change with the direction of water ingress (normal or parallel to the bedding planes). For the "brownish variety" measured values of rate of water ingress range from 0.008 $cm/s^{1/2}$ up to 0.015 $cm/s^{1/2}$ in directions perpendicular and parallel to the bedding, respectively.

[35] The free swelling strain in the direction parallel to the bedding averages 1.2×10^{-3} (or, 1200 μm/m) (Figure 3). It is substantially higher, about 2900 μm/m, in the direction perpendicular to the stone stratification (Figure 3). The 90% confidence limits, shown in Figure 3, are about ±200 μm/m. This value is slightly lower than the 3200 μm/m we previously reported [*Jiménez González and Scherer*, 2004]. The difference is, however, much larger with the 4000 μm/m reported by *Sebastian et al.* [2007] for the brown sandstone variety. This large discrepancy is probably due to natural variations in the structure and composition of the blocks from which the samples were obtained. Indeed, we find that swelling measurements are quite reproducible on a given sample, but that sample-to-sample variations are much larger. These are also larger in the direction parallel to bedding (standard deviation 26% of the average) than in the direction of maximum swelling (standard deviation 10% of the average). This can be seen in Figure 3, where the 90% confidence intervals on swelling strain averages in both directions are also shown.

[36] The sample-to-sample variations can be problematic for the validation of the warping technique where an independent measurement of swelling strain is needed. For this reason, we directly measured the swelling strain (in the direction normal to the bedding planes) on the thin plates used for warping tests. We find values of around 2600–2800 μm/m, which are slightly lower than the overall average of 2900 μm/m reported above.

[37] On samples of Portland brownstone treated with the selected swelling inhibitors, the swelling strain (measured in the direction normal to the sample bedding) was reduced by 50% [*Jiménez González and Scherer*, 2004].

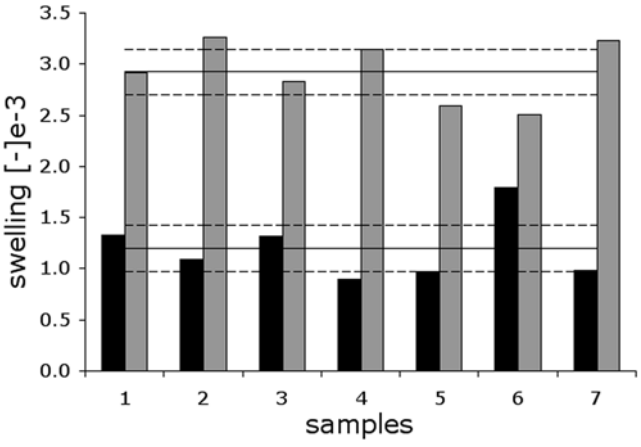

Figure 3. Free swelling strain measurements. Black and gray bars are averages of samples measured perpendicular and parallel to the bedding, respectively. The solid lines are the averages in both directions. The dashed lines show the associated 90% confidence interval on these averages.

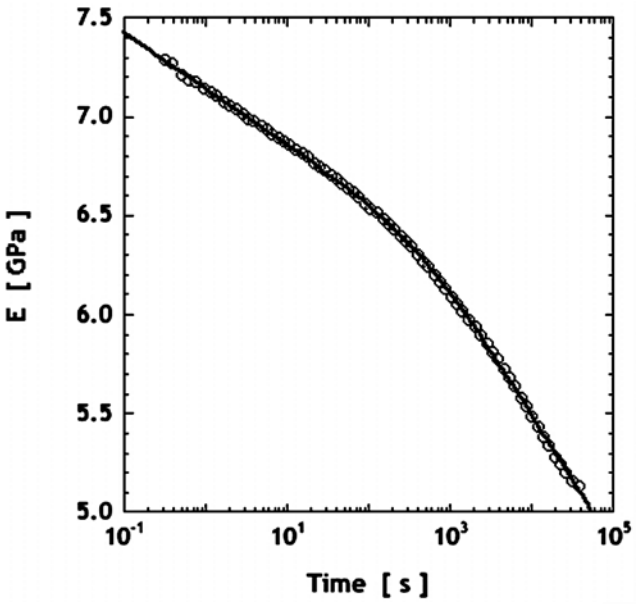

Figure 4. Stress relaxation of dry and untreated Tarifa sandstone (the sample bedding is parallel to the displacement applied). Circles indicate data points, and the solid curve indicates the fit by using equation (4).

3.2. Mechanical Properties

[38] In the direction perpendicular to the bedding, the average tensile strength is 5.3 MPa. In the parallel direction, an average value of 6.9 MPa was obtained.

[39] We have shown [*Jiménez González and Scherer*, 2004] the existing discrepancy between dynamic and static elastic modulus on clay-containing stones. In the case of the Tarifa sandstone, this difference is very big: dynamic moduli are about 2 times greater than the static moduli for the dry stones (average of at least 5 samples, giving a standard deviation of about 15%). In the direction perpendicular to the bedding the dry static modulus is on average about 9.4 GPa while the dynamic modulus is 15.4 GPa. For water saturated samples the difference is much bigger, around 20 times. The average static modulus of the saturated stone is 0.9 GPa (average of two samples, standard deviation of about 15%) compared to the 19.6 GPa obtained from ultrasound velocity measurements.

[40] Samples treated with swelling inhibitor show no change of static dry modulus with respect to the untreated. For the saturated samples, the treatment seems to raise the static modulus by about 0.17 GPa, (around 20%) which is not negligible, given the very low wet modulus of this stone.

[41] In the direction parallel to the bedding, only the dynamic elastic modulus was measured. The dry and wet moduli are 28.4 and 27.5 GPa, respectively. These measurements once again confirm the anisotropic character of this stone. However, these values should not be used to calculate stresses, because they drastically overestimate the elastic modulus.

[42] Stress relaxation measurements on dry samples (treated or untreated) show a bilinear relaxation rate on a logarithmic scale as represented in Figure 4.

[43] The stone relaxation involves two consecutive regimes, which can be fitted by using the following function:

$$E_d(t) = E_d(0) - a\ln\left(1+\frac{t}{\tau_1}\right) - b\ln\left(1+\frac{t}{\tau_2}\right), \qquad (4)$$

where $E_d(t)$ is the dry modulus at time t, $E_d(0)$ is the extrapolated dry modulus at $t = 0$, τ_1 and τ_2 are the characteristic times of the relaxation regimes of the dry stone and a and b are associated fitting constants.

[44] Early stress relaxation is governed by a and the later relaxation by b (Table 1). This implies that parameter a is the one that really characterizes the rate of stress relaxation in laboratory experiments (short test duration). The error for a is rather small (standard deviation of 15%, 2 samples treated, 4 samples untreated). Errors for the characteristic times, as well as for b, are larger (standard deviation between 38 and 75% of the average).

[45] In the case of water-saturated samples (Figure 5) subjected to bending, two relaxation processes occur: viscoelastic relaxation of stress in the solid and hydrodynamic relaxation of pressure in the pore fluid. The first process is similar in nature to that suffered by the dry samples, but with different kinetics. The extent of this relaxation continuously increases with time; on the other hand, the extent of the hydrodynamic relaxation is limited to a maximum value. When the sample is bent, the upper part of the sample is compressed (the water is squeezed out of that part) while the bottom is stretched (water is sucked into that part). This creates a pressure gradient and as a consequence the liquid in the sample redistributes. As this happens, the pressure gradient decreases, which means that the load needed to keep the sample bent decreases to a fixed value (for elastic materials). The rate at which the load decreases can be used to determine the sample permeability [*Scherer*, 2000, 2004; *Vichit-Vadakan and Scherer*, 2000, 2002].

[46] The stress relaxation measurement for wet samples is well fitted by a product of two functions, one describes the hydrodynamic relaxation and is denoted by $R(t)$, and

Table 1. Stress Relaxation Parameters for Dry and Saturated Tarifa Sandstone, Treated or Untreated

	Untreated							Treated						
	E_0 (GPa)	a (GPa)	b (GPa)	β (dimensionless)	τ_{VE}(s)	τ_1(s)	τ_2(s)	E_0 (GPa)	a (GPa)	b (GPa)	β (dimensionless)	τ_{VE}(s)	τ_1(s)	τ_2(s)
Dry	8.3	0.16	0.45	0.45	–	0.25	700	8.4	0.17	0.14	0.14	–	5.30E−4[a]	315
Wet	0.83	–	0.16	0.16	9.20E+7	–	–	0.84	–	0.57	0.57	1.30E+4	–	–

[a]Read 5.30E−4 as 5.30×10^{-4}.

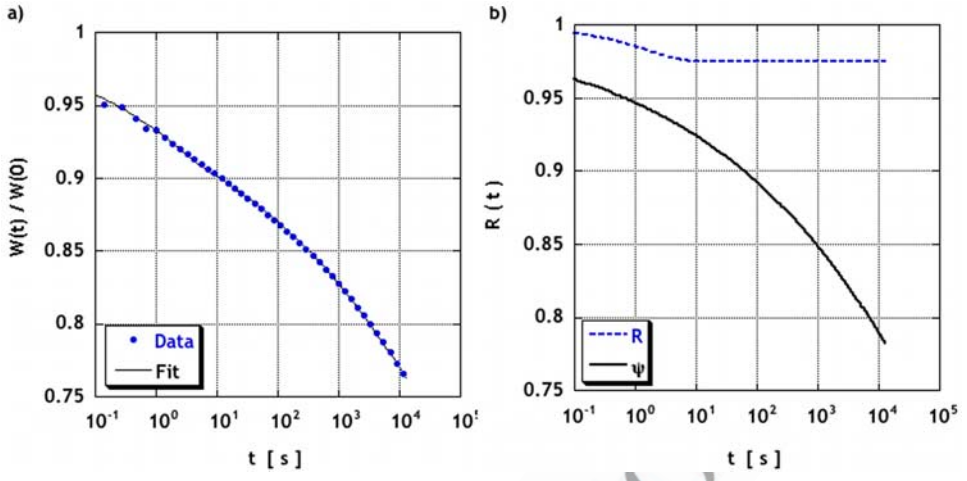

Figure 5. Stress relaxation of untreated water-saturated Tarifa sandstone that shows (a) the experimental data already fitted with equation (5) and (b) the deconvolution of the fitting function into the hydrodynamic (dashed curve) and the viscoelastic part (solid curve).

another that describes the viscoelastic relaxation and is denoted by $\psi(t)$

$$\frac{E_w(t)}{E_w(0)} = \frac{W(t)}{W(0)} = R(t)\psi(t), \tag{5}$$

where $W(t)$ and $E_w(t)$ are respectively the load and wet elastic modulus at time t, and $W(0)$ and $E_w(0)$ are respectively the load and wet elastic modulus at time $t = 0$. The type of function that is found to best fit the relaxation of wet samples is a stretched exponential

$$\psi(t) = \exp\left(-\left(\frac{t}{\tau_{VE}}\right)^{\beta}\right), \tag{6}$$

where τ_{VE} is the characteristic time for the viscoelastic relaxation of the wet sample and β is a fitting parameter of the viscoelastic relaxation function.

[47] Results of stress relaxation tests performed on saturated and untreated Tarifa samples are shown in Figure 5. In Figure 5a, the experimental curve is shown to be well fitted with equation (5). In Figure 5b, the theory is used to deconvolve the data to show separately the hydrodynamic, $R(t)$ and viscoelastic relaxation, $\psi(t)$. A repetition of this test with the same sample gave errors of the fitting parameters between 1 and 7%. Larger values are obtained for sample to sample variation. For this reason the same sample was treated and measured again to see the effect of treatment.

[48] Relaxation rate averages for the saturated sample before and after treatment are given in Table 1 along with the corresponding moduli. In the saturated case, which we discuss later, the treatment with swelling reducing agents leads to a spectacular increase in the rate of relaxation as can be seen in Figure 6. We expect that this is due to a lubrication of the contacts between clay particles and/or layers by the swelling inhibitors. As discussed later, this should limit the maximum stresses reached during wetting and reduce damage. However, the effect of this treatment on the strength of the wet stone (in particular at slow loading rates) should also be evaluated. As an example of the importance of this issue, *Dunning et al.* [1980] and *Dunning and Huf* [1983] report significant time of failure reductions under compressive stress for sandstones impregnated with DTAB, which they attribute to interfacial energy reduction.

3.3. Warping

[49] From the warping curves (Figure 7), we extract values of swelling strain, ratio of wet to dry modulus and sorptivity. The maximum deflection can be used to calculate the free swelling strain from equation (3), which yields values of 2000 to 2500 μm/m. Direct measurements of free swelling strain on two samples used for warping gave similar results, lower than the overall average of 2900 μm/m obtained with smaller samples. For these two samples, the

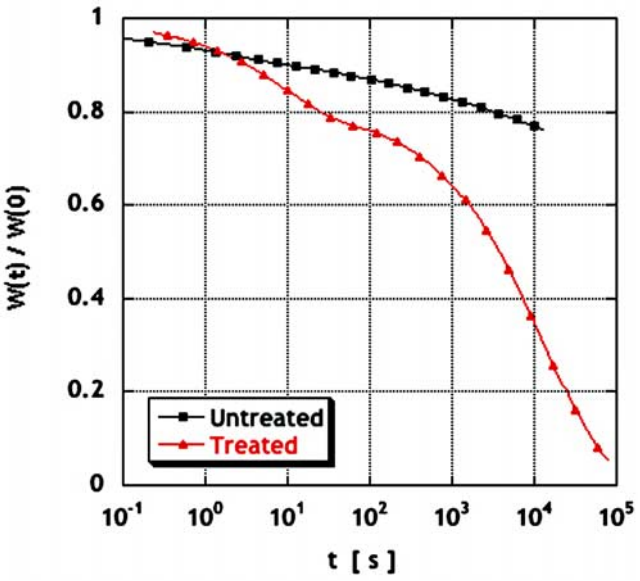

Figure 6. Fitted stress relaxation curves of untreated (squares) and treated (triangles) water-saturated Tarifa sandstone. Both curves are obtained from the same sample before and after treatment.

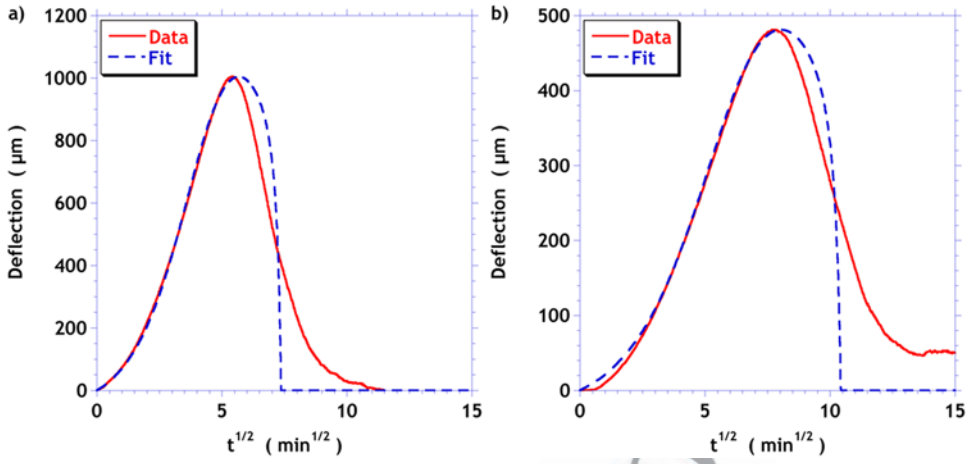

Figure 7. Warping curves of two Tarifa samples. (a) Bedding parallel to the water ingress. (b) Bedding perpendicular to the water ingress. The solid curve indicates the data points, and the dashed curve indicates the fit.

differences with the values obtained from warping were between 3 and 20%.

[50] With those values of maximum swelling, the first part of the warping curve is then very well fitted with equations (1) and (2) by adjusting sorptivity and modulus ratio. However, this is not the case for the second part, as already found for other stones [*Jiménez González and Scherer*, 2006]. That discrepancy is a consequence of the kinetics of swelling and softening of the stone, together with effects of capillary pressure in the pores (P. Duffus et al., Swelling damage mechanism for clay-bearing sanstones, paper to be presented at the 11th International Congress on Deterioration and Conservation of Stone, Torun, Poland, 15–20 September, 2008, hereinafter referred to as Duffus et al., paper to be presented, 2008).

[51] For the three samples measured, the average fitted values of the swelling strain, ratio of wet to dry modulus (E_w/E_d), and sorptivity in directions parallel, and perpendicular to the bedding are given in Table 2.

3.4. Swelling Pressure

[52] The result of the direct swelling pressure measurement is shown in Figure 8. The final pressure is about 0.84 MPa. In that plot, the two vertical dashed lines are estimations of the time to saturation. The first one is the intersection between the horizontal line of the plateau and the dashed line of the maximum slope. The second one is a visual estimate of when the plateau pressure is reached. These estimates of saturation time, t_{sat} can be used to calculate sorptivity from the following equation [*Scherer and Jiménez González*, 2005]:

$$t_{sat} \cong \frac{1}{4}\left(\frac{r_o - r_i}{S}\right)^2, \qquad (7)$$

where r_i and r_o are the inside and outside radius of the sample respectively.

[53] Equation (7) and the saturation times estimated from Figure 8 give sorptivities of 0.0065 and 0.0082 cm/s$^{1/2}$. These values are very similar to the ones obtained from warping measurements, but smaller than the ones obtained from direct sorptivity measurements (0.013 cm/s$^{1/2}$). The possible cause of this difference is discussed in section 4.1.

4. Discussion

[54] In the first part of this section, we examine the warping and swelling pressure measurements using a mechanical analysis of differential stresses and strains in a swelling sample. This analysis accounts for these measurements very well, so we have confidence in the general validity of this treatment of a swelling stone.

[55] In the second part of this discussion section, we use that same analysis to evaluate under what conditions the Tarifa sandstone can be damaged by wetting and drying cycles. We also discuss the quantitative benefit of swelling inhibitor treatments for reducing damage.

[56] Finally, we discuss the implications of this study for better understanding of physical weathering due to wetting/drying of sandstones in both urban environments and on the Earth's surface (and beyond).

4.1. Warping

[57] As already shown by *Jiménez González and Scherer* [2006], we cannot provide yet a total good fitting for the whole plot, but only for the first part of the curve which corresponds to the time at which the sample reaches the maximum deflection. The further sample relaxation could be probably explained by delayed expansion of the clays,

Table 2. Average Values of Swelling Strain, Ratio of Wet to Dry Static Modulus (E_{wet}/E_{dry}), and Sorptivity Obtained From the Fit of the Warping Curves[a]

	Swelling Strain (μm/m)	E_{wet}/E_{dry} (dimensionless)	Sorptivity (cm/s$^{1/2}$)
Bedding parallel to the water ingress	2254	0.088	0.0072
Bedding perpendicular to the water ingress	1000	0.081	0.0039

[a]Results are given for samples with the bedding parallel and perpendicular to the direction of water ingress.

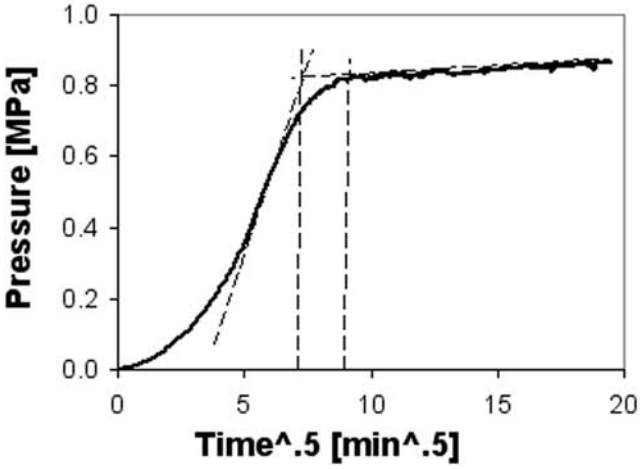

Figure 8. Swelling pressure evolution versus square root of time for a hollowed Tarifa cylindrical sample with 10.8 and 19.9 mm inner and outer radii, respectively.

together with the effect of capillary pressure, but we do not have yet a good way of accounting for this.

[58] From the maximum deflection, we calculate the maximum free swelling strain of the stone by using equation (3). That value, as already mentioned, agrees within 3–20% with the ones obtained by directly measuring that property on the same samples used to perform warping tests. Such a good agreement has not been reached with other stones (e.g., Portland Brownstone), although it is expected that the agreement should improve with thicker and longer samples.

[59] With the free swelling strain estimated from the maximum deflection, we then fit the first part of the warping curve by using equations (1) and (2) and adjusting the values of wet to dry modulus ratio and sorptivity.

[60] We find relatively good agreement between the ratio of wet to dry modulus extracted from warping measurements (0.088) and the one measured directly (0.095). The latter value is an average of beam bending measurements performed on different samples than the ones used for warping.

[61] Last, the sorptivity value that is extracted from warping (about 0.0072 cm/s$^{1/2}$) is consistent with the range estimated from swelling pressure tests (0.0065 to 0.0082 cm/s$^{1/2}$). However, these values differ substantially from the separate sorptivity measurements (around 0.013 cm/s$^{1/2}$). This discrepancy could be due to delayed swelling. Indeed, the analyses of both the swelling pressure and warping experiments assume instantaneous swelling, so that the progress of swelling can be determined directly by sorptivity. If the swelling were delayed, then the sorptivity calculated from these experiments would be lower, which is indeed the case. Sample to sample variation is not thought to explain this sorptivity difference, since independent measurements by *Sebastian et al.* [2007] were very similar to ours (0.016–0.018 cm/s$^{1/2}$).

[62] The largely nonlinear shape of the warping curve versus square root of time and the shift of the maximum deflection to longer times are due to the severe softening of the stone. It shows that the maximum swelling is only reached when a large part of the sample has been saturated. In terms of monument durability, it implies that large pressures only develop during wetting when a very large part of the block gets wet. These aspects are further discussed below.

4.2. Swelling Pressure and Stress Relaxation

[63] As mentioned in the previous section, sorptivity values extracted from swelling pressure measurements are consistent with the ones obtained from warping but not with the ones directly measured. Apart from this, the analysis of this experiment suggests that the pressure should increase linearly with the square root of time, which is not the case in Figure 8. This might be due to the top surface of the sample not being flat. If that is the case and because of the stone softening, the sample surface would first be pushed into (better) contact with the platens before being able to exert pressure.

[64] This possible issue of contact (smaller contact surface than sample surface) could also explain in part why the maximum pressure is only 0.83 MPa, which does not agree with the stress expected from the product of the wet modulus and free swelling strain (2.62 MPa). Even if stress relaxation is taken into account [*Scherer and Jiménez González*, 2005], the calculated pressure is still substantially higher (2.18 MPa).

[65] Sample to sample variation in material properties does not seem a sufficient reason to explain this difference since the 90% confidence interval on this pressure is about 0.7 MPa.

[66] However we observe that part of the curve is linear with square root of time as expected from the theory. This might correspond to the moment where the platens have a good contact with the sample. Extrapolation of this portion of the curve gives a pressure increase of 1.43 MPa between time zero and saturation. This corresponds to an intercept of −0.6 MPa that is just interpreted as a problem of setting the proper zero in a sample that does not have a perfect contact with the platens. This represents an attempt to obtain a more reliable estimate of the true swelling pressure (if the contact between the sample and the platens were perfect). This is much closer to the pressure calculated using viscoelastic relaxation and almost in range with the 90% confidence interval. However, the discrepancy remains large, which reflects the difficulty in achieving perfect experimental conditions for this type of measurement.

4.3. Stress Evaluation

[67] In this section we calculate the stresses that can develop during cycles of wetting and drying on clay-bearing stones. The hypotheses behind the equations presented are similar to those that led to the equation for analyzing the warping and swelling pressure experiments, which have been largely validated in the previous sections.

4.3.1. Compressive and Shear Stresses

[68] The maximum compressive stresses during wetting, σ_w, in the outer layer of an otherwise dry stone block can be estimated by (see Appendix A)

$$\sigma_w = \frac{E_w \varepsilon_S}{1 - \nu_w}. \quad (8)$$

Assuming a Poisson's ratio for the wet stone, ν_w of 0.2, and using the previously determined values of free swelling

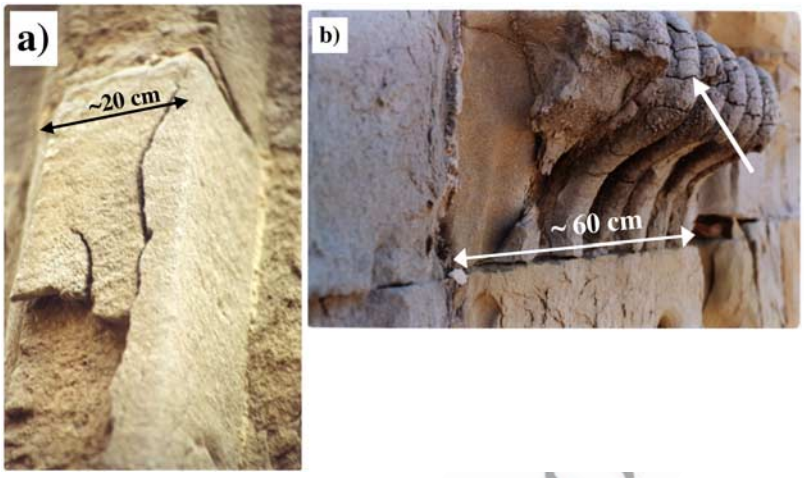

Figure 9. Possible damage patterns due to wetting and drying cycles on Tarifa sandstone. (a) Buckling of the stone surface during wetting. (b) Cracking of the stone surface following a mud-cracking pattern. The dimensions indicated are approximate.

strain, ε_S and elastic modulus of the wet stone, E_{wt}, the calculated stress is 3.3 MPa.

[69] As explained before, damage during wetting could happen if those stresses overcome the wet compressive strength of the stone. This is not the case since the compressive strength normal to bedding planes was measured to be about 14 MPa in the wet state, (information provided by G. Cultrone (unpublished data, 2007)). It is important, however, to emphasize that this compressive strength could be substantially lower if determined with very slow loading rate because of the viscoelastic behavior of the stone. In view of Figure 6, which shows a strong acceleration of stress relaxation of treated samples, it appears that the role of loading rate on wet compressive strength on such samples is a subject to examine carefully in future studies.

[70] On the other hand, shear forces that develop during wetting could be responsible for cracks opening parallel to the stone surface. This can create a disruption between the dry and wet layers producing the buckling of the wet outer surface [*Scherer*, 2006] and resulting in scaling, or contour scaling. This is indeed observed in Figure 9, which is a strong indication that clay swelling is contributing to the degradation of the stone. For this mechanism of damage the quantification is unfortunately not very easy. What can be said is that buckling damage is facilitated by the presence of preexisting flaws (Duffus et al., paper to be presented, 2008). These can be inherent to the stone (e.g., bedding planes of face-bedded blocks). Indeed *Sebastian et al.* [2007] report not only that the church of Tarifa shows the detachment of plates several centimeters wide but also that this is particularly pronounced in face-bedded blocks. Alternatively these flaws maybe produced by other degradation mechanisms. Given the climate of Tarifa, freezing is not an issue. Furthermore *Sebastian et al.* [2007] concluded that salt crystallization was not relevant, since the façade was only found to contain minor amounts of sodium chloride. However, considering that salt crystallization would only have to initiate damage, the role of this mechanism maybe much more important than one can conclude when considering it as a unique cause of damage.

4.3.2. Tensile Stresses

[71] During drying cycles, maximum tensile stresses, σ_d, in the outer layer of an otherwise wet stone can be estimated in a similar way as with equation (8) (see Appendix A)

$$\sigma_d = \frac{E_d \varepsilon_S}{1 - \nu_d}. \tag{9}$$

[72] Assuming a Poisson's ratio for the dry stone, ν_d of 0.2 (as for the wet stone) and using the previously determined swelling strain and dry modulus, we find stresses of about 34.4 MPa in the direction parallel to the bedding. This value exceeds by far the tensile strength of the stone (5.3 MPa). The same is true in the direction of the bedding planes. However, in this case, we have to estimate the dry static modulus since no measurements are available. Using the same modulus as perpendicular to the bedding, stresses of 14 MPa are obtained, which exceed the tensile strength in that direction (6.9 MPa). These stresses rise to 26 MPa if we assume that the ratios of static and dynamic modulus are the same in both directions.

[73] These calculations seem to indicate that damage should always happen during drying. However, for tensile stress to develop, the stone must first be sufficiently expanded, which will only occur if a block or ornamental piece is almost completely saturated. For a block of thickness L we can calculate the depth of wetting L_w that must be achieved for drying stresses to reach the tensile strength of the stone in a thin external layer by using equation (10) (see Appendix A)

$$\sigma_{d,2} = \frac{E_d \varepsilon_S}{1 - \nu_d} \left(\frac{r}{r + \dfrac{L - L_w}{L_w}} \right), \tag{10}$$

where $\sigma_{d,2}$ is the tensile stress in the drying outer layer; ν_d is the Poisson ratio of the dry stone, $r = E_w/E_d$; E_d and E_w are the dry and wet static modulus, respectively, and ε_s is the free swelling strain of the stone.

[74] In the case where swelling takes place perpendicular to the bedding and for a 25 cm thick block, we find that the depth of wetting would have to be about 16 cm for drying

stresses to reach the stone tensile strength in that direction. This is an improbably large extent of wetting, since *Sebastian et al.* [2007] estimated that capillary rise of the waterfront is not very high in Tarifa sandstone and that water only penetrates superficially to a depth estimated to be about 2 cm. This mode of failure therefore only seems probable for thin ornamental elements that can get fully saturated. Such situations are illustrated in Figure 9, where the cracks are of mud-cracking type, as would be expected if drying stresses are indeed causing damage. It is also important to note that *Sebastian et al.* [2007] described exactly this type of damage on ornamental features of the Tarifa Church façade.

[75] Other factors that can reduce the calculated stresses are slow drying (which permits viscoelastic relaxation) and a humid environment (which inhibits drying). However, the Town of Tarifa is known to be one of the windiest places in Europe, so that slow drying is no issue. In addition the climate of the city is rather dry for a coastal location (average 75% RH according to *Hoyos et al.* [1999]). Overall, the main factor limiting drying stresses really appears to be the depth of wetting.

[76] Our calculations are based on the assumption of the stone having homogeneous properties. In fact, we believe that the scatter of data shown in Figure 3 reflects true heterogeneity of the stone. In consequence, it must be pointed out that very high local stresses could develop from differential strains on a millimeter scale.

4.3.3. Swelling Inhibitors

[77] The major effect of swelling inhibitors is to reduce the swelling strain. Consequently, with a 50% reduction in dilation, we expect a 50% reduction in stresses (tensile, compressive or shear). In the case of swelling pressure, the change in modulus of the wet stone, although small, is not negligible. Therefore the reduction of ε_s in equation (9) is partially offset by the increase in E, so the effective reduction in swelling pressure would be only 33%. On the other hand, the increase in viscoelastic relaxation would partially compensate this: in the swelling pressure measurements, it would contribute to an overall pressure reduction of about 44%. For similar reasons, the same type of changes might be expected for the shear forces.

[78] However, as far as drying stresses are concerned, the stress reduction resulting from surfactant treatment should be about 50% since there is no detectable change in the dry modulus. This is true for blocks that previously get fully saturated. For blocks that are partially saturated, the tensile stresses can decrease by 40% at the most, but the stresses in this case are expected to be small unless the saturation is deep.

[79] Overall, these reductions in stresses, whether compressive, shear or tensile, are important in terms of avoiding or reducing the number of situations that can lead to damage. Such treatments should be considered as an option for monuments under the conditions discussed here. In addition, it is worth noting that if consolidation with ethyl silicates is to be considered, then a preliminary treatment with swelling reducing agents appears to be particularly advised. This should not be carried out without further testing; in particular, the effect that these products have on the stone strength at low loading rates should be investigated. However, applying swelling inhibitors to Portland brownstone before consolidation does indeed increase resistance to cycles of wetting and drying (this study).

[80] The reduction in swelling strain as well as in swelling stresses observed following the treatment with the swelling inhibitor, which adsorbs specifically on the clay minerals [*Snethlage and Wendler*, 1991], unambiguously demonstrates that the damage is associated with the expansion/shrinkage of these minerals. This is not a trivial conclusion, since controversy exists in the field of geomorphology as to the ultimate cause of wetting/drying damage in clay-containing sandstone, which has often been attributed to other weathering mechanisms, such as salt hydration/dehydration [*McGreevy and Smith*, 1984; *Turkington and Paradise*, 2005].

[81] Finally, it should be indicated that porosity and permeability of reservoir sandstones is drastically reduced because of swelling of clays, representing a significant problem in water injection or "squeeze" oil recovery [*Morris and Shepperd*, 1982; *Houseknecht and Pittman*, 1992; *Baker et al.*, 1993]. Different remediation treatments for this so-called formation damage, including the use of brines and surfactant polymer solutions, have been thoroughly studied and applied [*Borchardt*, 1989]. Our results suggest that the application of a diaminoalkane swelling inhibitor could be a potential solution for enhancing oil recovery in reservoir sandstones.

4.4. Implications for Understanding Sandstone Weathering in Nature

[82] The formation of several weathering forms observed in sandstone natural outcrops as well as in historic structures is poorly understood. This is the case of spalling and/or scaling/contour scaling, as well as polygonal cracking. Our results show that situations where damage can occur during wetting (and clay swelling) can lead to the formation of scales parallel to the exposed surface, as observed in Tarifa Church (Figure 9). Such a situation can explain why spalling and scaling/contour scaling are ubiquitous weathering forms in the sandstone monuments [*Snethlage and Wendler*, 1997] and in sandstone outcrops [*Campbell*, 1991; *Robinson and Williams*, 1994; *Turkington and Paradise*, 2005]. Previous theories suggesting that salt weathering is responsible for sandstone contour scaling [*Smith and McGreevy*, 1988], should therefore be reconsidered in lieu of these results. In addition, our results suggest that weathering phenomena associated with wetting events may contribute to tafoni development in salt-free sandstones, as has been suggested elsewhere [e.g., *Johnson*, 1974; *Martini*, 1978].

[83] On the other hand, drying stresses can lead to surface crack development (with cracks planes normal to the exposed surface), as observed in Tarifa Church (Figure 9b) and in nature [*Williams and Robinson*, 1989]. The latter striking weathering form, also-called "polygonal cracks" has also been observed in reworked evaporitic sandstones on Mars [*McLennan et al.*, 2005]. Figure 10 shows examples of such polygonal cracks developed on Martian rocks within Endurance Crater. The surface features are highly similar to those observed at Tarifa Church (Figure 9b). Those features point to stress development upon drying as a possible mechanism responsible for their formation.

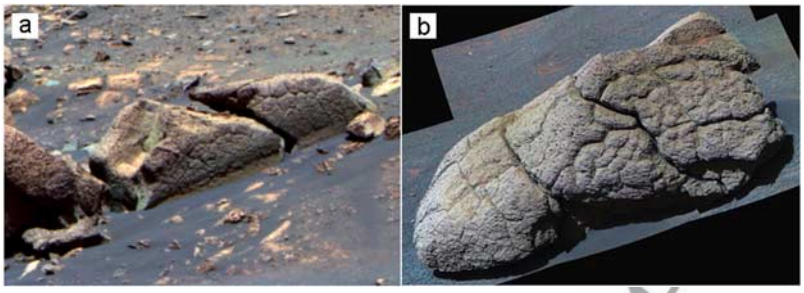

Figure 10. Polygonal cracks on sandstone rocks at Endurance crater, Meridiani Planum, Mars. (a) Pancam false color image of Earhart rock. Image is approximately 4 m across. This image was taken on Sol 219, sequence P1306, using 750, 530, and 430 nm filters. (b) False color Pancam mosaic of rock Wopmay within Endurance crater. Image is approximately 1 m across. Image was taken on Sol 251, sequence P2432, using 750, 530, and 430 nm filters. Image credits NASA/JPL/Cornell.

Potential minerals that could have been involved in the development of drying stresses could be magnesium sulfates [*Squyres et al.*, 2006] or clays, such as nontronite, chamosite, and montmorillonite, that several reports suggest are abundant on Martian surface rocks and sediments [*Poulet et al.*, 2005]. Interestingly, our theoretical analysis indicates that cracks would only develop when a significant portion of the rock is wet. This suggests that water could have been abundant on Mars' surface at the time of the formation of such weathering features.

[84] Note that controversy exists as to the origins of polygonal cracking in natural sandstone outcrops [*Williams and Robinson*, 1989]. It has been suggested that surface crusting due to deposition of secondary minerals and structural discontinuities between the crust and the substrate is the dominant process responsible for such a weathering form [*Turkington and Paradise*, 2005]. However, neither secondary minerals formation, nor crust development was observed in sandstone block displaying polygonal cracking in Tarifa Church [*Sebastian et al.*, 2007]. In contrast, crack formation upon drying appears to be sufficient to explain the formation of this striking weathering form.

[85] It should be stated that sandstones display a wide variation in mineralogy and texture, expanding from quartz arenites to arkoses, litharenites, and greywackes [*Tucker*, 1991]. In this respect, the Tarifa sandstone (an arkose) might not be fully representative of sandstones in general. However, nearly all sandstones include clays within the matrix, in proportions ranging from a few percent up to ~60 wt %, with an average value of ~10 wt % [*Tallman*, 1949]. The observed swelling/shrinking phenomena and the associated damage in Tarifa sandstone, with only 7 wt % clays, could thus be common for many of the sandstones on Earth's surface. In fact, extensive studies on swelling strains of a large number of sandstone types (~35) from many different locations show that nearly all sandstones experience some degree of hydric expansion, with values in the range 500–1000 μm/m on average, and maximum values of 5000–7000 μm/m for the clay-rich greywackes [*Felix*, 1983; *Esbert et al.*, 1997; *Snethlage and Wendler*, 1997; *Jiménez González et al.*, 2002; *Heinrichs*, 2005].

[86] The extent of sandstone damage experienced upon wetting/drying cycles would depend, among other parameters, on exposure, textural anisotropy, clay content and type (i.e., presence of expandable clays as opposed to nonexpandable clays), and the interplay of other weathering phenomena. However, it is expected that the damage mechanism due to cyclic wetting and drying will in general terms follow the model presented here. In addition, this model may help explain many field observations regarding sandstone weathering: for instance, why weathering rates of sandstone landscapes typically show a positive correlation with the number of wetting/drying events [*Pentecost*, 1991], and why damage resulting in continuous scaling typically concentrates at the limit of rising damp [*Snethlage and Wendler*, 1997], where wetting/drying events are more frequent. The latter may explain the formation of large-scale sandstone weathering forms such as pedestal rocks, which have often been attributed to salt weathering [*Selby*, 1993].

5. Conclusions

[87] In this work we have determined many material properties of Tarifa sandstone with the objective of supporting the analysis and validation of novel techniques used to characterize the swelling behavior of such a stones. These consist of the warping or 3 in 1 test on thin stone plates and an accelerated version of a swelling pressure measurement. Results show that the theory used to analyze these tests is valid, so that we may also apply it to calculate stresses than can develop in the field. Results of these calculations suggest that damage can take play in the two following ways:

[88] 1. Buckling and scaling/contour scaling development during wetting due to shear forces. This is enhanced by preexisting flaws that can be inherent to the stone (e.g., bedding planes) or result from other damage mechanisms, such as salt crystallization. It causes the detachment of rather large stone layers and is indeed something very evident on the façade that is the object of this study. Similar weathering forms are commonly observed in sandstone landscapes.

[89] 2. Tensile failure during drying. This type of damage only seems probable for thin ornamental elements that can get fully saturated or in sandstone outcrops where periods of wetting (rain showers, or capillary moisture uptake from the ground) are followed by intense drying. In those cases, the damage follows a mud-cracking pattern. This is also something that is observed on the ornaments of the San Mateo main Façade and on sandstone rocks, both on Earth and on Mars.

[90] Our stress analysis does not account for other types of damage reported by *Sebastian et al.* [2007], such as granular disintegration. In that case, those authors propose that the partially carbonatic nature of the cement in this sandstone could suffer chemical degradation caused by acid depositions from local traffic. The fact that wetting and drying would not account for that damage is supported by the fact that the same authors report it to occur in sheltered zones.

[91] Overall, our study clearly confirms that clay swelling and shrinkage is an important issue in the degradation of this monument and that swelling inhibitors have the potential of substantially reducing this type of damage. Similar weathering phenomena can also occur in natural sandstone outcrops, contributing to landscape modeling and evolution.

[92] Finally, it should be emphasized that the testing methodology and data analysis here presented and discussed might be a valuable tool for studying the response of different sandstone types to wetting/drying damage.

Appendix A: Drying Stress in Swelling Stone

[93] In this appendix we analyze the stresses generated during the drying of a partially wet stone block. We calculate what should be the depth of wetting in a stone block for these drying stresses to reach the tensile strength of the material. Consider a stone with thickness L that is wetted by water to a depth of $L_w + L_d$, after which the surface dries to a depth of L_d, as indicated in Figure A1. We calculate the stress in each zone. The x-y plane (which is the surface through which moisture passes) runs into the page, and the z axis is perpendicular to that surface. Since that surface is free, $\sigma_z = 0$; by symmetry, $\sigma_x = \sigma_y$ and $\varepsilon_x = \varepsilon_y$. If the free swelling strain is ε_s, then the constitutive equation of the stone is

$$\varepsilon_x = \varepsilon_f + \frac{1}{E_f}\left[\sigma_x - \nu_f\left(\sigma_y + \sigma_z\right)\right] = \varepsilon_f + \frac{\sigma_x\left(1-\nu_f\right)}{E_f}. \quad \text{(A1)}$$

[94] In the dry zone, $\varepsilon_f = 0$, $\nu_f = \nu_d$ and $E_f = E_d$; in the wet zone, $\varepsilon_f = \varepsilon_s$, $\nu_f = \nu_w$ and $E_f = E_w$. If the plate is wide compared to its thickness, L, then the strain ε_x will be the same in each region. We assume that the plate is prevented from warping (which is strictly true only if the wet region is exactly in the middle, so that the stresses are symmetrical), and that the edges are free. If there is no net force on the edges, then

$$\int_0^L \sigma_x dz = 0 \quad \text{(A2)}$$

the stress is

$$\sigma_x = \left(\frac{E_f}{1-\nu_f}\right)\left(\varepsilon_x - \varepsilon_f\right) = \begin{cases} \left(\frac{E_d}{1-\nu_d}\right)\varepsilon_x, 0 \le z \le L_d \\ \left(\frac{E_w}{1-\nu_w}\right)\left(\varepsilon_x - \varepsilon_s\right), L_d < z \le L_d + L_w, \\ \left(\frac{E_d}{1-\nu_d}\right)\varepsilon_x, L_d + L_w \le z \le L \end{cases} \quad \text{(A3)}$$

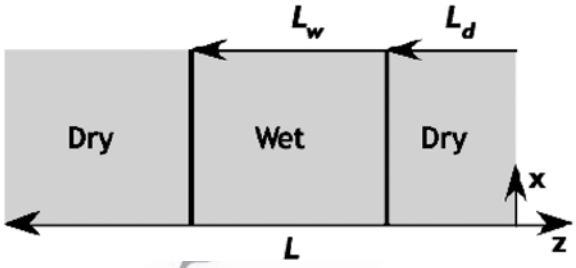

Figure A1. Illustration of the wet and dry parts of the stone block considered to analyze drying stresses in a partially wet block.

so if the Poisson ratio is assumed to be the same in both regions, equation (12) leads to

$$\varepsilon_x = \varepsilon_s\left(\frac{r}{r + \left(\frac{L - L_w}{L_w}\right)}\right), \quad \text{(A4)}$$

where $r = E_w/E_d$. The stress in the drying region is

$$\sigma_{d,2} = \frac{E_d \varepsilon_S}{1-\nu_d}\left(\frac{r}{r + \frac{L - L_w}{L_w}}\right), \quad \text{(A5)}$$

which is equation (10) in section 4.3.2.

[95] When $L_w = 0$, there is no swelling, so $\sigma_{d,2} = 0$; as L_w approaches L, the dry region is very thin so the contraction is completely suppressed and the stress in the dry region achieves its maximum value

$$\sigma_d = \left(\frac{E_d \varepsilon_s}{1-\nu_d}\right), \quad \text{(A6)}$$

which is equation (9) in section 4.3.2.

Notation

a, b	fitting constants for the dry viscoelastic modulus (GPa).
A	sample base in a sorptivity experiment (cm^2)
d	relative depth of water penetration in a warping sample (dimensionless)
E_f	elastic modulus, E_d in the dry zone and E_w in the wet zone (see Appendix A) (GPa)
$E_d(t)$, $E_w(t)$	viscoelastic modulus respectively of the dry and wet stone at time t (GPa)
E_d, E_w	elastic modulus respectively of the dry and wet stone, corresponding also to $E_d(t)$ and $E_w(t)$ at $t = 0$ (GPa)
h	plate thickness in a warping experiment (cm)
h_w	wet part of the sample thickness in a warping experiment (cm)
L	stone thickness of a partially saturated stone (cm)
L_d, L_w	depth of dry and wet part of a partially saturated stone of thickness L (cm)
r	ratio of wet to dry modulus (E_w/E_d) (dimensionless)

r_i, r_o inner and outer radius respectively of a swelling pressure measurement sample (cm)

$R(t)$ hydrodynamic relaxation function of a wet stone in a bending experiment (dimensionless)

S sorptivity (cm/s$^{1/2}$)

t time (s)

t_{sat} saturation time in swelling pressure test (s)

w span in a warping test (cm)

$W(t)$, $W(0)$ load in a beam bending experiment at time t and $t = 0$ respectively (g)

β fitting parameter of the viscoelastic relaxation function (dimensionless)

Δ warping deflection (cm or μm)

Δ_{max} maximum warping deflection (cm or μm)

Δh average height of water rise in a sorptivity experiment (cm)

Δm mass change in a sorptivity experiment (g)

ε_f swelling strain in a zone of a partially saturated stone; equals to zero in the dry zone and to ε_S in the wet zone (dimensionless)

ε_S free swelling strain (dimensionless or μm/m)

ε_x strain in an (x-y) plane parallel to the drying surface (dimensionless)

ϕ porosity

ν_d, ν_w Poisson's ratio of the dry and wet stone respectively (dimensionless)

ν_f Poisson's ratio in a zone of a partially saturated stone; equals to ν_d, in the dry zone and toν_w in the wet one (dimensionless)

ρ_L liquid density (g/cm^3)

σ_d maximum tensile stresses expected during drying (MPa)

σ_w maximum compressive stresses during wetting (MPa)

$\sigma_{d,2}$ tensile stress in the drying part of a partially saturated stone (MPa)

σ_x, σ_y, σ_z stresses in the plane parallel to the drying surface (x-y) and in the direction perpendicular to it (z) (MPa)

τ_1, τ_2 characteristic times of the first and second relaxation regimes of the dry stone (s)

τ_{VE} characteristic time for viscoelastic relaxation of the wet stone (s)

$\psi(t)$ viscoelastic relaxation function of the wet stone (dimensionless)

[96] **Acknowledgments.** Financial support for Inmaculada Jiménez González was provided by the Samuel Kress Foundation and VIP Restoration, Inc. The authors would also like to thank Dr. Giuseppe Cultrone, the corresponding author of the paper by *Sebastian et al.* [2007], for sharing very useful information from that paper before its publication. One of us (C.R.-N.) acknowledges the financial support provided by the Spanish Government under contract MAT2006-00578 and by the Research Group RNM-179 (Junta de Andalucia, Spain).

References

Baker, J. C., P. J. R. Uwins, and I. D. R. Mackinnon (1993), ESEM study of illite/smectite freshwater sensitivity in sandstone reservoirs, *J. Petrol. Sci. Eng.*, *9*, 83–94, doi:10.1016/0920-4105(93)90069-Q.

Beloyiannis, N., P. Theoulakis, and L. Haralambides (1988), Causes and mechanism of stone alteration at the temple of Apollo Epicuros, in *Engineering Geology of Ancient Works, Monuments and Historic Sites*, edited by P. Marinos and G. Koukis, pp. 763–770, Balkema, Rotterdam, Netherlands.

Borchardt, J. K. (1989), Chemicals used in oil-field operations, *ACS Symp. Ser.*, *396*, 3–54.

Bradley, W. C. (1963), Large-scale exfoliation in massive sandstones of the Colorado plateau, *Geol. Soc. Am. Bull.*, *74*, 519–528, doi:10.1130/0016-7606(1963)74[519:LEIMSO]2.0.CO;2.

Campbell, I. A. (1991), Classification of rock weathering at Writing-on-Stone Provincial Park, Alberta, Canada: A study in applied geomorphology, *Earth Surf. Processes Landforms*, *16*, 701–711, doi:10.1002/esp.3290160804.

Caner, E. N., and N. J. Seeley (1978), The clay minerals and the decay of limestone, paper presented at International Symposium on Deterioration and Protection of Stone Monuments, UNESCO-RILEM, Paris.

Cruikshank, K. M., and A. Aydin (1994), Role of fracture localization in arch formation, Arches National Park, *Utah, Geol. Soc. Am. Bull.*, *106*, 879–891, doi:10.1130/0016-7606(1994)106<0879:ROFLIA>2.3.CO;2.

Delgado Rodrigues, J. (2001), Swelling behaviour of stones and its interests in conservation: An appraisal, *Mater. Constr.*, *51*, 263–264.

Dragovich, D. (1978), Building stone and its use in rock weathering studies, *J. Geol. Educ.*, *27*, 21–25.

Dunn, J. R., and P. P. Hudec (1966), Water, clay and rock soundness, *Ohio J. Sci.*, *66*, 153–168.

Dunning, J. D., and W. L. Huf (1983), The effects of aqueous chemical environments on crack and hydraulic fracture propagation and morphologies, *J. Geophys. Res.*, *88*(B8), 6491–6499, doi:10.1029/JB088iB08p06491.

Dunning, J. D., W. L. Lewis, and W. L. Huf (1980), Chemomechanical weakening in the presence of surfactants, *J. Geophys. Res.*, *85*(B10), 5344–5354, doi:10.1029/JB085iB10p05344.

Esbert, R. M., J. Ordaz, F. J. Alonso, M. Montoto, T. González Limón, and M. Alvarez de Buergo Ballester (1997), *Manual de Diagnosis y Tratamiento de Materials Pétreos y Cerámicos*, 130 pp., Coll. Aparelladors Arquitectes Tèc. Barcelona, Barcelona, Spain.

Felix, C. (1983), Sandstone linear swelling due to isothermal water sorption, in *Materials Science and Restoration*, edited by F. H. Wittmann, pp. 305–310, Tech. Akad. Esslingen, Ostfildern, Germany.

Félix, C. (1988), Comportement des grès en construction sur le plateau Suisse, in *Conservation et Restauration des Biens Culturels*, edited by R. Pancella, pp. 833–841, Ecole Polytech. Fed. Lausanne, Montreux, Switzerland.

Félix, C. (1995), Choix de gres tenders du Plateau Suisse pour les travaux de conservation, in *Conservation et Restauration des Biens Culturels*, edited by R. Pancella, pp. 45–71, Ecole Polytech. Fed. Lausanne, Montreux, Switzerland.

Félix, C., and V. Furlan (1994), Variations dimensionnelles des gres et calcaires liees a leur consolidation avec un silicate d'ethyle, in *Proceedings of the 3rd International Symposium on the Conservation of Monuments in the Mediterranean Basin*, edited by V. Fassina and F. Zezza, pp. 855–859, Graffo, Venice, Italy.

Fookes, P. G., and A. B. Poole (1981), Some preliminary considerations on the selection and durability of rock and concrete materials for breakwaters and coastal protection work, *Q. J. Eng. Geol. Hydrogeol.*, *14*, 97–128, doi:10.1144/GSL.QJEG.1981.014.02.03.

Gill, E. D., E. R. Segnit, and N. H. McNeill (1980), Rate of honeycomb weathering features (small scale tafoni) on the Otway Coast, S.E. Australia, *Proc. R. Soc. Victoria*, *92*, 149–154.

Goudie, A. S., and H. Viles (1997), *Salt Weathering Hazards*, 241 pp., John Wiley, Oxford, UK.

Hall, K., and A. Hall (1996), Weathering by wetting and drying: some experimental results, *Earth Surf. Processes Landforms*, *21*, 365–376, doi:10.1002/(SICI)1096-9837(199604)21:4<365::AID-ESP571>3.0.CO;2-L.

Heinrichs, K. (2005), Diagnose der Verwitterungsschäden an den Felsmonumenten der antiken Stadt Petra, Jordanien, Ph.D. dissertation, Aachener Geowiss. Beitr., Aachen, Germany.

Hoke, G. D., and D. L. Turcotte (2002), Weathering and damage, *J. Geophys. Res.*, *107*(B10), 2210, doi:10.1029/2001JB001573.

Houseknecht, D. W., and E. D. Pittman (Eds.) (1992), *Origin, Diagenesis, and Petrophysics of Clay Minerals in Sandstones*, *SEMP Spec. Publ.*, vol. 47, SEMP, Tulsa, Okla.

Hoyos, M., S. Sanchez-Moral, E. Sanz-Rubio, and J. C. Cañaveras (1999), Alteration causes and processes in the stone material from the pavement in Baelo Claudia archaeological site, Cádiz/Spain, *Mater. Constr.*, *49*, 5–18.

Iñigo, A. C., J. García-Talegón, R. Trujillano, E. Molina, and V. Rives (2003), Evolution and decay processes in the Villamayor and Zamora sandstones, in *Applied Study of Cultural Heritage and Clays*, edited by J. L. Perez-Rodríguez, pp. 47–57, Cons. Super. Invest. Cient., Sevilla, Spain.

Jiménez González, I., and G. W. Scherer (2004), Effect of swelling inhibitors on the swelling and stress relaxation of clay bearing stones, *Environ. Geol.*, *46*, 364–377, doi:10.1007/s00254-004-1038-8.

Jiménez González, I., and G. W. Scherer (2006), Evaluating the potential damage to stones from wetting and drying cycles, in *Measuring, Monitoring and Modeling Concrete Properties*, edited by M. S. Konsta-Gdoutos, pp. 685–693, Springer, Dordrecht, Netherlands.

Jiménez González, I., M. Higgins, and G. W. Scherer (2002), Hygric swelling of Portland Brownstone, *Mater. Res. Soc. Symp. Proc.*, *712*, 21–27.

Johnson, A. R. M. (1974), Cavernous weathering at Berowra, N.S.W., *Aust. Geogr.*, *12*, 531–535, doi:10.1080/00049187408702665.

Kühnel, R. A., S. J. Van der Gaast, J. Brych, G. J. Laan, and H. Kulnig (1994), The role of clay minerals in durability of rocks observation on basaltic rocks, *Appl. Clay Sci.*, *9*, 225–237, doi:10.1016/0169-1317(94)90001-9.

Madsen, F. T., and M. Müller-Vonmoos (1985), Swelling pressure calculated from mineralogical properties of a jurassic opalinum shale, Switzerland, *Clays Clay Miner.*, *33*, 501–509, doi:10.1346/CCMN.1985.0330604.

Madsen, F. T., and M. Müller-Vonmoos (1989), The swelling behaviour of clays, *Appl. Clay Sci.*, *4*, 143–156, doi:10.1016/0169-1317(89)90005-7.

Martini, I. P. (1978), Tafoni weathering, with examples of Tuscany, Italy, *Z. Geomorphol.*, *22*, 44–67.

McGreevy, J. P. (1981), Some perspectives on frost shattering, *Prog. Phys. Geogr.*, *5*, 56–75, doi:10.1177/030913338100500103.

McGreevy, J. P., and B. J. Smith (1984), The possible role of clay minerals in salt weathering, *Catena*, *11*, 169–175.

McGreevy, J. P., and W. B. Whalley (1984), Weathering, *Prog. Phys. Geogr.*, *8*, 543–569, doi:10.1177/030913338400800404.

McLennan, S. M., et al. (2005), Provenance and diagenesis of the evaporite-bearing Burns formation, Meridiani Planum, Mars, *Earth Planet. Sci. Lett.*, *240*, 95–121, doi:10.1016/j.epsl.2005.09.041.

Meierding, T. C. (1981), Marble tombstone weathering rates: A transect of the United States, *Phys. Geogr.*, *2*, 1–18.

Meybeck, M. (1987), Global chemical weathering of surficial rocks estimated from river dissolved loads, *Am. J. Sci.*, *287*, 401–428.

Morris, K. A., and C. M. Shepperd (1982), The role of clay minerals in influencing porosity and permeability characteristics in the Bridport Sands of Wytch Farm, Dorset, *Clay Miner.*, *17*, 41–54, doi:10.1180/claymin.1982.017.1.05.

Mottershead, D., A. Gorbushina, G. Lucas, and J. Wright (2003), The influence of marine salts, aspect and microbes in the weathering of sandstone in two historic structures, *Building Environ.*, *38*, 1193–1204, doi:10.1016/S0360-1323(03)00071-4.

Mustoe, G. E. (1982), The origin of honeycomb weathering, *Geol. Soc. Am. Bull.*, *93*, 108–115, doi:10.1130/0016-7606(1982)93<108:TOOHW>2.0.CO;2.

Paradise, T. R. (2002), Sandstone weathering and aspect in Petra, Jordan, *Z. Geomorphol.*, *46*, 1–17.

Pentecost, A. (1991), The weathering rates of some sandstone cliffs, central Weald, England, *Earth Surf. Processes Landforms*, *16*, 83–91, doi:10.1002/esp.3290160109.

Pope, G. A., T. C. Meierding, and T. R. Paradise (2002), Geomorphology's role in the study of the weathering of cultural stone, *Geomorphology*, *47*, 211–225, doi:10.1016/S0169-555X(02)00098-3.

Poulet, F., et al. (2005), Phyllosilicates on Mars and implications for early Martian climate, *Nature*, *438*, 623–627, doi:10.1038/nature04274.

Pye, K., and D. N. Mottershead (1995), Honeycomb weathering of Carboniferous sandstone in a sea wall at Weston-super-Mare, UK, *Q. J. Eng. Geol.*, *28*, 333–347, doi:10.1144/GSL.QJEGH.1995.028.P4.03.

Robinson, E. S. (1970), Mechanical disintegration of the Navajo sandstone in Zion Canyon, Utah, *Geol. Soc. Am. Bull.*, *81*, 2799–2806, doi:10.1130/0016-7606(1970)81[2799:MDOTNS]2.0.CO;2.

Robinson, D. A., and D. A. Williams (1994), Sandstone weathering and landforms in Britain and Europe, in *Weathering and Landform Evolution*, edited by D. A. Robinson and R. B. G. Williams, pp. 371–391, John Wiley, Chichester, UK.

Rodríguez-Navarro, C., and E. Doehne (1999), Salt weathering: Influence of evaporation rate, supersaturation and crystallization pattern, *Earth Surf. Processes Landforms*, *24*, 191–209, doi:10.1002/(SICI)1096-9837(199903)24:3<191::AID-ESP942>3.0.CO;2-G.

Rodríguez-Navarro, C., E. Hansen, E. Sebastián Pardo, and W. S. Ginell (1997), The role of clays in the decay of ancient Egyptian limestone sculptures, *J. Am. Inst. Conserv.*, *36*, 151–163, doi:10.2307/3179829.

Rodríguez Navarro, C., E. Sebastián, E. Dohene, and W. S. Ginell (1998), The role of sepiolite-palygorskite in the decay of ancient Egyptian limestone sculptures, *Clays Clay Miner.*, *46*, 414–422, doi:10.1346/CCMN.1998.0460405.

Sancho, C., and G. Benito (1990), Factors controlling tafoni weathering in the Ebro Basin (NE Spain), *Z. Geomorphol.*, *34*, 165–177.

Scherer, G. W. (2000), Stress from crystallization of salt in pores, in *Proceedings of the* 9th *International Congress on Deterioration and Conservation of Stone*, edited by V. Fassina, pp. 187–194, Elsevier Sci., Amsterdam.

Scherer, G. W. (2004), Measuring permeability of rigid materials by a beam-bending method: part IV. Transversely isotropic plate, *J. Am. Ceram. Soc.*, *87*, 1517–1524.

Scherer, G. W. (2006), Internal stress and cracking in stone and masonry, in *Measuring, Monitoring and Modeling Concrete Properties*, edited by M. S. Konsta-Gdoutos, pp. 633–641, Springer, Dordrecht, Netherlands.

Scherer, G. W., and I. Jiménez González (2005), Characterization of swelling in clay-bearing stone, in *Stone Decay in the Architectural Environment*, *Geol. Soc. Am. Spec. Pap.*, vol. 390, edited by A. V. Turkington, pp. 51–61, Geol. Soc. of Am., Boulder, Colo.

Sebastian, E., G. Cultrone, D. Benavente, C. Rodríguez Navarro, and L. Linares (2007), Swelling damage in clay-rich sandstones used in Architectural Heritage, *J. Cult. Herit.*, *9*, 66–76.

Selby, M. J. (1993), *Hillslope Materials and Processes*, 2nd ed., 451 pp., Oxford Univ. Press, Oxford, UK.

Smith, B. J., and J. P. McGreevy (1988), Contour scaling of sandstone by salt weathering under simulated hot desert conditions, *Earth Surf. Processes Landforms*, *13*, 697–705, doi:10.1002/esp.3290130804.

Smith, B. J., R. W. Magee, and W. B. Whalley (1994), Breakdown patterns of quartz sandstone in a polluted urban environment, Belfast, Northern Ireland, in *Rock Weathering and Landform Evolution*, edited by D. A. Robinson and R. B. G. Williams, pp. 131–150, John Wiley, Chichester, UK.

Snethlage, R., and E. Wendler (1991), Surfactants and adherent silicon resins—New protective agents for natural stone, *Mater. Res. Soc. Symp. Proc.*, *185*, 193–200.

Snethlage, R., and E. Wendler (1997), Moisture cycles and sandstone degradation, in *Saving Our Architectural Heritage: The Conservation of Historic Stone Structures*, edited by N. S. Baer and R. Snethlage, pp. 7–24, John Wiley, London.

Squyres, S. W., et al. (2006), Two years at Meridiani Planum: Results from the Opportunity Rover, *Science*, *313*, 1403–1407, doi:10.1126/science.1130890.

Tallman, S. L. (1949), Sandstone types: Their abundance and cementing agents, *J. Geol.*, *57*, 582–591.

Timoshenko, S. (1925), Analysis of bimetal thermostats, *J. Opt. Soc. Am.*, *11*, 233–255.

Trenhaile, A. S. (1987), *The Geomorphology of Rock Coasts*, 384 pp., Clarendon, Oxford, UK.

Tucker, M. E. (1991), *Sedimentary Petrology: An Introduction to the Origin of Sedimentary Rocks*, 2nd ed., 260 pp., Blackwell Sci., Oxford, U. K.

Turkington, A. V., and T. R. Paradise (2005), Sandstone weathering: A century of research and innovation, *Geomorphology*, *67*, 229–253, doi:10.1016/j.geomorph.2004.09.028.

Veniale, F., M. Setti, C. Rodríguez-Navarro, and S. Lodola (2001), Role of clay constituents in stone decay processes, *Mater. Constr.*, *51*, 163–182.

Vicente, M. A. (1983), Clay mineralogy as the key factor in weathering of 'Arenisca dorada' (Golden sandstone) of Salamanca, Spain, *Clay Miner.*, *18*, 215–217, doi:10.1180/claymin.1983.018.2.11.

Vichit-Vadakan, W. (2002), Measuring permeability, young modulus and stress relaxation by the beam-bending technique, Ph.D. Dissertation, Princeton Univ. Princeton, N. J.

Vichit-Vadakan, W., and G. W. Scherer (2000), Measuring permeability of rigid materials by a beam-bending method: part II. Porous glass, *J. Am. Ceram. Soc.*, *83*, 2240–2245.

Vichit-Vadakan, W., and G. W. Scherer (2002), Measuring permeability of rigid materials by a beam-bending method: part III. Cement paste, *J. Am. Ceram. Soc.*, *85*, 1537–1544.

von Engeln, O. D. (1942), *Geomorphology: Systematic and Regional*, 655 pp., Macmillan, New York.

Wangler, T. P., A. K. Wylykanowitz, and G. W. Scherer (2006), Controlling stress from swelling clay, in *Measuring, Monitoring and Modeling Concrete Properties*, edited by M. S. Konsta-Gdoutos, pp. 703–708, Springer, Dordrecht, Netherlands.

Warke, P. A., and B. J. Smith (1998), Effects of direct and indirect heating on the validity of rock weathering simulation studies and durability tests, *Geomorphology*, *22*, 347–357, doi:10.1016/S0169-555X(97)00078-0.

Wendler, E., D. D. Klemm, and R. Snethlage (1991), Consolidation and hydrohobic treatment of natural stone, in *Durability of Building Materials and Components: Proceedings of the 5th International Conference*, edited by J. M. Baker et al., pp. 203–212, Chapman and Hall, London.

Wendler, E., A. E. Charola, and B. Fitzner (1996), Easter Island tuff: Laboratory studies for its consolidation, in *Proceedings of the 8th International Congress on Deterioration and Conservation of Stone*, edited by J. Riederer, pp. 1159–1170, Elsevier Sci., Berlin.

Williams, R., and D. Robinson (1989), Origin and distribution of polygonal cracking of rock surfaces, *Geogr. Ann. Ser. A*, *71*, 145–151, doi:10.2307/521386.

Wilson, M. J. (1987), *A Handbook of Determinative Methods in Clay Mineralogy*, 308 pp., Chapman and Hall, New York.

Winkler, E. M. (1997), *Stone in Architecture: Properties, Durability*, 3rd ed., 313 pp., Springer-Verlag, Berlin.

Wust, R. A. J., and J. McLane (2000), Rock deterioration in the royal tomb of Seti I, Valley of the Kings, Luxor, Egypt, *Eng. Geol.*, *58*, 163–190, doi:10.1016/S0013-7952(00)00057-0.

Yatsu, E. (1988), *The Nature of Weathering: An Introduction*, 624 pp., Sozosha, Tokyo.

Young, A. R. (1987), Salt as an agent in the development of cavernous weathering, *Geology*, *15*, 962–966, doi:10.1130/0091-7613(1987)15<962:SAAAIT>2.0.CO;2.

I. J. González, University of Granada, Fuentenueva s/n, 18002 Granada, Spain. (inmajimenez@ugr.es)

C. Rodríguez-Navarro, Department of Mineralogy and Petrology, University of Granada, Fuentenueva s/n, 18002 Granada, Spain. (carlosrn@ugr.es)

G. W. Scherer, Princeton Institute for the Science and Technology of Materials, Department of Civil and Environmental Engineering, Princeton University, 321 Bowen Hall, 70 Prospect Avenue, Princeton, NJ 08540, USA. (scherer@princeton.edu)

Anexo 7. Publicación nº.6

"Factors Affecting Portland Brownstone Durability – a Review"

Jiménez González, I.; Flatt, R.J. and Scherer, G.W.

(Enviado para su publicación, en periodo de revisión)

FACTORS AFFECTING PORTLAND BROWNSTONE DURABILITY – A REVIEW.

Inmaculada Jiménez González[1], Robert J. Flatt[2], and George W. Scherer[3]

[1] *University of Granada, Spain;*
[2]*Sika Technology AG. Switzerland*
[3]*Princeton University, Dept of Civil & Env. Eng/ Princeton Materials Institute, Eng. Quad. E-319, Princeton, NJ 08544 USA*

ABSTRACT

Portland brownstone was the *star* building material during the Brownstone Boom that happened in the USA during the 1850-80 decades. It has been largely used mainly in the northeastern USA since the second half of the 17th century, principally as a veneer stone for civil and religious building facades. Reviewing the literature about this stone, it is common to find statements about the poor durability of Portland Brownstone. The available information mostly refers to causes of decay of sandstones or of *brownstones* in general. This paper attempts to contribute to the knowledge of this particular sandstone by presenting a review of what is known about Portland Brownstone, both from field observation and laboratory studies. We review situations in which Portland Brownstone was most used and the types of degradation that are reported. In the first part, we remain very descriptive and the information given about decay remains largely at the macroscopic scale of visual observation on site. We then discuss a proposed sequence of events in the degradation of Portland Brownstone, which leads us into a more detailed description of the main degradation mechanisms. Finally, we attempt to highlight which material properties of Portland Brownstone make this stone more or less susceptible to those mechanisms, which would lead to faster or slower degradation on site and therefore are worth characterizing.

Key words: Brownstone, clays, swelling, wetting/drying cycles, stone degradation,

TABLE OF CONTENTS

1 INTRODUCTION

Portland brownstone has been used in the northeastern USA (mainly around Connecticut, Boston, New York and Philadelphia) since the second half of the 17th century, when the Portland Quarries of Connecticut (MA) started extracting the stone[1] (Mckee 1973-in Matero and Teutonico 1982, Merrill 1887). It came to be so much requested as a building material that soon its use extended far away to places such as Milwaukee and San Francisco (Merrill 1887) or across the border to Canada. Building with it reached the maximum popularity from 1850 into the 1880s. During that period up to 1500 men were working in the quarries [considered among the oldest and largest of the country, according to Crosby and Loughlin (1904)]. The stone production was so big that a fleet of 25 ships was used to transport it down the Connecticut River, according to Merrill (1887).

Due to its intrinsic properties, Portland brownstone is not the most suitable stone for carvings exposed to the elements (Merrill 1890) and, although one can find many figurative ornaments or sculptures, this stone has been chiefly used for veneering facades of civil and religious buildings, as well as in monuments.

When reviewing the literature about Portland brownstone conservation, one can find such statements as: …*the stone weathers in layers and ends up looking like a clumsily peeled onion* (Burns 1999) or…*you can take your hand and pull off chunks as big as apple pies*… (Rozhon 2000). This last particular case refers to the state of conservation of the cathedral of the Immaculate Conception in Albany (New York). This question of the poor durability of the

[1] It seems that Portland Brownstone beds were extensively outcropping and therefore obtaining stone from them was relatively easy and free of any cost. This practice *assumed such proportions as early as 1665* that at that time it was decided to start paying to get it (Merrill, 1887).

brownstone buildings is something that authors have referred to from an early date (Julien 1883a and Merrill 1891- in Meierding 2000; Loughlin 1903), some of them rather dramatically[2].

In contrast, one can also find more positive statements about Portland Brownstone durability. For example, Crosby and Loughlin (1904) consider that Portland Brownstone *is reasonably strong for sandstone, being fully up to the average, so those instances of crushing, cracking and transverse fracture or shearing due to overloading are rather infrequent and that it is not subject to chemical deterioration or detrimental change of color*. Merrill (1890) also wants to play down criticism about Portland Brownstone durability by saying that: *no stone that is capable of absorbing so large a percentage of water as is much of the Connecticut and other of our Triassic stones, can be more than very moderately durable in the very trying climate of our Northern States.* Nevertheless, today the general consensus is that Portland Brownstone does not weather well. This has led to many repairs and treatments applied to decayed buildings, many of which have been unsatisfactory. As a consequence, the *New York Landmarks Conservancy* decided to conduct the *Sandstone Restoration Study* in 1982[3] in response to this problem in New York City. This triggered greater demand for this stone in restoration projects[4] to such an extent that the Portland Brownstone Quarries in Connecticut were reopened around 1992, after having been closed since 1930 (Hart 2001). These quarries are recognized as an American National Historic Landmark since May 2000 (Larson 2000).

Unfortunately, this growth in the use of Portland Brownstone in restoration has not been paralleled by an increased knowledge of the causes that lead to its degradation and of the means

---

[2] *Several of the fronts along Fifth Avenue, some of them less than ten years old, already look frightful to the experienced eye of an honest stonecutte*r (unknown author from the N. York Tribune, 1869).

[3] Due to the current interest of conserving Brownstone buildings, the same Institution has published in 2002 the *Brownstone Guide: Maintenance & Repair Facts for Historic Property Owners.*

[4] As is the case of the Osborne Apartments and the Cooper Union for the Advancement of Science and Art Foundation Building in NYC or the Chapel at Gallaudet University (Washington D.C.). In this last building twenty tons of Portland Brownstone blocks replaced disintegrated stone (Guinness 2002).

by which to mitigate them. The available information mostly refers to causes of decay of sandstones or of *brownstones* in general. Prescriptions in the USA are to some extent based on results of studies on the deterioration of European ferruginous sandstones with the same type of cement (iron oxide rich) as brownstones (Roblee 1998).

This paper attempts to partially remedy this problem by presenting a review of what is known about Portland Brownstone, both from field observation and laboratory studies. More specifically, we attempt to highlight, from a materials science perspective, how the basic understanding of decay mechanisms needs to be taken a step further to meet concerns of field practitioners about durability prediction. At the same time, we also try to highlight which material properties are really the ones that control degradation and are worth characterizing. We do not go into the details of more basic research work aimed at preventing degradation mechanisms from occurring, as for example the application of surface treatments that should cancel crystallization pressures (Scherer et al. 2001, Houck and Scherer 2006). By adopting this form of presentation, we hope to draw the attention of both conservators and scientists to what we see as the main challenges remaining to achieve durability prediction.

While preparing this review, we were confronted by a rather loose use of nomenclature for designating what we refer to as “Portland Brownstone”: an arkosic sandstone with characteristic brown-red color that belongs to the uppermost Portland Formation unit and that is mainly obtained from the Portland Brownstone quarries, along the east bank of the Connecticut River (Olsen et al. 2005).

A first issue that readers should be aware of is the change in denomination of the geological period that this stone comes from. Sources seem to indicate that this occurred around the 1990’s. As a result, literature prior to that date defines this stone as being from the Triassic (Merrill 1887, Crosby and Loughlin 1904, Ries 1912, Krynine 1950, Matthias 1967) or Upper Triassic period (Matero and Teutonico 1982). On the other hand, literature after this date indicates it is from

Early Jurassic (Hubert et al. 1992, Guinnes, 2003, Olsen et al. 2005 and Powell 2005) or Early to Middle Jurassic (Meierding 2000).

The other main source of confusion is the rather loose use of terminology that has been common ever since the advent of Portland Brownstone as a building material. We found terms such as *brownstone, brown stone, brown-stone, brown sandstone, ordinary brownstone,* etc. that might overlap with what we designate as Portland Brownstone. However, those other designations could also refer more generally to any sandstone of brown color, as seems to be the case of the term **brownstone** (Ries 1912). On the other hand, other terminology such as ***Brown freestone, Connecticut stone*** *and* ***Portland arkose brownstone*** appear to refer more specifically to Portland brownstone[5].

As can be seen, the terminology used throughout the centuries has been quite ambiguous. However, confusion does not end here, since according to Ries (1912) one also finds sources that classify sandstones only according to their geographical provenance. Thus, not only the Portland-type and other brown-colored stones coming from other eastern states are considered *brownstones*, but also stones that <u>are not brown</u> but are found in the same Jurassic (Triassic in text) formation of the Connecticut Valley. In preparing this paper, we have been particularly careful to select only information that appeared to be clearly related to Portland Brownstone from the different characteristics provided by the authors, excluding those works that appeared to us to be mixing terminologies such that we could not be sure of their real origin. On the occasions where we use the term brownstone alone, we are placing ourselves in the general context referring to any of those famous brown sandstones used for decades in New York City.

[5] Two other terms that seem to refer to Portland Brownstone are: Connecticut sandstone (lithological term) and Connecticut Freestone (stone-cutters denomination) according to Knight (1895); Triassic or New Red sandstone (geological denomination) according to Merrill (1888)

Given these specifications, we proceed throughout the paper with the terminology of "Portland Brownstone" as a stone of brown color from the Early Jurassic period of the Portland formation.

In reviewing the available literature, it was difficult to find studies dedicated to the durability of Portland Brownstone, particularly ones with a sufficient grade of detail and quantification. Matthias in 1967 refers to the rate of face recession of 66 Portland arkose tombstones in Middletown, CT, found to be 1.1 mm/100 years. Meierding (2000) observed on brownstone tombstones that surfaces and inscriptions appeared fresh (little granular weathering) until large portions of the face fall off as layers larger than 3 mm thick. This type of degradation is referred to as contour scaling. It probably accounts for the fact that previously very few quantitative surface recession rate measurements on sandstone monuments have been reported. It highlights a problem of durability that studies often mention but never quantify, which is the non-linearity of degradation processes. This problem is highlighted in the following hypothetical example. Imagine one compares two stones. The first degrades by contour scaling, so that it may appear as rather unaltered until that stone suddenly loses a whole part of its surface. During that time, it may be diagnosed as altering much less than another stone that might have a constant recession rate, but which over a long period of time would lose less material than the first stone.

Bearing this in mind and having a better definition of what we understand by Portland Brownstone, we proceed to the next section where we present an overview of this stone and descriptive reports about its durability.

2 PORTLAND BROWNSTONE USE AND DURABILITY

In this section, we review situations in which Portland Brownstone was most used and the types of degradation that are reported. At this stage, we remain very descriptive and keep

information about decay largely at the macroscopic scale of visual observation on site. The last part of this section outlines a proposed sequence of events in the degradation of Portland Brownstone. It leads to a more detailed description of the main degradation mechanisms presented in section 3. Based on this, we highlight in section 4 the material properties of Portland Brownstone that can alter the rate and extent of the type of degradation seen on site.

2.1 The *Brown decades* Architecture

Portland Brownstone was the first sandstone quarried in the USA and obtaining it was cheap and relatively easy (Bell 1985). These reasons, together with the ease of shipping via river and train, made it very popular for use in facings and trims of buildings. Later, it was used in religious architecture and began to be a symbol of luxury and sophistication when used in residential buildings. Its use became fashionable when, in the late 1840's, America adopted the Gothic Revival style, expressing a romantic interest to bring aspects of nature into urban life by using the brown color of this material to evoke *the soils, rocks, wood and the bark of tress* (Downing 1850- in Matero and Teutonico 1982).

From the second half of the 19th century to the early 20th century brownstones reached great popularity. The Tenth Census of the U.S. (1880) determined that about 90% of the stone buildings in New York City were made of sandstones, and that close to 80% were brownstone (particularly in Brooklyn, 96% of the brownstone buildings used the Connecticut Brownstone).

Many buildings used to have a Portland brownstone veneer covering their brick walls, or a front of about 8 to 15 cm thick as indicated in Figure 2-1 (Lockwood 2005, Berry 2002, Cole 2004). Monuments, outdoor sculptures (e.g. Newport Church), decorative reliefs (e.g. Victoria Mansion, Manhattan houses), gravestones, and over 50,000 row houses (Rozhon 2000) were built with brownstones in many east coast cities of the USA, especially in New York City, where the

Brown Decades architecture (Mumford 1955) had its boom. Good examples can still be seen in Manhattan, Queens and Brooklyn boroughs in New York City.

Figure 2-1 Picture of a Portland Brownstone front at St. Mary's showing the masonry wall behind the stone façade (Picture provided by Ivan Myer)

By the end of the 19th century, brownstones were less requested as a building material due not only to the general change in Victorian tastes towards the use of more clear stones such as Indiana limestone (Smock 1890 and Volney Lewis 1908), but also due to the early decay suffered by facings and structures built with that stone. Later, around the 1920's, brownstone stopped being used as a material building and all quarries were closed by the 1930s.

2.2 Some examples of important buildings in Portland Brownstone

Among the buildings made of Portland Brownstone, the ***Cooper Union for the Advancement of Science and Art Foundation Building*** must be mentioned as one of the most important examples. Frederick A. Peterson designed it in 1858 for the city of New York (Figure 2-2).

Figure 2-2. Cooper Union for the Advancement of Science and Art Foundation Building (1858) after restoration

During the century and a half since its construction, this building suffered from all types of alterations and, in recent decades, the lack of maintenance developed into substantial stone damage. Conservators identified this as delamination, spalling and exfoliation of exterior masonry elements, such as pilasters, arches, bases, capitals, and decorative carved stones. As a result of the extent of degradation, a massive restoration program for the exterior building was concluded in 2001.

With respect to the origin of this degradation, Hart (2001) has underlined the presence of swelling of clays and the orientation of stone blocks as the main causes. Portland brownstone blocks were *face-bedded* (Figure 4-6b) in the façades, following the common 19th century aesthetic principle (Hart 2001). This orientation leads to worse durability than natural bedding and although some sources indicate this was already known at the time (Julien 1883a, Merrill 1890), esthetical, technical and economical considerations prevailed (see section 2.3). During the building restoration, the report of the Platt Byard Dowell Architects (2002) mentions how the entire ashlar on the north portico had to be replaced with new brownstone as a result of the extensive deterioration (exfoliations up to around 5 cm) suffered. Furthermore, the south portico was disassembled and reassembled using a combination of original and new stones. Some stone elements of this portico were covered by so much stucco during former interventions that they have had to be removed and the whole replaced.

This practice of replacing original stone is rather common in building restoration/preservation in the USA. In some cases, it is even done using new stone that does not correspond geologically to the original one. This was the case for the Cathedral of the Immaculate Conception in Albany (New York) built between 1848-52. For its restoration it was decided not to use Portland Brownstone, but sandstones from the Ruhr valley in Germany and southern Scotland that, according to architects and conservators, are more durable than Portland Brownstone. This was not the case for the restoration of the Cooper Union, since the new stone came from an original quarry that fortunately reopened before this major project started (Hart 2000). Overall, more than 85 cubic meters (3000 cubic feet) of new stone were used in the restoration of the Cooper Union Building.

In regard to this building, it should be noted that deterioration had been enhanced to some extent by inappropriate restoration/conservation decisions made during the 1950-60s. Indeed, it had then been decided to *remove anything that might spall* from the building façade. To achieve

this, the whole Portland brownstone front was jack-hammered. As a consequence of this intervention, it is reported that water ingress was increased (Hart 2001), probably as a result of the formation of cracks and/or microcracks that would also have weakened the surface. During the restoration completed in 2001, all these surfaces were smoothed down as much as possible (Figure 2-3).

Figure 2-3 Portland Brownstone jack-hammered surface of the Cooper Union for the Advancement of Science and Art Foundation Building (picture provided by Ivan Myer)

Another example of a Portland Brownstone building is the ***Morse-Libby House*** also known as ***Victoria Mansion, a*** National Historic Landmark in Portland (Maine). It was built in 1858-60 by Henry Austin. Further general information can be found at (www.victoriamansion.org) and (www.aroundmaine.com/04/victoria/default.asp)

It has been studied for 30 years, but despite this long history of survey, there is little published detailed information available about its degradation. The information we were able to obtain

regarding this was communicated by Myjer (2005)[6]. He has indicated that the observed damage can be categorized as:

- Blind and visible exfoliations of face bedded blocks (see Figure 4-6, case B for corresponding orientation). Myjer states this *may be* related to case hardening of the exposed surface.
- Separation of bedding planes in naturally bedded blocks (see Figure 4-6, case C for corresponding orientation).
- Contour scaling, mainly of the naturally bedded blocks and to a lesser extent on face bedded and end bedded stones (see Figure 4-6 for corresponding orientation).
- Granular disintegration of naturally bedded blocks that project from the building line and are frequently wetted. Myjer indicates that, unlike in calcareous stones, granular disintegration of brownstones is not related to a loss of binder.

These alteration patterns occur in most monuments and buildings made of Portland Brownstone. These include St. Mary's Church in Newport (Rhode Island, NY) whose sculptures are extensively deteriorated (Ivan Myjer, personal communication); the Immaculate Conception Cathedral in Albany (NY); St. Peter and Paul Cathedral in Providence (Rhode Island, NY) and the Cathedral of the Holy Cross (Boston, MA). All were built by Patrick Charles Keely, the most prolific church architect in the country during the second half of the 1800s and who used Portland Brownstone in many of his projects (www.keelysociety.com). Other important Portland Brownstone buildings are the Ascension Church and the Osborne Apartments, both in New York City. The Ascension Church, designed by Richard Upjohn in 1841 is a typical case where blocks of Portland Brownstone can be found in all orientations. As a result, this building shows quite

[6] Ivan Myer is a leading consultant to stone preservation projects. Prior to establishing his own firm he was Director of the Conservation Center of the Society for the Preservation of New England Antiquities (now Historic New England) from 1994-1997, and from 1991 to 1994 was Director of Restoration for the Cathedral of St. John the Divine in New York City.

different types of degradation patterns for reasons discussed later. As to the Osborne Apartments, they date back to 1885 and their exterior was designated a landmark in 1991. The flooding of the roof caused serious degradation of the stone in the top levels and led to the need for extensive stone replacement (Roblee 1998, Gray 1994).

To give a broader sense of the importance of Portland Brownstone in North East USA, we also mention, but without further description, other buildings made of this stone (Guinness 2002, 2003; Julien 1883a, Matero and Teutonico 1982, Ries 1912 and Roblee 1998):

- Italianate-style row houses built during 1820-90 along the northeast coast (some of which can still be seen in historical districts of NYC, such as Brooklyn)
- The Ascension Church (1841), NYC (NY)
- Part of the Astor Library (1853-81), NYC (NY)
- The entrance portal of Castle Clinton (1808-11), Battery Park, NYC (NY)
- Academy of Design, in Brooklyn, NYC (NY)
- Lowe stories of Waldorf-Astoria Hotel, in NYC (NY)
- Trinity Church, in Boston (MA)
- The Union Institute for Savings, in Boston (MA)
- Church of the Messiah (and Chapel), in Boston (MA)
- Harvard Church, Boston (MA)
- Roger Building at MIT, Cambridge (MA)
- Boston Society of Natural History, Boston (MA)
- Wesleyan University Buildings, in Middletown (CT)
- The Aetna Life and Casualty Building, Hartford (CT)

- Yale's Sterling Memorial Library, New Haven (CT)
- Library and Stock Building, Princeton University, Princeton (NJ)
- The Chapel at Gallaudet University, Washington D.C.
- James Flood Mansion (today the Pacific Union Club) (1880s), Nob Hill, San Francisco (CA)
- Parliament Building, Toronto (Canada)

2.3 Patterns of Portland Brownstone alteration and degradation

Before entering the discussion about the patterns of degradation most commonly seen on Portland Brownstone, two important points must be mentioned. The first one is that Portland Brownstone shows rather poor durability that is especially noticeable when it is used for decorative ornaments. The second is that, at the time most buildings of Portland Brownstone were constructed, it was customary to place the striated stones in the face-bedded orientation (Figure 4-6b). The reasons for this choice are both aesthetic and technical. Aesthetically, face bedded blocks expose a uniform surface on the façades, which was preferred. Technically, quarrying to produce blocks with their shortest direction perpendicular to bedding planes was easier, faster, more economical and less wasteful (Bell 1985; Rude 2000*)*. The same is true for the face-bedding placement of such blocks on façades (Rozhon 2000).

Unfortunately, this orientation also allows faster capillary rise of ground water, enhancing accumulation of water and salts. It is also the orientation in which the stone has the lowest mechanical resistance to support the weight above it. As a result, it is the worst orientation in which the stone can be placed for durability purposes. Evidence that this was known early on can be found in several sources (Loughlin 1903; Crosby and Loughlin 1904; Julien 1883a, 1883b;

Egleston 1887; Unknown author 1890; Hopkins 1897 and Smock 1890- both in Weiss et al. 1982). In an 1869 article in the New York Tribune, an unknown author emphasizes the generally bad weathering of the brownstone and mentions the crumbling of the lintels of the houses in some older streets of New York City, stating that: *it does not make very great difference whether the stone is laid parallel or perpendicular to its grain. In the former case, its destruction is more rapid. In the latter, rottenness, soon appears in the lintels, columns, cornices and other projecting portions of the edifices.*

An interesting approach to studying decay of Portland Brownstone is due to Meierding (2000). He chose to examine the state of conservation of tombstones made of Portland Brownstone, arguing that it is a simplified situation in that only one block at a time is involved. Furthermore, virtually all the tombstones he examined were cut such that the bedding planes were vertical, which is consistent with the widely used face bedding orientation used in buildings of the *Brown decades*. In this study, he observed various manifestations of alteration and degradation and proposed a general scheme of deterioration that brownstone seems to follow. Few other studies present this degree of detail, so little discussion of the proposed scheme could be found. Questions arise however, about the mechanisms proposed by the author to explain the observed scheme. While these questions do not alter the value of Meierding's observations, they imply that some care must be taken in using his conclusions to devise conservation measures or interventions. With this in mind, we now present at some length the proposed scheme of alteration.

Meierding (2000) distinguishes four steps in the deterioration process of Brownstone: case hardening, formation of face-parallel cracks, contour scaling and interior weathering of stone. He states that each of these could have a different causative environmental and weathering mechanism.

A case-hardened surface is said to exist in the outer layers of brownstones and is attributed to a process of dissolution-precipitation in which dissolved minerals can be reprecipitated as secondary minerals at the stone surface during drying events (Winkler 1997). This is an extension of a process known to occur with limestones and which is attributed mainly to the high solubility of calcite. In the case of sandstones, it is claimed that silica can be leached from clays and precipitate as amorphous silica, modifying porosity, permeability, strength and stiffness of the surface layers (Robinson and Williams 1987, Smith et al. 1994, Winkler 1975, 1979– in Meierding 2000). It is also worth pointing out that Viles and Goudie (2004) found that case hardening does not require microorganisms, contrary to some statements on this subject.

Concerning Portland Brownstone, Meierding (2000) found no differences in the mineralogical composition of the cementing phase between the case hardened layer and the inner part of the stone after analyzing samples by SEM and optical microscope. Indeed it is unlikely that there is any significant amount of soluble material in a typical brownstone and Meierding concludes that deposition of dissolved ions is most likely not the main cause for the formation of this hardened layer in Brownstones.

Meierding's assessment of the case hardening of stone exposed to the elements is rather qualitative. He seems to use the hardness of the stone that gets exposed once a layer of case hardened material falls off as reference for the hardness of the unaltered material. This may be misleading because the alteration process may weaken the freshly exposed stone surface before the external layer detaches. Thus, it is not certain that the detached layer is indeed harder than the unweathered stone.

However, whether hardening of the exterior layer or weakening below the surface constitutes the first stage does not alter the importance of Meierding's observations concerning the subsequent progress of damage. Indeed, he indicates that this then develops (continues) by the occasional formation of face-parallel cracks at the interface between the outer crust and weak

inner region. He further states that this is sometimes followed by contour scaling and weathering of the stone interior (Meierding 2000). As will be explained in section 5, this could result from the combination of freezing or salt crystallization, which causes damage at some distance below the surface, and the swelling of clays extending that damage by propagating defects parallel to the surface.

In relation to stones on buildings, the most frequently quoted alterations and/or patterns of degradation observed in Portland Brownstone are delaminations (Figure 2-4a), contour scaling also termed spalling or exfoliation by some authors (Figure 2-4b), and granular disintegration. Guinness (2002) who presents the point of view of the Society for the Preservation of New England Antiquities (SPNEA) shows a more synthetic picture about Brownstone degradation consisting of: weathering down (the loss of detail), spalling (loss of coherence), and crumbling (the loss of stability). For a more descriptive definition of these alteration/degradation patterns at the macroscopic level, multiple sources can be consulted (Alcalde y Martín 1990; Arnold et al. 1980; ASTM C 119-74; ASTM D 653-78; Delgado Rodrigues 1991; NORMAL 1-88; Ordaz and Esbert 1988).

a) b)

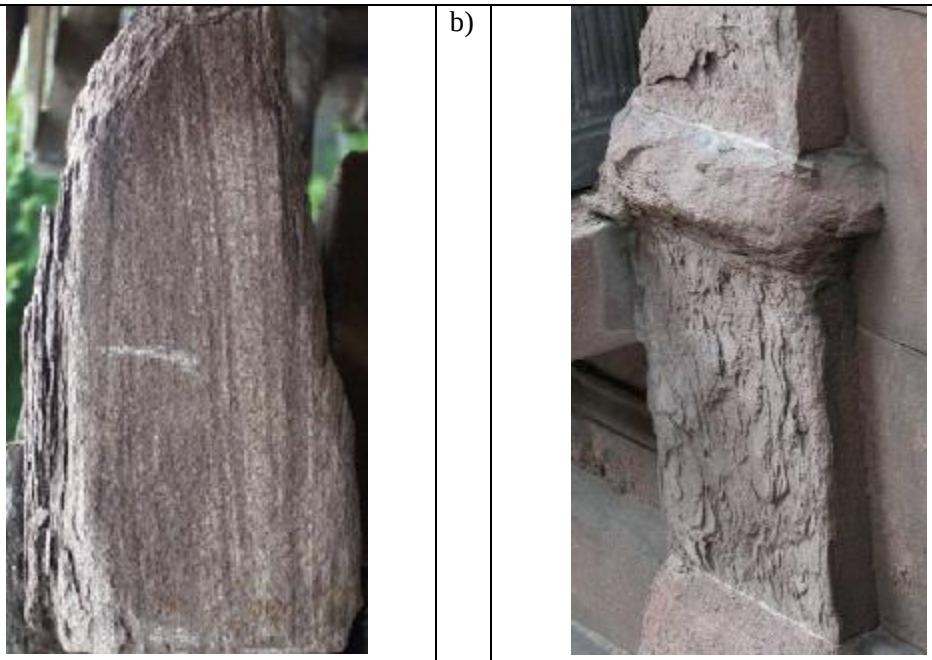

Figure 2-4. Example of some deterioration patterns shown by Portland Brownstone: a) delamination (exfoliation), b) contour scaling,

2.4 Seasoning and/or drying of Portland Brownstone

In Meierding's scheme of alteration, case hardening is indicated as a step in degradation. In contrast, a similar process referred to as *seasoning* is said to be beneficial for durability (Winkler 1997). The term seasoning is used to describe a period of time during which stones are left to age (alter, dry) after having been quarried and before they are used. Winkler indicates that during this time, the surface hardens and that this is a fact well known to sculptors and architects. He further states that the same practice was used nearly 2000 years ago by Vitruvius. In reality, what Vitruvius refers to is something quite different from allowing the stone surface to harden in order to obtain better properties. It is rather a period during which stones are allowed to weather and at the end of which the ones that resisted best are selected. This is clearly indicated in the following translation of an extract from his 2nd book on architecture: **"***Two years before the commencement*

of the building, the stones should be extracted from the quarries in the summer season; by no means in the winter; and they should then be exposed to the vicissitudes and action of the weather. Those which, after two years' exposure, are injured by the weather may be used in the foundations; but those which continue sound after this ordeal, will endure in the parts above ground" (Thayer 2006).

The benefit resulting from Vitruvius' selection procedure was recognized in the Brown decades. This was also the case in England during the construction of St. Paul's Cathedral (London) for which stones were previously seasoned, laying them on the sea beach for three years, is often mentioned (Julien 1983, 1990; Hawes 1885). Furthermore, the good state of conservation of that cathedral implied that such a procedure would also be beneficial to brownstones. However, at the same time, there is a clear drift in the literature from seeing seasoning as a selection procedure to seeing it as a way to improve stone properties by mineral deposition (Julien 1883b, 1990; Unknown author 1890; Merrill 1887, Hopkins 1897-in Weiss et al. 1982). Even if that might have been true for St-Paul's limestone, it is much less likely to be the case for Portland Brownstone that does not contain a significant quantity of soluble species. So, unless its clays are mobile, or the quarry water is rich in salts, surface hardening from mineral deposition is not expected for Portland Brownstone. However, it could be a result of drying since, as detailed in section 5, Portland Brownstone is harder dry than wet, as a result of the clays it contains (Jiménez González and Scherer 2004). Thus, there is no need to invoke transport and deposition of dissolved minerals in order to account for a strengthening of the stone surface subsequent to quarrying as reported by Merrill (1891) and Guinness (2002).

Other advantages of drying during seasoning should not be overlooked. It is probably why Merrill (1890) considers that: *a week or 10 days of good drying weather is a sufficient period of seasoning so as to place it* (the stone) *beyond danger from frost.* This issue of freezing was clearly a concern and is manifested in different ways:

1) The freshly quarried stones exposed to freezing are said to damage because of the always present variable amount of "quarry water": *they are, if not actually burst and ruined, at least rendered less tenacious*. (Merrill 1887). This was well recognized by field practitioners (Bayne 1884 in Guinness 2002).

2) Portland Brownstone quarries were not active the whole year around, but only from May to November (Merrill 1887). Allbee 1894-in Guinness 2002) also says that *the stones were not quarried in weather below twenty-two degrees F* (-5.5° C).

3) According to Merrill (1887): *...in many localities it is necessary to flood the quarries with water or cover them with earth, on the approach of cold weather, to prevent serious damage for this cause*.

4) Allbee, 1894 (in Guinness 2002) indicates that the stones are covered with soil for at least several months (about four). This could simply be achieving more controlled drying (i.e., slow drying and under conditions that limit freezing of the stone while it is still saturated).

3 DECAY MECHANISMS

In the previous section, we reviewed the use and typical macroscopic degradation of Portland Brownstone. The observed alterations can result from a number of different mechanisms, the most important of which are outlined in this section. In addition to these mechanisms, a number of additional causes should not be forgotten, which in many cases enhance the rate of the degradation mechanisms we will discuss. According to Amoroso (1995), these include:

- Inadequate choice of stone source (bad quality)
- Harmful means of extraction

- Careless shipment, inappropriate storage
- Bad workmanship
- Inadequate placing
- Inappropriate treatments[7]
- Vandalism

3.1 Salt crystallization

The crystallization of salts has been known for a long time as a cause of the degradation of porous materials (Arnold and Zenhder 1990, Scherer et al. 2001, Winkler 1997). The salts in question can be of endo- or exogeneous source, meaning that they can be present in the quarried stone from the start or that they can have been transported into the stone during its service life. In the later case, this can occur by capillary rise from ground water, which might have been enriched by deicing salts. It can also occur by deposition of aerosols (particularly in marine areas), by leaching from mortar, or by reaction with atmospheric pollutants (particularly in urban environments).

The reasons why the growth of salts inside porous materials can cause damage have been studied for many years. The first studies we are aware of go back to the 1850s and are due to Lavalle (1853). Two of the most important papers on the subject are from Taber (1916) and Correns (1949), who laid the basis of what is now known as crystallization pressure.

Crystallization pressure expresses the desire of a crystal to grow from a supersaturated solution, despite the fact that it encounters resistance from the pore walls. It does not require an

[7] Described by Scherer et al. (2001) as *"Good intentions"* and bad choices

increase in volume. The belief that such a volume increase is needed to cause damage is, however, still present in many minds, and has not changed much since the following statement by Thompson (1862) reported by Evans (1969): "*That solidification of crystalline matter in porous stones, whether that be ice formed by freezing from water, or crystals of salts formed from their solutions, usually produces disintegration – not, as implied in the views commonly accepted on this subject, by expansion of the total volume of the liquid and crystals jointly, producing a fluid pressure in the pores – but, on the contrary, by a tendency of crystals to increase in size when in contact with a liquid tending to deposit the same crystalline substance in the solid state, even where, to do so, they must push out of their way the porous walls of the cavities in which they are contained"*. With respect to that statement, Evans (1969) commented that: *"to this day, all too many writers on rock weathering have ignored these profound conclusions"*.

The confusion about the necessity of needing a volume increase for salt crystallization to cause damage has been enhanced by the work of Mortensen (1933) on sodium sulfate. This salt can be found in different states of hydration, which have rather different molar volumes. Mortensen's statement was that damage comes from the hydration, which increases the salt volume and thereby causes damage. It turns out that a more detailed analysis shows that it is once again a situation of crystallization pressure (Flatt and Scherer 2002) and that the transformation takes place through dissolution and reprecipitation (Rodríguez-Navarro and Doehne 1999).

The main aspects of the current understanding of crystallization pressure, which are pertinent to this paper, are the following:

- For salt crystallization to damage a stone, crystallization must take place inside the porous network. In this case one talks of cryptoflorescence (or subflorescence).
- When crystallization takes place outside the stone (efflorescence), little material damage is expected, although aesthetically this alteration may be disturbing.

- The location of crystallization is influenced by the transport properties of the stone in the specified environment. Where evaporation is faster (e.g., in a sunny and/or windy location), precipitation of salts occurs deeper inside the stone.
- The magnitude of the crystallization pressure increases with supersaturation.
- The magnitude of supersaturation can be increased
    - With fast drying rates (Scherer 2000, Flatt 2002)
    - When salts are trapped in small pores (Scherer 1999)
    - When wet zones become isolated during the stone drying owing to the pore structure (Scherer 2000)
    - When water enters a stone containing an anhydrous phase (e.g., thenardite, a sodium sulfate anhydrate) which can reprecipitate as a higher hydrate (e.g., mirabilite, a sodium sulfate decahydrate) (Flatt and Scherer 2002)
- When subjected to crystallization pressure the stone fails in tension rather than in compression (Scherer 1999)
- The tensile resistance of the stone is linked to the size of the largest defects, provided stresses are exerted on a large enough zone to propagate those defects. If this is the case, the tensile strength is the relevant mechanical property to consider when evaluating a stone's resistance to crystallization pressure.
- When the stresses are exerted over a smaller area (for example during drying, where crystallization pressure is localized near the wet/dry boundary), higher stresses must develop to damage the material. Smaller defects are propagated and the degradation should be much more by powdering than by formation of larger cracks.

- Crystallization pressures could in principle be avoided by a treatment that would change the pore wall surface energy. More specifically such a treatment should render the contact of the salt crystal with the pore wall favorable (Scherer 1999, Houck and Scherer 2006)

From the above, we can state that the resistance of a stone to salt crystallization depends on its strength, pore size and exposure conditions. It is, however, rare to find studies discussing all these factors at once with a clear materials science insight into the problem. The challenge for improving assessments of durability, therefore, is to understand under which conditions sufficient pressures can develop to cause damage, depending on the mechanical properties of the stone and exposure conditions.

3.2 Freezing

From the above statement by Thompson we understand that, as for salt crystallization, freezing damage does not require a volume expansion. This certainly goes against the general ideas about this damage mechanism, but is supported by a rather large body of experiments. For example, it has been shown that liquids that shrink upon freezing can induce stresses analogous to those caused when water freezes (Litvan 1972, Beaudoin and MacInnis 1974).

In the case of water, one also finds many references that discuss the so-called hydraulic pressure. This concept was introduced by Powers for explaining freezing damage to concrete (Powers 1949). In this case the damage is understood to come from ice crystals growing in the pores and pushing yet unfrozen water ahead of the growing crystals. The water viscosity causes a resistance to this displacement, which is the origin of hydraulic pressure. The importance of this mechanism with respect to crystallization pressure depends very much on the rates of cooling (Scherer et al. 2001). More recent analysis suggests that under most circumstances this mechanism is probably not as important as generally believed and that crystallization pressure is

the most likely source of damage (Scherer and Valenza 2005). This is in line with later work by Powers himself who had reached a similar conclusion (Powers and Helmuth 1953).

The thermodynamic analysis of freezing is very similar to the one of salt crystallization, except that undercooling replaces supersaturation as the driving force for growth (Scherer 1999). Consequently the factors that dictate a stone's resistance to freezing are quite similar to those for salt crystallization.

The main difference probably lies in the fact that it is easier to undercool a system over a broad area than to supersaturate it. This means that the defects that freezing can propagate will be larger and the associated damage will be seen at a larger scale (cracking and spalling, rather than powdering). Another important aspect about freezing is linked both to conditions of exposure and water and vapor transport characteristics. Indeed, situations which favor the accumulation of water at some distance below the surface should lead to rather large scale damage from freezing.

3.3 Atmospheric pollution

Atmospheric pollution can cause aesthetic problems as well as true material degradation. In the first case, one would tend to speak of soiling, a process mainly linked to deposit of particulate matter such as dust, soot, etc. The true material degradation triggered by atmospheric pollution comes mainly from acid attack by sulfur dioxide on carbonate stones. This process involves the oxidation, probably through solution, of sulfur dioxide, which leads to the formation of sulfuric acid. In the presence of carbonate minerals, this leads to an acid-base reaction, with the departure of carbon dioxide and the formation of a salt, gypsum ($CaSO_4 \cdot 2H_2O$), when the reacted mineral is calcite.

This acid/base reaction alone can weaken the stone. However, subsequent transport of gypsum through solution and its recrystallization is said to exacerbate this damage due to crystallization pressure. The acid-base reaction will not be of concern to most sandstones, unless their binding

phase is rich in carbonates. In the absence of such reactions, the accumulation of gypsum and associated crystallization pressure is limited to the reaction of sulfur dioxide with carbonate deposits at the stone surface and therefore of much more limited importance.

In summary, a crucial factor in terms of resistance to sulfur dioxide is the stone's content of carbonates. The resistance to recrystallization of gypsum, once it has been formed, is rather more difficult to establish. It is linked to the factors already stated above, but is also very strongly influenced by exposure conditions (Camuffo 1998) which can lead to gypsum accumulation, formation of black crusts by incorporation of particulate deposits, and leaching (Bromblet and Verges-Belmin 1996).

3.4 Swelling clays

Salt crystallization, freezing and atmospheric pollution are mechanisms of degradation that are all quite well documented and have been demonstrated by numerous laboratory studies. This contrasts strongly with the damage assumed to arise in stones containing swelling clays, such as montmorillonites or smectites. In this case, it is assumed that the swelling of clays during wetting or their shrinkage during drying can develop damaging stresses. Apart from stones that exhibit tremendous swelling and which essentially decompose upon wetting (Rodríguez-Navarro et al. 1998), there is little experimental evidence that this mechanism, which is said to be deleterious by fatigue, is of true concern for durability. To the best of our knowledge, only one study clearly establishes the importance of such damage. It is the work of Wendler et al. (1996) who studied stone from Easter Island. They subjected samples of this stone to cycles of wetting and drying and showed that the surface strength, measured by drill resistance, decreased quite substantially during these cycles. Furthermore, they showed that the application of a swelling inhibitor leads to a significant decrease of that damage.

In recent work, we have undertaken systematic studies of this damage mechanism in order to introduce some means of quantifying its importance. We have shown for instance that a simple evaluation of the expected stresses by multiplying the swelling strain by the elastic modulus is not sufficient and that the viscoelastic properties of the stone must be taken into account (Jiménez González and Scherer 2004). More specifically, clay-containing stones do not behave as strictly elastic solids. They can relax stresses, probably by a slippage among clay surfaces, and this reduces the magnitude of the stresses that develop during such wetting and drying cycles. Nevertheless, using a device that subjects stones to cycles of wetting and drying demonstrates evident damage (reflected in an increase in swelling) after hundreds of cycles (Jiménez González and Scherer 2006).

Thus, in a first approximation, the damage from wetting and drying can certainly be stated to increase with increased swelling. However, more complex material characteristics and exposure conditions are needed to evaluate the stresses that can arise. From the practical point of view, the first thing to consider, if one wants to reduce damage from this mechanism, is the application of so-called swelling inhibitors (Snethlage and Wendler 1991, Wendler et al. (1991), Jiménez González and Scherer 2004).

3.5 Biodegradation

The term biodegradation covers many sources that involve bacteria, algae, fungi or lichens. Their action can be either chemical or mechanical. More detailed information on all these sources is given by Koestler et al. (2003). Here we review only the most general knowledge about this mode of degradation.

In the case of algae, the chemical action comes from acidic compounds that some of these organisms can produce. It is also stated that the chelating nature of these molecules, as well as of other products of algal metabolism, such as sugars and proteins, can enhance the solubility of

minerals containing nutritionally important elements such as calcium, magnesium, potassium and iron.

The mechanical action is generally described to come from the growth of filaments, roots or bacteria themselves in between grains causing important disrupting pressures. Another aspect linked to biodegradation concerns the coupling with other degradation mechanisms, in particular freezing. Indeed, the formation of patina is known to promote water retention at the surface of stones; as a consequence it is expected that freezing damage may be enhanced.

3.6 Good intentions and bad choices

In relation to the Cooper Union building, we already mentioned that some conservation treatments may turn out to be detrimental in the long term. In particular, we mentioned the case where jack-hammering the surface enhanced degradation. Other examples of questionable interventions and inappropriate treatments can be found. For example, the common practice of filling missing parts in blocks or replacing damaged pieces of stone by applying different patching products[8] or stucco[9] has been really harmful for the stone in a number of cases (Rude 2000).

In the light of such problems, one can clearly see how enhanced knowledge of the decay mechanisms and their relation to measurable stone properties should allow better selection of stone sources, conservation materials and treatments. Achieving this will require continued

---

[8] In 1884 sources suggest that treatments such as a mixture of paraffin wax and carboxylic acid should be applied to obtain a *protective surface* with a depth of 1.5 inches (3.8 cm). Another treatment that was advocated consisted in applying 3 parts of glass, 3 parts of broken marble, 2 parts of anhydrous clay and 2 parts of freshly slaked lime, still warm (Roblee 1998). In addition, patching with a mixture of cement, sand, lime and mortar colours became the preferred fix (Berry 2002).

[9] Berry (2002) reports that: *Currently masonry contractors are persuading some row houses owners to chip away everything and replace the whole brownstone facades with a brown-coloured stucco that includes cement.*

research in the materials science of conservation. For the time being, only the main trends can be outlined as we attempt to do in the specific case of Portland Brownstone in the next section.

4 INFLUENCE OF PORTLAND BROWNSTONE PROPERTIES ON DURABILITY

Stone weathering is a natural and irreversible phenomenon produced by the continuous interactions between the stone and the environment. In the former section we gave a brief overview of the main mechanisms that can cause stone degradation. We indicated that the prediction of the actual extent and rate of degradation is not yet possible, even though the basic principles that govern these mechanisms, as well as the factors that affect their magnitudes, are known. This arises from the fact that the observed macroscopic degradation depends on additional factors. For example, in the case of salt crystallization, the location in the stone where salts crystallize is of crucial importance. An optimal combination of stone transport properties and environmental conditions might, for instance, lead salts to crystallize outside the stone in what is known as efflorescence. Although this can be detrimental in terms of aesthetical appearance, it does not lead to degradation of the stone itself. On the other hand, if the salts crystallize inside the stone (cryptoflorescence), this could lead to damage. The depth at which this occurs influences the type of damage that is observed macroscopically (powdering versus granular disintegration, for instance).

In this section, we attempt to determine which properties of Portland Brownstone lead this stone to be more or less sensitive to the different degradation mechanisms discussed previously. In doing so, we combine information found in the literature with our personal attempt to shed some light on this complex materials science topic.

4.1 Mineralogy and chemical composition

As mentioned in the introduction, Portland Brownstone is understood to be a type of *brownstone* that dates geologically from the Early Jurassic period and is obtained mainly from the quarries of Portland (CONN, USA). This stone comes from intermediate geological age beds deposited quite horizontally with a total thickness of about 200 m (Guinness 2003). The quarries, which descended vertically were between 50-60 m deep (Merrill 1890, Crosby and Loughlin 1904), with beds between several centimeters and 6 m (Merrill 1890). These were regularly divided, at wide intervals by vertical joints (Crosby and Loughlin 1904). Natural blocks of up to 30 m x 15 m x 6 m occurred, which in practical terms means that virtually any block size could be obtained (Merrill 1890).

Among the most obvious characteristics of Portland Brownstone, apart from its characteristic brown-reddish color, is the clear definition of bedding planes, which is visually enhanced by the presence of muscovite mica that also gives this stone a certain sparkling appearance. These marked bedding planes confer rather anisotropic properties and weaken the stone, as is discussed in following sections devoted to anisotropy and mechanical properties, respectively.

In terms of the actual mineralogical composition and characterization of Portland Brownstone given in this section, most information was gathered from two main sources: Hubert et al. (1982) and Crosby and Loughlin (1904).

Hubert et al. (1982) give an average mineralogical composition of Brownstones coming from different quarries in the Portland Formation in the Connecticut Valley. Nine specimens come from the Brownstone Quarries of Portland and eight from the Bucklan (Manchester, CT) ones. Four additional redstone specimens belong to the East Longmeadow Quarry (MA) and two more samples come from two other Connecticut quarries, Cromwell and East Windsor. The

compositions they report (see Figure 4-1) are volumetric proportions based on point modal analysis of thin sections from 23 samples.

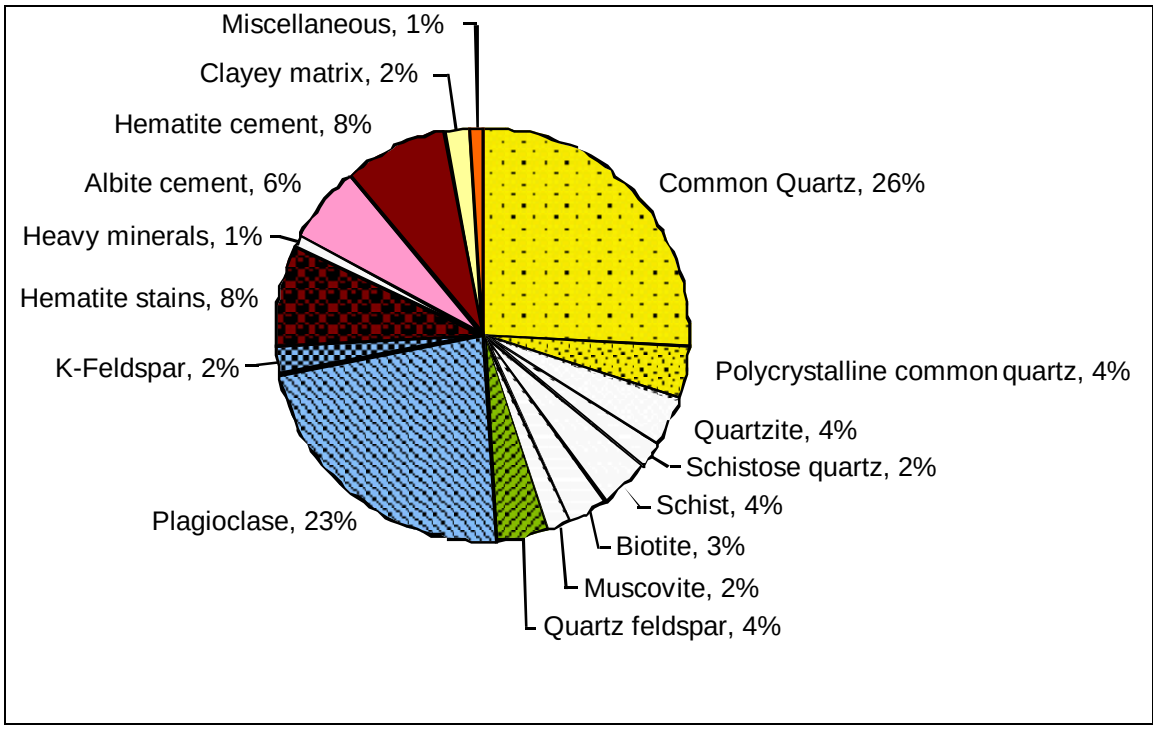

Figure 4-1. Average volume percent composition from 23 brownstone thin sections coming from various quarries (mainly Portland Brownstone and Bucklan Quarries) in the Connecticut River Valley. Graph adapted from Hubert et al. (1982).

From Figure 4-1 we determine that the framework grains are composed of quartz, feldspars and micas and that these amount to about 75% by volume of the stone composition. Furthermore, quartz and feldspars are about equally abundant, as illustrated in Figure 4-1 and also in accordance with Crosby and Loughlin (1904). Between those framework grains, a matrix of clay is present and the cementing phase is hematite and albite, which according to Hubert et al. (1982) is responsible for the *toughness and durability* of Portland Brownstones.

The detrital quartz grains are mostly common quartz, while the feldspar grains are predominantly plagioclase, entirely albite ($NaAlSi_3O_8$) to calcic oligoclase (~

$Na_{0.7}Ca_{0.3}Al_{1.3}Si_{2.7}O_8$) with minor amount of microcline ($KAlSi_3O_8$). These feldspars represent more than 25% of the sandstone composition. In fact, due to this high content of feldspars, one can refer to Portland Brownstone as an ***arkose*** brownstone because it agrees with the general characteristics of this typology of coarse-grained stones, that are usually derived from the rapid weathering of granitic rocks (Roblee 1998) and contain more than 25% by volume of feldspars. More specifically, when using the classification triangle of Folk (1980), Hubert et al. (1982) found that 2/3 of their Portland brownstone compositions were classified as ***lithic arkoses*** and the rest as arkoses. Arkoses and lithic arkoses ***in sensu*** Folk, both have less than 75% of quartz in the framework grains, but differ in their ratios of feldspar to rock fragments. For arkoses this ratio is greater than 3:1, whereas for lithic arkoses it is between 3:1 and 1:1 (Folk 1980).

Portland Brownstone also contains distinct amounts of micas (~5%), mainly muscovite (white mica) and biotite. These minerals are agglomerated by a binding/cementing phase, which represents around 15 % by volume and that includes mainly hematite (Fe_2O_3), albite, and various clay minerals most often kaolinite, sometimes sericite-illite and Gibbsite (Roblee 1998) that could be the weathering products of the feldspathic cement (Winkler 1997).

Hematite, a possible alteration product of limonite (hydrous iron oxide, $FeO(OH)•nH_2O$), magnetite (Fe_3O_4) or siderite ($FeCO_3$) (Klein 2002), is found as fine-grained hematite stains on some surfaces of the detrital and cementing grains (Hubert et al. 1982). Because of this staining, the binding phase of Portland Brownstone has been described by authors as Crosby and Loughlin, (1904) as a ferruginous clay cement.

As is seen in Figure 4-1, neither the detrital grains, nor the cement, contain calcite or other carbonates. Furthermore, the same figure indicates that the content of expandable clays is not high, although not nonexistent (Scherer and Jiménez González 2005).

In reference to earlier literature on Portland Brownstone, where mineralogical compositions could be inferred on the basis of chemical analysis, it must be noted that this can lead to incorrect

conclusions. For instance, strict consideration of the elemental analysis of this stone (Table 1) can misleadingly imply that the stone does have very large contents of clays, because of its high alumina content. This conclusion is reached if the CaO and MgO analyzed are attributed to carbonate phases. In fact, the alkali content of this stone, which approximates that of granite, indicates that most of the alumina is not present as expandable clays but rather as undecomposed feldspars, as well as mica. Consequently, the amount of expandable clays is indeed not excessively high and the analyzed calcium and magnesium should be considered as associated with feldspars rather than carbonates (Crosby and Loughlin 1904), which is consistent with Figure 4-1.

Table 1 Chemical composition of Connecticut Brownstone given by Crosby and Loughlin (1904).

Compounds	**weight** %		
Silica (SiO_2)	70.11	72.95	69.94
Ferric oxide (Fe_2O_3)	4.85	4.12	2.48
Alumina (Al_2O_3)	13.49	12.82	13.15
Manganese oxide (MnO_2)	0.35	-	0.7
Lime (CaO)	2.39	5.57	3.09
Magnesia (MgO)	1.44	2.4	Trace
Soda (Na_2O)	7.37	-	5.43
Potash (K_2O)		-	3.3
Loss	-	2.14	1.01

The same mineralogical composition is also generally consistent with an XRD analysis of samples we examined and that identifies quartz and albite as the most abundant phases by far (Figure 4-2). This XRD patterns also reveals the presence of smaller amounts of clays, such as smectites and vermiculites. More importantly, we also reach the conclusion that this stone has a very low content of carbonate minerals. Nevertheless, reports that calcite is a cementing material in Portland brownstone can be found in the literature (Matthias 1967, Olsen et al. 2005). While this might hold for some Portland Brownstone sources, our own experience as well as that of

Meierding (2000) and of Krynine (1950) is that this stone does not effervesce in acid, implying that calcite cannot be present in large amounts.

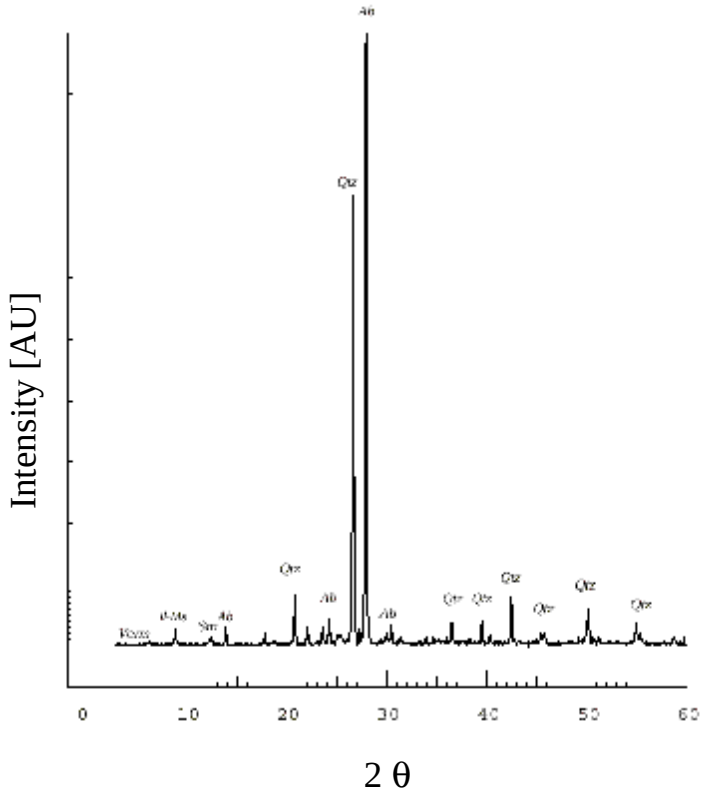

Figure 4-2. XRD pattern of Portland Brownstone used for our investigations. Peaks highlighted correspond to Albite (Ab), Quartz (Qtz), Vermiculite (Verm), Smectite (Sm), Illite (Il) and Muscovite-mica (Ms).

An implication of this absence of carbonate minerals is that Portland Brownstone cannot be expected to suffer much from acid attack of atmospheric pollution, in agreement with Meierding (2000) and Hubert et al. (1982), but in contrast with Draper (1872). In the context of this debate on the role of atmospheric pollution on Portland brownstone degradation, the work of Julien (1883a) is very important, since its shows that brownstone weathering was well advanced before anthropogenic SO_2 acid rain and deicing salts were prevalent. All things considered, it therefore

appears that acid attack, in whatever form it may occur, is not an important source of Portland brownstone alteration. Thus, in contrast with limestones, Portland brownstone should be much less susceptible to degradation due to atmospheric pollution and biological attack.

The absence of calcite in this stone does not, however, completely rule out the possibility that gypsum formation may occur and lead to subsequent damage through cycles of dissolution and precipitation. Nevertheless, for this to happen an exogeneous source of calcium would be needed, typically in the form of particulate deposits (Roblee 1998) or of lime leached from adjacent mortars.

As far as the swelling clays are concerned, although their total content by volume is rather low (2%) with respect to the whole stone, it becomes considerable (8.3%) when reported with respect to the binding phase in which most of the clays appear to be located. The nature of these clays is given by Scherer and Jiménez González (2005), who indicate the presence of montmorillonite, kaolinite and illite. Scanning electron microscope images of these clays can be seen in Figure 4-3 a and b. A thin section of Portland Brownstone acquired on an optical microscope using cross polarization also shows evidence of mica beds and probably some clays (as indistinct material at grain boundaries) in Figure 4-4. The parallel colored lines result from the birefringence of these layered minerals (principally muscovite).

The consequence of the presence of these clays is discussed in more detail later in the paper. For the time being we just point out that they decrease the stone strength when wet, and that their expansion and shrinkage during wetting and drying cycles is often quoted to be a possible source of degradation (Weiss et al. 1982, Roblee 1998, Myjer 1999, Hart 2001 and Gilley 2004). In fact, this issue of the swelling of the clays was already indicated early on as a possible problem for some sandstones (Egleston 1887).

The binding phase may be viewed as the weakest link in stone microstructure, particularly when swelling clays are present. Consequently, one may be tempted to try relating the binding

phase composition to stone durability. However other factors such as porosity and grain size should be at least as important as the mineralogy of the binding phase, so that no simple relation is expected. However, what can be stated, and is pertinent in the case of Portland Brownstone, is that a stone is weakened by a high content of swelling clays in the binder. In a following section we take the approach of examining how overall mechanical strength can be related to durability, since this is a more readily accessible parameter. Before that, we first examine the role of anisotropy in stone weathering.

a)

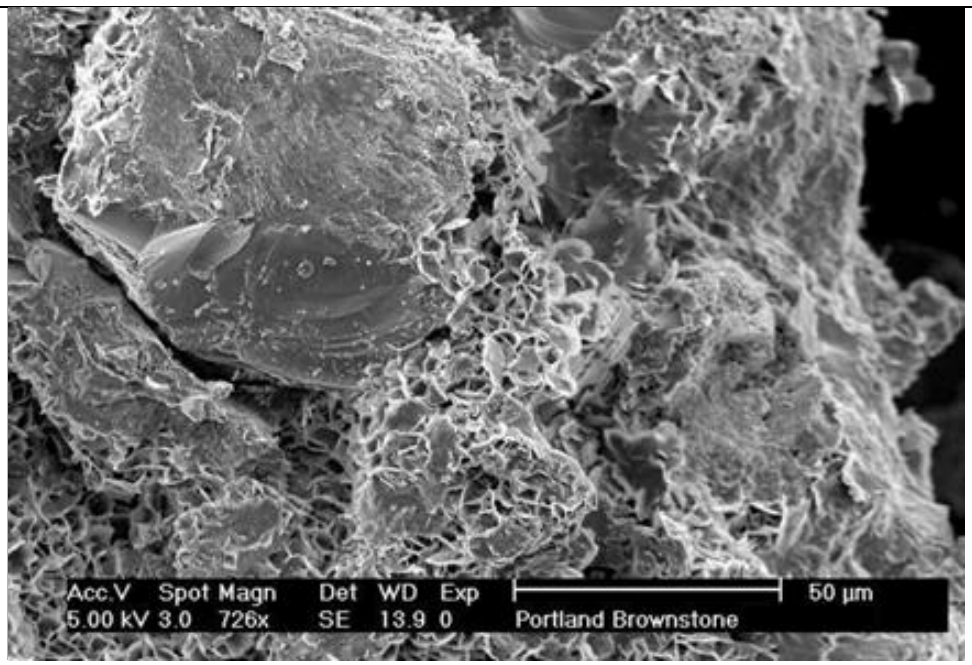

b)

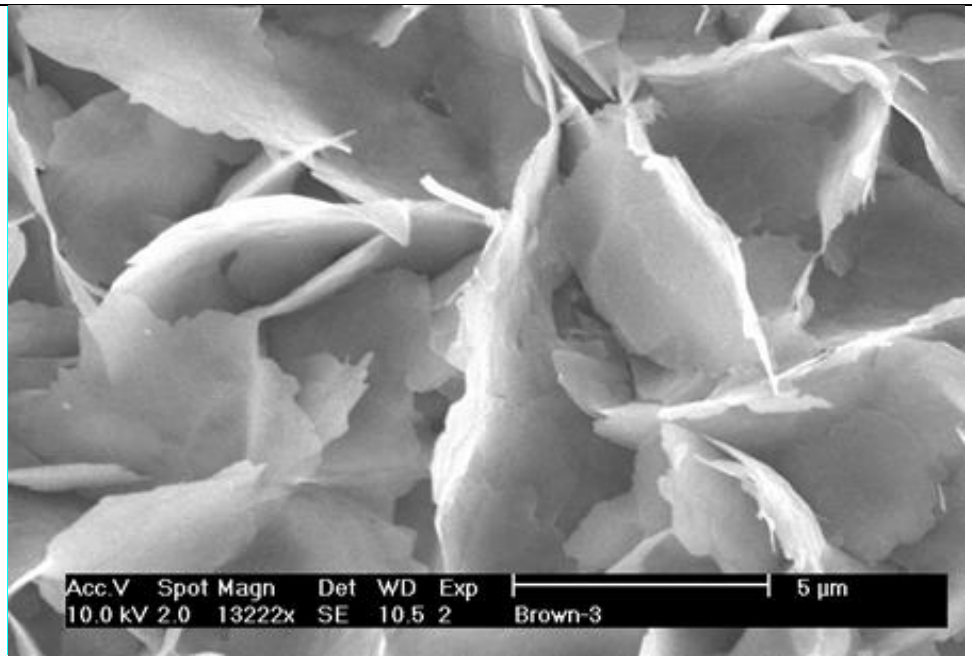

Figure 4-3. SEM images of Portland Brownstone showing presence of clay minerals. a) large view with clays surrounding grains. b) detailed view of clays minerals.

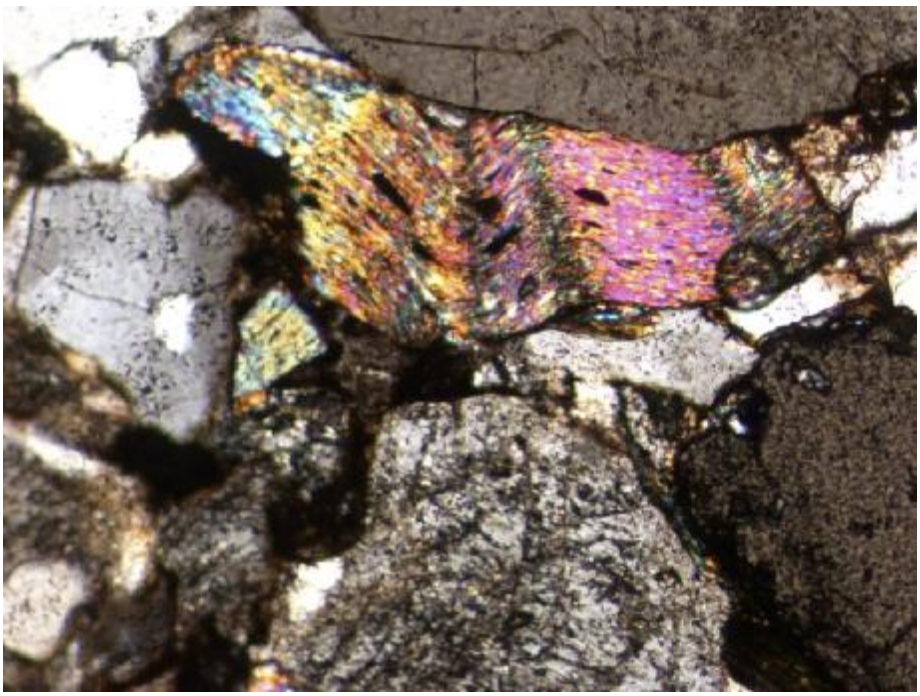

Figure 4-4. Optical microscope image of a thin section of Portland brownstone taken under polarized light. The birefringence of the mica beds is evident in the coloured layers seen in the top part of the image.

4.2 Anisotropy and heterogeneity

Portland Brownstone exhibits a very pronounced **stratification** (bedding planes) that

is often accompanied by an alternation of fine and coarse grains. This heterogeneity, perfectly apparent to the naked eye, not only poses an experimental challenge, but also limits the extent to which results obtained with one source of Portland Brownstone can be generalized to other sources. Furthermore, quarried stones show little homogeneity, which is explained by the variability in the Mesozoic climate, erosion and depositional environments, as well as diagenesis conditions. It was shown that both composition and grain size vary systematically from north to south of the valley. In addition rock colors of the southern part of the valley are more yellowish brown and purple than in the northern part.

Crosby and Loughlin (1904) indicate that this variation in stone quality and inappropriate stone selection could be a cause for various cases of enhanced degradation of Portland Brownstone. They distinguish four grades of quarried brownstone:

a) medium-grained (first quality) brownstone, used in high-class architectural work;

b) fine-grained (second quality) brownstone, richest in clay and mica, and most subject to injury by frost action;

c) brownstone of uneven, laminated and shaly texture (third quality)

d) coarse brownstone (conglomerate), used for rough stone work and bridges.

On the experimental front, the **heterogeneity** of Portland Brownstone (Figure 4-5) enhances the need for non-destructive testing of samples. For example, it is advantageous to measure a specific sample before and after a given treatment rather than different sets of samples untreated and treated. The same holds for durability tests, where the evolution is more reliably captured if samples can be measured over and over again. In terms of generalization of results, we expect that products identified as efficient on one source of PB should also be efficient on others, although the absolute values of these effects may vary.

Figure 4-5. Illustration or Portland Brownstone heterogeneity and anisotropy

Another experimental issue with Portland brownstone is its **anisotropy** (Figure 4-5). Whereas for heterogeneity the use of large samples or a large number of samples should reduce errors, anisotropy causes systematic differences according to the direction in which a property is measured. This is true however large the samples are or however many samples are measured. In this stone, anisotropy comes from the pronounced stratification and has a significant effect on swelling, sorptivity, elastic modulus and tensile strength as shown in Table 2 (Jiménez González and Scherer 2004).

Table 2. Properties of Portland Brownstone and their dependence on anisotropy.

TECNIQUE	Bedding orientation	conditions	Portland Brownstone
Static Modulus [GPa]	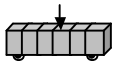	Dry	11.5
		Wet	4.1
	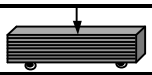	Dry	14.3
		Wet	7.7
Dynamic Modulus [GPa]	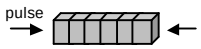	Dry	23
		Wet	38
		Dry	35
		Wet	44
Tensile Strength [MPa]	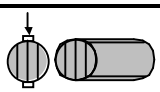	Dry	4.5
		Wet	n.a.
	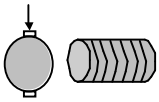	Dry	6.7
		Wet	5.2
Sorptivity [cm/s $^{1/2}$]			0.010
			0.005
Swelling [µm/m]			460
			170

Because all these properties matter in durability, we expect that Portland Brownstone durability is linked to the orientation in which blocks are placed. In fact, as already mentioned, many sources identify the face-bedded set up (bedding vertical and parallel to the wall surface) as a major cause of the stone deterioration (mainly on buildings from the *Brown Decades*). In this configuration (Figure 4-6, case B) the stone has the lowest mechanical resistance to support the mass above it. Furthermore, it has the fastest rate of capillary rise (same as A and faster than C in Figure 4-6). It also has the lowest rate of humidity exchange between the stone and the atmosphere. This would favor either accumulation of salts or water below the surface and contribute to damage from salt crystallization or freezing.

When blocks are laid either in end-bedded or naturally bedded orientation (case A or C in Figure 4-6), the rate of rainwater ingress is higher. Although this might enhance freezing damage, it would probably not lead to large scale spoiling seen in face-bedded blocks.

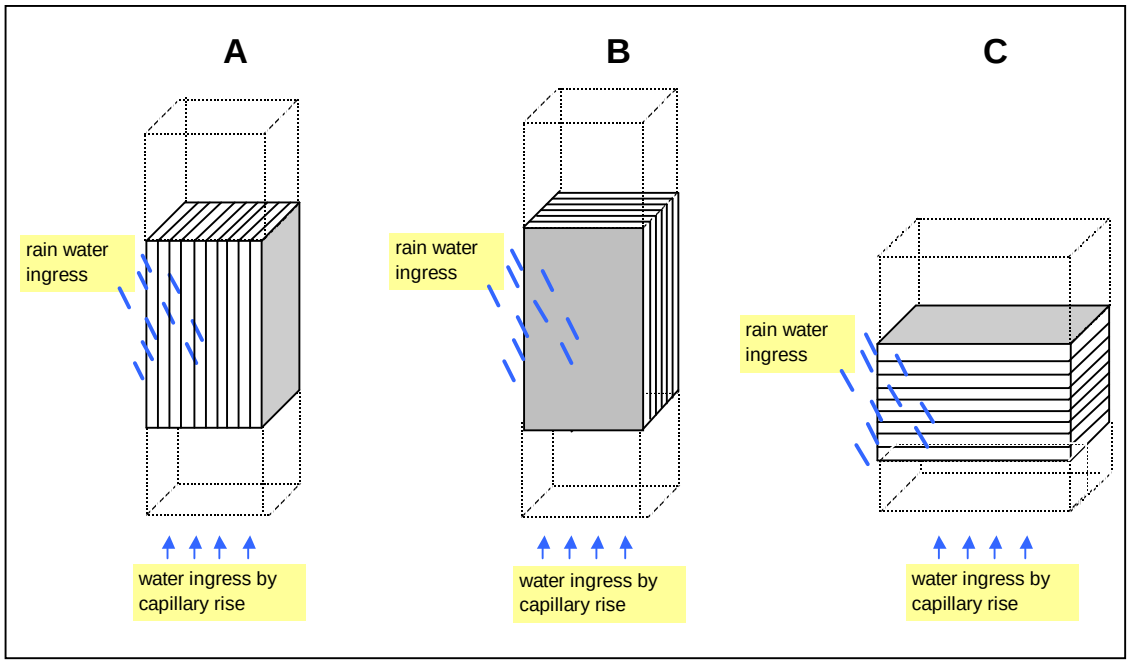

Figure 4-6. Illustration of the three orientations that stones with clear bedding planes can adopt on a building. A) end bedded, B) face bedded, C) naturally bedded. The choice of this orientation affects durability because of different rates of water transport as explained in section 4.2. For example, the rate of water ingress by capillary rise in A and B is obviously the same, but higher than in C. The rate of rainwater ingress or humidity exchange between the stone and the atmosphere is higher in A and C than in B.

4.3 Mechanical properties

We have seen previously that stone failure during degradation processes is expected to take place because of tensile rather than compressive stresses. Thus it is more relevant to examine the tensile strength of a stone rather than its compressive strength when discussing durability.

This rather general statement overlooks the fact that when stress develops very locally, the tensile strength that is relevant is not the macroscopic one, but the strength on the length scale of the volume in which those stresses develop. In first approximation, this can be understood in terms of propagation of flaws of different sizes. The larger the flaws are, the lower are the stresses needed to propagate them. However, this only holds if the volume over which those stresses develop is large enough (i.e., larger than the size of the flaws in question). Thus, in many durability cases, the use of macroscopic tensile strength as the failure criterion is not necessarily relevant.

In summary, this means that the relation between mechanical properties and durability is not a trivial issue, particularly when the damage mechanism only causes stresses to develop very locally.

The material properties that matter are those measured at the length scale where degradation mechanisms operate. Despite this, as a first approximation, we assume that the role of mechanical resistance follows the same trends as macroscopic mechanical strengths, all other things remaining equal. With this assumption, we outline the following links between durability and measured macroscopic mechanical strength:

- Flaw size distribution plays an important role in accounting for durability with respect to mechanisms that induce mainly localized stresses, as is often the case with salt crystallization.

- Values of mechanical strength of Portland Brownstone vary depending on the source of the stone. This is illustrated by the range of compressive strengths in Table 3.
- Owing to its strong anisotropy, Portland Brownstone's strength is not the same in all directions. In particular, we have reported differences on the order of 50% depending on the direction of testing.
- The presence of swelling clays in the cementing matrix leads to a softening of the material when wet. We typically find a decrease of the static elastic modulus by a factor of about 2 (see Table 2).
- The presence of clear bedding planes introduces specific defects that decrease the stone strength.

Table 3. Compressive strength of Portland Brownstone. Data from Crosby and Loughlin (1904)

	Compressive strength MPa (psi)
Transverse section	43 (6,200)
	74 (10,700)
First quality	94 (13,700)
Second quality	96 (13,900)
Third quality	104 (15,000)
Bridge stone	66 (9,600)

From the above it appears that if one macroscopic mechanical property should be used for assessment of durability it should be tensile strength. The two simplest measurements of tensile strength on stones are indirect. The one we have used is called the Brazilian test or the splitting test. It consists in compressing a cylinder laid on its side and using a well-established expression

to relate the load at failure to tensile strength (Mindess and Young 1981). Alternatively, a bending strength test or modulus of rupture can also be performed.

4.4 Petrophysical properties

In the former sections we alluded to the fact that the ***in situ*** resistance of a stone to degradation mechanisms is strongly influenced by porosity and transport properties. In this section, we briefly cover these properties for the Portland Brownstone, mentioning which experimental techniques are most readily applicable and appropriate.

In terms of porosity one distinguishes total porosity from water-accessible porosity. The difference between the two gives an indication about the degree of connectivity of the porous network. Both porosities are obtained with very simple and affordable experiments. Water accessible porosity is determined from the final mass gain of a sample subjected to capillary rise. For the total porosity, vacuum saturation of the sample is used (Jiménez González and Scherer 2004). Alternatively, mercury intrusion can also be used.

The water accessible porosity of the Portland Brownstone is on the order of 8% by volume, while the total porosity is slightly higher, about 11% (Scherer and Jiménez González 2005). In general a larger pore volume means more space for salts to crystallize or water to freeze, as well as a decrease in mechanical strength. On this front, the porosity of the Portland Brownstone is not very high for a sedimentary rock, but clearly much higher than metamorphic rocks.

However, pore volume alone is insufficient for durability classifications. What is much more important is the pore size distribution. Mercury intrusion porosimetry determines the distribution of pores sizes and such results have been used, together with mechanical strength, to propose a criterion for resistance to salt crystallization (Benavente et al. 2001). The pore size distribution of the Portland Brownstone we studied is shown in Figure 4-7. It shows a bimodal distribution of

pore sizes with about a third of the pore volume centered around 1 µm and the remainder averaging about 0.05 µm in diameter.

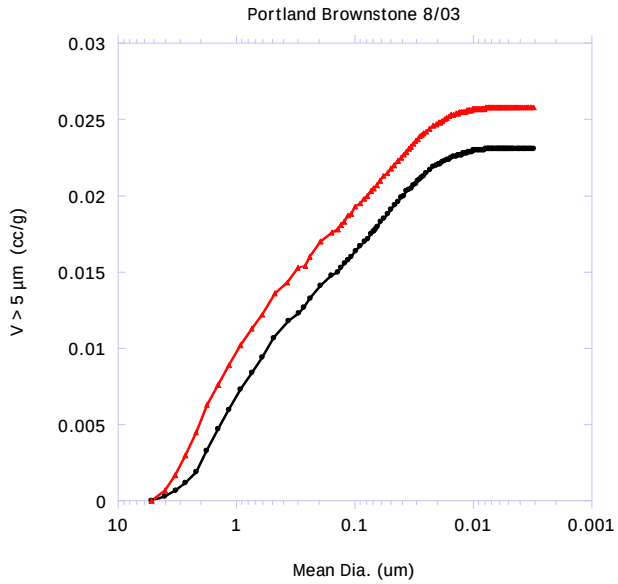

Figure 4-7 Mercury intrusion data for two samples of Portland Brownstone showing pores sizes centred both around 1 and 0.05 microns.

While results obtained by mercury intrusion porosimetry give a more complete picture of pore sizes, other techniques that are much more readily accessible provide information about average pore sizes. Sorptivity, for instance, can be analyzed to obtain an average pore size. The classical analysis of this experiment assumes a porous network composed of a series of cylindrical pores all parallel to the direction of water transport. This is clearly an over-simplification and does unfortunately not lead to reliable estimates of pore sizes. A better approach is described by Scherer and Jiménez González (2005). It uses an independent measurement of a transport coefficient termed permeability. With this separately determined parameter, it is then possible to estimate the pore size most pertinent to water transport. For the Portland Brownstone, and in the direction parallel to the bedding planes, Scherer and Jiménez González found this pore diameter

to be about 80 nm. With respect to the pore size distribution obtained by mercury porosimetry, this suggests that transport occurs mainly through or is limited by the smaller pores. Furthermore this size is also compatible with values obtained by nitrogen desorption, which is a more reliable technique in this range of small pore sizes.

The relatively large amount of small pores in Portland Brownstone should increase the susceptibility of this stone to freezing and salt crystallization. We found that submitting the stone to capillary rise of a sodium sulphate solution in a dry and controlled environment (39% RH) leads to damage at the base of the sample as illustrated in Figure 4-8a (Scherer 2004). In this case, the low permeability of the stone combined with salt accumulation probably leads to a fast blocking of the pore network, which could be an explanation for the apparently moderate height reached by the salts in this stone. In comparison, salts rise much higher in the Berea sandstone (on the right in Figure 4-8a) that has much higher permeability. In Figure 4-8b, we can see in closer detail that the salt accumulation and crystallization in the sample base causes substantial damage.

a) **b)**

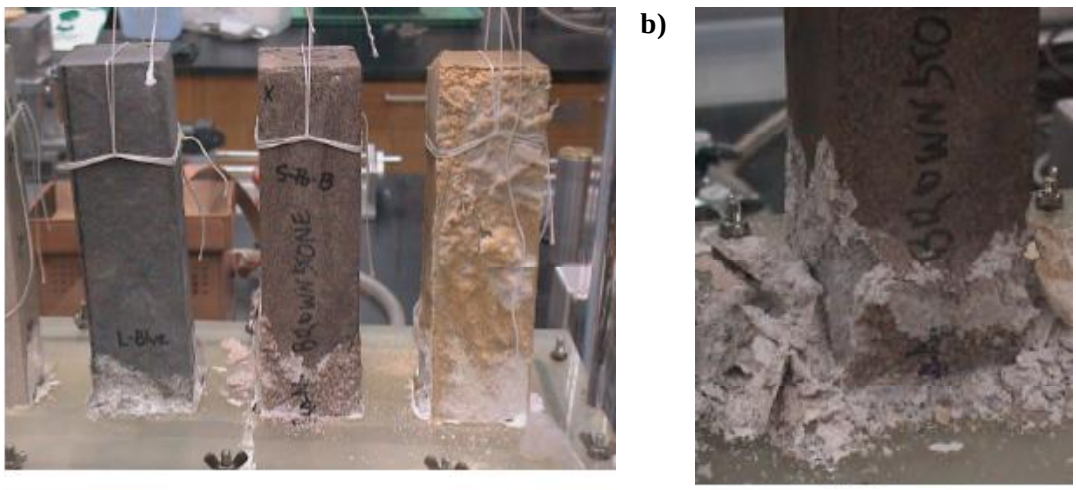

Figure 4-8. Salt damage in a capillary rise experiment of sodium sulphate in a humidity chamber at about 39% RH, a) Comparison between a Portland brownstone (center), a bluestone sandstone (left) and a berea sandstone (right) after 4 days, the low permeability of both the Portland brownstone and the bluestone result in a low level of salt rise in the image, b) detail at base of Portland brownstone after 21 days. Sample size is 5 x 5 x 25 cm.

4.5 Texture

Meierding (2000) pointed out that contour scaling increases with the grain size of Portland Brownstones. Based on the observations of many tombstones, he mentions for instance that the very fine-grained stone most common in the northern Connecticut River Valley does not contour scale at all and also shows little granular weathering.

These observations contrast somewhat with a much earlier article by Crosby and Loughlin (1904) who report that: *The student of this stone quickly discovers that it is not the coarse, irregular and seemingly friable brownstone which shows more injury by frost action, but rather the fine-grained, argillaceous and micaceous variety, the latter holding water tenaciously, while the former dries out quickly and usually before the water has time to freeze in it.*

The contrast between these two observations is rather typical of what can happen when attempting to generalize field study observations using very limited material properties or, as in this case, rather a property that can be affected by changes in a number of other material properties more directly linked to durability. For instance, in the case of texture, Meierding (2000) mentions that changes in permeability may be the cause for the enhanced degradation of the coarse grained stones. We could also include modification of mechanical strength. The other issue to bear in mind is that while Meierding (2000) centers his study on tombstones, Crosby and Loughlin (1904) speak about stones in buildings. In the first case, the accumulation of salts from capillary rise is much more important than in the second. Furthermore both studies are about one century apart and since we know that aging properties of stone are nonlinear, an inversion of tendency to degrade cannot be excluded.

Another interpretation of why these authors reach different conclusions regarding the role of texture is that one might have been observing damage from salt crystallization (Meierding) and

the others (Crosby and Loughlin) damage from freezing. Indeed, salt damage requires drying of the stone, while frost damage requires a high degree of saturation. Thus the discrepancy might be a result of a problem of damage mechanism diagnosis.

This example highlights the difficulty in this field and makes a case for the need for work aimed at quantifying durability in terms of measurable material properties. This is certainly a complex issue, as we try to outline in this paper. However, we believe that serious research efforts can lead to providing field practitioners with more rational tools that would benefit their day-to-day decision-making.

Another aspect of texture that is reported to be relevant to the durability of Portland Brownstone is the formation of black crusts. Indeed, the deposition of particulate matter from the atmosphere increases with surface roughness and thus with grain size of the stones. In the case of Portland Brownstone, these crusts are however much less of an indication of a serious deterioration beneath, owing to the fact that it is not a calcareous stone. Black crusts can, however, also be of biological origin, in which cases they can be observed in zones exposed to rain (Figure 4-9). Such biocoatings may develop more easily on coarse grained than on fine-grained stones. Apart from aesthetic issues, the negative impact of these biological crusts on durability is attributed to moisture retention, which leads to enhanced freezing damage (Young et al 1995).

Figure 4-9. Northeast corner of Edwards Hall at Princeton University. The image shows the presence of black crusts in zones exposed to rain where gypsum crusts tend to be washed away. Such crusts in exposed zones are expected to be of biological origin and to contribute to moisture retention, thus increasing freezing damage, Young et al. (1995).

5 SPECIFIC ISSUE OF WETTING AND DRYING

In recent years we have investigated the role of wetting and drying cycles on the durability of clay-bearing stones and in particular of Portland Brownstone. Although the swelling of this stone is rather moderate compared to some other stones, a number of interesting results were obtained that have implications for our general understanding of stone durability. As already mentioned, this work was motivated by the occurrence of several unquantified statements about a possible role of swelling clays in the literature on stone degradation. This section therefore aims at providing some quantification about the role of wetting and drying cycles in the degradation of building stone and Portland Brownstone in particular.

5.1 General issues

The fact that certain clays swell in the presence of water and contract during drying is well established and so is the fact that stones containing such clays do the same (Madsen 1985). It is also known that stones with extremely high contents of clays and coming from very dry environments, such as Egypt, can virtually decompose when submerged in water (Rodríguez-Navarro et al. 1998). However, as already said, there is to our knowledge only one study that convincingly shows that this can be an issue over time in stones that have lower amounts of such clays (Wendler et al. 1996, see also Figure 5-7). Despite this, many studies and conservation reports mention cycles of wetting and drying as a possible cause for degradation, including for Portland Brownstone. At this stage we do not discuss stones consolidated with ethyl silicates, for which a number of studies have shown that a limited number of wetting and drying cycles virtually cancel the mechanical benefit of consolidation (see for example Félix 1998, 1994, 1995 and Félix and Furlan 1994). Results of ours, still to be published, have confirmed this for Portland Brownstone.

In the case of unconsolidated stone, most articles discuss the role of the swelling pressure of clays (Madsen 1985). The key idea can be summarized as follows. The surface of an otherwise completely dry stone gets wet (Figure 5-3a). The clays in the wet zone begin to expand. Overall, this expansion is limited by the larger dry zone, which does not expand (Figure 5-3b). As a result, the wet layer is confined by the dry part, which puts the wet layer in compression (Figure 5-3c). We refer to this as a swelling pressure. From this perspective, the stone is expected to be damaged if the swelling pressure exceeds the compressive strength of the wet stone. For Portland Brownstone our calculations show that this should not occur, because this pressure reaches only 1-2 MPa and the compressive strength of the stone is about 35 MPa (Jiménez González and Scherer 2004). However, other stones weaken substantially more than Portland Brownstone when wet and might therefore fail during wetting if their compressive strength decreases enough.

Another situation that must be considered as a possible source of damage during the wetting cycles is where the exterior layer - which is in compression (Figure 5-3c) – buckles, because cracking occurs parallel to the surface (Figure 5-3d). An illustration of a possible case of buckling of the surface of Portland Brownstone is shown in Figure 5-1.

Figure 5-1. Possible case of buckling due to clay swelling. Surface of Portland Brownstone front in the Victoria Mansion, Portland (Maine). The picture was kindly provided by I. Myjer.

From a mechanical point of view, this type of failure requires the propagation of flaws parallel to the surface. These may be preexisting in the material or caused by other damage mechanisms. In the first case, bedding planes that weaken the material could constitute such flaws when blocks are face-bedded. In the second case, salt damage or freezing might may cause the weakness. With regard to Portland Brownstone, gypsum resulting from atmospheric pollution is rather unlikely.

This contrasts with another swelling stone we have studied (Swiss molasse with properties similar to the stones used on the Cathedral of Lausanne in Switzerland), for which gypsum crystallization is probably an important initiator of damage, which then gets amplified by clay swelling. In Portland Brownstone, salts more probably come from capillary rise or joining mortars. Figure 5-2 illustrates a possible situation where salts leached from the mortar lead to

localized damage at joints between stone blocks. It should however be noted that, in this specific case, accumulation of water running down the joint and keeping the stone wet could, together with freezing, also explain this localized damage.

Figure 5-2 Detail of deteriorated Portland Brownstone blocks that belong to the façade of the Victoria Mansion (MA, USA). The damage originates where the vertical mortar joint meets the block below. This could indicate that salts leach from the mortar and initiate damage in the stone (however, it might also mean that water runs down the joint and keeps the stone wet at that location).

On the other hand if we take the reciprocal situation, in which an otherwise fully saturated wet stone (Figure 5-3e) begins to dry from its surface, it is the drying layer that will be prevented from shrinking (Figure 5-3f). As a result, that layer would tend to fail in tension (Figure 5-3g). Because tensile strengths of stones are lower than compressive strengths, we expect in first approximation that wetting and drying cycles should cause damage during the drying rather than during the wetting cycles.

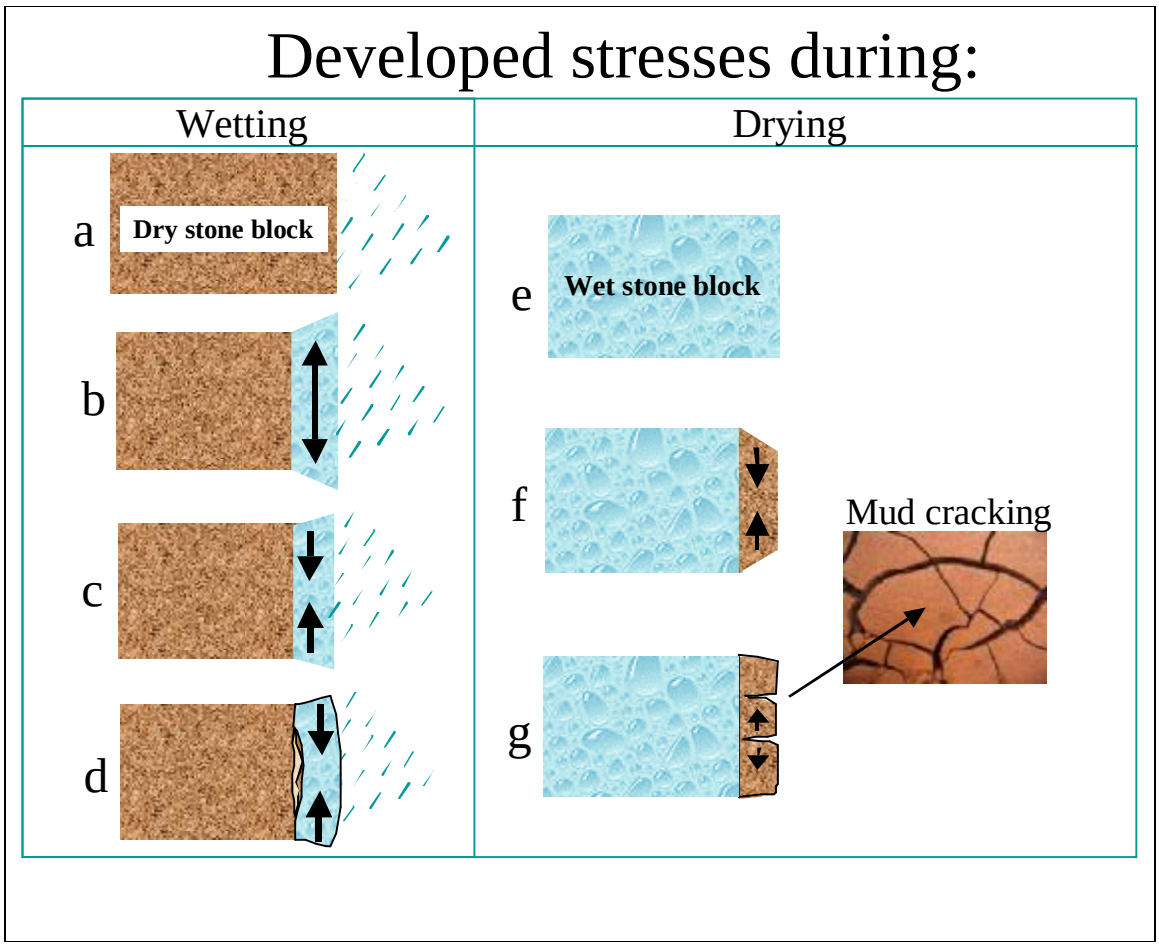

Figure 5-3 Illustration of both ways in which maximum stresses develop during wetting and drying cycles: During the wetting of a dry stone (a) the very thin outer layer will try to expand (b) but it is prevented from doing so by the big dry part that puts the thin layer in compression (c). Damage by compressive failure is possible only if the stones become very weak due to wetting. Instead, during wetting, the damage more likely involves shear forces that may cause buckling of the outer exposed layer (d). During the drying of a saturated block of stone (e) the very thin dry layer tries to shrink (f) but the much bigger wet part opposes this and puts the drying layer into tension (g), therefore cracks would develop perpendicular to the surface.

However, if this occurs, the type of damage observed should be similar to mud cracking (Figure 5-3g, Figure 5-4 a and b) in which cracks form perpendicular to the surface in random directions but forming patches of a characteristic size between each other.

a) b)

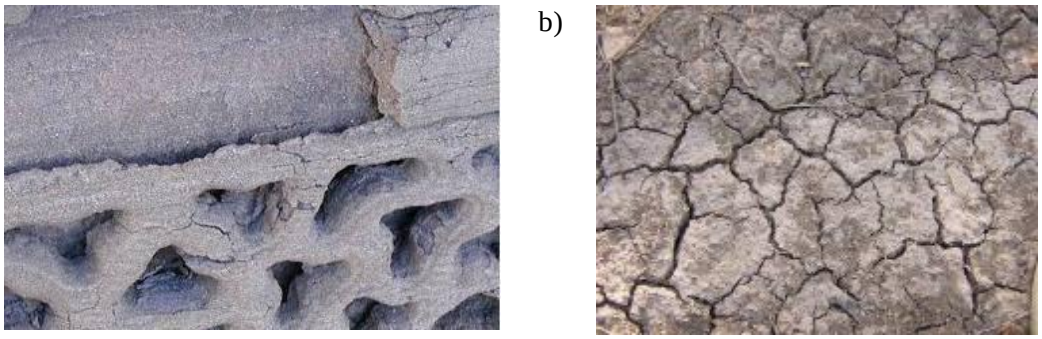

Figure 5-4 Portland Brownstone quoin belonging to one of the Victoria Mansion facades (Maine). a) Damage possibly due to drying stresses that develop a damage pattern consistent with mud (photo provided by I. Myjer). b) Typical case of mud cracking (photo provided by A. Jiménez González).

Mud-cracking patterns are not the usual damage seen on Portland Brownstone buildings fronts. The reason for that could be that, in the field, the drying stresses are limited by a series of factors. One of them is the viscoelastic behavior of this stone, which as explained in section 5.2, reduces the magnitude of the predicted stresses.

Apart from that, it is important to emphasize that the stresses calculated previously assume that the stone blocks are initially fully expanded and then dry by evaporation from the surface. The combination of both conditions in practice is probably rather rare, reducing the number of situations in which damage could occur. For instance, a stone block in a building wall does not have a specially water-exposed and/or protruding position that favors getting fully saturated. A different situation is found in the case of a protruding block, a relief or a thin tombstone placed in the ground, where all its faces are exposed to the rain or capillary raise water. In these situations, it is more likely to get fully saturated blocks and therefore cracking during drying. Interestingly the poor performance of Portland Brownstone in projections was already noted by Loughlin (1903) who states: "… the Portland Brownstone ought never to be used as projections, even when

properly laid, because of their structure. … Here the brownstone has disintegrated so far that all resemblance to a window sill has gone."

Furthermore, as atmospheric humidity increases, the extent of shrinkage during drying decreases. This is shown in Figure 5-5, where the shrinkage is given as a fraction of the maximum shrinkage obtained in a completely dry atmosphere. The elastic modulus of the stone varies with humidity as illustrated in the same figure. In those tests the samples were stabilized in atmospheric chambers before the tests, but the measurement could not be performed under regulated humidity, so the values should be taken as indicative only.

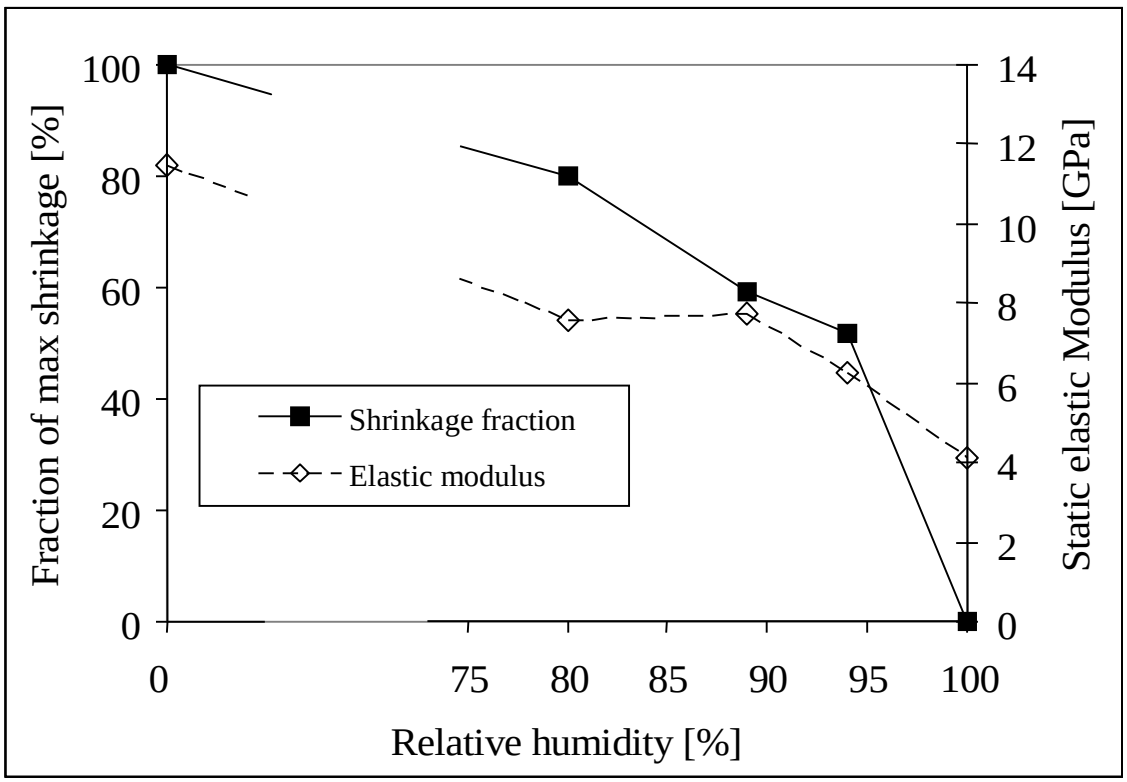

Figure 5-5 Fraction of maximum shrinkage (and drying stress) of Portland Brownstone given as a function of the relative humidity of the atmosphere at the time of drying. The elastic modulus is also represented and is seen to increase with decreasing relative humidity.

In the cases where the damage occurs during drying, the cracking is probably distorted from a typical mud cracking pattern as shown in Figure 5-3g, because of the strong anisotropy of Portland Brownstone. A first approximation of the distance *L* between cracks is that they scale as:

$$L \approx \frac{s}{(eE)^2} \tag{1}$$

where σ is the tensile strength, ε is the free swelling strain and *E* is the elastic modulus. Using values reported in Table 2, we find that the ratio between the spacing of cracks parallel and perpendicular to the bedding is about 10. This seems to be consistent with the type of damage shown in Figure 5-6. With smaller blocks one might therefore not see cracks perpendicular to the bedding.

Figure 5-6. Portland Brownstone anisotropy should result in an anisotropic crack spacing, departing from typical mud-cracking pattern. This capitol from the Victoria Mansion shows damage consistent with this interpretation (Picture provided by I. Myjer).

Concerning those blocks on buildings that do not protrude, it is also worth noting that the weight supported by a given stone will generally not prevent expansion. Indeed, based on experimentally measured swelling pressures (~1 MPa including stress relaxation), a height of about 50 m of stone would be needed to prevent expansion.

Overall, since buckling is the type of damage most commonly observed on site, we expect that wetting and drying cycles can indeed contribute to degradation and that they affect weathered stones more than fresh ones. A more detailed analysis of this problem is, however, needed to determine the real significance of this process on site. Such an analysis needs to incorporate the extent and rate of softening that stone undergoes during wetting.

5.2 Viscoelasticity

Clay bearing stones exhibit viscoelastic relaxation of stress, probably as a result of sliding of the clays. This can be demonstrated by bending a piece of stone and measuring the force needed to hold it in a fixed shape: the force will gradually decrease as the shape of the stone adapts to the imposed curvature; if held indefinitely, the stone would become permanently warped and no force would be required to keep it bent. In our case, we can think about the deformation as being the restriction of the swelling (or shrinkage) that the stone would like to exhibit when wetted (or dried). The stress needed for this restraint will decrease over time because of the viscoelastic nature of the material that can be characterized by stress relaxation experiments we described elsewhere (Jiménez González and Scherer 2004). It might also imply that fatigue may be a bigger issue, in that cumulative internal rearrangement of the material may cause a slow but net decrease of mechanical resistance over time.

This ability of clay bearing stones to relax stresses is much greater in the wet than in the dry state (Jiménez González and Scherer 2004). We have been able to demonstrate quantitatively the importance of this stress relaxation by measuring the time evolution of the load needed to prevent a stone suddenly wetted from swelling. The pressures we measured were consistent with other studies on swelling stones, but they were much lower than what could be expected from the product of the elastic modulus of the stone and the free swelling strain. The most important part in this finding was the fact that independent measurements of stress relaxation could be used to account for the kinetics of softening; that is, the small stress required to suppress expansion was quantitatively explained by taking account of the independently measured rate of stress relaxation. This confirms the important role that viscoelastic properties of clay bearing stones can play in their durability processes in general. For instance, in cases of salt crystallization or freezing where the small pores among clay particles probably remain wet, stress relaxation might be quite important, owing to possible slippage between clay particles or clay layers.

5.3 Swelling inhibitors

The swelling of clays and of clay-bearing stones can be drastically reduced by the application of well chosen organic molecules. A very demonstrative illustration of this can be found in the work of Wendler et al (1996). In that study the authors examined the aging of stones from Easter Island. They first observed that the drill resistance of exposed stone is much less at the outside than in the inside. To test whether such an alteration could be induced by cycles of wetting and drying, they subjected samples to 12 hour cycles in which there was 1 hour complete submersion in water at 20°C, followed by 11 hours at 40°C and 18% RH. After 600 cycles, the samples showed a drastic drop in the drill resistance of the first 1-1.5mm. The core of the sample remained unchanged (Figure 5-7).

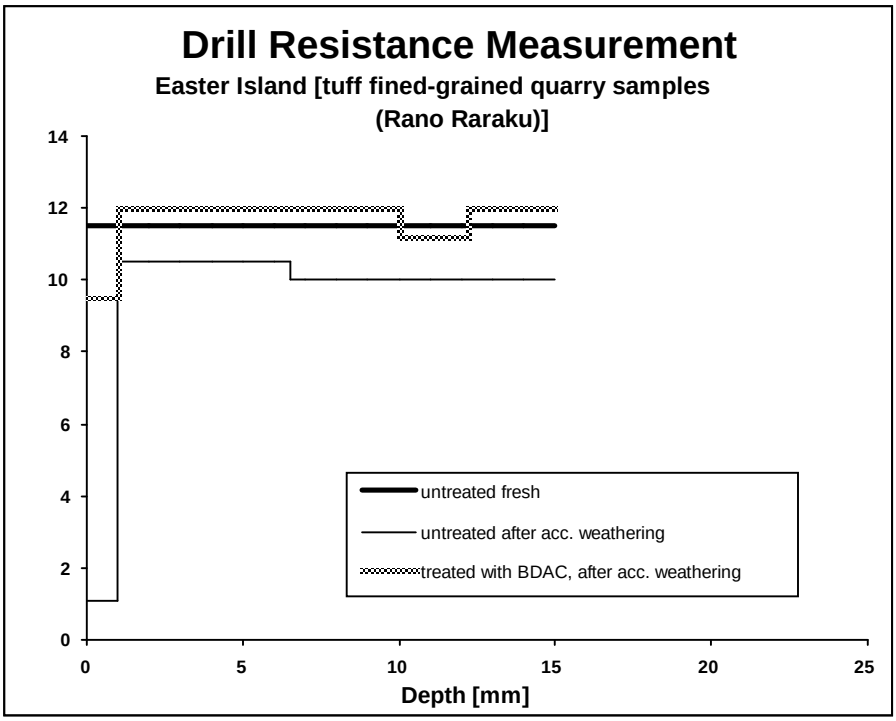

Figure 5-7. Adapted graph from Wendler et al (1996). Drill resistance measurement comparison between untreated, treated, weathered and unweathered tuff fined-grained quarry samples from (Rano Raraku), Easter Island. The weathering was composed 600 cycles in which the stones were 11h at 40°C/18%RH followed by 1 hour total immersion in water at 20°C.

More interestingly, they treated another series of samples of the same stone with a swelling reducing agent, a di-aminobutane di-hydrochloride (Wendler et al. 1991; Snethlage and Wendler 1991). This did not modify the water ingress or porosity of the sample, but significantly reduced the swelling. At the end of the same number of cycles, these samples only showed a slight reduction of the drill resistance in the outer part (Figure 5-7). This experiment clearly establishes that wetting and drying cycles can damage clay-bearing stones. Furthermore it demonstrates that swelling inhibitors may actively contribute to the reduction of this damage.

In our attempt to mitigate the consequences of wetting and drying cycles on the durability of clay bearing stones, and in particular of Portland Brownstone, we examined the use of diamino alkanes and amino alcohols (Jiménez González and Scherer 2004). The effectiveness of diamino alkanes as swelling inhibitors was first reported by Snethlage and Wendler (1991), who attributed this to a bridging of clay layers as illustrated in Figure 5-8. Recent X-ray diffraction experiments by Wangler (personal communication) indicate this interpretation may not be strictly correct (*viz*., the molecules lie parallel to the clay sheets) and that further research is needed to elucidate the mode of action of such molecules.

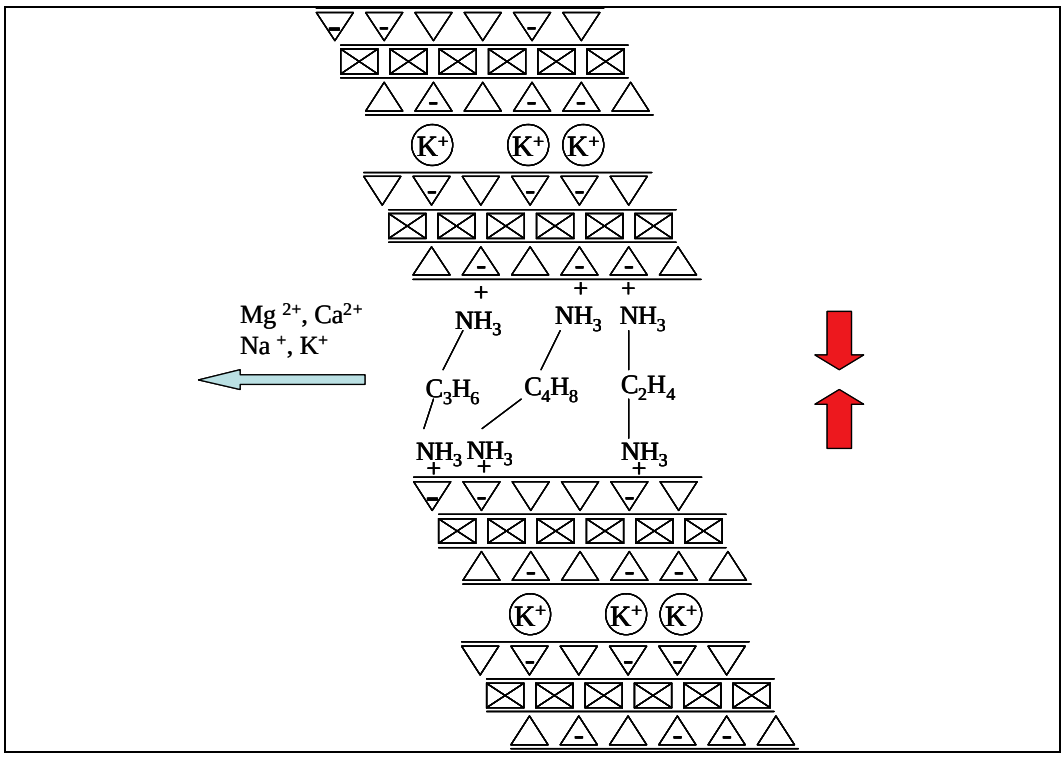

Figure 5-8. Illustration of the action in swelling inhibition as proposed by Snethalge et al (1991), where the diamino alkanes bridge the clay surfaces.

In our experiments, the diaminoalkanes used were 1,3 diaminopropane and ethylenediamine. These molecules are represented in Figure 5-9 both in the neutral and acidic form (with 2 HCl per molecule). In addition, we used a commercial corrosion inhibiting admixture based on aminoalcohols. This type of molecule is believed to enhance the resistance to wetting and drying cycles of stones that are subsequently consolidated with ethylsilicates (see section 6.4).

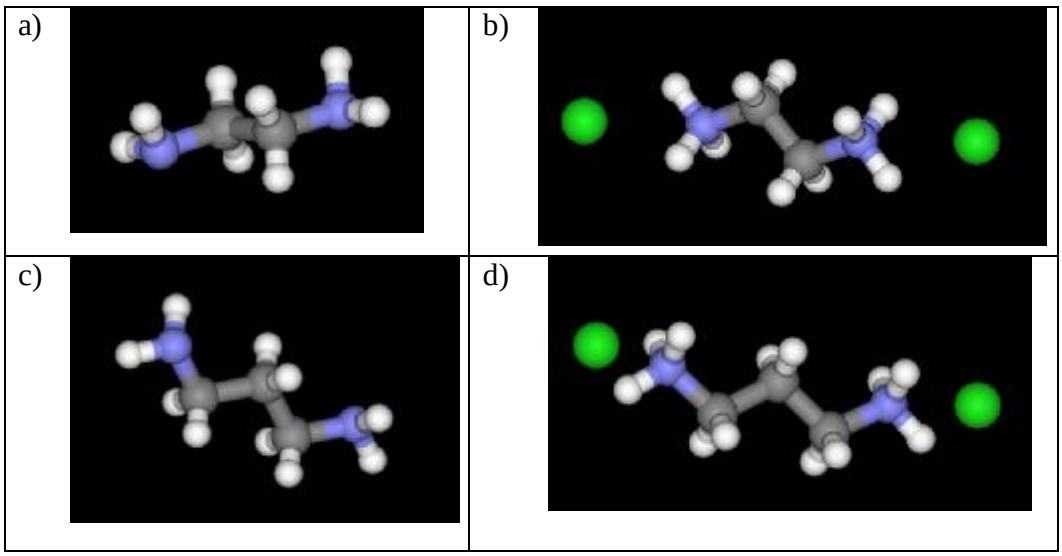

Figure 5-9. Structure of the diaminoalkanes used as swelling inhibitors.

(a) diaminoethane or ethylenediamine ($C_2H_8N_2$),
(b) acidified version of (a): ethylenediamine dihydrochloride ($C_2H_8N_2$. 2HCl)
(c) 1-3 diaminopropane ($H_2N(CH_2)3NH_2$).
(d) acidified version of (c):1,3 diaminopropane dihydrochloride ($H_2N(CH_2)3NH_2$. 2HCl).

In our experiments, we systematically find that larger proportional reductions are found for the stones with the largest swelling. This is rather good news in general for mitigating swelling, but also means that in the specific case of the Portland Brownstone, the swelling reduction (about 50%) is not as spectacular compared with other stones that have a swelling around three times higher (Wangler et al. 2006) and for which swelling reduction up to 80-90% can be obtained. Fortunately, these molecules are localized in the clays, so they do not make the stone hydrophobic, as indicated by the fact that the sorptivity is almost identical before and after such treatments. This means that they will not contribute to trapping water (coming, for instance, from capillary rise) and enhance freezing damage.

Measurements for selecting treatments can be accurately performed with an LVDT (Linear Variable Differential Transformer) or a DMA (Differential Mechanical Analyzer). In practical terms, the issue of whether such treatments remain effective over time is obviously of first importance. A partial answer to this question is to examine whether the products will wash out

over time when stones are subjected to cycles of wetting and drying. We have done this by building a specially designed machine to subject thin stone samples to multiple cycles of wetting and drying, after which the stone swelling was remeasured (Jiménez González et al 2006). We found that the swelling of the treated stones was slightly increased after 700 cycles, but remained well below the initial values of the untreated stone, indicating that the treatment does not get washed out during these cycles (Figure 5-10).

While the swelling experiments we have conducted are sufficient for us to infer durability differences, a more direct measure of degradation could be obtained with drill resistance as done by Wendler et al. (1996). It therefore appears that combining that measuring technique with our accelerated tests may be a way of delivering more readily interpretable results to conservators.

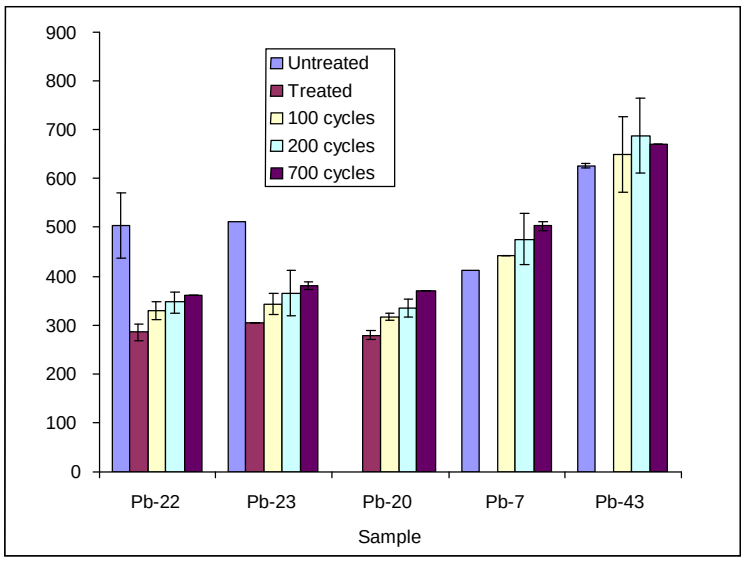

Figure 5-10. Evolution of the free swelling strain (direct measure) during the cycling (Jiménez González and Scherer 2006).

6 CONSOLIDANTS

6.1 General properties of stone consolidants

The term consolidant is used to describe products that conservators use to restore the mechanical strength (i.e. reestablishing the cohesion within the altered material and adhesion between the decayed and unaltered substrate) of weathered stones in a hope to increase the durability of the altered/deteriorated object or monument.

Many different types of products have been tested as consolidants (Amoroso and Fassina 1983; Price 1996; Wheeler 2005), including waxes, inorganic materials, silicones, vinyl and acrylic polymers and epoxy resins, among others. Nevertheless, their use is not always recommended and careful decisions have to be taken before performing such interventions, since they have been reported in some cases to lead to more damage than benefit over the long term (Wendler et al. 1991; Snethlage and Wendler 1991; Price 1996).

Some of the major properties that a consolidant must have are:

- Low viscosity in order to penetrate to a certain depth the porous stone
- Ease of application
- Hardening inside the stone
- Physical and mechanical properties that are compatible with the stone and prevent the consolidant from damaging the stone (e.g. thermal dilatation mismatch, etc.)
- No modification of the stone's appearance.

Two major types of consolidants have been most widely used by conservators. They are acrylic polymers (e.g. Acryloid or Paraloid B72) and ethylsilicates (e.g. Conservare OH).

In the first group, an acrylic thermoplastic resin is dissolved in a solvent and develops adhesive properties upon its evaporation. It is considered a reversible product, in that it can be

redissolved in the solvent at a later age; however, there are cases where, depending on the exact polymer structure, UV exposure can lead to cross-linking that prevents this redissolution and compromises reversibility (Laurenzi Tabasso 1995). Disadvantages of Paraloid B72 include a low penetration depth in stones, even very porous ones, and increased soiling in urban environments (Laurenzi Tabasso 1995). In addition, Furlan and Pancella (1983) found that after prolonged exposure to water, clay-bearing stones treated with such products exhibited a much higher swelling strain than the untreated ones. This suggests that these polymers intercalate between the clays and induce steric repulsion between the layers once these hydrate. This is clearly detrimental in terms of the associated stresses experienced by the stone as discussed previously.

Ethyl silicates are based on sol-gel chemistry. They consist of organosilane molecules, which undergo a condensation to produce an inorganic polymer (see Annex C for details). These consolidants are essentially the only class of product that conservators still have to restore mechanical properties of weathered stone. Nevertheless, it has been indicated by various authors, in particular by Félix (Félix 1988, 1994, 1995; Félix and Furlan 1994), that the effect induced by these products on clay-containing stones is rapidly lost when the stone is subjected to cycles of wetting and drying.

6.2 Consolidation progress

Ethyl silicate consolidants are applied in such a way that the product may soak into the stone's pores. After that, the stone is left exposed to the atmosphere. Water vapor molecules then trigger hydroysis and condensation reactions of the silicate oligomers. Ethanol is formed in this process and eventually evaporates. In field practice, the consolidant is generally applied either by brush or by spraying, and in more than one application. In the laboratory, samples are often fully saturated by immersion (total or partial) into a large enough amount of consolidant. This is the case of the

Portland Brownstone samples discussed below that were cut into thin (about 4 mm thick) and long plates in order to measure, among other properties, the elastic modulus by beam bending.

The advancement and extent of consolidation is often examined by ultrasonic methods, because of their non-destructive character. However, in view of the limitations of this technique already reported, we evaluated its pertinence for this purpose. Results in Figure 6-1 show the evolution of the dynamic elastic modulus measured by ultrasound (squares), the static elastic modulus measured by beam bending (diamonds) and weight fraction of consolidant lost over time (triangles). The two figures represent a stone sample previously treated with a swelling inhibitor (Figure 6-1b) and one not treated with it (Figure 6-1a).

The data clearly show that the static modulus continues to evolve, when the dynamic modulus has already stabilized. More interestingly, we observe that this evolution of the static modulus is more consistent with weight loss. Therefore, either of those measurements appears to be a better indicator of the progress of silicate condensation reactions than ultrasound.

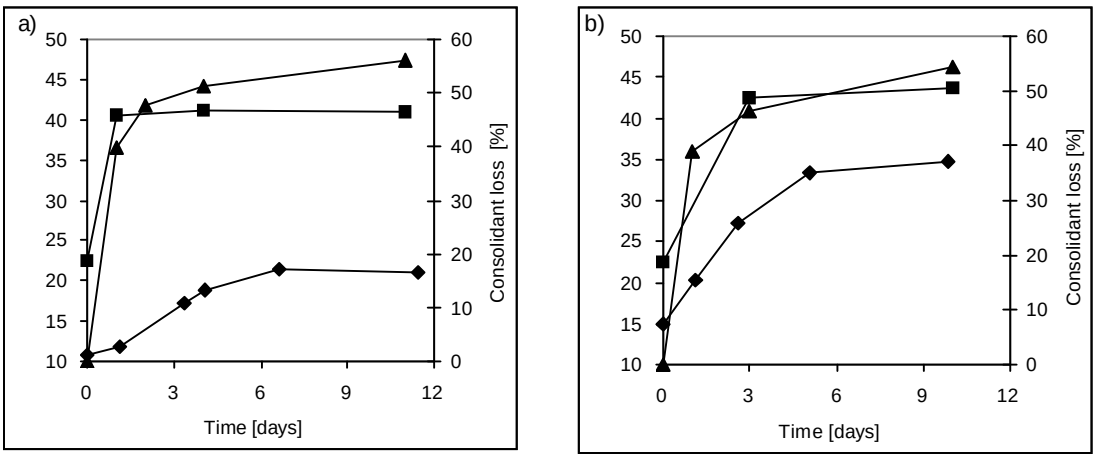

Figure 6-1. Evolution of the consolidation process of Portland Brownstone with an ethyl silicate. Triangles show the fraction of the weight of the added consolidant that is lost. Squares and diamonds respectively represent the dynamic and static elastic modulus.

It is clear that on a monument, neither beam bending nor weight loss are an option. Nevertheless, to judge how many consolidant applications are needed to achieve the required mechanical strength, one could consider carrying out beam bending and weight loss measurements in the laboratory ahead of time. In such a case, this ought to be done under representative environmental conditions (temperature, humidity, rate of air circulation, etc.) and using similar conditions of consolidant application.

6.3 Loss of consolidation

As indicated before, Félix studied quite extensively the loss of consolidation in clay-bearing stones of the Swiss plateau, showing that a couple of cycles of wetting and drying could be sufficient to cancel almost any benefit from consolidation. The same is true for Portland Brownstone as shown in Figure 6-2. Recently Wheeler (2005) has reported similar results for Portland Brownstone, although in that case the loss of consolidation required about 10 cycles, rather than the 2-3 indicated below. In Wheeler's experiments it is also worth noting that no difference of consolidation loss was seen between a *normal* ethyl silicate consolidant (Conservare-OH) and a partially hydrophobic one (Conservare-H).

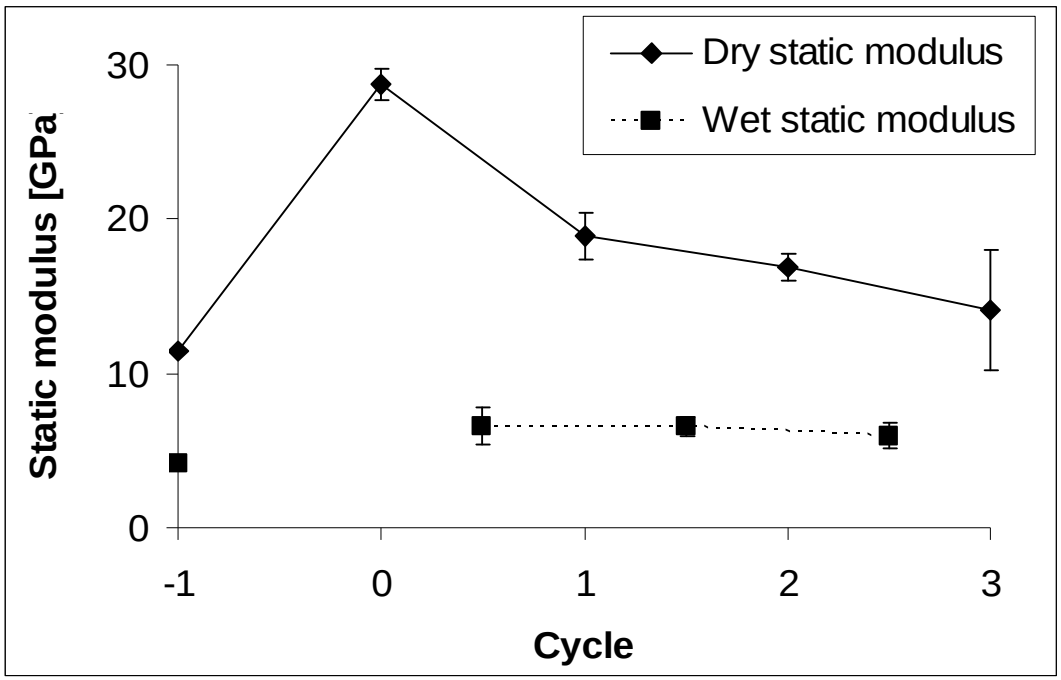

Figure 6-2. Evolution of the static elastic modulus of consolidated Portland Brownstone during wetting and drying cycles. The cycle –1 shows the stone modulus before the consolidation treatment. The cycle 0 shows the stone modulus after consolidation. Wet modulus measurements are reported at half cycles.

6.4 Effect of swelling inhibitors

Swelling inhibitors are effective in reducing the swelling strain of untreated stones as shown in section 5. Here we show the role that such treatments can play in increasing the resistance of consolidated Portland Brownstone to cycles of wetting and drying. The results illustrated in Figure 6-3 concern the evolution of the static modulus of thin plates. The average values from Figure 6-2 are reported with error bars corresponding to 95% confidence interval. These data, that represent samples not previously treated with a swelling inhibitor, are reported with open symbols. Two other data series are also illustrated. Both series were treated with mixtures of amino alcohol and diaminoalkane. The amount of diaminoalklane was constant but the aminoalcohol amount varied. The low aminoalcohol samples are indicated by gray symbols and

the high aminoalcohol series by black symbols. These swelling inhibitor treatments were applied prior to consolidation. The data plotted are the average of two samples (except for the last dry modulus value for the high amino alchohol). The error bars give the range of the two values measured.

It is apparent from the results below that the wetting and drying cycles reduce the static modulus of the consolidated stone whether it is dry (Figure 6-3a) or wet (Figure 6-3b), even if it has been treated with a swelling inhibitor prior to consolidation. Nevertheless, the modulus of the sample that received the treatment with the higher aminoacohol content shows better behavior than the reference. In addition, it is also apparent that the static modulus of the wet stone also remains substantially higher for the sample with a single swelling inhibitor treatment.

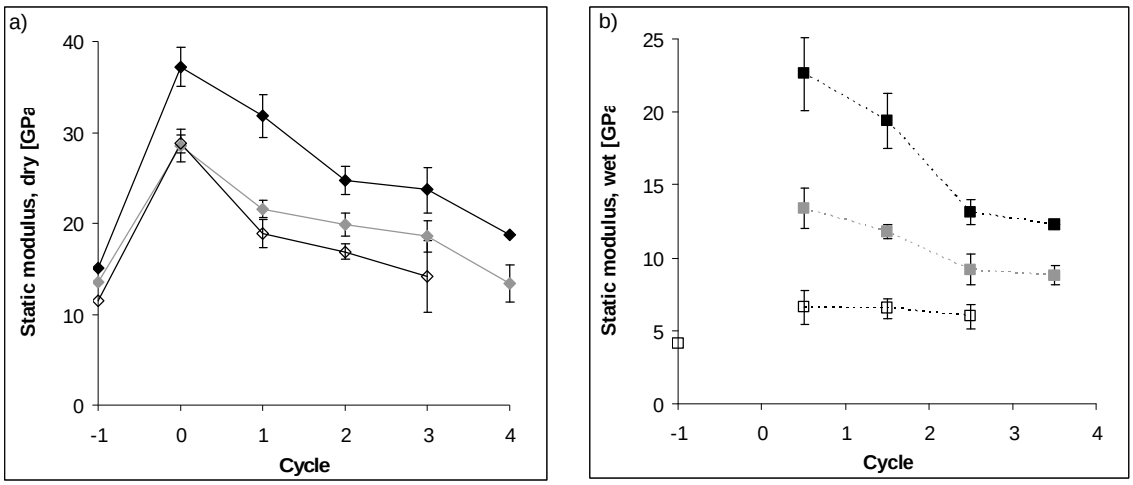

Figure 6-3. Evolution of the dry and wet static modulus of consolidated Portland Brownstone during wetting and drying cycles. a) dry samples, b) wet samples. The empty symbols represent stones that received no swelling inhibition treatment before consolidation. Error bars are a 95% confidence interval determined for the average of the fours samples measured at each cycle. The gray symbols represent samples that received a swelling inhibition treatment with a low amino alcohol content and the black symbols are those samples treated with a swelling inhibition mixture having a higher aminoalcohol content. In both cases, data are averages of two samples and the error bars give the range of values. (except for the last dry modulus at high amino alcohol content, where only one sample was measured).

In terms of field application, the long-term benefit of the swelling inhibition treatment prior to consolidation still needs to be confirmed, since these results only concern the first few cycles. However, since these are always the most devastating, there are good reasons to expect that such treatments can be beneficial. In addition, the tests were done using vacuum impregnation for the wetting and drying at 60°C, which are more dramatic conditions than what stones would be exposed to on a building.

The fact that the sample would remain stronger (as suggested by its greater stiffness), particularly in the wet state, could be beneficial in badly deteriorated samples, where the compressive failure during wetting may be an issue. It may also be useful in avoiding propagation of flaws in the process of buckling. In that case, a critical factor for the success of such treatments is to insure that the consolidant is applied in such a way that it will be effective at the depth where the flaw propagation is taking place.

7 CONCLUSIONS

In this work we have attempted to present a very general overview of the use and degradation of Portland Brownstone, indicating as much as possible to what extent various materials properties can be linked to observed damage patterns. By attempting this rather ambitious task, we wanted to highlight the multiple factors that affect degradation of buildings, taking the specific case of Portland Brownstone for its importance in the northeastern United States.

The link from field observations to established mechanisms of degradations is thus not trivial, since different mechanisms can lead to similar pathologies. However, establishing the correct mechanism is a crucial step in adopting adequate preventive conservation methods. One of the challenges for the future appears to be to understand the kinetics of damage, which requires coupling of chemistry, mechanics and transport in a multiscale model that will be capable of

representing adequately the alteration that can be expected on site. The necessity of including transport, for instance, is highlighted by the different degradation pathologies of Portland Brownstone blocks, according to the orientation of their bedding planes once placed on the buildings.

Given the complexity of this task, it is not surprising that contradictory conclusions can be reached when rather descriptive properties, such as granular texture, are used for classification of durability. Although within a restricted range of exposure conditions and for a given stone such approaches may prove useful, their generalization may be hazardous. Indeed, these *descriptive* properties may be associated with various material and/or transport properties, all of which may impact durability in different ways depending on exposure conditions.

Despite the complexity of the task we describe, increased understanding of decay mechanisms and their kinetics from laboratory studies can provide useful information on how to mitigate the extent of various degradation mechanisms. For instance, in the case of wetting and drying cycles, laboratory tests can perfectly identify the best candidate molecules to limit the extent of swelling. However, in order to avoid cases of so-called degradation by *good intentions and bad choices*, the ability to quantify behavior appears essential. Here again, we refer to the case of wetting and drying cycles. Our tests demonstrated for the first time that swelling pressures are largely limited by the viscoelastic character of these stones. It follows that conservation treatments should in principle also be studied for their impact on viscoelasticity.

The case of wetting and drying has been used to illustrate how quantification of degradation mechanisms can and should be developed. In our opinion, concerted efforts of this type between the scientific community and conservators are essential. We believe that it will lead to identifying reliably, from site to site, which degradation mechanism is most harmful and which treatment will prove most efficient. Although this is a very challenging task, we are convinced it can be met long before the standing buildings of Portland Brownstone will have disappeared.

ACKNOWLEDGEMENTS

The authors would like to thank Dr. George Wheeler (Metropolitan Museum of Art, NY) and Ivan Myjer for supplying very useful information about Portland Brownstone. We thank Dr. John Valenza and Tim Wangler for beam bending measurements on the consolidated samples, and Dr. Lucia Fernández Linares (formerly at the Geology Faculty of the University of Granada) and Dr. Thomas Füelman (EPFL) for the XRD analysis of the Portland Brownstone. The authors would also like to thank Mr. Fred Girardet for extremely useful discussions on the durability of clay-bearing stones. Support for Inmaculada Jiménez González was kindly provided by the Samuel Kress Foundation.

ANNEX A: GEOLOGICAL AND GEOGRAPHICAL PROVENANCE OF PORTLAND BROWNSTONE

As explained in the introduction, the literature abounds with different terminologies to designate Portland Brownstone. Because our study attempts to relate material properties of this stone to durability, some precision is needed to define what is referred to by "Portland Brownstone". For some people this might simply be any stone of brown color used in the late 1800s in the northeast USA. As stated also in the introduction, we designate Portland Brownstone as an arkosic sandstone with a characteristic brown-red color that belongs to the uppermost strata of the *Park River Member* of the Portland Formation and that is mainly obtained from the Portland quarries.

More detailed information about this stone is given in this annex, which summarizes essential information and key references on the subject. While not pretending to be exhaustive, we attempt to give a clear and synthetic picture about the geological and geographical provenance of this stone. In doing so, our main sources for depositional environments, sedimentology, stratigraphy and tectonic history of Portland Brownstone were basically Hubert et al. (1982); Krynine (1950) and Olsen et al. (2005). Some of the bibliographic sources consulted are based on paleontological findings. The study of plants and animal fossils allow reconstructing original environments (Abrams and Riley 2002) that give very valuable information also about sedimentology and stratigraphy of geographical units. In that respect, Olsen et al. (2005) say that Portland Brownstone quarries have provided numerous reptile footprints (Hitchcok 1865) and dinosaur bone casts (Colbert and Baird 1958).

Lastly it is worth pointing out that the stratigraphic information gathered from the sources after 1990s is very reliable since it comes from the analysis of cores drilled on the lowermost part

of the Portland Formation (Olsen et al. 2005) during the *Newark Basin Coring Project* (LeTourneau 2003). In contrast, there is relatively little information existing about the Portland Brownstone sandstones structure and sedimentology, which Olsen et al. (2005) attribute to the difficult accessibility of the quarries since the 1930s floodings.

To find the geological origin of Portland Brownstone, we follow a linear chronological path that takes us back to the end of the Paleozoic Era. At that time, one of the first mountain-building processes results in the formation of the Appalachian Mountains (around 680 million years ago) which are the basis for the Eastern and Western Highlands as well as the Central Lowland of the Connecticut valley (Abrams and Riley 2002). It is a period of numerous plate collisions that initiates with the birth of these mountains and culminates with the formation of the supercontinent Pangea (Alter 1995). The following Era, the Mesozoic, also continued to be very dynamic in terms of plate tectonics, the forces of which this time, through a reversal process, lead to the break up of Pangea. As a consequence, intense deformation processes (folding, faulting, etc) result in a new earth morphology. In that period, a series of rift basins or half-graben are created along the eastern coast of the present USA. According to Hubert et al. (1992), they extend for more than 2000 km from the southeastern USA (North Carolina) into eastern Canada (Nova Scotia) and are known as the Newark Supergroup (Figure A-7-1). Such rift valleys were eventually filled with continental deposits (lacustrine, fluvial, paludal and playa) strata of Upper (late) Triassic age (Krynine 1950; McInerney and Hubert 2003).

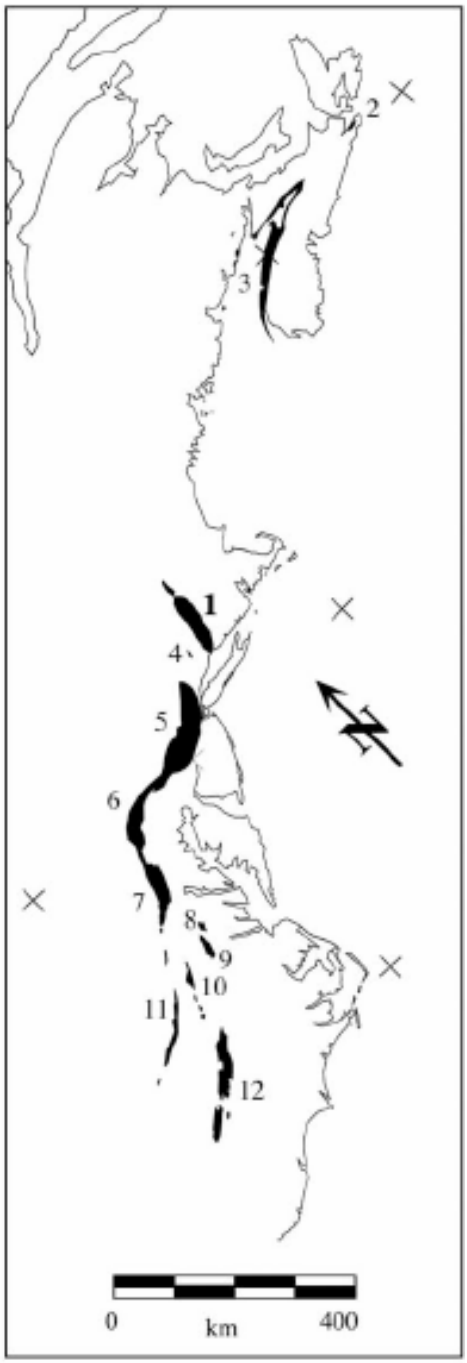

Figure A-7-1. Illustration of the location of the Newark Supergroup.(reproduced from Olsen et al, 2005)

1) Hartford and Deerfield basins

2) Chedabucto or Orpheus basin

3) Fundy basin

4) Pomperaug basin

5) Newark basin

6) Gettysburg basin and mostly buried

7) Culpeper basin

8) Taylorsville basin

9) Richmond basin

10) Farmville and associated basins

11) Dan River basin;

12) Deep River basin.

One of the largest exposed rifts is the Hartford Basin (Figure A-7-1, #1, Figure A-7-2), formed around 220-195 million years ago (Late Triassic / Early Jurassic). It extends 140 km north to south and 30 km east to west and has a thickness of about 4 km (Guinness 2003). Olsen et al.

(2005) report in detail the geographical location of this formation, which is reproduced in Figure A-7-2. A detailed description of the stratigraphy and paleogeography of the basin is reported by Hubert et al. 1992. The uppermost sediments of this basin comprise what is currently known as the *Portland Formation*.

Prior to the 1970's the *Portland Formation* was known under other names. For example, Krynine (1950) denominated it *Portland Arkose* but in 1977 Leo et al. (in Olsen et al. 2005) point out that various lithofacies could be distinguished in it and a new denomination of *Formation* was found to be more appropriate.

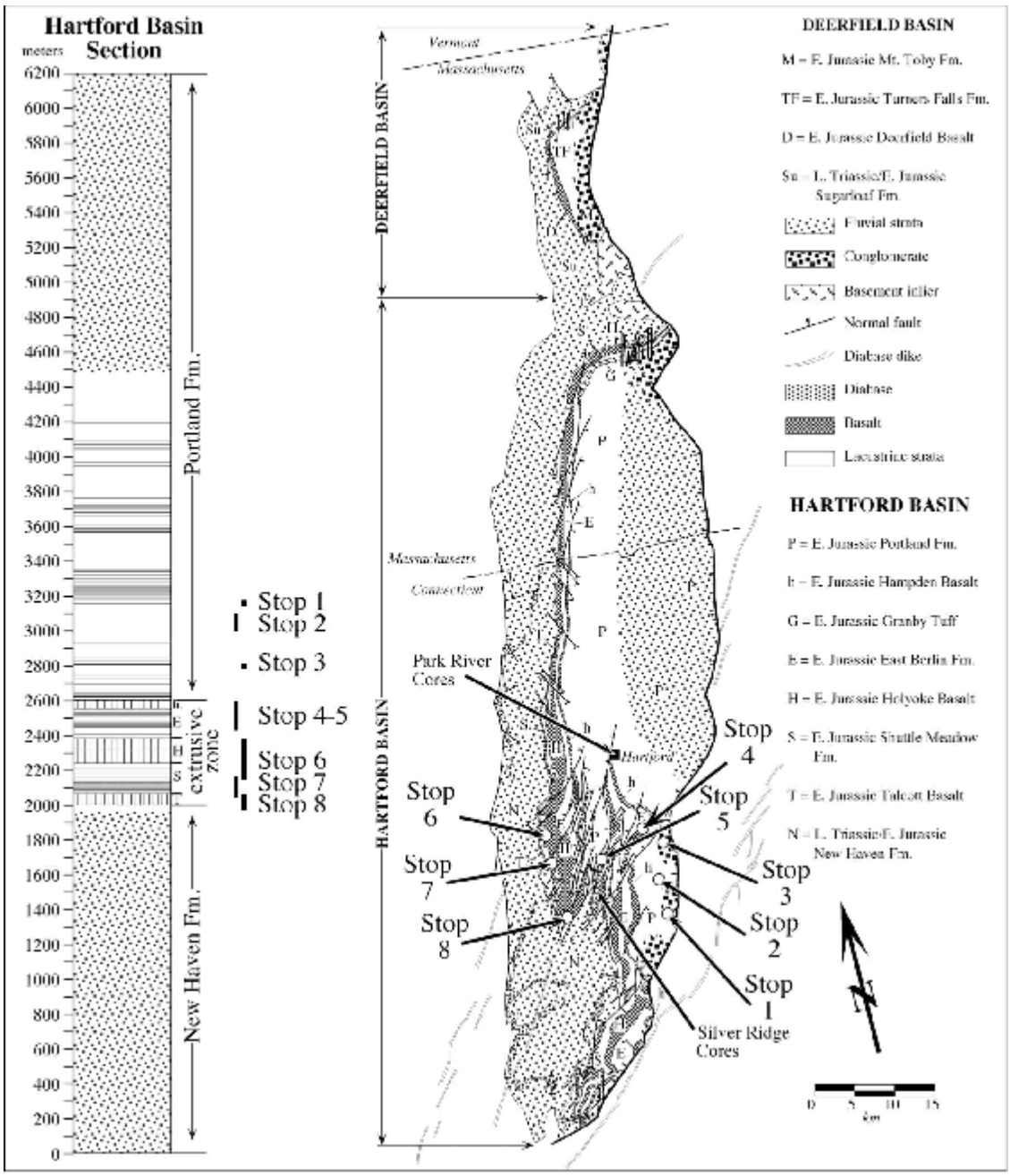

Figure A-7-2. Location of the Hartford Basin reproduced from Olsen et al. 2005. It can be seen how this formation overlaps the states of Vermont, Massachusetts and Connecticut. Furthermore the location of the main Portland Brownstone quarries are indicated on the stop n.2

According to Olsen et al. (2005), this formation is of Hettangian age (200 Ma) and ranges in thickness from ≅ 450 m in Southern Connecticut to ≅ 1 km in the vicinity of Middletown, to as

much as ~4 or 5 km thick in the central portion of the Hartford basin north of Hartford and in south-central Massachusetts. In a first stage, it can be divided into an upper and a lower part of similar thickness (about 2 km each). The Portland Brownstone sandstone we are interested in crops out in red and brown fluvial and eolian[10] strata that alternate in intervals about 15 m thick (Olsen et al. 2005). It belongs to the lower (older) part of this Portland Formation, which in its complex comprises cyclical lacustrine and marginal fluvio-lacustrine red, gray and black clastic rocks. This older part is subdivided into five informal members (Olsen et al 2005). The fourth lowest is known as the Park River member, whose Upper part is the source for Portland Brownstone (Figure A-7-3). The red beds of Portland Brownstone can be found mainly near Middletown in the well-known Portland Brownstone Quarries. The same beds but in the northern and southern portions of the Hartford basin are outcropping also in the quarries of South Hadley, Massachusetts (Olsen et al. 2005).

[10] Eolian deposits are a significant component of this sequence, which means that Portland Brownstone contains sedimentary features attributable to sands sheets and dunes. Eolian beds were preferred for building stone, because of their grain size and texture. (Olsen et al. 2005)

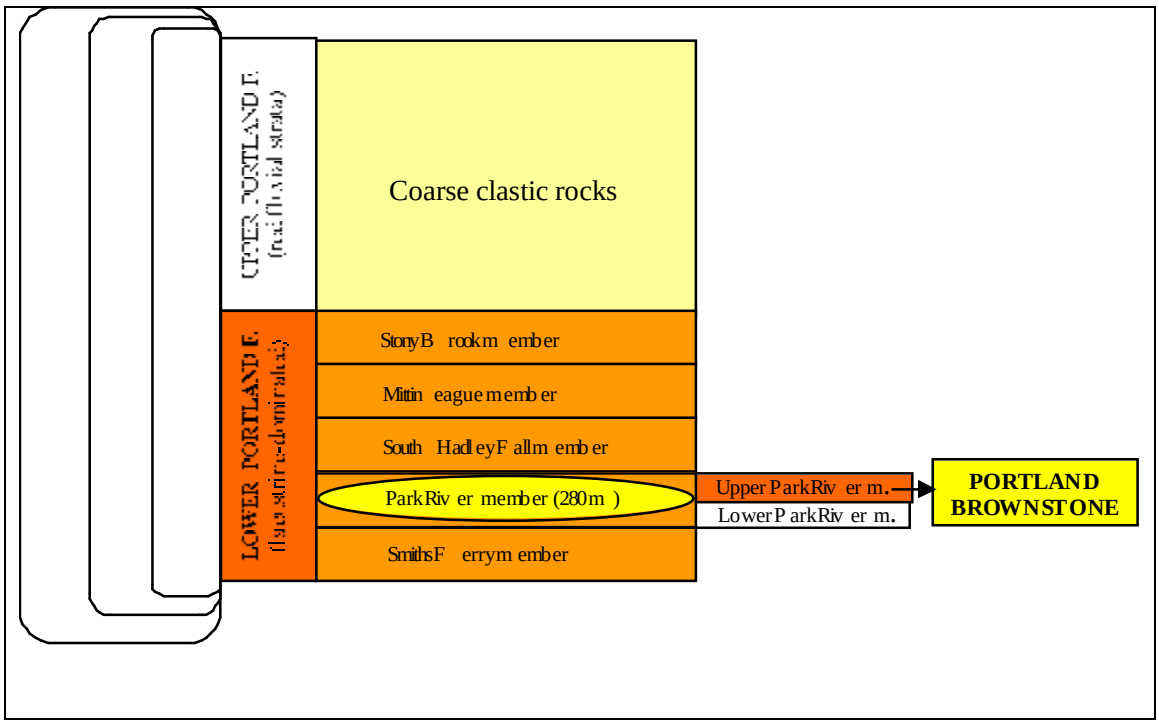

Figure A-7-3. Schematic representation of the position of the Portland Brownstone sandstone in the stratigraphy of the Newark Supergroup. Informal division of the Lower part of the Portland Formation into members. The upper part of the Park River Center exposes Portland Brownstone

ANNEX B CLAY STRUCTURE AND SWELLING

B.1 Introduction

This section explains what clays are and why some clay minerals can swell or shrink depending on whether water is added or removed. Not all clays behave like this. Those that do are referred to as swelling or expandable clays. Their behavior is linked to the surface properties of clay minerals, which in turn, depends on their structure. The understanding of what causes the swelling helps to indicate ways to avoid or reduce it, in particular what additives (swelling inhibitors) might help to mitigate the swelling and prevent damage of stones that contain swelling clays.

Much of what is presented in this annex is based on Madsen and Müller-Vonmoos (1989) and course notes by Eslinger and Pevear (1988).

B.2 Formation of clay minerals

To begin this section, the terminology “clays” and “clay minerals” must be clarified. The term “clays”, as used by most geologists according to the Atterberg or International and USDA (United State Department of Agriculture) granulometric standards of soils components, refers to all kind of material, independently of its chemical or mineralogical composition, that has a grain size smaller than typically 2 µm.

A more recent definition proposed in a joint report of the AIPEA (Association Internationale Pour l’Études Argiles) and the CMS (Clay Minerals Society) does not include particle size. The version reproduced is the result of various revisions and was given by Guggenheim and Martin (1995):

The term “clay” refers to a naturally occurring material composed primarily of fine-grained minerals which is generally plastic at appropriate water contents and will harden with dried or

fired. Although clay usually contains phyllosilicates, it may contain other materials that impart plasticity and harden when dried or fired. Associated phases in clay may include materials that do not impart plasticity and organic matter.

On the other hand, from the mineralogical point of view, clay minerals are crystalline aluminosilicates with a layered structure, sheet-like habit and with colloidal particle sizes ranging from nanometers to a couple microns. They "can" contain various amounts of water and allow more ionic substitutions than other minerals within in the same group of phyllosilicates. The terminology "clay minerals" only applies to the later definition. In the report of Guggenheim and Martin (1995) clay minerals are defined in a way to incorporate any yet unknown minerals that might exhibit plasticity and harden upon drying or firing. Their definition is:

The term "clay mineral" refers to phyllosilicate minerals and to minerals which impart plasticity to clay and which harden upon drying or firing.

In this manuscript, the term "clay" always follows the mineralogy definition (otherwise it is specified).

Clays are products of the water-rock interaction processes. Most of them find their origin in instabilities in other silicate minerals and result from weathering of primary silicate minerals or other clay minerals (incongruent dissolution, hydrolysis, erosion), burial diagenesis (effects of chemical and thermal changes), recrystallization processes, hydrothermal alterations (occurring at temperatures between 100-250 °C) and precipitation from concentrated solutions (Velde 1992).

The formation of important clay minerals is illustrated in Table 4a, which shows how montmorillonite, illite and kaolinite can form from the alteration of feldspars. The process is, however, more general and leads from primary minerals such as mica, muscovite, feldspar, etc., to intermediate ones, such a vermiculite, and finally to secondary clay minerals, such as kaolinite,

illite, montmorillonite, etc. The more specific case of the transformation of potassium feldspar to kaolinite is also illustrated in Table 4b.

Table 4. Illustration of weathering processes, where primary minerals, such as feldspars, can transform into clay minerals, such as montmorillonite, illite or kaolinite. a) General scheme adapted from Smith (1999), b) Kaolinite formation scheme showing more chemical details, adapted from Velde (1992).

a)

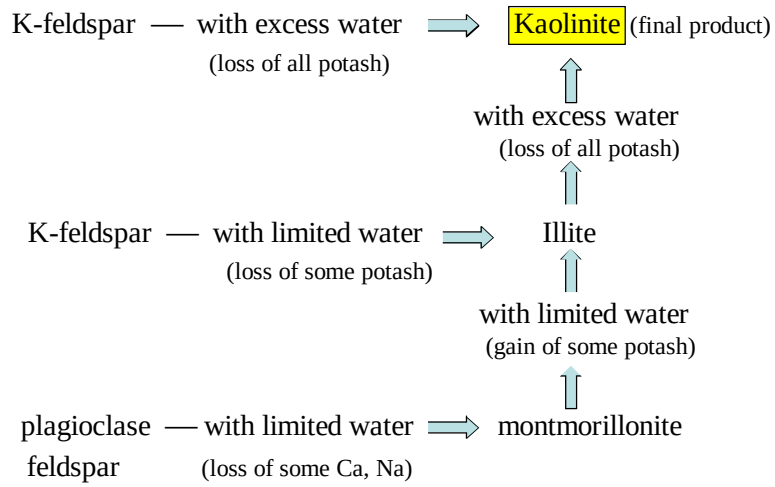

b)

$$K-\text{feldspar} + H^+ \rightarrow \text{hydrous clay} + K^+ + \text{Si ions}$$

$$3\,KAlSi_3O_8 + 6H^+ \rightarrow Al_3Si_3O_{10}(OH)_6 + 3\,K^+ + 6\,\text{Si ions}$$

feldspar — kaolinite

B.3 Structure of clay minerals

B.3.1 General structure

Clay minerals have a phyllosilicate or layered structure. These layers are composed of silicon or aluminum cations, which are respectively coordinated tetrahedrally or octahedrally by oxygen atoms (Figure A-7-4). These tetrahedra or octahedral arrange themselves in periodic 2D arrays, sharing oxygen atoms. This is illustrated for the case of a silicate sheet in Figure A-7-5.

The arrangement of layers of silicate and aluminate can be explained starting with Figure A-7-5. On top of the silicate sheet illustrated, an aluminate sheet can be placed that shares the upper oxygen atoms. These oxygen atoms form hexagonal rings at the center of which comes an OH group shared between aluminates as illustrated in Figure A-7-6. On the outer side of the silicate layer (lower side in Figure A-7-5), hexagonal rings of smaller dimension can also be seen in Figure A-7-6. This forms a cavity that can stabilize some cations, in particular potassium, through optimum sharing of electrons from the oxygens in those rings. A symbolic representation of one of these types of clays is given in Figure A-7-7. One distinguishes two main classes:

1) 1:1 layer clays or T-O

   In these clays, a layer is composed of the superposition of a sheet of tetrahedrally coordinated silicon, T or S, and a sheet of octahedrally coordinated aluminum, O (termed also gibbsite sheet, G) and/or magnesium (also called brucite, B). This gives the notation T-O, S-G or S-B for these clay minerals.

2) 2:1 layer clays or T-O-T

   In these clays, a layer is composed of the superposition of a sheet of octahedrally coordinated aluminum, O, or magnesium, M, sandwiched between two sheets of tetrahedrally coordinated silicon, T. This gives the notation T-O-T, S-G-S or S-B-S to these clay minerals.

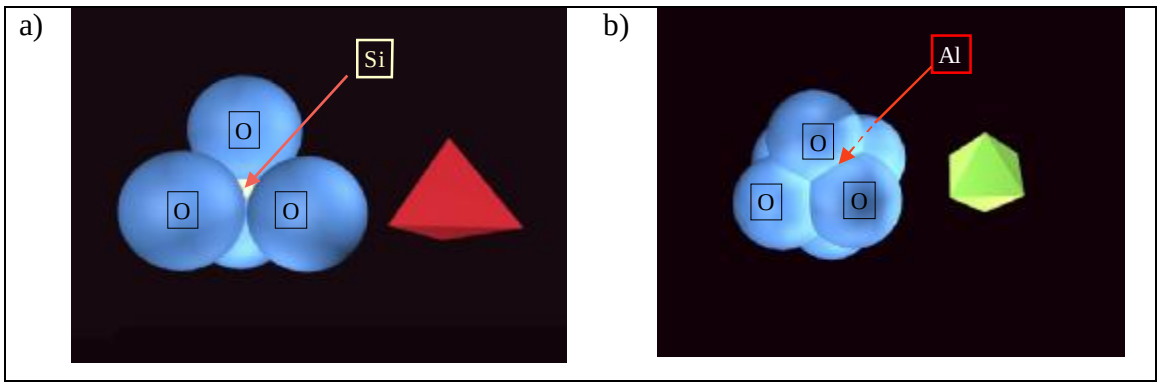

Figure A-7-4. Illustration of the basic units that form a clay sheet: a) the tetrahedrally coordinated silicon, and b) octahedrally coordinated aluminium.

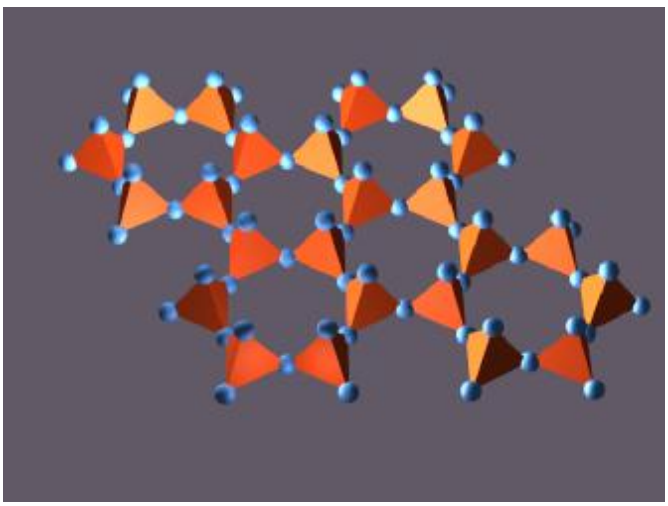

Figure A-7-5. Illustration of a silicate sheet.

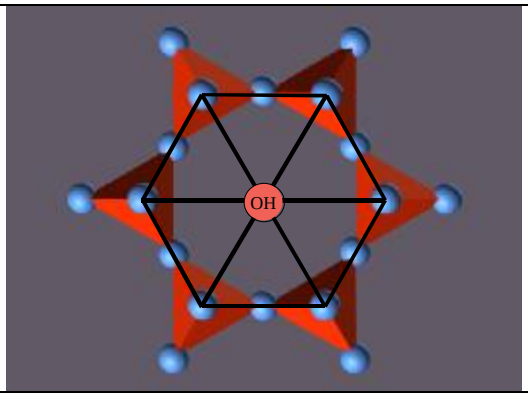

Figure A-7-6. Illustration of hexagonal rings formed by a silicate sheet. At the bottom a smaller ring is formed and its dimension can stabilize potassium ions as explained later. Above, a larger hexagonal ring of oxygen atoms is shared with the aluminate sheet and an OH group from that layer fits in the centre of it.

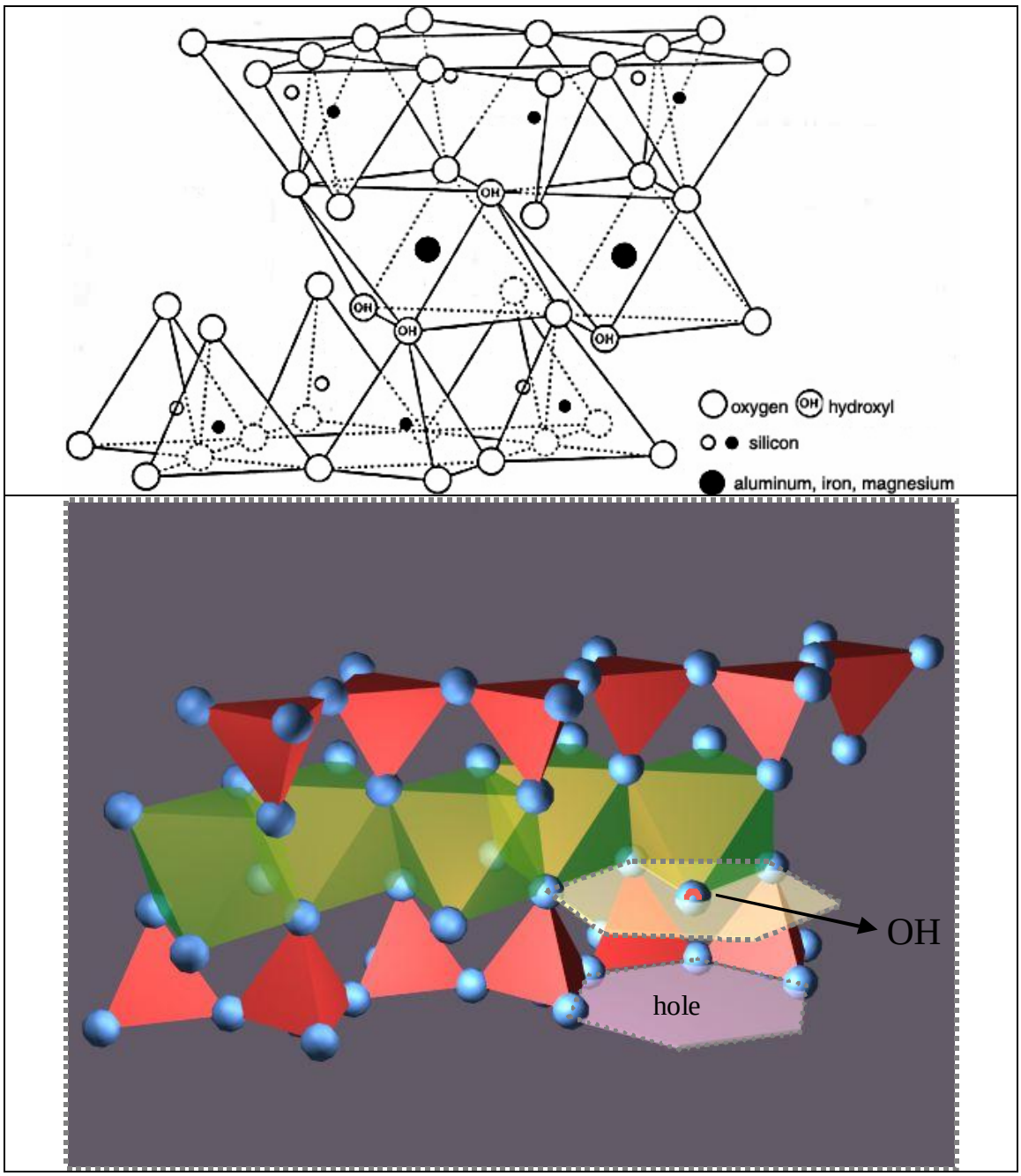

Figure A-7-7. Illustration of a layer of a T-O-T clay. The location of an OH group from the aluminate layer in the hole left in the upper part of the silicate layer is illustrated.

In Figure A-7-7, the disposition of a layer of a T-O-T type clay is shown. The positioning of the OH group is highlighted, as well as the hole left in the bottom part of the silicate sheet. Based on this structure, various definition of clay groups can be found. A broadly accepted classification

can be found in the "Report of the clay minerals society nomenclature committee". The proposed classification for planar hydrous phylosilicates is given Table 5, adapted from Martin et al. (1991). It is based on: a) the type of silicate layer present (1:1 or 2:1), b) the magnitude of the net charge (x) per formula unit, and c) the interlayer material that compensates the layer charge. The terms di- and tri-octahedral define the cases where, for a unit cell, the 6 charges of the octahedral layer (from the three oxygens) are balanced respectively by two trivalent cations (case considered up to now with Al^{3+}) or by three divalent cations.

Table 5. Clay of planar hydrous phyllosilicats as proposed by Martin et al (1991). The groups that were found in Portland Brownstone are indicated in bold as well as the species when identified.

Layer type	Interlayer Material*	Group	Octahedral Character	Species
1:1	None or H_2O only (x ~ 0)	Serpentine-kaolin	Trioctahedral	Lizardite, berthierine, amesite, cronstedtite, nepouite, kellyite, fraipontite, brindleyite
			Dioctahedral	Kaolinite, dickite, nacrite, halloysite (planar)
			Di-trioctahedral	Odinite
2:1	None (x ~ 0)	Talc-pyrophyllite	Trioctahedral	Talc, willemseite, keolite, pimelite
			Dioctahedral	Pyrophyllite, ferripyrophyllite,
	Hydrated exchangeable cations (x ~ 0.2-0.6)	**Smectite**	Trioctahedral	Saponite, hectorite, sauconite, stevensite, swinefordite
			Dioctahedral	Montmorillonite, beidellite, nontronite, volkonskoite
	Hydrated exchangeable cations (x ~ 0.6-0.9)	**Vermiculite**	Trioctahedral	Trioctahedral vermiculite
			Dioctahedral	Dioctahedral vermiculite
	Non-hydrated monovalent cations (x ~ 0.6-1.0)	**True (flexible) mica**	Trioctahedral	Biotite, phlogopite, lepidolite, etc.
			Dioctahedral	**Muscovite, illite**, glauconite, celadonite, paragonite, etc.
	Non-hydrated divalent cations (x ~ 0.6-1.0)	Brittle mica	Trioctahedral	Clintonite, kinoshitalite, bityite, anandite
			Dioctahedral	Margarite
	Hydroxide sheet (x = variable)	Chlorite	Trioctahedral	Clinochlore, chamosite, pennantite, nimite, baileychlore
			Dioctahedral	Donbassite
			Di-trioctahedral	Cookeite, sudoite
2:1	Regularly interstratified (x = variable)	Variable	Trioctahedral	Corrensite, aliettite, hydrobiotite, kulkeite
			Dioctahedral	Rectorite, tosudite

B.3.2 Ion Substitutions

The structure described above gives the generic structure and composition of clay minerals. Most clay minerals, as well as other phyllosilicate structures, during their genesis have some extent of isomorphous substitution of either silicon or aluminum by various other ions. These can be Mg^{2+}, Fe^{2+}, and less frequently Fe^{3+} for the Al^{3+}. For the Si^{4+}, substituting ions can be Al^{3+}, or Fe^{3+}. These substitutions are dictated by the size of the ions as illustrated in Figure A-7-8.

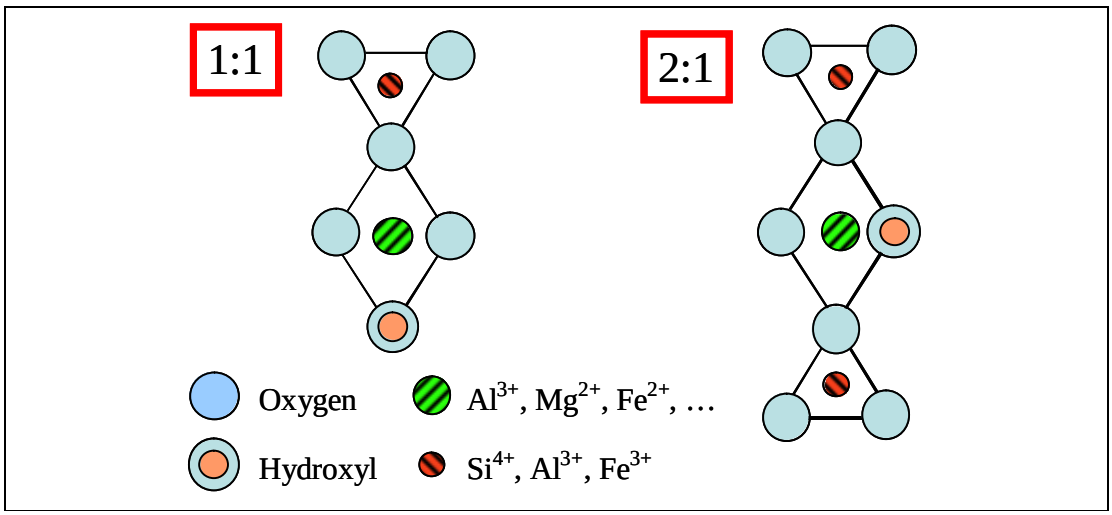

Figure A-7-8. Illustrations of the type of ion substitution that can take place in the structure of 1:1 or 2:1 clay minerals.

The most important result of these substitutions is that they introduce a charge deficiency. In the case of a clay mineral, this means that a layer with substituted ions has a net negative charge. This negative charge is compensated by various cations taken from the surroundings during formation and possibly exchanged with it after that. They arrange themselves at the surface of the clay layers and are called counterions or compensating ions. The ensemble clay plus counterions is neutral. However, these balancing ions are not fixed into the layer structure by covalent bonds as the other atoms are, but by electrostatic bonds (coulomb forces). These bonds are subject to dissociation in presence of water and the consequences of this are discussed later.

The other result of ion substitution in clays is a destabilization of the structure, because it deforms their crystalline arrangement. Clay minerals with extremely low substitutions can be very large, while those with more substitutions are smaller. The higher the extent of substitution, the smaller is the size of the layer. Thus most clays have a highly disorganized structure (poorly crystalline) and high specific surfaces in the range of 15 m^2/g to 300 m^2/g.

B.3.3 Surface area

Because of their platy shape and small size, most clays have rather large surface areas. In addition, for some processes, the internal surface area (between the layers of a given particle/ interlayer surfaces) is important. This part of the surface area cannot be measured by the traditional nitrogen adsorption technique. This is because sample preparation leads to a collapse of the layer such that no N_2 molecules can enter. Internal surface area can, however, be measured by the adsorption of some polar molecules, such as water or ethylene glycol.

B.3.4 Surface charge

It was mentioned before that one does not only need to consider swelling between layers of a given particle, but also interparticle swelling. The charge of the interlayer space in a given particle is of structural origin and is therefore permanent. The charge at the exterior surfaces of these particles can be structural or result from the presence of potential determining ions. The latter is a non-permanent charge.

The term “potential determining ions” refers to ions whose presence modifies the potential of a given surface. The charge of most surfaces is sensitive to pH, so H^+ and OH^- are then considered as potential determining ions. Because this is the case for so many oxide surfaces, the pH at which their charge is zero is used as a characteristic of these surfaces, called the zero point of charge (ZPC). At pH values above the ZPC the surface is negative (more OH^- than H^+ at the surface) and below the ZPC the surface charge is positive (more H^+ than OH^- at the surface).

In clays, the basal surfaces do not have the same ZPC as their edges. Below the lowest ZPC or above the highest ZPC, basal and edge surfaces have the same sign and repel each other. Between the two ZPC, basal and edge surfaces have opposite charges and attract each other. For example if the side and edge ZPC were 4 and 6, then repulsion would be observed below pH 4 and above pH 6, while attraction would be seen among basal and edges surfaces between pH 4 to pH 6.

Experimentally the ZPC is determined by titration, measuring zeta potential versus pH. This technique cannot separate the contributions from the different surfaces to the measured potential. It therefore gives a ZPC, which is an average between the different surfaces of the titrated mineral. Finally, it must be noted that this pH dependent charge accounts for less than 1% of the total charge in 2:1 swelling clays such as smectites, which are of primary interest with respect to swelling of stone.

B.4 Swelling of clays

B.4.1 Crystalline swelling

The hydration of cations in the interlayer, or so-called cohesion layer, causes clays to swell. This first part of clay swelling is a crystalline swelling (also known as innercrystalline, interlayer or intraparticle swelling). It is experienced by clays denominated as swelling or expandable clays (e.g. smectites). The magnitude of the swelling strain depends on the number of layers of water that are coordinated around the charge compensating cations. This is why it takes place in more-or-less discrete steps and why its extent is limited. Indeed, after the first hydration layer, the coordination of more water molecules becomes much less favorable. Some hydrogen bonding to the inner layer is possible because of the orientation of the water molecules around the cations. However, the importance of this is limited and crystalline swelling rarely causes layers to move apart by more than about four water molecules layers (about 1 nm).

This swelling is resisted by the attractive forces that, in the absence of water, hold the clay layers together and are both of van der Waals (electromagnetic) and electrostatic origin. Crystalline swelling takes place if the hydration of cations and pushing apart of the layers is more favorable than keeping the layers together and not hydrating the cations.

Kaolinite, for example, does not undergo crystalline swelling. The reason is that this clay mineral has an almost zero structural charge. Thus, it does not have enough hydratable counterions to make it favorable to move layers apart.

Other "non-swelling" clays typically have potassium (K^+) as charge balancing cations. This is because the potassium cation has just the correct size to fit between the hexagonal cavities at the exterior of the silicate sheets (bottom ring in Figure A-7-6). It therefore already interacts with many oxygen atoms that can stabilize its charge. As a result, the hydration of potassium by water molecules is not favorable and crystalline swelling does not take place, or is at least much reduced, in clay minerals with that counter ion (ex: illite).

B.4.2 Osmotic swelling

It was mentioned above that the extent of crystalline swelling is limited. However, clays can swell considerably more than the approximately four water molecule layers mentioned above. The process responsible for this additional expansion is osmotic swelling, also referred to as electrostatic or double layer repulsion. It can take place between clay layers or particles. Therefore, it concerns both "swelling" and "non-swelling" clays, such as kaolinite for instance. Although the charge-compensating cations in kaolinite are too few to make their hydration favorable between clay layers, at the exterior of particles, where the contact with other particles is less strong, cations hydrate and surface charging can take place more easily. It is explained below that the origin of osmotic swelling is the dissociation of these cations. The principle behind this mechanism of repulsion is as follows.

If a salt solution is put in contact with pure water, the natural spontaneous process is for the two to mix. Pure water molecules would move towards the salt solution and dissolved salt (anions and cations) would move towards the pure water until the composition becomes homogeneous. In the case of clays, there are more mobile cations than anions needed to balance the structural charge of the clay surfaces. Because of electrostatics, the excess of cations cannot move out and away from the clay surface unless other cations come in. If the system is in contact with pure water, then the natural process of mixing mainly takes place by water moving into the interlayer space. This is what causes the so-called osmotic swelling.

The calculation of the osmotic force requires determining the distribution of charges in solution away from the surfaces. The so-called Double layer Theory is used for this (Figure A-7-9). It assumes that those ions can be separated into two layers. In the first layer, called the Stern layer, the ions are largely fixed. In the second layer, called the Gouy-Chapman layer, the ions are mobile. It is from the distribution of charges in that second layer that the osmotic force can be calculated. That distribution is affected by the electrostatic potential (charge) of the Stern layer[11], the overall ionic concentration and the valence of the ions.

[11] Physically, the electrostatic potential of a surface represents the energy (work) that has to be provided to move (transfer) a negative charge from the surface to an infinite distance from it, where the charge and the surface will not interact. A negative value means that this process is favorable and corresponds to negative surfaces (it is favorable to move a negative charge away from a negative surface). A positive value means that moving the charge away is not favorable. This corresponds to positively charged surfaces that do not want to let negative charges be moved away from them.

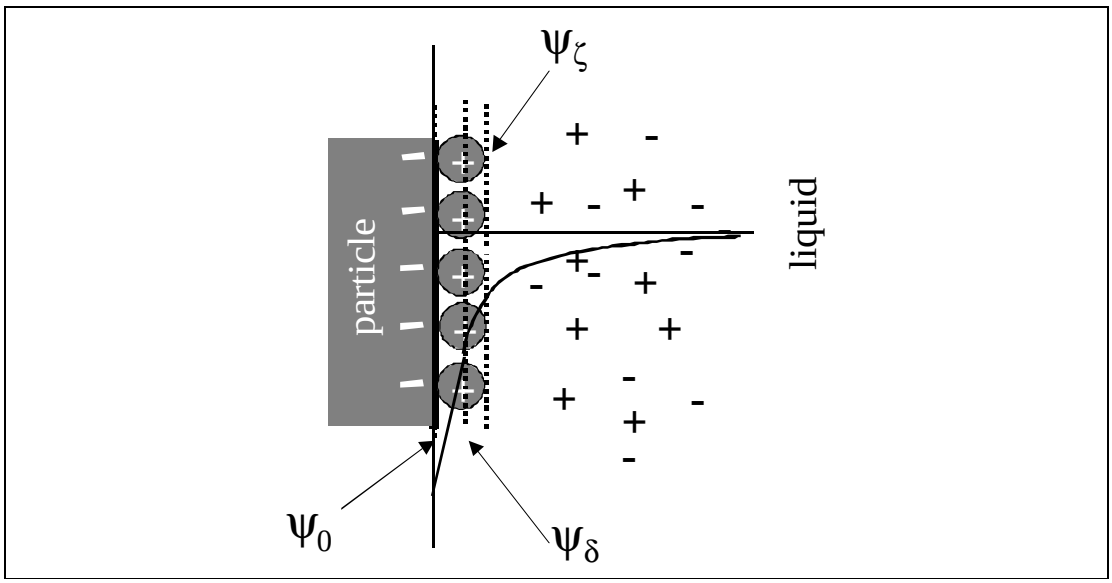

Figure A-7-9. Distribution of charges away from a negatively charged surface. The circles marked + represent the cations in the Stern layer and are considered fixed to the surface. The electrostatic potential is negative at the surface (ψ_0) and becomes progressively less negative as the distance from the surface increases (continuous line). In the Stern layer the potential changes linearly until it reaches the Stern potential (ψ_δ). After that, the decrease is nonlinear. The zeta potential (ψ_ζ) is the potential that can be measured experimentally and corresponds to a distance farther away from the surface than the Stern potential.

An important parameter in the calculations of the osmotic force is the electrostatic double layer thickness. It is noted κ^{-1} and is calculated from the ionic concentrations as follows:

$$k^{-1} = \sqrt{\frac{e_r e_0 k_B T}{e^2 \sum_i z_i^2 n_i}} \tag{2}$$

where e_0 is the permitivity of vacuum (8.854 10^{-12} $C^2N^{-1}m^{-2}$), ε_r is the relative permitivity of the liquid (80 for water), z_i and n_i are respectively the valence and the concentration (per unit volume in m^{-3}) of ions of species i, N_A is Avogadro's number (6.02 10^{23}) and e is the charge of an electron (1.602 10^{-19} C). One can also write this expression as a function of the ionic strength:

$$I = \frac{1}{2} \sum_i z_i^2 c_i \tag{3}$$

(where c_i is the concentration in moles per liter) which gives:

$$k^{-1} = \sqrt{\frac{e_r e_0 k_B T}{2000\, N_A\, e^2 I}} \tag{4}$$

Equations (2) and (4) indicate that the double layer thickness decreases when the concentration of ions in the pore or bulk solution increases. The osmotic force F between two surfaces of area S can be written as below, when the separation distance D is larger than the Debye length and the electrostatic potential y_0 (of the Stern layer) is lower than 25 mV (Israelachvili 2002):

$$F / S_{(D)} \cong 2 e_r e_0 y_0^2 \exp(-kD) \tag{5}$$

In practice, one usually uses the zeta potential instead of y_0 because it is the value that can be determined experimentally. Equation (5) shows that the osmotic force decreases with the double layer thickness. So having more ions in the system should reduce the swelling. On the other hand, it also indicates that this force increases with the absolute value of the electrostatic potential. In the case of clays, this means that more negatively charged surfaces will lead to a larger repulsion.

The initial explanation of this osmotic force can now be taken a little further by introducing the notion of double layer overlap. Indeed, if two surfaces each having their double layer are brought together, the zone between both surfaces gets an “overpopulation” of ions with respect to the ideal distribution of a Gouy-Chapman layer. To reestablish the “ideal distribution”, water is drawn in by osmosis and a repulsive force results between the surfaces. This is the real origin of the repulsive force between charged surfaces and is why it is also referred to as double layer overlap.

The van der Waals force resists this electrostatic repulsion. A balance between the two determines whether surfaces approach, separate, or stay at the same distance one from the other.

B.5 Other cases of *swelling*

The literature mentions other processes that can cause swelling of stone. For instance Madsen and Müller-Vonmoos (1989) indicate the case of stones containing the mineral anhydrite, which "transforms" into gypsum when in contact with water. This is basically a case of crystallization pressure, where one mineral dissolves and another precipitates under a high supersaturation. This has nothing to do with clay swelling. Thus, we are in line with Velde (1992) who stresses that the only components of a stone that can really swell are clay minerals. Finally, we can mention that macroscopic dilatation of stones can result from temperature changes, but that this once again is a completely different question than clay swelling.

ANNEX C GENERAL ISSUES ON CONSOLIDATION WITH ETHYL SILICATES

C.1 Hydrolysis and condensation reactions

The chemistry of ethyl silicates was discovered in the middle of the 19th century by the German scientist von Ebelman (Grissom and Weiss, 1981). The reference molecule in the family of organosilanes is tetraethyl orthosilicate, also called tetra ethoxysilane and denoted TEOS. Its chemical formula is: $Si(-O-CH_2-CH_3)_4$.

In the absence of water, TEOS is stable and its viscosity is very low, very close to that of water. When it is exposed to water, the reaction known as condensation begins. This leads to the formation of larger molecules containing increasing numbers of silicon atoms and ultimately to a rigid network. The first step in the series of reactions that leads to this is hydrolysis. It involves the elimination of an ethoxy ($–O-CH_2-CH_3$) group by a molecule of water and leads to the formation of a molecule of ethanol and an –OH group linked to the silicon atom (Brinker and Scherer, 1990):

$$Si(-O-CH_2-CH_3)_4 + H_2O \rightarrow Si(-O-CH_2-CH_3)_3(-OH) + CH_3-CH_2-OH \quad (6)$$

The reaction can proceed in a similar way, leading to the replacement of the other ethoxy groups by hydroxyl groups. The next type of reaction that can take place is condensation. In this reaction, two hydroxyl groups (or a hydroxyl and an ethoxy group) on different silicon atoms react together. This leads to elimination of a water (or ethanol) molecule and the sharing of an oxygen atom between the two silicon atoms.

$$2\ Si(-O-CH_2-CH_3)_3(-OH) \rightarrow (CH_3-CH_2-O-)_3Si-O-Si(-O-CH_2-CH_3)_3 + H_2O \quad (7)$$

The released water molecule can contribute to the hydrolysis of another ethoxy group. The succession of these reactions eventually leads to a network of Si-O bonds and the formation of a so-called silica gel. This is a solid material, which has a large porosity, typically on the order of more than 50%, with extremely small pore sizes (in the nanometer range).

C.2 Commercial ethylsilicate consolidants

TEOS as such is a rather volatile compound and its direct application would lead to important losses by evaporation. Consequently, commercial ethyl silicate consolidants are most often partially pre-hydrolyzed, so that the product contains small oligomers with up to 3 or 4 silicon atoms. With such small oligomers, the consolidant remains fluid, but does not evaporate much.

These oligomers can be diluted or not with an organic solvent. The condensation reactions can take place using water from the humidity of the atmosphere. If solvent is present, it will evaporate at the same time. To facilitate the hydrolysis reaction, commercial products most often contain small amounts of a catalyst, the most common of which is a dibutyltindilaurate. Further information on these consolidants is best found in the book by Wheeler (2005).

C.3 Efficiency in sandstone versus limestone

The efficiency of ethyl silicate consolidants is known to be much higher in sandstones than in limestones and tuffs (Wendler 1997). The main reason for this difference is believed to be that the surface quartz grains in sandstone offer hydroxyl groups to which the ethyl silicate consolidants can bind. No such bonding would be possible in limestone. Therefore in silicate rocks, the consolidant can chemically bind the grains one to another, while in limestone the bonding

between grains would rely on surface irregularities (mechanical adhesion). Wheeler (2005) for instance states that:

"Alkoxysilianes do not bond to calcite, but they do bond to silicate minerals, particularly quartz and feldspars. This bonding (or lack of bonding) is the single most important factor that influences the performance of consolidated stone in mechanical testing: quartz-rich samples experience much higher strength increases than do stone samples that contain only calcite."

However, another alkoxysilane (Brethane™), a system developed by the English Heritage Research during the 1970s-80s, proved more efficient on limestones than sandstones (Martin et al. 2002). This was one of the results of an 18 years survey of the application of this product to British monuments, mainly based on a collection of visual observations. The authors attribute this unexpected behavior to several possible reasons. In our opinion, the most significant could be that the silica network formed, although weak, may have "protected" these limestones from chemical decay (e.g. acid attack). As a result, the treated stones would appear less weathered than the untreated ones.

Recently, a chemical treatment has been proposed which is meant to enhance the adhesion of ethyl silicate consolidants to limestone (Weiss et al. 2000). In consists in applying a solution containing tartaric acid to the limestone before applying the consolidant. This acid is meant to react with the limestone to create a layer of calcium tartrate. The tartrate molecules contain two —OH groups that are meant to allow condensation with the silicates.

However, in the case of Portland Brownstone, which barely contains any calcite, the poor adhesion of the consolidant is not an issue.

C.4 Cracking from drying shrinkage

A high degree of condensation of the consolidant and good binding to the surface of the stone grains are two necessary conditions for good consolidation. They are not sufficient, however, since other factors can intervene. This is the case in particular of stresses from drying which can cause the consolidant to crack (Scherer and Wheeler 1997).

It is indeed reported that microscopy observations of consolidated stones reveal extensive cracking in the consolidated stone (Félix 1995; Scherer and Wheeler 1997). This clearly limits the efficiency of such treatments.

Drying shrinkage leads to stresses which increase with decreasing pore sizes. They are related to the capillary pressure that develops from the meniscus (Brinker and Scherer 1990, Ch. 8):

$$P = -\frac{2\,g_{LV}\,\cos(q)}{r} \tag{8}$$

where g_{LV} is the liquid/vapor interfacial energy and q is the wetting angle.

For a wetting liquid, q can usually be taken to be 0˚, making cos (q) equal to unity. This leads to a negative pressure for a wetting liquid:

$$P = -\frac{2\,g_{LV}}{r} \tag{9}$$

The solid network (stone and consolidant) is therefore subjected to negative pressure by the liquid in the pores, which means that the solids want to shrink. The stone has a stiff 3D network, which can resist this tendency but the consolidant is much softer. This leaves the consolidant with a tendency to shrink, but it is prevented from doing so by its binding to the pore walls. As a result, the consolidant finds itself in tension. If this results in stresses that exceed the tensile strength of the consolidant, then cracking will result, particularly in consolidant applied in thick rather than

in thin layers. Owing to the small amount of strain energy in a thin film, gel films thinner than about 0.5-1 micron usually do not crack, but thicker ones do (Brinker and Scherer 1990, Ch. 8).

As an example, we can use the water liquid vapor interfacial energy of 70 mN/m. With the pore size of silica gel, in the range of 10 nm or smaller, this leads to stresses of at least 14 MPa. These are largely in excess of the consolidant tensile strength, which is on the order of only 2 MPa.

It must be emphasized that during the initial drying of the stone, the contact angle of the solvent with the silicate consolidant might be quite different from zero and the surface tension of organic solvents is much lower than that of water. Therefore the initial drying could lead to stresses that would be much lower than estimated above and not result in damage of the consolidant. However, when water subsequently wets the stone and invades it, the drying that will follow may then lead to such stresses.

To limit damage from drying on consolidated stones, Scherer has proposed to introduce small particles into the consolidant. Such consolidants are referred to as Particle Modified Consolidants (PMC) and encouraging results have been reported (Escalante et al. 2000, Aggelakopoulou et al. 2002).

C.5 Ethyl silicates as hydrophobic treatments

Finally, it must be noted that incomplete hydrolysis of the ethyl silicate consolidant can lead to making the stone hydrophobic. In circumstances when this result is desired, the ethyl silicates can be made to contain some non-hydrolyzable groups such as methyl groups (as is the case in Conservare-H). This might be done to prevent water ingress into the stone (i.e. protective treatments). The danger of this however is that if water does ultimately enter the stone by another way, such as capillary rise, it will accumulate behind the consolidated zone and freezing events may then lead to serious damage.

References

Abrams and Riley (2002), "A reconstruction of the biodiversity of the Connecticut river valley using fossil and geologicl history evidence", The Traprock, Vol. 1, Dec. 2002, pp.18-22.

Aggelakopoulou, E., Charles, P.; Acerra, M.E.; Garcia, A.I.; Flatt, R.J and Scherer G.W. (2002): "Rheology Optimization of Particle Modified Consolidants", in Materials Issues in Art and Archaeology VI, 2001 MRS Fall meeting Proceedings (Eds: P.B. Vandiver, M. Goodway, J.L. Mass), Volume 712, II.6.

Alcalde, M. and Martin, A. (1990): "Examen visual de las alteraciones que presentan las obras de piedra de interes historico artistico". In Ensayos y Experiencias de Alteracion en la Conservacion de Obras de Piedra de Interes Historico Artistico, ed. A. Martin. Centro de Estudios Ramon Areces, Madrid. Ch. 3 p.117-239.Matero F.G. and Teutonico J.M.

Allbee, B. H. (1894): "The famous Connecticut Brownstone" Stone Magazine no 9, pp.1-31 (in Guinness, 2002)

Alter L. (1995)), http://www.yale.edu/ynhti/curriculum/units/1995/5/95.05.01.x.html#q

Amethyst Galleries (2006)

Amoroso, G.G. (1995): "Il restauro della pietra nell'architettura monumentale: posa in opera, degrado, pulitura", Dario Flaccovio ed., Florence, 220p.

Arnold, A.; Jeanette, D. and Zehnder, K. (1980): Proposal for a terminology of weathering phenomena on building stones. Meeting of Petrology group of ICOMOS. Strasbourg. p.1-26.

Arnold, A. and Zehnder, K. (1990): "Salt weathering on monuments". In First International Symposium on the Conservation of Monuments in the Mediterranean Basin, ed. F.Zezza. Brescia: Grafo. 31–58

ASTM C 119-74: Standard definitions of terms relating to natural building stones

ASTM D 653-78: Standard definitions of terms and symbols relating to soils and rock mechanics

Beaudoin, J.J. and MacInnis, C. (1974): "The mechanism of frost damage in hardened cement paste", Cem. Concr. Res. 4 [2] pp. 139-147

Bell, M. (1985): "The Face of Connecticut: People, Geology and Land". State Geological and Natural History survey of Connecticut, Bulletin 110 (in Guinness, 2002), available online at: http://tmsc.org/face_of_ct/index.html

Benavente, D.; García del Cura, M.A.; Bernabéu, A. and Ordóñez, S. (2001): "Quantification of salt weathering in porous stones using an experimental continuous partial immersion method". Eng. Geol. 59 pp. 313-325.

Berry, N.E. (2002) "Saving Face; Offsetting the march of time in brownstone façades", Old House journal online, June 2002, (http://www.oldhousejournal.com/magazine/2002/june/savingface.shtml)

Brinker, C.J. and Scherer G.W. (1990): “Sol-Gel Science”, Academic Press, San Diego

Bromblet, P. and Verges-Belmin, V. (1996) : "L’élimination des sulfates sur la statuaire calcaire de plein air: une habitude discutable", Le dessalement des materiaux poreux (SFIIC, Champs-sur-Marne, France)

Burns E. (1999): “The City Rocks. Explore the Hidden World of Building Stone; The Connecticut River Valley”, http://homepage.mac.com/ebandpck/cityrocks/connecticut.html.

Camuffo, D. (1998): “Microclimate for cultural Heritage”, in developments in Atmospheric Science, 23. Elsevier.

Colbert, E.H. and Baird, D. (1958): “Coelurosaur bone casts from the Connecticut Valley Triassic”. In America Museum Novitates, n. 1901, July 22. Ed by the American Museum of Natural History, N.Y.pp.1-11

Correns, C.W. (1949): “Growth and dissolution of crystals under linear pressure”, Disc. Faraday Soc. 5: 267–271.

Crosby, W.O and Loughlin, G.F. (1904): “The Building Stones of Boston and Vicinity”, Tech. Quarterly, 17, 165-185.

Delgado Rodrigues, J. (1991): “Proposal for a terminology of stone decay forms on monuments”. G.P. News Letter, Group Petrography of the ICOMOS Stone Committee, pp. 2 4. l/91. Lisboa.

Draper, J.C. (1872): “The Decay of Stone and Brick”, The Manufacturer and Builder, vol. 4 [8], pp 170-171.

Egleston, T. (1887): “The Cause and Prevention of the Decay of Building-Stones”, The Manufacturer and Builder, vol. 19 [11], November 1887, p. 251

Esbert, R. M. and Marcos, R. (1982): “La deterioration de las piedras de la Catedral de Oviedo. 2ª part: Formas y fenomenos de alteracion”. Materiales de construccion 186, pp. 79-88.

Eslinger, E. and Pevear, D.(1988): “Clay Minerals for Petroleum Geologists and Engineers”, SEPM Short Course No. 22.

Escalante M., Valenza J., Scherer G.W. (2000) “Compatible consolidants for ‘particle modified gels’”, In Proc. 9th Int. Congr. on Deterioration and Conservation of Stone, Venice, 19-24 June, 2000, Vol. 2, Ed V. Fassina, pp.459-65. Amsterdam: Elsevier.

Evans, I.S. (1969-70): “Salt crystallization and rock weathering”, Rev Géomorphologie dynamique XIX 4, pp. 153–177.

Félix, C., (1988), Comportement des grès en construction sur le plateau suisse (Performance of Sandstones in Construction on the Swiss Plateau). In *LCP Publications 1975-1995*, Montreux, R. Pancella Ed., EPFL, 833-841

Félix, C. (1995): “Peut-on consolider les grès tendres du Plateau suisse avec le silicate d’éthyle? (Can one consolidate the soft sandstones of the Swiss plateau with ethyl silicate?)”, pp. 267-274

in Preservation and restoration of cultural heritage, ed. R. Pancella, Proc. LCP Congress, Montreux.

Félix C. (1994) "Déformation des grès consecutive à leur consolidation avec un silicate d'ethyle", in 7th Int. Congress of the association of engineering geology, Lisboa, Ed. R. Oliveria, L.F. Rodrigues, A.G. Coehlo and A.P. Cunha, pp.3543-50. Rohterdam: A.A. Balkema.

Félix, C.; Furlan, V., 1994, Variations dimensionnelles des gres et calcaires liees a leur consolidation avec un silicate d'ethyle (Dimensional changes of sandstones and limestones related to their consolidation with an ethyl silicate). In *3rd international Symposium on the conservation of Monuments in the Mediterranean Basin*. Edited by V. Fassina, F. Zezza. Venice, 22-25-June

Flatt, R.J. (2002): "Salt damage in porous materials: how high supersaturations are generated" in J. Crystal Growth 242:435–454.

Flatt R.J. and Scherer G.W. (2002) "Hydration and Crystallization Pressure of Sodium Sulfate: a Critical Review", Mat. Res. Soc. Symp. Proc. 712:29-34.

Folk R.L. (1980): "Petrology of sedimentary rocks", Hemphill Publishing Company, Austin TY, USA, p.184.

Furlan V. and Pancella R. (1983) "Effects of water on the properties of a calcareous sandstone consolidated with synthetic resins". *Proc. Int. Conf. on Material Science and Restoration.* (ed. F.H. Wittmann) Esslingen, Germany: Technische Akademie, 335-339.

Gilley C. (2004) http://www.aroundmaine.com/04/victoria/default.asp

Grissom, C.A. and Weiss, N.R. (1981): "Alkoxysilanes in the conservation of art and architecture: 1861-1981", Art and Archaeology Technical Abstracts 18 [1] 150-202

Guggenheim S. and Martin R.T. (1995) "Definition of clay and clay mineral: Joint report of the AIPEA nomenclature and CMS nomenclature committees", *Clays Clay Miner*. 43:255-256.

Guinness A.C. (2002) "The Portland Brownstone Quarries". In The Chronicle of the Early American Industries Association. vol. 55 [3]. September pp.95-111.

Guinness A.C. (2003) "Heart of stone: The Brownstone industry of Portland, Connecticut" in "The great rift valleys of Pangea in Eastern North America", Ed. LeTourneau P.M. and Olsen P.E., Columbia Press, NY, pp.224-247.

Gray, C (1994): "Streetscapes/ The Osborne. Restoring a Stone Dealer's Idiosyncratic Building". The New York Times, Feb 6th, 1994

Hart S. (2001) "Healing exteriors injured by time", Architectural record (continuing education) http://archrecord.construction.com/resources/conteduc/archives/0111healing-1.asp

Hawes (1885) account by unknown author in: "The Building Stones", in The Manufacturer and Builder, 17 [9], 202

Hitchcok, E. (1865): "Supplement to the Ichnology of New England. A report to the Government of Massachusetts in 1863", Wright & Potter, State Printers, N. 4 Spring Lane, Boston 1865.

Hopkins, T. C. (1897): "Brownstones" in Stone Magazine [15], September 1897: 364-369; 257-265, 147-155 (in Weiss et al. 1982)

Houck, J. and Scherer, G.W. (2006): "Controlling stress from salt crystallization" to be published in proceedings of 16th European Conference Fracture, Alexandroupolis, Greece 2006.

Hubert, J.F., Gildhirst J.M. and Reed A.A (1982), Jurassic Redbeds of the Conneticut Valley: (1) brownstones of the Portland formation, Guidebook for fieldtrips in Conneticut and south Central Massechussets: 74th New England Intercollegiate Geological Conference: Conneticut Geological and Natural History Survey Guidebook. Eds:Joeston and Quarrier , V.5, pp. 1-39 and 103-141

Hubert, J.F., Feshbach-meriney, P.E. and Smith, M.W. (1992): "The Triassic-Jurasic Hartford Rift Basin, Connecticut and Massachussetts: Evolution, Sandstone diagenesis, and hydrocarbon history", The American Association of Petroleum Geologists Bulletin, 76 [11], pp. 1710-1734.

Israelachvili J.N. (1992) "Intermolecular & surface forces", 2nd Ed., Academic Press, Amsterdam, 450p.

Jiménez González, I. and Scherer, G.W. (2004): "Effect of swelling inhibitors on the swelling and stress relaxation of clay bearing stones" in Environmental Geology, 46: 364-377.

Jiménez González, I. and Scherer, G.W. (2006): "Evaluating the potential damage to stones from wetting and drying cycles", to be published in proceedings of 16th European Conf. Fracture, Alexandropoulis, Greece.

Julien, A.A. (1883a): "The Decay of Building Stones of New York City", Trans. N.Y. Ac. Sci., section of Geology, pp. 67-79 and 120-138 (part II).

Julien, A.A. (1883b): "The decay of the building stones of New York City", The Manufacturer and Builder, vol. 15 [2], pp. 43 [account of Julien, 1883]

Julien, A.A (1890): "The Decay of Building Stones of New York City and Vicinity", The Manufacturer and Builder. Vol. 22 [9], pp. 200.

Klein, C. (2002): "The 22nd edition of the manual of Mineral Science (after James D, Dana)". John Wiley Sons, INC. 641p.

Knight, F.E. (1895): "Compressive Resistance of Connecticut Brownstone", Stone Magazine, Vol. XII, No. I, December, 1895, pp 32-33.

Koestler, R.J., Koestler, V.H., Charola, A.E. and Nieto-Fernandez, F.E. (2003): "Art, Biology, and Conservation: Biodeterioration of Works of Art", eds. (Metropolitan Museum of Art, New York,)

Krynine, P.D. (1950): "Petrology, stratigraphy, and origin of the Triassic sedimentary rocks of Connecticut". Connecticut Geological and Natural History Survey Bulletin 73, 247 p.

Larson, J.B. (2000): "Larson announces major historic recognition for town or Portland", US House of Representatives press release of May 23rd 2000. (http://www.house.gov/larson/pr_000523.htm)

Laurenzi Tabasso, M. (1995): "Acrylic Polymers for the Conservation of Stone: Advantages and Drawbacks" APT Bulletin, Vol. 26, No. 4, Preservation of Historic Masonry, pp. 17-21

Lavalle, J. (1853): "Recherches sur la formation lente des cristaux à la température ordinaire" (Research on the slow growth of crystals at ambient temperature), Compt Rend 34: 493–495.

Leo, G.W.; Robinson, P. and Hall, D.J. (1977): "Bedrock geologic map of the Ludlow quadrangle Hampden and Hampshire Counties, south-central Massachusetts: U.S. Geol. Surv. Geol. Quad. Map, GQ-1353 (in Olsen et al. 2005)

LeTourneau, P.M. (2003): "Introduction Chapter" in "The great rift valleys of Pangea in Eastern North America", Ed. LeTourneau P.M. and Olsen P.E., Columbia Press, NY, pp.1-4.

Litvan, G.G. (1972): "Phase transitions of adsorbates: III. Heat effects and dimensional changes in nonequilibrium temperature cycles" in J. Colloid Interface Sci 38 (1): 75–83.

Lockwood, C. (2005): "Q and A column on the Brownstoner" in "Brownstoner; Brooklyn inside out", http://www.brownstoner.com/brownstoner/archives/2005/01/index.html

Loughlin, G.F. (1903), "The building stones of Boston and vicinity", PhD Thesis, MIT.

McInerney, D. P. and Hubert, J.F. (2003): "Meandering-River Facies in the Upper Triassic New Haven Arkose, South-Central Connecticut: Early Evolution of the Hartford Rift Basin". In "The Great Rift Valleys of Pangea in Eastern North America", vol 2. Sedimentology, Stratigraphy and Paleontology. Ed. Peter M. LeTourneau and Paul E. Olsen.

Madsen, F.T. and Müller-Vonmoos, M. (1985): "Swelling pressure calculated from mineralogical properties of a jurassic opalinum shale, Switzerland" in *Clays Clay Miner.*, 33 [6]: 501–509.

Madsen, F.T. and Müller-Vonmoos, M. (1989): "The swelling behavior of clays". *Applied Clay Science* 4:143–56

Martin, B.; Mason, D.; Teutonico, J. M. and Chapman S. (2002): "Stone consolidants: Brethane™". Report of an 18-year review of Brethane™-treated sites. English Heritage Research Transactions, vol 2, pp 3-18

Martin R.T.; Bailey, S.W.; Eberl, D.D.; Fanning, D.S.; Guggenheim, S.; Kodama, H.; Pevear, D.R.; Srodon, J. and Wicks, F.J. (1991): "Report of the clay minerals society nomenclature committee: Revised classification of clay minerals". *Clays Clay Miner*. 39: 333-335.

Matero, F.G. and Teutonico, J. M.(1982): "The use of architectural sandstone in New York City in the 19th century", Bull. of the Association for Preservation Technology, 14 [2], pp.11-17.

Matthias, G.F. (1967): "The weathering rates of Portland arkose tombstones" in Journal of Geological Education, 15: 140-144.

Meierding T.C. (2000) “Arkose (Brownstone) Tombstone Weathering in the Northeastern USA.” In Stone Decay Its Causes and Controls, Bernard J. Smith and Alice V. Turkinton, Proceeding of Weathering 2000, An international symposium held in Belfast, June 26-30, 2000.

Merrill, G.P. (1887): “Our Building Stone Supply”, The Manufacturer and Builder, vol. 19 [5], p. 106

Merrill, G.P. (1888): “The Portland Sandstone Quarries”, The Manufacturer and Builder, vol. 20 [2], p.35 (Account on a report by Prof. Merill)

Merrill, G.P. (1890) accounts by unknown author in: “The Physical Properties of Rocks”, The Manufacturer and Builder, vol. 22[4], pp.78-80; “The Triassic Sandstone of Connecticut”, The Manufacturer and Builder, vol. 22 [5], p 105

Merrill, G.P. (1891): “Stones for Building and Decoration”, J. Wiley & Sons, NewYork. (in Meridering, 2000)

Mindess, S. and Young, J.F. (1981): “Concrete”. Prentice-Hall, Englewood Cliffs, NJ, 425–427.

Mortensen, H. (1933): “Die Salzsprengung“ und ihre Bedeutung für die regiona1klimatische Gliederung der Wüsten”. Petermanns Geogr. Mitt. 5/6: 130-135

Mumford, L. (1955): “The Brown Decades” New York: Dover Publications, p.3 (in Matero and Teutonico, 1982)

Myjer, I. (1999): “In-kind replacement of Brownstone” In traditional building. Division:4 Special report: Masonry restoration. July/August

Myjer, I. (2005): Personal communication.

NORMAL 1-88 Alterazioni macroscopiche dei materiali lapidei: lessico. (CNR-ICR, Italy) Centro Stampa ICR, Roma.

Olsen, P.E., Smith, J.B. and McDonnald, N. G. (1998): “Type material of the type species of the classic theropod foorprint genera Eubrontes, Anchisauripus and Grallator (Early Jurassic, Hartford and Deerfield basins, Connecticut and Massachusetts, Usa)”. Journal of Vertebrae Paleontology 18: 586-601

Olsen, P.E.; Whiteside, J.H.; LeTourneau, P.M.; and Huber, P. (2005): “Jurassic cyclostratigraphy and paleontology of the Hartford basin”. In B.J. Skinner and A.R. Philpotts (eds.), 97th New England Intercollegiate Geological Conference, Department of Geology and Geophysics, Yale University, New Haven, Connecticut, p. A4-1 – A4-51.

Ordaz, J. and Esbert, R. M. (1988): “Glosario de terminos relacionados con el deterioro de las piedras de construccion”. Mat. Constr. 38, pp. 39-45.

Platt Byard Dovell Architects (2002) “The Cooper Union for the Advancement of Science and Art”, Building Stone Magazine, April/May/June 2002, pp. 58-64.

Powell, W.G. (2005): “Portland Brownstone” (http://academic.brooklyn.cuny.edu/geology/powell/613webpage/NYCbuilding/PortlandBrownstone/PortlandBrownstone.htm)

Powers, T.C. (1949): “The air requirement of frost-resistant concrete”, in Proc. Highway Res Board 29: 184–211

Powers, T.C. and Helmuth, R.A. (1953): "Theory of volume changes in hardened Portland-cement paste during freezing" in Proc. Highway Res. Board 32: 285-297.

Ries, H. (1912): “Building Stones and Clay-Products: a Handbook for Architects”,1st ed., J. Wiley & Sons, NY, p.415.

Robinson, D.A. and Williams, R.B.G. (1987): “Surface crusting of sandstones in southern England and Northern France” in International Geomorphology 1986, Part II. Edited by V. Gardiner. John Wiley & Sons Ltd, pp. 623-635

Roblee, E. (1998): Support article of a stone conservation course given at NYU by Dr. G. Wheeler.

Rodríguez-Navarro, C. and Doehne, E. (1999): “Salt weathering: Influence of evaporation rate, supersaturation and crystallization pattern” In Earth Surf. Process. Landforms, vol. 24, no 3, pp. 191-209.

Rodríguez-Navarro, C.; Sebastián Pardo, E.; Doehne, E. and Ginell, W. S. (1998): “The role of sepiolite-palygorskite in the decay of ancient Egyptian limestone sculptures” in Clays and Clay Minerals 46(4): 414-422.

Rozhon, T. (2000): “Brownstone is back, but its use is debated”, NY Times, July 4th 2000, Late Edition - Final, Section A, Page 1, Column 2.

Rude, D. (2000): “Brownstone Restoration: common Mistakes, Practical Solutions”, Concrete Repair Bulletin, pp. 4-5.

Scherer, G.W. (1999): “Crystallization in pores” in Cem. Concr. Res. 29: 1347–1358.

Scherer, G.W. (2000): “Stress from crystallization of salt in pores”, in Proc. 9th Int. Cong. Deterioration and Conservation of Stone, ed. V. Fassina, Elsevier, Amsterdam, Vol. 1: 187-194.

Scherer, G.W. (2004): “Stress from crystallization of salt”, Cem. Concr. Res. 34, pp. 1613-1624.

Scherer, G.W.; Flatt, R. and Wheeler, G. (2001): “Materials science research for the conservation of sculpture and monuments”, MRS Bull. 26 [1], pp.44-50

Scherer, G.W. and Jiménez González, I. (2005): “Characterization of swelling in clay-bearing stone” in Turkington A.V., ed. Stone decay in the architectural environment: Geological Society of America Special Paper 390: 51-61.

Scherer, G.W. and Valenza, II, J.J. (2005): “Mechanisms of Frost Damage” in Materials Science of Concrete, eds. J. Skalny and F. Young (American Ceramic Society) Vol. VII: 209-246

Scherer G.W. and Wheeler, G.E. (1997): “Stress Development Drying of Conservare OH” in Fourth Int. Symp. Conservation Mediterranean Basin, ed. A. Moropoulou, F. Zezza, E. Kollias and I. Papachristodoulou, pp.355-62, Athens: Technical Chamber of Greece.

Smith, B.J.; Magee, R.W. and Whalley, W.B (1994): "Breakdown patterns of quartz sandstone in a polluted urban environment, Belfast, Northern Ireland". In Rock Weathering and Landform Evolution. Ed. By D.A. Robinson and R.B.G. Williams. J. Wiley & Sons, New York, pp.131-150.

Smith, M.R. [ed].(1999): "Stone: Building stone, rock fill and armourstone in construction". Geological Society, London. Engineering Geology Special Publications, 16

Smock, J.C. (1890): "Building Stone in New York", New York State Museum and Science Service. Bulletin 10, p.289 (in Matero and Teutonico, 1982 and Weiss et al., 1982)

Snethlage, R., Wendler, E. (1991): "Surfactants and adherent silicon resins—New protective agents for natural stone" in Mat. Res. Soc. Symp. Proc., Pittsburgh, PA, 185, pp. 193–200.

Taber, S. (1916): "The growth of crystals under external pressure" in Am J. Sci 41: 532–556.

Tenth Census of the United States (1880): "Building Stones of the United States and Statistics of the Quarry Industry for 1880", vol. 10 (Washington Government Printing Office, 1884) 314.

Thayer, B. (2006): Translation of Vitruvius ten books on Architecture. (www.penelope.uchicago.edu/Thayer/E/Roman/Texts/Vitruvius/home.html)

Unknown author from the N. Y. Tribune (1869): "Brown-Stone" in The Manufacturer and Builder, vol. I, [November], pp. 332-333

Velde B. (1992) "Introductions to clay minerals: Chemistry, origins, uses and environmental significance", Chapman & Hall, London,198p.

Viles, H. A. and Goudie, A. S. (2004): "Biofilms and case hardening on sandstones from Al-Quwayra, Jordan". In Earth Surface Process Landforms 29, John Wiley & Sons, Ltd, pp 1473-1485.
Volney Lewis, J. (1908): "Buildings Stones of New Jersey", New Jersey Geological Survey, Annual Report of the State Geologist for 1908. p. 108 (in Matero and Teutonico, 1982)

Wangler, T., Wylykanowitz, A. and Scherer, G.W. (2006): "Controlling stress from swelling clay" to be published in proceedings of 16th European Conf. Fracture, Alexandropoulis, Greece.

Weiss, N.R.; Slavid, I. and Scherer G.W. (2000): "Development and assessement of a conservation treatment for calcareous stone" in 9th Int. Congr. Deterioration and Conservation of Stone, (Ed. V. Fassina), Elsevier, Amsterdam, Vol 2, pp. 533-540.

Weiss, N.; Teutonico, J.; Matero, F. and Pepi, R. (1982): "Sandstone Restoration Study", The New York Landmarks Conservancy, NY.

Wendler, E.; Klemm, D.D. and Snethlage, R. (1991): "Consolidation and hydrohobic treatment of natural stone" in Proc. 5th Int. Conf. on Durability of Building Materials and Components, eds. J.M. Baker, P.J. Nixon, A.J. Majumdar, and H. Davies (Chapman & Hall, London), 203–212.

Wendler, E., Charola, A.E. and Fitzner, B. (1996): "Easter Island tuff: Laboratory studies for its consolidation" in Proceedings of the 8th International Congress on Deterioration and Conservation of Stone, ed. J. Riederer. Berlin, Germany, 2: 1159-1170.

Wendler, E. (1997) "New materials and approaches for the conservation of stone", in *Saving our architectural heritage: The conservation of historic stone structures*, (Ed. Baer N.S. and Snethlage R.), John Wiley & Sons.

Wheeler, G. (2005): "Alkoxysilanes and the Consolidation of Stone", Getty Conservation Institute, Los Angeles, 196 pp.

Winkler, E.M. (1975): "Stone: Properties, Durability in Man's Environment". New York: Springer (in Meridering, 2000)

Winkler, E.M. (1979): "Effect of case hardening in stone", 3rd Int. Congr. on the Det. And Pres. of Stone, Venice 24-27.10.1979, pp.55-63.

Winkler, E.M. (1997): "Stone in architecture", 3rd Ed. Springer, Berlin.

Young, M.E., Wakefiled, R., Urquhart, D.C.M. Nicholson, K. and Tonge, K. (1995): "Assessment in a field setting of the efficacy of various biocides on sandstones" In international colloquium on Methods of Evaluating Products for the Conservation of Porous Building Materials in Monuments, Rome 19/21 june 1995 (ICCROM ed) pp. 93-99

Anexo 8. Glosario

Este glosario esta dirigido al lector no familiarizado con algunos de los temas de los que esta tesis se ocupa. Ha sido confeccionado con el propósito de ofrecer una definición breve de algunos términos usados en este trabajo, estén o no descritos en el cuerpo fundamental de la tesis. De esta forma, se ofrece la posibilidad de hacer una consulta rápida. No consiste por tanto en una recopilación exhaustiva de la terminología técnica empleada.

Las principales fuentes consultadas en la elaboración del mismo han sido las siguientes: Bailey (1980), Camuffo (1998), Esbert et al. (1997), Folk (1980), Glosario de geología del Instituto de Geología americano (AGI), Velde (1996), Winkler (1997), Alcalde y Martín (1990) y WIKIPEDIA.

TÉRMINO	SINÓNIMOS	DEFINICIÓN
abombado *(buckling)*	combado, abombamiento	Véase combado
absorción *(absorption)*		Asimilación o incorporación de fluidos (líquidos o gases) en la estructura porosa de un sólido (AGI). (ej. absorción de agua o absorción de consolidante por parte de la piedra)
adsorción *(adsorption)*		Adhesión de moléculas gaseosas o moléculas en solución a las superficies de cuerpos sólidos con los que están en contacto (AGI). (ej. adsorción de vapor de agua, adsorción de nitrógeno). Puede ser de tipo químico o físico.
agentes inhibidores de la expansión *(swelling inhibitors agents)*	reductores de la expansión	Productos capaces de disminuir o evitar la expansión hídrica y/o hígrica de los minerales de la arcilla del sustrato pétreo.
agua		
cristalina *(crystalline water)*		Moléculas de H_2O en el interior del mineral. Según Velde (1996) se elimina por encima de los 500 °C.
estructural *(structural)*	de constitución	Grupos hidróxidos (OH^-) que forma parte de la estructura química y cristalina del mineral de la arcilla (capa octahédrica). Se eliminan a los 1000-1200 °C. Su desprendimiento provoca la destrucción de la arcilla y su transformación en un producto cerámico.
zeolítica *(zeolitic)*		Agua presente en los vacíos de la red cristalina de la arcilla, su desprendimiento no produce la rotura de la molécula. Se elimina entre los 300-400 °C, aunque según Velde (1996) esto se

		produciría entre los 100-150 °C.
alcano *(alcane)*		Molécula orgánica formada exclusivamente por átomos de carbono e hidrógeno de reducida reactividad.
altura de succión capilar *(height of capillary rise)*		Altura alcanzada por el agua que accede al material por succión capilar. Esta altura aumenta con el tiempo hasta que se produce la saturación de la probeta o hasta que el agua llegue a una altura máxima que depende del tamaño de los poros del material.
amina *(amine)*		Grupo orgánico funcional muy polar derivado del amoniaco y que resulta de la sustitución de al menos un hidrógeno por un radical alquilo. En esta tesis sólo se trata de aminas monosustituidas.
protonada *(protonated amine)*		Amina que ha adquirido un protón por una reacción ácido-base. En esta tesis, la protonación de diaminas se supone necesaria para que se produzca una buena interacción de estos agentes inhibidores de la expansión con los minerales de la arcilla.
aminoalcohol *(amino alcohols)*		Compuesto orgánico que contiene un grupo alcohol y otro de tipo amina.
anisotropía *(anisotropy)*		Es la propiedad general de la materia según la cual determinadas propiedades físicas varían según la dirección en que son examinadas.
arcosa *(arkose)*		Roca arenisca de textura granular formada principalmente por procesos de agregación mecánica. Esencialmente esta formada por grandes granos de cuarzo y de feldespatos. Ambos minerales se presentan comúnmente mezclados en cantidades casi iguales aunque es más frecuente que el cuarzo sea predominante (AGI). Según Folk (1980) se trata de una roca donde predominan los feldespatos (> 25%).
ascenso capilar *(capillary rise)*	succión capilar, capilaridad	Forma que tiene el agua de acceder a un material poroso por presión capilar. Esto se debe a un balance de energías interfaciales que favorece el mojado del material pétreo por el agua.
celda de carga *(load cell)*		Es un transductor (dispositivo electrónico) que convierte una fuerza en una señal eléctrica.
cemento (de la roca) *cement (rock)*		Fase aglomerante entre los granos minerales de la piedra que consiste en material cristalino o amorfo neoformado in situ (precipitado) [Esbert et al. 1997].
ciclos de expansión/contracción *(swelling and shrinkage cycles)*	ciclos de expansión/retracción; (en ciertos casos: ciclos	Periodos sucesivos y alternantes donde el material pétreo sufre continuas deformaciones como consecuencia de las oscilaciones en su

	de humedad/sequedad)	contenido de humedad.
coeficiente de absorción capilar *(sorptivity)*	coeficiente de absorción de agua, de capilaridad o capilaridad	Se define como la masa de agua absorbida por unidad de superficie en relación con la raíz cuadrada del tiempo.
coeficiente de penetración capilar *(sorptivity)*	Coeficiente de succión capilar	Cuantifica la altura alcanzada por el agua succionada, en relación con la raíz cuadrada del tiempo.
coeficiente de hinchamiento lineal ***(e_S)*** *(free swelling strain)*	coeficiente de: expansión lineal, expansión hídrica, expansión libre, deformación por expansión	Relación entre el incremento de longitud de la muestra en una dirección determinada y la longitud inicial en la misma.
coeficiente de Poisson *(Poisson ratio)*		Cociente entre las deformaciones laterales y axiales sufridas por un sólido cuando se le aplica una tracción. Dicha tracción provoca un alargamiento elástico en la dirección de la carga aplicada y contracciones en las direcciones perpendiculares a la misma.
colorimétricos (cambios) *(colorimetric changes)*		Modificación de color (tono, luminosidad y saturación) que sufren algunas piedras como consecuencia de su exposición ambiental, degradación o aplicación de tratamientos de conservación/restauración.
combado *(buckling)*	abombado, abombamiento	Deformación sufrida por la superficie de una piedra que consiste en la separación de placas de material como consecuencia de esfuerzos de compresión generados durante la saturación del mismo. Tales placas presentan una superficie curva (convexa hacia el exterior).
condensación (reacción de) *condensation (reaction of)*		Etapa en el proceso de formación de un gel de sílice donde se forma un enlace Si-O-Si a partir de dos grupos Si-OH con liberación de una molécula de agua.
consolidación *(consolidation)*		Tratamiento encaminado a reestablecer las propiedades físico/mecánicas (rigidez y resistencia mecánica) originales del material pétreo. Esto se consigue a través de la aplicación de productos llamados consolidantes.
consolidantes *(consolidants)*		Productos químicos que mejoran tanto la cohesión entre la fracción alterada como la adhesión de esta a la parte no deteriorada del material. En esta tesis, el consolidante usado ha sido un silicato de etilo (Conservare® OH).
curación del consolidante *(curing of the consolidant)*		Periodo durante el cual un consolidante sigue reaccionando después de ser aplicado en la piedra. Para silicatos de etilo, estas reacciones son de condensación entre los mismos silicatos o entre silicatos y grupos hidroxilos en la superficie del material pétreo.
defectos *(flaws, defects)*	desperfectos, grietas	Imperfecciones, irregularidades o impurezas, que reducen la resistencia mecánica del material

		a la tracción.
deformación *(strain)*		Medida del cambio de tamaño experimentado por un cuerpo cuando un esfuerzo actúa sobre el mismo. Se expresa como la relación del cambio respecto a la dimensión original.
elástica *(elastic strain)*		Aquella que es reversible, es decir, el material recupera su forma inicial una vez que cesa el esfuerzo responsable de tal deformación.
plástica *(plastic strain)*		Aquella que no es o es parcialmente reversible, es decir, el material no recupera o sólo recupera parcialmente su forma inicial una vez que cesa el esfuerzo responsable de la deformación.
por retracción *(shrinkage strain)*		Disminución en la dimensión del material pétreo como consecuencia de su pérdida de agua.
densidad aparente *(apparent density)*	densidad de la roca seca o en bloque, densidad global	Masa del material seco por unidad de volumen total, es decir, el volumen incluyendo su parte sólida y todos sus espacios vacíos.
densidad real *(skeletal density)*	densidad verdadera o de la fracción sólida	Densidad de los granos minerales o “la masa del material seco por unidad de volumen de la parte sólida” es decir, el volumen excluidos sus espacios vacíos.
desecación *(drying)*	evaporación, secado, desorción	Véase desorción
del consolidante *(of the consolidant)*		Periodo en el que el producto consolidante, una vez aplicado al material pétreo, pierde masa. Esto puede ser debido a la evaporación del disolvente o a la producción de alcohol durante las reacciones de condensación de los silicatos de etilo.
desorción *(desorption)*	evaporación, secado o desecación	Proceso que consiste en la cesión de moléculas (ej. vapor de agua) por parte de una interfase (ej. el material pétreo) a una fase líquida o gaseosa.
desprotonacion *(deprotonation)*		Pérdida de un protón. En esta tesis se usa en el contexto de diaminas protonadas usada como inhibidores de la expansión.
desvío *(deflexion or deflection)*	flecha, flecha de flexión	Desplazamiento máximo de una probeta sometida a la flexión en un tiempo determinado.
por pandeo *(warping deflection)*		Desvío de una probeta durante un ensayo de pandeo.
diamino-alcano *(diamino-alkane)*		Alcano con dos funciones aminas. En esta tesis estas aminas se encuentran en cada extremo de las moléculas de alcanos lineares que tienen 2, 3 o 4 carbonos (etano, propano o butano).
diamino-alcano di-hidroclórico *(diamino-alkane dihydrochloride)*	clorhidrato de diamino-alcano	Diamino-alcano combinado con 2 moléculas de ácido clorhídrico para protonar cada función amina de la molécula.
durabilidad *(durability)*		Aptitud o capacidad de un material para resistir la acción agresiva de los agentes de alteración

		una vez colocado en obra.
elasticidad *(elasticity)*		Propiedad de ciertos materiales de recuperar su forma original después de la actuación de un esfuerzo.
enfriamiento evaporativo *(evaporative cooling)*		Reducción en la temperatura de un material (poroso) debido a la evaporación de un líquido (contenido en el material).
ensayo		
brasileño *(Brazilian test)*	ensayo de resistencia indirecta a la tracción	Véase ensayo de resistencia a la tracción indirecta.
de flexión estática por tres puntos *(3 point beam bending)*		Procedimiento que consiste en aplicar una deflexión a una placa de material en el punto medio entre los dos soportes donde se apoya y medir la carga necesaria para producir ese desvío. Con la relación entre la carga y la deflexión se obtiene el módulo de elasticidad estático (en flexión) de la probeta. Este ensayo también se usa en esta tesis para medir relajaciones de esfuerzos. En este caso, se mide la reducción de la carga correspondiente a una determinada deflexión mantenida durante un largo periodo de tiempo.
de pandeo *(warping test)*		La técnica consiste en colocar una placa de piedra que contiene minerales de la arcilla sobre dos soportes e impregnar de agua su superficie superior. La expansión de dichos minerales provoca el pandeo de la probeta. Con la medida de la deflexión se calcula el coeficiente de expansión lineal, aquel de penetración capilar y la relación de módulo de elasticidad saturado respecto de aquel seco.
de resistencia a la tracción indirecta *(indirect tensile strength)*	ensayo brasileño	Procedimiento que consiste en aplicar una carga a una probeta cilíndrica perpendicularmente a su eje de rotación hasta llegar a su rotura. La carga a la que se produce el fallo se relaciona con la resistencia a la tracción.
de resistencia a la compresión *(compressive strength)*		Experimento donde una probeta es sometida a un esfuerzo uniaxial de compresión hasta conseguir la rotura del material. En probetas cilíndricas, el esfuerzo se aplica en la dirección del eje de rotación.
esfuerzos *(stresses)*	tensiones, solicitaciones mecánicas	Fuerza aplicada por unidad de superficie.
de compresión *(compressive)*		Esfuerzo que resulta de la aplicación de dos fuerzas (de la misma dirección y magnitud pero de sentido contrario) perpendicularmente a dos superficies paralelas de un material con la intención de acortarlo.
cortante *(shear)*	de cizalla	Esfuerzo que resulta de la aplicación de dos fuerzas (de la misma magnitud pero de sentido

		contrario) paralelamente a dos superficies, también paralelas, de un material.
de tracción *(tensile)*	de tensión, tensional	Esfuerzo que resulta de la aplicación de dos fuerzas (de la misma dirección y magnitud pero de sentido contrario) perpendicularmente a dos superficies paralelas de un material con la intención de alargarlo.
esfuerzo-deformación (curvas de) *(stress-strain)*		Relación que define el comportamiento mecánico de un material a través de la relación entre esfuerzo y deformación.
esmectitas (smectites)		Grupo de minerales de la arcilla de estructura T-O-T o 2:1, con una carga de capa entre 0.2 y 0.6 (por fórmula unidad) que es compensada por la incorporación de cationes hidratados que se sitúan en la intercapa. Estos minerales son expansivos.
espaciado basal o d_{001} *(basal space or c-spacing)*		Distancia entre un plano en la capa de un mineral de la arcilla y el correspondiente plano en la próxima capa del mismo según la dirección [001].
expansión *(swelling)*	hinchamiento, dilatación	
cristalina *(crystalline, intra, inner-crystalline or interlayer)*	expansión intracristalina	Hinchamiento debido a la incorporación de moléculas de agua de forma ordenada (generalmente hasta un máximo de 4 capas de moléculas) en la intercapa de los minerales de la arcilla de tipo expansivo. Se produce a nivel intracristalino.
hídrica *(hydric)*		Hinchamiento debido al contacto con agua en estado líquido.
hígrica *(hygric)*		Hinchamiento debido al contacto con agua en estado gaseoso o vapor (HR %).
libre *(libre)*		Incremento de dimensión de una probeta medido en una o varias direcciones respecto a la dimensión original de la misma sin hacer uso de constricciones.
osmótica *(osmotic, electrostatic or double layer repulsion)*	Expansión electrostática, repulsión de la doble capa	Hinchamiento debido a la incorporación de moléculas de agua de forma desordenada en o entre los minerales de la arcilla. Se produce a nivel intercristalino o interparticular y puede darse tanto en presencia de arcillas expansivas como no.
retardada *(delayed)*		Hinchamiento del material pétreo que se produce de forma no inmediata una vez este ha alcanzado la saturación por agua.
uniaxial *(uniaxial)*	expansión lineal	Incremento de dimensión medido en una única dirección determinada en relación a la dimensión original de la probeta en esta dirección.

fallo (del material pétreo) *(stone failure)*	rotura, fractura	Rotura del material debido a que los esfuerzos generados son superiores a la resistencia del material.
fatiga mecánica *(mechanical fatigue)*		Fenómeno por el cual la rotura de un material se produce más fácilmente bajo cargas cíclicas dinámicas que bajo cargas estáticas.
filosilicatos *(phyllosilicates)*		Minerales del grupo de los silicatos que presentan una estructura típicamente hojosa. Las hojas son bidimensionales y continuas y están formadas por una (o dos) capas de silicio tetraédricamente coordinados por átomos de oxígeno compartidos, y una capa octaédrica de Al o Mg (con distinto tipo y grado de sustitución). Los minerales de la arcilla son un tipo de filosilicatos.
fisuras de secado *(drying cracking, mud cracking)*	craquelado, grietas poligonales	Fisuras generadas durante el secado del material pétreo. Consiste en un entramado característico de grietas de forma poligonal y se encuentra comúnmente por ejemplo en los terrenos de secano.
flexión *(bending)*		Deformación que presenta un elemento estructural alargado en una dirección perpendicular a su eje longitudinal. En esta tesis se trata de la flexión de pequeñas viguetas o placas largas y finas de piedra.
fluencia lenta *(creep)*	arrastramiento, fluencia viscosa	Incremento de deformación que sufre un material cuando le es aplicado un esfuerzo constante. Este fenómeno se presenta en materiales viscoelásticos.
fragilidad *(brittleness)*		Capacidad de un material de fracturarse con escasa deformación o sin (o casi sin) deformación plástica y con relativamente poca absorción de energía, a diferencia de la rotura dúctil.
frecuencia *(frequency)*		Medida que indica el número de repeticiones de cualquier fenómeno o suceso periódico en una unidad de tiempo.
función de estiramiento exponencial (función de Kohlrausch-Williams-Watts) *(stretched exponential function)*		Función frecuentemente utilizada para describir empíricamente la relajación de sistemas viscoelásticos.
gel de sílice *(silica gel)*		Material sólido amorfo de alta superficie especifica y con poros extremadamente pequeños producto de las reacciones de hidrólisis y condensación de silicatos como el ortosilicato tetraetílico (TEOS).
hidratación de cationes *(cation hydration)*		Coordinación de moléculas de agua por parte de los cationes situados en la intercapa de los minerales de la arcilla. Esto produce la expansión intracristalina de dichos minerales.

humedad relativa
(relative humidity)
Humedad de una masa de aire en relación con la máxima cantidad de humedad que admite sin que se produzca condensación y conservando las mismas condiciones de temperatura y presión atmosférica.

intercapa
(interlayer)
Espacio entre dos capas en los minerales de la arcilla. Cada capa esta formada por un conjunto de las denominadas "hojas" tetra y octaédricas.

interfase
(interphase)
Zona de conexión física y funcional entre dos aparatos o sistemas independientes (ej. entre un sólido y un líquido).

luz
(span)
Distancia entre dos puntos de apoyo en ensayos mecánicos. En esta tesis, se usa para ensayos de flexión o de pandeo.

matriz (de la roca)
(matrix)
Fase aglomerante en una roca formada por material fino depositado (Esbert et al. 1997).

meteorización
(meteorization)
Desintegración y descomposición de una roca en la superficie terrestre o próxima a ella como consecuencia de su exposición a los agentes atmosféricos. Puede ser de origen físico, químico y biológico.

microclima
(microclimate)
Clima local de características distintas a las de la zona en que se encuentra. Una definición más elaborada la ofrece Camuffo (1998): *"Microclima es la síntesis de condiciones físicas ambientales (ej. distribuciones de tiempo y espacio, valores fluctuantes y tendencias, valores medios y extremos, gradientes espaciales y frecuencia de la oscilaciones) debida a cada una de las variables atmosféricas (ej. emisión infrarroja, calefacción, iluminación, ventilación) durante un periodo de tiempo representativo de todas las condiciones determinadas por factores forzados naturales o por aquellos creados por el hombre"*.

minerales de la arcilla
(clay minerals)
Aluminosilicatos de estructura laminar/hojosa (filosilicatos) y con partículas de tamaño coloidal (desde nanómetros a micras). Pueden contener cantidades variables de agua y permiten más substituciones iónicas que otros filosilicatos. En su estructura se distinguen hojas de átomos de silicio y aluminio tetraédricamente coordinados y otros de aluminio o cationes de metales de transición (Fe, Mg, Mn, etc.) octaédricamente coordinados.

expansivos
(swelling)
Aquellos minerales de la arcilla que tienen la capacidad de adsorber agua en su intercapa y por lo tanto expandirse (ej. montmorillonitas sódicas).

no expansivos
(non-swelling)
Aquellos minerales de la arcilla que no experimentan expansión cristalina. No obstante

		pueden hincharse por procesos osmóticos entre partículas. Ejemplos de estos serían las illitas y kaolinitas.
módulo *(modulus)*		Medida de la rigidez de un material.
de elasticidad *(of elasticity)*	De Young	Parámetro que caracteriza el comportamiento de un material elástico según la dirección en la que se aplica un esfuerzo. Para un material elástico lineal e isótropo, el módulo de Young tiene el mismo valor para una tracción que para una compresión; siendo una constante independiente del esfuerzo siempre que no exceda de un valor máximo denominado límite elástico.
de elasticidad estático *(static elastic)*		Aquel módulo de elasticidad obtenido a través de métodos estáticos como la flexión estática por tres puntos.
de elasticidad dinámico *(dynamic elastic*)		Aquel módulo de elasticidad obtenido a través de métodos dinámicos como la medida de velocidad de pulsos ultrasónicos a través del material.
molasa *(molasse)*		Arenisca de cemento calcáreo, en ocasiones margoso.
montmorillonitas *(montmorillonite)*		Tipo de esmectita con una estructura tipo "sándwich" (una capa central de átomos de aluminio y magnesio octaédricamente coordinados entre dos capas de átomos de silicio tetraédricamente coordinados).
pandeo *(warping)*		Combado de una placa de piedra fina y larga como consecuencia de su expansión tras aplicar agua en su superficie superior.
pasta de cemento *(cement paste)*		Fase aglutinante en el hormigón compuesta principalmente por silicatos de calcio hidratados (C-S-H), que son el principal producto de la reacción química (hidratación) entre el agua y el cemento Portland.
permeabilidad *(permeability)*		Capacidad de un material para permitir que un fluido lo atraviese sin alterar su estructura interna.
planos de sedimentación *(bedding planes)*	planos de estratificación	Capas de sedimentos en una roca sedimentaria. Son por lo tanto elementos de anisotropía textural de la piedra. Sus interfases pueden ser también zonas de debilidad del material.
polaridad *(polarity)*		Propiedad de ciertas moléculas que tienen una distribución espacial asimétrica de cargas (positivas y negativas), formando dipolos eléctricos que influyen en varias propiedades como la solubilidad.
porosidad *(porosity)*		Volumen ocupado por los espacios vacíos por unidad de volumen de un material.

presión de capilaridad
(capillary pressure)
Disminución de presión en un líquido que accede por succión capilar en un medio poroso. Es proporcional a la tensión superficial e inversamente proporcional al radio de la interfase.

presión de hinchamiento
(swelling pressure)
Esfuerzo de compresión necesario para prevenir la expansión de un material. En esta tesis se trata de expansión debida a los minerales de la arcilla contenidos en materiales pétreos.

presión de cristalización
(crystallization pressure)
Esfuerzo de compresión necesario para prevenir el crecimiento de un cristal en una solución sobresaturada. Se refiere al esfuerzo ejercido por un medio poroso en oposición al crecimiento de sales en sus poros.

regresión linear
(linear regression)
Método matemático que expresa la relación entre una variable dependiente Y y una (o más) variable independiente X, como la suma de dos términos. El primero es el producto de X por una constante denominada pendiente y el segundo es una constante denominada intersección (u ordenada en el origen). Los valores de la intersección y la pendiente son los que minimizan los errores en dicha relación.

relajación de esfuerzos o tensiones
(stress relaxation)
Disminución del esfuerzo necesario para mantener un desvío fijo bajo una determinada carga. Este fenómeno se presenta en materiales viscoelásticos.

reproducibilidad
(reproducibility)
Capacidad que tiene un ensayo o experimento para ser reproducido.

resiliencia
(compliance)
Capacidad de un material para absorber energía elástica cuando es deformado por la aplicación de una carga y de cederla cuando la carga se deja de aplicar.

resistencia mecánica
(*mechanical strength*)

- **a la compresión**
  (compressive)
  Esfuerzo máximo de compresión soportado por un material antes de romperse.
- **a la tracción**
  (tensile)
  Esfuerzo máximo de tensión/tracción soportado por un material antes de romperse.
- **al taladrado**
  (drilling resistance)
  Resistencia que presenta un material a determinadas condiciones de taladrado. En esta tesis, el término hace referencia al tipo de medidas usadas por Wendler et al. (1996) quienes usan unidades arbitrarias que parecen correlacionarse bien con la resistencia a la flexión del material.

rigidez
(stiffness)
Capacidad de un objeto sólido para soportar esfuerzos sin sufrir grandes deformaciones o desplazamientos.

saturación (con un líquido) *(saturation)*		Absorción máxima de agua en un cuerpo poroso.
separación de placas *(contour scaling)*		Alteración por disyunción que implica la separación o levantamiento de placas (laminas extensas y de varios milímetros de espesor, generalmente rígidas), paralelas a la superficie de la piedra e independientes de su estructura.
silicatos de etilo *(ethyl silicates)*		Son productos silicoorgánicos usados como consolidantes. La molécula de base presenta la formula $Si(O\text{-}CH_2\text{-}CH_3)_4$. En algunos casos, una función etoxi puede ser sustituida por una alquilo. Además, en presencia de agua se producen reacciones de hidrólisis y de condensación.
sistema poroso *(porous system)*		Parte de la roca formada por espacios vacíos. Su estudio es muy importante para determinar la durabilidad de los materiales pétreos.
solicitaciones mecánicas *(stresses)*	esfuerzos, tensiones	Véase esfuerzos
soluciones acuosas *(aqueous solutions)*		Disolución donde la parte disolvente es agua.
succión capilar *(capillary rise)*		Véase ascenso capilar
tensoactivos *(surfactants)*		Son productos formados por moléculas que tienen una parte hidrófoba (no polar) y una hidrófila (polar o iónica). Su adsorción en interfases cambia algunas propiedades de las mismas.
técnica "3 en 1" *("3 in 1 technique or warping)*	ensayo de pandeo	Véase ensayo de pandeo
tensiones *(stresses)*	esfuerzos, solicitaciones mecánicas	Véase esfuerzos
cortantes *(shear stresses)*	esfuerzos, tensiones de cizalladura	Véase esfuerzos cortantes
de secado *(drying stresses)*		Esfuerzos desarrollados durante el proceso de evaporación. En el caso de un bloque pétreo saturado que comienza a secarse, se desarrollaran esfuerzos de tracción.
Transductor diferencial variable lineal (TDVL) *(Lineal variable differential transformer, LVDT)*		Transductor de desplazamiento que convierte un desplazamiento en un cambio de tensión alterna en proporción a la magnitud del mismo.
toba volcánica *(volcanic tuff)*		Roca ligera, de consistencia porosa y origen volcánico.
vidrios Vycor® *(Vycor® glass)*		Vidrio poroso de alto contenido en sílice (95 %) de porosidad bien caracterizada.
viscoelasticidad *(viscoelasticity)*		Propiedad de algunos materiales que presentan un comportamiento tanto elástico como viscoso. En ellos, la deformación sufrida tras aplicar una carga no es totalmente reversible y además esta

varía con respecto al tiempo de aplicación de la misma.

viscosidad
(viscosity)

La viscosidad es la oposición de un fluido a las deformaciones tangenciales.

Anexo 9. Traducción de términos ingleses

absorption	absorción
absorption	adsorción
alkane	alcano
amine	amina
amino alcohols	aminoalcoholes
anisotropy	anisotropía
apparent density	densidad aparente, densidad de la roca seca o en bloque, densidad global
aqueous solutions	soluciones acuosas
arkose	arcosa
basal space or C-spacing	espaciado basal (001)
bedding planes	planos de sedimentación, planos de estratificación
bending	flexión
brazilian test	ensayo Brasileño, ensayo de resistencia indirecta a la tracción
brittleness	fragilidad
buckling	abombado, combado, abombamiento
capillary pressure	presión de capilaridad
capillary rise	ascenso capilar, succión capilar, capilaridad
cation hydration	hidratación de cationes
cement paste	pasta de cemento
cement (rock)	cemento (de la roca)
clay minerals	minerales de la arcilla
colorimetric changes	colorimétricos (cambios)
compliance	resiliencia
compressive strength	resistencia mecánica a la compresión
compressive strength test	ensayo de resistencia a la compresión
compressive stresses	esfuerzos de compresión
condensation, reaction of	condensación (reacción de)
consolidants	consolidantes
consolidation	consolidación
contour scaling	separación de placas
creep	fluencia lenta, arrastramiento, fluencia viscosa
crystalline water	agua cristalina

crystalline, intra, inner-crystalline or interlayer swelling	expansión cristalina, expansión intracristalina
crystallization pressure	presión de cristalización
curing of the consolidant	curación del consolidante
deflexion or deflection	desvío, flecha, flecha de flexión
delayed swelling	expansión retardada
deprotonation	desprotonacion
desorption	desorción, evaporación, secado o desecación
diamino-alkane	diamino-alcano
diamino-butane dihydrochloride	diamino-alcano di-hidroclórico
drilling resistance	resistencia mecánica al taladrado
drying	desecación, evaporación, secado, desorción
drying cracking, mud cracking	fisuras de secado, craquelado, grieta
drying of the consolidant	desecación del consolidante
drying stresses	tensiones de secado
durability	durabilidad
dynamic elastic modulus	módulo de elasticidad dinámico
elastic strain	deformación elástica
elasticity	elasticidad
ethyl silicates	silicatos de etilo
evaporative cooling	enfriamiento evaporativo
failure (stone)	fallo (del material pétreo), rotura, fractura
flaws, defects	defectos, desperfectos, grietas
free swelling	expansión libre
free swelling strain	coeficiente de hinchamiento lineal (ε_S), coeficiente de expansión lineal
frequency	frecuencia
height of capillary rise	altura de succión capilar
hydric swelling	expansión hídrica
hygric swelling	expansión hígrica
indirect tensile strength test	ensayo de resistencia a la tracción indirecta
interlayer	intercapa
interphase	interfase
Lineal Variable Differential Transformer (LVDT)	Transductor Diferencial Variable Lineal (TDVL)
linear regression	regresión linear
load cell	celda de carga
matriz (rock)	matriz (de la roca)

mechanical fatigue	fatiga mecánica
mechanical strength	resistencia mecánica
meteorization	meteorización
microclimate	microclima
modulus	módulo
modulus of elasticity	módulo de elasticidad, De Young
molasse	molasa
montmorillonite	montmorilonitas
mud cracking	fisuras de secado, craquelado, grieta
non-swelling clay minerals	minerales de la arcilla no expansivos
osmotic swelling, electrostatic swelling or double layer repulsion	expansión osmótica, expansión electrostática, repulsión de la doble capa
permeability	permeabilidad
phyllosilicates	filosilicatos
plastic strain	deformación plástica
Poisson ratio	coeficiente de Poisson
polarity	polaridad
porosity	porosidad
porous system	sistema poroso
protonated amine	amina protonada
relative humidity	humedad relativa
reproducibility	reproducibilidad
saturation	saturación (con un líquido)
shear stresses	esfuerzos o tensiones cortantes o de cizalladura
shrinkage strain	deformación por retracción
silica gel	gel de sílice
skeletal density	densidad real, densidad verdadera o de la fracción sólida
smectites	esmectitas
sorptivity	coeficiente de absorción capilar, de absorción de agua, de capilaridad, de penetración capilar o capilaridad
span	luz
static elastic modulus	módulo de elasticidad estático
stiffness	rigidez
strain	deformación

stress relaxation	relajación de esfuerzos o tensiones
stresses	esfuerzos, tensiones , solicitaciones mecánicas
stress-strain	esfuerzo-deformación
stretched exponential or Kohlrausch-Williams-Watts function	función de estiramiento exponencial (función de Kohlrausch-Williams-Watts)
structural water	agua estructural o de constitución
surfactants	tensoactivos
swelling	expansión, hinchamiento, dilatación
swelling and shrinkage cycles	ciclos de expansión/retracción
swelling clay minerals	minerales de la arcilla expansivos
swelling inhibitors agents	agentes inhibidores o reductores de la expansión
swelling pressure	presión de hinchamiento
tensile strength	resistencia mecánica a la tracción
tensile stresses	esfuerzos de tracción, de tensión, tensional
test	ensayo
three point beam bending test	ensayo de flexión estática por tres puntos
uniaxial swelling	expansión uniaxial, expansión lineal
viscoelasticity	viscoelasticidad
viscosity	viscosidad
volcanic tuff	toba volcánica
Vycor® glass	vidrios Vycor®
warping	pandeo
warping deflection	desvío por pandeo
warping test	ensayo de pandeo
zeolitic water	agua zeolítica
“3 in 1” technique or warping	técnica del "3 en 1" o ensayo de pandeo